BNL-52643
Formal Report

Proceedings of RIKEN BNL Research Center Workshop Volume 35

RIKEN Winter School

Quarks, Hadrons and Nuclei

~QCD Hard Processes and the Nucleon Spin~

December 1-5, 2000

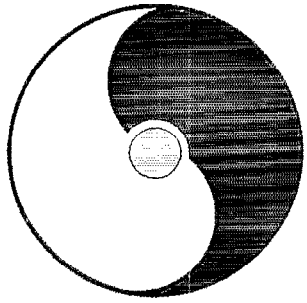

Organizers:

Naohito Saito, Toshi-Aki Shibata, and Koichi Yazaki

RIKEN BNL Research Center

Building 510A, Brookhaven National Laboratory, Upton, NY 11973-5000, USA

DISCLAIMER

This report was prepared as an account of work sponsored by an agency of the United States Government. Neither the United States Government nor any agency thereof, nor any employees, nor any of their contractors, subcontractors or their employees, makes any warranty, express or implied, or assumes any legal liability or responsibility for the accuracy, completeness, or any third party's use or the results of such use of any information, apparatus, product, or process disclosed, or represents that its use would not infringe privately owned rights. Reference herein to any specific commercial product, process, or service by trade name, trademark, manufacturer, or otherwise, does not necessarily constitute or imply its endorsement, recommendation, or favoring by the United States Government or any agency thereof or its contractors or subcontractors. The views and opinions of authors expressed herein do not necessarily state or reflect those of the United States Government or any agency thereof.

Available electronically at-

`http://www.doe.gov/bridge`

Available to U.S. Department of Energy and its contractors in paper from-

U.S. Department of Energy
Office of Scientific and Technical Information
P.O. Box 62
Oak Ridge, TN 37831
(423) 576-8401

Available to the public from-

U.S. Department of Commerce
National Technical Information Service
5285 Port Royal Road
Springfield, VA 22131
(703) 487-4650

Printed on recycled paper

Preface to the Series

The RIKEN BNL Research Center (RBRC) was established in April 1997 at Brookhaven National Laboratory. It is funded by the "Rikagaku Kenkyusho" (RIKEN, The Institute of Physical and Chemical Research) of Japan. The Center is dedicated to the study of strong interactions, including spin physics, lattice QCD, and RHIC physics through the nurturing of a new generation of young physicists.

During the first year, the Center had only a Theory Group. In the second year, an Experimental Group was also established at the Center. At present, there are seven Fellows and eight Research Associates in these two groups. During the third year, we started a new Tenure Track Strong Interaction Theory RHIC Physics Fellow Program, with six positions in the first academic year, 1999-2000. This program has increased to include ten theorists and one experimentalist in the current academic year, 2001-2002. Beginning this year there is a new RIKEN Spin Program at RBRC with four Researchers and three Research Associates.

In addition, the Center has an active workshop program on strong interaction physics with each workshop focused on a specific physics problem. Each workshop speaker is encouraged to select a few of the most important transparencies from his or her presentation, accompanied by a page of explanation. This material is collected at the end of the workshop by the organizer to form proceedings, which can therefore be available within a short time. To date there are thirty-four proceeding volumes available.

The construction of a 0.6 teraflops parallel processor, dedicated to lattice QCD, begun at the Center on February 19, 1998, was completed on August 28, 1998.

T. D. Lee
August 2, 2001

*Work performed under the auspices of U.S.D.O.E. Contract No. DE-AC02-98CH10886.

CONTENTS

Preface to the Series..... i

Introduction
N. Saito, T.-A. Shibata, & K. Yazaki..... 1

Probing the Nucleon with Hard Processes: an Introduction
X.-D. Ji..... 3

Experiments of Deep Inelastic Scattering
W.-D. Nowak..... 63

Spin Structure Functions in the Chiral Quark Soliton Model
M. Wakamatsu..... 163

Spin Physics at RHIC
G. Bunce..... 207

Physics of Proton-Antiproton Collisions at Tevatron CDF
F. Ukegawa..... 271

Heavy Quarkonium and QCD
H. Fujii..... 365

Organization of the School 407

List of the Students of the School 408

Program of the School 409

Photos

Additional RIKEN BNL Research Center Proceeding Volumes

Contact Information

Introduction

The RIKEN School on "Quarks, Hadrons and Nuclei — QCD Hard Processes and the Nucleon Spin" was held from December 1st through 5th at NASPA New Ohtani, Yuzawa, Niigata, Japan, sponsored by the RIKEN Accelerator Research Facility. The school was intended to be the first of a new series with a broad perspective of hadron and nuclear physics but was also meant to be a continuation of the previous two schools on QCD hard processes which had been held in 1996 and 1998.

The purpose of the school was to offer young researchers an opportunity to learn the exciting physics associated with hadrons and nuclei based on QCD in general and the structure of the nucleon probed by QCD hard processes and modeled by effective theories in particular. The subjects discussed in the school cover theoretical and experimental aspects of the hard processes and the nucleon structure functions, starting from the basics of the perturbative QCD.

We had 2 basic courses, one theoretical and one experimental, each consisting of 3 one-hour lectures, 4 topics courses each consisting of 2 one-hour lectures and 2 evening sessions for Q&A on the lectures and short talks by students. The list of the lecturers together with the titles of their lectures are given below.

Lecturers

X.-D. Ji (Maryland)	"Probing the nucleon with hard processes: an introduction"
H. Fujii (Tokyo)	"Heavy quarkonium and QCD"
M. Wakamatsu (Osaka)	"Spin structure functions in the chiral quark soliton model"
W.-D. Nowak (DESY)	"Experiments of deep inelastic scattering"
G. Bunce (BNL/RBRC)	"Spin physics at RHIC"
F. Ukegawa (Tsukuba)	"Physics of proton-antiproton collisions at Tevatron CDF"

17 students attended the school and actively participated in the program. The lecturers gave excellent courses which were both pedagogical and inspiring. They also attended the evening sesseions and were kind enough to respond to any questions asked either during the sessions or in smaller circles.

Profs. T. Hatsuda and J. Kodaira volunteered to be senior tutors of the school helping students in understanding the lectures and organizing "late evening sessions" for chutter-

ing in relaxed atmosphere. The young tutors, Drs. N. Ishii, K. Naito and Y. Yasui, also helped students during the lectures and the discussion sessions.

An excursion to Naeba skiing area was organized on the 3rd day in the afternoon and some of lecturers, students and organizers enjoyed early season skiing.

At the end of the school, we asked the students and the lecturers to write their opinions about the school. The responses were all positive. The students were satisfied by the well-prepared lectures, stimulating discussions with the lecturers and the nice environment, while the lecturers also enjoyed talking to students and pleasant atmosphere. The students wanted to have this kind of school regularly, every year if possible. The school is now planned to be held every two years but we are considering the possibility of organizing mini-schools in intermediary years.

We are grateful to the RIKEN Accelerator Research Facility for the generous financial support which enabled us to organize this school. The school was held as an activity related to the collaboration with the RIKEN BNL Research Center and we thank the director of the Center, Professor T.D. Lee, for general support. We also thank the members of the International Advisory Committee for suggesting lecturers and giving us useful comments. We are obliged to the lecturers, the tutors and the students for making the school exciting and fruitful.

Special thanks are due to Ms.Yoko Kishino who did most of the administrative works and took care of drinks and snacks during the coffee breaks and the evening sessions. Last but not least, we thank NASPA New Ohtani for their excellent service and comfortable atmosphere.

Naohito Saito, Toshi-Aki Shibata and Koichi Yazaki

RIKEN,
August, 2001

Probing the Nucleon Structure in High-Hnergy Processes

Xiang-dong Ji
University of Maryland

Summary

Lecture 1: Nucleon Physics and QCD

Summary: In this lecture, I first discuss why studying the nucleon structure is important and explain various recent experimental efforts in the field. Then I discuss a brief history of nucleon physics which led to the advent of quantum chromodynamics (QCD). Following this, I explain some salient features of QCD: chiral symmetry, asymptotic freedom, and color confinement. In particular, I consider the aspects of QCD as strongly-coupled quantum field theory. Finally the physical significance of renormalization is explored.

Lecture 2: High-Energy Probe of the Nucleon Structure

Summary: In this lecture, I start with a discussion of factorization theorems for various high-energy scattering processes. Then I focus on deep-inelatic scattering (DIS) as a special example. I introduce the light-cone coordinates and the collinear expansion. The leading-order handbag diagram is calculated in perturbation theory. The result can be expressed in terms of quark light-cone correlation functions. The corrections to the handbag include longitudinal gluon scattering, QCD radiative corrections, and higher twist contributions. The final result is a leading-twist factorization formula for DIS.

Lecture 3: The Nucleon Spin and Quark Orbical Motion

Summary: I start with an historical introduction to the studies of orbital motion. Then I explore the question what do we know about quark orbital motion in the proton. Following this, I consider quark orbital observables in the infinit momentum frame. Finally, I show how to probe the quark orbital motion in Compton scattering and to calculate relevant observables using lattice QCD.

核子物理

Nucleon Physics

Study the low & high energy structure and properties of the nucleon.

⇒ why do we care?

- Microscopic structure of matter.

  matter → atoms ('20~'30) → atomic nuclei ('60~'70) → nucleon

- A New Paradigm

  Relativistic, strongly coupled
  infinite-body system
  No example has been solved before

- Laboratory for New Physics

  Stable beam & target
  One must understand the structure
  to predict rates for t-quark, Higgs, ...
  production

A New wave of interest ...

⇒ Experimental facilities

- Jetterson Lab

  $\not{P}$ electron Scattering
  Polarized Structure functions
  Compton Scattering, Polarizabilities
  N^* physics
  ...

- $\overrightarrow{\text{RHIC}}$ Spin Physics

  Polarized & unpolarized Parton distributions

- HERA - HERMES Collaboration

  Deep inelastic Scattering
  hadron final state

- CERN - COMPASS Collaboration

  Polarized gluon distribution
  Off-forward Parton Distributions

- FANL, E866, Drell-Yan
- MIT-Bates Sample exp.
- MAINZ photo-pion physics, chiral symmetry
- ...

⇒ Theoretical efforts (Beyond Models)

- Lattice QCD

  Desy, Germany
  Kentucky (K. F. Liu)
  Tsukuba, Japan
  MIT (Negele)
  Triumf

- Large N_c

  Manohar et al.
  Witten

- χ-perturbation theory

  Meissner
  Holstein

- QCD Sum Rule

  Limited predictive power

A Brief History ...

- Measurement of the Proton magnetic moment $\mu_p = 2.8\,\mu_N$

  O. Stern 1933

  Nobel prize 1943

  ★ First evidence that the proton has a nontrivial internal structure.

- Measurement of electromagnetic form factors

  R. Hofstadter (mid 50's)

  Nobel prize 1961

  $G_M(Q^2)$

  $G_E(Q^2)$ $\langle r_p^2 \rangle^{1/2} = 0.862$ fm

  $= -0.112$ fm

- Quark Model

  Gell Mann & Zweig 1964

  Nobel prize 1969

- Discovery of Quarks

  Friedman, Kendall, Taylor 1967

  Nobel prize 1990

- <u>Advent of QCD (1972-1973)</u>

Quark model is unsatisfactory for a number of reasons

- Mass of pion ~ 140 MeV. pions are Goldstone Bozons resulted from spontaneous breaking of χ-symmetry. m_q cannot be as large as 300 MeV.

- Quarks have an internal degrees of freedom, color.

  existence of Ω^-, Δ^{++}, ..
  $\pi^0 \to 2\gamma$ decay
  $e^+e^- \to$ hadrons

  Why is the color there?

- No free quarks found in lab.

In 1972-73, Gell-Mann, Fritzch & Leutwyler "Nonabelian gauge theory with SU(3) color degrees of freedom" $\equiv$ QCD

QCD: a quantum field theory

$$\mathcal{L}_{QCD} = \bar{\psi}_i (i\not{\partial} - m_q)\psi_i - \frac{1}{4} F^a_{\mu\nu} F^{\mu\nu}_a - g\bar{\psi}\not{A}\psi$$

$i = 1, 2, 3 \qquad a = 1, 2, \ldots, 8$

$$F^a_{\mu\nu} = \partial_\mu A^a_\nu - \partial_\nu A^a_\mu - g f_{abc} A_{b\mu} A_{c\nu}$$

$$m_q = \begin{pmatrix} m_u & & 0 \\ & m_d & \\ 0 & & m_s \end{pmatrix}$$

- <u>Chiral symmetry</u>

$m_u \sim 5\,\text{MeV} \quad m_d \sim 9\,\text{MeV} \quad m_s \sim 150\,\text{MeV}$

$m_q \ll M_N$

To a good approximation

$$\psi_{L,R} = \tfrac{1}{2}(1 \mp \gamma_5)\psi$$

Can be rotated independently in flavor space.

- <u>Asymptotic freedom</u>

$\alpha_s(Q) \to 0$ as $Q^2 \to \infty$

an important condition for theory to make sense

- <u>Quark Confinement</u>

$Q \to \Lambda_{QCD}, \quad \alpha_s \to \infty$

strong coupling $\to$ quark confinement

QCD as a quantum field theory

QFT = Quantum Mechanics
+ Space-time Symmetry
(Poincaré Symmetry
Causality)

① **Causality**:

$$[\hat{O}_1(x), \hat{O}_2(y)] = 0 \quad \text{if} \quad (x-y)^2 < 0$$

Spacelike

$\Longrightarrow$

- Negative energy states or antiparticle
- Spin & Statistics

Dirac lecture by R. Feynman

★★★ Physical vacuum is a complicated dynamical system.

- In QED, the vacuum can be studied in perturbation theory
- In QCD, the vacuum is nonperturbative (χ-symmetry breaking, Color confinement)

Physical States (particles) appear as elementary excitations of the vacuum

→ One cannot understand the structure of a bound state without understanding the vacuum

→ physical observables

$$\langle O \rangle = \langle p|\hat{O}|p\rangle - \langle 0|\hat{O}|0\rangle$$

↑ Part of the state describes the vacuum

hadron structure → condensed matter

(Why is the hydrogen atom so simple?)

② <u>Lorentz Symmetry</u>:

particles with all possible momenta (pointli

local interactions

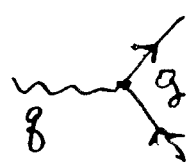

Same interaction g even if $q^2 \to \infty$

★★★ Ultraviolet Divergences

For <u>renormalizable quantum field theory</u>, all large momentum effects can be isolated and classified into a few types, and eventually can be absorbed in a few parameters. This type of theories has <u>minimal sensitivity</u> to physics at high-energy scales.

- Pointlike particles are an approximation of reality at low energy. Thus for an effective theory at low energy, the physics should be independent of the details of the high energy structure.

- Only physical observables can be rid of ultraviolet divergences. These include S-matrix elements and currents associated with symmetries of the lagrangian. Any other operators need <u>renormalization</u> and hence <u>scale & scheme dependent</u>.

Even for renormalizable theory such as QCD. the formal Lagrangian is meaningless. One must introduce <u>regularization</u> (cutoff) which In general will break some symmetries of the classical lagrangian.

Two popular regularizations:

- Dimensional regularization ($d=4-\epsilon$)
  Consistent in perturbation theory
  break scale & $U_A(1)$ symmetries.

- Lattice regularization (a)
  breake scale & $U_A(1)$ & Lorentz Symmetries
  Good for nonperturbative Calculation

After regularization (& renormalization — minimal subtraction in dimensional Reg.) The original theory becomes an effective theory with momentum scale $< \mu$.

All degrees of freedom above μ are integrated out. The remaining degrees of freedom with modified (renormalized) Lagrangian yield well-behaved Green's functions (free of divergences)

- Effective theory is entirely equivalent to original theory at any μ. In particular it is not necessary to let $a \to 0$ or $\mu \to \infty$.
- There are many different, but equivalent effective theories. (choice of different scheme)
- A choice of scheme & scale is like a choice of coordinates. Thus, the so-called quarks & gluons do not have definitive physical significance. They depend on your definition or choice.

Renormalization group equation

Although real physical observables are independent of μ, many auxiliary quantities are μ-dependent. Renormalization group equations are derived by considering renormalized theories with two different cutoff (μ) & $(\mu+d\mu)$.

A change of cutoff introduces a change of coupling $g(\mu)$ if physical observables are kept fixed. Change of the coupling can be calculated in perturbation theory. if $g(\mu)$ is small.

$$\mu \frac{dg(\mu)}{d\mu} = \beta(g(\mu))$$
$$= -\beta_0 \frac{g^3}{16\pi^2} - \beta_1 \frac{g^5}{(16\pi^2)^2} - \cdots$$

$\beta(g(\mu))$ is QCD β function. $\beta_0 = 11 - \frac{2n_f}{3} > 0$

One loop solution:

$$\alpha_s(\mu) = \frac{g(\mu)^2}{4\pi} = \frac{4\pi}{\beta_0 \ln \mu^2/\Lambda_{QCD}^2} \xrightarrow{\text{as } \mu\to\infty} 0$$

Asymptotic freedom.

Small coupling does not always imply that perturbation theory is applicable. For instance, the hadron mass

$$M \sim \mu e^{2\pi/\beta_0 \alpha_s(\mu)}$$

remains nonperturbative in the limit $\mu \to \infty$ and $\alpha_s(\mu) \to 0$.

Renormalization group equation for other quantities (Green's functions, composite operators, etc) can be derived in a similar way.

Gauge Symmetry

In perturbative calculation, it is necessary to make a gauge choice. A consistent choice is covariant gauge fixing which is done by adding $-\frac{1}{2\lambda}(\partial_\mu A^\mu)^2$ to QED lagrangian. This choice introduces extra degrees of freedom — Fadeev-Popov Ghost.

Using dimensional regularization the effective Lagrangian

$$\mathcal{L}_{eff} = -\frac{1}{4} F_{\mu\nu} F^{\mu\nu} + \bar{\psi}(i\not{\partial} - m)\psi$$
$$- \frac{1}{2\lambda}(\partial_\mu A)^2 - \partial_\mu \bar{\omega} D_\mu \omega$$

Formal solution of QCD is contained in the path integral

$$Z(\eta, \bar{\eta}, \xi, \bar{\xi}, J) = \int [D\psi\, D\bar{\psi}\, D\omega\, D\bar{\omega}\, DA]$$
$$e^{i S_{eff} + \bar{\omega}\eta + \bar{\eta}\omega + \bar{\psi}\xi + \bar{\xi}\psi + AJ}$$

Because of the gauge fixing, the formal gauge invariance is lost. However, for physical observables the gauge symmetry is guaranteed by generalized Ward identities associated with BRST symmetry

$$\delta_{BRST} \langle T \cdots \rangle = 0$$

$$\frac{dM}{d\mu} = 0$$

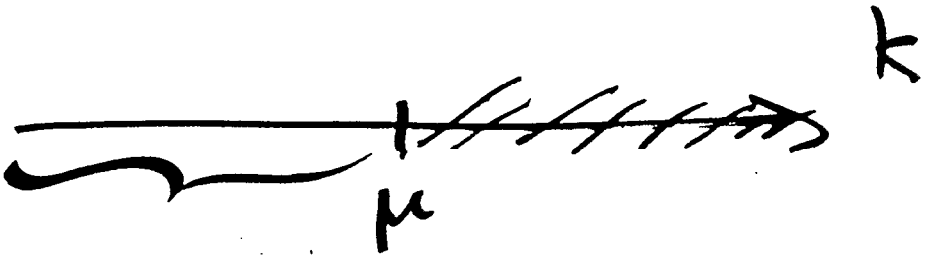

$$\mathcal{L}_{eff}\left(\psi(\mu), A(\mu)\right)$$

<u>physical observables</u>

$$\begin{cases} S\text{-matrix} \\ J_\mu \end{cases}$$

$$\begin{cases} \rightarrow \text{Parton Distributions} \\ \rightarrow \alpha_s(Q) \end{cases}$$

In the following lectures, I will not talk about how to solve QCD. Instead, I will focus on

$$\boxed{\text{High-Energy Probes of the Nucleon Structure}}$$

Experimental studies of the nucleon properties can be classified into <u>low & high energy frontiers</u>.

The low-energy studies involve:

- Electromagnetic form factors
  e.g. neutron charge form factor
- Neutral-Charge form factors
  F_1^Z, F_2^Z, measurable in P.V.E.S.
- Polarizabilities
  $\Delta E = \frac{1}{2}\alpha E^2$, $\Delta E = \frac{1}{2}\beta B^2$
  low-energy Compton Scattering
- Axial Current form factor:
  $G_A(Q^2)$: elastic neutrino Scattering <u>LSND</u>

...

High-Energy Probes:

- Deep inelastic Scattering
- Drell-Yan, W, Z production
- Direct photon production
- heavy quark production
- jet production

....

Thanks to asymptotic freedom, <u>Scattering mechanism</u> Can be understand in perturbative QCD. The general result can be expressed in term of factorization theorems:

$$d\sigma = \int \Gamma(x_1 \cdots x_n)\, \sigma_{parton}(x_1 \cdots x_n)\, dx_1 \cdots dx_n$$

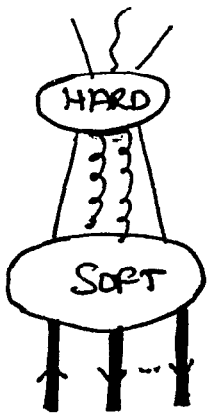

σ_{parton}: parton scattering, contain hard scales only. Calculable in perturbative QCD.

$\Gamma(x_1 \cdots x_n)$: Parton-hadron Vertex function, contain soft scale only.

Deep inelastic Scattering:

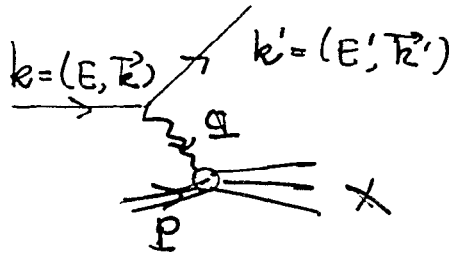

Total inclusive cross section:

$$\frac{d^2\sigma}{dE'd\Omega'} = \frac{\alpha_{em}^2}{MQ^4}\frac{E'}{E}\, l^{\mu\nu}W_{\mu\nu} \qquad (Q^2 = -q^2)$$

M: mass of the nucleon

$l^{\mu\nu}$: unpolarized lepton tensor

$$l^{\mu\nu} = k^\mu k'^\nu + k^\nu k'^\mu - g^{\mu\nu} k\cdot k'$$

$W^{\mu\nu}$: hadron tensor (unpolarized)

$$W^{\mu\nu} = \frac{1}{4\pi}\int e^{iq\cdot\xi} d^4\xi \, \langle p | [J^\mu(\xi), J^\nu(0)] | p\rangle \qquad \left(\nu = \frac{p\cdot q}{M}\right)$$

$$= W_1(Q^2,\nu)\left(-g^{\mu\nu} + \frac{q^\mu q^\nu}{q^2}\right) + W_2(Q^2,\nu)\frac{1}{M^2}\left(p^\mu - \frac{q^\mu p\cdot q}{q^2}\right)\left(p^\nu - \frac{q^\nu p\cdot q}{q^2}\right)$$

Bjorken limit: $Q^2 \to \infty$, $\nu \to \infty$

$x_B = \frac{Q^2}{2M\nu}$ fixed: $\quad 0 < x_B < 1$

A Special Choice of Coordinates:

Take 3-momentum of the nucleon in z-direction:

$$P = (P^0, 0, 0, P^3)$$
$$q^\mu = (\nu, 0, 0, -\sqrt{Q^2+\nu^2})$$
$$= (\nu, 0, 0, \nu) + \underbrace{(0, 0, 0, -Mx_B)}_{\text{finite}}$$

To isolate large kinematic factors, it is convenient to introduce two light-like vectors:

$$\begin{cases} p^\mu = \frac{\Lambda}{\sqrt{2}}(1, 0, 0, 1) \\ n^\mu = \frac{1}{\Lambda\sqrt{2}}(1, 0, 0, -1) \end{cases}$$

Λ has mass-dimension 1

$\Lambda \to \infty$: Infinite Momentum frame

$$\longrightarrow \quad p^2 = n^2 = 0, \quad p \cdot n = 1$$

Any four-vector can be expanded in terms of the two vectors plus unit vectors in two transverse directions

$$k^\mu = (k \cdot n)\, p^\mu + (k \cdot p)\, n^\mu + k_\perp^\mu$$

In particular,

$$\begin{cases} P^\mu = p^\mu + \frac{M^2}{2} n^\mu \\ q^\mu = \alpha p^\mu + \underline{\beta n^\mu} \end{cases} \qquad \begin{pmatrix} \alpha \sim -x \\ \beta \sim Q^2/2x \end{pmatrix}$$

We calculate $W^{\mu\nu}$ in the leading order in the Bjorken Limit. Because of the asymptotic freedom, it is legitimate to consider Impulse approximation:

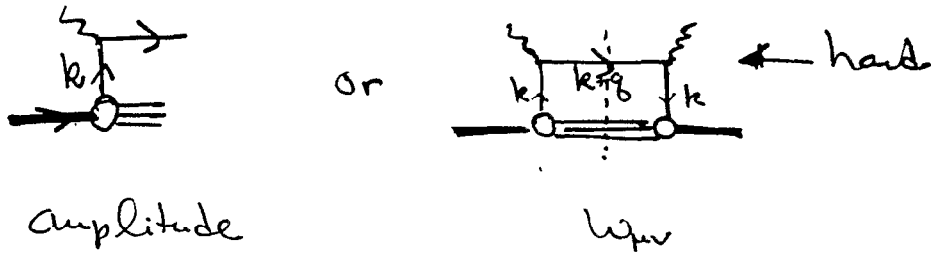

- The handbag diagram without cut is part of the Forward Compton amplitude:

$$T^{\mu\nu} = i \int e^{iq\cdot\xi} d^4\xi \, \langle P | T J^\mu(\xi) J^\nu(0) | P \rangle$$

It is easy to show

$$W^{\mu\nu} = \frac{1}{2\pi} \operatorname{Im} T^{\mu\nu} \qquad \text{(Optical theorem)}$$

In Impulse approximation:

$$W^{\mu\nu} = \frac{1}{2\pi} \operatorname{Im} i \int \frac{d^4k}{(2\pi)^4} \operatorname{Tr}\left[\gamma^\mu \frac{i(\not k + \not q)}{(k+q)^2 + i\epsilon} \gamma^\nu \Sigma(k)\right]$$

$$+ \text{ Crossing}$$

$M(k,p)$ is a forward quark-nucleon scattering amplitude, or <u>Single particle Green's function</u>

$$M_{\alpha\beta} = \int e^{ik\cdot\xi}\, d^4\xi \, \langle P | T\bar{\psi}_\beta(0)\psi_\alpha(\xi) | P \rangle$$

- To pick up the leading-order contribution, make a collinear expansion for k,

$$k^\mu = (k\cdot n)\, p^\mu + (k\cdot p)\, n^\mu + \cancel{k_\perp^\mu}$$

Since $q = \alpha p + \underline{\beta n}$ with $\beta \to \infty$, one can approximate $W^{\mu\nu}$ by

$$k^\mu \approx k\cdot n\, p$$

- Introduce $\int dx\, \delta(x - k\cdot n) = 1$, we have,

$$W^{\mu\nu} = -\frac{1}{2\pi}\, \mathrm{Im} \int_{-\infty}^{+\infty} dx\, \mathrm{Tr}\Big[\gamma^\mu \frac{x\not{p} + \not{q}}{(xp+q)^2 + i\epsilon}\gamma^\nu \cdot \underbrace{\int \frac{d^4k}{(2\pi)^4}\, \delta(k\cdot n - x)\, M(k,p)}_{M_{\alpha\beta}}\Big]$$

The loop-momentum can now be integrated to produce:

$$M_{\alpha\beta}(x) = \int \frac{d\lambda}{2\pi}\, e^{ix\lambda} \int e^{-ik\cdot n\lambda} \frac{d^4k}{(2\pi)^4}\, M_{\alpha\beta}(k,p)$$

$$= \int \frac{d\lambda}{2\pi}\, e^{ix\lambda} \langle P | \bar{\psi}_\beta(0)\, \psi_\alpha(\lambda n) | P \rangle$$

$M_{\alpha\beta}(x)$ contains two quark fields separated along the light-cone.

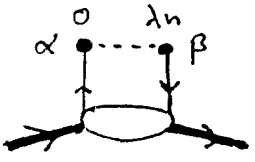

$M_{\alpha\beta}(x)$

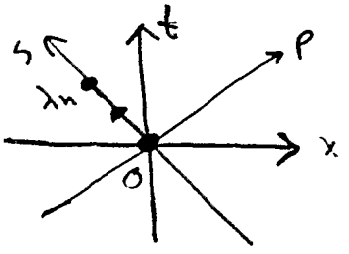

Struck quark propagates along the light-cone.

- $M(x)$ is a 4x4 matrix in the spinor space. It can be expanded in terms of 16 Dirac matrices.

$$M_{\alpha\beta}(x) = \sum_i (\Gamma_i)_{\alpha\beta} C_i$$
$$= \frac{1}{2} \not{P}_{\alpha\beta} f_1(x) + \cdots$$

where only the leading term is shown. One can project out $f_1(x)$ — quark distribution — by tracing both sides with $n\!\!\!/$

$$f_1(x) = \frac{1}{2} \int e^{ix\lambda} \frac{d\lambda}{2\pi} \langle P | \bar{\Psi}(0)\, n\!\!\!/\, \Psi(\lambda n) | P \rangle$$

$(g_1(x))$

Substituting $M(x)$ into $W^{\mu\nu}$,

$$W^{\mu\nu}(x) = -\frac{1}{4\pi} \mathrm{Im} \int_{-\infty}^{+\infty} dx \; \mathrm{Tr}\left[\gamma^\mu \frac{x\not{p}+\not{q}}{(xp+q)^2+i\epsilon} \gamma^\nu \not{p} f_1(x)\right]$$
$$+ \text{Crossing}$$

After performing the trace.

$$W^{\mu\nu}(x) = \frac{1}{2\nu}\left(f_1(x_B) - f_1(-x_B)\right)\left(2x_B p^\mu p^\nu + p^\mu q^\nu + p^\nu q^\mu - g^{\mu\nu}\nu\right)$$

Summing over quark flavors.

$$\begin{cases} W_1 = \frac{1}{2}\sum_i e_i^2 \left[f_1^i(x_B) - f_1^i(-x_B)\right] \\ W_2 = \frac{M}{\nu} x_B \sum_i e_i^2 \left[f_1^i(x_B) - f_1^i(-x_B)\right] \end{cases}$$

Defining the Scaling function

$$\begin{cases} F_1(x_B) = W_1 = \frac{1}{2}\sum_i e_i^2 \left[f_1^i(x_B) - f_1^i(-x_B)\right] \\ F_2(x_B) = \frac{\nu}{M} W_2 = x_B \sum_i e_i^2 \left[f_1^i(x_B) - f_1^i(-x_B)\right] \end{cases}$$

We immediately have Callan - Gross relation

$$\boxed{F_2(x_B) = 2x_B F_1(x_B)}$$

$$\Rightarrow \quad R = \frac{\sigma_L}{\sigma_T} \to 0 \quad \text{as} \quad Q^2 \to \infty$$

The above result coincides with Feynman's Parton model. However, no assumption is made about the initial state quark interactions. Thus, Feynman's parton model is <u>a model for the Scattering Process</u>, not for the internal dynamics of the nucleon.

Corrections to the hand-bag process:

- Longitudinal gluon Scattering
  $\Rightarrow$ gauge invariant quark distribution
- QCD radiative Corrections
  $\Rightarrow$ leading-twist factorization formula
- Multiparton Scattering
  $\Rightarrow$ higher-twist Corrections

- Longitudinal gluon Scattering

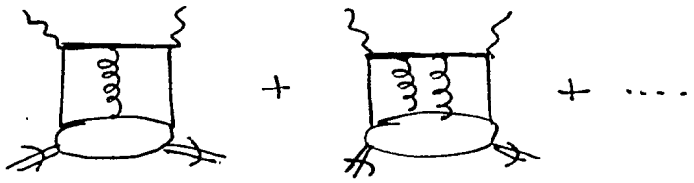

$$A^\alpha = p^\alpha n\cdot A + n^\alpha p\cdot A + A^\alpha_\perp$$

In the leading order, only $p^\alpha n\cdot A$ contributes

$$A^\alpha \sim p^\alpha n\cdot A$$

Summing over all diagrams, one gets a gauge link,

$$L = \underset{\substack{\uparrow \\ \text{Path ordering}}}{P}\, e^{-ig\int_\lambda^0 n\cdot A(\lambda' n)\,d\lambda'} = 1 \quad \text{if } n\cdot A = 0 \text{ gauge is chosen}$$

Thus, the modification to the handbag result is just a change of quark distribution

$$\underset{(f_1(x))}{\underline{q}(x)} = \frac{1}{2}\int_{-\infty}^{+\infty} e^{ix\lambda}\frac{d\lambda}{2\pi}\langle \underline{p}|\,\bar{\Psi}(0)\,\not{n}\,\underset{\sim}{L}\,\Psi(\lambda n)\,|\underline{p}\rangle$$

$\uparrow$ gauge invariant

- QCD Radiative Corrections

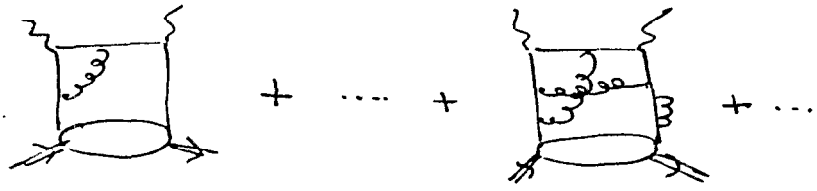

These diagrams cannot be calculated entirely in perturbative QCD due to infrared divergences.

- Soft divergences. $k^\mu \sim 0$
- Collinear divergences. $k \sim p$

$\Rightarrow$ When summing over all diagrams, the soft divergences cancel.

- Collinear-divergent contribution can be factorize into:
  - Hard contribution $C(Q^2, \mu^2)$, with gluon virtuality $\mu^2 < k^2 < Q^2$
  - Soft contribution $\underline{\delta q(\mu^2, x)}$, with virtuality $< \mu^2$.

quark dis. in a bare quark.

Renormalized quark distribution

★ $$F_1(x_B, Q^2) = \frac{1}{2} \sum_i e_i^2 \int \frac{dy}{y} C_i\left(\frac{x_B}{y}, \frac{\mu^2}{Q^2}\right) q_i(y, \mu^2)$$

$$\boxed{q_i(y, \mu^2) = \delta q_i(\mu^2, y)\, q_i(y)}$$

- Higher-twist Contribution.

$O(\frac{1}{Q^2})$ ... Corrections

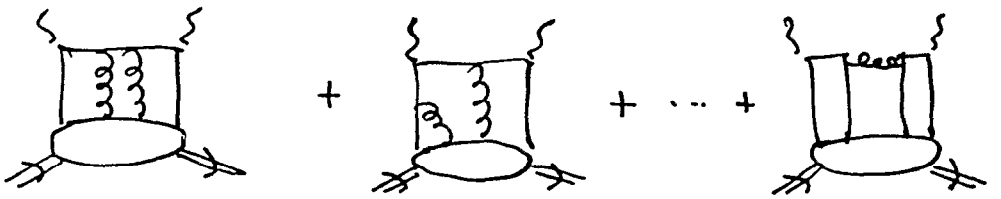

These Corrections can be taken into account by introducing multiparton Correlation functions e.g.

$$\int \frac{d\lambda}{2\pi}\frac{d\mu}{2\pi}\, e^{ix\lambda + i(y-x)\mu} \langle P_s | \bar{\psi}(0)\, iD^{\alpha}(\mu n)\, n\!\!\!/\, \psi(\lambda n) | P_s \rangle$$

...

Due to infrared renormalon in the leading twist Coefficient function. $C_i(\alpha_s) = \sum_i C_i^n (\alpha_s)^n$ the higher-twist contribution is not well-defined. It is scheme-dependent.

$\Longrightarrow$ The status of higher-twist physics is not satisfactory at present.

Summary:

In leading-order in $1/Q^2$, the deep inelastic Structure function can be expressed as

$$F_1(x_B, Q^2) = \frac{1}{2}\sum_i e_i^2 \int \frac{dy}{y}\, C_i\left(\frac{x_B}{y}, \frac{\mu^2}{Q^2}\right) q_i(y, \mu^2) + (\text{gluon})$$

- $C_i\left(\frac{x_B}{y}, \frac{\mu^2}{Q^2}\right)$ is the coefficient function and has been calculated to order α_s in QCD perturbation theory.

- $q_i(y, \mu^2)$ is the unknown quark distribution in the nucleon and is scheme & scale dependent. Experimental data on $F_1(x_B, Q^2)$ allow us to extract

$$q_i(y, \mu^2) = \frac{1}{2}\int_{-\infty}^{+\infty} e^{ix\lambda}\frac{d\lambda}{2\pi}\, \langle p | \bar{\psi}(0) \not{n}\, e^{-ig\int_\lambda^0 n\cdot A(\lambda' n)\, d\lambda'}\, \psi(\lambda n) | p \rangle$$

Light-cone Correlation

Stalking Quark's Orbital Motion: In the Lab and On the Lattice

Xiangdong Ji

- Historical Introduction
- What Do We Know About Quark Orbital Motion in the Proton?
- Quark Orbital Observables in the Infinite Momentum Frame
- Probing Quark Orbital Motion in Compton Scattering
- Studying Quark Orbital Observables in Lattice QCD

Johannes Kepler (1571-1630)

"By the study of the orbit of Mars, we must either arrive at the secrets of astronomy or forever remain in ignorance of them"

Three laws of planet motion (1609,1619)
$\Rightarrow$ **Inverse square law of gravity**
(Hooke & Newton, 1679)

Niels Bohr (1885-1962)

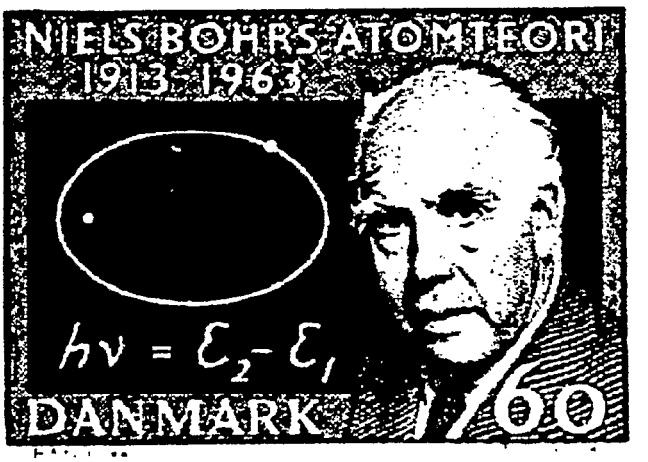

> " It could be that I've perhaps found out a little bit about the structure of atoms. You must not tell anyone about it. "
>
> Letter to his brother, 1912.

The electrons move in stable orbits around the nuclei just like the planets move around the sun.

$\Rightarrow$ Atomic Spectra, Quantum Mechanics

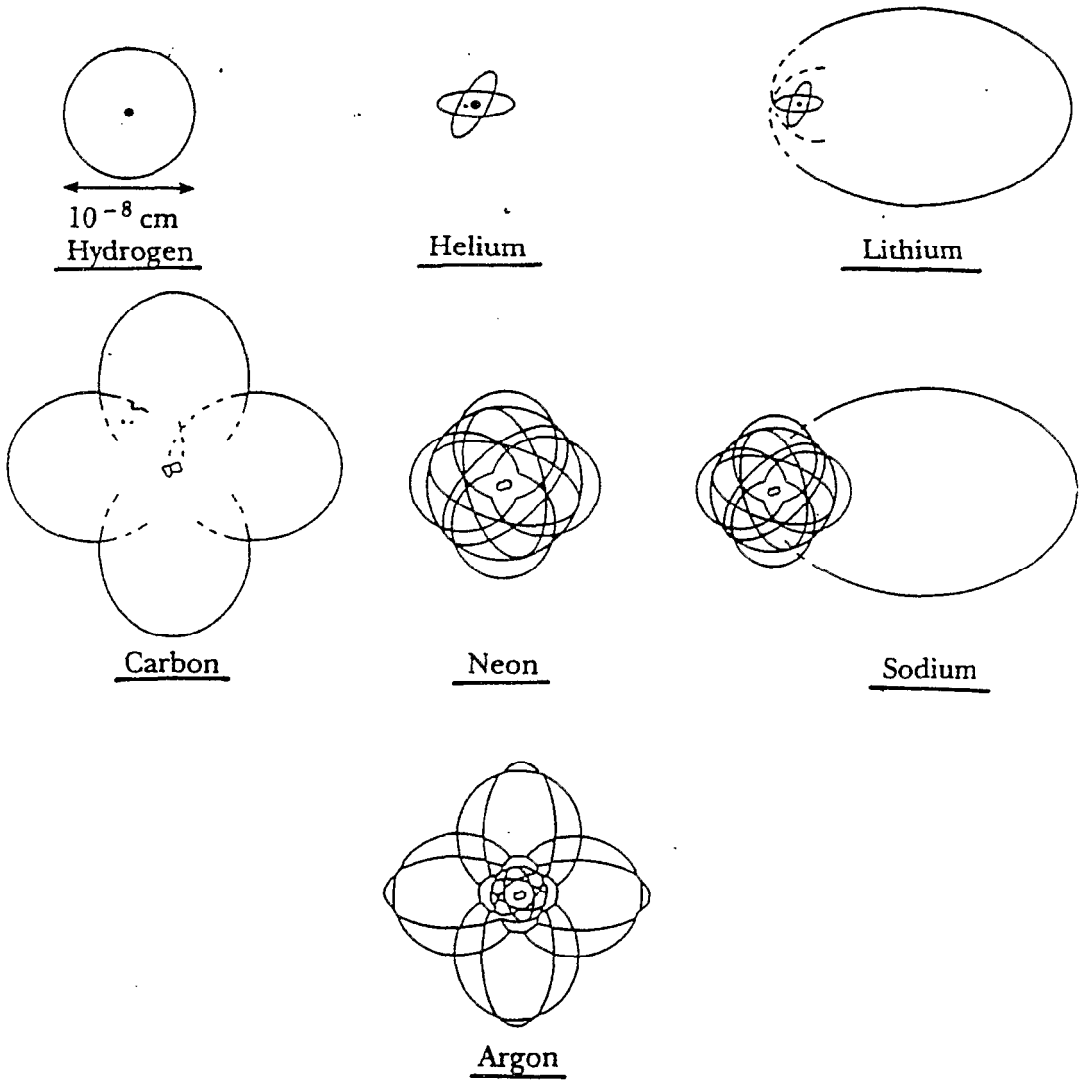

Bohr's sketches of electronic orbits.

Electron's Orbital Density in ^1H

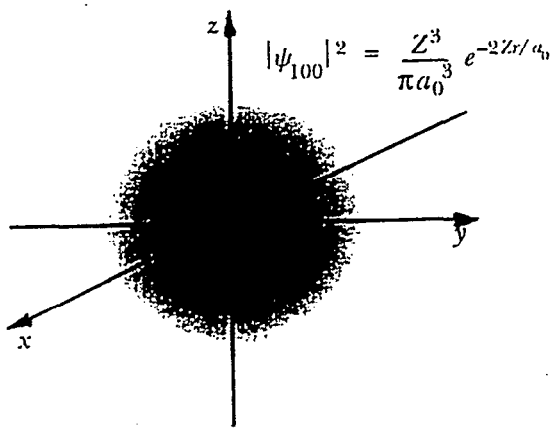

(a)

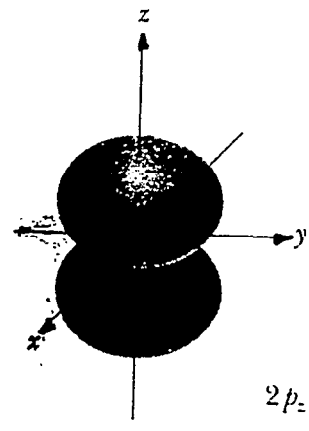

(b)

$l = 0$

$l = 1,\ m_l = 0$

★ Do not mean there is no orbital motion ★

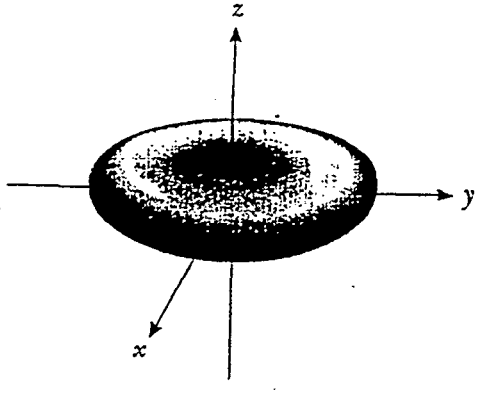

$n = 2,\ \ell = 1,\ m_\ell = \pm 1$

(a)

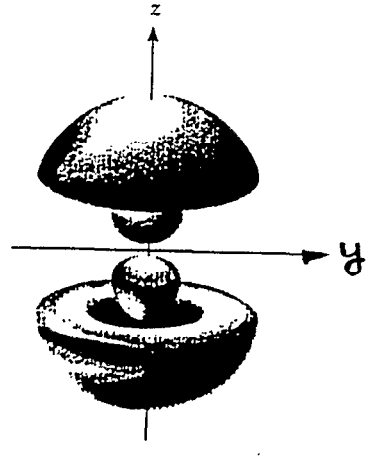

$n = 3,\ \ell = 1,\ m_\ell = 0$

(b)

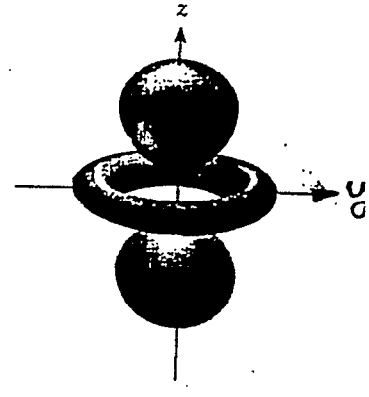

$n = 3,\ \ell = 2,\ m_\ell = 0$

(c)

What Do We Know About Quark's Orbital Motion In a Proton?

- The proton has three valence quarks: two ups and one down.
- Since $J^P=1/2^+$, assuming there is nothing else

$$S = 1/2, 3/2 \Rightarrow L = 0, 2$$

- Most of the quark models allege the dominance of L=0 over L=2.

$$|P\rangle = 0.9\,|^2S_S\rangle - 0.34\,|^2S_S\rangle - 0.27\,|^2S_M\rangle - 0.06\,|^2D_M\rangle$$

(Isgur & Karl, '78)

- **Is the quark orbital motion really spherically-symmetric?**

1. Magnetic Moment

- Orbital motion of charged particles contributes to the magnetic moment:

$$\vec{\mu} = g_s \vec{S} + g_l \vec{L}$$

- Proton's magnetic moment was first measured in by O. Stern in 1932. (Nobel prize 1943)

$$\mu_p = 2.913\ \mu_N \quad (= e\hbar/2m_N c\ )$$

- How much of this is from the quark orbital current?

$$\mu_P = \frac{e\hbar}{2(m_N/3)c}$$

This can be interpreted as entirely from a quark with mass $m_N/3$ and L=0!

- Caveats:
  - μ_p can also be explained with $L \neq 0$.
  - For a relativistic particle, $\vec{\mu} \neq g_s \vec{S} + g_\ell \vec{L}$
  - Beside valence quarks, there are many quark-antiquarks pairs (sea quarks).

2. N→Δ Electromagnetic Transitions

- The electromagnetic transitions are known to provide useful information about the orbital motion of charged particles.

  Angular distribution of photon intensity and polarization in the 2p ⇒ 1s Lyman transition in ^{1}H atom.

- **Δ is an excited state of the proton with spin J=3/2.** When it makes a transition to the proton, it emits electric quadrupole (E2) & magnetic dipole (M1) radiations.

- **Experimentally, the E2/M1 transition ratio is found to be 2~3%.**

- The data seem to favor small L=2 components in the proton and Δ wave functions. But the caveats in explaining the magnetic moment also apply here.

3. Form Factors:

- In elastic electron (photon) scattering on a system, one can measure the spatial distributions of the charged particles ⇒ **Form Factors (or Structure Sactor)**

$$F_c(\vec{q}) = \int \rho(\vec{r}) e^{i\vec{q}\cdot\vec{r}} d^3\vec{r}$$

e.g. The structure of crystals (Bragg, Laue)

- The **charge form factor of the nucleon** has been measured in the 50's by Hofstadter et al. (Nobel Prize, 1961)
- Because the nucleon is J=1/2, there is only one charge form factor which is **spherically symmetric and does not distinguish L=0, 2**. A quadrupole form factor has ΔJ=2 and is forbidden by the Wigner-Eckart theorem.
- For J≠0 target, there is the **magnetic form factors $F_M(q)$** which measures the current density distribution.

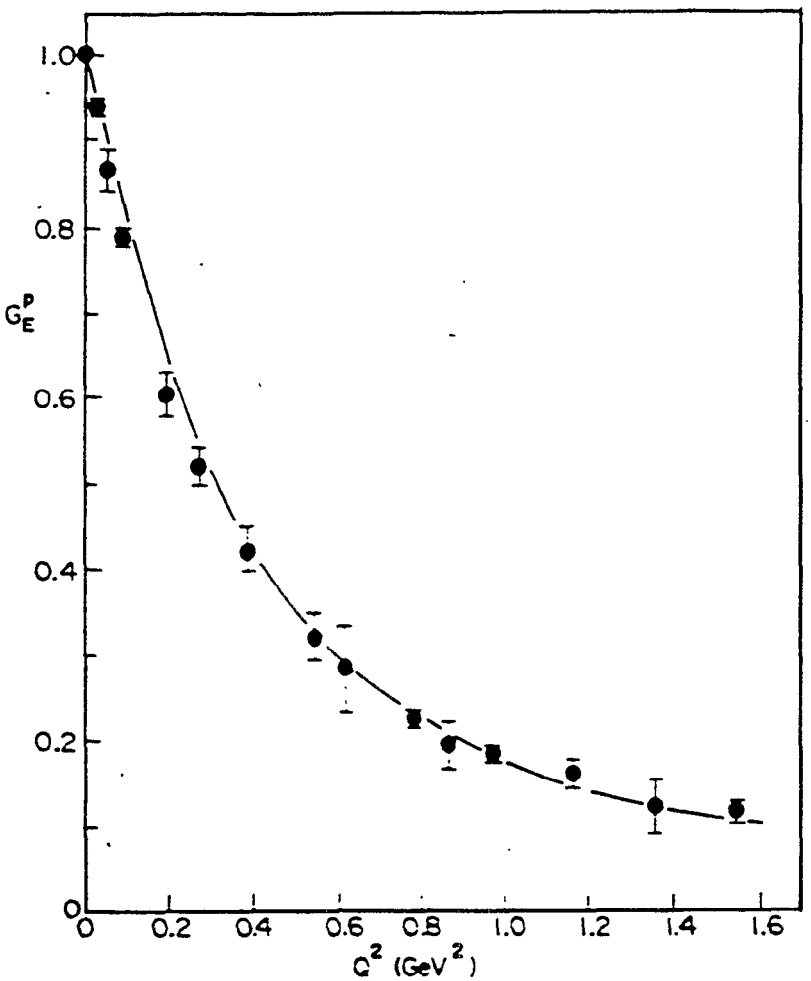

The elastic form factor, G_E^P, of a proton

4. Momentum Distribution:

- In high-energy knock-out scattering, *under certain conditions*, the scattering probability depends on the density of particles with fixed momentum **k**,

$$n(\vec{k}) = \left| \int e^{i\vec{q}\cdot\vec{r}} \psi(\vec{r}) d^3\vec{r} \right|^2$$

e.g. The momentum distribution of ^{4}He atoms in liquid helium has been obtained from neutron scattering.

- Quark momentum distributions **q(x)** in the proton have been measured in high-energy scattering for over 30 years.

What the physics of q(x)? (R.P.Feynman)

- Imaging the nucleon is moving with $P \to \infty$ along the z-direction.
- q(x) is the density of quarks with momentum $k_z = xP$, and arbitrary $k_\perp = (k_x, k_y)$

No clear orbital information can be obtained from data on q(x).

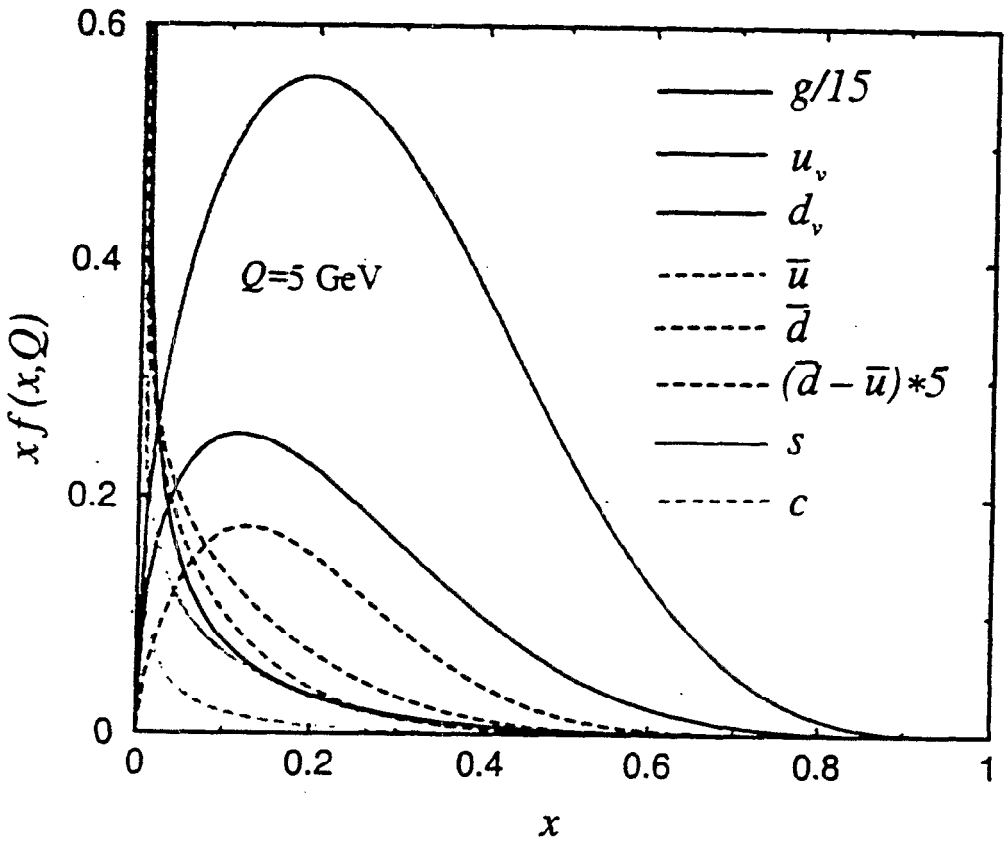
0.6
0.4
0.2
0
0
0.2
0.4
0.6
0.8
1
x
x f(x,Q)
Q=5 GeV
g/15
u_v
d_v
ū
d̄
(d̄ − ū)*5
s
c

Indirect info about the quark orbital motion from

Polarized deep-inelastic scattering:

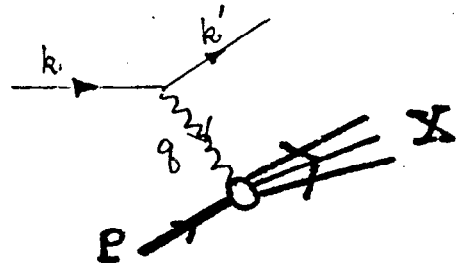

Measure the polarized quark distribution

$$\Delta q(x) = q_+(x) - q_-(x)$$

where $q_\pm(x)$ is the density of quarks with the spin aligned in and opposite to the spin of the proton.

The fraction of the nucleon spin carried in the quark spin is

$$\int_0^1 dx \sum_q \Delta q(x) = \Delta\Sigma$$

The data from last ten years: $\Delta\Sigma$=**0.2±0.1**

A comparison of data on the spin structure Function of the proton.

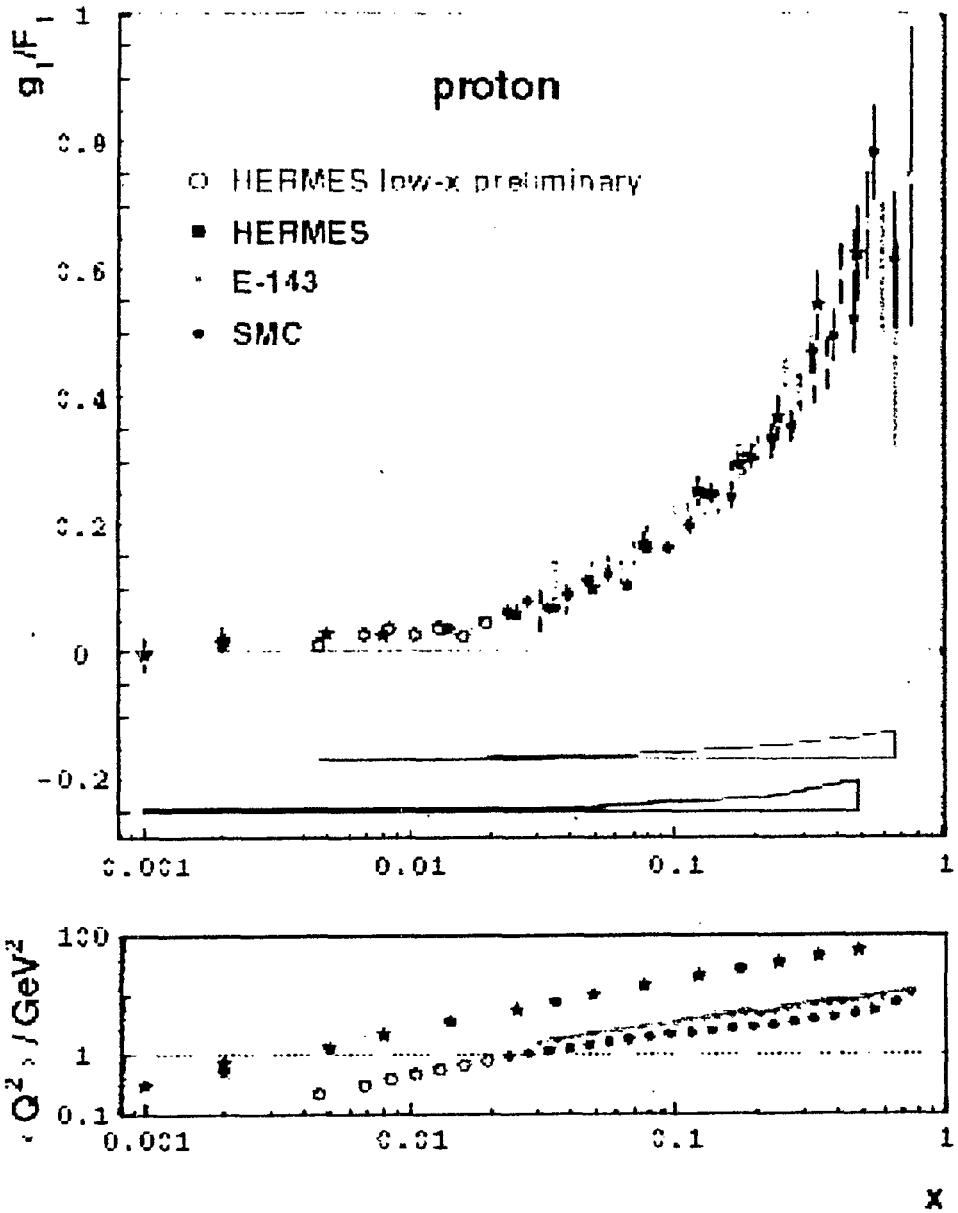

- 70% of the proton spin is in either the orbital motion of the quarks or gluon!

- <u>Theoretical arguments that the orbital ang. mom. might be important</u>:
  - Quarks are relativistic. The lower component of the Dirac wave function is important; it is a ***p***-wave.
  - When a quark is split into a quark plus a gluon, the angular momentum conservation implies that the quark and gluon obtain orbital angular momentum.

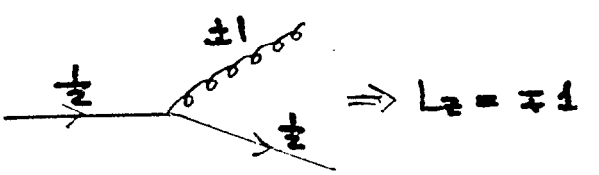

$$\underset{\Delta\Sigma}{\frac{1}{2}} = \underset{\Delta\Sigma}{\frac{1}{2}} \underset{\Delta G}{\pm 1} \underset{L_z}{\mp 1}$$

How do we find this out directly?

Quark Orbital Angular Momentum Distribution $L_q(x)$

- Consider quarks in the nucleon $P \to \infty$. Beside the longitudinal momentum xP, they have transverse momentum
- For a given x, expand the $k_\perp$ part of the wave function in terms of partial waves with $m=0, \pm 1, \pm 2 \ldots$, from which we can get the orbital angular momentum L_z carried in the quarks.
- Thus we can define the Orbital Angular Momentum Distribution $L_q(x)$:

  Density of L_z carried by quarks of flavor q and longitudinal momentum xP.

  Hoodbhoy, Ji & Lu, PRD59, 1999

- **Quark Angular Momentum Distribution:**

  $$J_q(x) = L_q(x) + \Delta q(x)/2$$

Angular Momentum Sum Rules

- The fraction of the proton spin carried in quark orbital motion,

$$\int_0^1 dx L_q(x) = L_q$$

- The fraction of the proton spin carried in quarks

$$\int_0^1 dx J_q(x) = J_q$$

  – Total quark angular momentum.

$$J_q \quad L_q + \Delta\Sigma/2$$

- Sum rule for the spin structure of the nucleon,

$$L_q + \Delta\Sigma/2 + J_g = 1/2$$

J_g is the angular momentum of the gluons.

Field Theoretical Content of $J_q(x)$ and $L_q(x)$

In QCD, the x-moments of $J_q(x)$ are the matrix elements of the <u>spatial moments of the generalized momentum densities.</u>

- Generalized quark momentum densities:
  $$O_q^{\beta\mu_1\cdots\mu_n}(\xi) = \overline{\psi}\gamma^{(\beta}iD^{\mu_1}\cdots iD^{\mu_n)}\psi(\xi)$$

- Generalized angular momentum densities:
  (spatial moments of $O_q^{\beta\mu\cdots}$)
  $$M_q^{\alpha\beta\mu_1\cdots\mu_n}(\xi) = \xi^\alpha O_q^{\beta\mu_1\cdots\mu_n}(\xi) - \xi^\beta O_q^{\alpha\mu_1\cdots\mu_n}(\xi) - \text{trace}$$

- The proton matrix elements
  $$\langle PS|\int d^4\xi M_q^{\alpha\beta\mu_1\cdots\mu_n}(\xi)|PS\rangle$$
  $$= 2J_{qn}(2S_\rho P_\sigma/(n+1)M^2)(\varepsilon^{\alpha\beta\rho\sigma}P^{\mu_1}\cdots P^{\mu_n}+\cdots)(2\pi)^4\delta^4(0)$$

- J_{qn} defines the x-moments of $J_q(x)$
  $$\int_0^1 dx x^{n-1} J_q(x) = J_{qn}$$

Thus, $J_q(x)$ is a well-defined observable in QCD.

Relation to Form Factors

- The matrix elements of the spatial moments of momentum densities are difficult to calculate and measure directly.
- On the other hand, the matrix elements can be extracted from the form factors of the momentum densities:

Magnetic Moment μ

$$\vec{\mu} = \frac{1}{2}\int d^3\vec{r}\ \vec{r}\times\vec{j}$$

$$\langle p'|j^\mu|p\rangle = \bar{U}(p')\left[F_1(q^2)\gamma^\mu + F_2(q^2)\frac{i\sigma^{\mu\alpha}q_\alpha}{2M}\right]U(p)$$

$$\mu = F_1(0) + F_2(0)$$

Angular Momentum J_q X. Ji, PRL78, 610 1997

$$\vec{J}_q = \int d^3\vec{r}\ \vec{r}\times\vec{T}_q$$

$$\langle p'|T_q^{\mu\nu}|p\rangle = \bar{U}(p')\Big[A(q^2)\gamma^{(\mu}P^{\nu)} + B(q^2)\frac{i\sigma^{\mu\alpha}q_\alpha}{2M}P^{\nu)} + C(q^2)\Delta^{(\mu}q^{\nu)}\Big]U(p)$$

$$J_q = \frac{1}{2}[A(0) + B(0)]$$

How to Measure the Quark Orbital Motion?

- The quark angular momentum distribution is found to be measurable through **virtual Compton scattering.**

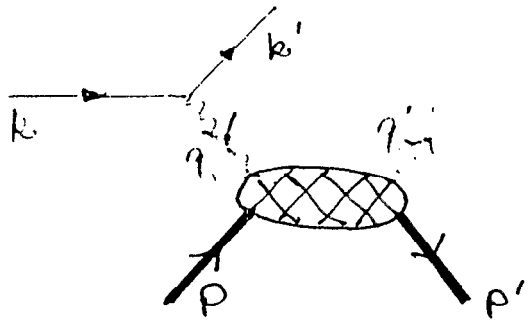

- In the special kinematic limit, $Q^2 \to \infty$, $\nu \to \infty$, and the ratio stays fixed (Bjorken limit), the **scattering is through just a single quark.**

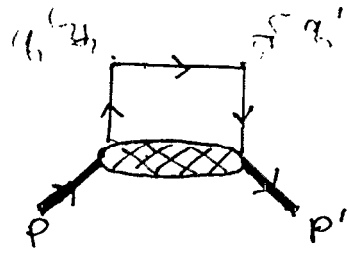

- **Deeply-virtual Compton scattering (DVCS)** X. Ji, PRL 78, 610 (1997).

A hand-waving answer to "How Is It Possible?"

- In the single quark scattering, the virtual photon hits a quark with transverse momentum. The scattered quark carries the information of the initial state.
- When the scattered quark radiates a real photon, the polarization and angular distribution of the radiation depends on the initial as well as final quark states, the latter must return to form a recoiling proton.
- The radiation pattern contains the information about quark orbital motion.

First Evidence of DVCS

- ZEUS Detector at HERA, Hamburg

DVCS event candidate:

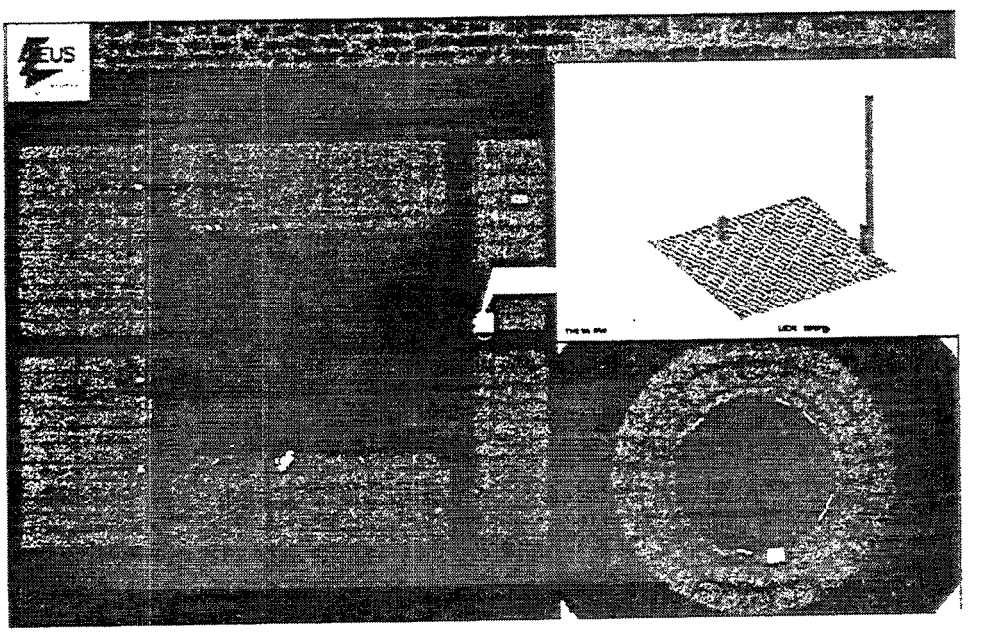

No tracks, contributions from both types of diagram.

(Wide-angle DIS positron events are almost exclusively QEDC.)

H1 Detector at HERA

Cross section

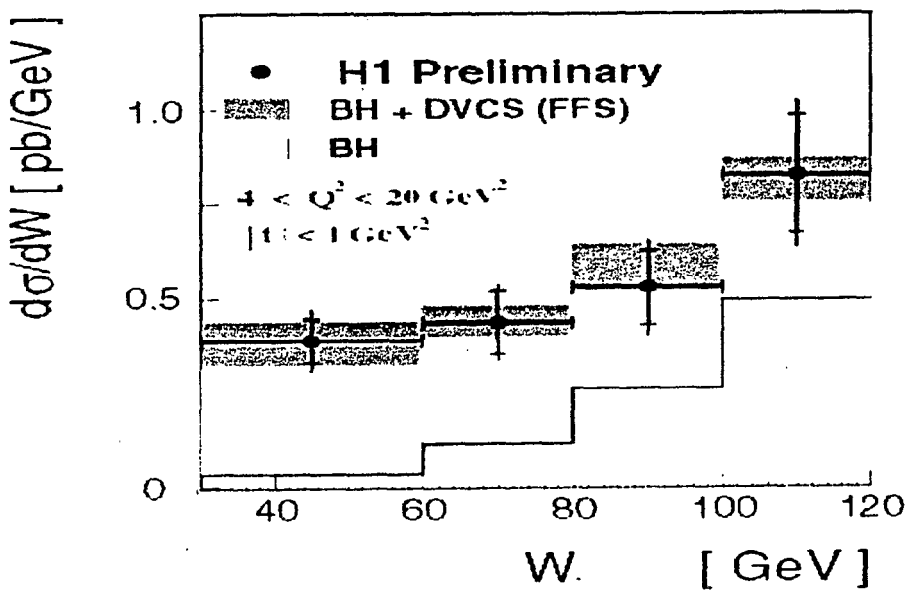

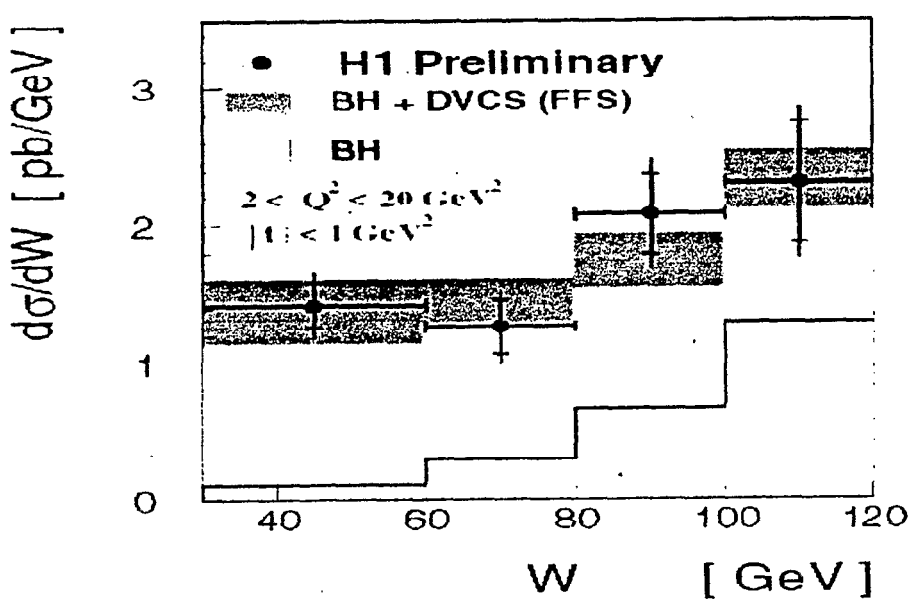

ZEUS DVCS Data

Look at θ_2:

ZEUS 1996/97 Preliminary

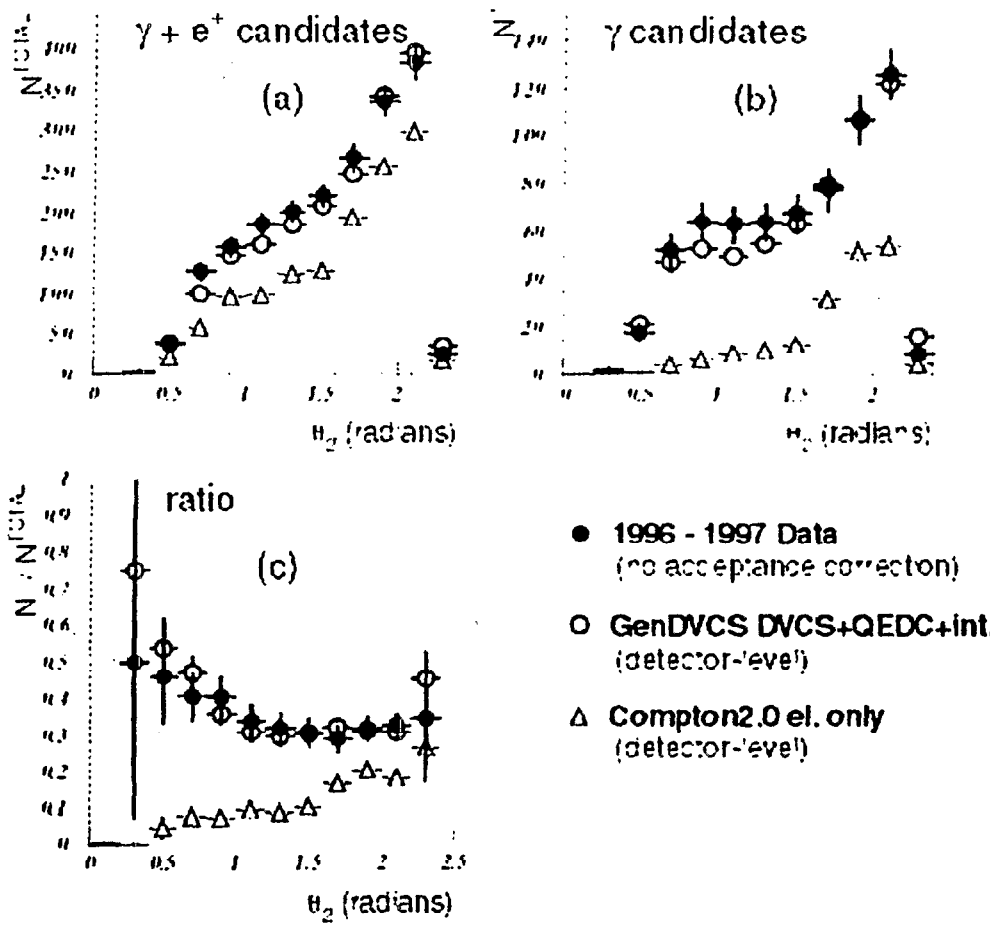

BUT, there may be π^0 etc background!

HERMES Exp. at HERA

ϕ Dependence of SSA

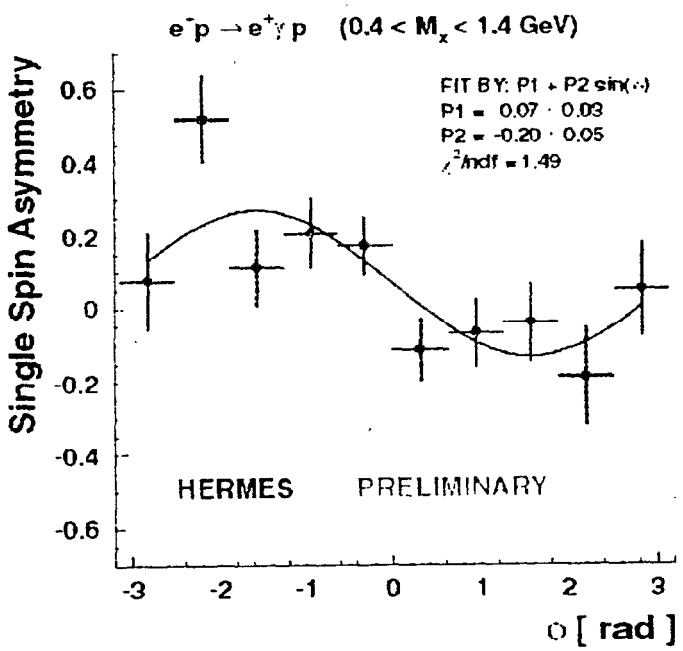

Experiments Under Considerations

- Jefferson Lab at 6 and 12 GeV
  - Measuring DVCS and Bethe-Heitler interference
- COMPASS experiment at CERN
  - To build a special recoil detector
- ELFE (European Lab for Electron)
  - 25~50 GeV high-intensity polarized electron beam, $L = 10^{35}$ and above.
  - Special detector for exclusive production.
- eRHIC and/or EPIC in USA
  - Electron-hadron collider at high luminosity ($L=10^{33}$).
  - Under consideration for the 5 year plan in Division of Nuclear Physics.

Studying quark orbital motion in lattice QCD

- Quantum chromodynamics (QCD) has been established as **the fundamental theory** of strong interactions.
  - F. Wilczek, Physics Today, August, 2000.
- To understand the structure of the proton, one need solve QCD in the strong coupling region. The only way we know how to do this is lattice QCD.
- **Lattice hadron physics Collaboration** (**LHPC**) is the largest collaboration in the world with the goal of

  Solving the structure of hadrons using Teraflop-scale computers.

  Understanding the orbital motion of quarks is an important part of the research program.

Lattice QCD Made Simple

- Step 1:

  Write the matrix elements of any operator between hadron states as **Feynman path integrals**. (∞^4 ordinary integrals)

- Step 2:

  Rotate the integrals related to the time variable to imaginary axis (**Euclidean space**), so that the integrals become real.

- Step 3:

  Approximate the continuum **spacetime as a set of discrete lattice points** in a finite 4-dimensional box. (e. g. 32^4)

- Step 4:

  Evaluate a large number ($\sim 32^4$) of integrals using the **Monte Carlo method**.

An Exploratory Calculation of Orbital Angular Momentum

N. Mathur et al., Hep-ph/9912289

- Lattice Parameters:
  - $16^3 \times 24$ lattice with $\beta=6.0$
  - Wilson quark with m_q=210,124,80 MeV
- Lattice and Physical Observables:
  - **Calculate** three-point correlation functions involving the proton current and quark's stress-energy tensor.
  - **Extract** <u>elastic form factors of the stress-energy tensor in the proton.</u>
- Result:
  - Dipole fit to get result at $q^2=0$.
  - Extrapolate to $m_q=0$ limit.

  $J_q = 0.30 \pm 0.07 \Rightarrow L_q = 0.17 \pm 0.07$

  <u>Quark orbital momentum is significant!</u>

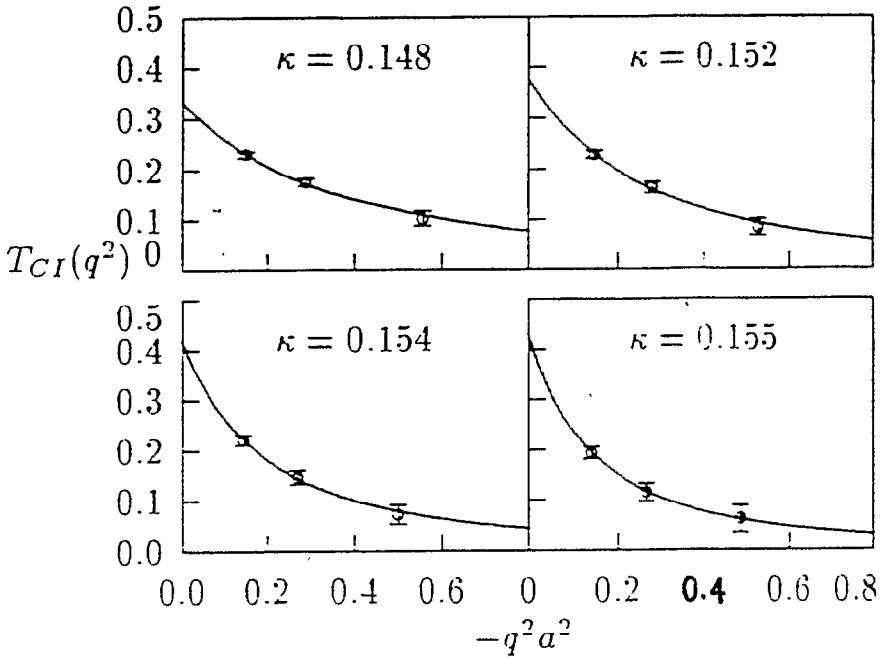

FIG. 2. Dipole fitting for $T_{CI}(q^2)$ at 4 different κ values.

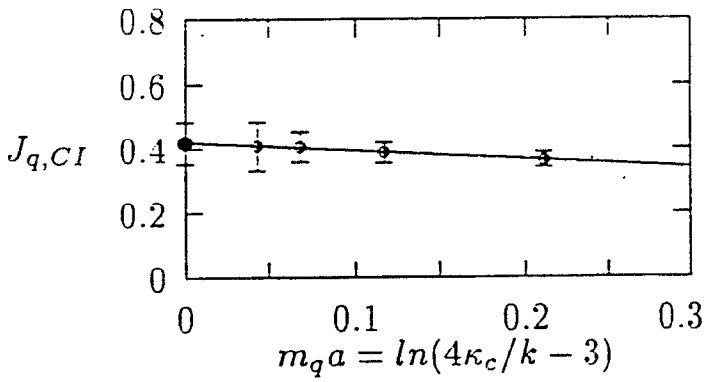

FIG. 3. Chiral extrapolation for $J_{q,CI}$ as a function of the quark mass. The value at the chiral limit is indicated by •.

The Momentum & Spin Structure of the Nucleon

– A Challenge for Several Generations of Experiments –

Wolf-Dieter Nowak [1] *– DESY Zeuthen*

RIKEN Winter School, Yuzawa/Japan, Dec. 2-5, 2000

Abstract

The 1st lecture is devoted to the history of Deep Inelastic Scattering (DIS) over the last 25 years. After an introduction to DIS kinematics main results achieved in often pioneering DIS experiments at SLAC, FNAL, CERN and DESY are discussed. At every step in history it is demonstrated to what extent the development of theoretical ideas (Quark-Parton model, Quantum Chromodynamics) was stimulated by the experimental results. The lecture is concluded by introducing the only presently running experiment studying the spin structure of the nucleon – HERMES at DESY.

The 2nd lecture describes the main results obtained at HERMES on the spin structure of the nucleon in the last few years. An inclusive analysis of 1997 proton data taken with both beam and target polarized shows a scaling behaviour of the spin structure function g_1^p very similar to that of the unpolarized structure function F_1^p. A flavor separation, based on a semi-inclusive analysis of the 1997-2000 data, led to fairly precise data on the polarized u- and d-quark distributions. A first indication for a positive polarized gluon distribution is obtained from an analysis of pairs of high-p_t hadrons representing the photon-gluon fusion subprocess. Finally, prospects are discussed on the planned future measurement of the u-quark transversity at HERMES in conjunction with the polarized fragmentation function.

The 3rd lecture looks into the long-term future of DIS. A promising project, TESLA-N, is discussed as the possible ultimate future experiment to measure very precisely the different polarized parton distributions that characterize a polarized nucleon. The experiment would utilize high-rate polarized electrons accelerated in one arm of the planned linear collider TESLA and hitting a stationary polarized target. An envisaged integrated luminosity of 100 fb^{-1} per effective year would allow for a precision mapping of the (Q^2, x)-dependence of both quark helicity and transversity distribution functions as well as of the polarized gluon distribution function. The axial and the tensor charge of the nucleon would be determined with accuracies on the percent level.

[1] Wolf-Dieter.Nowak@desy.de

The Momentum & Spin Structure of the Nucleon

A challenge for several Generations of Experiments

Wolf-Dieter Nowak - DESY Zeuthen

RIKEN Winter School
Yuzawa/Japan, Dec. 2-5, 2000

Lecture 1: Deep inelastic scattering at SLAC, CERN, FNAL & DESY

Lecture 2: HERMES results on the spin structure of the nucleon

Lecture 3: TESLA-N – the ultimate future experiment ?

Deep Inelastic Scattering at SLAC, FNAL, CERN & DESY

– Four Generations of Experiments –

Wolf-Dieter Nowak - DESY Zeuthen

RIKEN Winter School, LECTURE 1
Yuzawa/Japan, Dec. 2, 2000

- DIS kinematics
- DIS at SLAC, FNAL & CERN
  – a historical overview –
- the HERMES experiment at DESY

Inclusive Analysis of Polarized Deep Inelastic Scattering

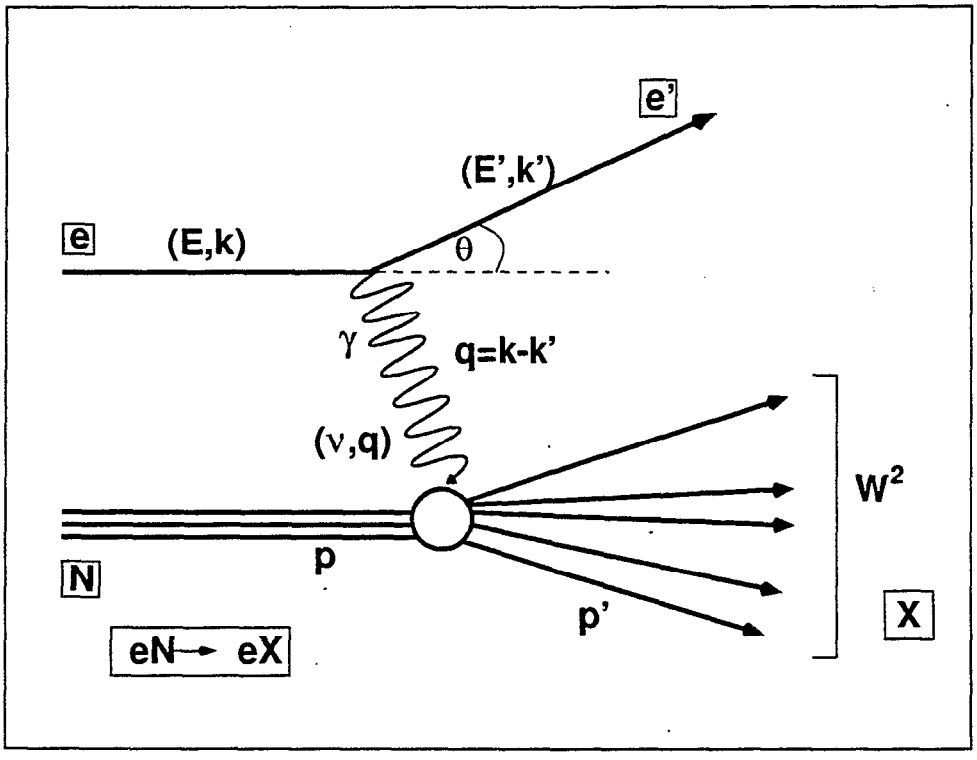

$$\frac{d^2\sigma}{d\Omega\, dE'} = \frac{\alpha^2}{2MQ^4}\,\frac{E}{E'}\,\mathcal{L}_{\mu\nu}\mathcal{W}^{\mu\nu}$$

$$\mathcal{W}_{\mu\nu} = -g_{\mu\nu}F_1 + \frac{p_\mu p_\nu}{\nu}F_2 + \frac{i}{\nu}\varepsilon_{\mu\nu\lambda\sigma}q^\lambda s^\sigma g_1$$
$$+ \frac{i}{\nu^2}\varepsilon_{\mu\nu\lambda\sigma}q^\lambda(p\cdot q s^\sigma - s\cdot q p^\sigma)g_2$$

DIS VARIABLES

q	VIRTUAL PHOTON 4-MOMENTUM $q = k - k'$
ν	VIRTUAL PHOTON ENERGY $\nu = E - e'$
Q^2	MOMENTUM TRANSFER $Q^2 = -q^2 \overset{lab}{=} 4EE' \sin^2 \frac{\vartheta}{2}$
W^2	HADRONIC SYSTEM INV. MASS $W^2 = p'^2 \overset{lab}{=} M^2 + 2M\nu - Q^2$
x	BJORKEN-X $x = \frac{Q^2}{2p\cdot q} \overset{lab}{=} \frac{Q^2}{2M\nu}$
y	FRACTIONAL ENERGY OF SCATTERED LEPTON $y = \frac{p\cdot q}{p\cdot k} \overset{lab}{=} \frac{\nu}{E}$
z	OBSERVED HADRON: γ^* ENERGY FRACTION $z = \frac{p\cdot p_h}{p\cdot q} \overset{lab}{=} \frac{E_h}{\nu}$

INCLUSIVE CROSS SECTION: 2 INDEPENDENT VARIABLES (OUT OF ν, Q^2, W^2, x, y).

VARIABLE z: RELEVANT FOR SEMI-INCLUSIVE ANALYSIS.

STRUCTURE FUNCTIONS, E.G. F_1 OR g_1, USUALLY GIVEN AS FUNCTIONS OF x AND Q^2.

1st Generation of DIS Experiments

~1960	: Hofstadter et al. $ep \to ep$, $eN \to eN$
$\sigma_{el}(Q^2)$	: the proton is not point-like
1967-72	: first generation of deep inelastic scattering (DIS) experiments
SLAC	: $ep(d,N) \to eX$ $\quad 1 \leq E_0 \leq 20$ GeV, $1 \leq Q^2 \leq 20$ GeV^2

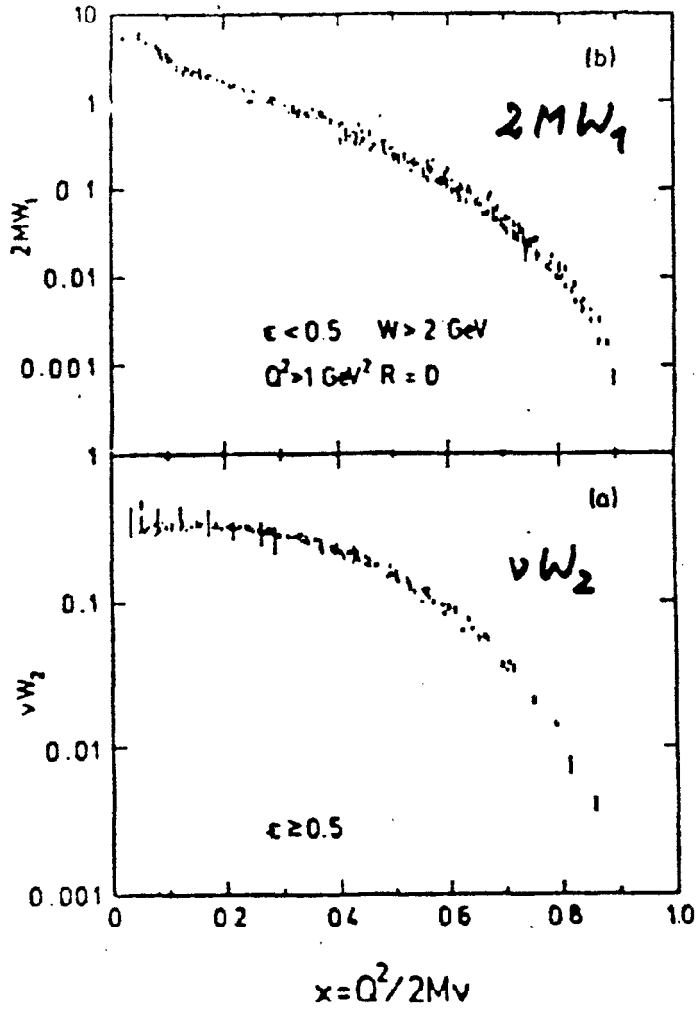

Most important result: Scaling of $2MW_1(\nu, Q^2)$ and $\nu W_2(\nu, Q^2)$ versus $x = Q^2/2M\nu$.

Pioneering SLAC Experiments

VOLUME 23, NUMBER 16 PHYSICAL REVIEW LETTERS 20 OCTOBER 1969

OBSERVED BEHAVIOR OF HIGHLY INELASTIC ELECTRON-PROTON SCATTERING

M. Breidenbach, J. I. Friedman, and H. W. Kendall
Department of Physics and Laboratory for Nuclear Science,*
Massachusetts Institute of Technology, Cambridge, Massachusetts 02139

and

E. D. Bloom, D. H. Coward, H. DeStaebler, J. Drees, L. W. Mo, and R. E. Taylor
Stanford Linear Accelerator Center,† Stanford, California 94305
(Received 22 August 1969)

Results of electron-proton inelastic scattering at 6° and 10° are discussed, and values of the structure function W_2 are estimated. If the interaction is dominated by transverse virtual photons, νW_2 can be expressed as a function of $\omega = 2M\nu/q^2$ within experimental errors for $q^2 > 1$ (GeV/c)^2 and $\omega > 4$, where ν is the invariant energy transfer and q^2 is the invariant momentum transfer of the electron. Various theoretical models and sum rules are briefly discussed.

In a previous Letter,[1] we have reported experimental results from a Stanford Linear Accelerator Center–Massachusetts Institute of Technology study of high-energy inelastic electron-proton scattering. Measurements of inelastic spectra, in which only the scattered electrons were detected, were made at scattering angles of 6° and 10° and with incident energies between 7 and 17 GeV. In this communication, we discuss some of the salient features of inelastic spectra in the deep continuum region.

One of the interesting features of the measurements is the weak momentum-transfer dependence of the inelastic cross sections for excitations well beyond the resonance region. This weak dependence is illustrated in Fig. 1. Here we have plotted the differential cross section divided by the Mott cross section, $(d^2\sigma/d\Omega dE')/(d\sigma/d\Omega)_{\text{Mott}}$, as a function of the square of the four-momentum transfer, $q^2 = 2EE'(1-\cos\theta)$, for constant values of the invariant mass of the recoiling target system, W, where $W^2 = 2M(E-E') + M^2 - q^2$. E is the energy of the incident electron, E' is the energy of the final electron, and θ is the scattering angle, all defined in the laboratory system; M is the mass of the proton. The cross section is divided by the Mott cross section

$$\left(\frac{d\sigma}{d\Omega}\right)_{\text{Mott}} = \frac{e^4}{4E^2}\frac{\cos^2\frac{1}{2}\theta}{\sin^4\frac{1}{2}\theta}$$

in order to remove the major part of the well-known four-momentum transfer dependence arising from the photon propagator. Results from both 6° and 10° are included in the figure for each value of W. As W increases, the q^2 dependence appears to decrease. The striking difference between the behavior of the inelastic and elastic cross sections is also illustrated in Fig. 1, where the elastic cross section, divided by the Mott cross section for $\theta = 10°$, is included. The q^2 dependence of the deep continuum is also consider-

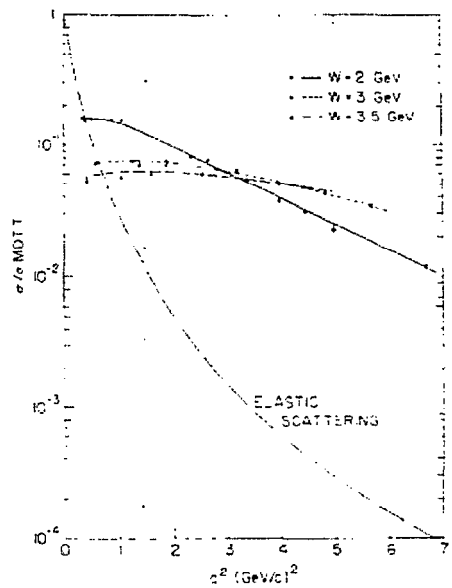

FIG. 1. $(d^2\sigma/d\Omega dE')/\sigma_{\text{Mott}}$, in GeV^{-1}, vs q^2 for $W = 2$, 3, and 3.5 GeV. The lines drawn through the data are meant to guide the eye. Also shown is the cross section for elastic e-p scattering divided by σ_{Mott}, $(d\sigma/d\Omega)/\sigma_{\text{Mott}}$, calculated for $\theta = 10°$, using the dipole form factor. The relatively slow variation with q^2 of the inelastic cross section compared with the elastic cross section is clearly shown.

Interpretation of the SLAC Data

1968 Bjorken : Scaling Hypothesis

$$W_i(Q^2,\nu) \underset{\substack{Q^2/M\to\infty \\ \nu\to\infty \\ x \quad finite}}{\longrightarrow} F_i(x)$$

1968 Feynman : Parton Model
Partons: charged, point-like, no self-interaction
parton $\xi \equiv$ Bjorken x

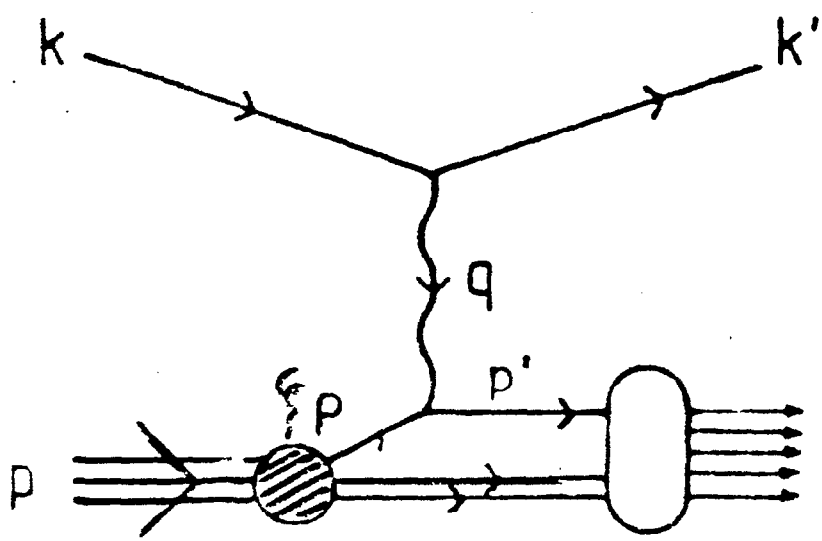

1971 Kuti/ Weisskopf : Quark-Parton Model
parton number density $q_i(x)$
parton momentum distr.$xq_i(x)$
nucleon structure function
$F_2(x) = \sum_i e_i^2 x q_i(x)$

Structure Function F_2 in Principle

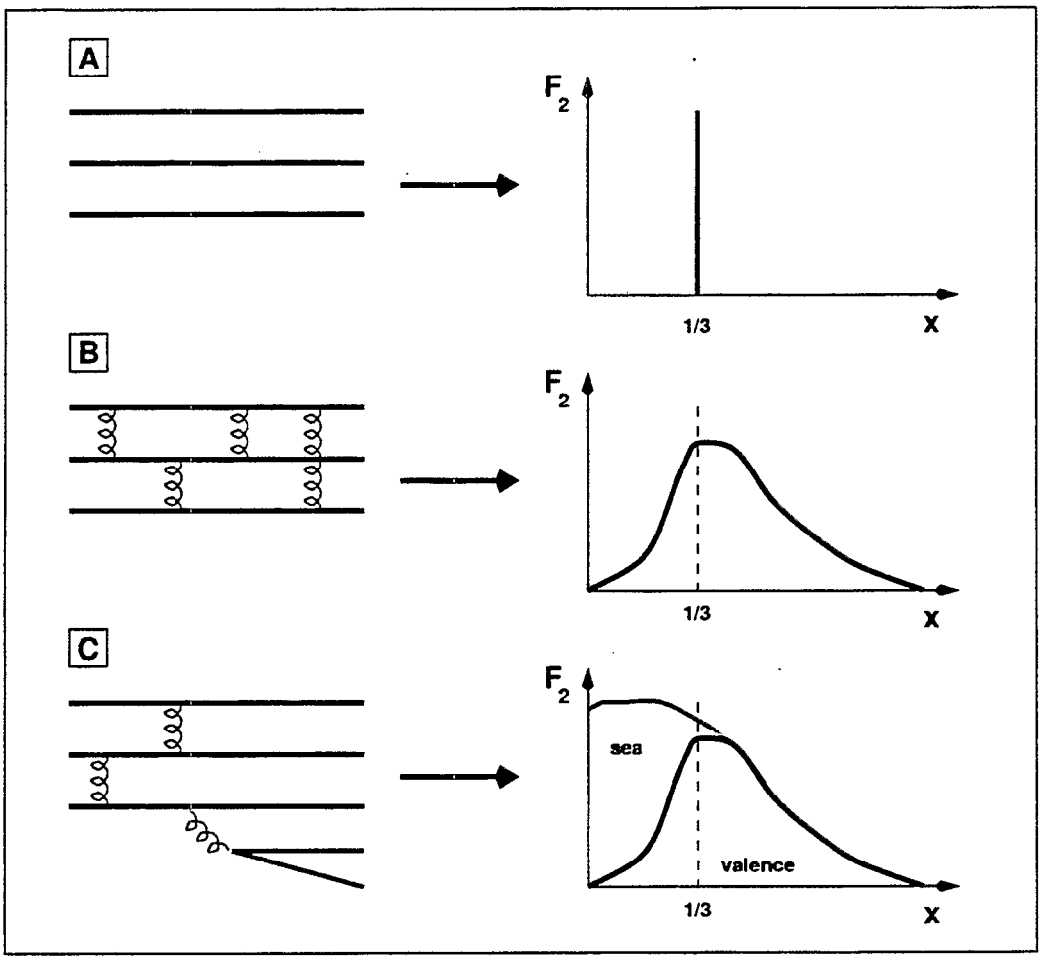

A 3 quarks without interaction

B with interaction in the form of gluons

C also with small x contribution from sea quarks

QPM: Proton in $SU(6)$

Simple quark model: nucleon consists of three valence quarks.
$\Rightarrow$ introduce $SU(6)$ wave functions as product of flavor $SU(3)$ and spin $SU(2)$:

$$|p\uparrow\rangle = \sqrt{\frac{1}{18}}[uud(2\uparrow\uparrow\downarrow - \uparrow\downarrow\uparrow - \downarrow\uparrow\uparrow)$$
$$+ udu(2\uparrow\downarrow\uparrow - \uparrow\uparrow\downarrow - \downarrow\uparrow\uparrow)$$
$$+duu(2\downarrow\uparrow\uparrow - \uparrow\downarrow\uparrow - \uparrow\uparrow\downarrow)]$$

$\rightarrow \mu_p, \mu_n, \mu_\Lambda \rightarrow \mu_u, \mu_d, \mu_s$
$\rightarrow$ calculate baryon magnetic moments:

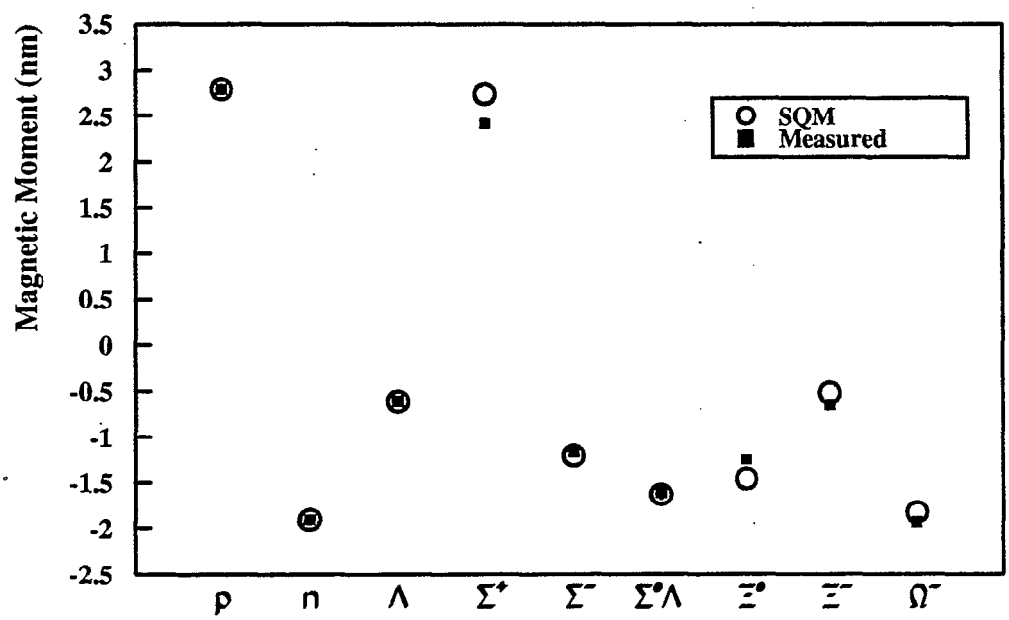

2nd Generation of DIS Experiments

1972-77 : second generation of deep inelastic scattering (DIS) experiments

FERMILAB : $\mu p(d, N) \to \mu X$ $100 \leq E_0 \leq 150$ GeV
$1 \leq Q^2 \leq 40$ GeV^2

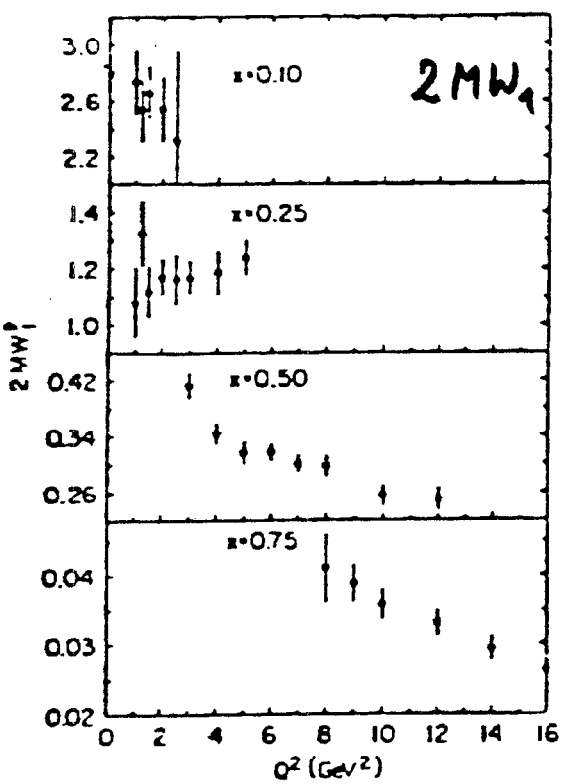

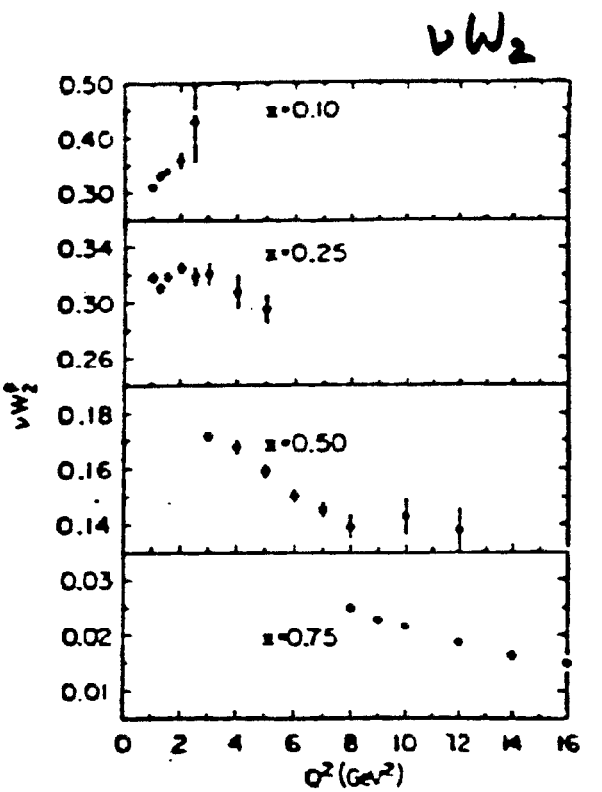

Most important result: $F_i(x) \Rightarrow F_i(x, Q^2)$
$\Rightarrow$ small violations of scaling behavior

Begin of the QCD Era

1973 : Quantum ChromoDynamics (QCD)

$$\alpha_s = \alpha_s(Q^2) \sim 1/\ln\left(\frac{Q^2}{\Lambda^2_{QCD}}\right)$$

running coupling constant

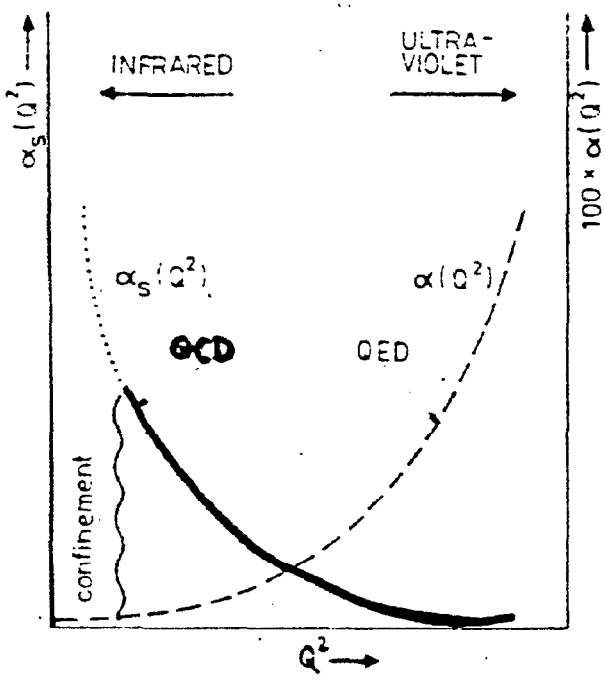

	QED	QCD
interaction	electromagnetic	strong
fundamental fields	leptons e,μ,τ,ν_e,ν_μ, ν_τ	quarks u, d, s, c, t, b
gauge field	photon γ	gluons g
coupling to	electric charge	color charge
renorm. group	U_1	SU_3^c
$Q^2 \to \infty$ (UV)	$\alpha(Q^2) \to \infty$	$\alpha_s(Q^2) \to 0$ asymptotic freedom perturbative QCD
$Q^2 \to 0$ (IR)	$\alpha(Q^2) \to 0$	$\alpha_s(Q^2) \to$? confinement lattice QCD

Illustration of QCD Processes

QPM

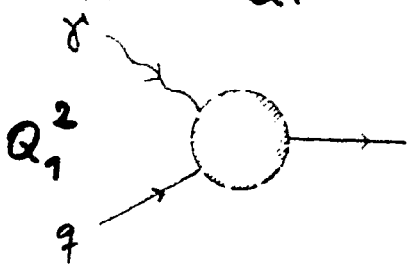

Gluon → Quark Pair

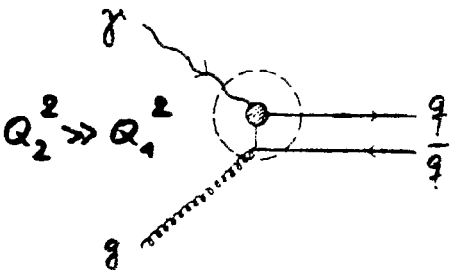

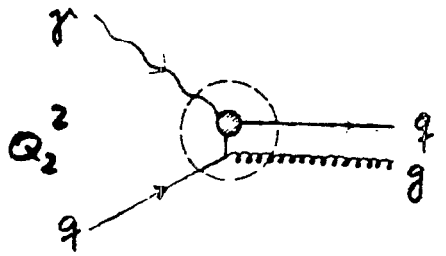

Gluon Bremsstrahlung

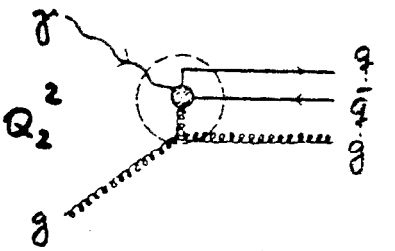

3-Gluon-WW

At $Q_2^2 >> Q_1^2$:

More (less) partons with smaller (larger) momentum.

$\Rightarrow$

'Shrinking' of all the parton distributions

Fig. shows it for $F_2 = \sum_i e_i^2 x q_i(x)$

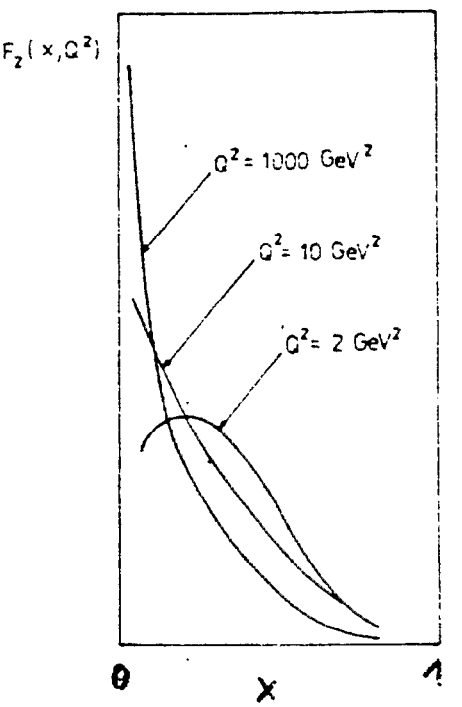

3rd Generation of DIS Experiments

1978-1990 : third generation of deep inelastic scattering (DIS) experiments

CERN (EMC, BCDMS) : $\mu p(d, N) \to \mu X$ $100 \leq E_0 \leq 280$ GeV
$1 \leq Q^2 \leq 280$ GeV^2

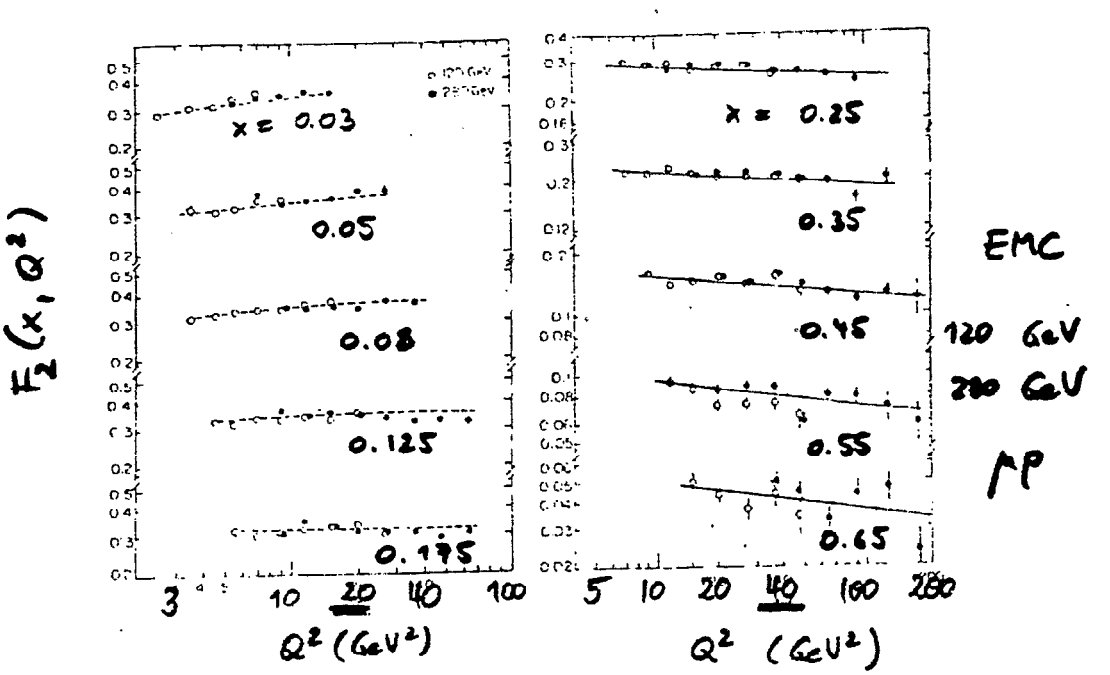

Most important results: Measurements of F_2, R, Λ_{QCD} (first quantitative QCD tests)

Also at CERN: $\nu N \to \nu X$, $\bar{\nu} N \to \bar{\nu} X$
Experiments: CDHS,CHARM,BEBC,Gargamelle

Results on F_2, xF_3, R, Λ_{QCD}, $g(x)$, $q_i(x)$, $\bar{q}_i(x)$, QPM

EMC Forward Spectometer (NA2)

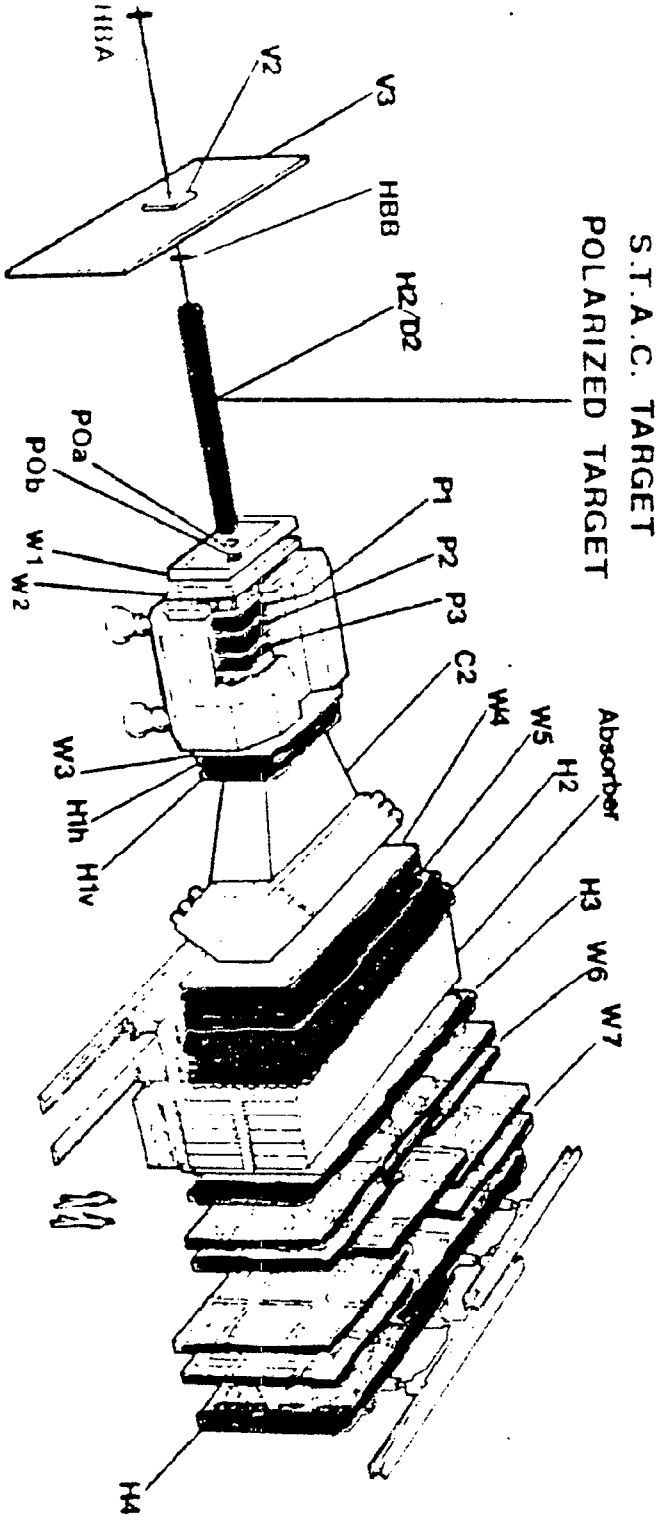

BCDMS Iron-Toroid Spectometer (NA4)

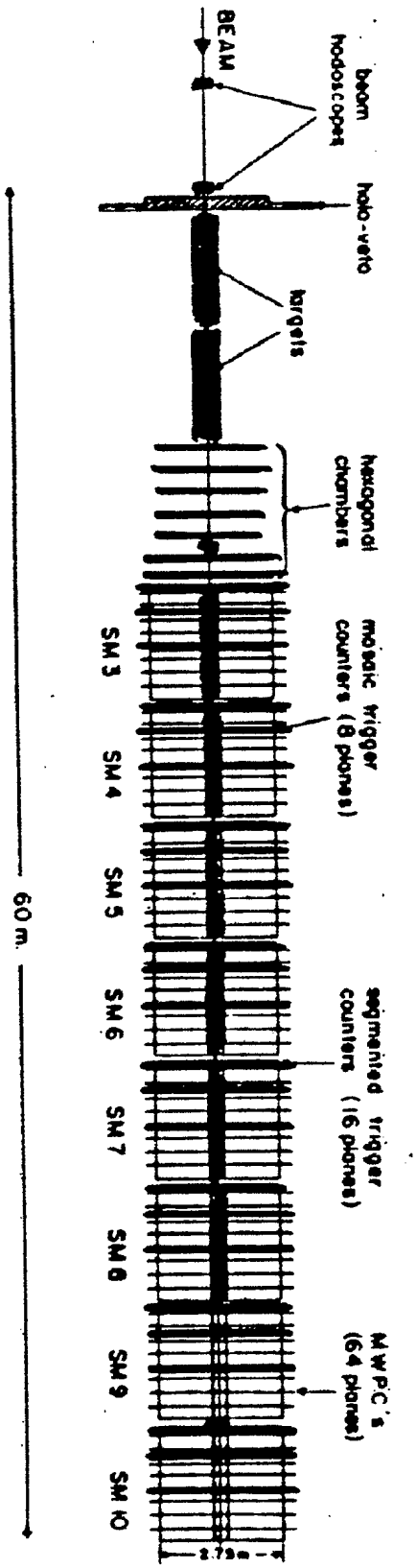

Kinematic Plane

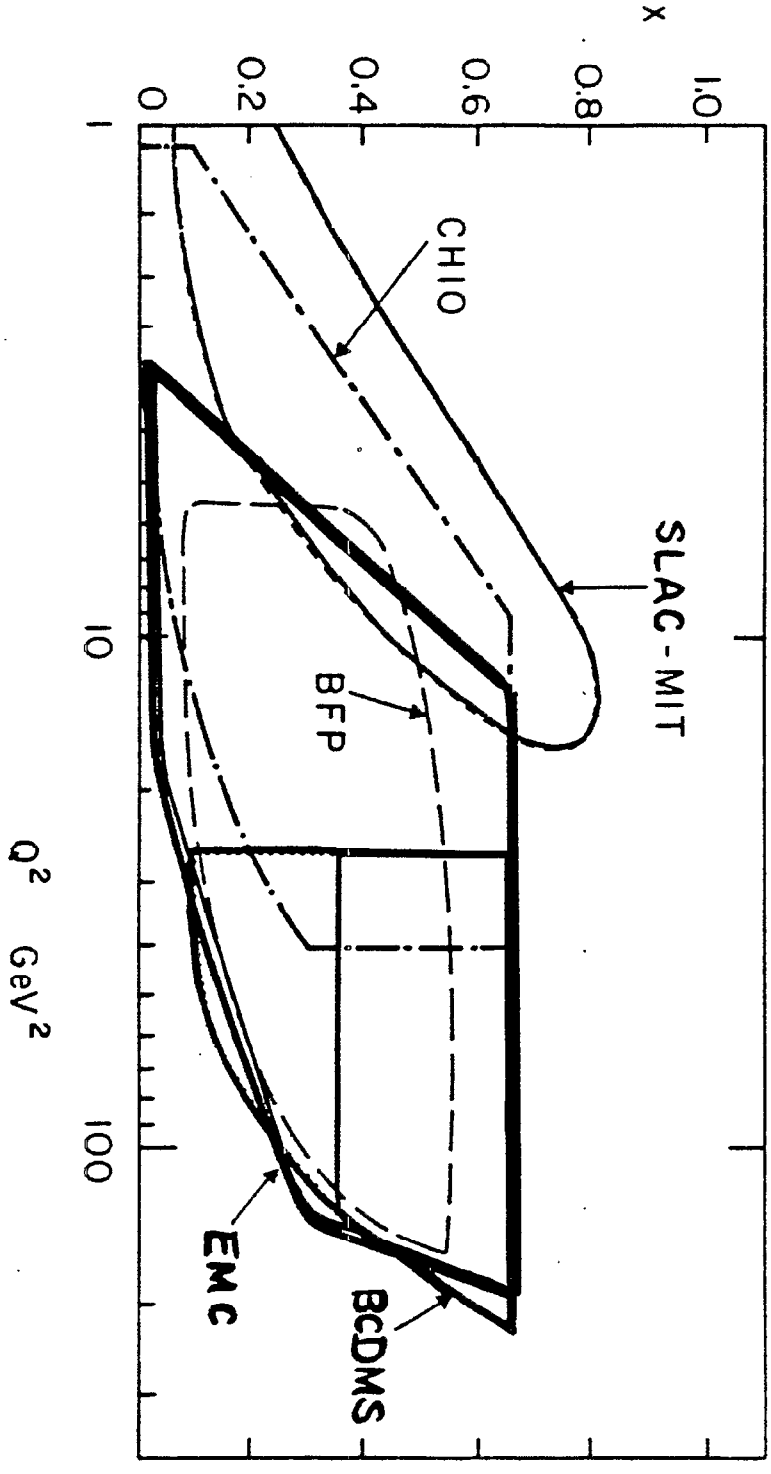

1983: Quark Spin and Transv. Mom.

$$R = \frac{\sigma_L}{\sigma_T} = \left[\left(1 + \frac{4M^2x^2}{Q^2}\right)\frac{F_2}{2xF_1}\right] - 1$$

$$\text{QPM: quark spin} = \begin{cases} 0 & : F_1 \equiv 0 \quad \Rightarrow R \to \infty \\ \frac{1}{2} & : F_2 = 2xF_1 \Rightarrow R = 4M^2x^2/Q^2 \end{cases}$$

$$k_T \neq 0 \qquad : \qquad R = \frac{4\langle k_T^2 \rangle}{Q^2}$$

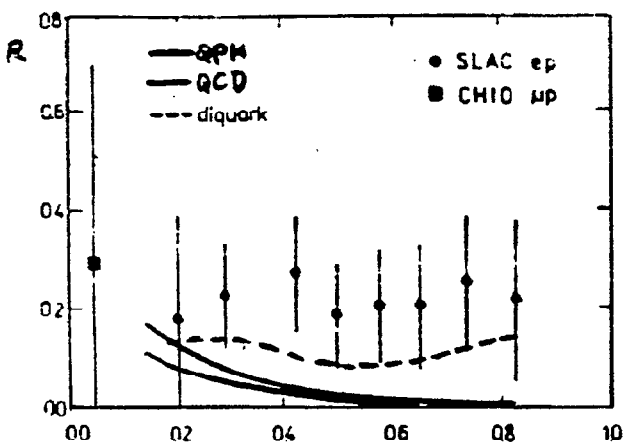

QCD LO : $R = 0$
QCD NLO : $R \sim \alpha_s(Q^2)$

SLAC (1979-83):
$1 \leq Q^2 \leq 18$ GeV^2

QPM + QCD + diquarks ($\tau = 4$) ok

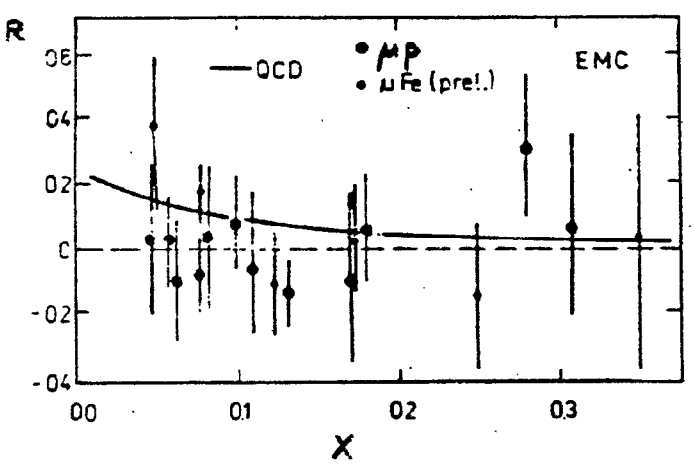

EMC (1983):
$\langle Q^2 \rangle \sim 55$ GeV^2

QPM: $R = 0$
QCD(NLO) :
$x \geq 0.2 \quad R \approx 0$ ok
$x \leq 0.2 \quad R > 0$ open

Results: (1) quark spin = 1/2
(2) QCD prediction is compatible
(3) $\langle k_T^2 \rangle \lesssim 0.5$ GeV^2

1982: Quark Charge 1/3 or 1 ?

QPM: $\dfrac{F_2^{\mu N}}{F_2^{\nu N}} = \begin{cases} \frac{5}{18} & \text{for } e_u^2 = 4/9 \qquad e_d^2 = 1/9 \\ 1 & \text{for } e_u^2 = e_d^2 = 1 \end{cases}$

1982: EMC (μFe) vs. CDHS (νFe):

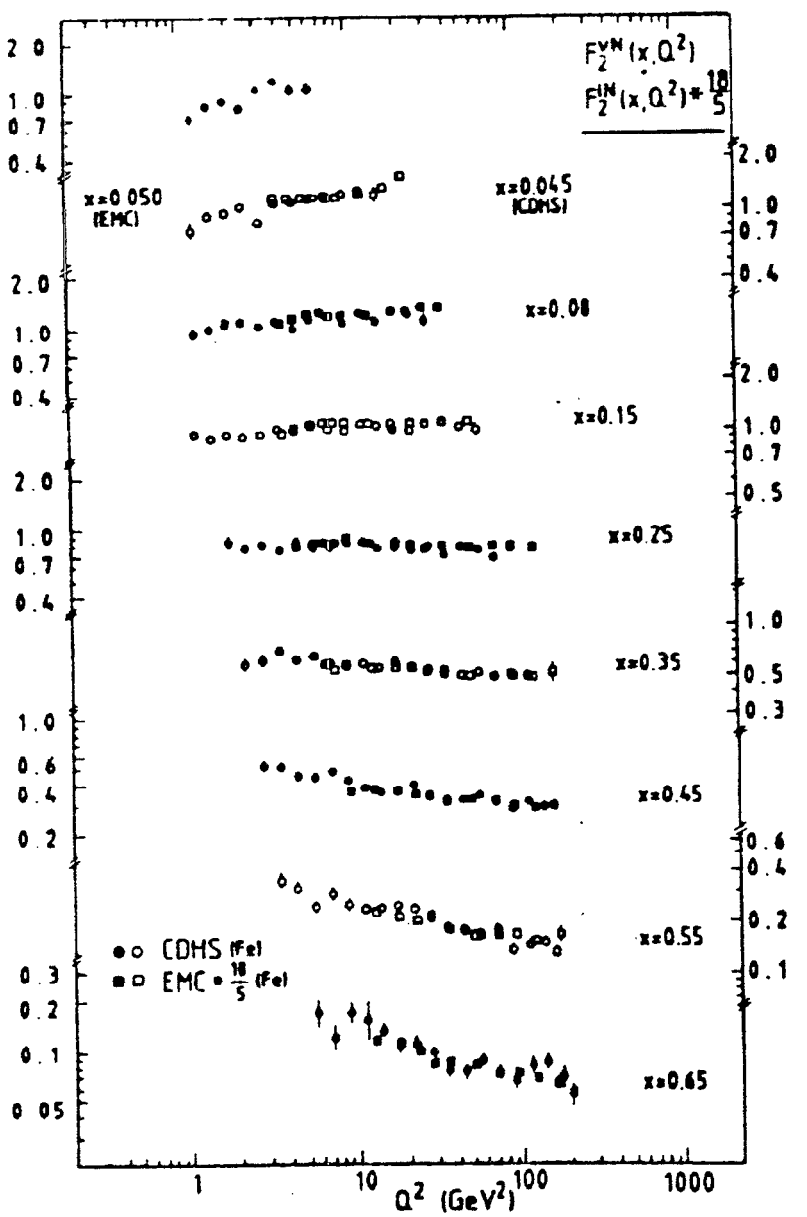

Result: Quark Charge is 1/3 !

1982: Number of Valence Quarks

QPM:

Number of Valence Quarks in the Nucleon =

$$\int_0^1 \frac{dx}{x} x F_3(x) = 3(1 - \frac{\alpha_s}{\pi})$$

with $1 - \alpha_s/\pi = 0.91$ for Q^2=10 GeV^2 and Λ_{QCD}=200 MeV

CHARM (1983)	: 2.56±0.41±0.10
CCFFR (1984)	: 2.83±0.15±0.15

Result: QPM ok, QCD corrections compatible
exp. (syst.) problem : small x !

1983: Valence Quarks in the Nucleon

QPM:
Difference between u- and d- Valence Quarks:

$$3\int_0^1 \frac{dx}{x}(F_2^p - F_2^n) = \underbrace{\int_0^1 dx(u_v - d_v)}_{1\ \text{(QPM)}} + \underbrace{\int_0^1 dx(\bar{u} - \bar{d})}_{0\ (SU_4\ \text{symm. sea})}$$

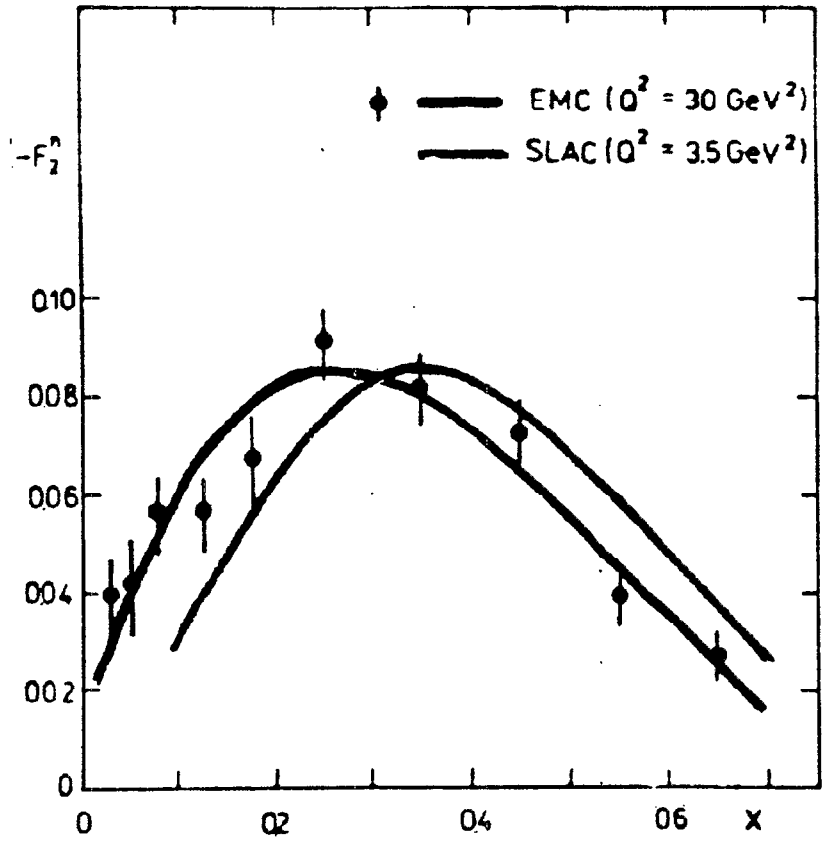

EMC (1983): 0.72±0.06±0.39
exp. (syst.) problem: low x

Result:
QPM is ok (proton: 2 u-quarks, 1 d-quark)

1985-90: Precision F_2 - Measurements

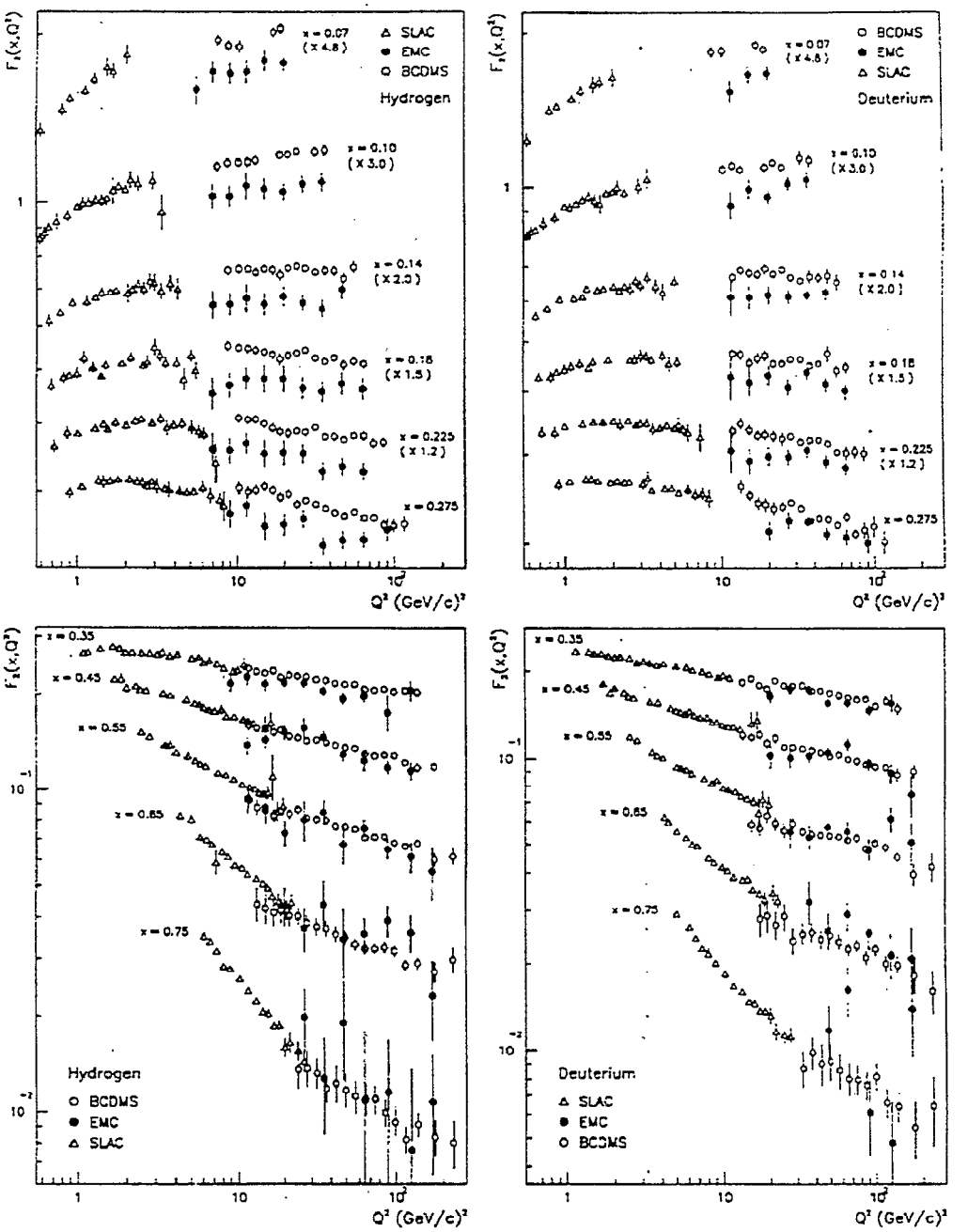

Precision data on $F_2(x, Q^2)$ published:
EMC: 1985 (Proton), 1987 (Deuterium)
BCDMS: 1989 (Proton), 1990 (Deuterium)
$\Rightarrow$ Determination of Λ_{QCD} possible

POLARIZED POSITRONS IN HERA

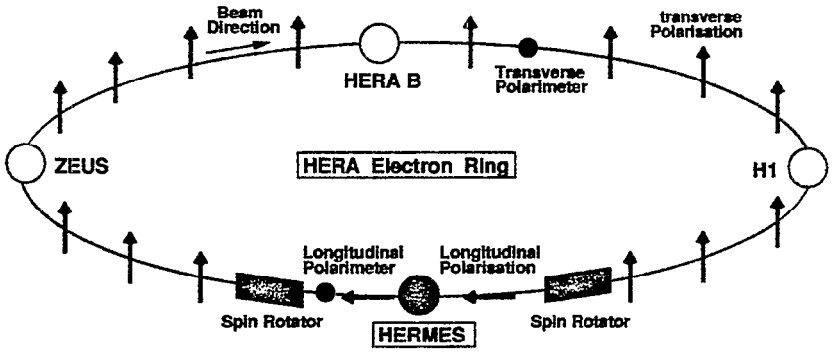

- SELF-POLARIZATION BY EMISSION OF SYNCHROTRON RADIATION [SOKOLOV-TERNOV EFFECT]:

$$P_b(t) = p_b^{max}[1 - exp(t/\tau)]$$

- LONGITUDINAL POLARIZATION AT HERMES
  $\Rightarrow$ SPIN ROTATORS
- POLARIMETERS BASED ON COMPTON BACK-SCATTERING
  - TRANSVERSE POLARIMETER: POSITION ASYMMETRY IN THE COMPTON CROSS SECTION
  - LONGITUDINAL POLARIMETER: ASYMMETRY IN THE INTEGRAL OF THE ENERGY WEIGHTED COMPTON CROSS SECTION
- AVERAGE BEAM POLARIZATION $\langle P_b \rangle \approx 55\%$

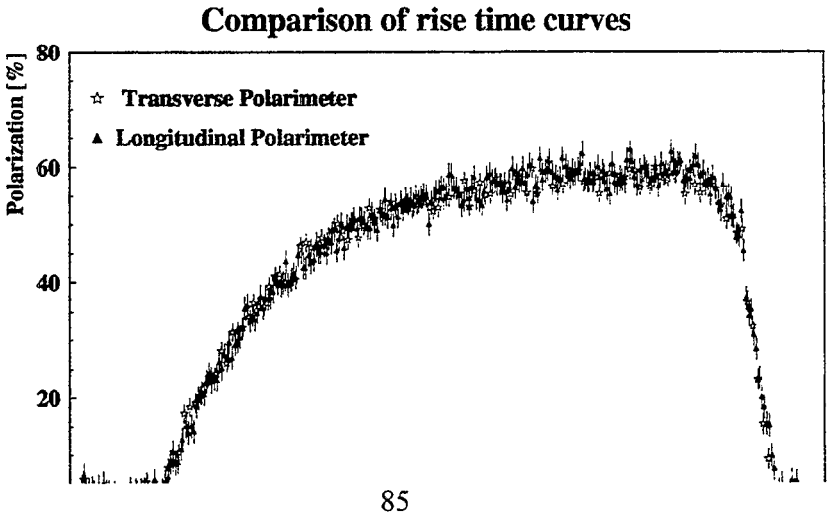

THE HERMES EXPERIMENT AT DESY

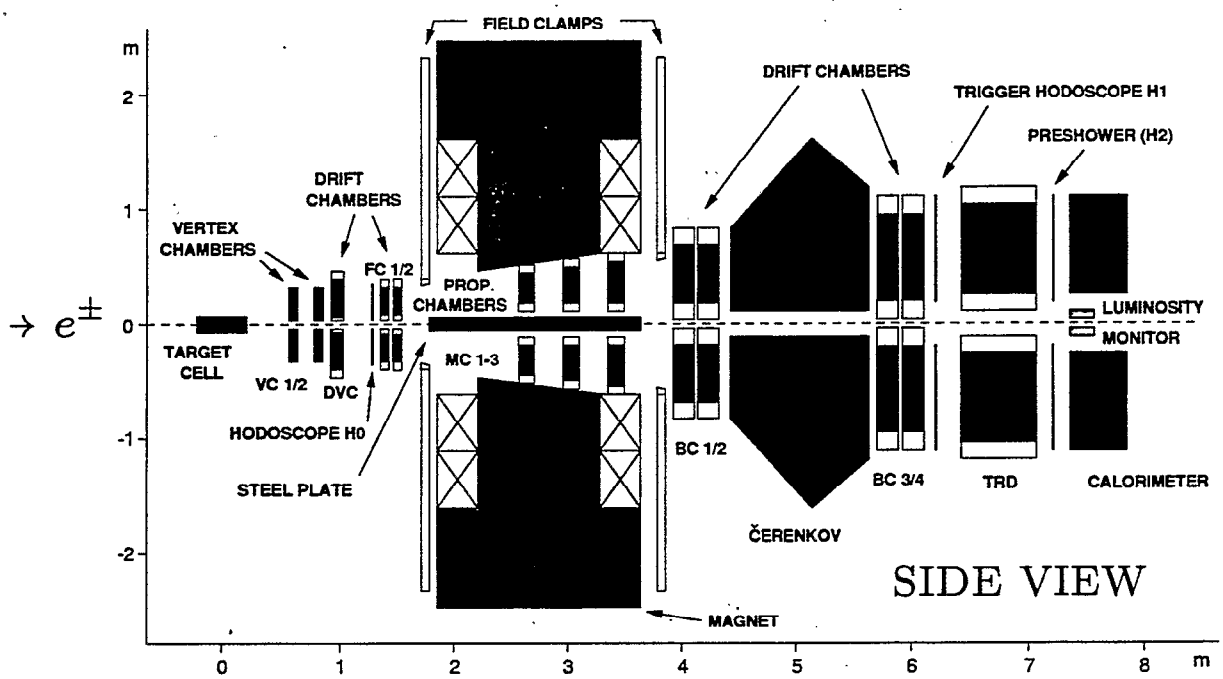

- Beam: transversely self-polarized 27.6 GeV $e^{\pm}$-beam of HERA, rotated to longitudinal spin orientation at the HERMES IP; $P_{\text{beam}} \approx 0.55 \pm 0.02$
- Target: cooled open-ended storage cell inside the beam pipe, longitudinally polarized pure (^{1}H, D, ^{3}He) gas atoms of $(7-33) \times 10^{13}$ nucleons/cm^2; $P_{\text{H}} = 0.88 \pm 0.04$, $P_{\text{D}} \approx P_{\text{H}}$, $P_{\text{He}} = 0.46 \pm 0.02$
- Tracking: forward dipole magnet spectrometer with 57 chamber planes (40 mrad $< \theta <$ 220 mrad); resolution: $\delta\theta < 0.6$ mrad, $\delta p/p < 1.5\%$
- Particle ID: threshold Cerenkov detector, TRD, preshower, lead-glass calorimeter; e/h misidentification $< 0.4\%$
- Fast Trigger: scintillator hodoscopes H0, H1, H2; calorimeter; energy threshold 1.4 (3.5) GeV

THE HERMES POLARIZED TARGET

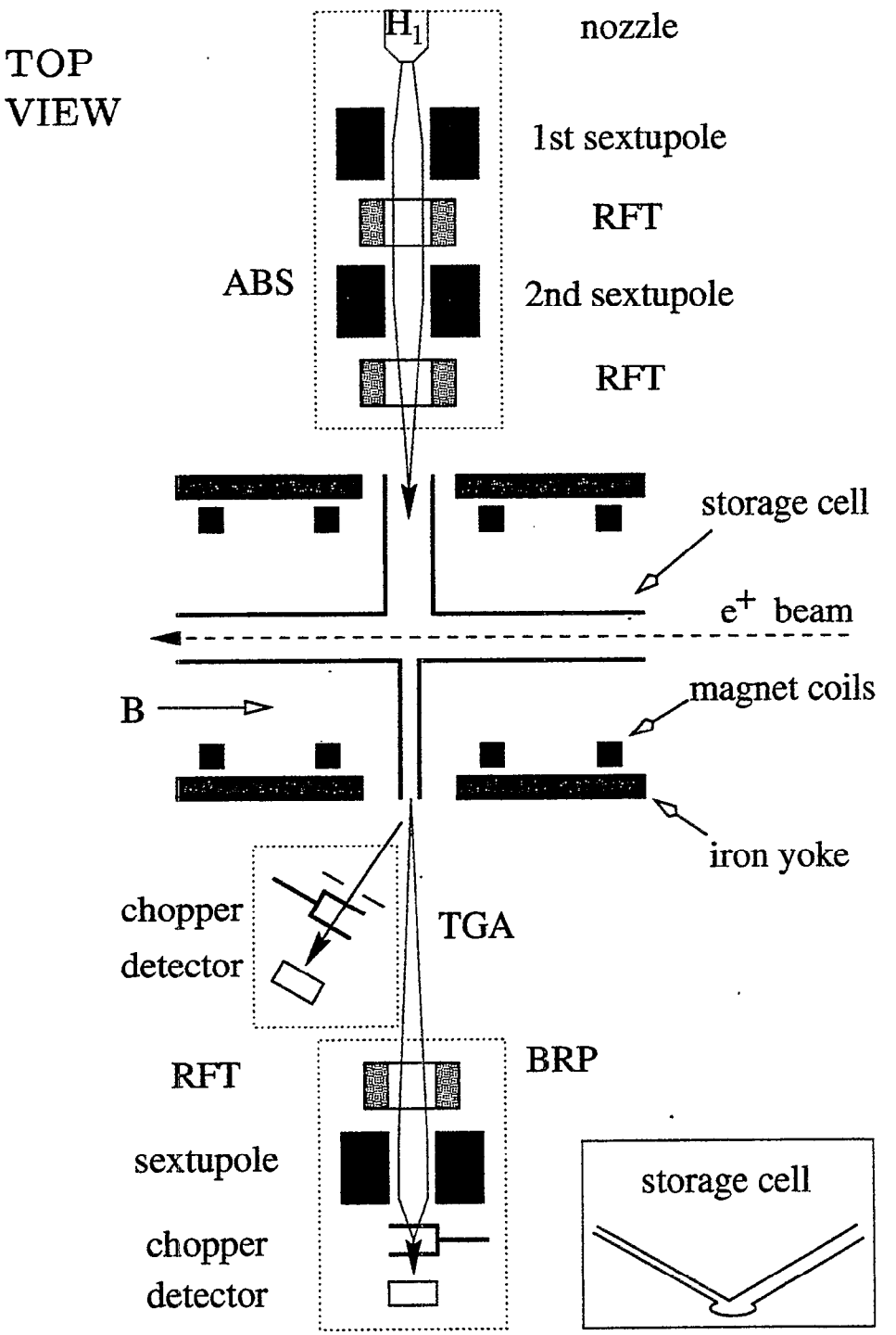

- CELL WALLS 75μ ALUMINUM, DRIFILM COATED
- CELL TEMPERATURE 35...260 K, HELIUM COOLED

TARGET PERFORMANCE 1996-2000

$$P^T = \alpha_0^T(\alpha_r^T + (1-\alpha_r^T)\beta)P_a^T$$

- P^T TARGET POLARIZATION (AVERAGED)
- α_0^T INITIAL DEGREE OF DISSOCIATION
- α_r^T RECOMBINATION INSIDE CELL
- β MOLECULE POLARIZATION: $\beta = P_a/P_m$
- P_a^T ATOM POLARIZATION

	1996/1997 HYDROGEN	1998/1999 DEUTERIUM	2000 DEUTERIUM
$< d^T >$	$7.5*10^{13}$	$7.5*10^{13}$	$14*10^{13}$
T_c (K)	100	90	65
B^T (mT)	335	335	335
α_0^T	0.99±0.02	0.94±0.03	0.953±0.014
α_r^T	0.93±0.04	1.00±0.03	0.997±0.013
P_a^T	0.92±0.03	0.99±0.01	0.99±0.01
β	0.60±0.40	0.60±0.40	0.60±0.40

The Hermes RICH Detector

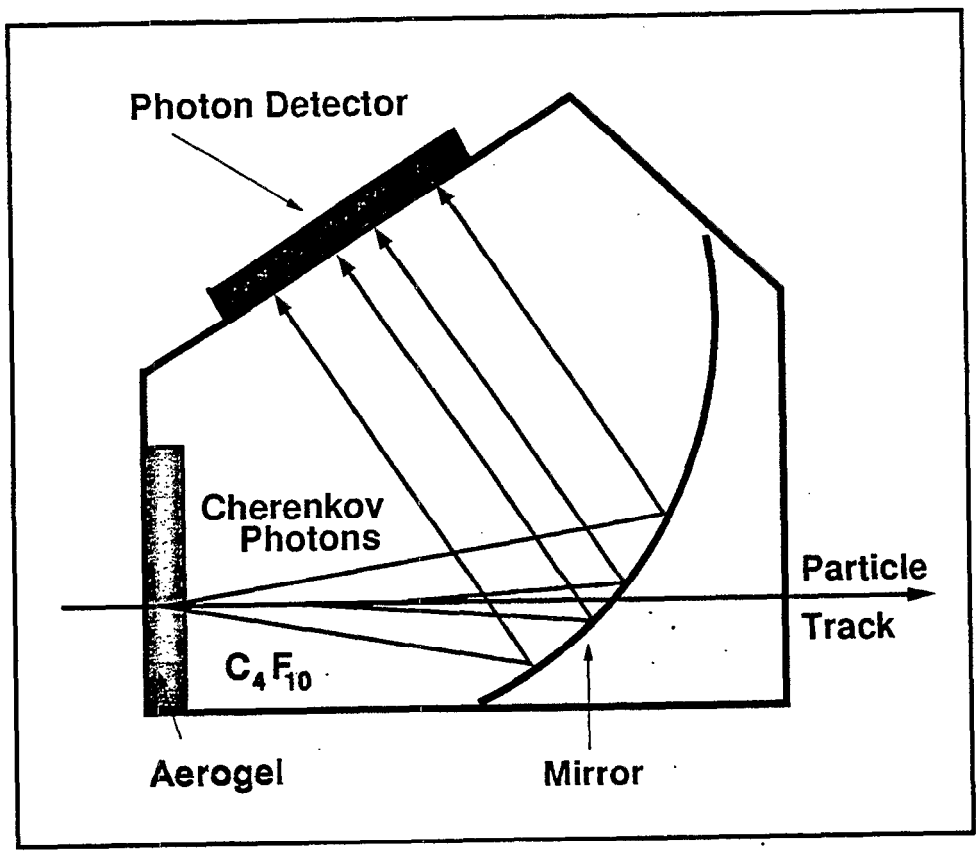

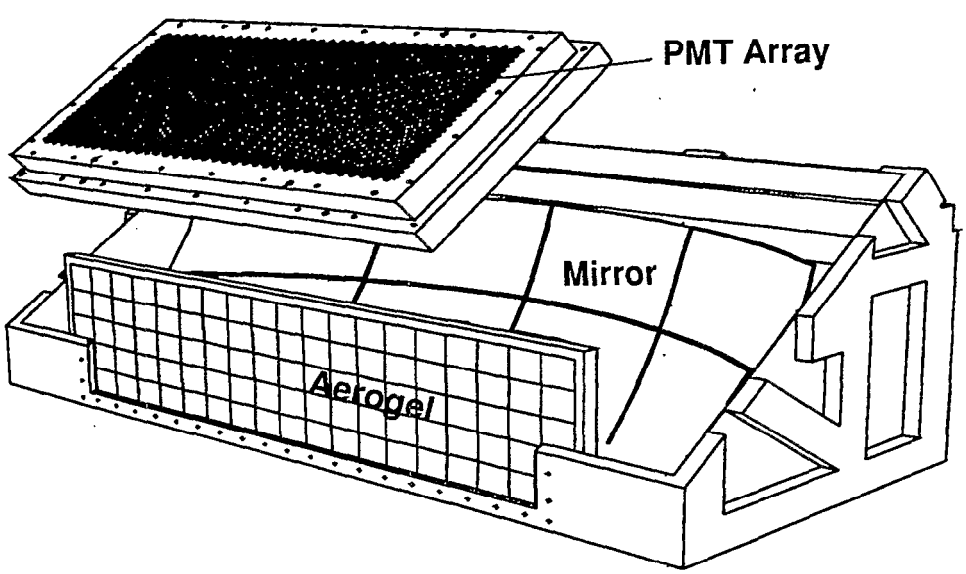

HERMES RICH - AVERAGE ANGLES

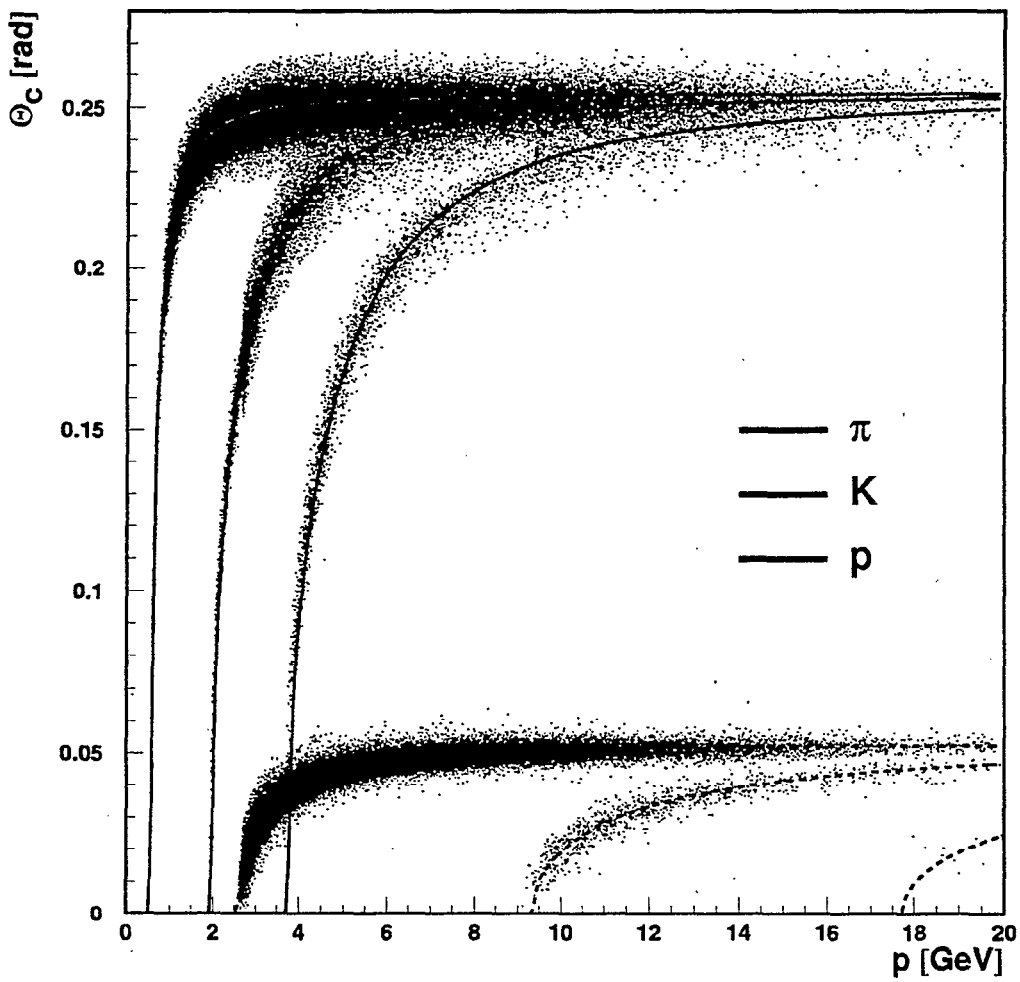

⇒ DESIGN RESOLUTION REACHED FOR GAS AND AEROGEL
(WITHIN 10%).

Charm Meson Candidate

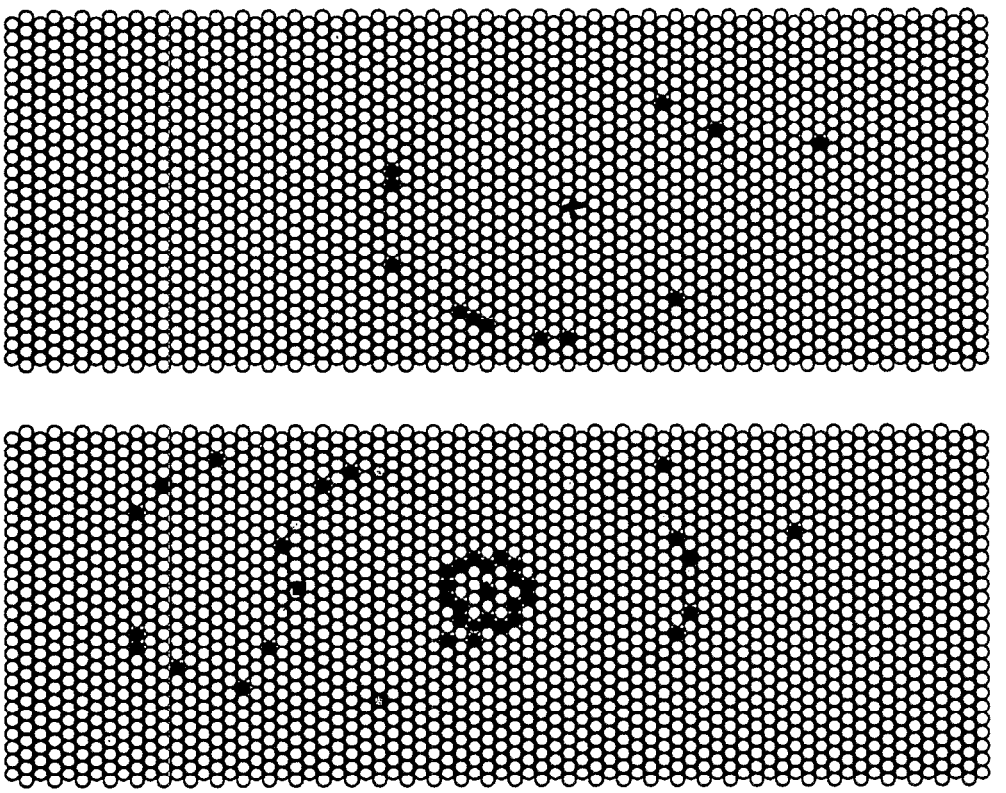

Run: 3360 Event: 20097411 Time: Mon Nov 23 05:39:09 1998 Number of tracks: 3

Particle	1 ✦	2 ■	3 ◆
Momentum(GeV/c)	5.54	1.52	14.61
Type(est)	Kaon+	Pion-	Electron
Position	Top	Bottom	Bottom

No hits 1 or more hits

Polarized DIS Experiments

Experiment	Beam	Period of Data Taking	Beam Energy (GeV)	Target
E80	e^-	1974-76	6-19	C_4H_9OH
E 130	e^-	1979-80	16.2-22.7	C_4H_9OH
EMC	μ^+	1984-85	100-200	NH_3
SMC	μ^+	1992	100	C_4D_9OD
	μ^+	1993	190	C_4H_9OH
	μ^+	1994	190	C_4D_9OD
	μ^+	1995	190	C_4D_9OD
	μ^+	1996	190	NH_3
E142	e^-	1992	19.4-25.5	^3He
E143	e^-	1993	29.1	NH_3, ND
E154	e^-	1995	50	^3He
E155	e^-	1996	50	NH_3, ND
HERMES	e^+	1995	27.5	^3He
	e^+	1996	27.5	H
	e^+	1997	27.5	H
	e^-	1998	27.5	D
	e^-, e^+	1999	27.5	D
	e^+	2000	27.5	D

HERMES Kinematic Plane

- Extended (and standard) kinematic range:

$$0.85 > x > 0.0021\ (0.0212)$$
$$0.1 < y < 0.91\ (0.85)$$
$$Q^2 > 0.1\ (0.8)\ \mathrm{GeV}^2$$

- 1997 Pol. hydrogen data, after quality cuts:
  $\Rightarrow 1.7 * 10^6$ events in 'standard' kin. range
  $\Rightarrow 0.8 * 10^6$ events in extended kin. range

- The HERMES kinematic plane:

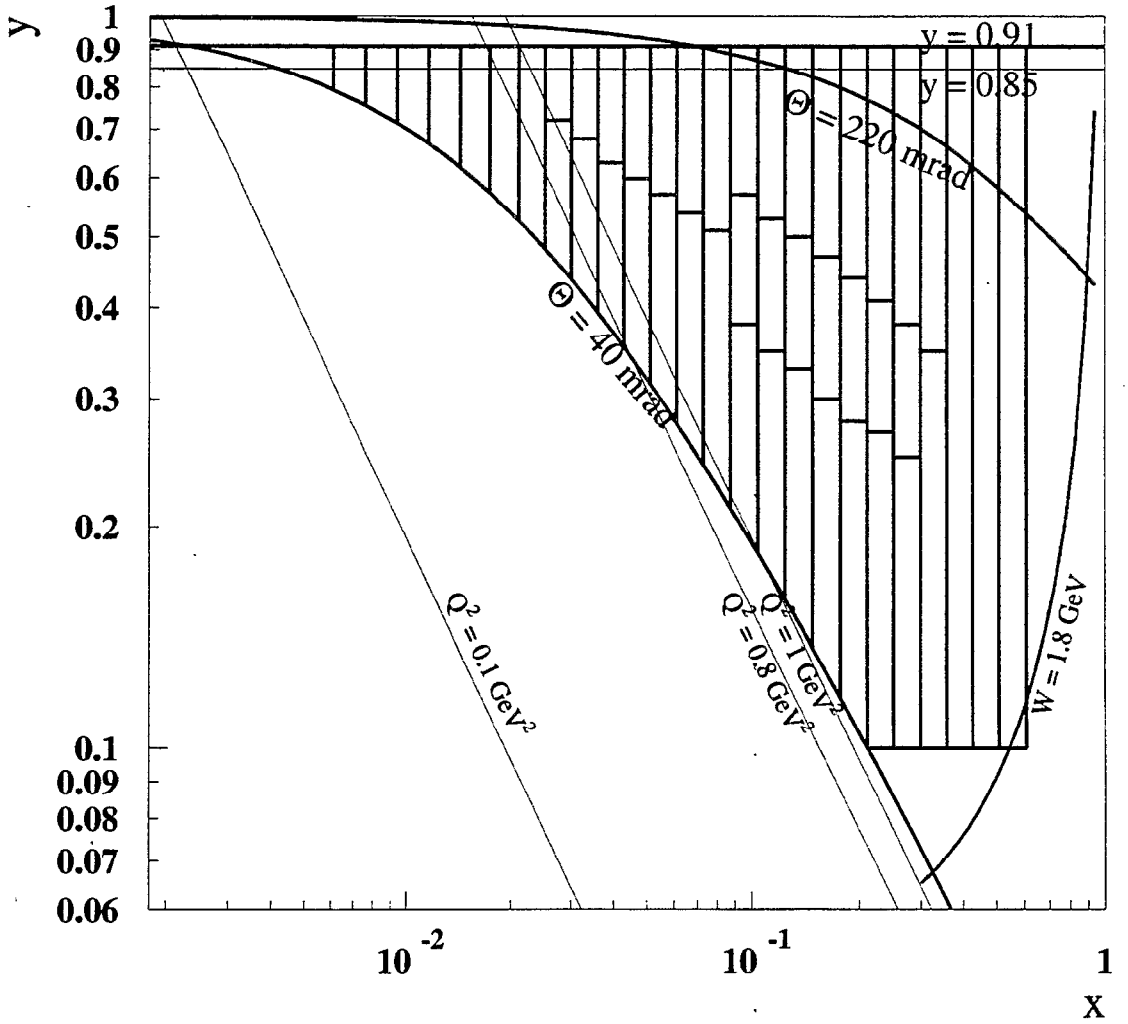

Summary of DIS History

- Analyzing the cross section of (polarized) inclusive deep inelastic lepton-nucleon scattering allows the extraction of unpolarized (and polarized) nucleon structure functions, i.e. the understanding of the momentum (and spin) structure of the nucleon.

- The 1st generation of experiments (electron scattering at SLAC) revealed the scaling of the nucleon structure functions and thus stimulated the development of Feynman's Parton Model.

- The 2nd generation (muon scattering at FNAL) confirmed the scaling violations and thus stimulated the development of QCD.

- The 3rd generation (muon- AND neutrino-scattering at CERN) allowed for various QPM tests and first quantitative tests of QCD.

Results with polarized targets initiated the study of the spin structure of the nucleon (→ Lecture 2).

- The 4th generation (electron/positron-scattering at DESY) allows for higher statistics semi-inclusive measurements thus opening access to the spin structure of the nucleon (→ Lecture 2).

- A 5th generation (electron-scattering at TESLA) may lead to the ultimate completion of the understanding of the full spin structure of the nucleon (→ Lect. 3).

TESLA-N
Polarized Electron-Nucleon Scattering at TESLA

Wolf-Dieter Nowak - DESY Zeuthen
On Behalf Of The TESLA-N Study Group

RIKEN Winter School, LECTURE 3
Yuzawa/Japan, Dec. 4, 2000

- Polarized eN-Scattering at TESLA
- Physics Program and Projections
- Possible Layout of the Experiment
- Monte Carlo Simulation
- Overall Conclusions

TESLA-N Study Group

G. v.d.Steenhoven, J. Steijger, NIKHEF Amsterdam

P.J. Mulders, Free University Amsterdam

M. Düren, University of Bayreuth

A. Meier, W. Meyer, K. Goeke, St. Goertz, J. Harmsen,
M.V. Polyakov, P.V. Pobylitsa, G. Reicherz, C. Weiss
Ruhr-University Bochum

A. Gute, E. Steffens, K. Rith, University of Erlangen

D. Ryckbosch, University of Gent

W. Bialowons, R. Brinkmann, N. Meyners, K. Oganessyan, K. Sinram
DESY Hamburg

E. Leader, Birckbeck College London

D. v.Harrach, E.M. Kabuss, University of Mainz

S. Belostotski, St. Petersburg Nuclear Physics Institute

V. Braun, B. Lehmann-Dronke, D. Müller,
L. Niedermeier, A. Schäfer
University of Regensburg

M. Anselmino, INFN Torino

L. Mankiewicz, Nicolaus Kopernicus Astronomical Center Warsaw

R. Jakob, P. Kroll, University of Wuppertal

E.C. Aschenauer, J. Blümlein, F. Ellinghaus,
R. Kaiser, V. Korotkov, W.-D. Nowak
DESY Zeuthen

A POLARIZED FIXED-TARGET EXPERIMENT AT TESLA

BASIC IDEA: USE ONE ARM OF THE TESLA COLLIDER FOR A POLARIZED FIXED-TARGET EXPERIMENT TO OPERATE IN PARALLEL TO THE COLLIDER EXPERIMENT(S).

- ☐ ELECTRON (SOUTH) ARM CANNOT BE USED, BECAUSE KICKER MAGNETS WOULD NOT BE FAST ENOUGH TO DIVERT ONLY PART OF THE BEAM.

⇒ USE POSITRON (NORTH) ARM FOR ACCELERATION

⇒ STATIC MAGNET SYSTEM FOR SEPARATION FROM THE POSITRONS.

- ☐ THE POLARIZED BEAM CONSTITUTES ONLY ABOUT 0.04% OF THE MAIN CURRENT

⇒ ADDITIONAL ENERGY CONSUMPTION IS NEGLIGIBLE.

ADDITIONALLY NEEDED FOR THE EXPERIMENT, BESIDES TARGET AND SPECTROMETER:

- ☐ POLARIZED SOURCE AND INJECTOR
- ☐ EXPERIMENTAL HALL AND SHORT TUNNEL
- ☐ BEAM DUMP

CIVIL ENGINEERING

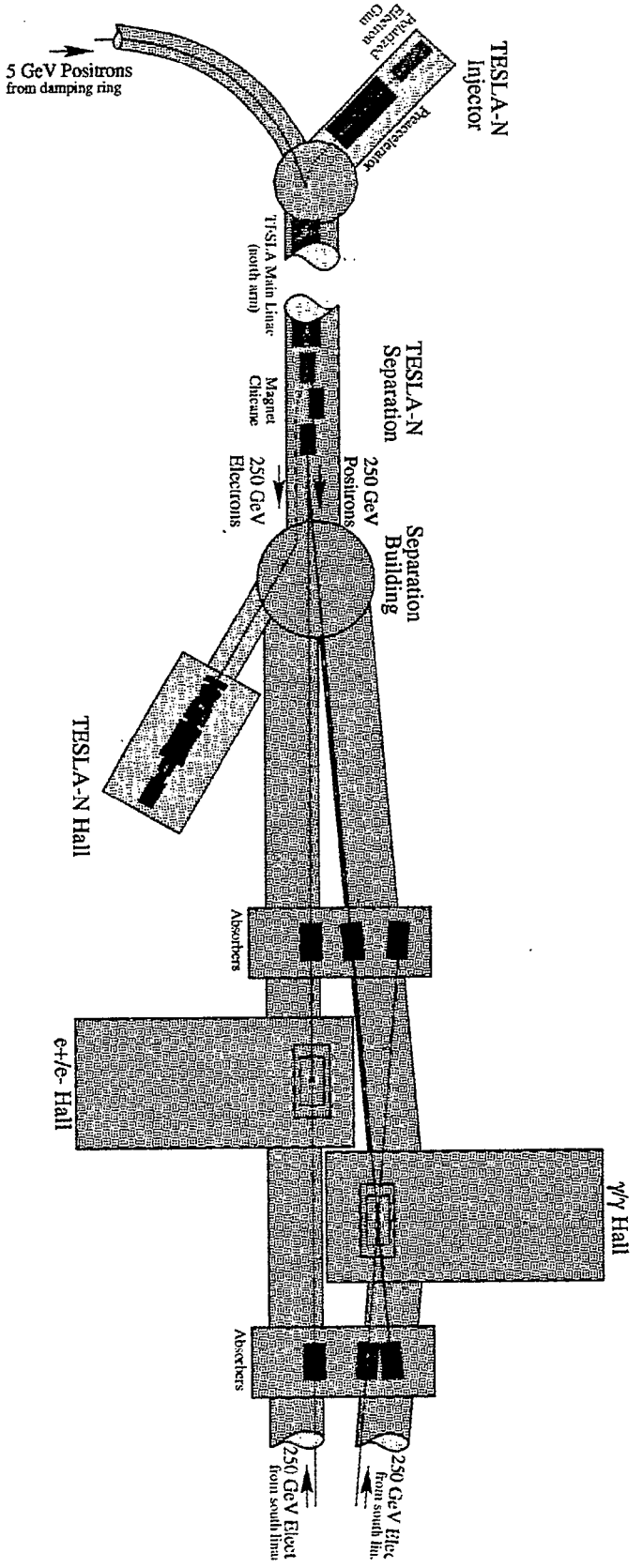

LUMINOSITY (I)

TESLA-N figures for 5 Hz operation:

LUMINOSITY L	$7.5 \cdot 10^{34}$ nucl/cm^2/s
$\int L\ dt$/s	7.5 nb^{-1}
$\int L\ dt$/e-bunch	12 mb^{-1}
$\int L\ dt$/eff. day	1.6 fb^{-1}
$\int L\ dt$/eff. year	600 fb^{-1}(upper limit)
C.M. ENERGY	22.3 GeV

TESLA-N ANSATZ FOR EFFICIENCIES:

$$\varepsilon_{lumi} = \varepsilon_{up-time} \cdot \varepsilon_{exp} = 0.33 \cdot 0.75 = 0.25$$

CONSERVATIVE ASSUMPTIONS:

- ☐ ONLY THE TIME RESOLUTION OF COMPASS CAN BE REACHED (2 ns)
- ☐ ONLY HALF OF THE MAXIMUM CURRENT IS USED TO KEEP THE MULTIPLE EVENT FRACTION SMALL

$\Rightarrow$ 100 fb^{-1} PER YEAR FOR PHYSICS

LUMINOSITY (II)

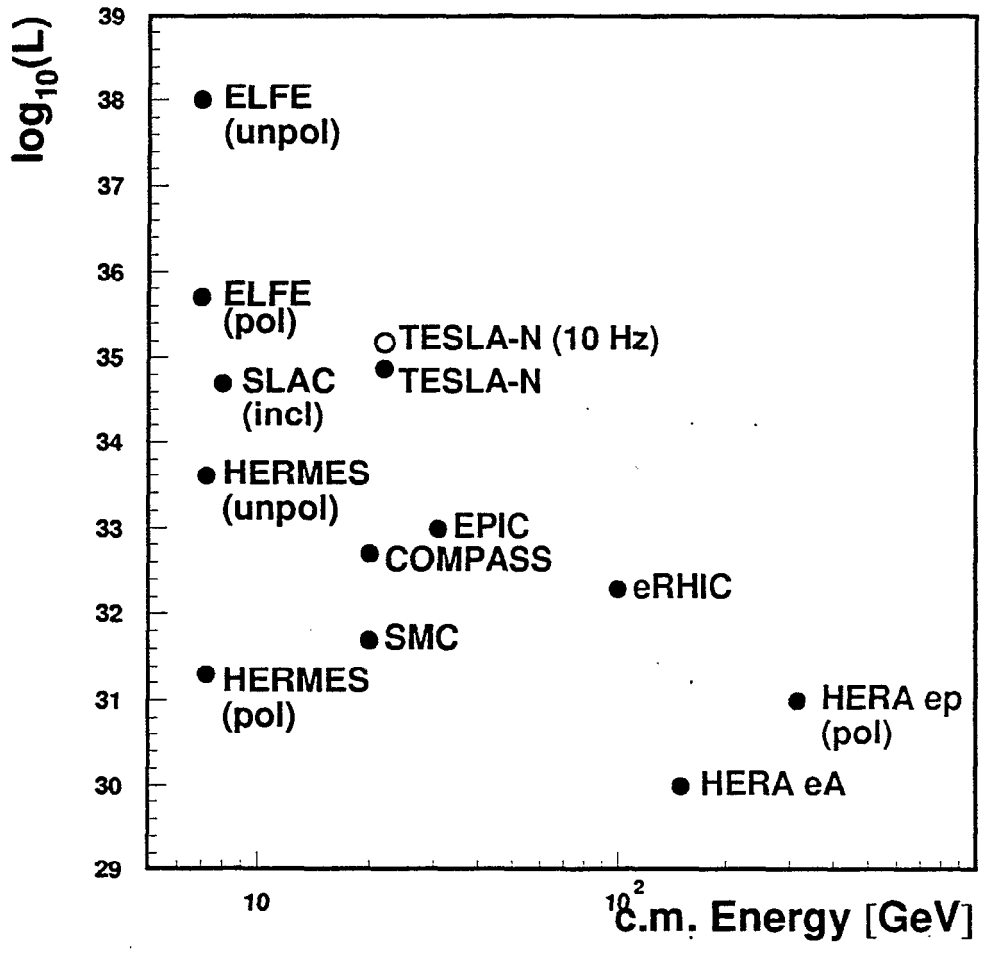

THE EFFECTIVE POLARIZED LUMINOSITY FOR A SOLID-STATE FIXED-TARGET EXPERIMENT IS A FACTOR OF ABOUT 25 LOWER THAN FOR POLARIZED ep-COLLIDERS.

Semi-Inclusive Deep Inelastic Scattering

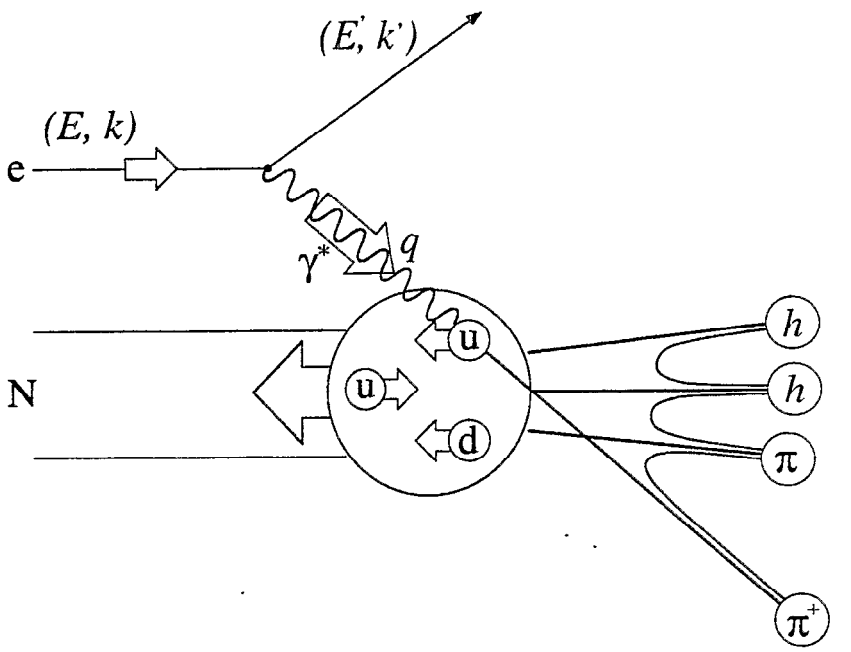

q	VIRTUAL PHOTON 4-MOMENTUM $q = k - k'$
ν	VIRTUAL PHOTON ENERGY $\nu = E - E'$
Q^2 W^2	MOMENTUM TRANSFER $Q^2 = -q^2 \stackrel{lab}{=} 4EE' \sin^2 \frac{\vartheta}{2}$ HADRONIC SYSTEM INV. MASS $W^2 = p'^2 \stackrel{lab}{=} M^2 + 2M\nu - Q^2$
x	BJORKEN-X $x = \frac{Q^2}{2p\cdot q} \stackrel{lab}{=} \frac{Q^2}{2M\nu}$
z	γ^* ENERGY FRACTION OF OBSERVED HADRON $z = \frac{p\cdot p_h}{p\cdot q} \stackrel{lab}{=} \frac{E_h}{\nu}$

Quark Transversity from semi-inclusive Pions (I)

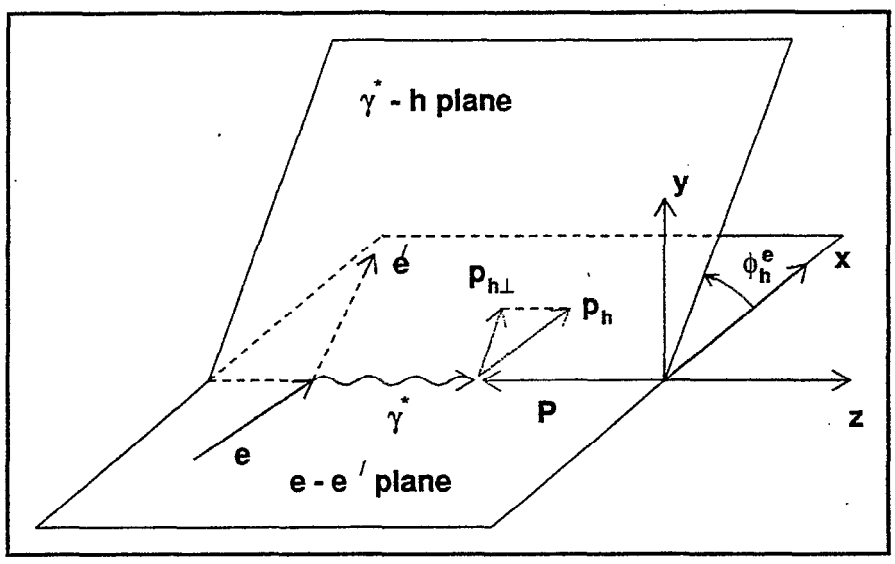

MEASURE WEIGHTED ASYMMETRIES:

$$A_T(x, Q^2, z) \equiv$$

$$\frac{\int d\phi^e \int d^2P_{h\perp} \frac{|P_{h\perp}|}{zM_h} \sin(\phi_s^e + \phi_h^e) \left(d\sigma^\uparrow - d\sigma^\downarrow\right)}{\int d\phi^e \int d^2P_{h\perp} (d\sigma^\uparrow + d\sigma^\downarrow)}$$

WITH FACTORIZATION (VALID FOR TESLA-N):

$$A_T(x, Q^2, z) =$$

$$P_T \cdot D_{nn} \cdot \frac{\sum_q e_q^2 \; \delta q(x, Q^2) \; H_1^{\perp(1)q}(z)}{\sum_q e_q^2 \; q(x, Q^2) \; D_1^q(z)}$$

Quark Transversity from semi-inclusive Pions (II)

DEFINE PURITIES:

$$P_q^h(x, Q^2, z) = \frac{e_q^2 \; q(x) \; D_1^q(z)}{\sum_q e_q^2 \; q(x) \; D_1^q(z)}$$

ASSUME FLAVOR-INDEPENDENT POLARIZED FRAGMENTATION FUNCTION $H_1^{\perp(1)}(z)$:

$$\frac{1}{P_T \cdot D_{nn}} \cdot A_p{}^{\pi^+} = \frac{\delta u(x, Q^2)}{u(x, Q^2)} \cdot \frac{H_1^{\perp(1)}(z)}{D_1(z)} \cdot P_{u(p)}^{\pi^+} + \frac{\delta \bar{d}(x, Q^2)}{\bar{d}(x, Q^2)} \cdot \frac{H_1^{\perp(1)}(z)}{D_1(z)} \cdot P_{\bar{d}(p)}^{\pi^+}$$

RESOLVE NORMALIZATION AMBIGUITY:
$\delta q = \Delta q$ at $x \simeq 0.25$, low Q^2

$4 \cdot N_{(x,Q^2)} \cdot N_z$ MEASUREMENTS $(A_{p,d}^{\pi^+(\pi^-)})$
$4 \cdot N_{(x,Q^2)} + N_z$ UNKNOWN PARAMETER
$(\delta u, \delta d, \delta \bar{u}, \delta \bar{d}(x, Q^2), \; H_1^{\perp(1)}(z)/D_1(z))$
$\Rightarrow$ OVERCONSTRAINED SYSTEM OF COUPLED EQUATIONS.

IF KAON ASYMMETRIES ARE MEASURED IN ADDITION, THE DISTRIBUTIONS $\delta s(x, Q^2)$ AND $\delta \bar{s}(x, Q^2)$ CAN BE INCLUDED AS WELL.

Quark Transversity from semi-inclusive Pions (III)

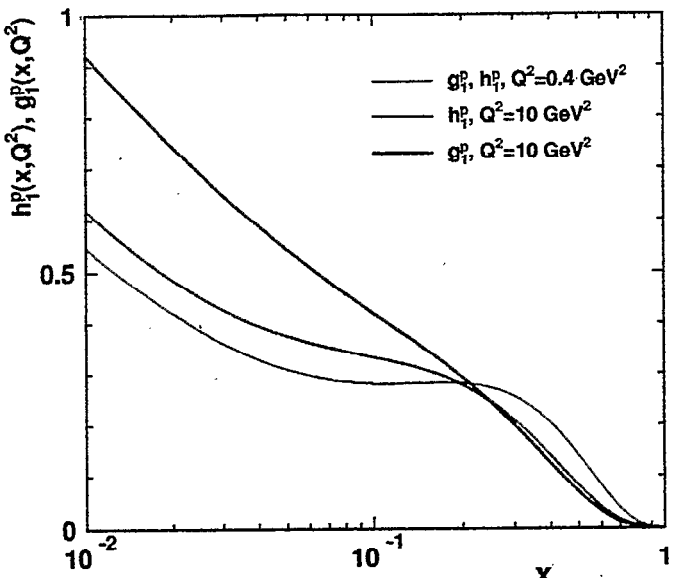

LO TRANSVERSITY AND HELICITY DISTRIBUTION AT $Q^2 = 0.4$ GeV^2 (SOLID), AND BOTH EVOLVED TO $Q^2 = 10$ GeV^2.

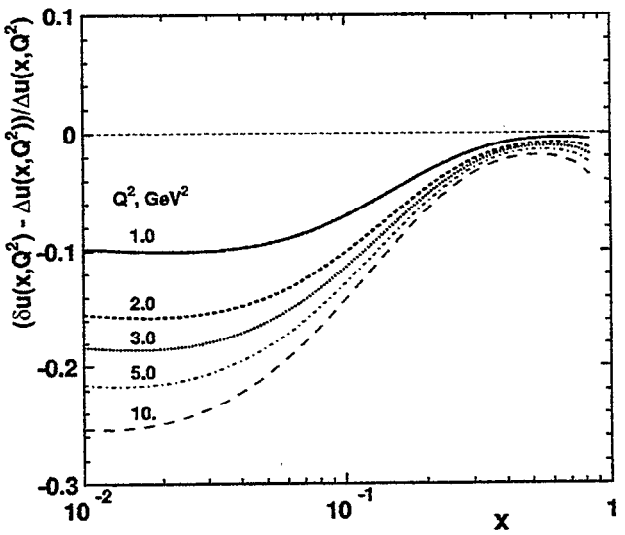

RELATIVE DIFFERENCE BETWEEN U-QUARK TRANSVERSITY AND HELICITY DISTRIBUTION VS. x AND Q^2.

QUARK TRANSVERSITY FROM SEMI-INCLUSIVE PIONS (IV)

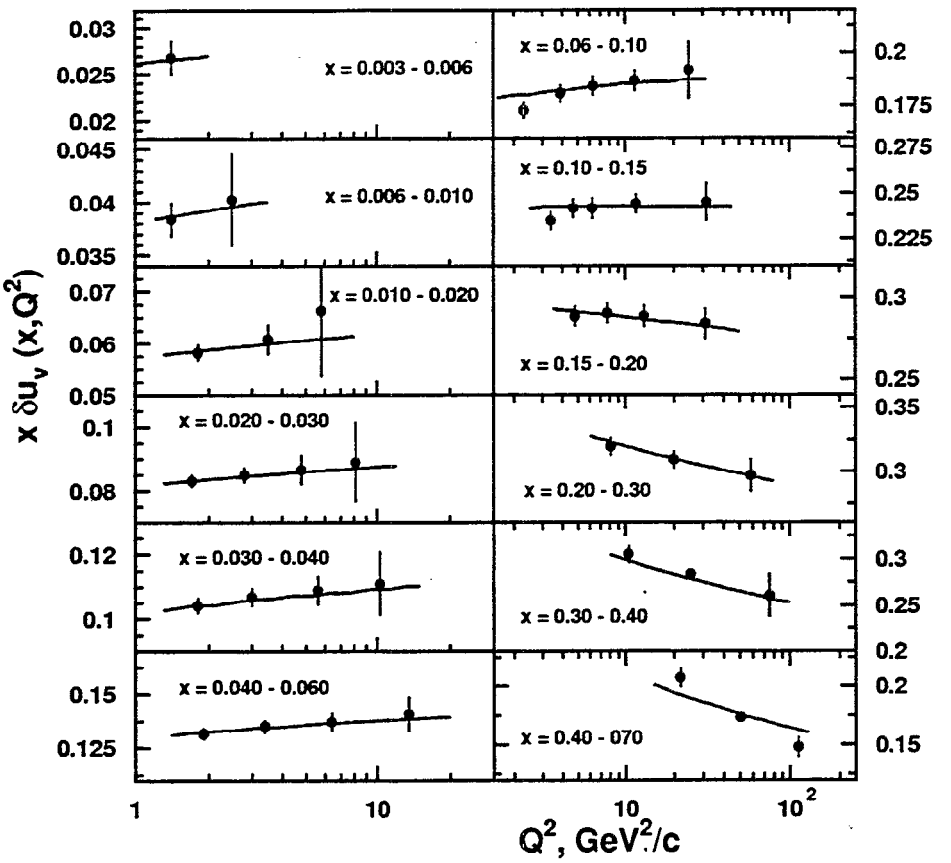

PROJECTION FOR THE VALENCE u-QUARK TRANSVERSITY DISTRIBUTION BASED ON 100 fb^{-1} AND A MINIMUM DETECTOR ACCEPTANCE OF 5 mrad.

TENSOR CHARGE / TRANSVERSE SPIN OF THE NUCLEON: ('ALL-VALENCE OBJECT')

$$\delta\Sigma(Q^2) = \sum_q \int_0^1 dx(\delta q(x, Q^2) - \delta\bar{q}(x, Q^2))$$

PROJECTED ACCURACIES AT $Q^2 = 1$ GeV^2:

$$\delta u = 0.88 \pm 0.01, \; \delta d = -0.32 \pm 0.02$$

Quark Transversity from Two-Meson Correlations (I)

THE REACTION

$$ep^{\uparrow} \to e'\pi^+\pi^- X$$

OFFERS AN ALTERNATIVE POSSIBILITY TO MEASURE THE QUARK TRANSVERSITY.

THE INTERFERENCE EFFECT BETWEEN THE S- AND P-WAVES OF THE TWO-MESON SYSTEM ALLOWS THE QUARK'S POLARIZATION TO BE CARRIED THROUGH $\vec{k}_+ \times \vec{k}_- \cdot \vec{S}_\perp$ [Jaffe et al., 1998].

PROTON/DEUTERON TARGET:

$$\begin{aligned} \mathcal{A}^p &\sim (\delta u_v(x) - \tfrac{1}{4}\delta d_v(x)) \cdot \delta\hat{q}_I(z) \\ \mathcal{A}^d &\sim (\delta u_v(x) + \delta d_v(x)) \cdot \delta\hat{q}_I(z) \end{aligned}$$

THE UNKNOWN CHIRALLY ODD INTERFERENCE FRAGMENTATION FUNCTION $\delta\hat{q}_I(z)$ CAN IN PRINCIPLE BE MEASURED IN

$$e^+e^- \to (\pi^+\pi^- X)(\pi^+\pi^- X)$$

NOTHING HAS BEEN PUBLISHED YET.

Quark Transversity from Two-Meson Correlations (II)

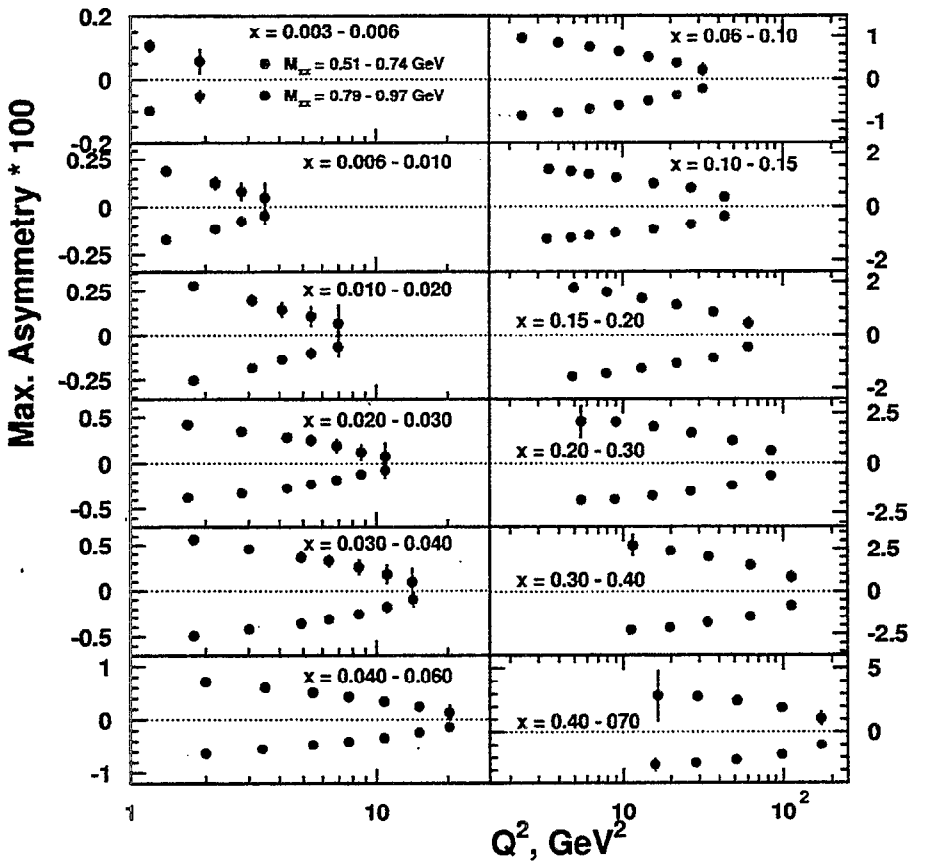

MAXIMUM ASYMMETRY FOR THE TWO-PION SYSTEM AS A FUNCTION OF x AND Q^2 AT TESLA-N WITH AN INTEGRATED LUMINOSITY OF 100 fb^{-1}. RESULTS ARE SHOWN SEPARATELY FOR BOTH TWO-PION MASS REGIONS.

Polarized Gluon Distribution (I)

Use pairs of high-p_T hadrons to isolate the photon gluon fusion process (PGF). The main background is due to QCD-Compton (QCDC).

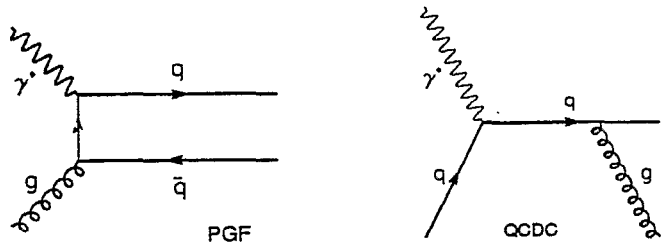

Measure the cross section asymmetry

$$A_{\parallel} = \frac{N^{\uparrow\downarrow}_{h^+h^-} L^{\uparrow\uparrow} - N^{\uparrow\uparrow}_{h^+h^-} L^{\uparrow\downarrow}}{N^{\uparrow\downarrow}_{h^+h^-} L^{\uparrow\uparrow}_P + N^{\uparrow\uparrow}_{h^+h^-} L^{\uparrow\downarrow}_P}$$

$$\approx \left(\hat{a}_{\mathrm{PGF}} \frac{\Delta G}{G} f_{\mathrm{PGF}} + \hat{a}_{\mathrm{QCDC}} \frac{\Delta q}{q} f_{\mathrm{QCDC}} \right) D$$

$\hat{a}_{\mathrm{PGF}} = -1 \qquad \hat{a}_{\mathrm{QCDC}} \approx 0.5$ (hard scattering asym.)

HERMES result 1996/97 data [PRL 84 (2000) 2584] (does not include systematic errors due to PYTHIA MC)

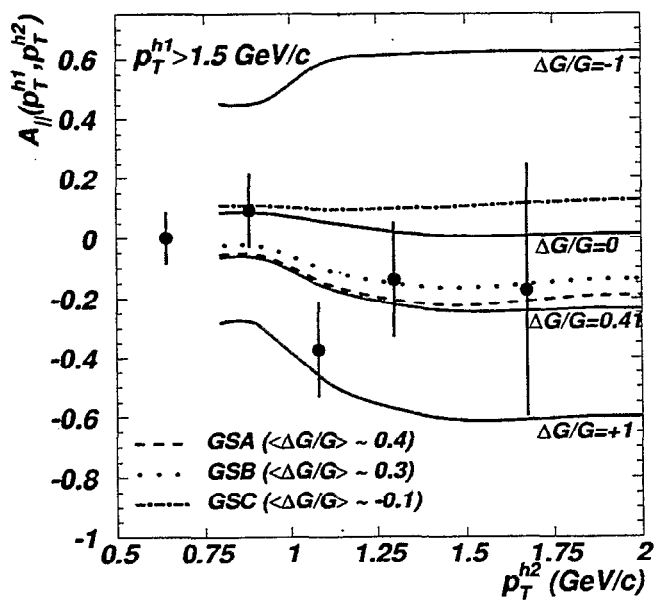

POLARIZED GLUON DISTRIBUTION(II)

TESLA-N PROJECTIONS FOR 100 fb^{-1}:

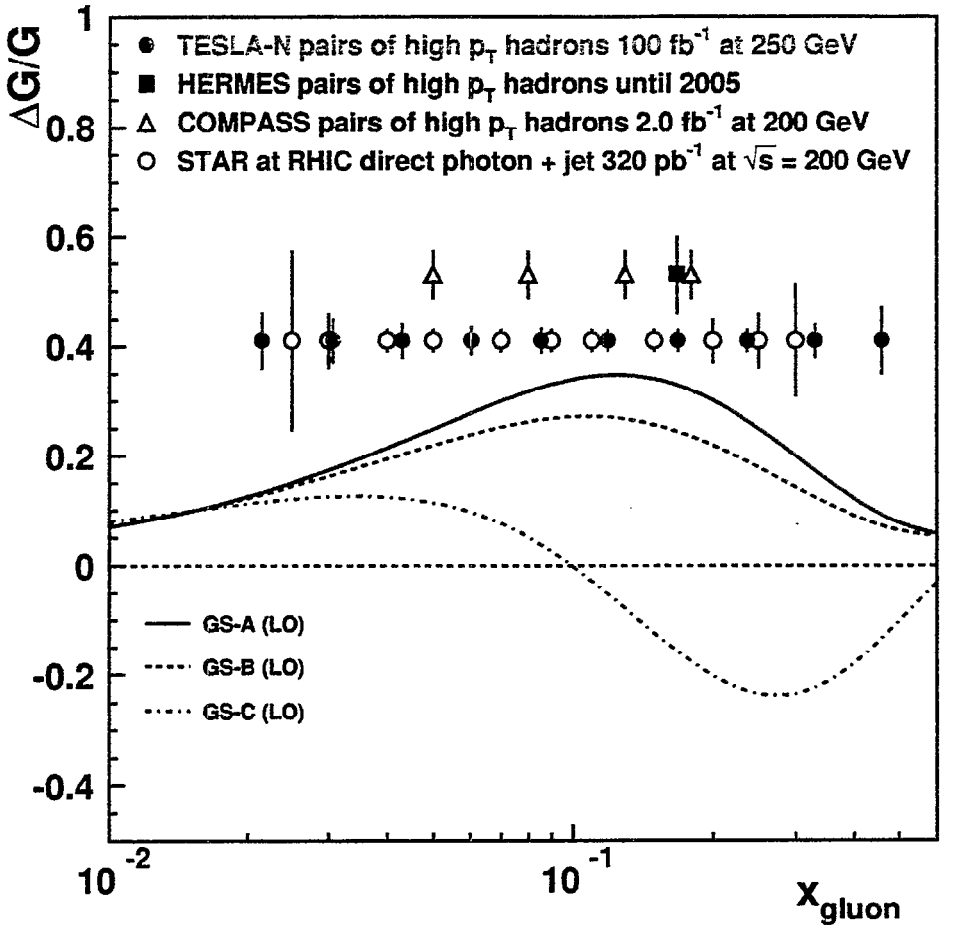

PROJECTED STATISTICAL ACCURACIES FOR THE DIRECT DETERMINATION OF $\Delta G(x)/G(x)$.

- ☐ VERY GOOD SENSITIVITY OVER LARGE x_{gluon} RANGE
- ☐ SYSTEMATIC EFFECTS UNDER STUDY

POLARIZED GLUON DISTRIB. (III)

QCD IMPROVED QUARK PARTON MODEL:

$$g_1^p = \frac{1}{2}\left(\frac{1}{n_f}\sum_{i=1}^{n_f} e_i^2\right)\left\{\delta C_{NS}\otimes\Delta q^{NS} + \delta C_S\otimes\Delta\Sigma + \delta C_G\otimes\Delta G\right\}$$

$\Rightarrow$ PARAMETRIC FORM OF $\Delta G(x)$
IS INDIRECTLY DETERMINED FROM
QCD NLO FITS TO $g_1(x, Q^2)$

$\Rightarrow$ THE FIT YIELDS $\Delta G(Q_0^2)$:
GLUON CONTRIBUTION TO NUCLEON SPIN:

	$\Delta G(Q_0^2)$
EXISTING DATA	0.43 ± 0.21
PLUS 100 fb^{-1} TESLA-N(p)	± 0.06
PLUS 100 fb^{-1} TESLA-N(d)	± 0.04

POLARIZED GLUON DISTRIB. (IV)

INCLUSIVE MEASUREMENT:
MAP OUT $g_1^p(x, Q^2)$ WITH HIGH PRECISION

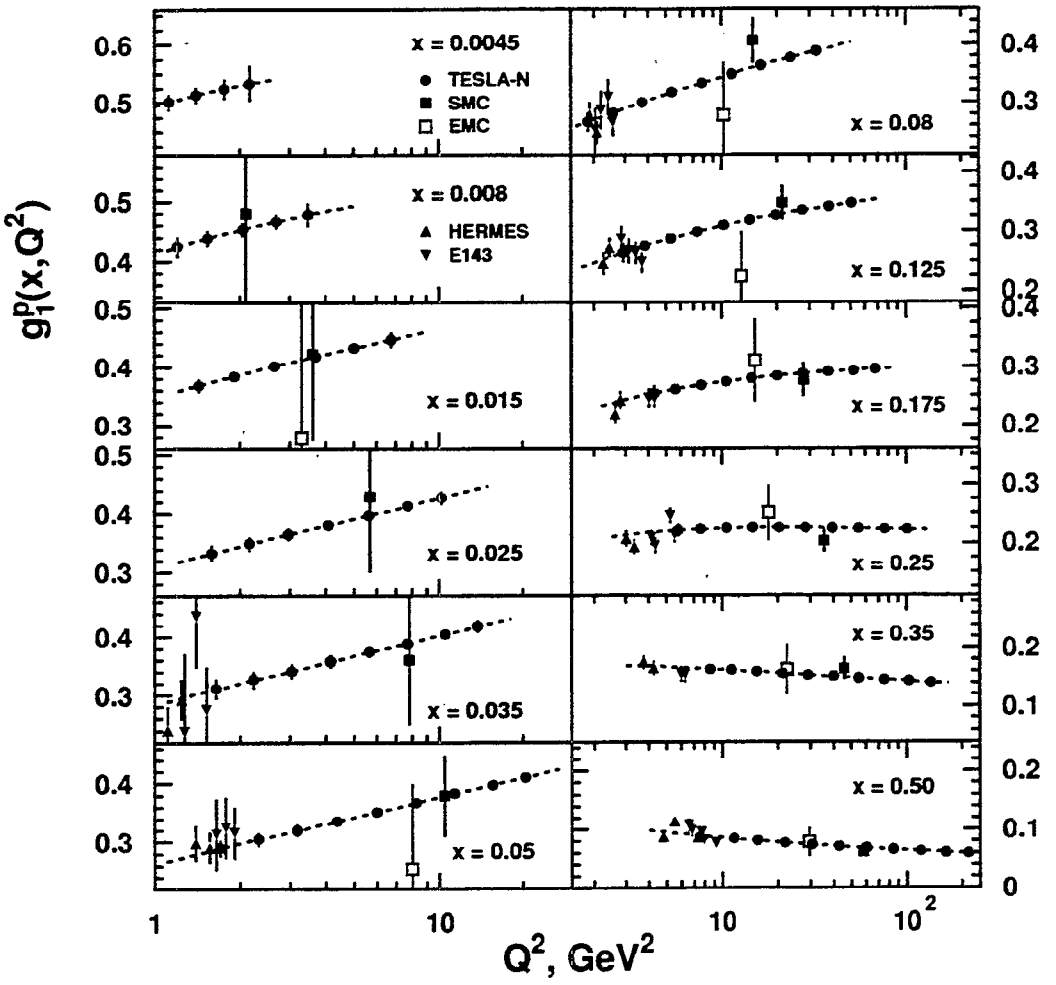

PROJECTED STATISTICAL ACCURACY FOR A MEASUREMENT OF $g_1^p(x, Q^2)$ AT TESLA-N, BASED ON A LUMINOSITY OF 100 fb^{-1} AND A MINIMUM DETECTOR ACCEPTANCE OF 5 mrad.

Further Physics Topics

- ☐ flavour separation of quark helicity distributions: $\Delta u_v(x,Q^2), \Delta d_v(x,Q^2)$, $\Delta\bar{u}(x,Q^2), \Delta\bar{d}(x,Q^2), \Delta s(x,Q^2)$
- ☐ measure $g_2(x,Q^2)$ down to x=0.005
- ☐ fragmentation functions (as input for B-factories and LHC)
- ☐ deeply virtual Compton scattering (DVCS); at lower beam energy
- ☐ unpolarized gluon distribution function $G(x)$ at high x
- ☐ specific deuteron structure functions $b_{1,2}(x,Q^2)$ and $\Delta(x,Q^2)$
- ☐ nuclear effects in eA scattering
- ☐ real photon scattering from nucleons and nuclei

for these topics TESLA-N projections have not been worked out yet

POLARIZED TARGET

- ☐ ^{4}He EVAPORATOR CRYOSTAT GUARANTEES TEMPERATURE OF 1 K FOR A HEAT LOAD OF 1 W

  ⇒ SUFFICIENT POLARIZATION ONLY IN A HIGH MAGNETIC FIELD OF 5 T

- ☐ TARGET POLARIZATION MUST SURVIVE HIGH RADIATION DOSES

  ⇒ DEUTERON TARGET MATERIAL: ^{6}LiD, ($^6\mathrm{Li} \leftrightarrow \alpha + \mathrm{D}$)
  TARGET DILUTION FACTOR 0.44,
  TARGET POLARIZATION 0.3

  ⇒ PROTON TARGET MATERIAL: NH_3,
  TARGET DILUTION FACTOR 0.176,
  TARGET POLARIZATION 0.8

- ☐ AREAL TARGET DENSITY $\sim 1\ \mathrm{g/cm^2}$

POLARIZED ELECTRON BEAM

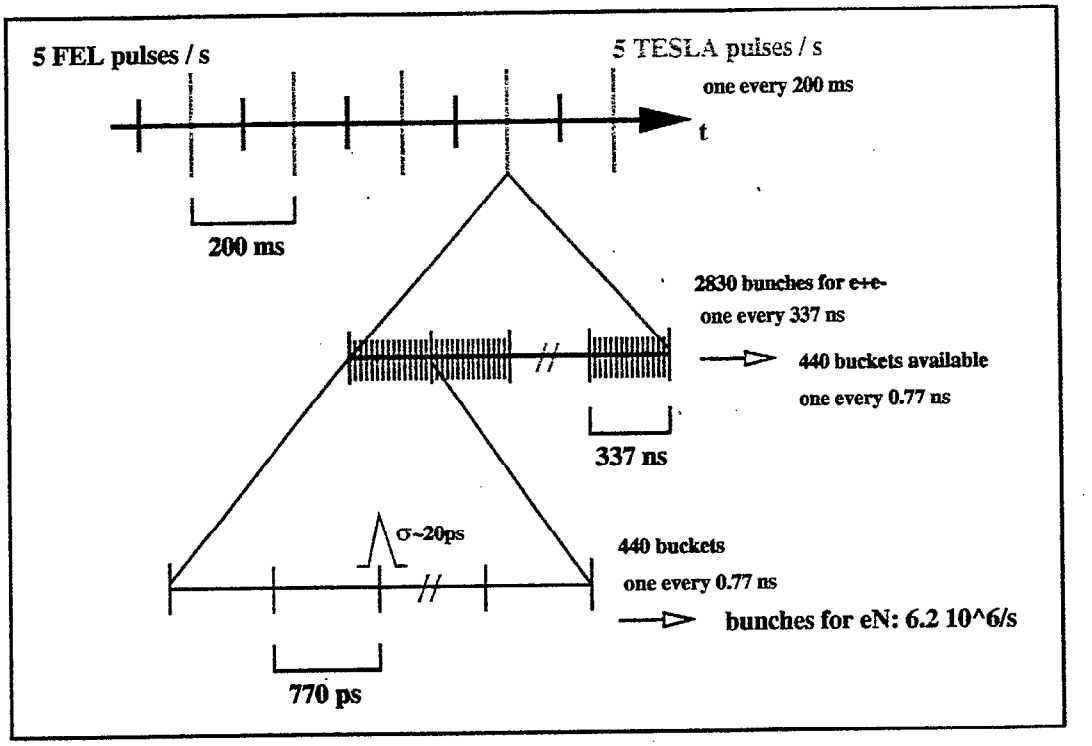

MACHINE FREQUENCY	1.3 GHz ⇒ ONE BUCKET EVERY 0.77 ns
eN-BUNCHES / S	$6.2 \cdot 10^6$
MAX. CURRENT	20 nA
# e^- / eN-BUNCH	20000

SOURCE	strained GaAs (SLAC TYPE)
ENERGY	250 GeV ALSO 25-100 GeV POSSIBLE
POLARIZATION	$\geq$ 90 %

Detector Design Considerations

- ☐ BEAM ENERGY 250 GeV

  ⇒ OVERALL DIMENSIONS SIMILAR TO COMPASS

- ☐ GOOD MOMENTUM RESOLUTION

  ⇒ 3-STAGE SPECTROMETER

  STAGE 1 'HADRON STAGE'
  STAGE 2 'ELECTRON STAGE'
  STAGE 3 'FORWARD SPECTROMETER'

- ☐ HORIZONTAL DIPOLE FIELDS, TO DIRECT 'SHEET OF FLAME' TO THE HALL FLOOR

  ⇒ TWO SYMMETRIC HALVES OF THE SPECTROMETER: LEFT AND RIGHT

- ☐ SEMI-INCLUSIVE MEASUREMENTS:

  ⇒ PID AS IN HERMES:
  RICH, TRD, ECAL
  FOR STAGE 1 AND STAGE 2,
  STAGE 3 ONLY WITH ECAL

Schematic Spectrometer Design

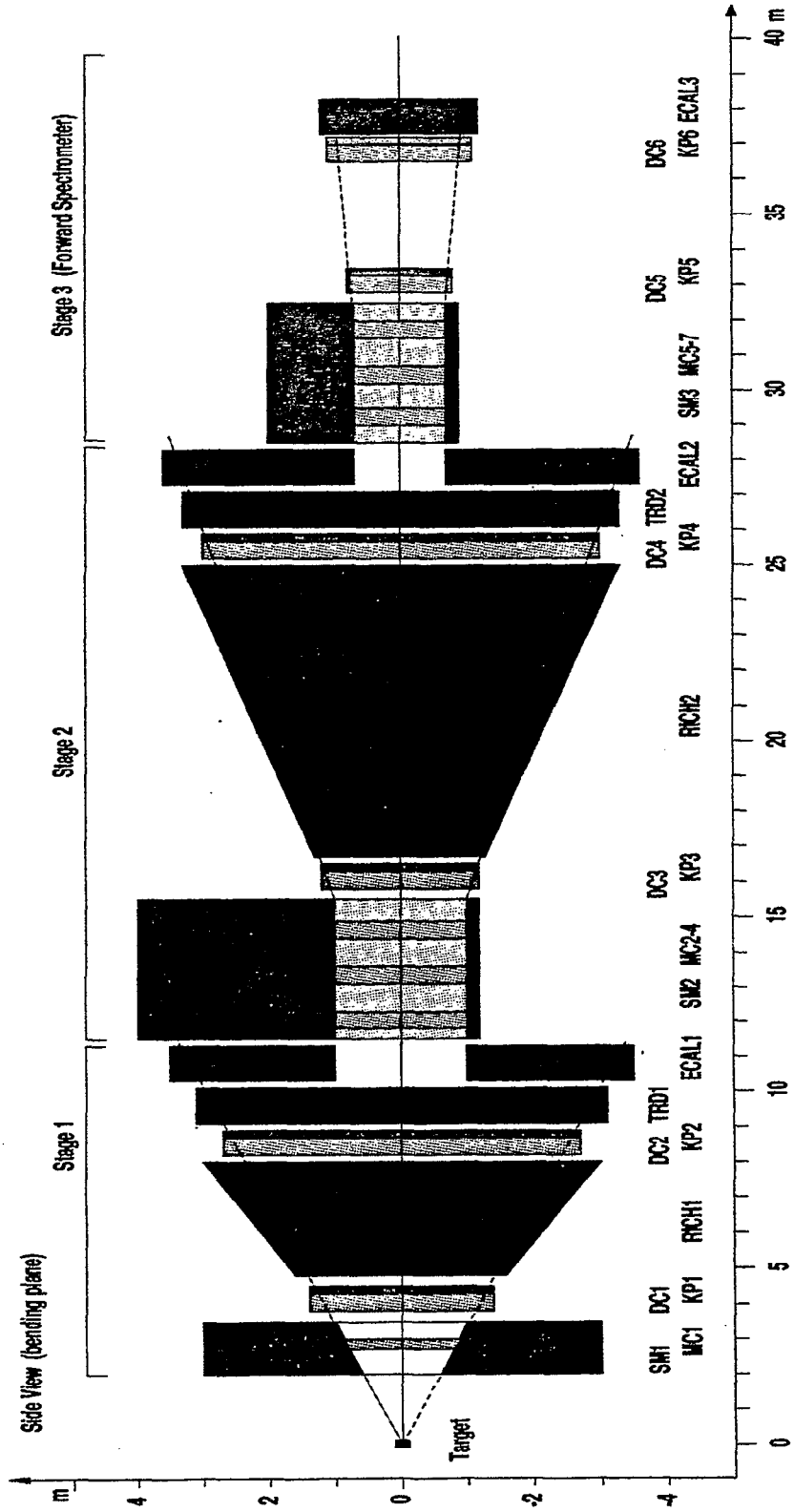

Detector Geometry in TMC

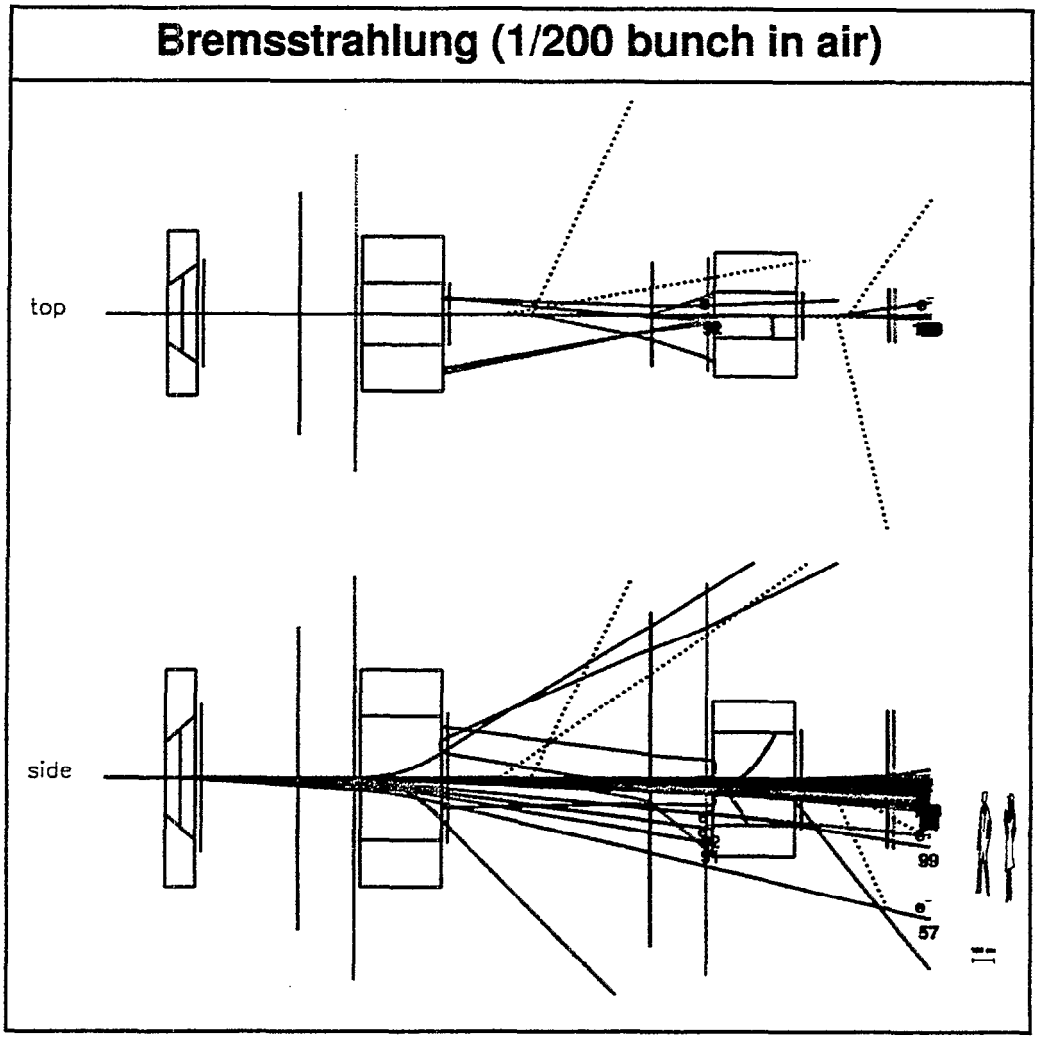

BLACK:	Dipole Magnets
GREEN:	DC 1-6
BLUE:	MC1 inside SM1
MAGENTA:	ECAL 1,2 and 3

Bremsstrahlung Events

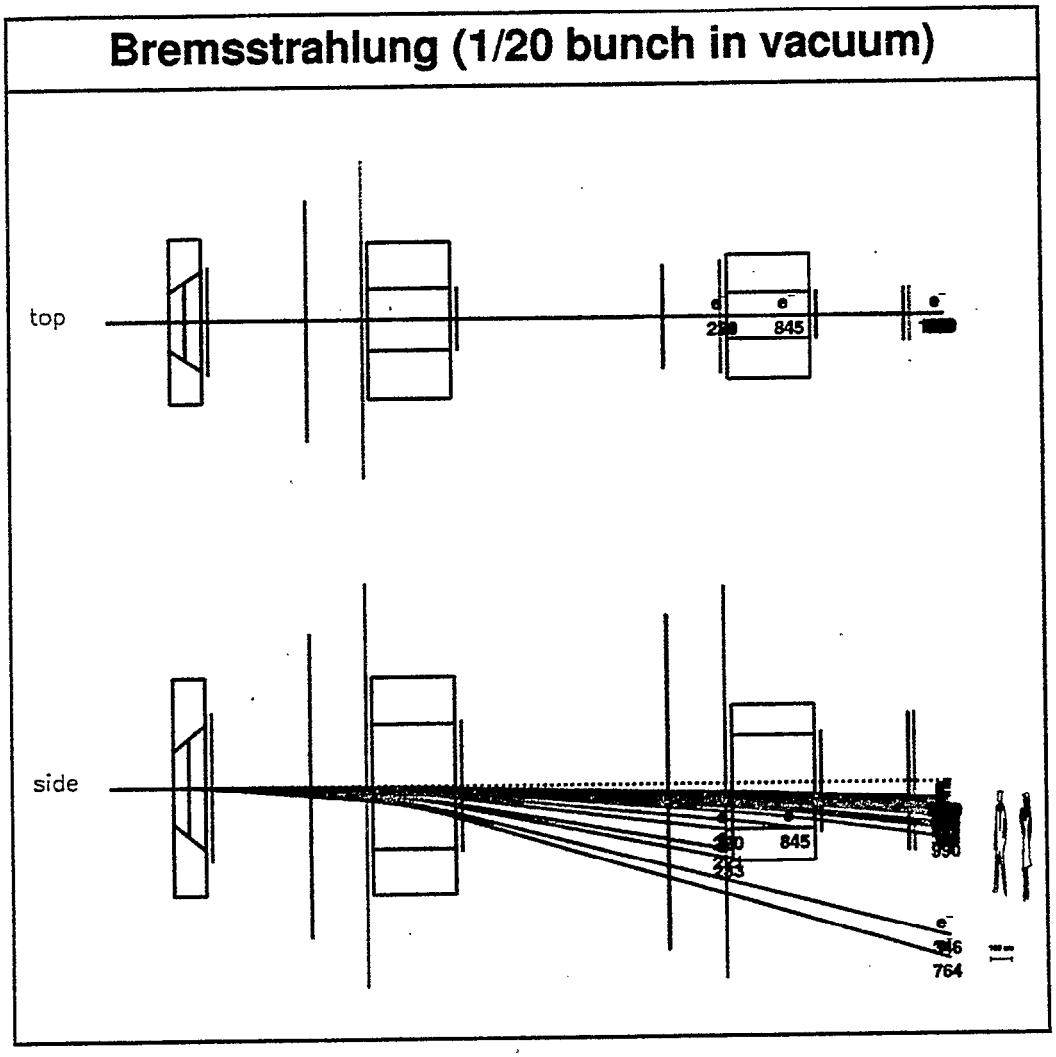

1000 electrons corresponding to 1/20 of one bunch. About 20% produce bremsstrahlung in the target.

Schematic Spectrometer Design

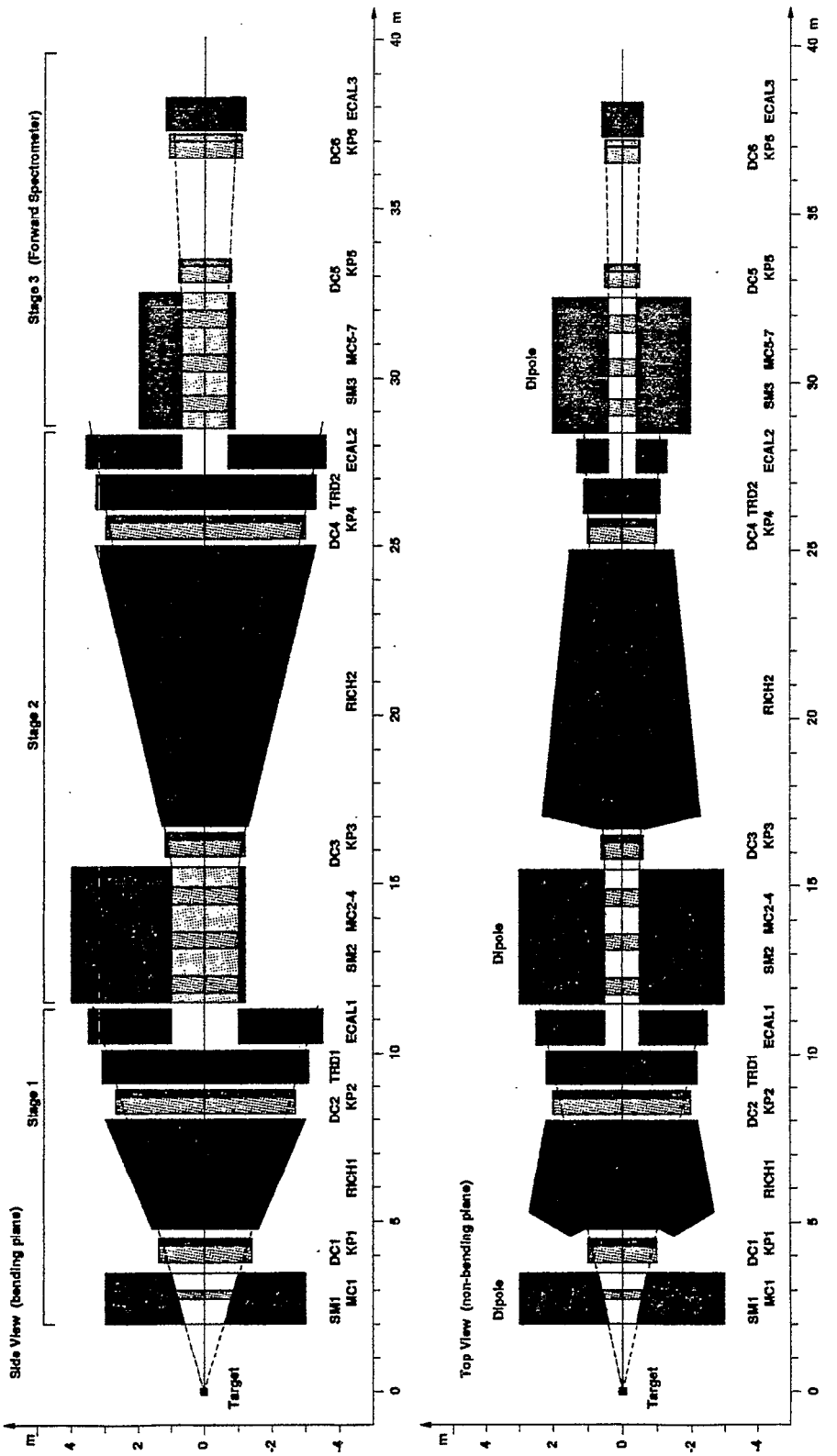

'Sheet of Flame'

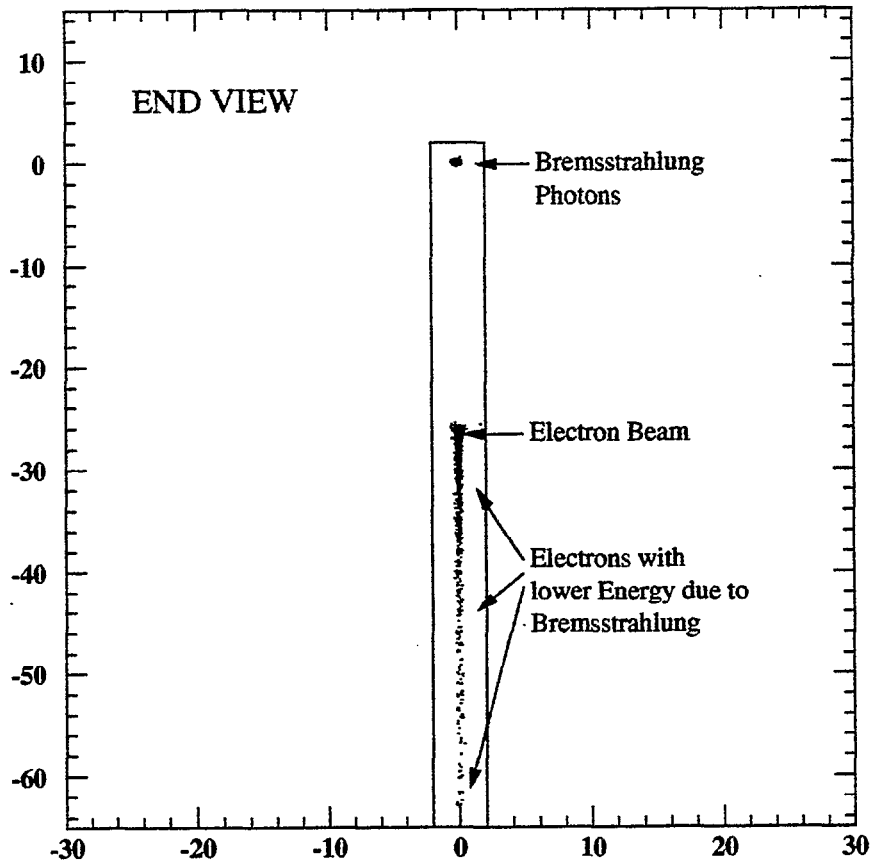

POSITION AT THE END OF THE DETECTOR

GEANT MC SIMULATION WITH 10,000 BREMSSTRAHLUNG EVENTS. WIDTH OF 'SHEET OF FLAME' DOMINATED BY THE BEAM PROFILE; THE ANSATZ FOR THE SIGMA OF THE BEAM IS 1 mm.

$\Rightarrow$ WIDTH OF VACUUM VESSEL CAN BE AS LOW AS $\pm$ 2 cm.

Bremsstrahlung in Magnet SM2

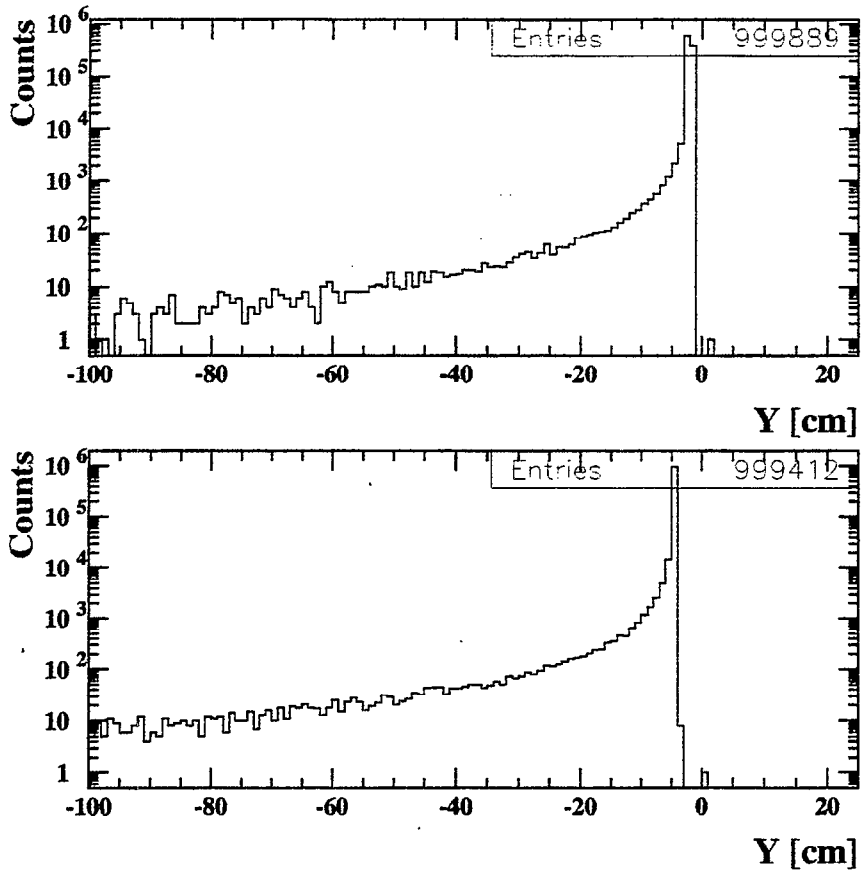

Geant MC Simulation with 1.000.000 Bremsstrahlung events $\simeq$ 40 ns TESLA-N running.

primary electrons at the entrance (Top) and exit (Bottom) of SM2:

Aperture of SM2: $y = \pm$ 1 m

$\rightarrow$ about 600 electrons scatter in SM2 within 40 ns

$\Rightarrow$ SM2 and SM3 will have to be C-Type Magnets.

DIS Event

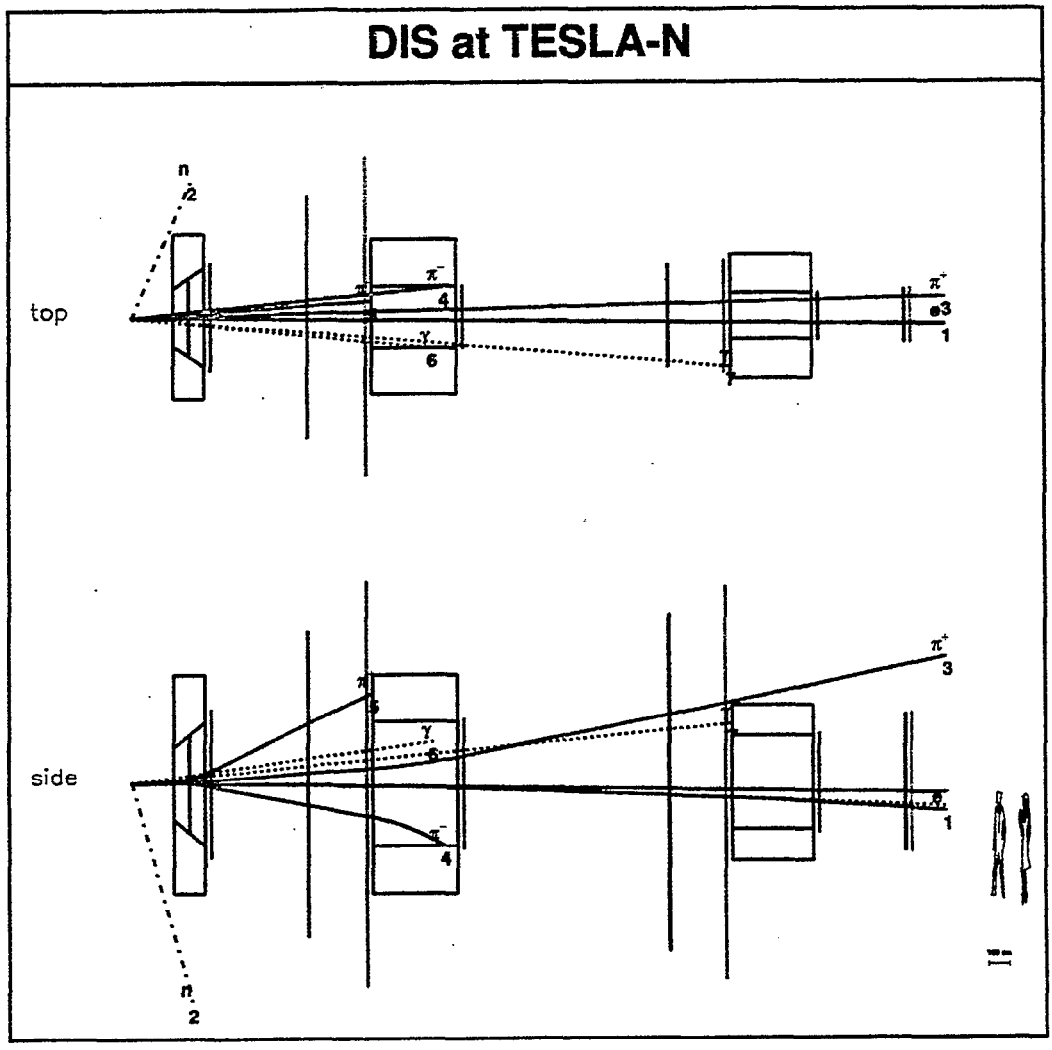

Number of Charged Hadrons per DIS Event with $Q^2 > 1$ GeV^2

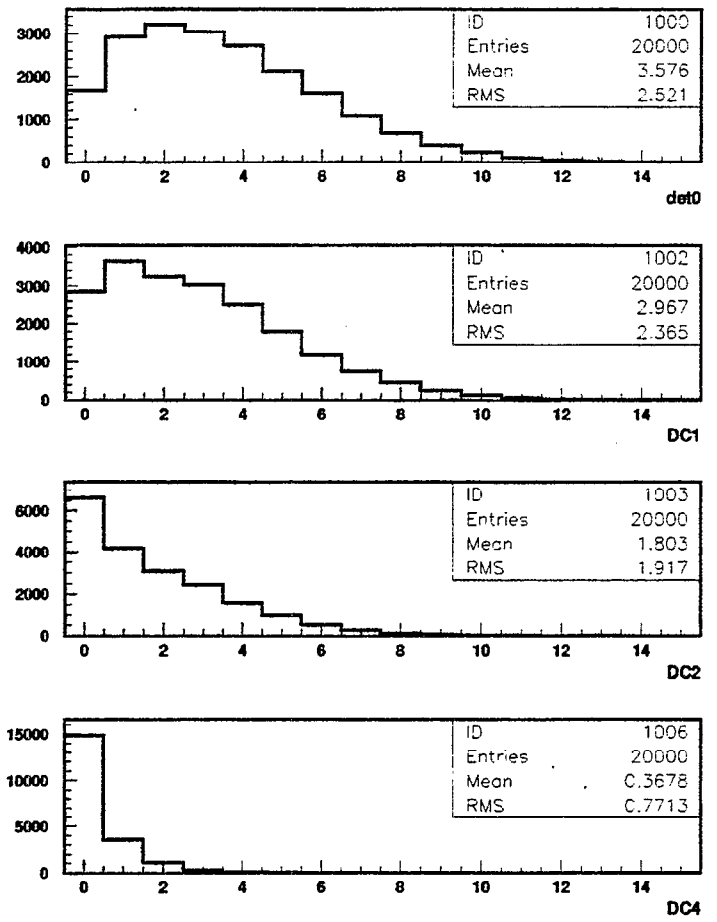

Top: In front of SM1
Second: DC1
Third: DC2 - Full Tracks in Stage 1
Bottom: DC4 - Full Tracks in Stage 2

$\Rightarrow$ 2-4 hadrons per event
(DIS, photoproduction)

Event Rates

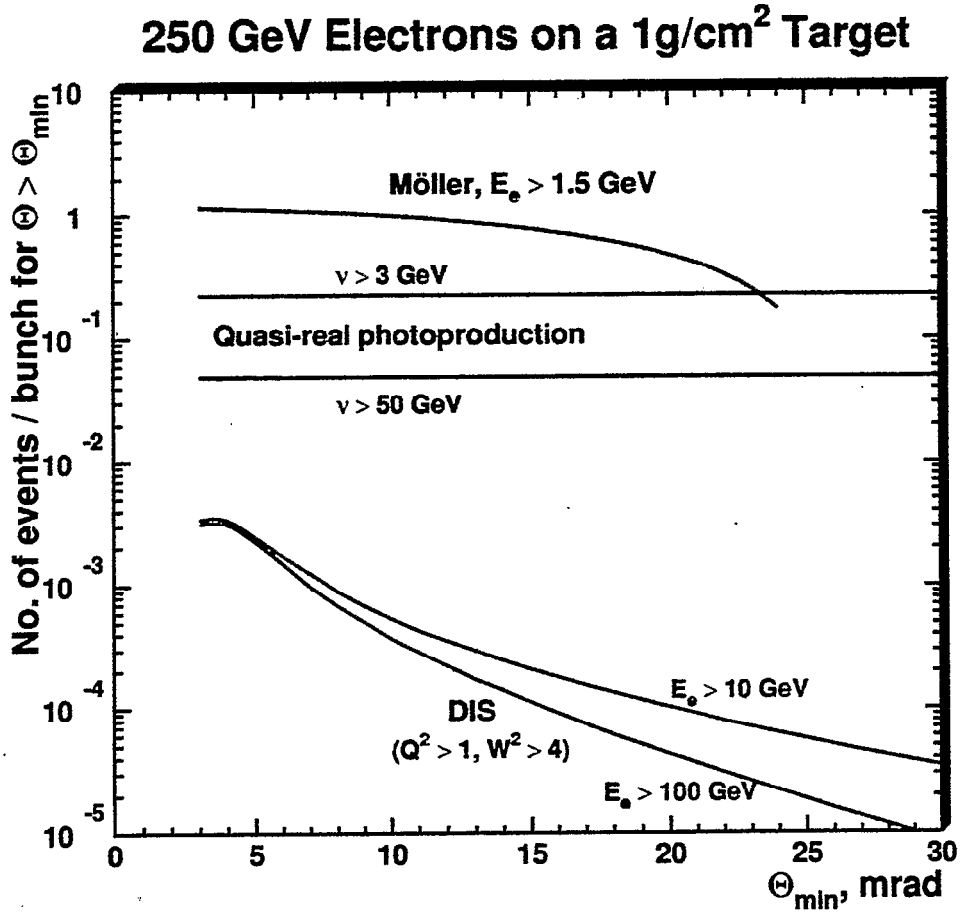

e.g. for $\Theta_{min} = 10$ mrad : $\frac{N_{DIS}(E_e > 10)}{N_{photo}(\nu > 3)} \approx 2.5 \cdot 10^{-3}$

Möller events are kinematically distinguishable from DIS events for $Q^2 > 1$ GeV^2.

A 'Recorded Event'

Assume the integration time for a 'recorded event' is about 150 ns, which is a typical time for drift chambers. Then a recorded event contains roughly 200 bunches with 20,000 electrons each.

⇒ 200 Möller events (electron tracks)

⇒ 40 photoproduction events
(on average 3 charged hadrons)

⇒ 0.2 DIS events

If the bremsstrahlung events can be neglected, because the electrons stay contained in the vacuum vessel, there are still about 320 charged tracks per recorded event.

⇒ The complexity of the experiment lies between HERMES (few tracks) and heavy-ion exp.'s (thousands of tracks)

Overall Summary & Outlook

- Fixed-target lepton-nucleon scattering exp.'s have initiated a many-decade study of the momentum and spin structure of the nucleon.

- Several generations of experiments have, in over 2 decades of close interaction with theory, revealed more and more pieces of the nucleon structure 'puzzle'.

- Further important impact to theoretical development in the context of the QCD picture of the polarized nucleon is clearly expected to emerge from upcoming results of HERMES@DESY & COMPASS@CERN in the years to come.

- A complementary set of results on the spin structure of the polarized nucleon will be obtained from pp-scattering at RHIC by PHENIX & STAR within this decade.

- The ultimate fixed-target lepton-nucleon scattering experiment may be realized in the next decade, possibly at TESLA. Based upon very high luminosity and variable energy there is good hope to eventually complete the understanding of the angular momentum

HERMES Results on the Spin Structure of the Nucleon

Wolf-Dieter Nowak - DESY Zeuthen
On Behalf Of The HERMES Collaboration

RIKEN Winter School, LECTURE 2
Yuzawa/Japan, Dec. 3, 2000

- Spin Structure Function g_1
- Polarized quark distributions
- Polarized gluon distribution
- Polarized fragmentation function

Published results are based on data taking periods 1995 [neutron target] and 1996-97 [proton target], preliminary results are mainly from 1998-99 [deuterium target].

MOTIVATION (I)

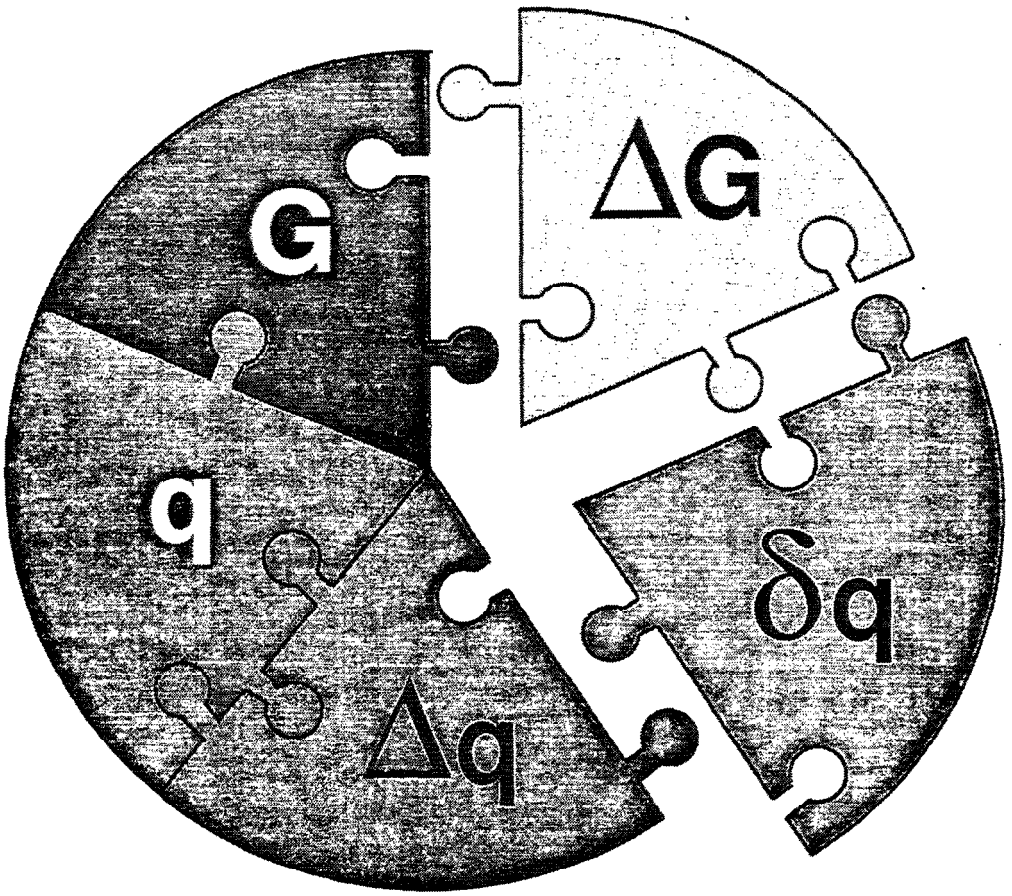

PARTON DISTRIBUTIONS OF THE NUCLEON

AT LEADING TWIST IN PQCD

$q(x, Q^2)$	QUARK NUMBER DENSITY DISTRIBUTION (f_1^q)
$\Delta q(x, Q^2)$	QUARK HELICITY DISTRIBUTION (g_1^q)
$\delta q(x, Q^2)$	QUARK TRANSVERSITY DISTRIBUTION (h_1^q)
$G(x, Q^2)$	GLUON NUMBER DENSITY DISTRIBUTION
$\Delta G(x, Q^2)$	POLARIZED GLUON DISTRIBUTION

$\delta q(x, Q^2)$ AND $\Delta G(x, Q^2)$ PRESENTLY NOT KNOWN !

MOTIVATION (II)

SPIN STRUCTURE OF A *longitudinally* POLARIZED PROTON:

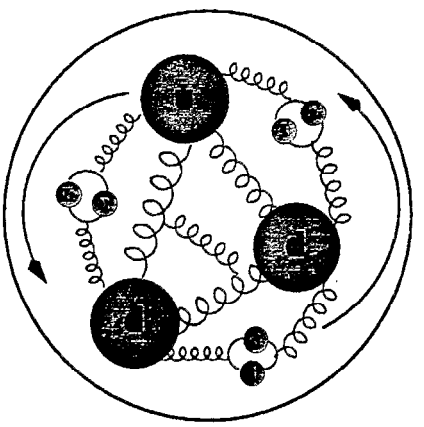

$$S_z = \frac{1}{2} = \frac{1}{2}\Delta\Sigma + \Delta G + L_z$$

$\Delta\Sigma$ EXPECTED TO BE ≈ 0.6 IN NR QPM
BUT WAS FOUND TO BE SMALL IN INCLUSIVE DIS EXPERIMENTS (EMC, SMC, SLAC, HERMES)
$\rightarrow$ SPIN 'CRISIS'

$$\Delta\Sigma = \sum_{i=1}^{n_{\text{flavors}}} (\Delta q_i + \Delta\bar{q}_i) \approx 0.2 \ldots 0.4$$

POSSIBLE CONTRIBUTIONS TO S_z:

- STRANGE SEA POLARIZATION Δs IS NEGATIVE?
- GLUON POLARIZATION ΔG IS POSITIVE?
- ORBITAL ANGULAR MOMENTUM L_z IS POSITIVE?

Polarized DIS in the Quark Parton Model

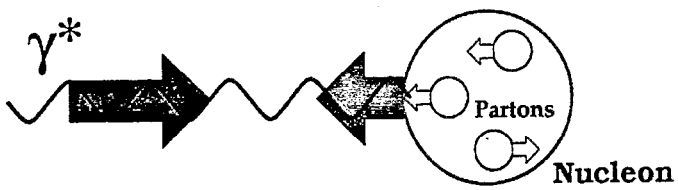

$\sigma_{1/2} \sim q_+(x)$

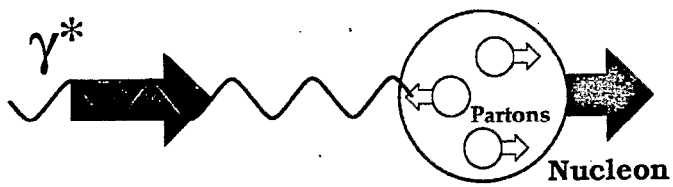

$\sigma_{3/2} \sim q_-(x)$

POLARIZED PHOTON (SPIN 1) CAN ONLY PROBE QUARKS WITH SPIN OPPOSITE TO ITS OWN:

QUARK SPIN PARALLEL TO NUCLEON SPIN:

$$\vec{S}_\gamma + \vec{S}_N = \frac{1}{2} \Longrightarrow \sigma_{\frac{1}{2}} \sim q^+(x)$$

QUARK SPIN OPPOSITE TO NUCLEON SPIN:

$$\vec{S}_\gamma + \vec{S}_N = \frac{3}{2} \Longrightarrow \sigma_{\frac{3}{2}} \sim q^-(x)$$

FLIPPING SPIN OF TARGET $\Rightarrow$ QUARK HELICITY DISTRIBUTIONS:

$$\boxed{\Delta q_f(x) = q_f^+(x) - q_f^-(x)}$$

$$(\ f = u, d, s, \overline{u}, \overline{d}, \overline{s}\ )$$

Asymmetries in Inclusive Polarized DIS

$2xF_1$ measures a weighted average of the quark momentum distributions:

$$F_1(x) = \frac{1}{2}\sum_i e_i^2 \; (q_i^+(x) + q_i^-(x)) = \frac{1}{2}\sum_i e_i^2 \; q_i(x)$$

g_1 measures a weighted average of the quark helicity distributions:

$$g_1(x) = \frac{1}{2}\sum_i e_i^2 \; (q_i^+(x) - q_i^-(x)) = \frac{1}{2}\sum_i e_i^2 \; \Delta q_i(x)$$

Virtual Photon Asymmetries:

$$A_1 = \frac{\sigma_{1/2} - \sigma_{3/2}}{\sigma_{1/2} + \sigma_{3/2}} = \frac{g_1 - \gamma^2 g_2}{F_1} \approx \frac{g_1}{F_1}$$

$$A_2 = \frac{\sigma_{TL}}{\sigma_T} = \frac{\gamma(g_1 + g_2)}{F_1}; \gamma = \frac{2Mx}{\sqrt{Q^2}}$$

Measurable Asymmetries:

$$A_{\parallel} = \frac{\sigma^{\rightleftarrows} - \sigma^{\rightrightarrows}}{\sigma^{\rightleftarrows} + \sigma^{\rightrightarrows}} \qquad A_{\perp} = \frac{\sigma^{\uparrow\rightarrow} - \sigma^{\uparrow\leftarrow}}{\sigma^{\uparrow\rightarrow} + \sigma^{\uparrow\leftarrow}}$$

$$A_{\parallel} = D(A_1 + \eta A_2) \qquad A_{\perp} = d(A_2 + \xi A_1)$$

D,d: Virtual photon depolarization factors

η, ξ: kinematic factors

WHY g_1 AT LOW x_{Bj} AND LOW Q^2 ?

WHY g_1 AT LOW x_{Bj}?

- LOW–x REGION IS IMPORTANT FOR DETERMINING THE QUARK CONTRIBUTION $\Delta\Sigma$ TO THE NUCLEON SPIN (EXTRAPOLATION INTO THE UNMEASURED REGION)

WHY g_1 AT LOW Q^2?

- PROVIDE NEW DATA FOR THE STUDY OF SCALING VIOLATIONS
  $\Longrightarrow$ INDIRECT ACCESS OF ΔG
- ALLOW FURTHER TESTS OF THE pQCD CONCEPT: DOWN TO WHICH Q^2 IS THE CONCEPT VALID?

$$
\begin{aligned}
xg_1(x,Q^2) \quad = \quad & xg_1^{tw-2}(x,Q^2) \\
& + \frac{1}{Q^2} h^{tw-4}(x,Q^2) \\
& + \frac{1}{Q^2}\left(h_{TMC}^{tw-2}(x,Q^2) + h_{TMC}^{tw-3}(x,Q^2) \right) \\
& + \mathcal{O}\left(\frac{1}{Q^4}\right)
\end{aligned}
$$

$\Longrightarrow$ FIELD IN PROGRESS [DIS '99: E.STEIN, NP **B79** (1999) 567]
[J.BLÜMLEIN, A.TKABLADZE, HEP-PH/98124

- UP TO NOW: ANALYSIS OF PROTON TARGET DATA IN THE EXTENDED KINEMATIC RANGE

SYST. UNCERTAINTIES AT LOW x AND Q^2

- EXPERIMENTAL SYSTEMATIC UNCERTAINTIES:

→ BEAM POLAR.: $\Delta_{P_B} = 3.4\ \%$

→ TARGET POLAR.: $\Delta_{P_T} = 4.7\ \%$

→ OTHER SOURCES: $\Delta_{\text{misc}} = 5.5\ \%$

(NORMALIZATION, HADRON CONTAMINATION, CUT STABILITY, Θ–SYSTEMATICS)

- SYSTEMATIC UNCERTAINTIES IN THE ITERATIVE EXTRACTION OF THE BORN ASYMMETRY:

→ RAD. CORR. [POLRAD: J. PHYS. G20(1994)513] + SMEARING CORR.:

$\Delta_{\text{corr}} \approx 5.0\ \%$ (11 % LOWEST x)

→ A_2–PARAMETRIZATION: $A_2 = 0.5 \cdot x/\sqrt{Q^2}$

[BASED ON E-143 DATA: PHYS. REV. D58(1998)112003]

$\Delta_{A_2} \leq 0.5\ \%$

FIXED: F2: ALLM97 [HEP-PH/9712415] WITH LOW-W MOD. (FOR W < 2.2 GeV AND $Q^2 < 0.5$ GeV^2) AND R1990 [PHYS. LETT. B250(1990)193]

⇒ TOTAL FOR LOW–x REGION: 9.4 %

(13.6 % LOWEST x BIN)

---

g_1^p/F_1^p : Comparison to E143 & SMC

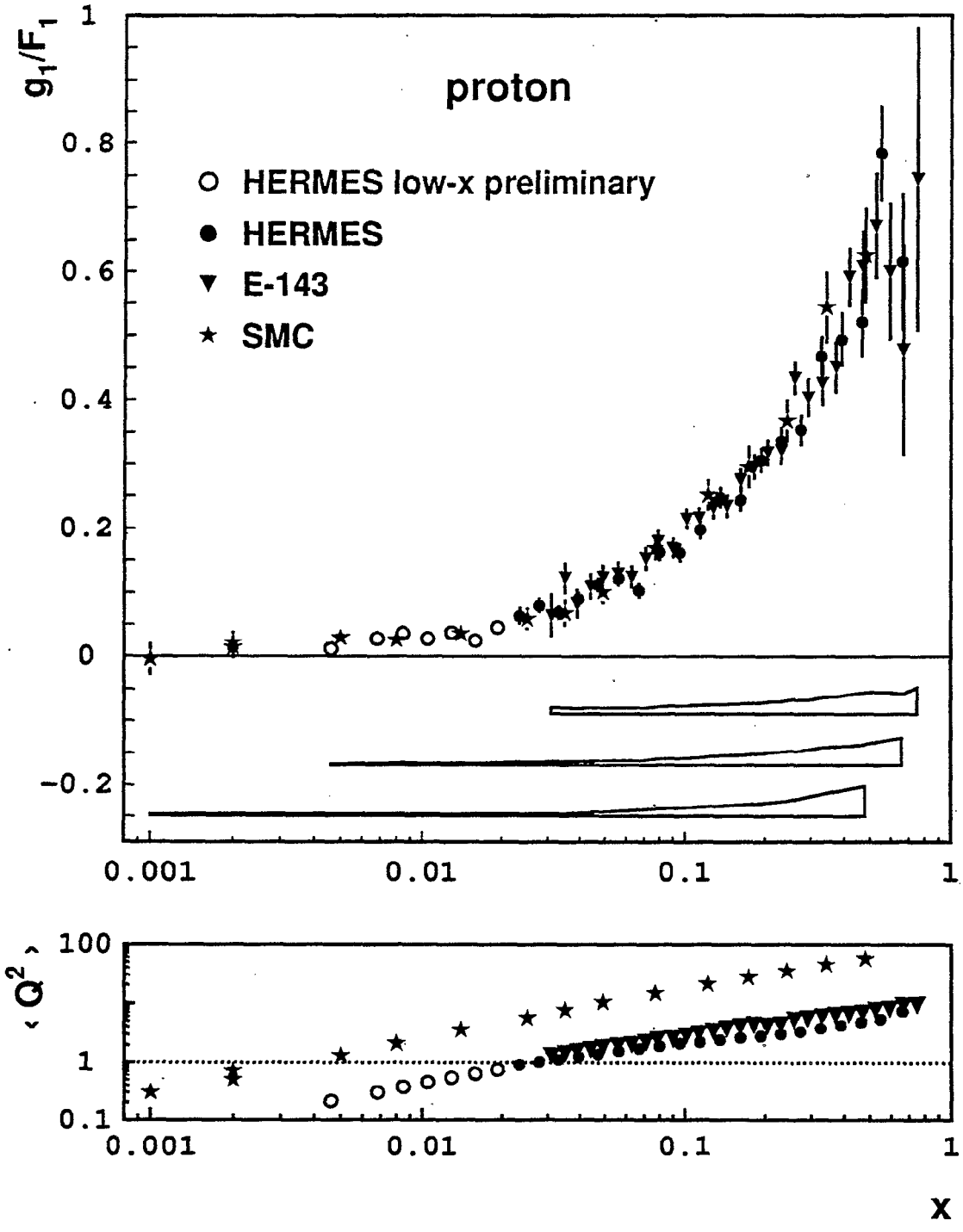

$\Rightarrow$ No statistically significant Q^2 dependence

g_1^{p} VERSUS x AND Q^2

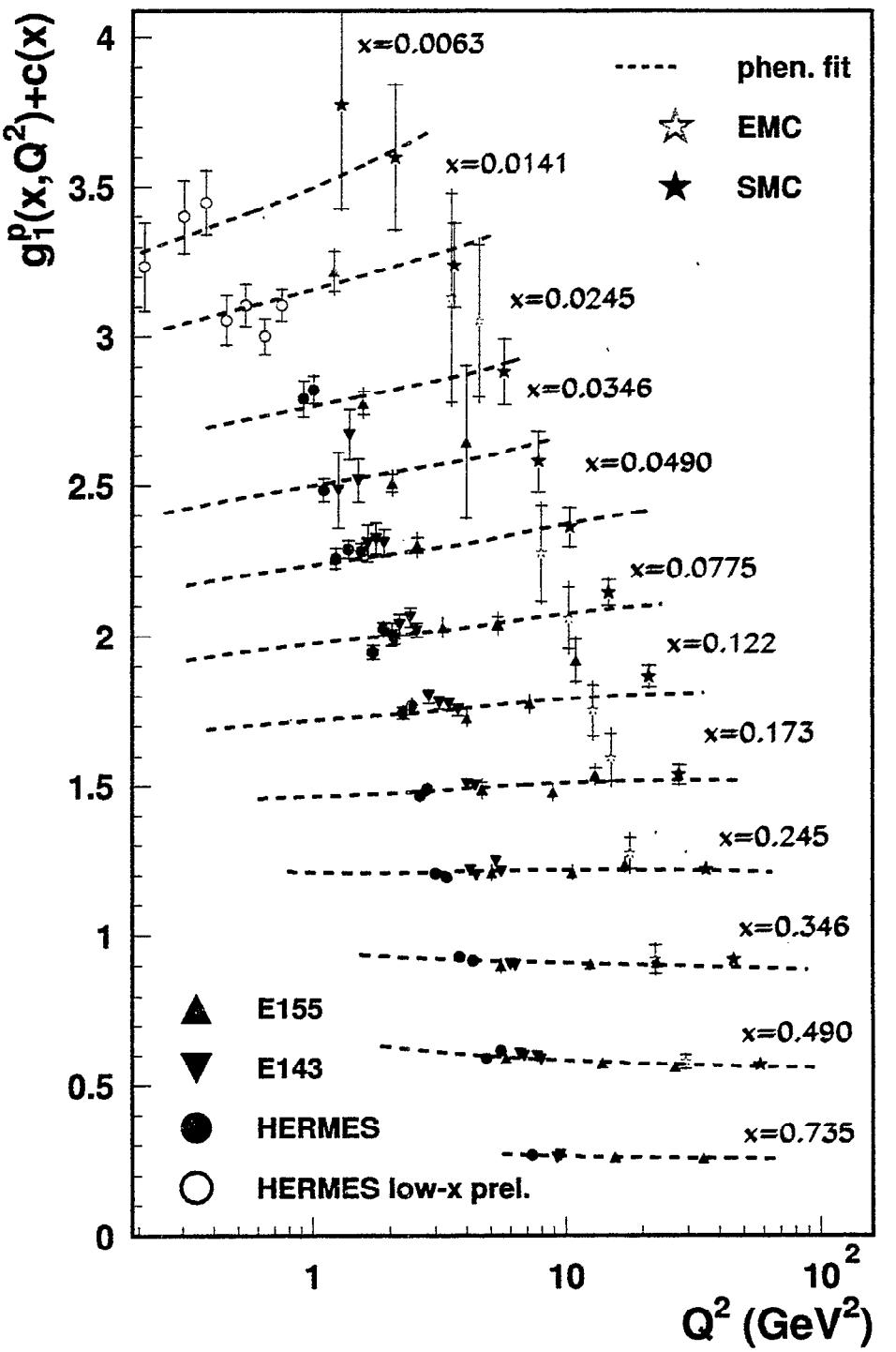

FIT BY E155 USING $Q^2 > 1$ GEV^2 WORLD DATA:

$g_1/F_1 = x^{0.7}(0.817+1.014x-1.489x^2)(1-0.04/Q^2)$ [HEP-PH/0007248].

SCALING VIOLATION IN g_1^p ?

- LOW–x REGION $(x < 0.05)$:

  LARGE STATISTICAL UNCERTAINTIES
  (ALL DATA SETS ARE STATISTICS DOMINATED)

  ONLY LIMITED CONCLUSIONS ON SCALING VIOLATIONS AND ΔG POSSIBLE

- MEDIUM–x REGION $(0.05 \leq x \leq 0.2)$:

  SIGNIFICANT SCALING VIOLATIONS OBSERVED

- LARGE–x REGION $(0.2 \leq x \leq 0.8)$:

  DATA CONSISTENT WITH NO SCALING VIOLATIONS

$\Rightarrow$ MORE PRECISE DATA NEEDED FOR $x < 0.05$ AT BOTH

- LOW Q^2 (HERMES DATA $>$ 1998)
- HIGHER Q^2 (COMPASS)

g_1^d/F_1^d – 1999 HERMES D DATA: COMPARISON WITH WORLD DATA

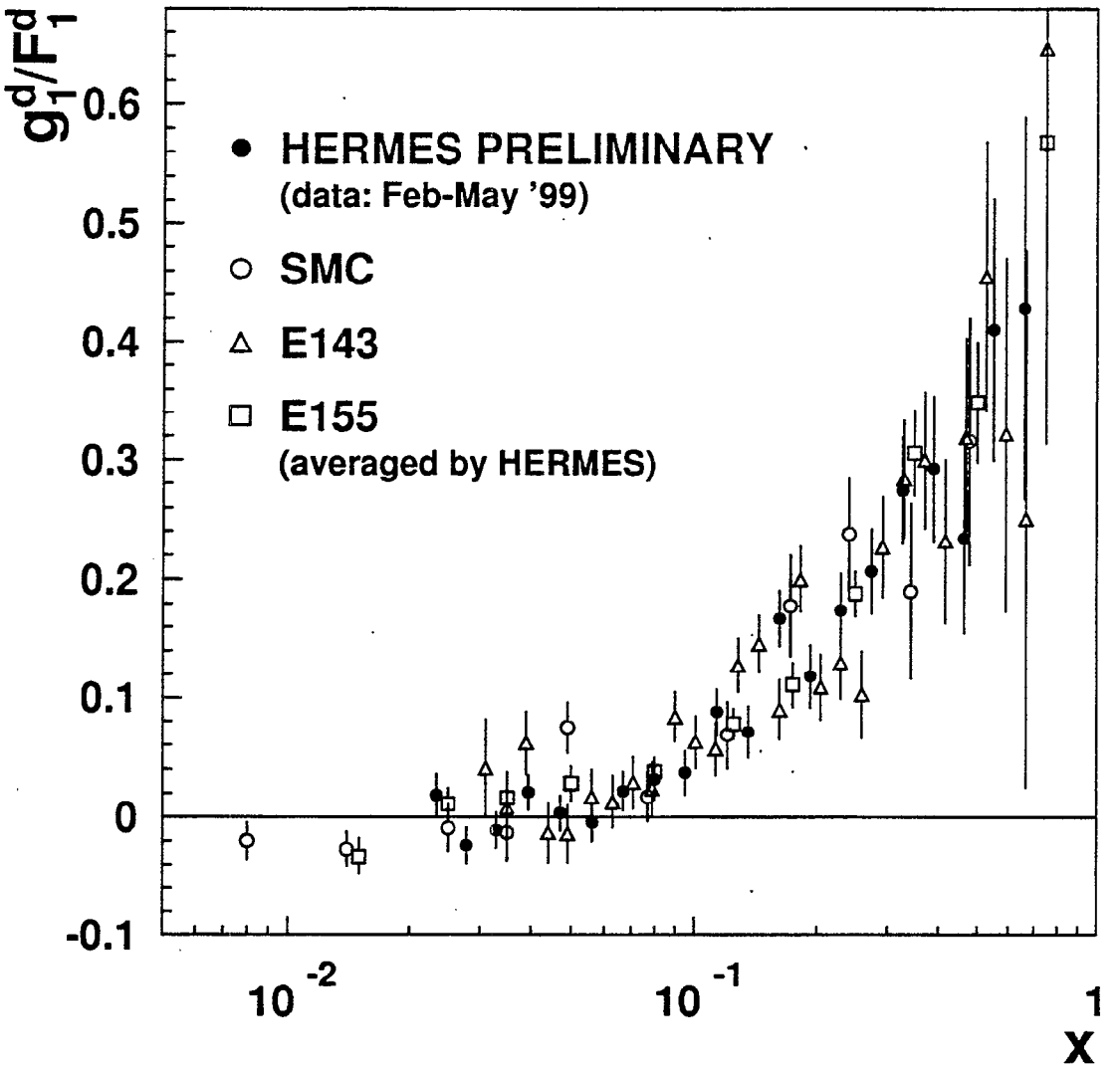

$\Longrightarrow$ NO STATISTICALLY SIGNIFICANT Q^2 DEPENDENCE

$\Longrightarrow$ MORE PRECISE DATA NEEDED:

▷ FACTOR 6 OF HERMES STATISTICS 'ON TAPE'

▷ ANALYSIS OF EXTENDED KIN. RANGE PLANNED

Spin Asymmetry in $SU(6)$-Model

$$|p\uparrow\rangle = \sqrt{\frac{1}{18}}[uud(2\uparrow\uparrow\downarrow - \uparrow\downarrow\uparrow - \downarrow\uparrow\uparrow)$$
$$+ udu(2\uparrow\downarrow\uparrow - \uparrow\uparrow\downarrow - \downarrow\uparrow\uparrow)$$
$$+ duu(2\downarrow\uparrow\uparrow - \uparrow\downarrow\uparrow - \uparrow\uparrow\downarrow)]$$

PROBABILITIES ON UP AND DOWN QUARKS TO HAVE THEIR SPIN PARALLEL ($\uparrow$) OR ANTIPARALLEL ($\downarrow$) TO THE NUCLEON SPIN:

$$\mathrm{P}(u^{\uparrow})=5/9 \quad \mathrm{P}(u^{\downarrow})=1/9$$
$$\mathrm{P}(d^{\uparrow})=1/9 \quad \mathrm{P}(d^{\downarrow})=2/9$$

THE SPIN ASYMMETRY A_1 FOR THE PROTON IS GIVEN BY THE SQUARE OF TH CHARGES OF EACH QUARK FLAVOR AND THESE PROBABILITIES:

$$A_1^p = \frac{4/9[P(u^{\uparrow}) - P(u^{\downarrow})] + 1/9[P(d^{\uparrow}) - P(d^{\downarrow})]}{4/9[P(u^{\uparrow}) + P(u^{\downarrow})] + 1/9[P(d^{\uparrow}) + P(d^{\downarrow})]}$$

THE PROTON ASYMMETRY BECOMES $A_1^p = 5/9$ AND THE NEUTRON ASYMMETRY $A_1^n = 0$.

World Data for g_1 versus x

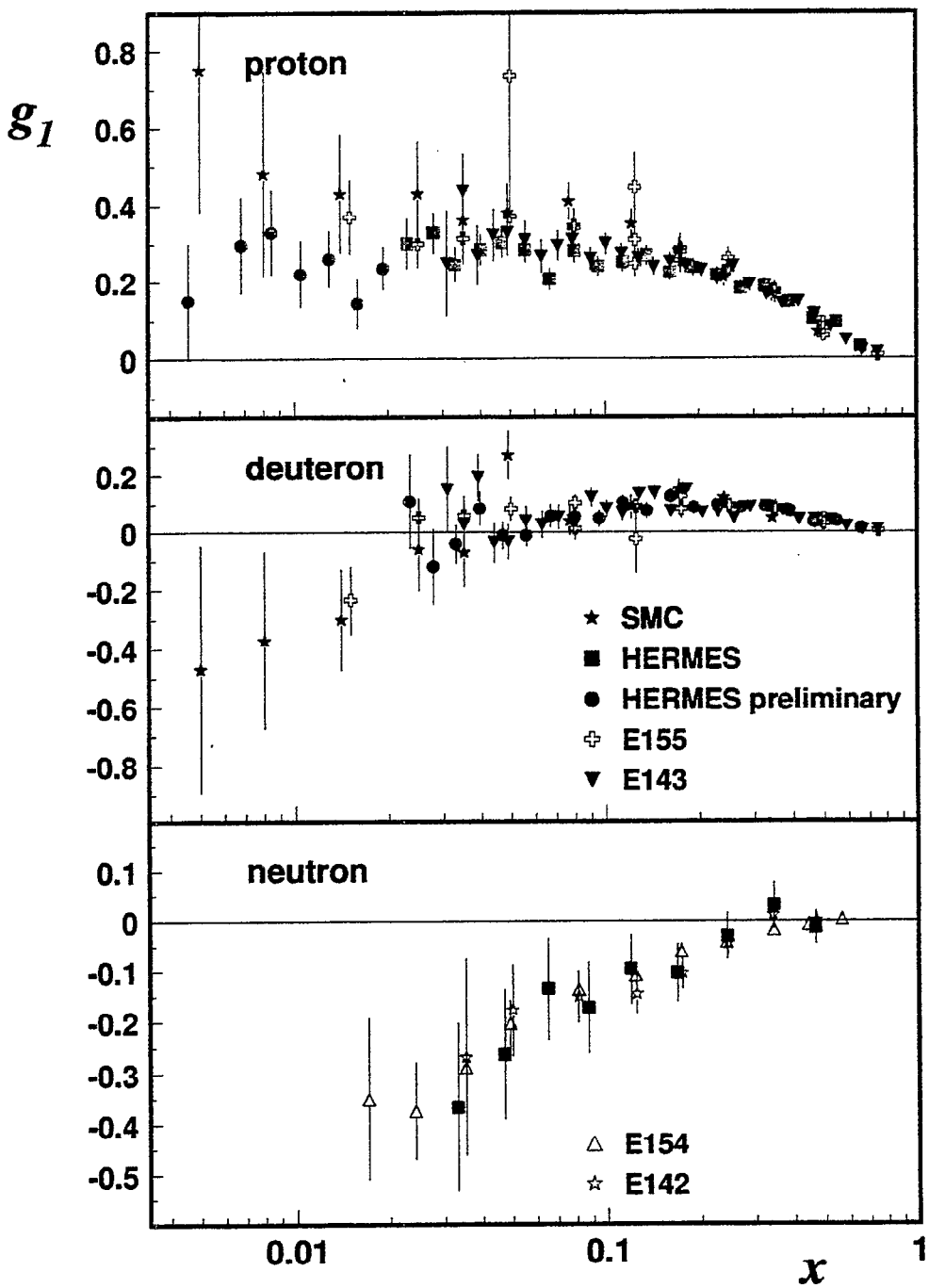

Data points shown at measured Q^2 values.

SMC data shown for $Q^2 > 1$ GeV^2.

World Data for xg_1 versus x

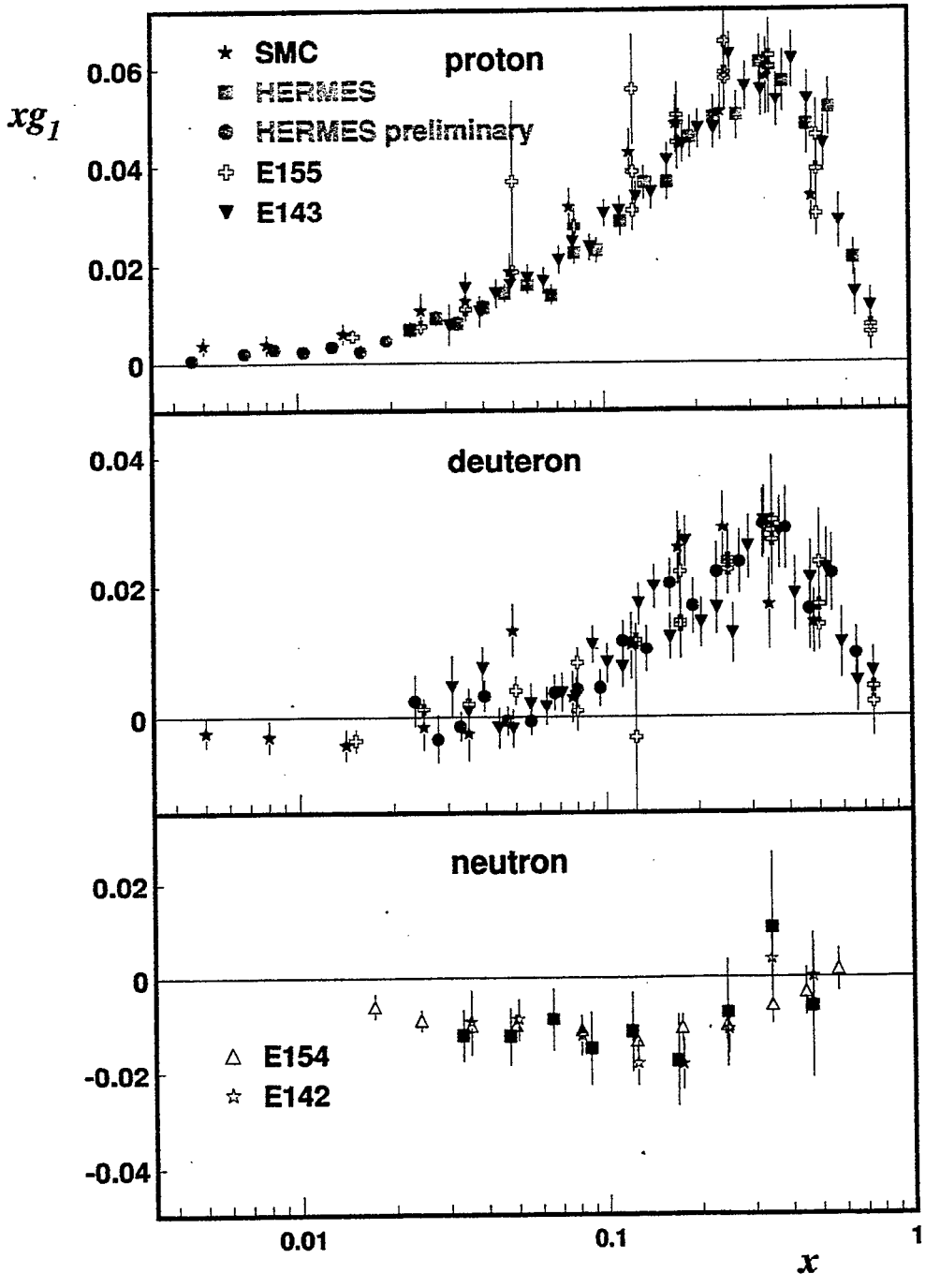

Data points shown at measured Q^2 values.

SMC data shown for $Q^2 > 1$ GeV^2.

SEMI-INCLUSIVE DIS

IN SEMI-INCLUSIVE DEEP INELASTIC SCATTERING A HADRON h IS DETECTED IN COINCIDENCE WITH THE SCATTERED LEPTON.

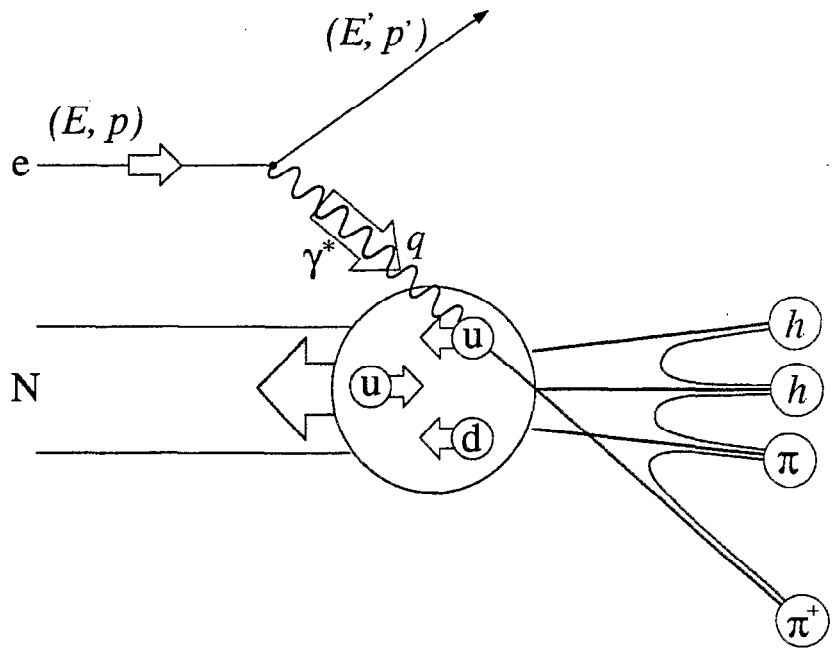

- SELECT HADRONS FROM THE CURRENT FRAGMENTATION REGION BY CUTS ON
  $z = E_h/\nu > 0.2$ AND $x_F = 2p_L^*/W \geq 0.1$

- IN LO QCD (ASSUMING SPIN INDEPENDENCE OF FRAGMENTATION):

$$\frac{g_1^h}{F_1^h}(x, Q^2) = \frac{\int_{z_{min}}^1 dz \sum_q e_q^2 \Delta q(x, Q^2) \cdot D_q^h(z, Q^2)}{\int_{z_{min}}^1 dz \sum_q e_q^2 q(x, Q^2) \cdot D_q^h(z, Q^2)}$$

$(\Delta q)q$: (POLARIZED) QUARK DISTRIBUTION

D_q^h: FRAGMENTATION FUNCTION

PROBABILITY FOR (STRUCK) QUARK OF FLAVOR f TO FRAGMENT INTO HADRON OF TYPE h

SEMI-INCLUSIVE ASYMMETRY A_1^h

MEASURED LEPTON NUCLEON ASYMMETRY:

$$A_{||}^h = \frac{\sigma_h^{\rightleftarrows} - \sigma_h^{\rightrightarrows}}{\sigma_h^{\rightleftarrows} + \sigma_h^{\rightrightarrows}}$$

$$= \frac{1}{\langle P_{\mathrm{T}} P_{\mathrm{B}} \rangle} \frac{(N^h/L)^{\rightleftarrows} - (N^h/L)^{\rightrightarrows}}{(N^h/L)^{\rightleftarrows} + (N^h/L)^{\rightrightarrows}}$$

$P_{\mathrm{T}}, P_{\mathrm{B}}$:	TARGET AND BEAM POLARISATION
N^h :	NUMBER OF SEMI-INCLUSIVE DIS EVENTS
L :	DEADTIME CORRECTED LUMINOSITY

IN ANALOGY TO THE INCLUSIVE CASE:

$$\frac{g_1^h}{F_1^h} = \frac{1}{1+\eta\gamma}\left[\frac{A_{||}^h}{D} + \gamma(\gamma-\eta)\cdot\frac{g_2^h}{F_1^h}\right]$$

ASSUMPTION $g_2^h = 0$: PHYSICS ASYMMETRY

$$A_1^h = \frac{g_1^h}{F_1^h} = \frac{A_{||}^h}{D(1+\eta\gamma)}$$

Semi-Inclusive Asymmetries

Inclusive and semi inclusive asymmetries on $^3\vec{He}$, $\vec{H}$ and $\vec{D}$ targets. Data shown at mean measured Q^2 in each bin.

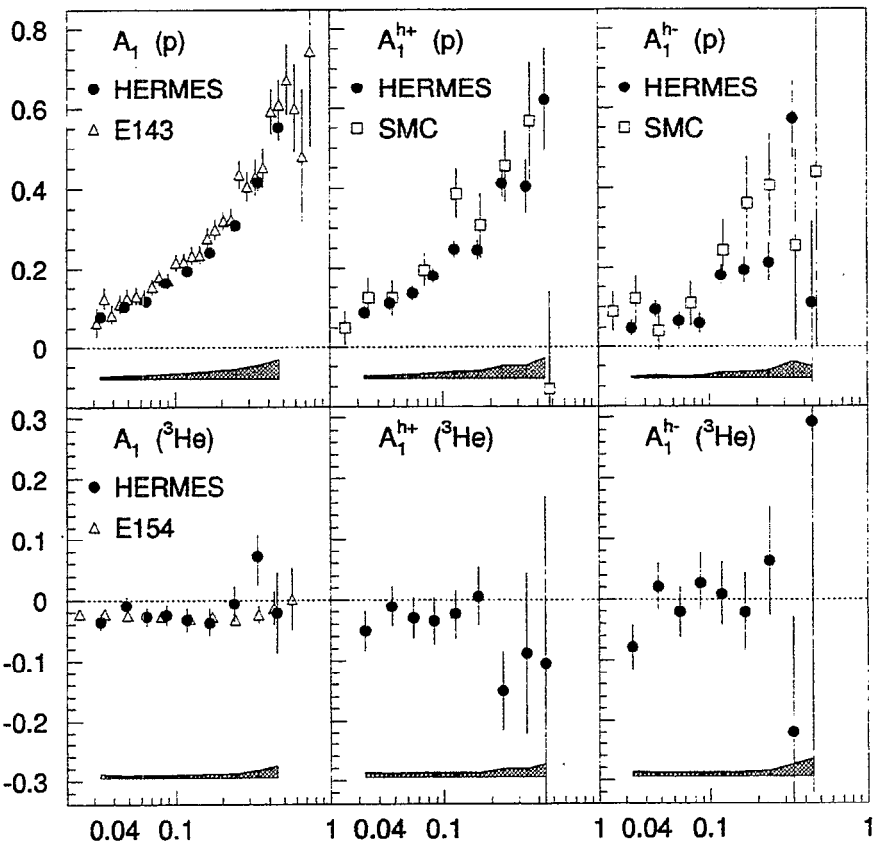

PUBLISHED IN Phys. Lett. B464 (1999) 123

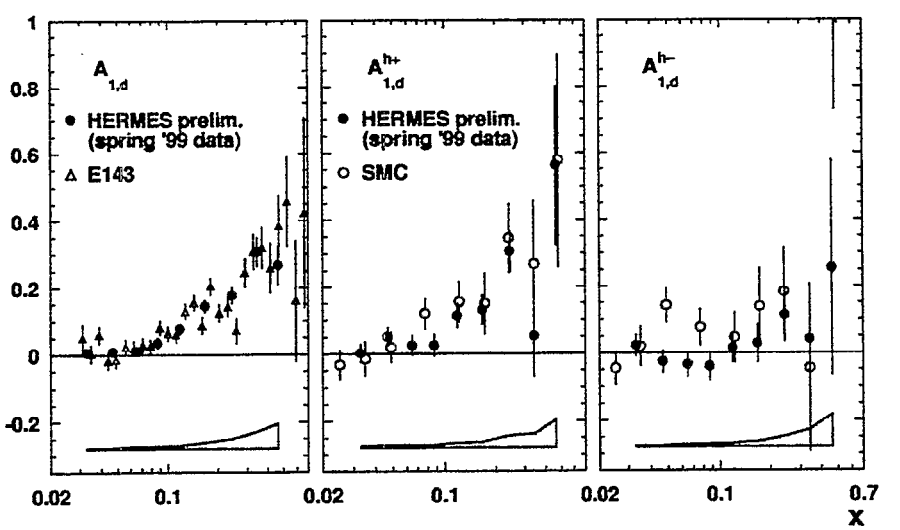

Δq-EXTRACTION

- REWRITE PHOTON-NUCLEON ASYMMETRY

$$A_1^h(x,z) = \sum_q \left[\underbrace{\frac{e_q^2\ q(x) \cdot D_q^h(z)}{\sum_{q'} e_{q'}^2\ q'(x) \cdot D_{q'}^h(z)}}_{P_q^h(x,z)} \cdot \frac{\Delta q(x)}{q(x)} \right]$$

- PURITY $P_q^h(x,z)$ GIVES PROBABILITY THAT A QUARK $q(x)$ WAS STRUCK WHEN A HADRON $h(z)$ IS DETECTED

- PURITIES ARE SPIN-INDEPENDENT QUANTITIES (FRAGMENTATION PROCESS SPIN-INDEPENDENT)

- DEFINE

$$\vec{\mathcal{A}} = \begin{pmatrix} A_1^{h_1(x)} \\ \dots \\ A_1^{h_m(x)} \end{pmatrix} \quad \mathcal{P} = \left[P_q^{h_j}(x) \right]_{mn} \quad \vec{Q} = \begin{pmatrix} \Delta q_1(x)/q_1(x) \\ \dots \\ \Delta q_n(x)/q_n(x) \end{pmatrix}$$

$$\text{WHERE } P_q^h(x) = \int_{z_{min}}^1 P_q^h(x,z)\ dz$$

- TO EXTRACT QUARK POLARIZATIONS SOLVE

$$\vec{\mathcal{A}} = \mathcal{P}\vec{Q}$$

Determination of Purities

- The Purities

$$P_f^h(x) = \frac{e_f^2\, q_f(x) \int \mathrm{d}z\, D_f^h(z)}{\sum_{f'} e_{f'}^2\, q_{f'}(x)\ \int \mathrm{d}z\, D_{q_{f'}}^h(z)}$$

are derived from the tuned *LUND* fragmentation model and from *(CTEQ4LQ)* parametrisations of $q_f(x)$

- Scheme at HERMES

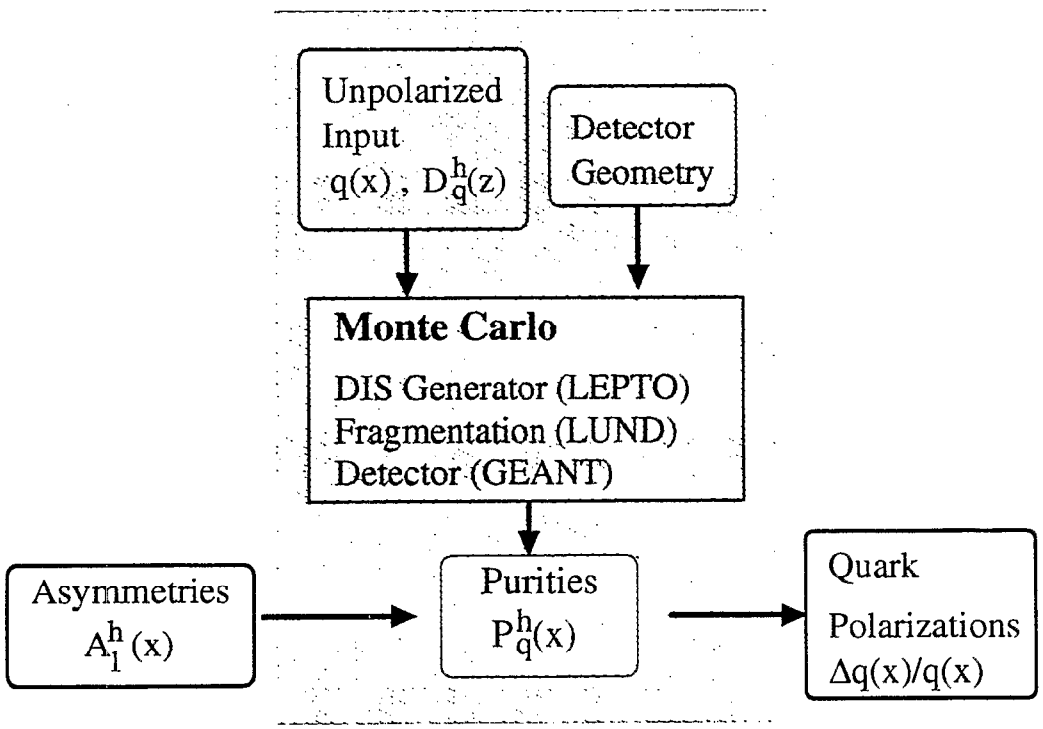

Purities from Monte Carlo

Purities $P^{h^{\pm}}_{u,d,\bar{u},\bar{d}}(x)$ for proton and neutron target:

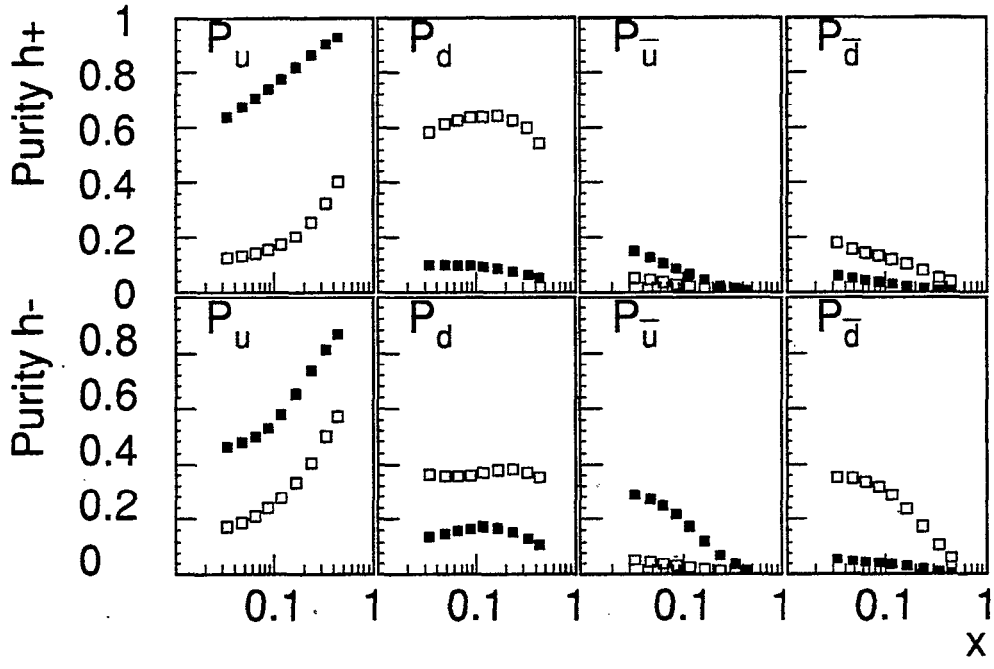

- h^+, h^- asymmetries on the proton dominated by $\Delta u(x)$
- h^+, h^- asymmetries on the neutron sensitive to $\Delta d(x)$
- Sensitivity to $\Delta\bar{u}(x)$ & $\Delta\bar{d}(x) \geq 10\%$ for $x \leq 0.2$

Flavor Decomposition

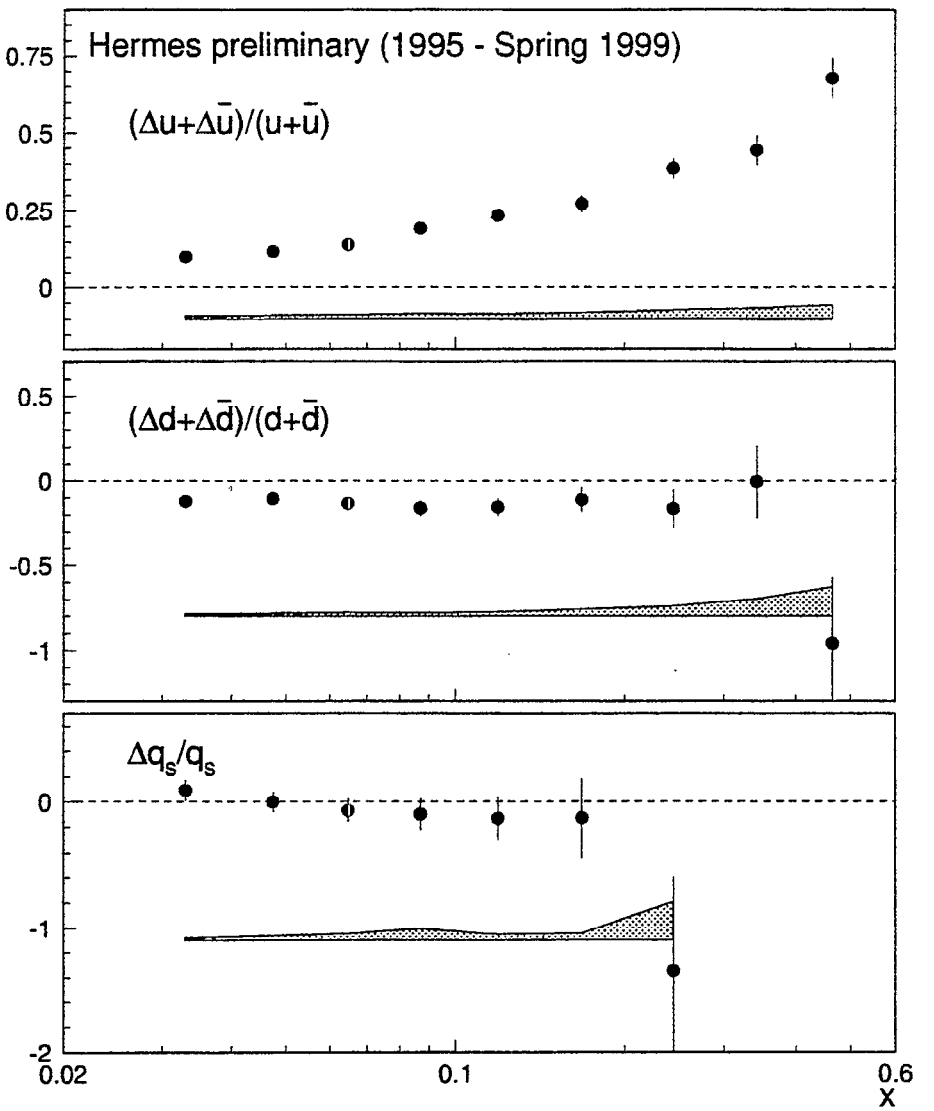

Flavour decomposition of quark polarisations as a function of x at measured Q^2.
Fit of sea contributions requires assumption:
Choose symmetric sea polarisation:

$$\frac{\Delta q_s(x)}{q_s(x)} \equiv \frac{\Delta u_s(x)}{u_s(x)} = \cdots = \frac{\Delta \bar{s}(x)}{\bar{s}(x)}$$

$\rightarrow$ direct determination of Δs not yet possible

Polarized Valence and Sea Quark Distributions

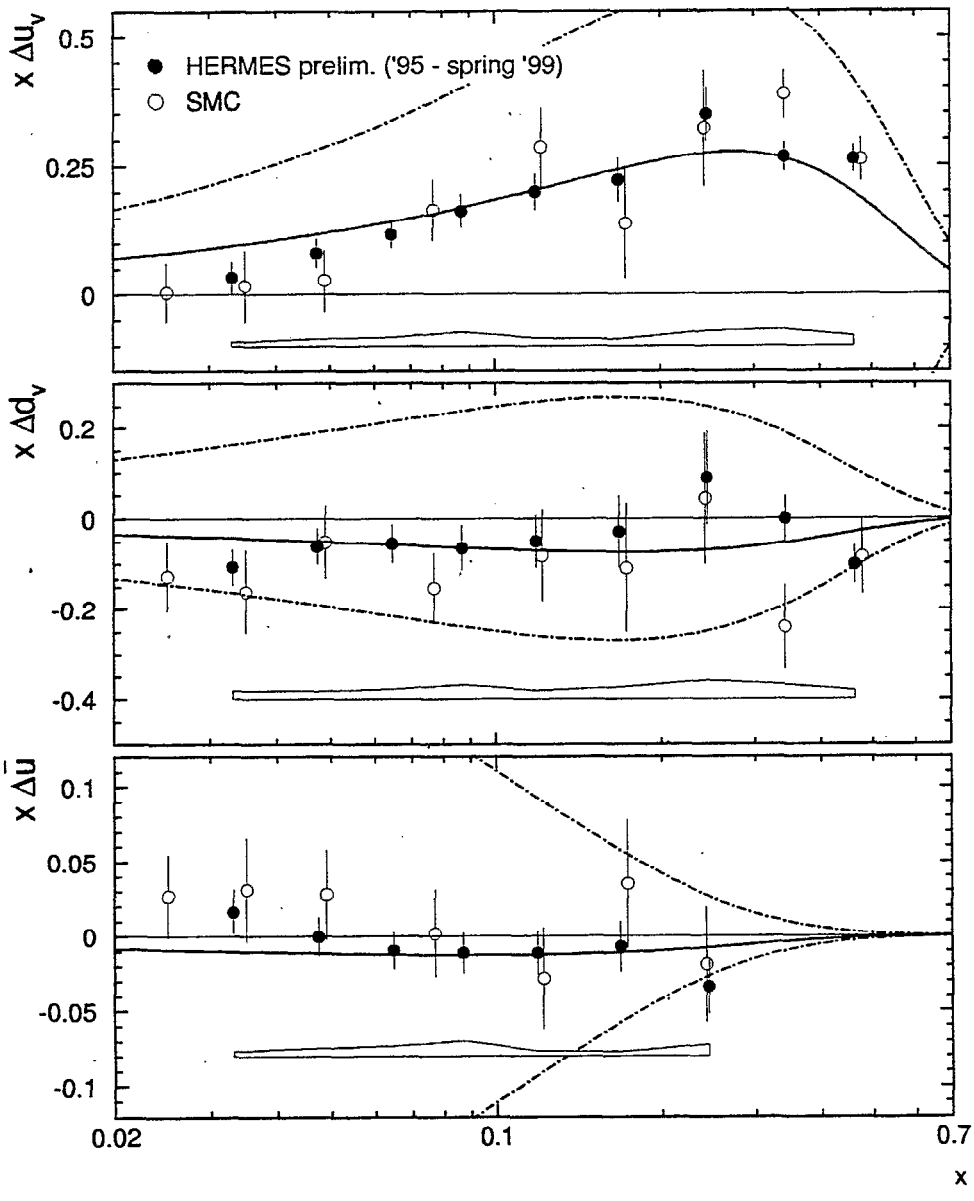

- Data points evolved to $Q^2 = 2.5$ GeV^2
- Solid lines: Gehrmann-Stirling ("Gluon A", LO)
- Dashed lines: positivity limits

Comparison of Publ. HERMES Data to Parameterizations

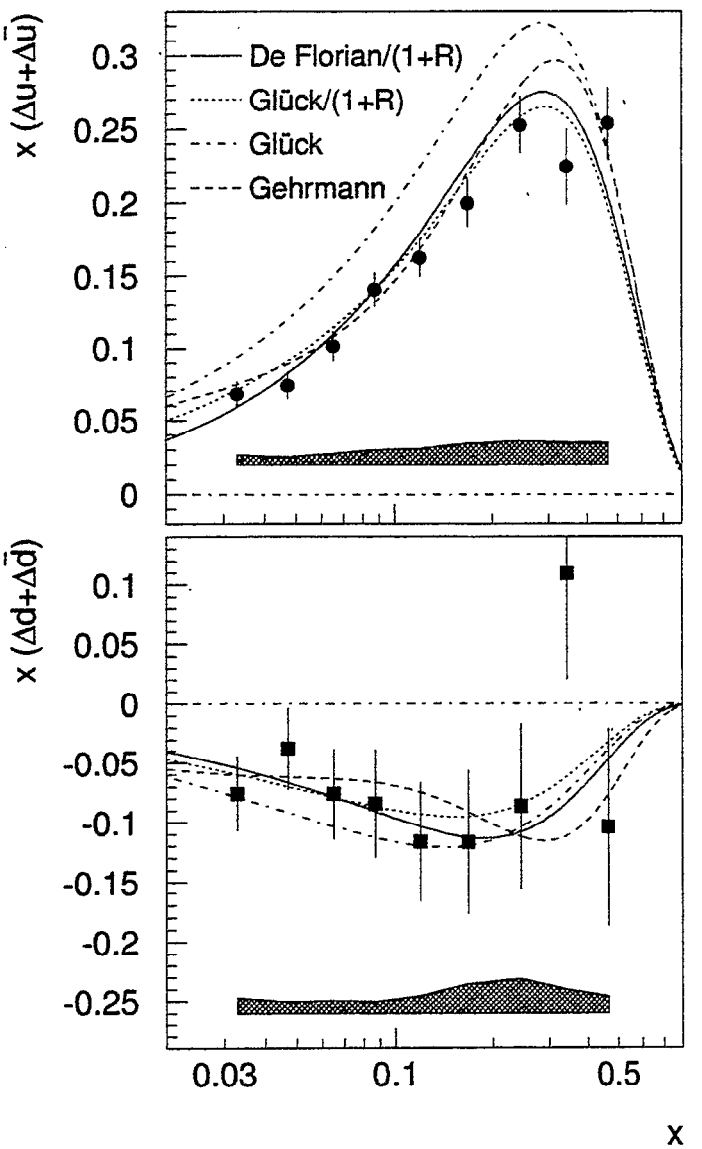

De Florian and Glück parametrizations corrected by a factor of $(1 + R)$ to allow for a direct comparison.

Flavour Contributions to Nucleon Spin (publ. data)

COMPARISON OF THE HERMES INTEGRALS WITH SMC RESULTS AT $Q^2 = 2.5$ GeV^2 AND IN THE HERMES x-RANGE OF $0.023 < x < 0.6$. THE UNCERTAINTY FOR THE LOW x EXTRAPOLATION IS NOT INCLUDED.

	HERMES	SMC
Δu_v	$0.52 \pm 0.05 \pm 0.08$	$0.59 \pm 0.08 \pm 0.07$
Δd_v	$-0.19 \pm 0.11 \pm 0.13$	$-0.33 \pm 0.11 \pm 0.09$
$\Delta \bar{u}$	$-0.01 \pm 0.02 \pm 0.03$	$0.02 \pm 0.03 \pm 0.02$
$\Delta \bar{d}$	$-0.02 \pm 0.03 \pm 0.04$	$0.02 \pm 0.03 \pm 0.02$

$\rightarrow$ AGREEMENT WITHIN 1 σ

TEST OF SU(3)$_f$ PREDICTIONS

	TOTAL INTEGRAL	SU(3)$_f$
$\Delta u + \Delta \bar{u}$	0.57 ± 0.04	0.66 ± 0.03
$\Delta d + \Delta \bar{d}$	-0.25 ± 0.07	-0.35 ± 0.03
$\Delta s + \Delta \bar{s}$	-0.01 ± 0.05	-0.08 ± 0.02

$\rightarrow$ A DEFINITE STATEMENT WHETHER THE INTEGRATED POLARIZED QUARK DISTRIBUTIONS VIOLATE SU(3)$_f$ OR NOT IS NOT POSSIBLE YET

$\rightarrow$ PRECISE SEPARATION OF STRANGE SEA CONTRIBUTION REQUIRED

Projected Δq-Accuracy for Existing Data (1995-2000)

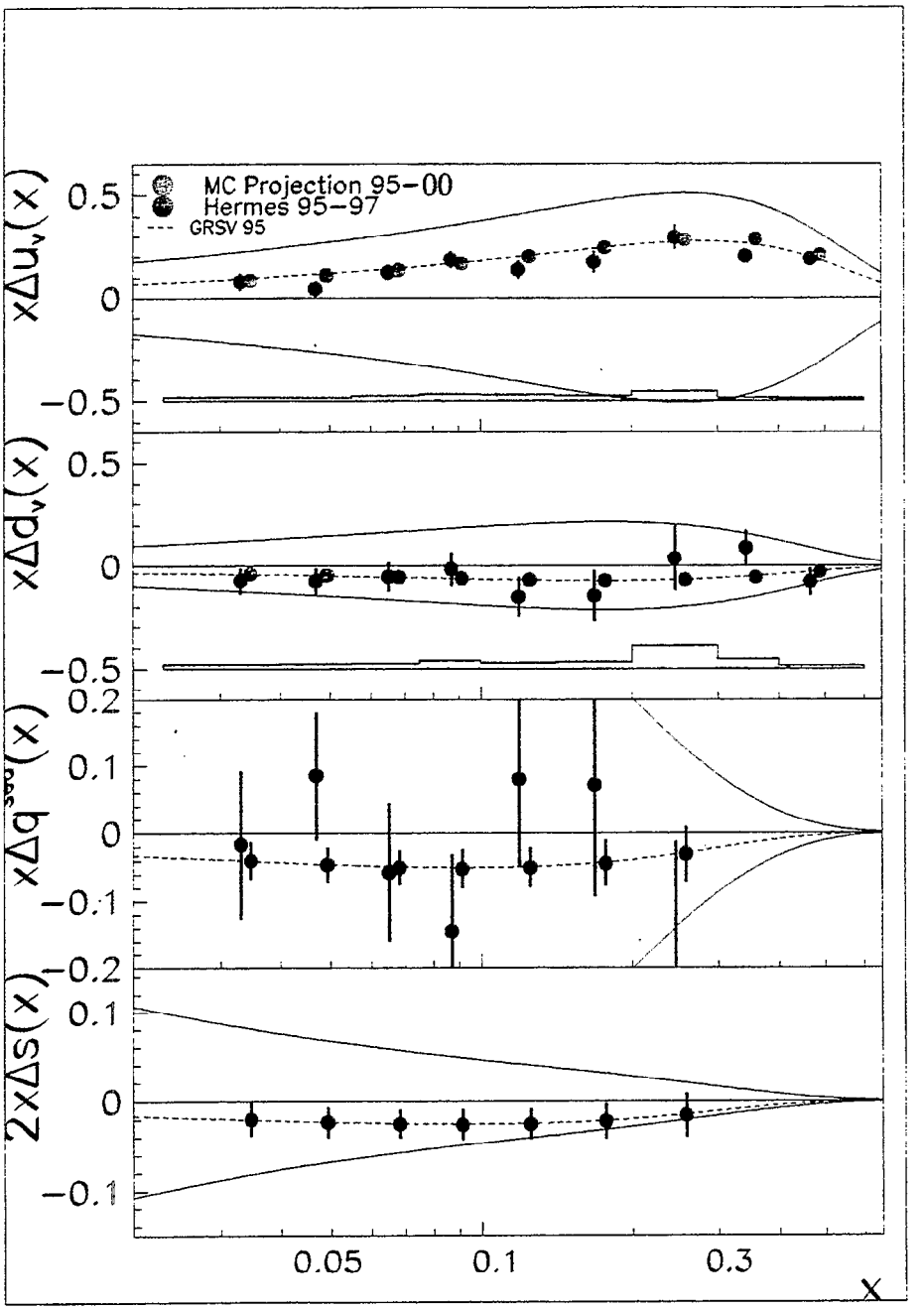

Prediction based on 8 x 10^6 DIS events including semi-inclusive $K^{\pm}$ asymmetries, based upon $\langle P_{target} \rangle = 0.88$ and $\langle P_{beam} \rangle = 0.5$

Indirect Determination of ΔG from $g_1(x, Q^2)$ Evolution

In NLO QCD the spin structure function $g_1(x, Q^2)$ additionally depends on the polarized gluon distribution $\Delta G(x, Q^2)$:

$$g_1 = \frac{1}{2}\sum_q^{N_f} e_q^2 \left[(\Delta q + \Delta\bar{q}) \otimes \left(1 + \frac{\alpha_s}{2\pi}\Delta C_q\right) + \frac{\alpha_s}{2\pi}\Delta G \otimes \Delta C_G \right]$$

$\Rightarrow$ the parametric form of $\Delta G(x, Q^2)$ can be indirectly determined from QDC NLO fits to the Q^2-evolution of $g_1(x, Q^2)$.

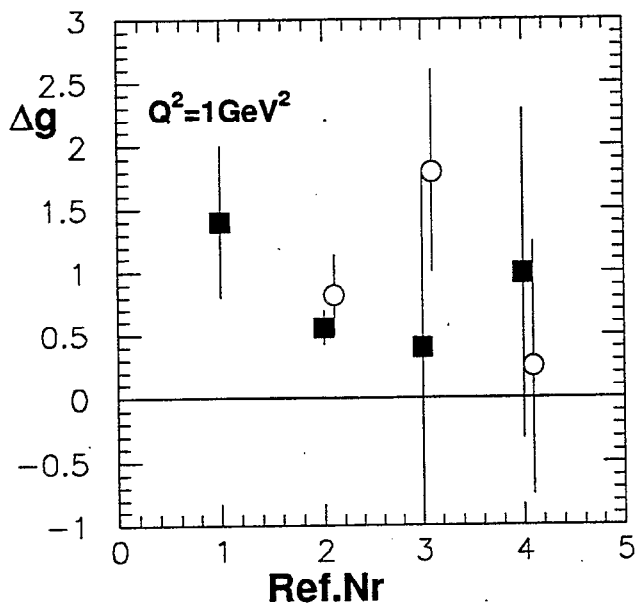

1 Altarelli et al., 1998
2 Leader et al., 1998
3 E154, 1997
4 SMC, 1998

[Presented by R. Windmolders at DIS-99.]

Open circles: $\overline{MS}$ scheme, full squares: AB scheme.

Errors are statistical and systematic errors in quadrature; theoretical uncertainty is not included in the errors of (2).

Direct Determination of $\Delta G/G$

Can determine $\Delta G/G$ directly from Photon-gluon fusion (PGF) since the gluon enters in LO:

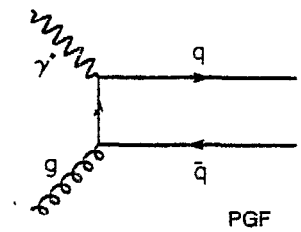

Experimental signatures of PGF:

OPEN CHARM

reconstruct D^*, D^0

$$A_{||} = \frac{N_{c\bar{c}}^{\rightleftarrows} - N_{c\bar{c}}^{\rightrightarrows}}{N_{c\bar{c}}^{\rightleftarrows} + N_{c\bar{c}}^{\rightrightarrows}}$$

$$A^{\gamma p \to c\bar{c}} \sim \Delta G/G$$

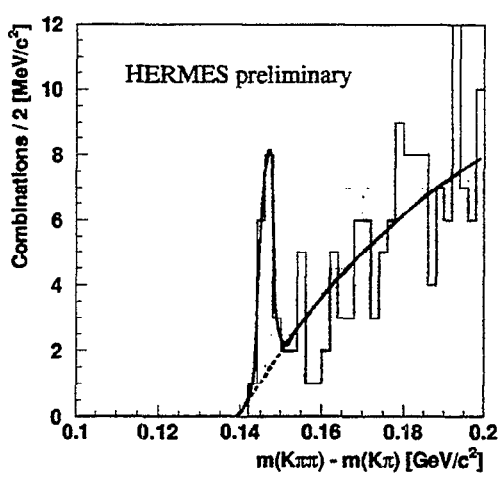

$$D^* \to K + \pi + \pi_{slow}$$

need data with RICH

HIGH-P_T

pairs of high-P_T hadrons

$$A_{||} = \frac{N_{h^+h^-}^{\rightleftarrows} - N_{h^+h^-}^{\rightrightarrows}}{N_{h^+h^-}^{\rightleftarrows} + N_{h^+h^-}^{\rightrightarrows}}$$

$$A^{\gamma p \to h^+h^-} \sim \Delta G/G$$

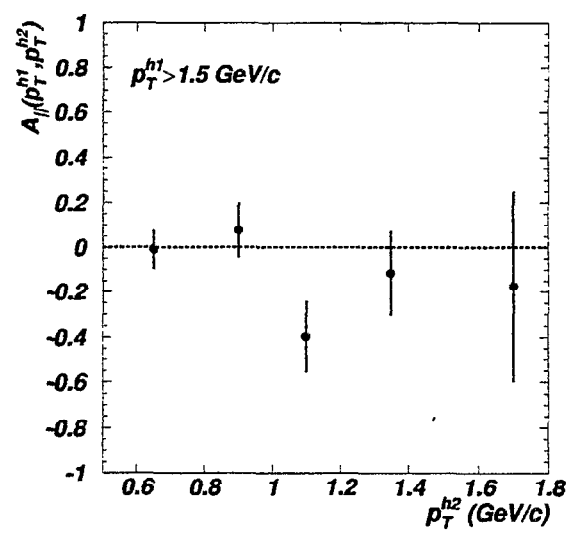

1997 data analyzed $\Rightarrow \cdots$

CONTRIBUTIONS TO $A^{\gamma p \to h^+ h^-}$

LO QCD: ASSUME THAT FOUR PROCESSES MAY CONTRIBUTE TO THE PRODUCTION OF HIGH-p_T h^+h^- PAIRS:

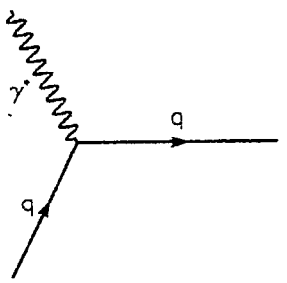

DIS

NEGLIGIBLE CONTRIBUTION

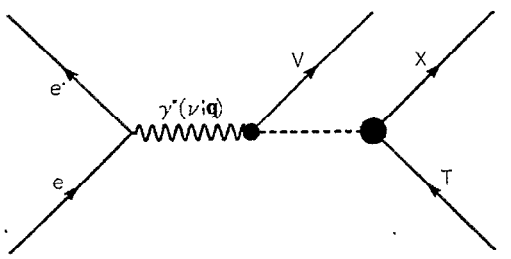

VMD

ASSUME $A_{VMD} = 0$

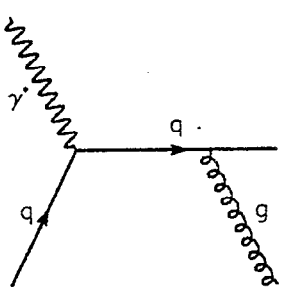

QCDC

$A_{QCDC} \sim \frac{\Delta q}{q}$

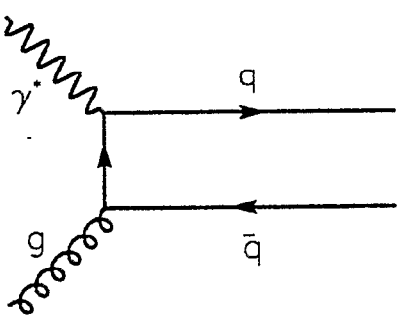

PGF

$A_{PGF} \sim \frac{\Delta G}{G}$

.. ESTIMATE THEIR RELATIVE CONTRIBUTIONS USING PYTHIA

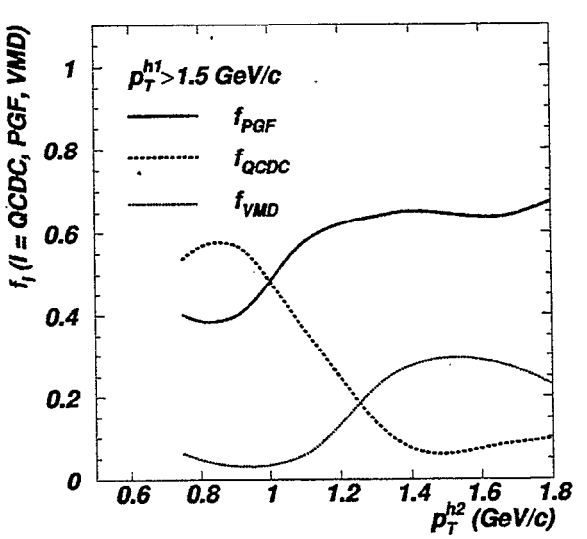

HERMES Result on $\Delta G/G$

Assuming no asymmetry in VMD contribution the cross section asymmetry can be simplified:

$$A_{\parallel} = \frac{N^{\uparrow\downarrow}_{h^+h^-} L^{\uparrow\uparrow} - N^{\uparrow\uparrow}_{h^+h^-} L^{\uparrow\downarrow}}{N^{\uparrow\downarrow}_{h^+h^-} L^{\uparrow\uparrow}_P + N^{\uparrow\uparrow}_{h^+h^-} L^{\uparrow\downarrow}_P}$$

$$\approx \left(\hat{a}_{\mathrm{PGF}} \frac{\Delta G}{G} f_{\mathrm{PGF}} + \hat{a}_{\mathrm{QCDC}} \frac{\Delta q}{q} f_{\mathrm{QCDC}} \right) D$$

$\hat{a}_{\mathrm{PGF}} = -1$ $\quad \hat{a}_{\mathrm{QCDC}} \approx 0.5$ (hard scattering asym.)

HERMES result 1996/97 data [PRL 84 (2000) 2584] (does not include systematic errors due to PYTHIA MC)

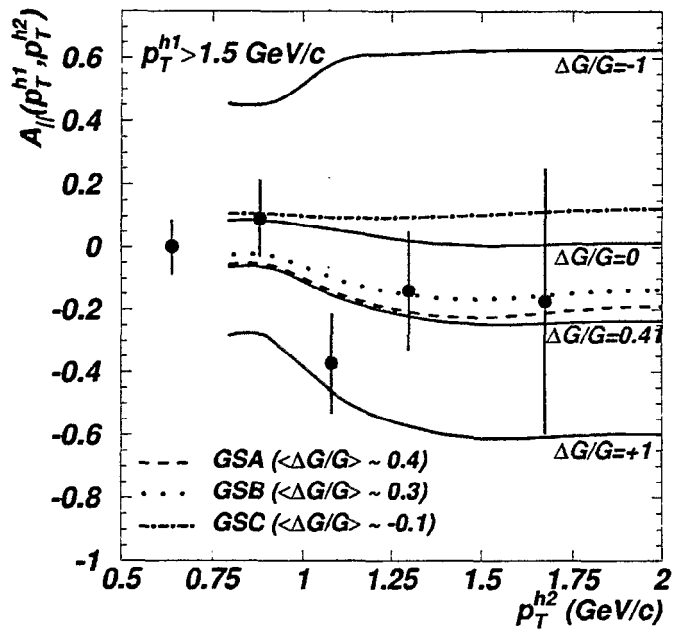

$\rightarrow \Delta G/G$ is positive

$$\Delta G/G = 0.41 \pm 0.18 \text{ (stat.)} \pm 0.03 \text{ (exp.syst.)}$$
$$\text{at } \langle x_G \rangle = 0.17 \text{ and } \langle \hat{p}_T^2 \rangle = 2.1 \text{ GeV}^2$$

NOTE: extraction strongly model dependent

Future Measurements of the Gluon Polarization

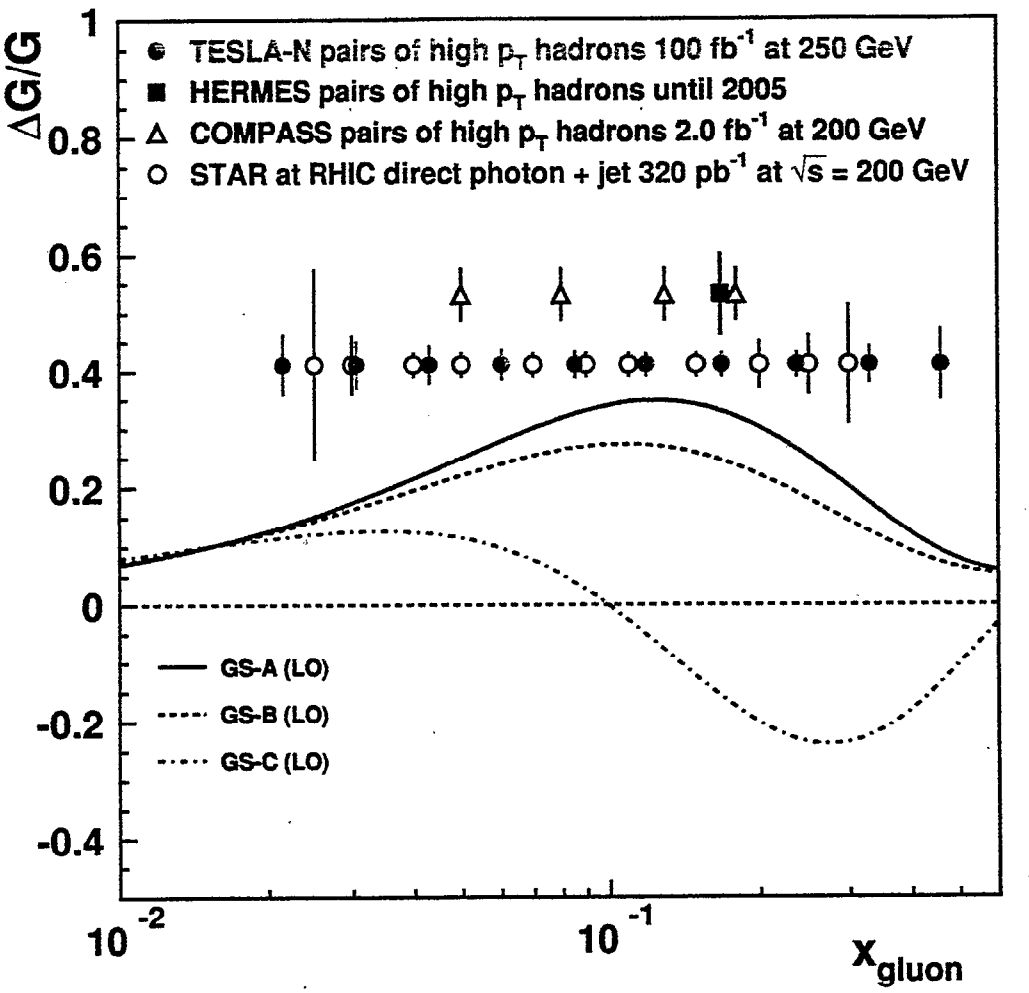

Phenomenological predictions for $Q^2 = 10$ GeV^2

HERMES points in the figure:
data with longitudinal target polarization, originally planned until 2005, are to about 80% already on tape thanks to excellent HERA conditions in 2000 and due to an improvement of the target density by about a factor of 2.

Transversity Measurement through the Collins effect

WEIGHTED ASYMMETRY

[Mulders, Tangermann 96, Kotzinian, Mulders 97]

$$A_T(x,y,z) \equiv \frac{\int d\phi^\ell \int d^2P_{h\perp} \frac{|P_{h\perp}|}{zM_h} \sin(\phi_s^\ell + \phi_h^\ell)\ (d\sigma^\uparrow - d\sigma^\downarrow)}{\int d\phi^\ell \int d^2P_{h\perp}(d\sigma^\uparrow + d\sigma^\downarrow)}$$

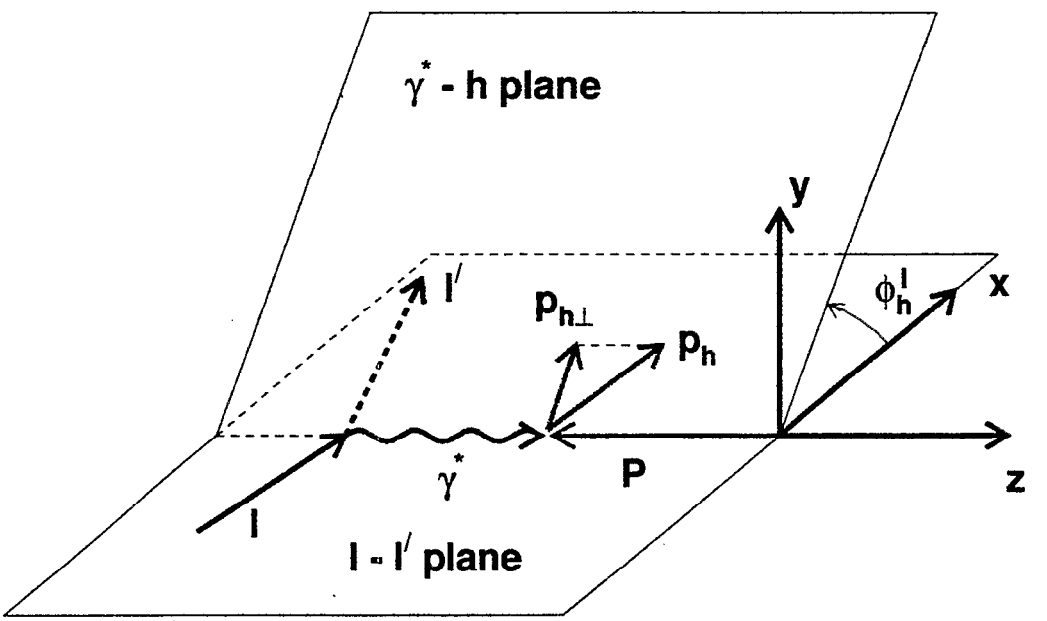

Factorization w.r.t. x and z:

$$A_T(x,y,z) = f \cdot P_T \cdot D_{nn} \cdot \frac{\sum_q e_q^2\ \delta q(x)\ H_1^{\perp(1)q}(z)}{\sum_q e_q^2\ q(x)\ D_1^q(z)}$$

$D_{nn} = (1-y)/(1-y+y^2/2)$: transverse spin transfer coefficient

Transversity Measurement at HERMES: Future Prospects

Projections for $\delta u(x)$ and $H_1^{\perp(1)u}(z)/D_1^u(z)$ on a proton target

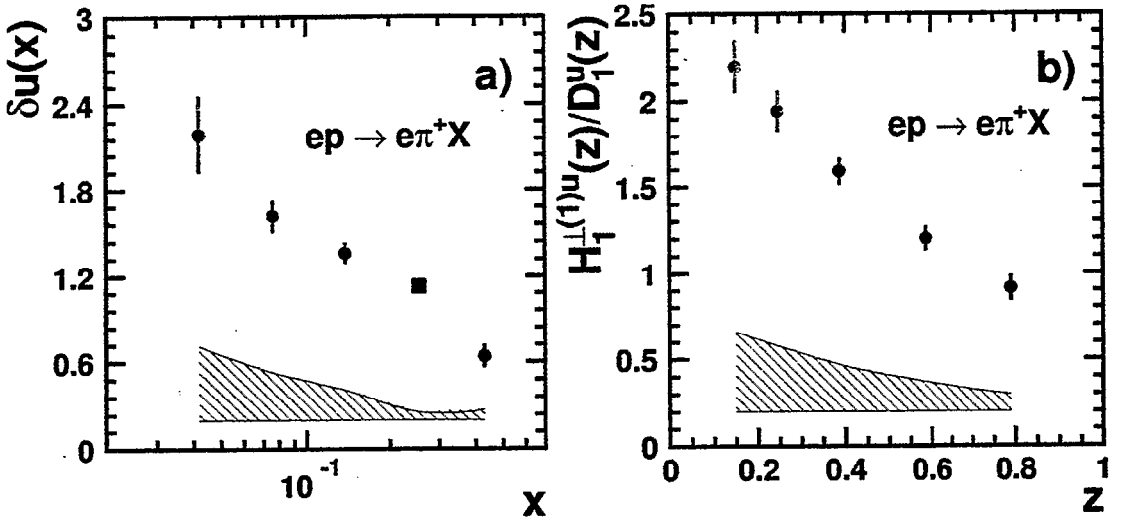

Projections for $\delta u(x)+\delta d(x)$ and $H_1^{\perp(1)u}(z)/D_1^u(z)$ on a deuteron target

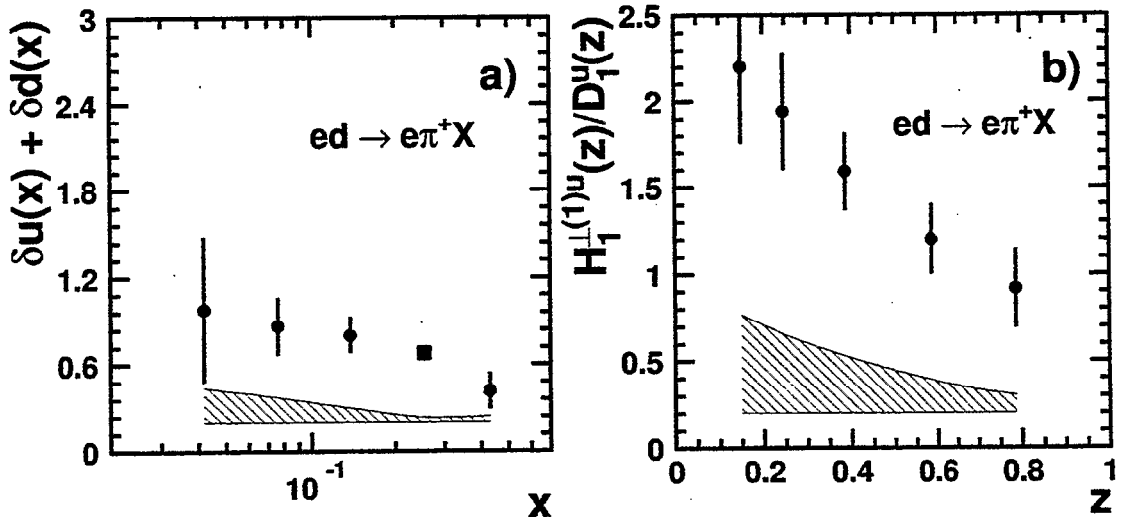

More hermes Data to Analyse...

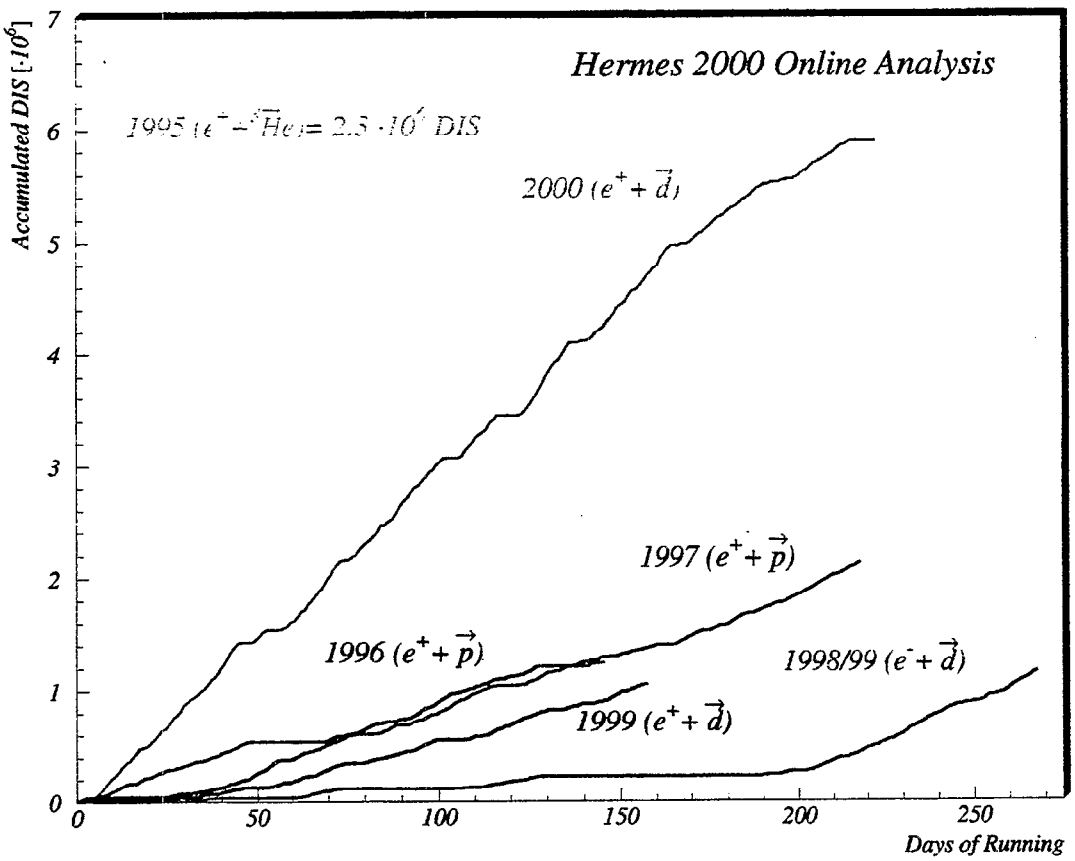

7 Million DIS events from polarised $\vec{D}$ on tape; are currently being analysed.

SUMMARY

- NEW PRELIMINARY HERMES RESULTS FOR THE SPIN STRUCTURE FUNCTION g_1
  - FOR THE PROTON IN THE EXTENDED KINEMATIC RANGE $0.0021 < x < 0.0212$ AND $0.1 < Q^2 < 0.8$ GeV^2
  - FOR THE DEUTERON IN THE KINEMATIC RANGE $0.0212 < x < 0.85$ AND $Q^2 > 0.8$ GEV^2
- VERY GOOD AGREEMENT FOR RESULTING g_1/F_1 VALUES WITH OTHER EXPERIMENTAL DATA

  $\Rightarrow$ NO STATISTICALLY SIGNIFICANT Q^2 DEPENDENCE OBSERVED FOR BOTH PROTON AND DEUTERON g_1/F_1 VALUES
  - FOR DEUTERON ANALYSIS 6 TIMES MORE STATISTICS FORTHCOMING IN FULL HERMES KINEMATIC RANGE
- $A_1^{(h)}$ MEASURED ON $^3\vec{\mathrm{He}}$, $\vec{\mathrm{H}}$ AND $\vec{\mathrm{D}}$ TARGETS
- QUARK POLARISATIONS EXTRACTED FOR UP AND DOWN QUARKS WITH GOOD STATISTICS. ALTERNATIVELY FOR VALENCE AND SEA QUARKS
- POLARISATION OF UP QUARKS POSITIVE, OF DOWN QUARKS NEGATIVE. POLARIZATION OF SEA QUARKS COMPATIBLE WITH ZERO WITHIN ERROR BARS OF PRELIMINARY ANALYSIS
- HADRON PAIR ANALYSIS INDICATES THAT SIGN OF POLARIZED GLUON DISTRIBUTION IS POSITIVE AT $x_{gluon} = 0.17$

Acknowledgements

For magnificent help in preparing the transparencies many thanks to

Ralf Kaiser (DESY Zeuthen).

For the kind permission to re-utilize tex-files of recent talks I'm grateful to

Elke Aschenauer (DESY Zeuthen)

Ralf Kaiser (DESY Zeuthen)

Vladislav Korotkov (DESY Zeuthen)

Thore Lindemann (DESY Hamburg)

Uta Stoesslein (U. Colorado)

Nucleon Spin Structure Functions in the Chiral Quark Soliton Model

M. Wakamatsu

Department of Physics, Faculty of Science,
Osaka University, Toyonaka, Osaka 560, Japan

Undoubtedly, the EMC measurement in 1988, which brought about the so-called "nucleon spin crisis", and the NMC measurement in 1991, which has established the flavor asymmetry of sea-quark distributions in the nucleon, are two of the most striking findings in the recent experimental studies of nucleon structure functions. A prominent feature of the chiral quark soliton model (CQSM) is that it can simultaneously explain the above two big discoveries in no need of artificial fine-tuning of the model. In this lecture, I will try to explain the reason why the model is so successful in explaining high-energy deep-inelastic observables of the nucleon.

In the first part of the lecture, I would like to recall you several basic facts about the CQSM, first confining to the standard low-energy observables of the nucleon. After that, how the model can be used to study parton distribution functions of the nucleon will be explained. Particularly emphasized here is the field theoretical nature of the model, which enables us to carry out nonperturbative evaluation of the parton distribution functions with full inclusion of the vacuum polarization effects. It is shown that an incomparable feature of the CQSM as compared with many other effective models of the nucleon like the MIT bag model is that it can give reasonable predictions not only for quark distribution functions but also for antiquark distributions as exemplified by the argument on the positivity constraint for $\bar{u}(x) + \bar{d}(x)$ and also on the Soffer inequality for antiquark distributions.

The second part of the lecture is devoted to the comparison of various model predictions with the existing high-energy data. It is shown that, without introducing any adjustable parameter except for the initial-energy scale of the Q^2-evolution, the model can explain all the qualitatively noticeable features of the recent high-energy deep-inelastic scattering observables. It naturally explains the excess of $\bar{d}$ sea over the $\bar{u}$ sea in the proton. It also reproduces qualitative behavior of the observed longitudinally polarized structure functions for the proton, neutron and the deuteron. The most puzzling observation, i.e. unexpectedly small quark spin fraction of the nucleon can also be explained in no need of large gluon polarization at the low renormalization point. As a further unique prediction of the model, I point out the possibility of large isospin asymmetry of the spin-dependent sea-quark distributions, which seems to be a natural consequence of the N_c-counting rule, but appears inconsistent with the naive meson cloud convolution model. Then, if this large asymmetry of the longitudinally polarized sea is experimentally established, it would offer a strong evidence in favor of nontrivial spin-isospin correlation imbedded in the "large N_c chiral soliton picture" of the nucleon. The model can give reasonable predictions also for the transversity distributions as well as the higher-twist parton distribution functions. It is hoped that these unique predictions of the CQSM will be tested through various experiments in the near future, which enables the flavor as well as the valence plus sea quark decompositions of distribution functions.

Nucleon Spin Structure Functions in the Chiral Quark Soliton Model

RIKEN School, Niigata, Yuzawa, Dec. 2-5, 2000

Plan of Lecture

— Part I —

1. Introduction
2. Fundamentals of Chiral Quark Soliton Model
3. CQSM and Parton Distribution Functions

— Part II —

4. Comparison with High Energy Data
5. Conclusion

Nucleon Spin Structure Functions in the Chiral Quark Soliton Model

M. Wakamatsu, Osaka University

1. Introduction

two big discoveries in nucleon structure function physics

- EMC measurement (1988) $\rightsquigarrow$ "**Nucleon Spin Puzzle**"
- NMC measurement (1991) $\rightsquigarrow$ "**Flavor Asymmetric Sea**"

nucleon spin puzzle

still unsolved completely

widely-accepted explanation of NMC observation

pion cloud effect

$\Downarrow$

manifestation of **nonperturbative QCD dynamics** (SχSB) in **high-energy deep-inelastic scattering observables** !

♣ A prominant feature of the **Chiral Quark Soliton Model** is that it can **simultaneously** explain the above **two big observations** in no need of artificial fine-tuning !

What is the Chiral Quark Soliton Model like ?

- it is a **relativistic field theoretical model** effectively incorporating the idea of **large N_c QCD**

- at large N_c, a nucleon is a composite of N_c **valence quarks** and infinitely many **Dirac sea quarks** bound by the self-consistent **pion field** of **hedgehog shape**

- cannonically quantizing the spontaneous **rotational motion** of the **symmetry breaking mean field configuration**, we can perform **nonperturbative evaluation** of any nucleon observables with full inclusion not only of N_c **valence quarks** but also of deformed **Dirac sea quarks**

$$\Downarrow$$

$$\boxed{\text{reasonable estimation of } \textbf{antiquark distributions}}$$

- **only 1 parameter** of the model (**dynamical quark mass** M) was already fixed by low energy phenomenology

$$\Downarrow$$

$$\boxed{\textbf{parameter-free predictions for PDF}}$$

at low renormalization scale

2. Fundamentals of Chiral Quark Soliton Model

milestone in the history of CQSM

[1988] D. Diakonov, V. Petrov and P. Pobylitsa

- **proposal of the model** based on

  instanton picture of QCD vacuum

  (Skyrme model, Hybrid chiral bag model, $\cdots$)

[1991] M. W and H. Yoshiki

- **numerical basis** for **nonperturbative evaluation** of nucleon observables including **vacuum polarization**
- **spin contents of the nucleon**

[1993] M. W and T. Watabe

- discovery of novel $\mathbf{1/N_c}$ **correction**

  — resolution of g_A-problem —

[1996,1997] D. Diakonov et al.

- application to **PDF** of the nucleon

basic lagrangian

$$\boxed{\mathcal{L}_{CQM} \;=\; \bar{\psi}\,(\,i\,\partial\!\!\!/ - M\,U^{\gamma_5}(x)\,)\,\psi \quad \text{with} \quad U^{\gamma_5}(x) \;=\; e^{\,i\,\gamma_5\,\boldsymbol{\tau}\cdot\boldsymbol{\pi}(x)\,/\,f_\pi}}$$

no kinetic term for $\boldsymbol{\pi}(x)$

effective action

$$\begin{aligned} Z \;&=\; \int \mathcal{D}\pi\,\mathcal{D}\psi\,\mathcal{D}\psi^\dagger\;\exp\left[\,i\int d^4x\;\mathcal{L}_{QCM}\,\right] \\ &=\; \int \mathcal{D}\pi\;e^{\,i\,S_{eff}[\boldsymbol{\pi}]} \end{aligned}$$

$$\Downarrow$$

$$\boxed{S_{eff}[U] \;=\; -\,i\,N_c\,\mathrm{Sp}\log\left[\,i\,\partial\!\!\!/ - MU^{\gamma_5}\,\right]}$$

where

$$\mathrm{Sp}\,\hat{O} \;\equiv\; \int d^4x\;\mathrm{tr}_f\,\mathrm{tr}_\gamma\,\langle x\,|\,\hat{O}\,|\,x\rangle$$

effective meson action from derivative expansion

$$\begin{aligned} S_{eff}[\boldsymbol{\pi}] \;=\;& \quad \textbf{Skyrmion action with W-Z term} \\ &+\quad \text{destabilizing 4-th deriv. term} \\ &+\quad \cdots\cdots\cdots \end{aligned}$$

Soliton construction without using derivative expansion

$\boxed{\text{1st step}}$: start with static $\boldsymbol{\pi}(\boldsymbol{x})$ of **hedgehog shape**

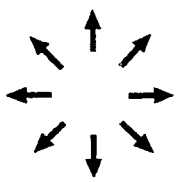

$$\boldsymbol{\pi}(\boldsymbol{x}) = \hat{\boldsymbol{r}}\, F(r)$$

M.F. for quarks

$$\left(\begin{array}{l} F(0) - F(\infty) = n\,\pi \\ n \ : \ \text{winding number} \end{array} \right)$$

Dirac eq.

$$\boxed{H\,|\,m\,\rangle \;=\; E_m\,|\,m\,\rangle}$$

$$H = \frac{\boldsymbol{\alpha}\cdot\nabla}{i} + M\beta\,(\cos F(r) + i\,\gamma_5\,\boldsymbol{\tau}\cdot\hat{\mathbf{r}}\sin F(r))$$

breaks "rotational" invariance

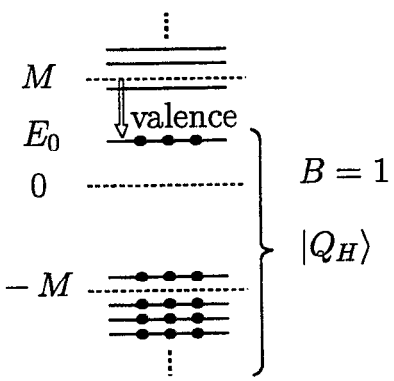

Energy of $|\,Q_H >$

$$\boxed{E_{static} \;=\; N_c\,E_0 \;+\; E_{v.p.}}$$

$$E_{v.p.} \;\sim\; N_c\,\Big(\sum_{m<0} E_m \;-\; \sum_{k<0} \epsilon_k\Big) \;\Longrightarrow\; \text{regularize} \quad \textbf{(physical cutoff)}$$

Hartree condition

$$\frac{\delta}{\delta F(r)}\, E_{static}[F(r)] \;=\; 0.$$

Numerical Method

- principle idea is **numerical diagonalization** of Dirac hamiltonian H by using **Kahana-Ripka's discretized plane-wave basis**

(1) **discretization** of plane-wave momentum is achieved by putting the soliton system into a **sphere** with

large enough radius D

(2) basis is **finitized** by truncating momenta

$$k_i \leq k_{max}$$

justification

♣ numerical check of $\left\{ \begin{array}{c} D \\ \\ k_{max} \end{array} \right\} \longrightarrow \infty$ limit

$$\Downarrow$$

need **some modification of K-R basis** for evaluating **next-to-leading order correction** in $\mathbf{1/N_c}$ **expansion** discussed later (M. W. and H. Yoshiki, 1991)

$$\Downarrow$$

$\boxed{\text{nonperturbative evaluation of vacuum polarization effects}}$

$\boxed{\text{2nd step}}$: **quantization** of **collective rotational motion**

- energy degeneracy under isospin (spatial) rotation

$$E_{static}[R\,U_0^{\gamma_5}R^\dagger] \;=\; E_{static}[U_0^{\gamma_5}] \quad : \quad R \in SU(2)$$

$$\Downarrow$$

- spontaneous rotation of hedgehog mean-field ("zero mode")

$$U^{\gamma_5}(\boldsymbol{x},t) \;=\; A(t)\,U_0^{\gamma_5}(\boldsymbol{x})\,A^\dagger(t) \quad : \quad A(t) \in SU(3)$$

then

$$\begin{aligned} S_{eff}[U] &= -i\,N_c\,\mathrm{Sp}\log\left[\,i\,\partial\!\!\!/ - M\,A(t)\,U_0^{\gamma_5}(\boldsymbol{x})\,A^\dagger(t)\,\right] \\ &= -i\,N_c\,\mathrm{Sp}\log\,A(t)\,\gamma^0\,(\,i\,\partial_t - H - \Omega\,)\,A^\dagger(t) \\ &= -i\,N_c\,\mathrm{Sp}\log\,(\,i\,\partial_t - H - \Omega) \end{aligned}$$

with

$$\Omega \;\equiv\; -i\,A^\dagger(t)\,\dot{A}(t) \;\equiv\; \frac{1}{2}\,\Omega_a\,\tau_a$$

: **collective angular velocity**

we then get

$$\begin{aligned} S_{eff}[U] &= S_{eff}[U_0] \;+\; \{\,S_{eff}[U] \;-\; S_{eff}[U_0]\,\} \\ &= S_{eff}[U_0] \;-\; i\,N_c\,\mathrm{Sp}\,\log\left(1 - \frac{1}{i\partial_t - H}\,\Omega\right) \end{aligned}$$

perturbative expansion in Ω

$$
\begin{aligned}
&\mathrm{Sp}\,\log\left(1-\frac{1}{i\partial_t-H}\,\Omega\right)\\
&= T\int_{-\infty}^{\infty}\frac{d\omega}{2\pi}\,\mathrm{Tr}\,\log\left(1-\frac{1}{\omega-H}\,\Omega\right)\\
&= T\int\frac{d\omega}{2\pi}\,\mathrm{Tr}\left(-\frac{1}{\omega-H}\,\Omega-\frac{1}{2}\,\frac{1}{\omega-H}\,\Omega\,\frac{1}{\omega-H}\,\Omega+\cdots\right)\\
&= -T\int\frac{d\omega}{2\pi}\sum_n\frac{1}{\omega-E_n}\,\langle n\,|\,\Omega\,|\,n\rangle \qquad (\Rightarrow\ \text{vanish}\,!)\\
&\quad -T\int\frac{d\omega}{2\pi}\sum_{m,n}\frac{1}{(\omega-E_n)(\omega-E_m)}\,\langle n\,|\,\Omega\,|\,m\rangle\langle m\,|\,\Omega\,|\,n\rangle+\cdots
\end{aligned}
$$

then

$$
\begin{aligned}
&\mathrm{Sp}\,\log\left(1-\frac{1}{i\partial_t-H}\,\Omega\right)\\
&= T\cdot\frac{1}{4}\,i\sum_{m>0,n\le 0}\frac{\langle n\,|\,\tau_a\,|\,m\rangle\langle m\,|\,\tau_b\,|\,n\rangle}{E_m-E_n}\,\Omega_a\,\Omega_b+\cdots\\
&\equiv T\cdot\frac{1}{2}\,i\cdot I_{ab}\cdot\Omega_a\,\Omega_b
\end{aligned}
$$

where

$$
I_{ab}\equiv\frac{1}{2}\sum_{m>0,n\le 0}\frac{<n\,|\,\tau_a\,|\,m><m\,|\,\tau_b\,|\,n>}{E_m-E_n}=\delta_{ab}\,I
$$

with

$$
I=\frac{1}{2}\sum_{m>0,n\le 0}\frac{<n\,|\,\tau_3\,|\,m><m\,|\,\tau_3\,|\,n>}{E_m-E_n}\ :\ \textbf{moment of inertia}
$$

effective lagrangian

$$S_{eff}[U] \equiv T \cdot L_{eff}[U]$$

with

$$L_{eff}[U] = -E_{static}[U_0] + \frac{1}{2} I \, \Omega_a^2$$

canonical quantization : (crude argument)

$\Omega_a \sim$ **time derivative** of **collective coordinate**

canonical momentum : $\hat{J}_a \sim \dfrac{\partial L_{eff}}{\partial \Omega_a} = I \, \Omega_a$

then

$$\begin{aligned} H_{eff} &= \hat{J}_a \Omega_a - L_{eff} \\ &= E_{static}[U_0] + \frac{\hat{J}_a^2}{2I} = E_{static}[U_0] + H_{rot} \end{aligned}$$

$\hat{J}_a$: collective angular momentum operator

H_{rot} : hamiltonian of classical **symmetric top**

eigenstate of H_{rot}

$$H_{rot} \Psi^{(J)}_{M_J M_T}[A] = \frac{J(J+1)}{2I} \Psi^{(J)}_{M_J M_T}[A]$$

$$\Psi^{(J)}_{M_J M_T}[A] = \sqrt{\frac{2J+1}{8\pi^2}} (-1)^{T+T_3} \cdot \underbrace{D^{(J)}_{-T_3 J_3}[A]}_{\text{Wigner rotation matrix}}$$

nucleon observables : (M.E. of **quark bilinear operator**)

$$
\begin{aligned}
\langle \bar{\psi} O^\mu \psi \rangle &= \int \mathcal{D}\psi \, \mathcal{D}\psi^\dagger \;\; \bar{\psi} \, O^\mu \, \psi \;\; e^{i \int d^4x \, \bar{\psi} (i \partial\!\!\!/ - M U^{\gamma_5}) \psi} \\
&= \frac{1}{i} \frac{\delta}{\delta A_\mu} \int \mathcal{D}\psi \mathcal{D}\psi^\dagger \;\; e^{i \int d^4x \, \bar{\psi} (i \partial\!\!\!/ - M U^{\gamma_5} + A_\mu O^\mu) \psi} \, |_{A_\mu \to 0} \\
&= \frac{N_c}{i} \frac{\delta}{\delta A_\mu} \, \mathrm{Sp} \log (i \, \partial\!\!\!/ - M U^{\gamma_5} + A_\mu O^\mu) \, |_{A_\mu \to 0} \\
&= \frac{N_c}{i} \, \mathrm{Sp} \, [\frac{1}{i \, \partial\!\!\!/ - M U^{\gamma_5}} \, O^\mu]
\end{aligned}
$$

collective rotation

$$
U^{\gamma_5}(\boldsymbol{x}, t) \;=\; A(t) \, U_0^{\gamma_5}(\boldsymbol{x}) \, A^\dagger(t)
$$

$$
\Downarrow
$$

$$
\langle \bar{\psi} O^\mu \psi \rangle \;=\; \frac{N_c}{i} \, \mathrm{Sp} \, [\frac{1}{i\partial_t - H - \Omega} \, \tilde{O}^\mu]
$$

with

$$
\tilde{O}^\mu \;\equiv\; A^\dagger(t) \, \gamma^0 \, O^\mu \, A(t)
$$

perturbative expansion in Ω : ($\sim 1/N_c$ expansion)

$$
\frac{1}{i\partial_t - H - \Omega} = \frac{1}{i\partial_t - H} + \frac{1}{i\partial_t - H} \, \Omega \, \frac{1}{i\partial_t - H} + \cdots
$$

final answer for nucleon observables

$$\langle J' M'_J M'_T \,|\, O \,|\, J M_J M_T \rangle \;=\; \int \mathcal{D}A \;\; \Psi^{(J')*}_{M'_J M'_T}[A] \; \langle O \rangle_A \; \Psi^{(J)}_{M_J M_T}[A]$$

with

$$\langle O \rangle_A \;=\; \langle O \rangle_A^{(0)} \;+\; \langle O \rangle_A^{(1)} \;+\; \cdots$$

$O\,(\Omega^0)$: leading N_c term

$$\langle O \rangle_A^{(0)} \;=\; N_c \sum_{n \leq 0} \langle\, n \,|\, \tilde{O} \,|\, n \,\rangle$$

diagonal sum over **occupied** states (valence + sea)

$O\,(\Omega^1)$: $1/N_c$ correction term

$$\langle O \rangle_A^{(1)} \;=\; \frac{N_c}{2} \sum_{m>0, n \leq 0} \frac{1}{E_m - E_n} \left[\langle n \,|\, \tilde{O} \,|\, m \rangle \langle m \,|\, \Omega \,|\, n \rangle + (\tilde{O} \leftrightarrow \Omega) \right]$$

transition from **occupied** to **nonoccupied** states

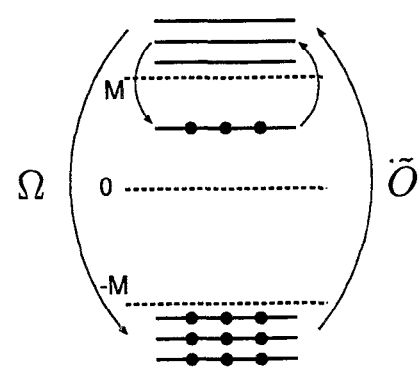

model needs **regularization**

$$
\begin{aligned}
S_{eff}[U] &= -i\, N_c \,\mathrm{Sp}\, \log\left[\, i\, \partial\!\!\!/ - M U^{\gamma_5}\right] \\
&= \frac{4N_c}{f_\pi^2}\, I_2(M) \cdot \frac{1}{2}\,(\partial_\mu \boldsymbol{\pi})^2 \;+\; \cdots
\end{aligned}
$$

where

$$
I_2(M) \;\equiv\; i \int \frac{d^4k}{(2\pi)^4} \frac{M^2}{(k^2 - M^2)^2} \quad : \quad \textbf{log divergence}
$$

Pauli-Villars regularization scheme

$$
\boxed{S_{eff}^{reg} \;\equiv\; S_{eff}^{M} \;-\; \left(\frac{M}{M_{PV}}\right)^2 S_{eff}^{M_{PV}}}
$$

then

$$
I_2^{reg} \;\equiv\; I_2(M) - \left(\frac{M}{M_{PV}}\right)^2 I_2(M_{PV}) \;=\; \frac{M^2}{16\pi^2} \log\left(\frac{M_{PV}}{M}\right)^2
$$

$$
\frac{N_c}{4\pi^2} M^2 \log\left(\frac{M_{PV}}{M}\right)^2 = f_\pi^2 \;\Longrightarrow\; \boldsymbol{M_{PV}}
$$

other observables

$$
\langle O \rangle^{reg} \;\equiv\; \langle O \rangle^{M} \;-\; \left(\frac{M}{M_{PV}}\right)^2 \langle O \rangle^{M_{PV}}
$$

3. CQSM and Parton Distribution Functions (PDF)

quark distribution functions

$$q(x) = \frac{1}{4\pi}\int_{-\infty}^{\infty} dz^0 \; e^{i\,x\,M_N\,z^0}$$

$$\times \; \underbrace{\langle N(\boldsymbol{P}=0)\,|\,\psi^\dagger(0)\,O\,\psi(z)\,|\,N(\boldsymbol{P}=0)\rangle}\;|_{z^3=-z^0,\,z_\perp=0}$$

nucleon matrix element of **bilocal operator**

$$\Downarrow$$

taking full account of this **nonlocality** !

Novel $\boldsymbol{N_c}$ **dependencies** of twist-2 distributions

$$\begin{cases} u(x)+d(x) & \sim \; N_c\,[\,O(\Omega^0) \;+\; 0\;] & \sim \; O(N_c^1) \\ u(x)-d(x) & \sim \; N_c\,[\;\mathbf{0}\;+\;O(\Omega^1)\,] & \sim \; O(N_c^0) \\ \Delta u(x)+\Delta d(x) & \sim \; N_c\,[\;\mathbf{0}\;+\;O(\Omega^1)\,] & \sim \; O(N_c^0) \\ \Delta u(x)-\Delta d(x) & \sim \; N_c\,[\,O(\Omega^0) \;+\; \underbrace{O(\Omega^1)}\,] & \sim \; O(N_c^1) \;+\; \underbrace{O(N_c^0)} \end{cases}$$

$$\boldsymbol{\Omega \;\propto\; 1/N_c}$$

$\boxed{\text{basis of analysis}}$

$$\langle N(\boldsymbol{P}) \,|\, \psi^\dagger(0)\, O\, \psi(z) \,|\, N(\boldsymbol{P})\rangle$$

$$\sim \int d^3x\, d^3y\; e^{-i\boldsymbol{P}\cdot\boldsymbol{x}}\, e^{i\boldsymbol{P}\cdot\boldsymbol{y}} \int \mathcal{D}\pi \int \mathcal{D}\psi\, \mathcal{D}\psi^\dagger$$
$$\times\; J_N(\frac{T}{2}, \boldsymbol{x}) \cdot \psi^\dagger(0)\, O_a\, \psi(z) \cdot J_N^\dagger(-\frac{T}{2}, \boldsymbol{y})\; e^{i\int d^4x\, \mathcal{L}_{CQSM}}$$

where

$$J_N(x) \;=\; \frac{1}{N_c!}\, \epsilon^{\alpha_1\cdots\alpha_{N_c}}\, \Gamma^{\{f_1\cdots f_N\}}_{JJ_3,TT_3}\; \psi_{\alpha_1 f_1}(x)\cdots\psi_{\alpha_{N_c} f_{N_c}}(x)$$

composite operator carrying the quantum numbers JJ_3, TT_3 of the nucleon

<u>rotational zero mode</u>

$$U^{\gamma_5}(\boldsymbol{x}, t) \;=\; A(t)\; U_0^{\gamma_5}(\boldsymbol{x})\; A^\dagger(t) \quad : \quad A(t) \in SU(2)$$

<u>variable transform</u> : $\psi(x) \;\to\; \psi_A(x) \;=\; A(t)\,\psi(t)$

$$e^{i\int d^4x\, \bar\psi\,(\,i\partial\!\!\!/ - MU^{\gamma_5}\,)\,\psi} \;=\; e^{i\int d^4x\, \psi_A^\dagger\,(\,i\partial_t - H - \Omega\,)\,\psi_A}$$
$$\psi^\dagger(0)\, O_a\, \psi(z) \;=\; \psi_A^\dagger(0)\; \underbrace{A^\dagger(0)\, O_a\, A(z_0)}\; \psi_A(z)$$

$$\Downarrow$$

perturbative expansion in $\boldsymbol{\Omega}$

2 new features in PDF calculation

$$\psi_A^\dagger(0)\,\underbrace{A^\dagger(0)\,O_a\,A(z_0)}\,\psi_A(z)$$

1. Ω can operate **between** 0 and z_0 !
2. **nonlocality** (in time) of $A^\dagger(0)\,O_a\,A(z_0)$

novel nonlocality correction

$$\begin{aligned} A^\dagger(0)O_aA(z_0) &= A^\dagger(0)\,O_a\,A(0) \;+\; z_0\,A^\dagger(0)\,O_a\,\dot{A}(0) \;+\; \cdots \\ &= A^\dagger(z_0)\,O_a\,A(z_0) \;-\; z_0\,\dot{A}^\dagger(z_0)\,O_a\,A(z_0) \;+\; \cdots \end{aligned}$$

in quantization : ($\Omega_a \to \hat{J}_a/I$)

$$\begin{aligned} A^\dagger(0)\,O_a\,A(z_0) &\to A^\dagger\,O_a\,A \;+\; \frac{1}{2}\,z_0\,(\,A^\dagger\,O_a\,A\,A^\dagger\,\dot{A} - \dot{A}^\dagger\,A\,A^\dagger\,O_a\,A\,) \\ &= \tilde{O}_a \;+\; i\;z_0\,\frac{1}{2}\,\{\Omega, \tilde{O}_a\} \end{aligned}$$

$$\Downarrow$$

2nd term : $O(\Omega^1)$ correction from **nonlocality**

schematically

$$q(x) \;=\; \frac{1}{4\pi}\int_{-\infty}^{\infty} dz_0\; e^{ix\,M_N\,z_0}$$
$$\times \int \mathcal{D}A \;\; \Psi^{(J)*}_{M_J M_T}[A] \;\; \langle O(0,z_0)\rangle_A \;\; \Psi^{(J)}_{M_J M_T}[A]$$

where

$$\langle O(0,z_0)\rangle_A \;=\; O(\Omega^0) \;+\; O(\Omega^1) \;+\; \cdots$$

with

$O(\Omega^0) =$

$O(\Omega^1) =$ 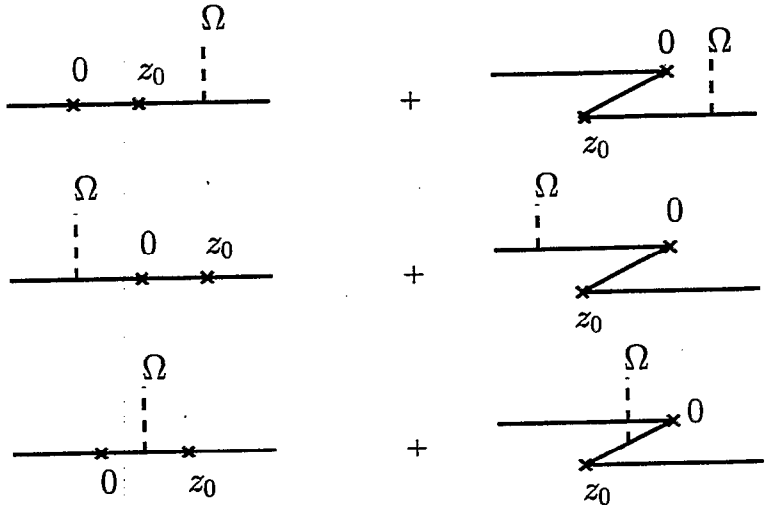

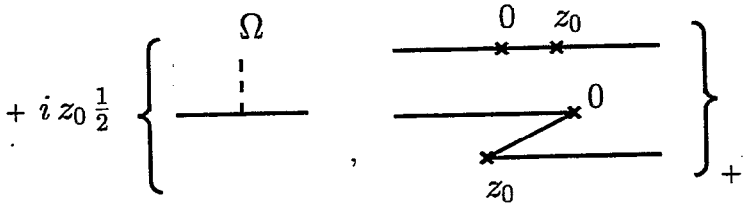

$O(\Omega^1)$ correction resulting from expansion of $A^\dagger(0)O_a A(z_0)$ in z_0

nonlocality correction in time

sample form of $O(\Omega^0)$ contribution

$$\Delta u(x) - \Delta d(x) \;=\; \langle D_{33}\rangle_{p\uparrow} \cdot M_N \; N_c \sum_{n\leq 0} \langle\, n \,|\, (1+\gamma^0\gamma^3)\,\gamma_5\,\delta_n \,|\, n\,\rangle$$

with

$$\delta_n \;\equiv\; \delta(xM_N - E_n - \hat{p}_3), \qquad (-1 < x < 1)$$

sample form of $O(\Omega^1)$ contribution

$$\Delta u(x) + \Delta d(x) \;=\; [\,\Delta u(x) + \Delta d(x)\,]^{(1)}_{\{A,B\}} + \underbrace{[\,\Delta u(x) + \Delta d(x)\,]^{(1)}_{C}}_{\text{nonlocality correction}}$$

with

$$[\,\Delta u(x) + \Delta d(x)\,]^{(1)}_{\{A,B\}} \;=\; \langle 2\,J_3\rangle_{p\uparrow} \cdot M_N \,\frac{N_c}{2I}$$
$$\times \sum_{m=all,n\leq 0} \frac{1}{E_m - E_n} \,\langle\, n \,|\, \tau_3 \,|\, m\,\rangle\, \langle\, m \,|\, \tau_3\,(1+\gamma^0\gamma^3)\,\gamma_5\,\delta_n \,|\, n\,\rangle$$

$$[\,\Delta u(x) + \Delta d(x)\,]^{(1)}_{C} \;=\; \langle 2\,J_3\rangle_{p\uparrow} \cdot \frac{N_c}{4I}$$
$$\times \frac{d}{dx} \sum_{n\leq 0} \langle\, n \,|\, \tau_3\,(1+\gamma^0\gamma^3)\,\gamma_5\,\delta_n \,|\, n\,\rangle$$

from

$$\frac{1}{2\pi} \int_{-\infty}^{\infty} dz_0 \; i\, z_0 \; e^{i\,(xM_N - E_n - \hat{p}_3)\,z_0} \;=\; \frac{1}{M_N}\,\frac{d}{dx}\,\delta(xM_N - E_n - \hat{p}_3)$$

♣ **naive expression** for $\Delta u(x) + \Delta d(x)$
obtained with ignorance of nonlocality effects

$$\Delta u(x) + \Delta d(x) \;=\; \langle 2J_3 \rangle_{p\uparrow} \cdot M_N \, \frac{N_c}{2\,I}$$
$$\times \sum_{m>0, n\leq 0} \frac{1}{E_m - E_n} \, \langle n| \, \tau_3 \, |m\rangle \langle m| \, \tau_3 \, (1 + \gamma^0 \gamma^3) \, \gamma_5 \, \delta_n \, |n\rangle$$

— from **occupied** to **nonoccupied** —

$$\Downarrow$$

<u>importance of **nonlocality effects** (NLE)</u>

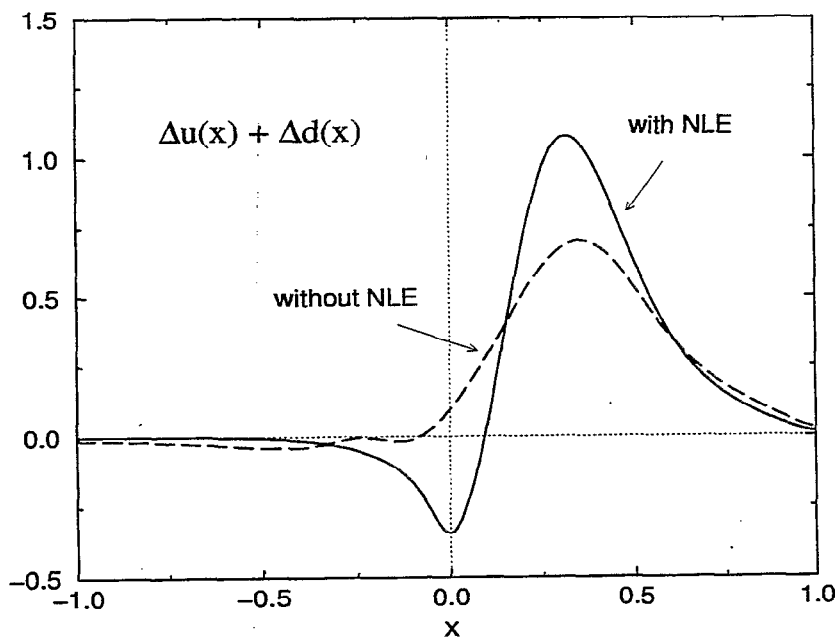

$$\Delta u(-x) \;+\; \Delta d(-x) \;=\; [\,\Delta\bar{u}(x) \;+\; \Delta\bar{d}(x)\,] \qquad (0 < x < 1)$$

4. Comparison with High Energy Data

- **only 1 parameter** of the CQSM (dynamical quark mass M) is fixed from the analyses of **nucleon LE observables**

$$M = 375\,\mathrm{MeV} \quad (\text{ this gives } M_{PV} \simeq 562\,\mathrm{MeV})$$

$$\Downarrow$$

parameter free predictions for PDF

- use predictions of CQSM as **initial-scale distributions**

$$u(x),\ \bar{u}(x),\ d(x),\ \bar{d}(x),\ \Delta u(x),\ \Delta\bar{u}(x),\ \Delta d(x),\ \Delta\bar{d}(x)$$

$$s(x) = \bar{s}(x) = 0,\ g(x) = 0,\ \Delta s(x) = \Delta\bar{s}(x) = 0,\ \Delta g(x) = 0$$

- **scale dependence of PDF** : (setting $N_c = 3$)

Fortran Program of DGLAP evolution eqs. at **NLO**

provided by Saga group

initial energy scale is fixed to be

$$Q^2_{ini} = 0.30\,\mathrm{GeV}^2 \simeq (550\,\mathrm{MeV})^2$$

model predictions for twist-2 PDF

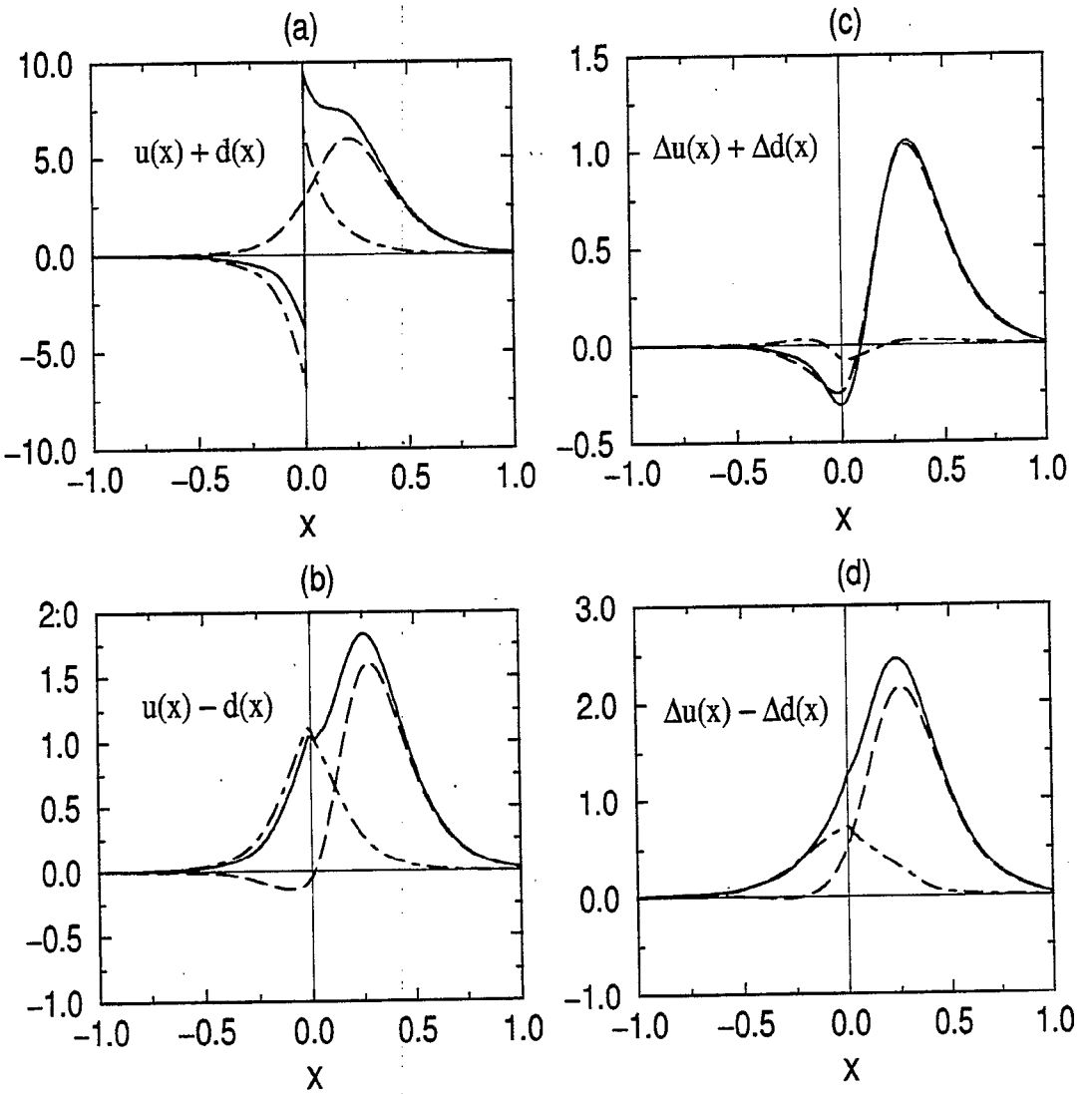

$$u(-x) \pm d(-x) = -[\bar{u}(x) \pm \bar{d}(x)] \qquad (0 < x < 1)$$

$$\Delta u(-x) \pm \Delta d(-x) = \Delta\bar{u}(x) \pm \Delta\bar{d}(x) \qquad (0 < x < 1)$$

complete set of twist-2 PDF

$$
\begin{aligned}
q(x) &: \text{ unpolarized distribution} \\
\Delta q(x) &: \text{ longitudinally polarized distribution} \\
\delta q(x) &: \textbf{ transversity distribution}
\end{aligned}
$$

Soffer inequality

$$
|\pm\, \delta q(x)| \;\leq\; \frac{1}{2}\,(\pm q(x) \;+\; \Delta q(x)) \qquad \begin{cases} x > 0 \\ x < 0 \end{cases}
$$

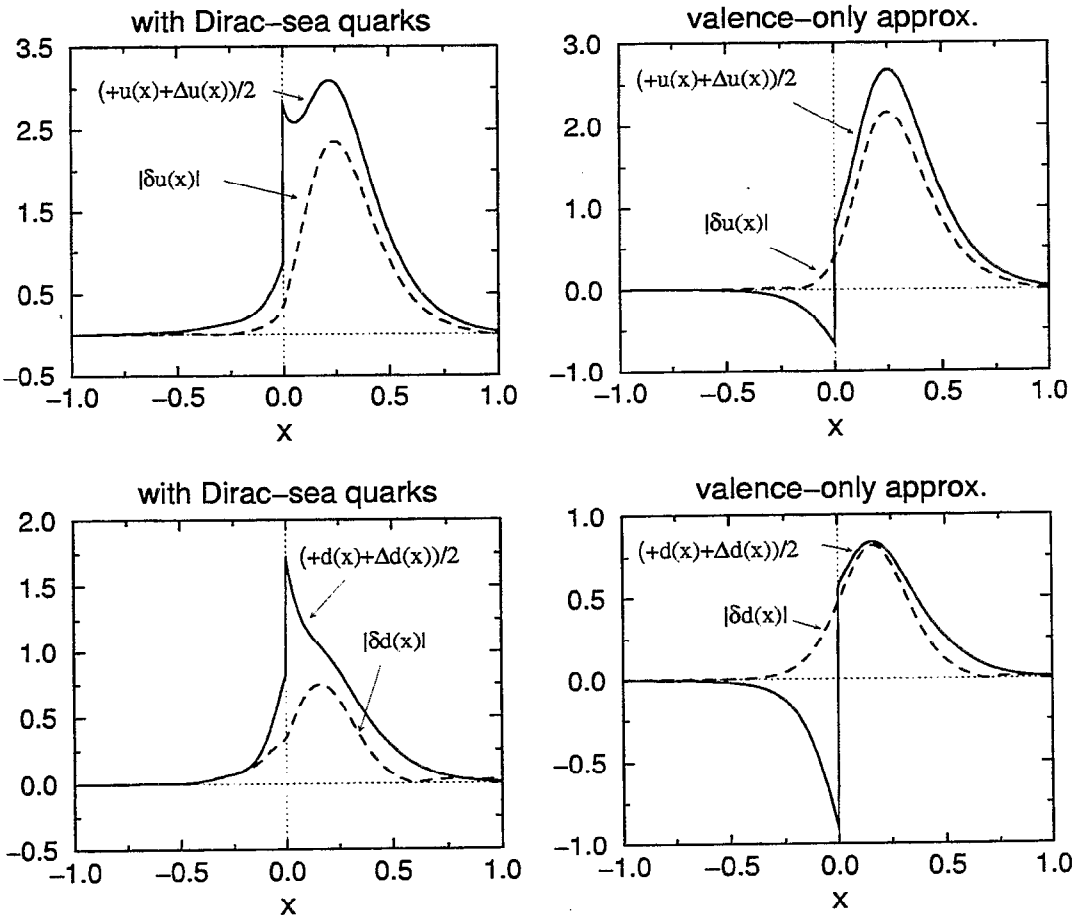

comparison with NMC data

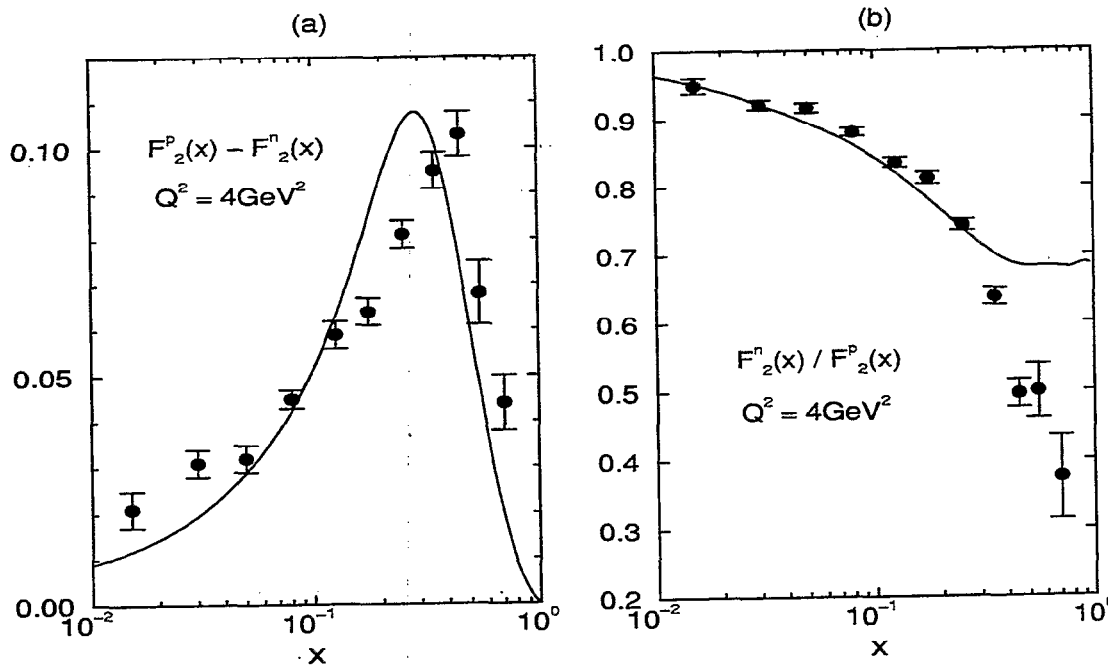

Gottfried sum

$$S_G = \int_0^1 \frac{F_2^p(x) - F_2^n(x)}{x}\, dx = \frac{1}{3} + \int_0^1 \{\, \bar{u}(x) - \bar{d}(x) \,\}$$

$$S_G^{th}(Q^2 = 4\,\mathrm{GeV}^2) \simeq \mathbf{0.204} < \frac{1}{3}$$

$$\Updownarrow$$

$$S_G^{exp}(Q^2 = 4\,\mathrm{GeV}^2) = \mathbf{0.228 \pm 0.007}$$

Fig.3

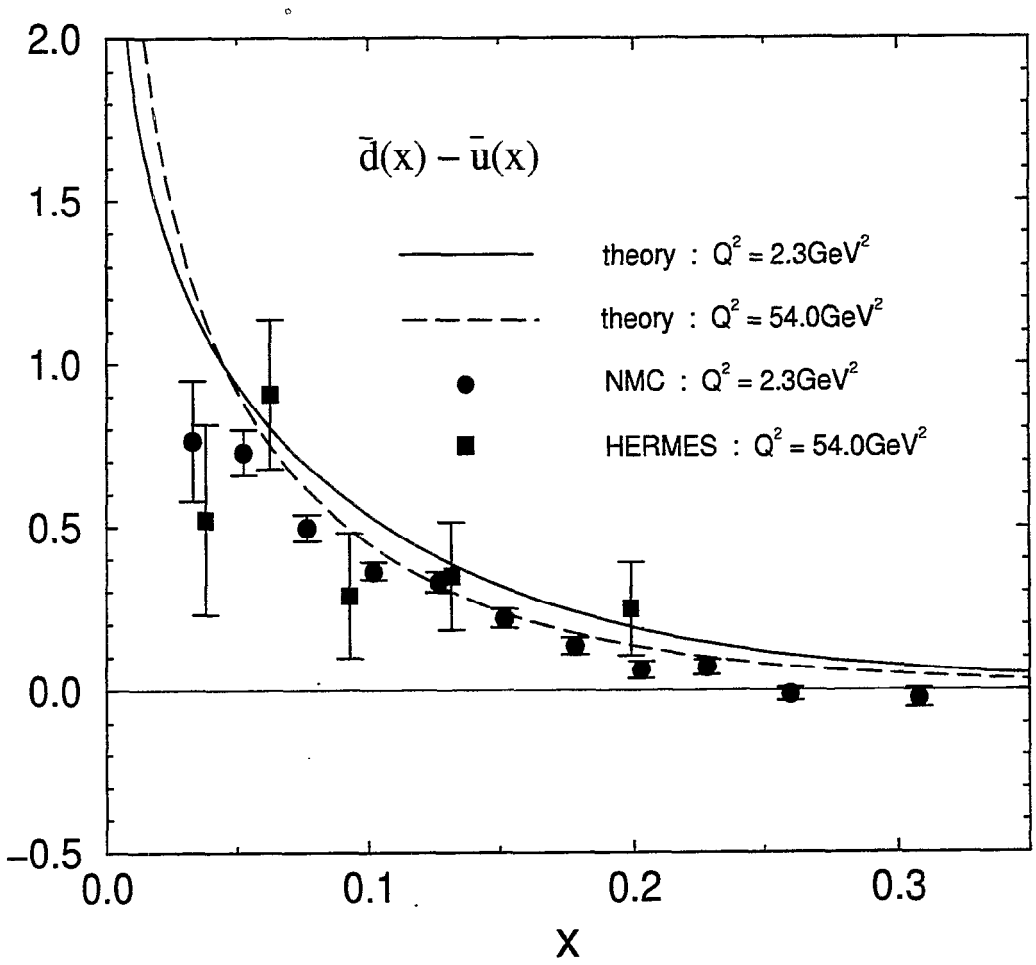

$$\Downarrow$$

$$\bar{d}(x) \;>\; \bar{u}(x) \quad \text{in the proton !}$$

comparison with EMC and SMC data

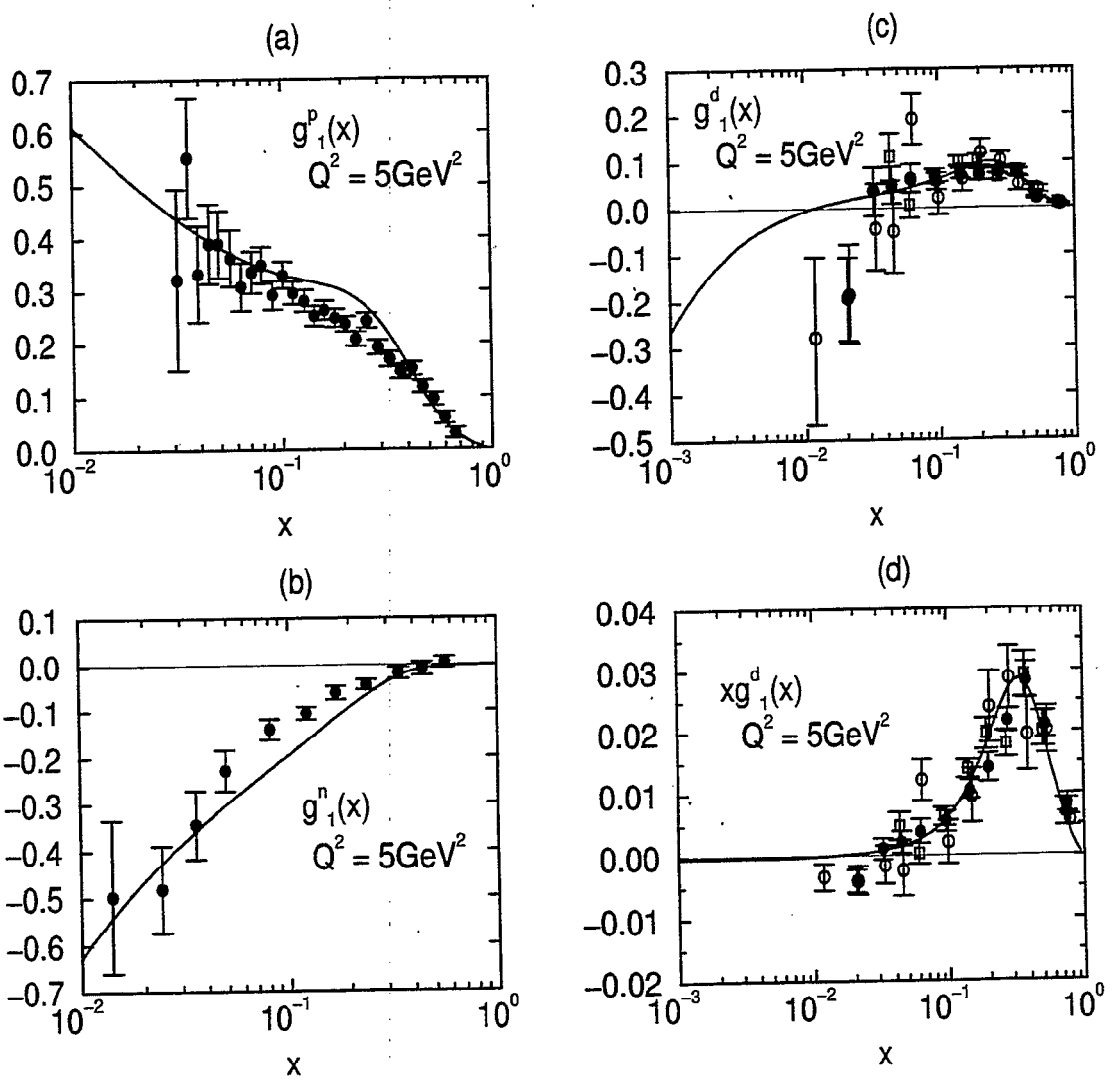

good reproduction of **neutron data**

$\Downarrow$

manifestation of **chiral symmetry** in high energy observables !

isospin asymmetry for spin-dependent sea quark distributions

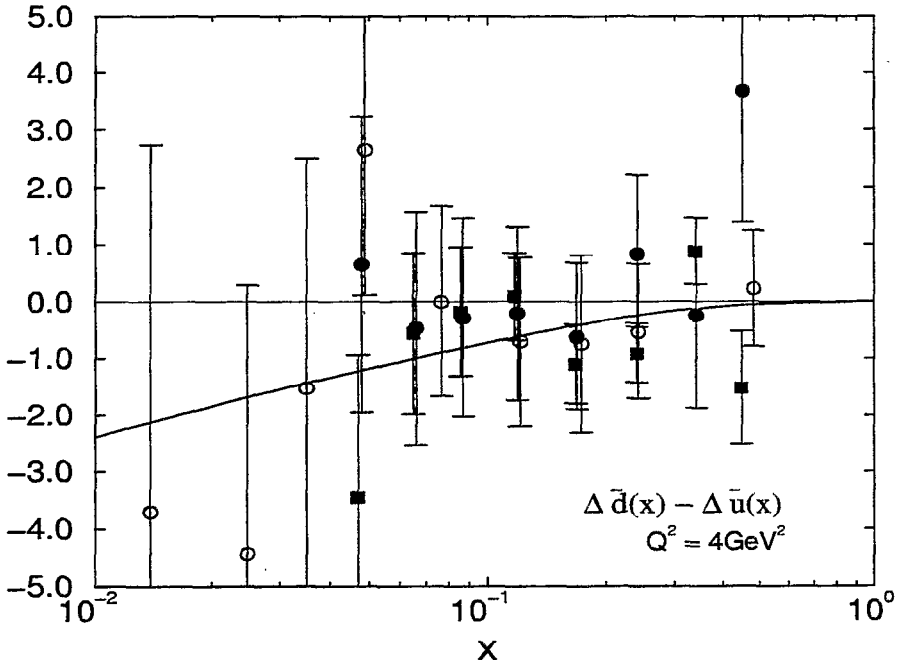

parametrization by Morii and Yamanishi

$$\boxed{\Delta\bar{d}(x) - \Delta\bar{u}(x) \;=\; \boldsymbol{C}\, x^{\alpha}\, \left(\bar{d}(x) - \bar{u}(x)\right)}$$

$$\boldsymbol{C} = \mathbf{-3.40}\ (<0), \quad \alpha \;=\; 0.567$$

fitting the prediction of CQSM

$$\boldsymbol{C} = \mathbf{-2.0}\ (<0), \quad \alpha \;\simeq\; 0.12$$

$|C| > 1$ is consistent with N_c - **counting**

$$\begin{cases} \Delta\bar{u}(x) - \Delta\bar{d}(x) & \sim \quad O(N_c^1) \\ \bar{u}(x) - \bar{d}(x) & \sim \quad O(N_c^0) \end{cases}$$

strong correlation between **spin** & **isospin** imbedded in the hedgehog configuration

$\Updownarrow$ compare !

Meson Cloud Convolution Model would not lead to large spin polarization of sea quarks, since

- **pion carries no spin**
- heavier meson clouds are much weaker

<u>Some other supports</u>

- D. de Florian and Sassot, P.R. D62 (2000) 094025

  NLO analysis of $\left\{ \begin{array}{c} \text{inclusive} \\ \text{semi-inclusive} \end{array} \right\}$ polarized DIS

  $\Downarrow$

  $\boldsymbol{\Delta\bar{u}(x) > 0}$, but $\Delta\bar{d}(x)$ undetermined !

- R.S. Bhalerao, hep-ph / 0003075

  semi-theoretical analysis (statistical model)

  $\Downarrow$

  $$\boldsymbol{\Delta\bar{u}(x) > 0 > \Delta\bar{s}(x) > \Delta\bar{d}(x)}$$

spin and orbital angular momentum distribution functions

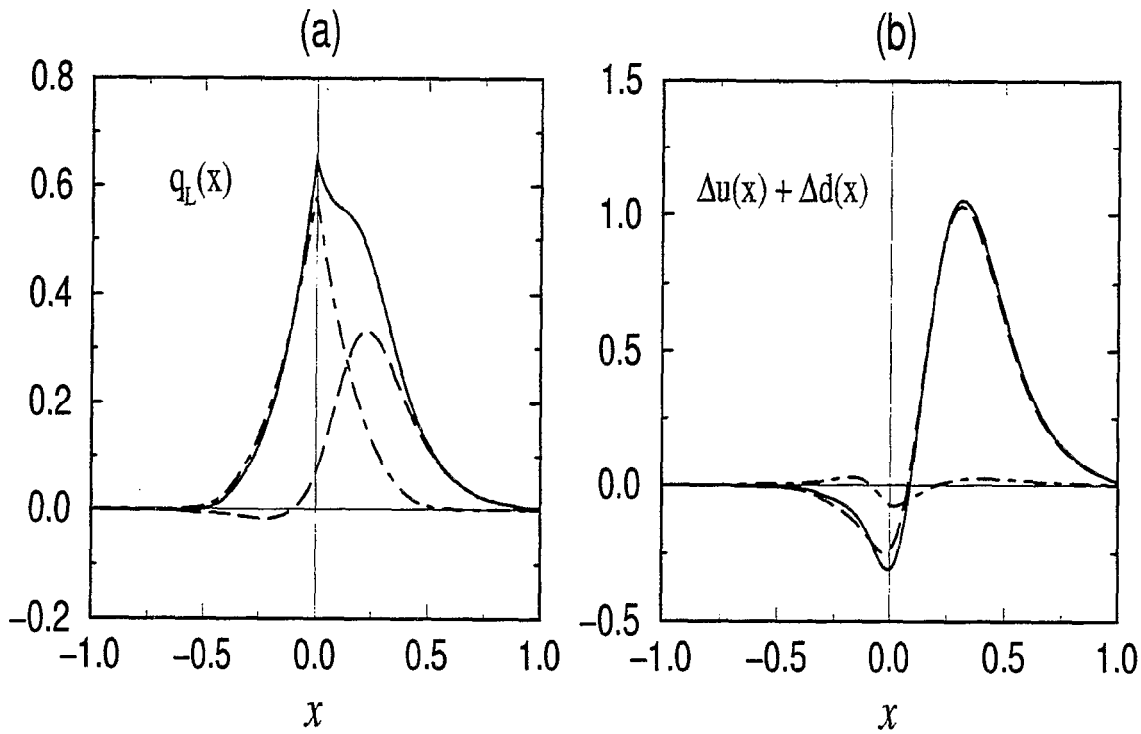

nucleon spin contents at low renormalization point

	quark	antiquark	total
$\Delta\Sigma$	0.40	- 0.05	**0.35**
$2\,L_q$	0.46	**0.19**	**0.65**
$\Delta\Sigma + 2\,L_q$	0.86	0.15	1.00

Comparison with recent lattice QCD calculation

N. Mathur et. al. , hep-ph / 9912289

from analysis of energy momentum tensor form factor

$$\langle J_{quark} \rangle \simeq \mathbf{60}\,\%$$

combining with the previous estimates for $\langle \Delta\Sigma \rangle$

$$\underset{\sim \mathbf{25}\,\%}{\langle \frac{1}{2}\Sigma \rangle} + \underset{\sim \mathbf{35}\,\%}{\langle L_q \rangle} + \underset{\sim 40\%}{\langle J_{gluon} \rangle} = \frac{1}{2}$$

Compare with

$$60\,\% \quad \text{of} \quad \langle \frac{1}{2}\Sigma \rangle^{CQSM} \simeq \mathbf{21}\,\%$$

$$60\,\% \quad \text{of} \quad \langle L_q \rangle^{CQSM} \simeq \mathbf{39}\,\%$$

interesting common feature

$$\langle L_q \rangle > \langle \frac{1}{2}\Sigma \rangle$$

scale dependencies of nucleon spin contents

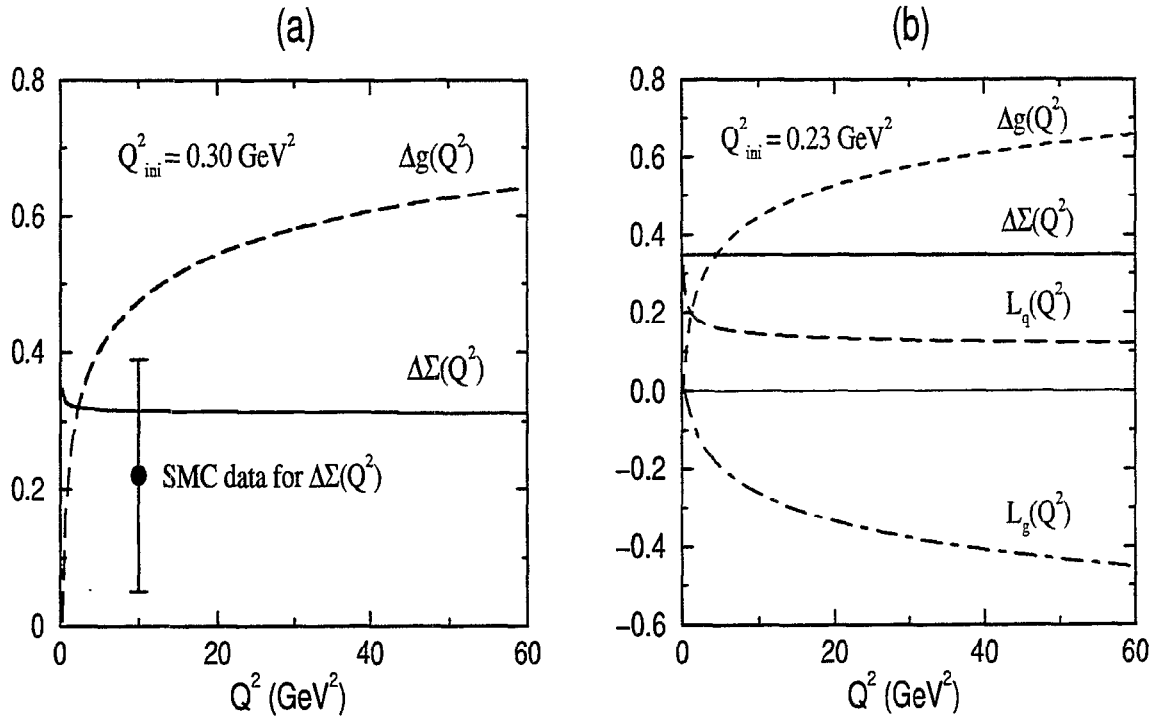

initial energy scale of DGLAP equation

$$Q^2_{ini}(NLO) \;=\; 0.30\,\mathrm{GeV}^2$$

$$Q^2_{ini}(LO) \;=\; 0.23\,\mathrm{GeV}^2$$

NLO

$$\Delta\Sigma\,(Q^2 = 10\,\mathrm{GeV}^2) \;=\; \mathbf{0.31} \;\Longleftrightarrow\; \Delta\Sigma_{SMC} \;=\; \mathbf{0.22 \pm 0.17}$$

1st moment sum rules (axial and tensor charges)

R.L. Jaffe and X. Ji, N. P. B375 (1992) 527

$$g_A^{(0,3)} = \int_0^1 dx \, \{ [\Delta u(x) + \Delta\bar{u}(x)] \pm [\Delta d(x) + \Delta\bar{d}(x)] \}$$
$$g_T^{(0,3)} = \int_0^1 dx \, \{ [\delta u(x) - \delta\bar{u}(x)] \pm [\delta d(x) - \delta\bar{d}(x)] \}$$

NRQM

$$g_A^{(3)} = g_T^{(3)} = \frac{5}{3}$$
$$g_A^{(0)} = g_T^{(0)} = 1$$

MIT bag model (with lower component)

$$g_A^{(3)} = \frac{5}{3} \cdot \int (f^2 - \frac{1}{3} g^2), \qquad g_T^{(3)} = \frac{5}{3} \cdot \int (f^2 + \frac{1}{3} g^2)$$
$$g_A^{(0)} = 1 \cdot \int (f^2 - \frac{1}{3} g^2), \qquad g_T^{(0)} = 1 \cdot \int (f^2 + \frac{1}{3} g^2)$$

where

$$\psi_{g.s.} = \begin{pmatrix} f(r)\, \chi_s \\ g(r)\, i\, \boldsymbol{\sigma} \cdot \hat{\boldsymbol{r}}\, \chi_s \end{pmatrix}$$

important observation

$$g_A^{(0)}/g_A^{(3)} = g_T^{(0)}/g_T^{(3)} = 3/5$$
$$\Downarrow$$

limit of **valence quark model** without chiral symmetry ?

axial versus tensor charges

	CQSM	MIT-bag	Lattice QCD*)	Experiment
$g_A^{(3)}$	**1.40**	1.06	0.99	**1.254** $\pm$ 0.006 (Q^2-indep.)
$g_A^{(0)}$	**0.35**	0.64	0.18	**0.31** $\pm$ 0.07 ($Q^2 = 10$ GeV^2)
$g_T^{(3)}$	**1.22**	1.34	1.07	–
$g_T^{(0)}$	**0.67**	0.80	0.56	–
$g_A^{(0)}/g_A^{(3)}$	**0.25**	0.60	0.18	**0.24**
$g_T^{(0)}/g_T^{(3)}$	**0.55**	0.60	0.52	–

*) Y.Kuramashi, at Quark Lepton Nuclear Physics, (RCNP), 1997

$\Downarrow$

- qualitative difference between **transversity distributions** and **longitudinally polarized distributions**

$$g_A^{(0)}/g_A^{(3)} = g_T^{(0)}/g_T^{(3)} \quad \text{(NRQM, MIT bag model)}$$

$$g_A^{(0)}/g_A^{(3)} << g_T^{(0)}/g_T^{(3)} \quad \text{(\textbf{CQSM}, Lattice)}$$

Single target-spin asymmetries in semi-inclusive pion electroproduction

$$e + \vec{p} \longrightarrow e' + \pi + X$$

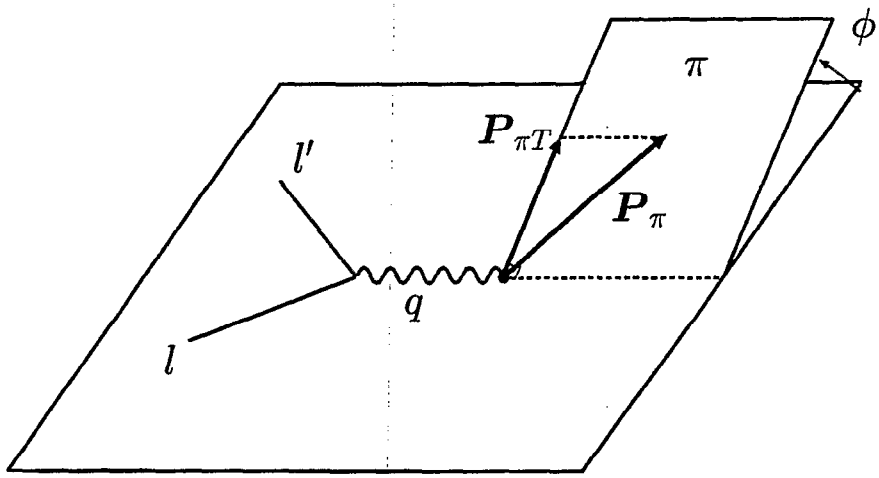

kinematics

$$s = 2P \cdot l,\ q = l - l',\ x = Q^2/2P \cdot q,\ y = 2P \cdot q/s$$

asymmetries measured by **HEREMES**

$$A_{UL}^W = \frac{\int d\phi\, dy\ W(\phi)\ (d\sigma^+/S_H^+\ dx\, dy\, d\phi\ -\ d\sigma^-/S_H^-\ dx\, dy\, d\phi)}{\frac{1}{2}\int d\phi\, dy\ (d\sigma^+/S_H^+\ dx\, dy\, d\phi\ +\ d\sigma^-/S_H^-\ dx\, dy\, d\phi)}$$

with

$$W(\phi) = \sin\phi \ \text{ or } \ \sin 2\phi$$

$$S_H^\pm \ : \ \text{nucleon polarization}$$

theoretical analysis

- A. Kotzinian, N. P. B441 (1995) 234
- P.J. Mulders and R.D. Tangerman, N. P. B461 (1996) 197
- K.A. Oganessyan et al., hep-ph/9808368, hep-ph/0010261

$$A^{\sin\phi} \simeq \frac{2\,M_\pi}{\langle P_{\pi T}\rangle}\cdot\langle\frac{|P_{\pi T}|}{M_\pi}\,\sin\phi\rangle = \frac{2\,M_\pi}{\langle P_{\pi T}\rangle}\cdot\frac{I_2(x,y,z)}{I_1(x,y,z)}$$

$$A^{\sin 2\phi} \simeq \frac{2\,M\,M_\pi}{\langle P_{\pi T}^2\rangle}\cdot\langle\frac{|P_{\pi T}|^2}{M\,M_\pi}\,\sin 2\,\phi\rangle = \frac{2\,M\,M_\pi}{\langle P_{\pi T}^2\rangle}\cdot\frac{I_3(x,y,z)}{I_1(x,y,z)}$$

where

$$I_1(x,y,z) = \frac{1}{2}\left[1+(1-y)^2\right]\sum_a e_a^2\,x\,f_1^a(x)\,D_1^a(z)$$

$$\begin{aligned} I_2(x,y,z) &= 2\,(2-y)\sqrt{1-y}\,\frac{M}{Q}\,\sum e_a^2 \\ &\times\left\{x^2\,h_L^a(x)\cdot z\,H_1^{\perp(1)a}(z) - x\,h_{1L}^{\perp(1)a}(x)\cdot\tilde{H}^a(z)\right\} \\ &+(1-y)\,\sqrt{1-y}\,\frac{2\,M\,x}{Q}\,\sum_a e_a^2\,x\,h_1^a(x)\cdot z\,H_1^{\perp(1)a}(z) \end{aligned}$$

$$I_3(x,y,z) = 4\,(1-y)\,\sum_a e_a^2\,x\,h_{1L}^{\perp(1)a}(x)\cdot z^2\,H_1^{\perp(1)a}(z)$$

$\Downarrow$ I_1, I_2, I_3 depend on

4 distribution functions **3 fragmentation functions**

$$f_1(x),\ \underbrace{h_1(x),\ h_L(x),\ h_{1L}^{\perp(1)}(x)}_{\textit{chiral odd}} \qquad D_1(z),\ \underbrace{H_1^{\perp(1)}(z),\ \tilde{H}(z)}_{\textit{time-reversal odd}}$$

fragmentation function $D_1^a(z)$

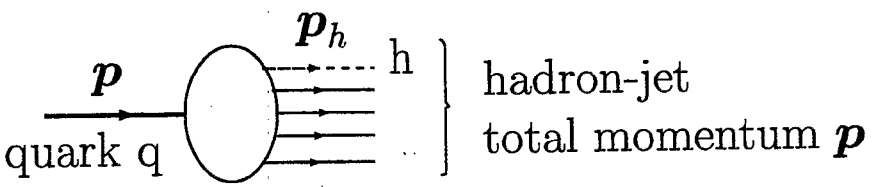

- longitudinal momentum fraction of a hadron h with momentum $\boldsymbol{p}_h$

$$z \equiv \frac{\boldsymbol{p}_h \cdot \boldsymbol{p}}{|\boldsymbol{p}|^2}$$

- probability of finding the hadron h with the momentum fraction between z and $z + dz$

$$D_1^{q \to h}(z)\ dz$$

relatively well-determined from

$$e^+ e^- \longrightarrow \left\{ \begin{array}{c} \pi \\ K \end{array} \right\} + X$$

see, for example

- J. Binnewies, B.A. Kniehl and G. Kramer, Z. Phys. C65 (1995) 471.

time reversal-odd fragmentation function

$$H_1^{\perp(1)a}(z) \;=\; \int d^2\boldsymbol{k}'_T \; \frac{|\boldsymbol{k}_T|^2}{2\,M_h^2} \; H_1^{\perp\,a}(z, \boldsymbol{k}'_T)$$

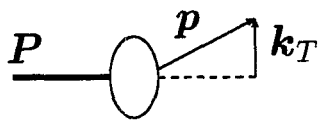

$$\boldsymbol{p} \;=\; x\boldsymbol{P} \;+\; \underbrace{\boldsymbol{k}_T}_{\textit{transverse momentum}}$$

$$\boldsymbol{k}'_T \;=\; -\,z\;\boldsymbol{k}_T$$

$H_1^{\perp}$ = 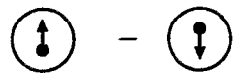

T-odd leading twist F.F, giving the probability of a spinless or unpolarized hadron to be created from a transversely polarized scattered quark

subleading T-odd fragmentation function : $\tilde{H}^a(z)$

$$\tilde{H}^a(z) \;=\; z\,\frac{d}{dz}\left(z\;H_1^{\perp(1)a}(z)\right)$$

$$\Downarrow$$

- existence of **T-odd fragmentation functions** (**Collins mechanism**) opens up new possibility to measure **chiral-odd PDF** in semi-inclusive deep-inelastic scatterings

chiral odd distribution functions

$$h_1^a(x) \;:\; \text{transversity distribution function}$$

$$h_L^a(x) = \underbrace{2\,x \int_x^1 dy\, \frac{h_1^a(y)}{y^2}}_{twist-2\ part} + \underbrace{\bar{h}_L^a(x)}_{interaction-dep.\ part}$$

$$h_{1L}^{\perp(1)a}(x) = \int_x^1 dy\, \left[h_L^a(y) - h_1^a(y) \right]$$

2 frequently used approx.

approximation (i) : **W-W type-approximation**

$$\bar{h}_L^a(x) \simeq 0$$

$$\Downarrow$$

$$h_L^a(x) = 2\,x \int_x^1 dy\, \frac{h_1^a(y)}{y^2}$$

$$h_{1L}^{\perp(1)a}(x) = -\,x^2 \int_x^1 dy\, \frac{h_1^a(y)}{y^2}$$

approximation (ii)

$$h_L(x) \simeq h_1(x)$$

$$\Downarrow$$

$$h_{1L}^{\perp(1)a}(x) = 0 \;:\; \text{adovocated by HERMES group}$$

theoretical predictions of CQSM at $Q^2 = 2.5\,\mathrm{GeV}^2$

using model predictions for $h_1^a(x)$ and $h_L^a(x)$ $\quad (a = u, d, \bar{u}, \bar{d})$

$$\Downarrow$$

$$\bar{h}_L^a(x) = h_L^a(x) - 2x \int_x^1 dy \, \frac{h_1^a(y)}{y^2}$$

$$h_{1L}^{\perp(1)a}(x) = \int_x^1 dy \, [h_L^a(y) - h_1^a(y)]$$

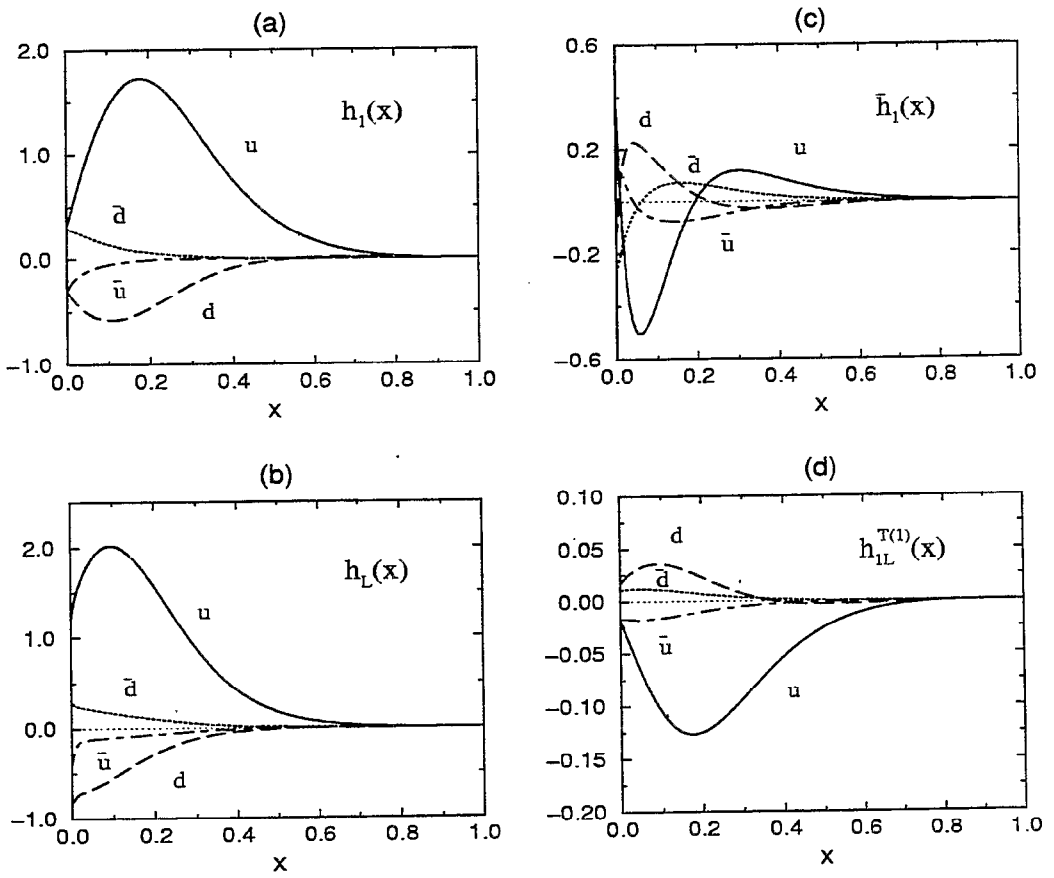

HERMES experiments : $\sin\phi$ and $\sin 2\phi$ asymmetries

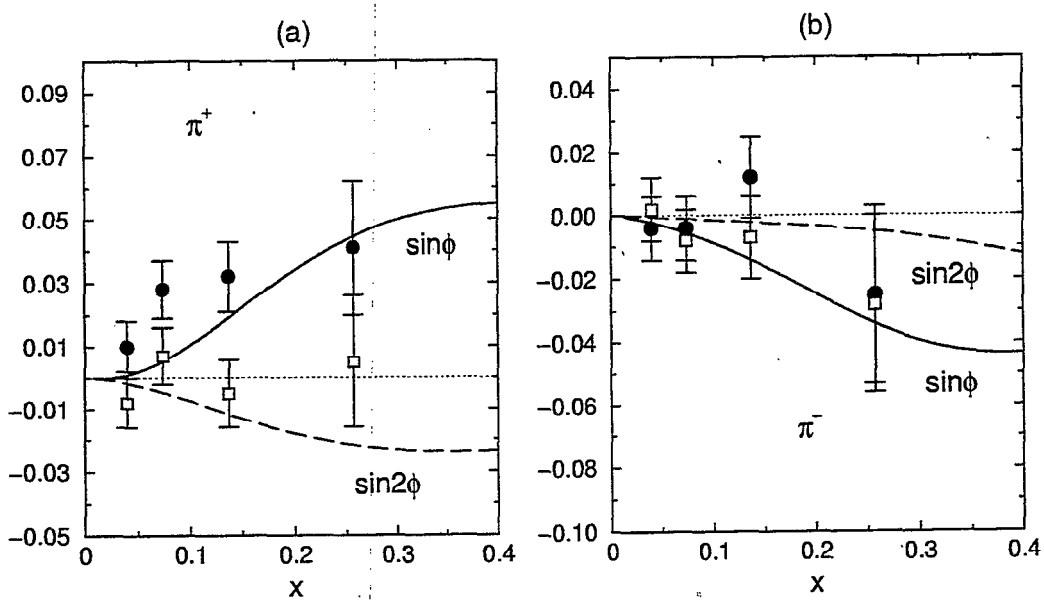

- HERMES group advocates that observed small $\sin 2\phi$ asymmetry is consistent with the ansatz

$$h_{1L}^{\perp(1)}(x) \simeq 0, \quad \text{or} \quad h_L(x) \simeq h_1(x)$$

- while CQSM (as well as MIT bag model) indicates

$$h_L(x) \neq h_1(x)$$

$$\Downarrow$$

need more accurate measurements !

Asymmetry for a target polarized transversely to electron beam

$$A_{OT}^{W} \sim \left\langle \frac{Q_T}{M_\pi} \sin\phi \right\rangle_{OT}$$
$$= \frac{4\,\pi\alpha^2\, s}{Q^4}\, |S_T|\, (1-y) \sum_a e_a^2\, x\, \underbrace{h_1^a(x)}\, H_1^{\perp(1)a}(z)$$

$$\Downarrow$$

more direct measurement of $h_1(x)$!

under dominant-flavor-only approximation for F.F.

$$\pi^+ \;:\; \frac{4}{9}\, h_1^u(x) + \frac{1}{9}\, h_1^{\bar{d}}(x)$$
$$\pi^- \;:\; \frac{1}{9}\, h_1^d(x) + \frac{4}{9}\, h_1^{\bar{u}}(x)$$

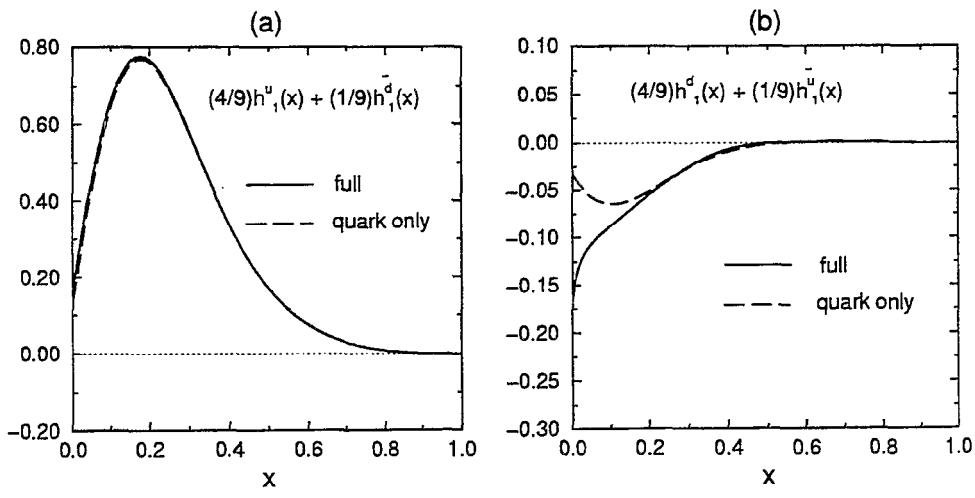

5. Conclusion

♣ An **incomparable** feature of the Chiral Quark Soliton Model as compared with other effective models like the MIT bag model is that it can give reasonable predictions also for the **antiquark distribution functions** as exemplified by the argument on

- **possitivity constraint** for $\bar{u}(x)+\bar{d}(x)$
- **Soffer inequality** for **antiquarks**

<u>it can explain</u>

without any adjustable parameter

- **excess** of $\bar{d}$**-sea**, over $\bar{u}$**-sea** in the proton
- qualitative behavior of experimentally measured polarized structure functions $g_1^p(x), g_1^n(x), g_1^d(x)$
- **small quark spin fraction of the nucleon**

in **no need of large gluon polarization**
at **low renormalization scale**

further unique prediction

- **large isospin asymmetry** of **spin-dependent sea-quark** distributions

$$\Delta\bar{d}(x) - \Delta\bar{u}(x) < 0$$

$$\Updownarrow$$

a natural consequence of $\boldsymbol{N_c}$ - **counting rule**

$$\Updownarrow$$

but seems **inconsistent** with naive

Meson Cloud Convolution Model

CQSM can give reasonable predictions also for

- transversity distribution : $\boldsymbol{h_1^q(x)}$
- twist-3 PDF : $\boldsymbol{e^q(x), g_T^q(x), h_L^q(x)}$

which will be tested by near-future experiments of various kinds, which enables

$$\left\{ \begin{array}{c} \textbf{flavor} \\ \textbf{valence} \oplus \textbf{sea} \end{array} \right\} \textbf{decomposition} \text{ of PDF}$$

RHIC Spin Physics

Gerry Bunce
RIKEN-BNL Research Center

Summary

RHIC begins a program colliding polarized protons at high energy, root(s)=200 GeV, next year, 2001, and at energy root(s)=500 GeV in following years. This will be the first polarized proton collider. The high energy, and the high luminosity of RHIC spin, will provide polarized quark probes of the spin structure of the proton which are well into the domain where perturbative QCD describes the scattering processes.

RHIC spin will complement the beautiful work on proton spin structure using lepton probes. The RHIC spin probes, polarized quarks, and possibly polarized gluons, are strongly interacting and, thus, directly access the spin structure due to the gluons in the proton. And, RHIC will separately measure u, d, ubar, and dbar quark polarizations in the polarized proton through parity violating W boson production.

The first lecture focuses on three RHIC measurements:

--gluon polarization using direct photon production;
--u, dbar, ubar, d polarization using parity violating W production;
--searches for quark substructure and new Z' bosons by searching for parity violation in jet production.

The second lecture discusses the physics of polarized proton acceleration, including the successful acceleration and storage of polarized protons at RHIC this September, which was the first use of a Siberian Snake at high energy. A new method of measuring proton polarization was developed for RHIC. The lecture introduces the RHIC detectors for spin, PHENIX, STAR, and pp2pp. Finally, the RHIC sensitivities are compared with deep inelastic scattering measurements.

Many RHIC spin topics have not been included. During the school, Professor Jiandong Ji told me of a remark by Professor Weisskopf for lecturers: "Discovering a little is better than covering a lot." To list a few of the missing: ubar/dbar ratio from W production and measuring the gluon distribution using directly produced photons, both for unpolarized (spin-averaged) data; transversity quark polarizations which, when compared with longitudinal polarizations, will not have a gluon contribution; single transverse spin asymmetries in the BRAHMS experiment; jet and fragmentation probes of the gluon polarization, and also others. Many are discussed in, and these lectures are based on, "Prospects for Spin Physics at RHIC", written by Gerry Bunce, Naohito Saito, Jacques Soffer, and Werner Vogelsang, published in the Annual Reviews of Nuclear and Particle Science 2000, page 525-575, or see http://arXiv.org/abs/hep-ph/0007218.

December 2000
RIKEN School
Niigata, Japan

RHIC Spin – 2 Lectures

G. Bunce

1. Spin and the physics of RHIC spin

2. Accelerating polarized protons, measuring polarization, RHIC detectors, comparisons of sensitivities

---

These lectures are based on
"Prospects for Spin Physics at RHIC"
by GB, Naohito Saito, Jacques Soffer, and Werner Vogelsang

http://arXiv.org/abs/hep-ph/0007218
Dec. 2000, Annual Reviews of Nuclear and Particle Science

Lecture 1: Spin and the physics of RHIC spin

① Spin – a powerful and elegant tool

- spin signals are a direct result of quantum mechanics
- spin effects often violate our intuition
- spin provides direct tests of symmetry
  - parity for example
- large spin signals imply order
  - collisions at high energy
    ⇒ expected disorder!
- spin signals are beautiful!

- deep inelastic scattering of pol. electrons + muons from pol. p, n
  ⇒ $(q + \bar{q})$ only carry ~25% of the proton spin on average!

Proton-deuteron double scattering

1970-71

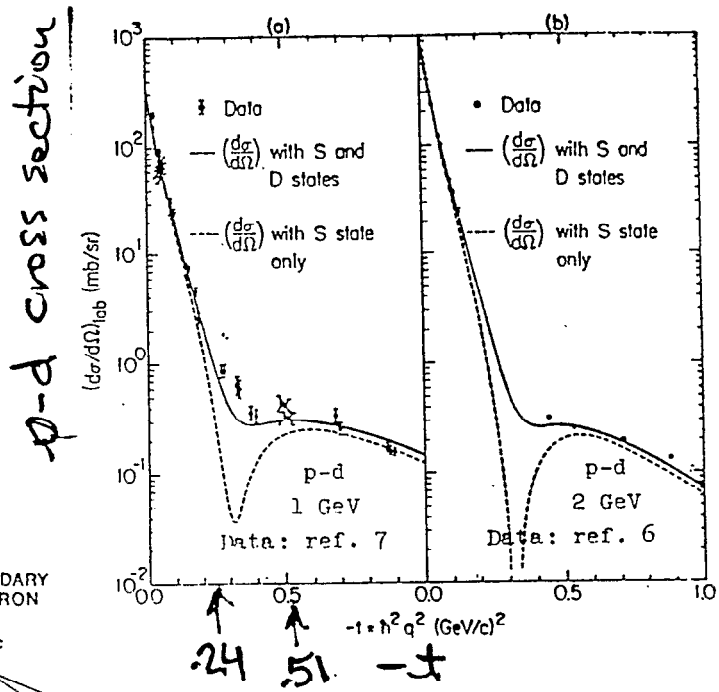

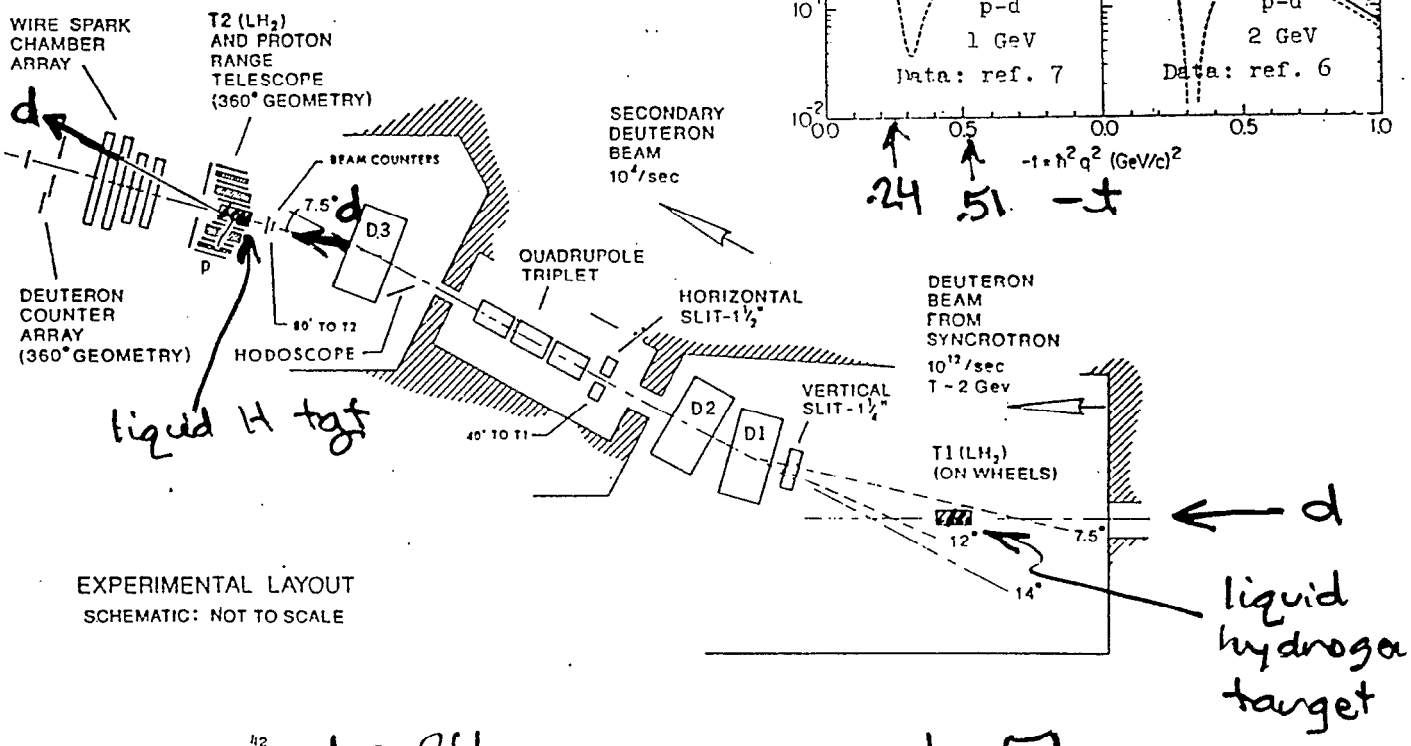

EXPERIMENTAL LAYOUT
SCHEMATIC: NOT TO SCALE

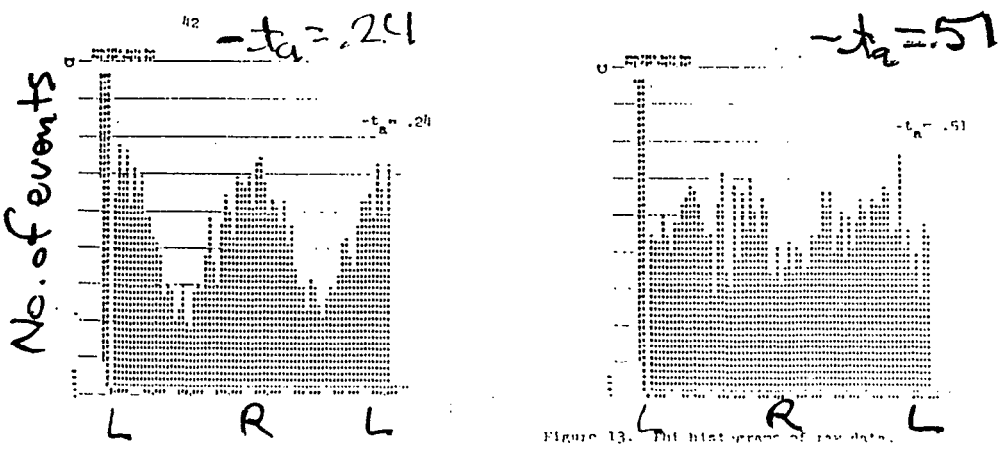

Figure 13. The histograms of raw data.

Azimuthal angle of secondary d

pp elastic scattering ~1976

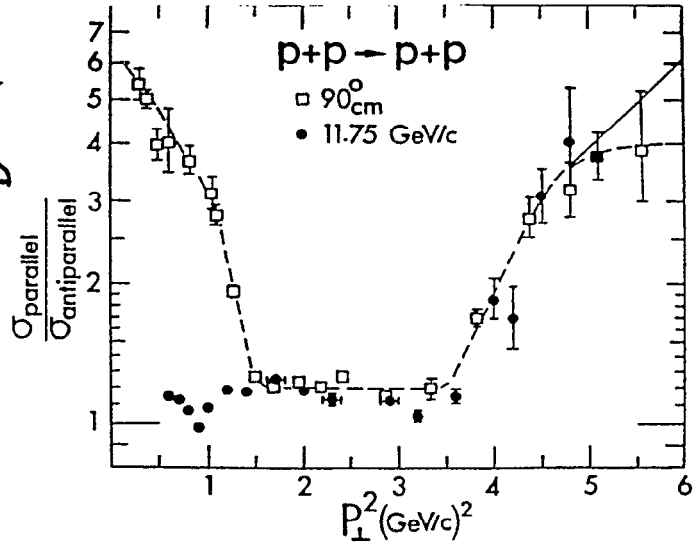

Fig. 3. Ratio of spin-parallel to spin-antiparallel p-p elastic cross-sections plotted against $P_\perp^2$ for fixed energy and fixed angle experiments.

$p^{\uparrow} + p \to \pi + X$ at 200 GeV

$A_N = \frac{1}{P_{beam}} \frac{N_{left} - N_{Right}}{sum}$

N_{left}/N_{Right}

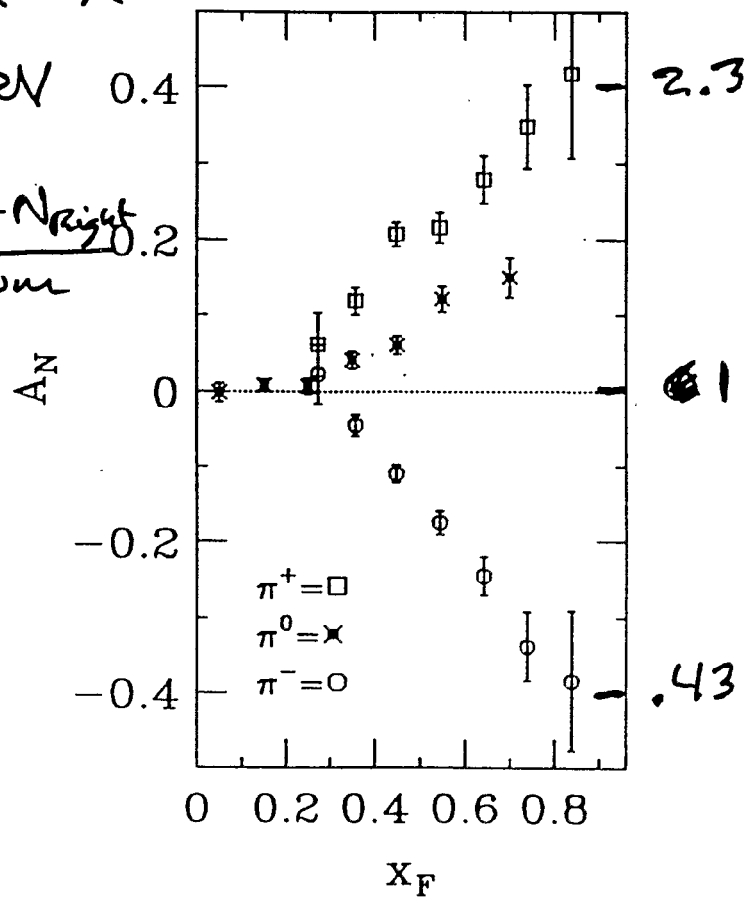

Fig. 4. A_N versus x_F for π^+, π^- and π^0 data.

$p + Be \to \Lambda + X$
at 300 GeV

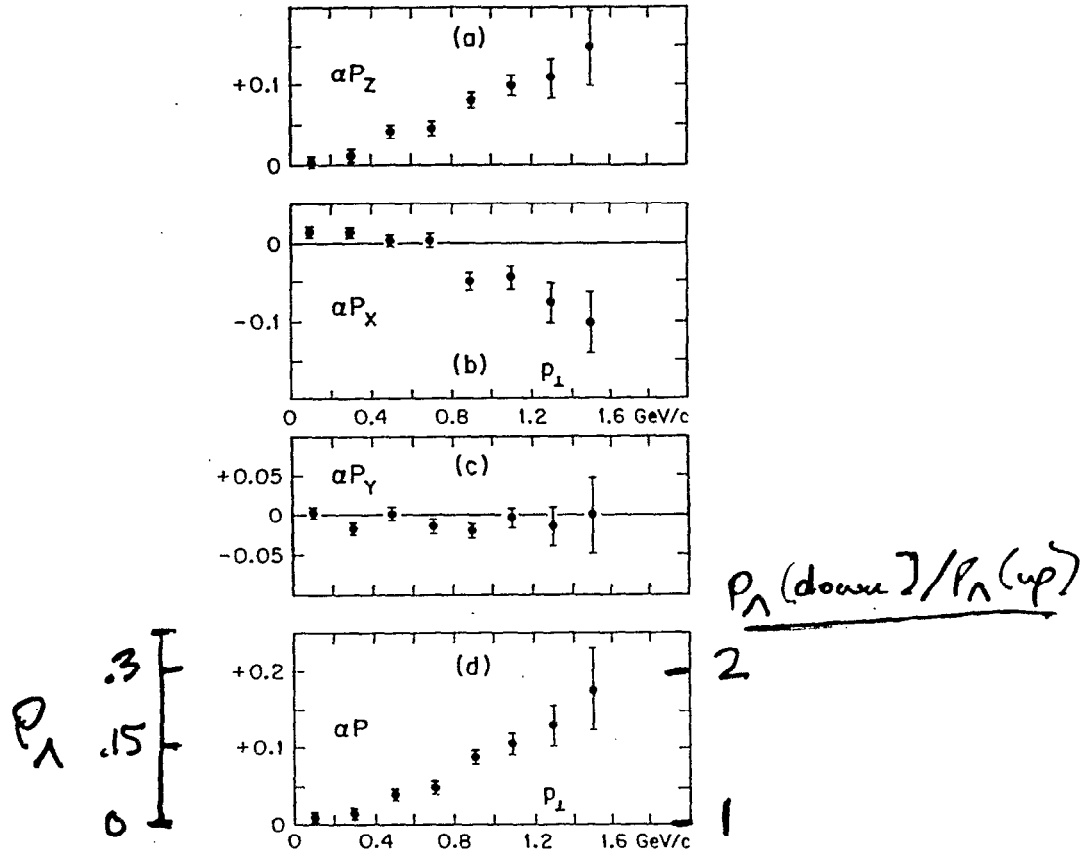

FIG. 3. Three components and magnitude of the $\Lambda^0 \to p + \pi^-$ asymmetry as a function of Λ^0 transverse momentum.

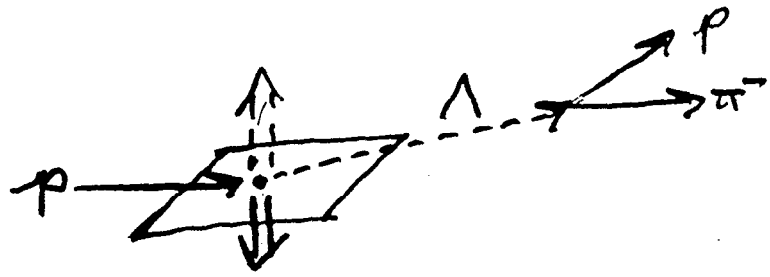

3.1 GeV $\mu^+ \to e^+ + 2\nu$

$E_{e^+}/E_\mu \geq 0.6$

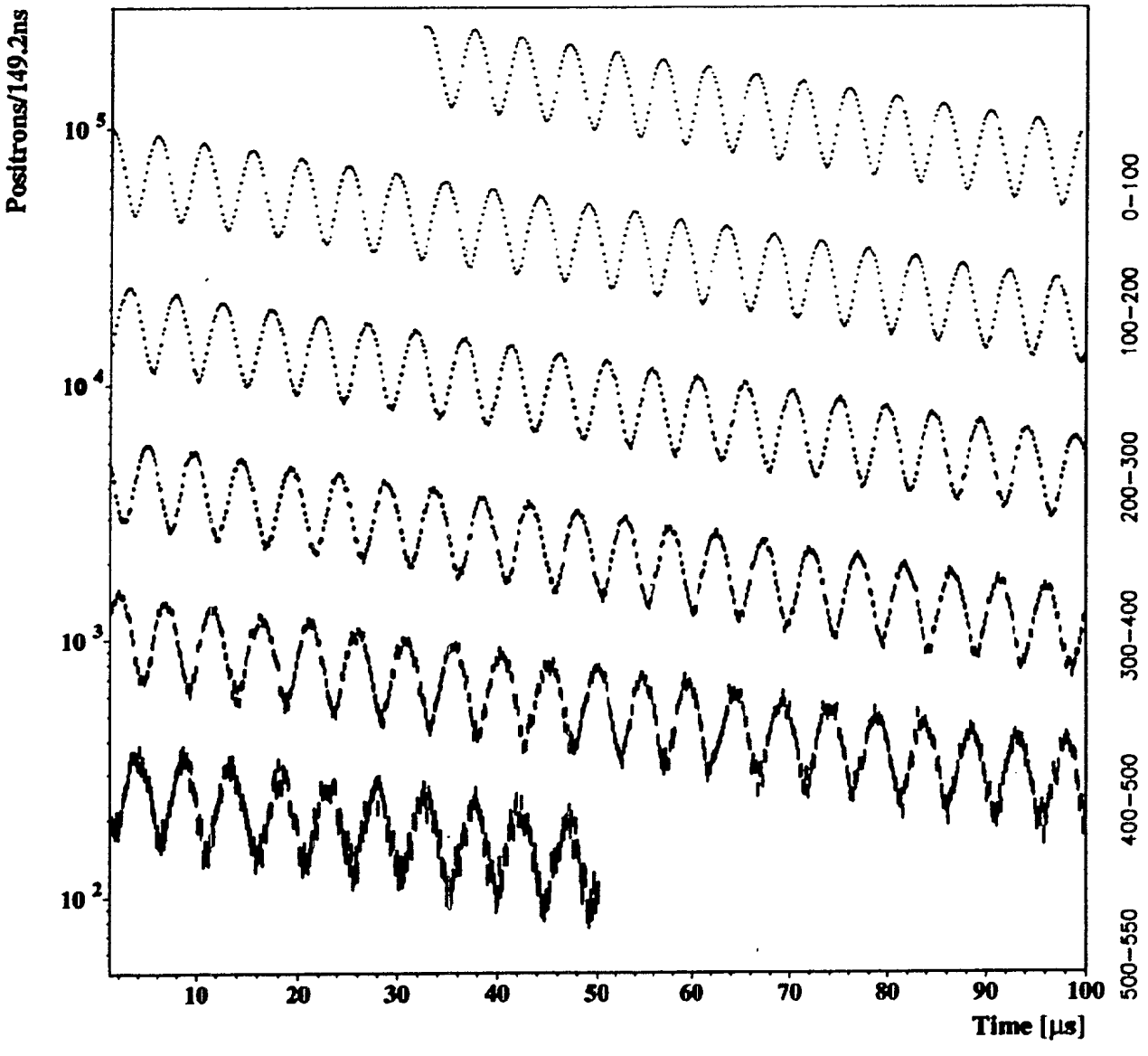

(2) RHIC spin – collide beams of polarized protons 250 × 250 GeV

1. "because it was there" – qualitatively new physics reach

– previous $p\Uparrow$ used
$p \to \Lambda \to p\Uparrow$, fixed target expt:
$\sqrt{s} \approx 20$ GeV <u>vs. 500 GeV at RHIC</u>

2. because $\overrightarrow{DIS}$ was there : $\Delta\Sigma \approx 0.25$

$$\frac{1}{2} = \int_0^1 dx \left[\underbrace{\frac{1}{2}\sum_q (\Delta q + \Delta\bar{q})(x,\mu^2)}_{\sim 0.25} + \Delta g(x,\mu^2) \right] + L(\mu^2)$$

$$\vec{p} \longrightarrow \longleftarrow \vec{p}$$

Use polarized quarks (and gluons?) of one polarized proton to probe the spin structure of the other $\vec{p}$.

Complementary to $\overrightarrow{DIS}$: $\vec{\gamma}^*$ vs. $\vec{q}$ probe

Polarized Proton Collisions at BNL

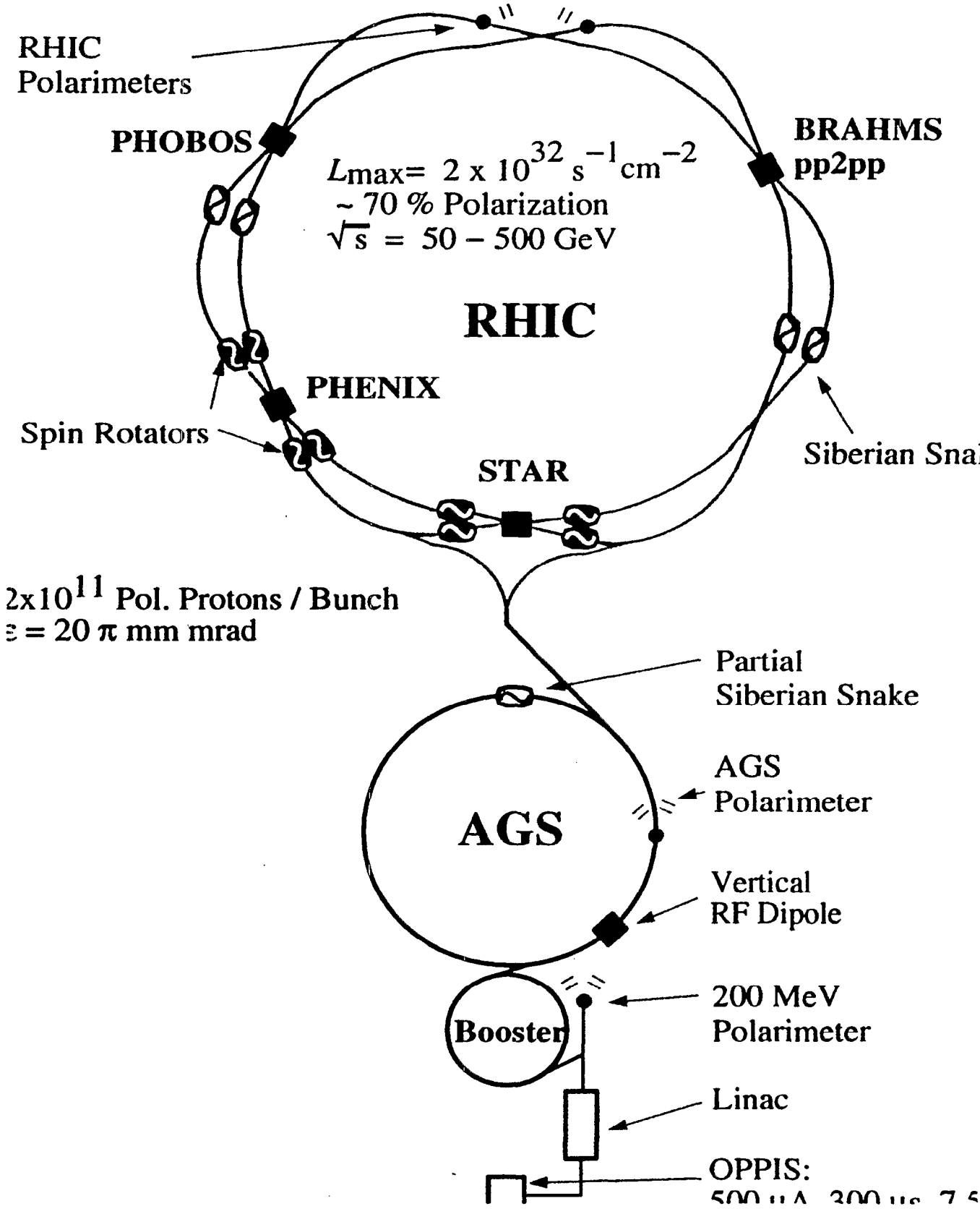

Physics with $p\vec{p}$ at RHIC

$\sqrt{s} = 500$ GeV
$L = 2\times10^{32}\ cm^{-2}\ s^{-1}$ } high p_T accessible

Hard scattering ⇒ factorization

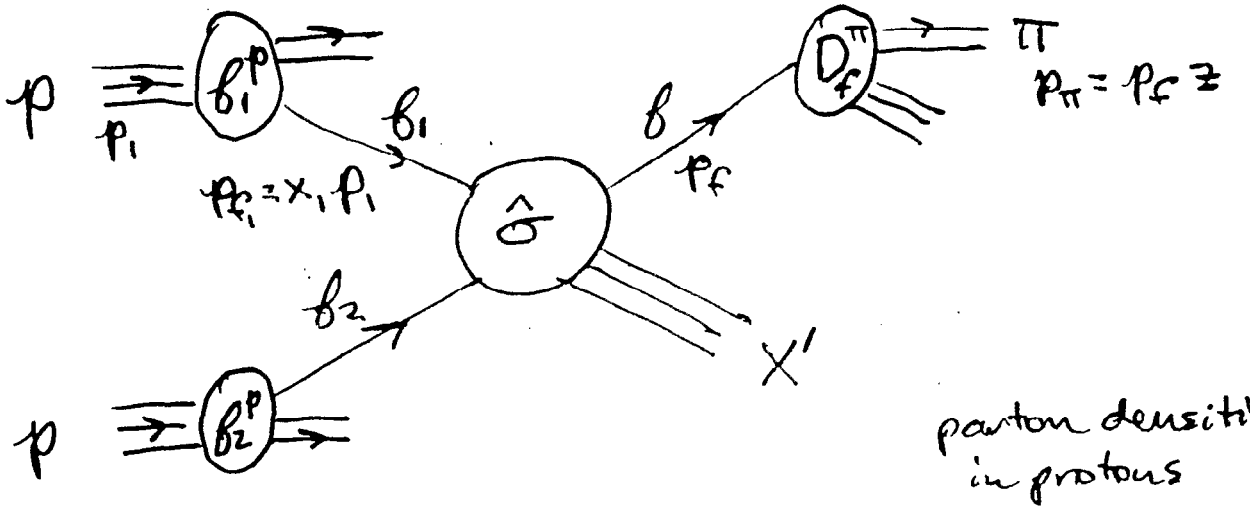

parton densities in protons

$$\frac{d\sigma^{pp\to\pi X}}{dP} = \sum_{f_1,f_2,f} \int dx_1\, dx_2\, dz\, f_1^p(x_1)\, f_2^p(x_2)$$

$$\times \underbrace{\frac{d\hat{\sigma}^{f_1 f_2 \to f X'}}{dP}(x_1, x_2, z)\,(p_{f_1}, p_{f_2}, p_f)}_{\text{parton-parton subprocess}}\ D_f^\pi(z)$$

fragmentation of parton f to π

Spin: $p_1 \Rightarrow \longrightarrow X \longleftarrow \Leftarrow p_2$ $\qquad$ $p \Rightarrow \longrightarrow X \longleftarrow \Rightarrow p$

σ_{++} ← helicity of p_2

helicity of p_1

σ_{+-}

Asymmetry:

$$A_{LL} \equiv \frac{\sigma_{++} - \sigma_{+-} - \sigma_{-+} + \sigma_{--}}{\sigma_{++} + \sigma_{+-} + \sigma_{-+} + \sigma_{--}}$$

longitudinal spin, both beams

Factorization ⇒ polarized parton densities

quark + helicity

$$p_+ : \; q_+^+ \,,\; q_+^- \,,\; g_+^+ \,,\; g_+^-$$

proton + helicity

$$\boxed{\begin{aligned} \Delta q &\equiv q_+^+ - q_+^- \\ \Delta g &\equiv g_+^+ - g_+^- \end{aligned}}$$

$$A_{LL}^{\pi} = \frac{\sum_{f_1 f_2 f} \Delta f_1 \, \Delta f_2 \left[d\hat{\sigma}^{f_1 f_2 \to f X'} \, \hat{a}_{LL}^{f_1 f_2 \to f X'} \right] D_f^{\pi}}{\sum_{f_1 f_2 f} f_1 f_2 \, d\hat{\sigma} \, D_f^{\pi}}$$

Subprocess analyzing power:

$$\boxed{\hat{a}_{LL}^{f_1 f_2 \to f X'} \equiv \frac{\hat{\sigma}_{++} - \hat{\sigma}_{+-} - \hat{\sigma}_{-+} + \hat{\sigma}_{--}}{\hat{\sigma}_{++} + \hat{\sigma}_{+-} + \hat{\sigma}_{-+} + \hat{\sigma}_{--}}}$$

Sensitivity to parton spin is from angular momentum conservation:

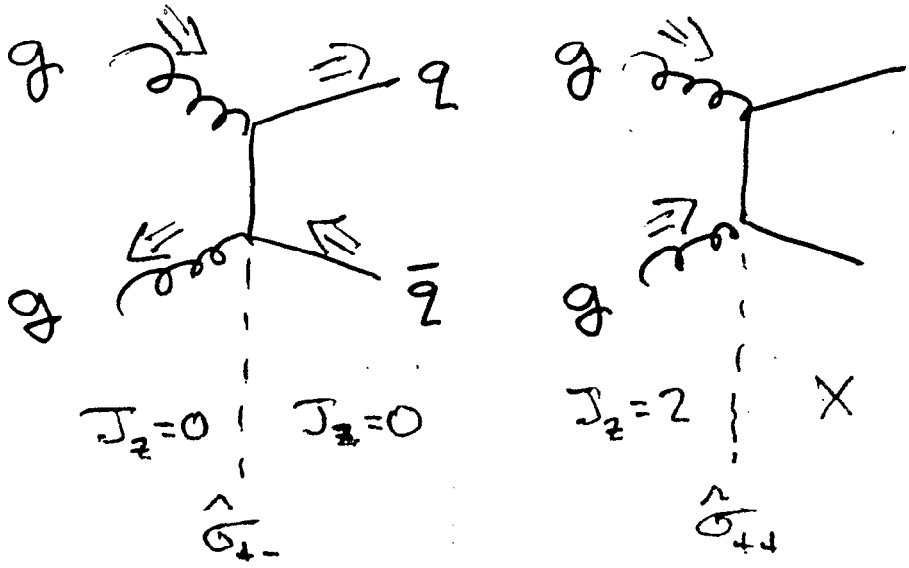

$$\hat{a}_{LL}^{gg\to q\bar{q}} = \frac{\hat{\sigma}_{++} - \hat{\sigma}_{+-}}{\hat{\sigma}_{++} + \hat{\sigma}_{+-}} = \frac{-\hat{\sigma}_{+-}}{\hat{\sigma}_{+-}} = -1$$

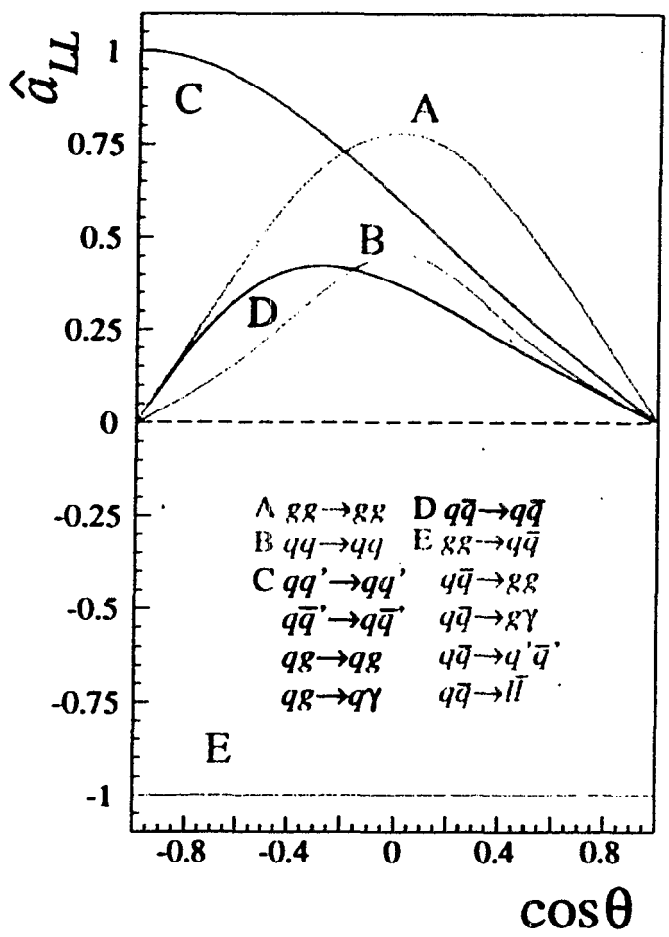
$\hat{a}_{LL}$
1
0.75
0.5
0.25
0
-0.25
-0.5
-0.75
-1
-0.8
-0.4
0
0.4
0.8
cosθ
A
B
C
D
E
A $gg \to gg$
B $qq \to qq$
C $qq' \to qq'$
$q\bar{q}' \to q\bar{q}'$
$qg \to qg$
$qg \to q\gamma$
D $q\bar{q} \to q\bar{q}$
E $gg \to q\bar{q}$
$q\bar{q} \to gg$
$q\bar{q} \to g\gamma$
$q\bar{q} \to q'\bar{q}'$
$q\bar{q} \to l\bar{l}$

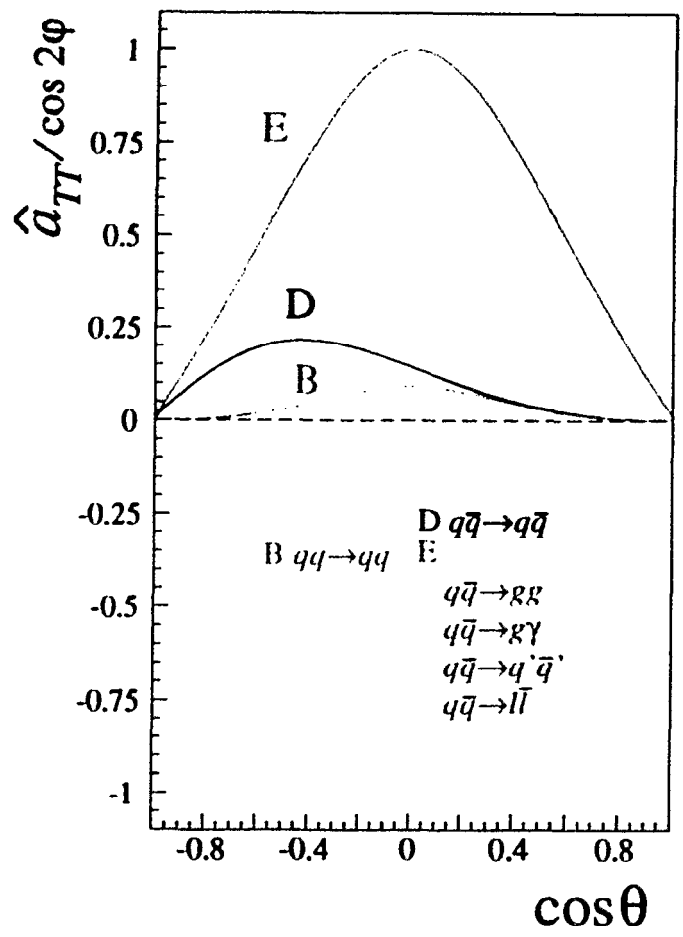
$\hat{a}_{TT}/\cos 2\varphi$
1
0.75
0.5
0.25
0
-0.25
-0.5
-0.75
-1
-0.8
-0.4
0
0.4
0.8
cosθ
E
D
B
B $qq \to qq$
D $q\bar{q} \to q\bar{q}$
E
$q\bar{q} \to gg$
$q\bar{q} \to g\gamma$
$q\bar{q} \to q'\bar{q}'$
$q\bar{q} \to l\bar{l}$

Proton spin sum rule:

$$\frac{1}{2} = \int_0^1 dx \left[\frac{1}{2} \underbrace{\sum_q (\Delta q + \Delta \bar{q})(x)}_{\Delta\Sigma \approx 1/4\,!} + \Delta g(x) \right] + L$$

A major focus of RHIC spin: $\Delta g(x)$

Probe $\Delta g(x)$ directly with prompt γ:

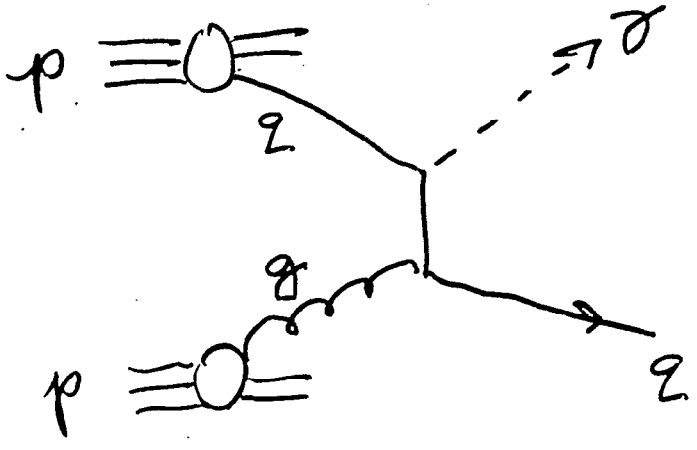

$$\hat{a}_{LL}^{qg \to \gamma X}(90^\circ) = 0.6$$

A_1^p of DIS

1. large subprocess analyzing power
2. $q\bar{q} \to \gamma g$ only $\sim 10\%$ of $qg \to \gamma X$
3. $A_{LL} \approx \frac{\Delta g(x_1)}{g} \cdot \boxed{\frac{\sum e_q^2 [\Delta q(x_2) + \Delta \bar{q}(x_2)]}{\sum e_q^2 [q(x_2) + \bar{q}(x_2)]}} \hat{a}_{LL}^{qg \to \gamma X}$

$$A_1 = \frac{\sigma_{1/2} - \sigma_{3/2}}{\sigma_{1/2} + \sigma_{3/2}} = \frac{\sum e_i^2 [q_i^\uparrow - q_i^\downarrow]}{\sum q_i} \quad \text{May, 1995}$$

WORLD PROTON A_1^p

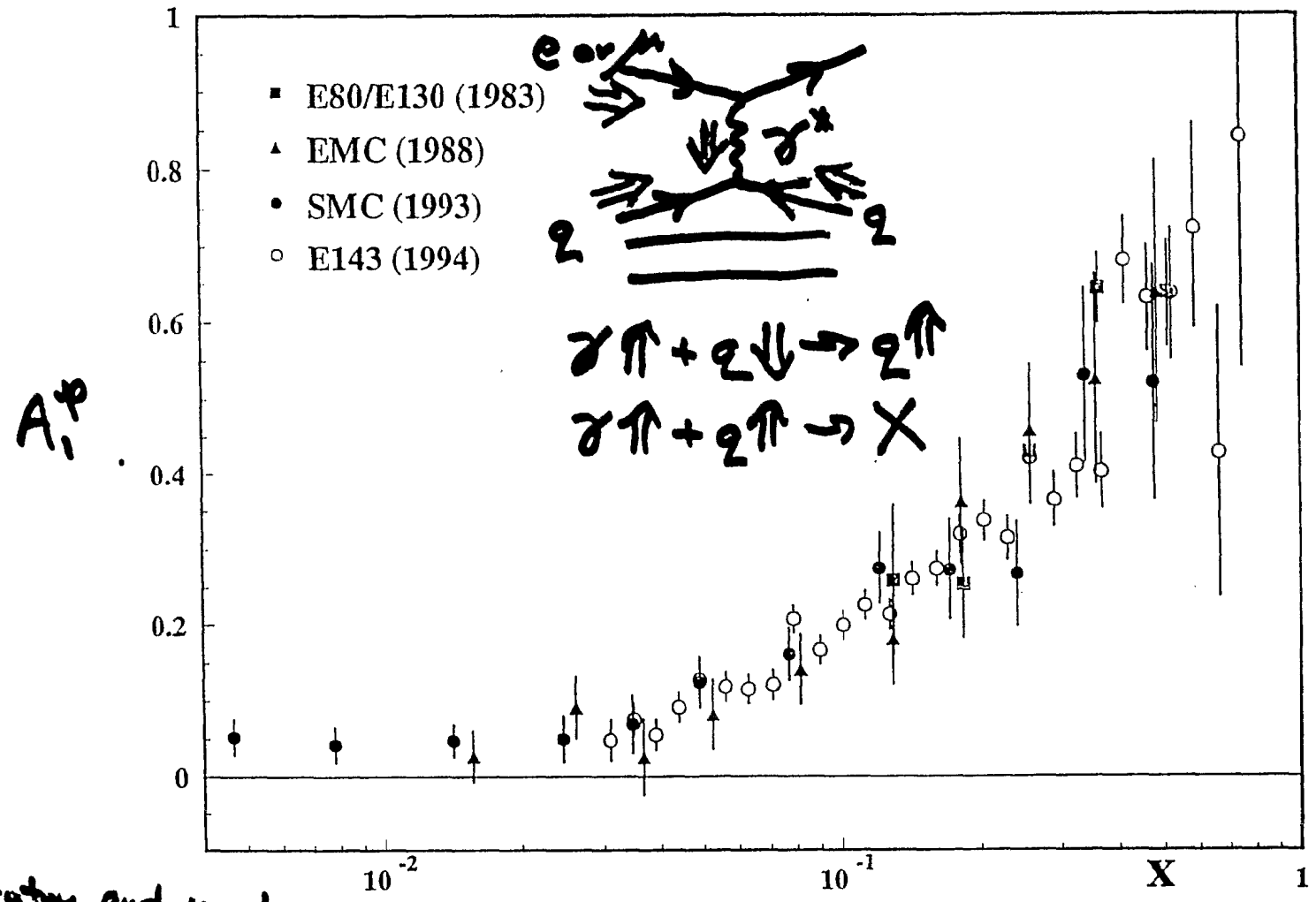

⇒ 2/3 proton spin is in gluons and/or L_z

Proton and n, d,

Integral over x → $\Delta\Sigma = \Delta(u+\bar{u}) + \Delta(d+\bar{d}) + \Delta(s+\bar{s}) = \underline{.27 \pm .05}$

Recipe to measure gluon polarization

1. collide $(+,+)$, $(+,-)$, $(-,+)$, $(-,-)$ p

2. observe isolated γ in detector

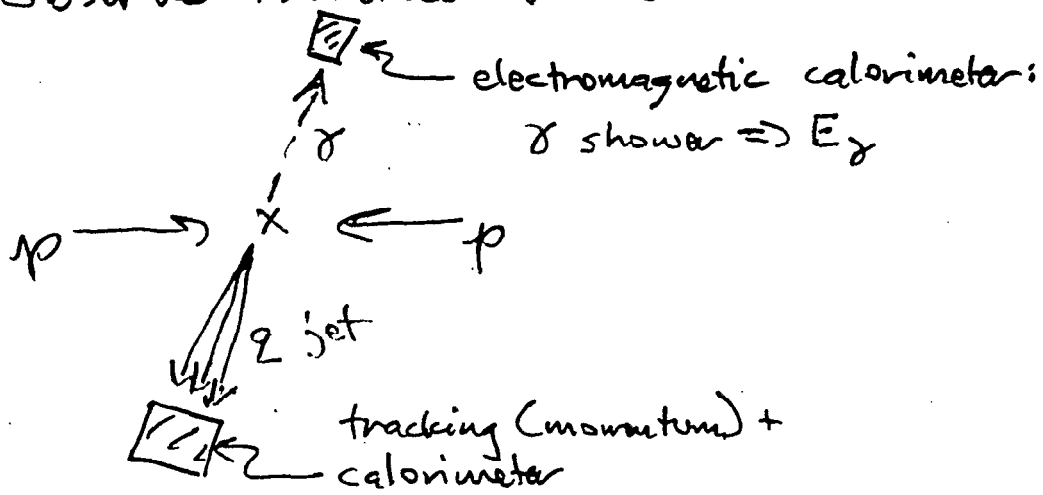

3. $$A_{LL} = \frac{1}{P^2_{beams}} \frac{N_{++} - N_{+-} - N_{-+} + N_{--}}{\text{sum}}$$

4. $$A_{LL} = \boxed{\frac{\Delta g}{g}(x_1)} \, A_1^p(x_2) \, \hat{a}_{LL}^{qg \to \gamma X}$$

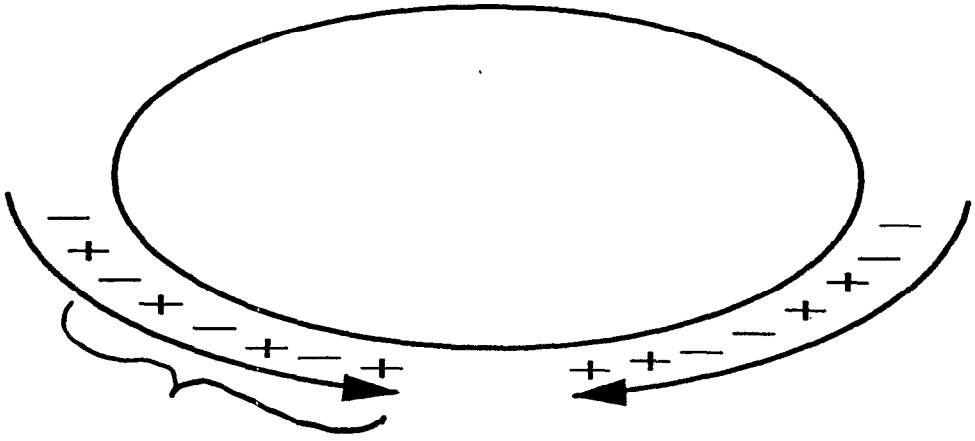

Commissioning:
loaded 6 bunches
- 2 μsec apart

2001 Spin run:
load 60 bunches
- 200 nsec apart

2002 Spin run:
load 120 bunches
- 100 nsec apart

PHENIX Experiment at RHIC:

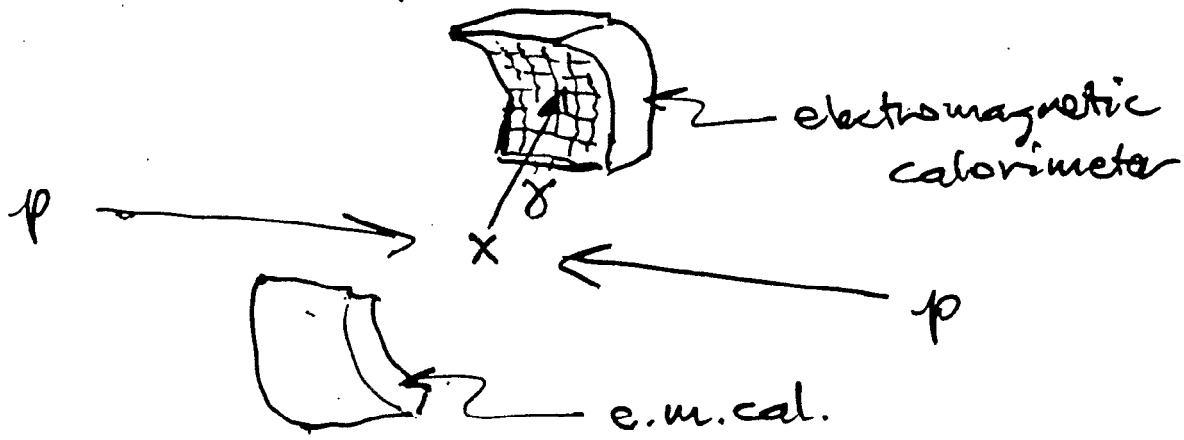

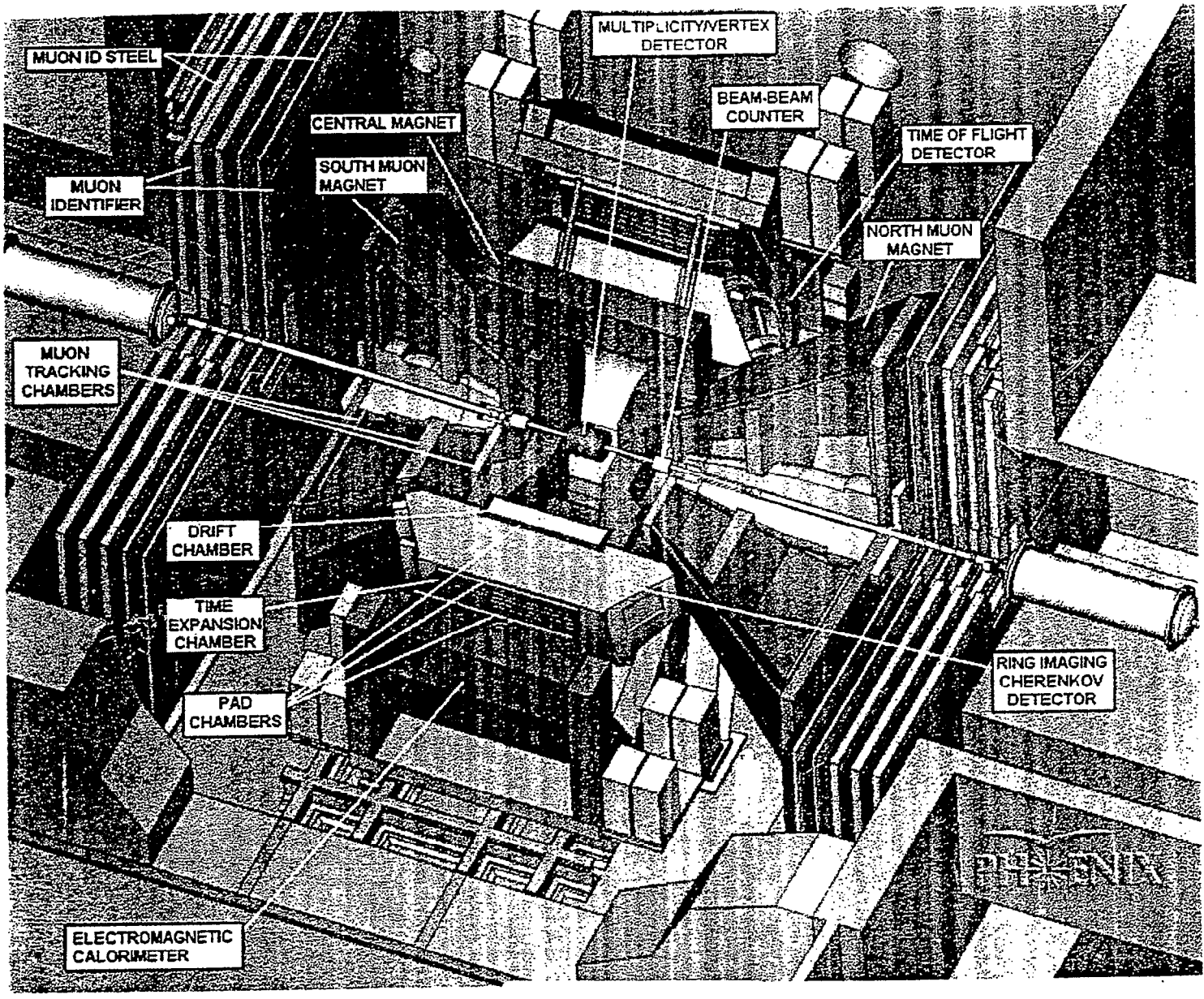

Sensitivity at PHENIX for gluon pol.

$\int L\,dt = 320\ pb^{-1}$ $\sqrt{s} = 200$
$= 800\ pb^{-1}$ 500

$P_{beams} = 70\%$

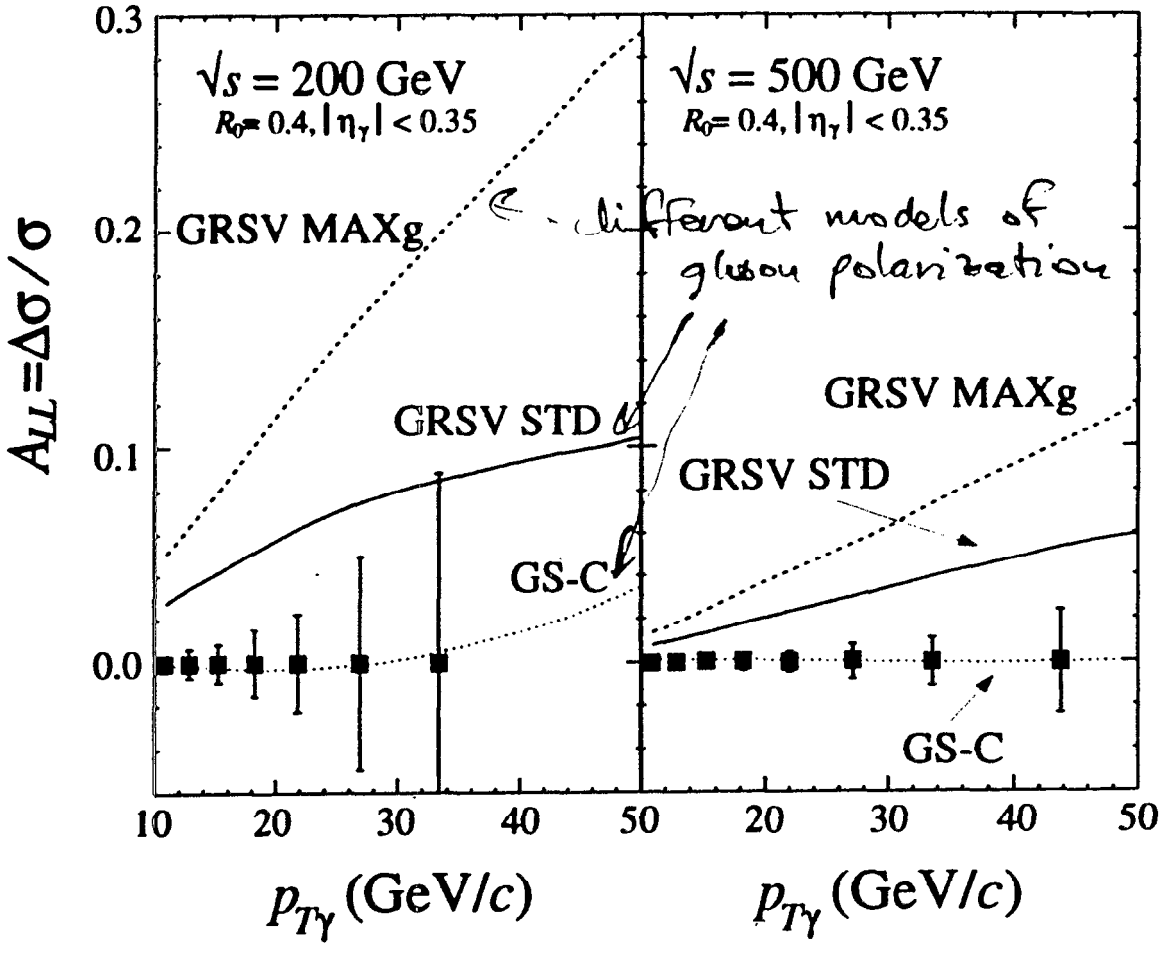

Parity Violation in W^+ Production

One beam is longitudinally polarized : $A_L = \frac{1}{Pol.} \frac{N_+ - N_-}{N_+ + N_-}$

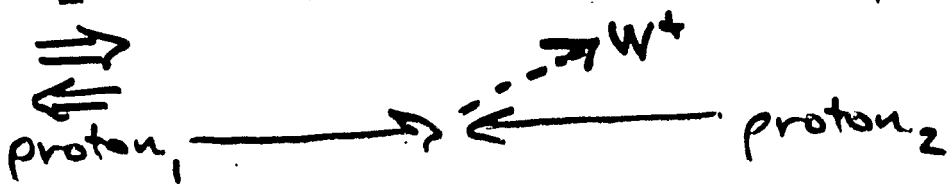

- if W^+ is produced to $+y \Rightarrow$ large x_1, small x_2

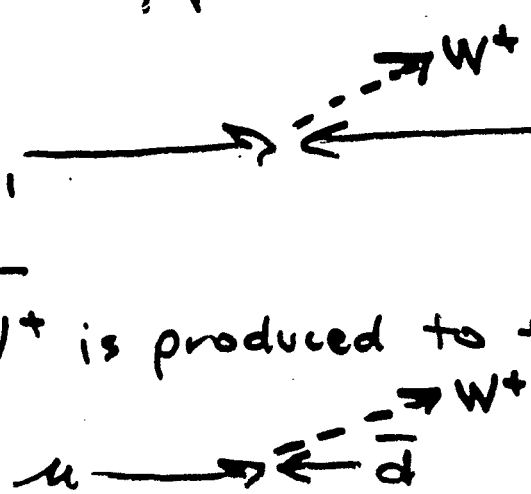

- but proton 1 is polarized $\Rightarrow$ <u>u quark is polarized</u> and

$$A_L(+y) = \frac{\Delta u}{u}$$

- if W^+ is produced to $-y \Rightarrow$ small x_1, large x_2

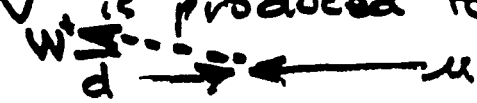

- proton 1 is polarized $\Rightarrow$ <u>$\bar{d}$ is polarized</u> and

$$A_L(-y) = \frac{\Delta \bar{d}}{\bar{d}}$$

I. Shestermanov 5/23/95

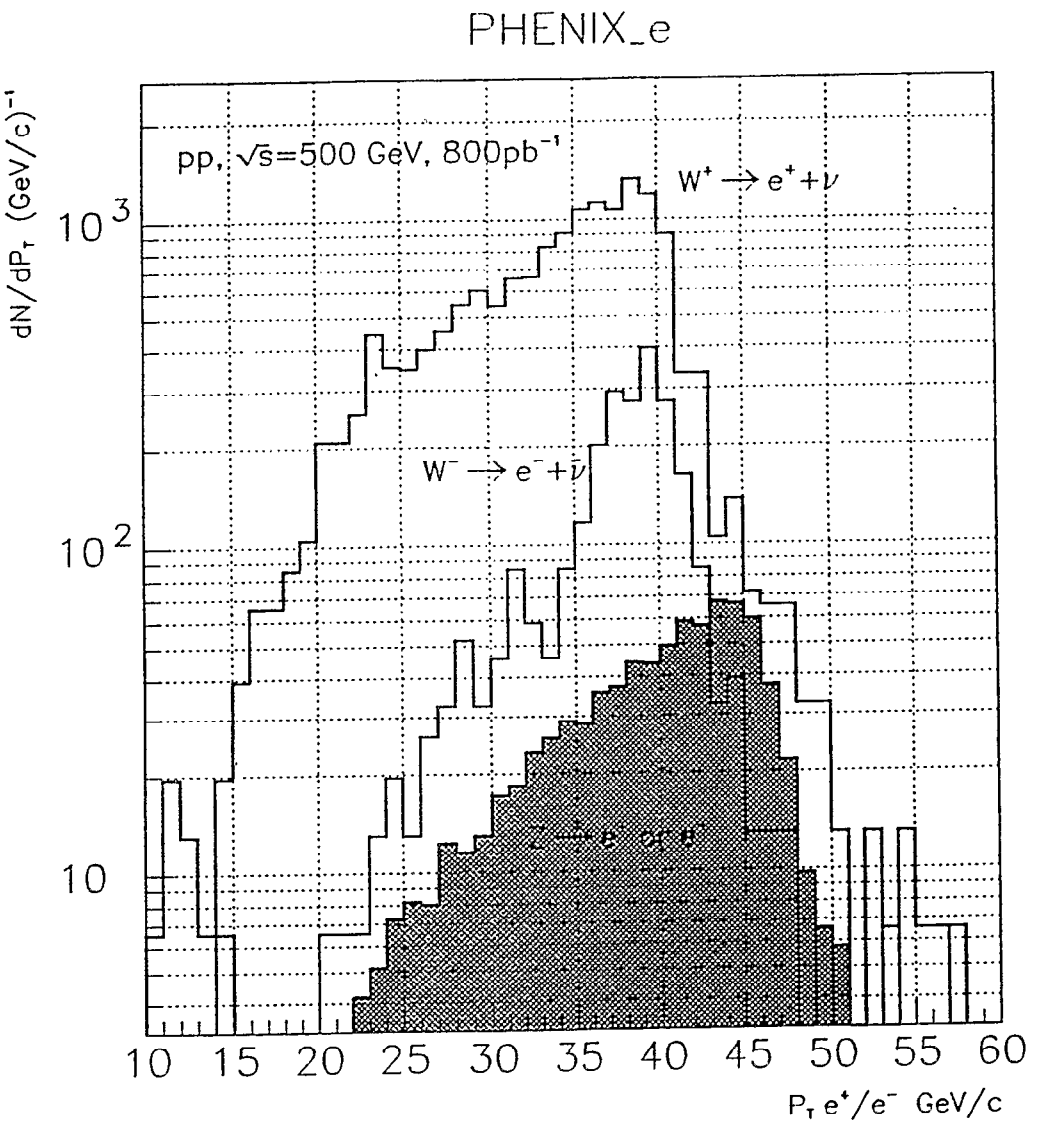

$W^+ \to e^+ + \nu_e$ ~ 15700 events

$W^- \to e^- + \bar{\nu}_e$ 2500 events

$Z \to e^+$ or e^- ~ 830 e^+ and ~ 830 e^-

$= \frac{e^+ + e^-}{2}$

But you see the lepton – what is correlation to y_W?

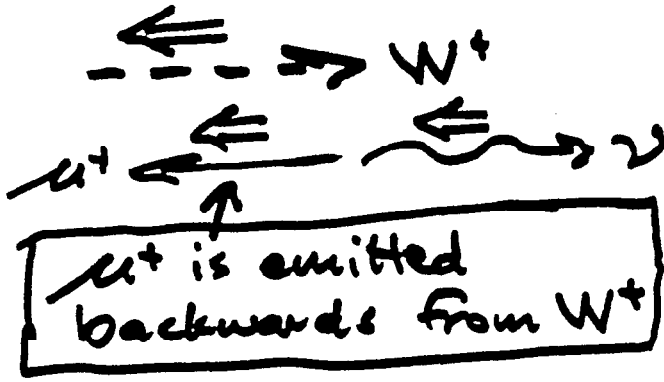

W is left-handed.

ν is left-handed, emitted in direction of W^+

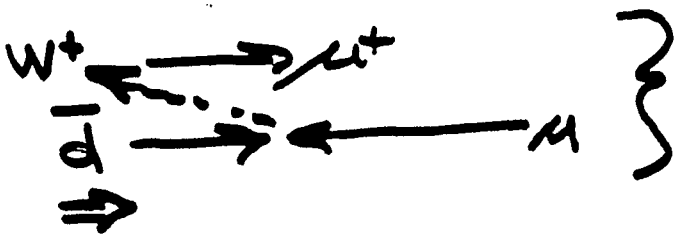

detector on this side sees lower energy μ^+ ⇒ polarised $\bar{d}$

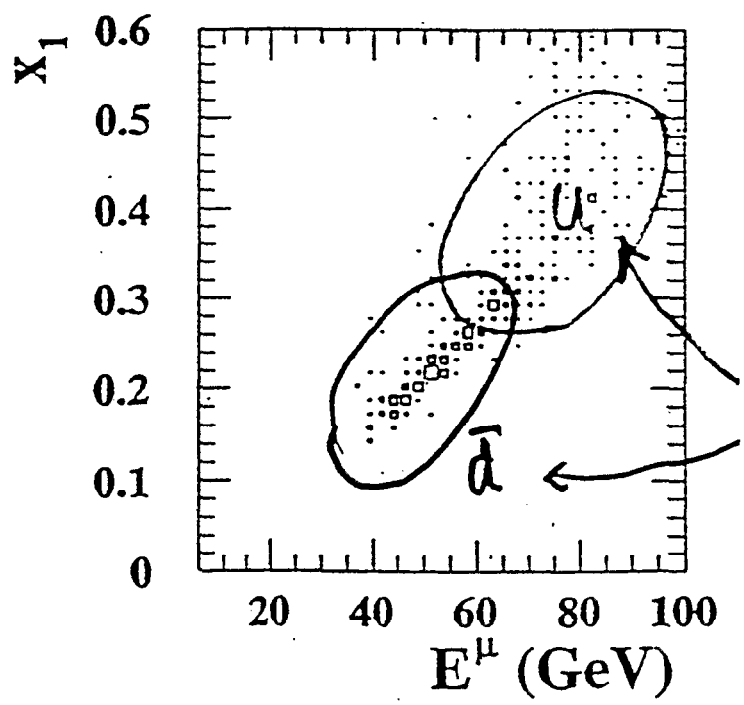

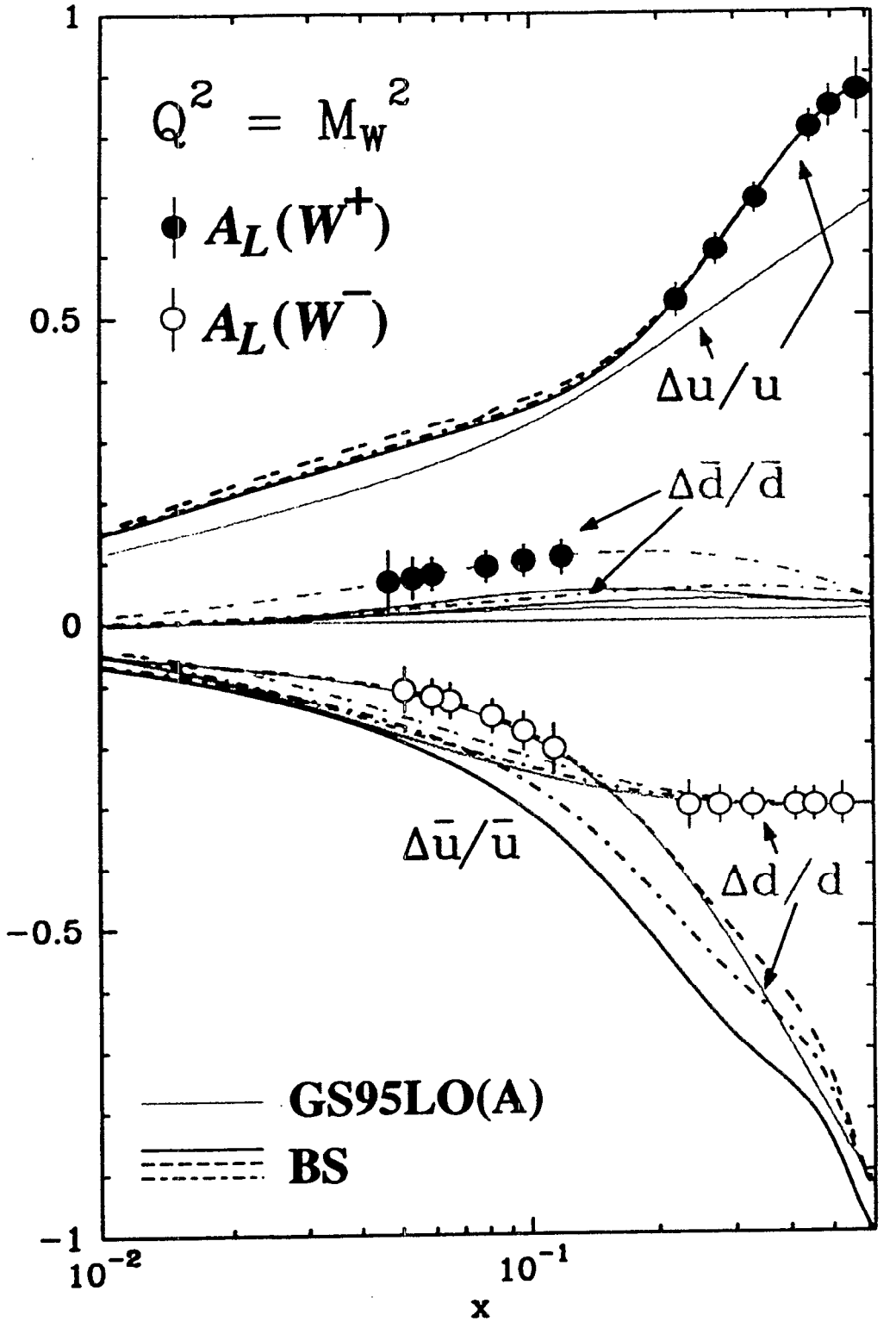

courtesy of Jacques Soffer & Claude Bourrely

Search for new physics using parity violation

From M. Tannenbaum:

Criteria for The Maximum Discovery Potential:

- Look where most theorists predict that nothing will be found.
- Look in a channel where the known rates from conventional processes are small, since low background implies high sensitivity for something new.
- Be the first to explore a new domain—something that has never been measured by anybody else.

Almost any model for new physics violates parity since any new mass scale $\Lambda > M_W$.

Example: CDF search for quark substructure in high p_T jet production...

INCLUSIVE JET CROSS SECTION AT CDF TO LOOK FOR QUARK SUBSTRUCTURE.

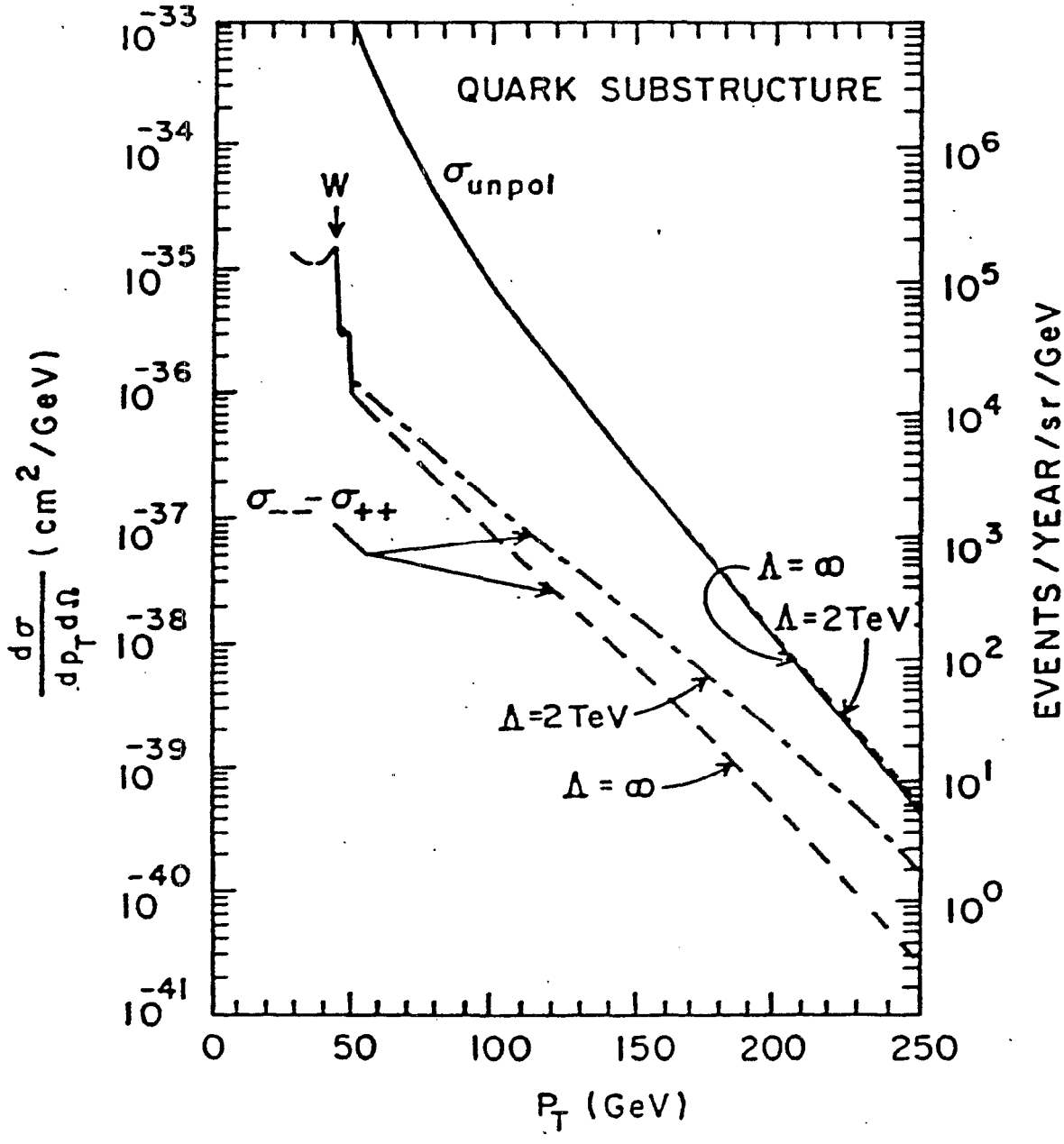

$$\hat{t} \simeq 2P_T^2$$

$$A_{LL} = \underbrace{K(QCD)}_{0.20-0.30} \times \frac{\hat{t}}{\alpha_s \Lambda^2}\left(1 + \frac{21}{32}\frac{\hat{t}}{\alpha_s \Lambda^2}\right)$$

Inclusive Jet Cross Section in $\bar{p}p$ Collisions at $\sqrt{s} = 1.8$ TeV

(CDF Collaboration)

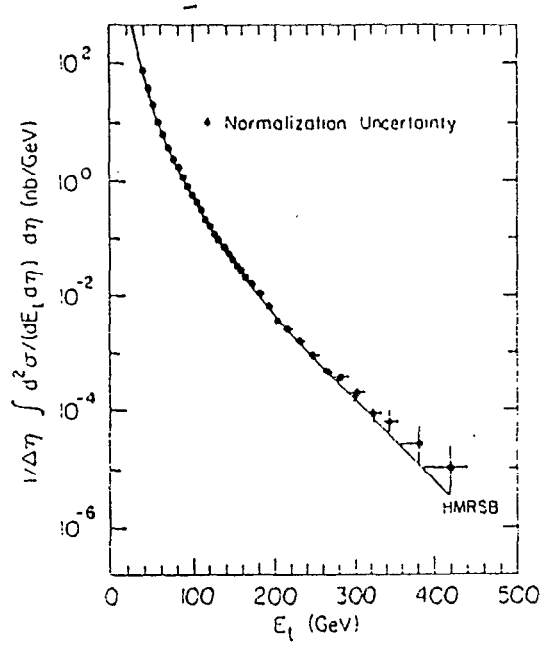

FIG. 1. Inclusive E_t spectrum for a cone size of $R = 0.7$, averaged over the pseudorapidity interval $0.1 \leq |\eta| \leq 0.7$. The curve represents the predictions of a next-to-leading-order QCD calculation by Ellis, Kunszt, and Soper [3]. The error bars on the data represent statistical and E_t-dependent systematic errors. An overall normalization uncertainty is also indicated.

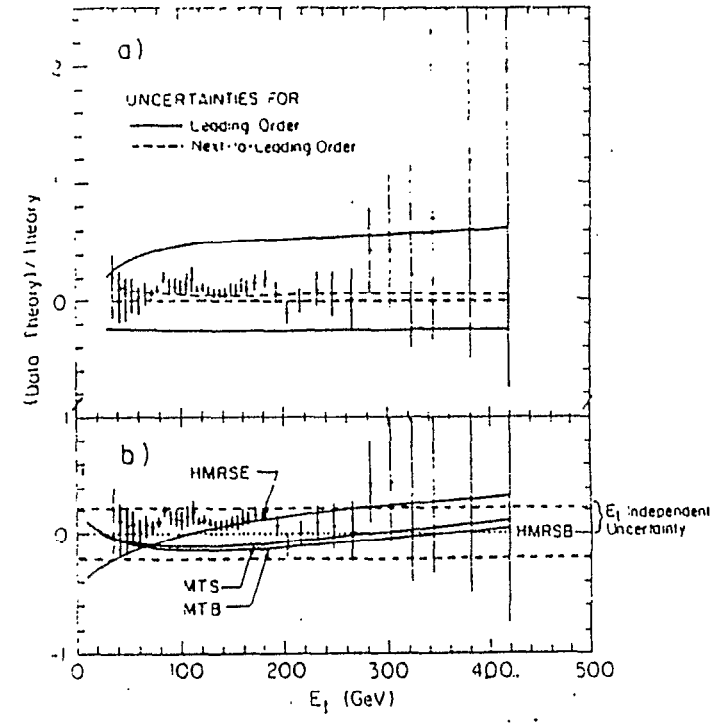

FIG. 2. The inclusive jet E_t spectrum for $R = 0.7$ compared to theory as the ratio of (data − theory)/theory. The upper plot (a) illustrates the theoretical uncertainty associated with variation of the renormalization scale μ ($E_t \geq \mu \geq E_t/4$) for both leading order and next-to-leading order. The data have both the statistical and the E_t-dependent parts of the systematic uncertainties indicated. The lower plot (b) illustrates the dependence on the choice of parton distribution function. The $O(\alpha_s^3)$ prediction using the HMRS set B [14] structure function is used as a reference.

Sensitivity at STAR to "new" physics:

2 jet production:

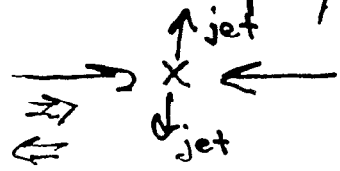

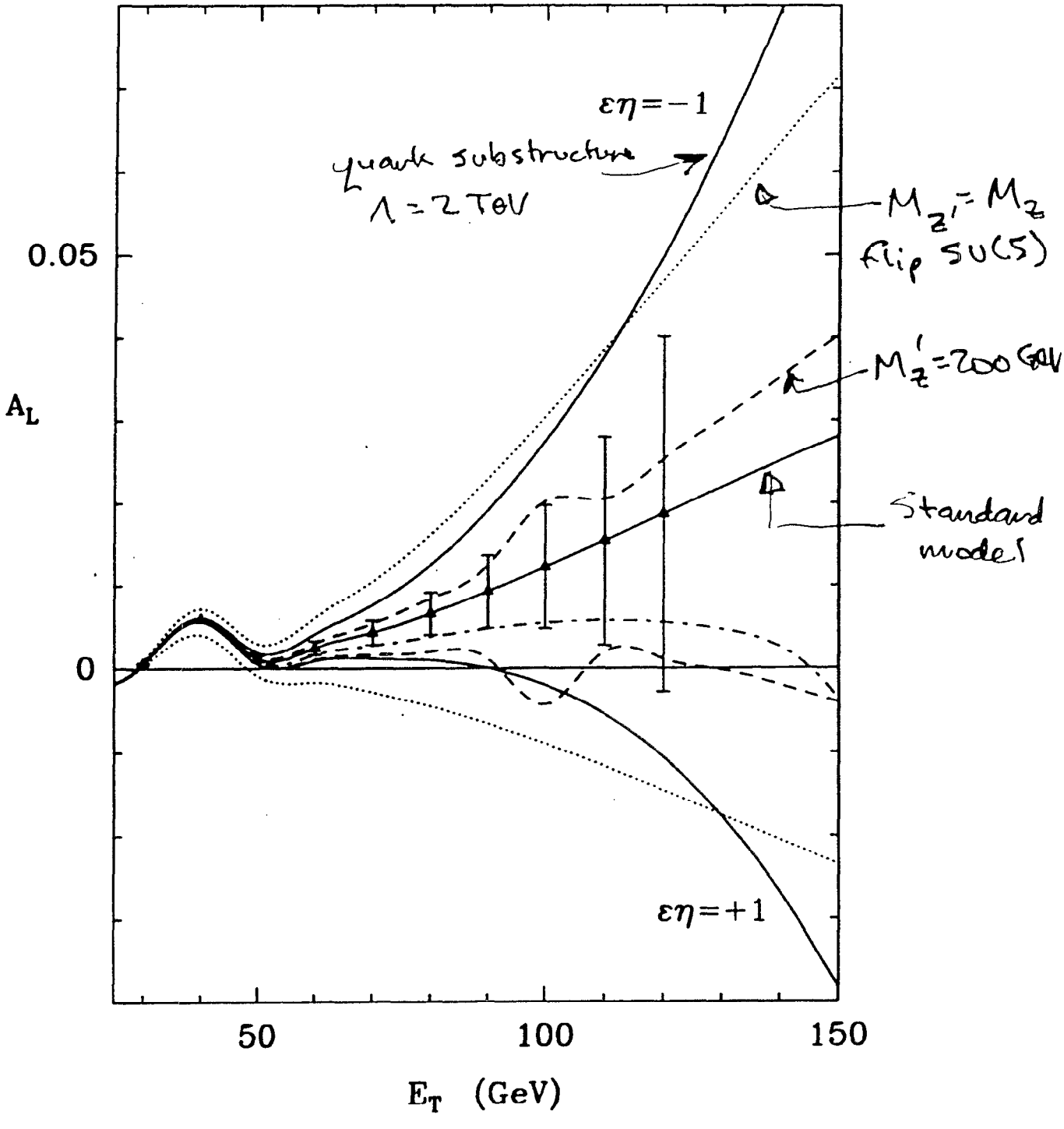

$\sqrt{s} = 500$ GeV, 70% pol., $\int L dt = 800$ pb^{-1}

RHIC Spin Milestones

Nov. 1990	Polarized Collider Workshop at Penn State
Jan. 1991	RSC formed
Aug. 1991	AGS partial snake approved
Aug. 1992	Proposal to PAC
June 1993	Accelerator spin issues reviewed - enthusiastic endorsement Partial snake installed in AGS
Oct. 1993	RSC (2 experiments) approved STAR/Spin, PHENIX/Spin
Jan. 1994	Eng. design of helical snake prototype begins
April 1994 – Dec. 1994	Pol. proton acceleration in AGS with partial snake
Jan. 1995	RIKEN joins → supports accel., enhanced Phenix/Spin
1999/2000	1st polarized proton run in RHIC

December 2000
RIKEN School
Niigata, Japan

RHIC Spin – 2 Lectures

G. Bunce

1. Spin and the physics of RHIC spin

2. Accelerating polarized protons, measuring polarization, RHIC detectors, comparisons of sensitivities

---

These lectures are based on
"Prospects for Spin Physics at RHIC"
by GB, Naohito Saito, Jacques Soffer, and Werner Vogelsang

http://arXiv.org/abs/hep-ph/0007218
Dec. 2000, Annual Reviews of Nuclear and Particle Science

Lecture 2 on RHIC Spin

1. accelerator spin physics is beautiful too!
   - crossing spin resonances in AGS with a coherent β tron oscillation
   - Siberian Snakes
   - measuring beam polarization in RHIC
   - it works! ← September commissioning

2. RHIC detectors + comparisons to DIS

3. What I skipped

Polarized proton collisions in RHIC

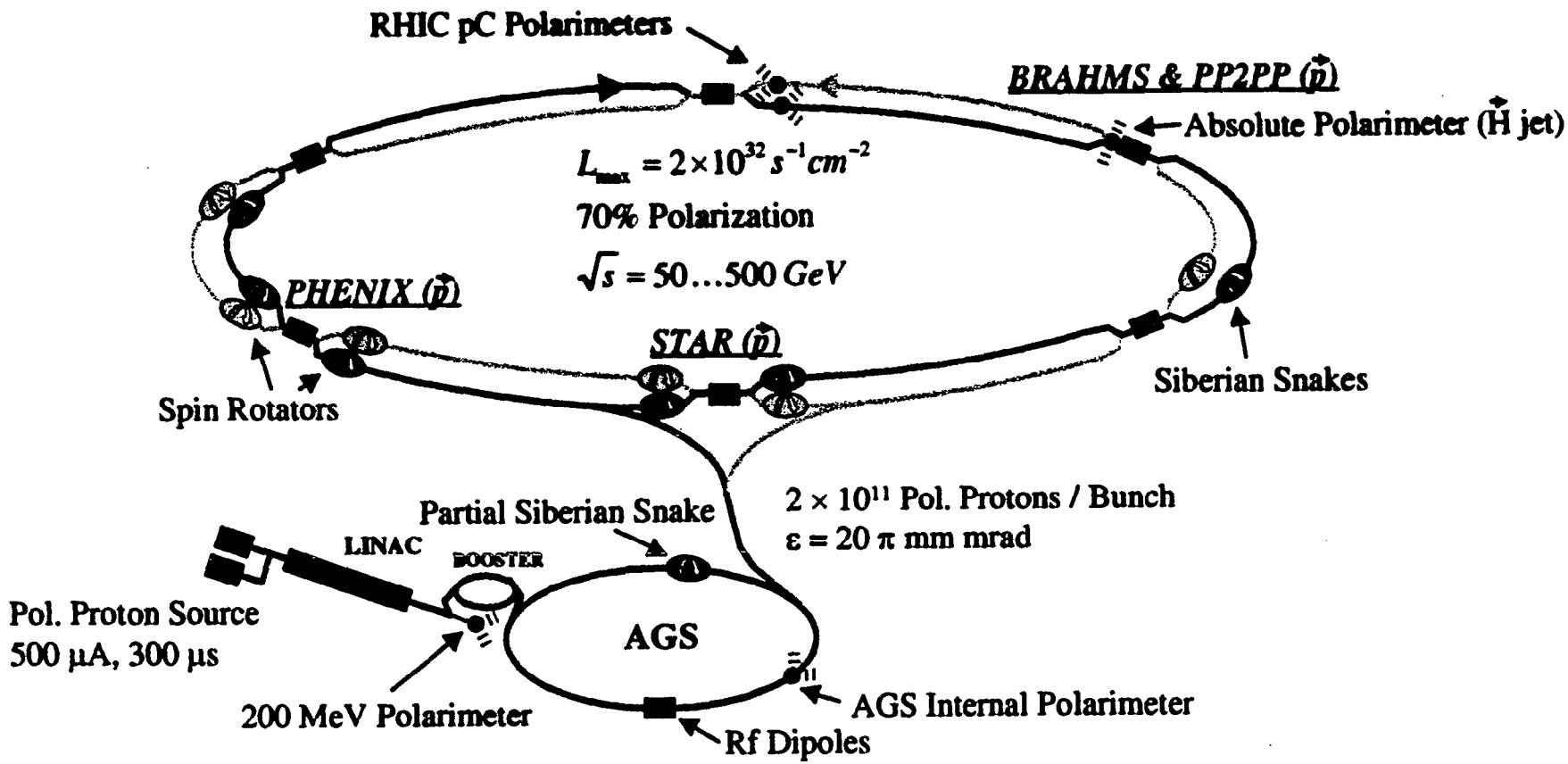

BROOKHAVEN
NATIONAL LABORATORY

D0070799

What are spin resonances?

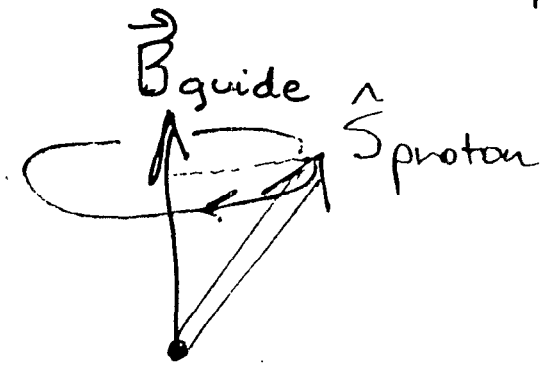

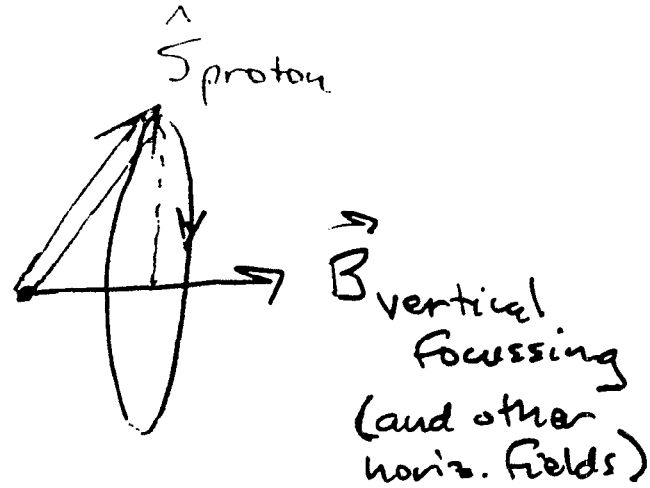

When the two are in phase → spin resonance.

Several solutions:

- jump past energies of spin resonances
  → non-adiabatic, blows up beam size

→ - for a strong resonance, spin flips but polarization is not lost if all the beam sees the resonance

→ - Siberian Snakes

Crossing Intrinsic Resonance using RF Dipole

Adiabatically generate a Coherent Betatron Oscillation to increase the resonance strength seen by every particle; thus, all will flip spin

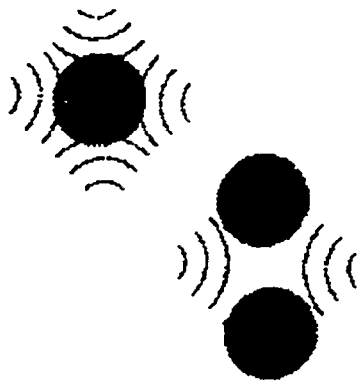

In frame rotating at the RF dipole frequency:

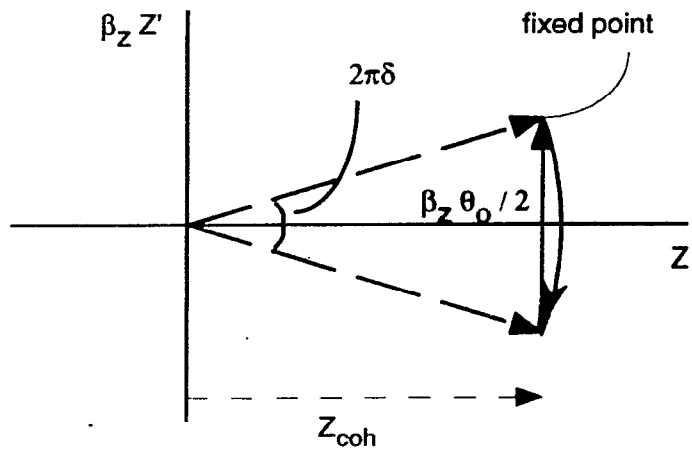

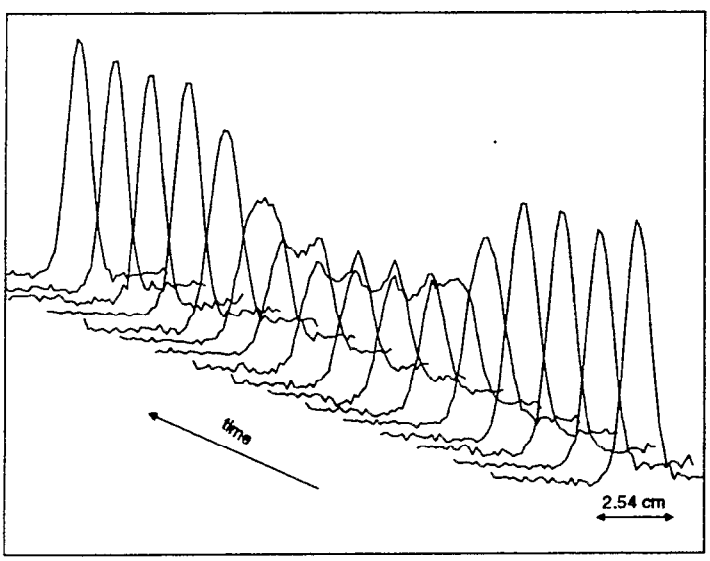

$$Z_{coh} = \beta_z \theta_0 / 4\pi\delta$$

$$\delta = \nu_{rf} - \nu_\beta$$

Emittance is preserved throughout the process

Vertical Beam Response with the RF Dipole

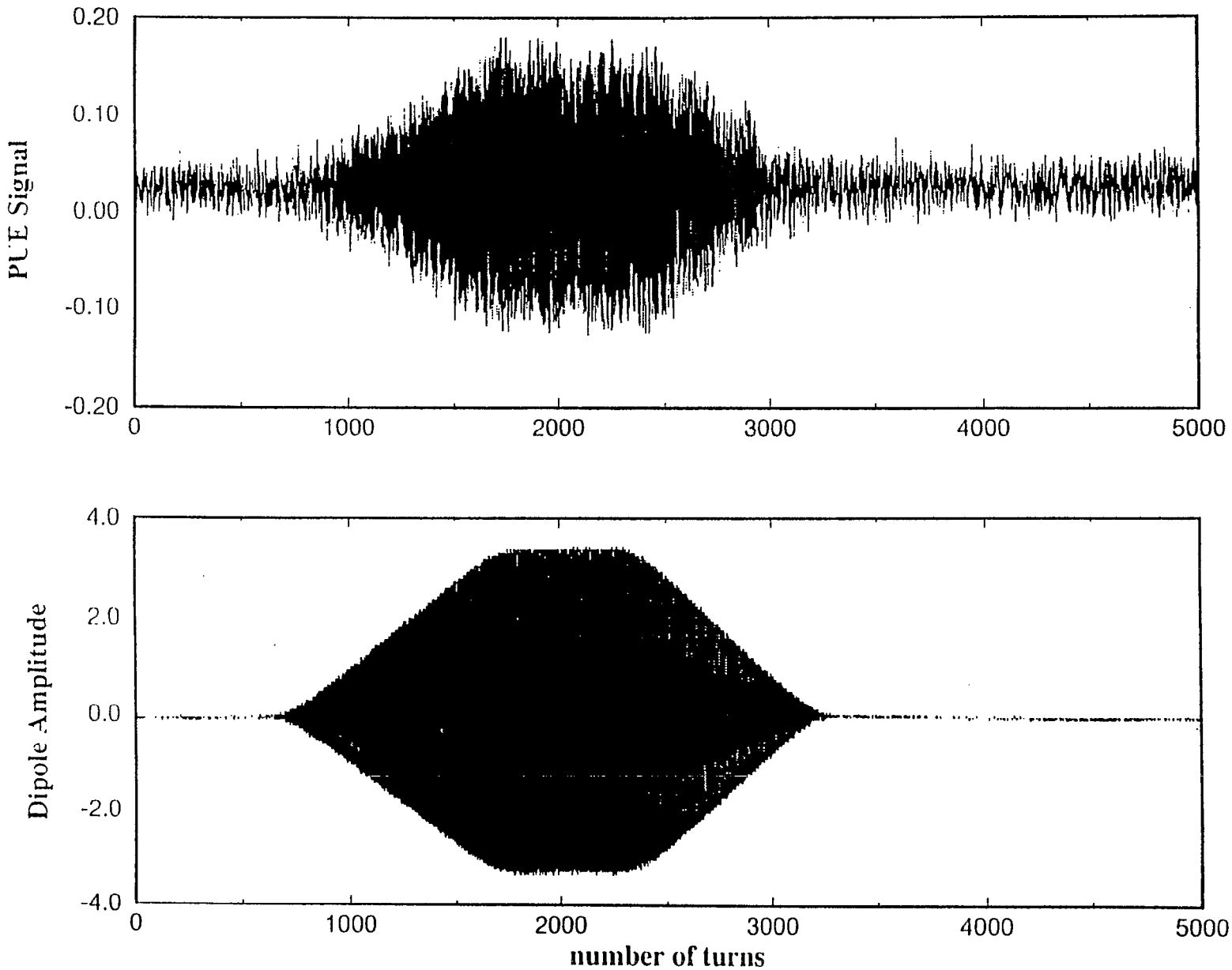

Crossing of intrinsic resonance in AGS using RF dipole magnet...

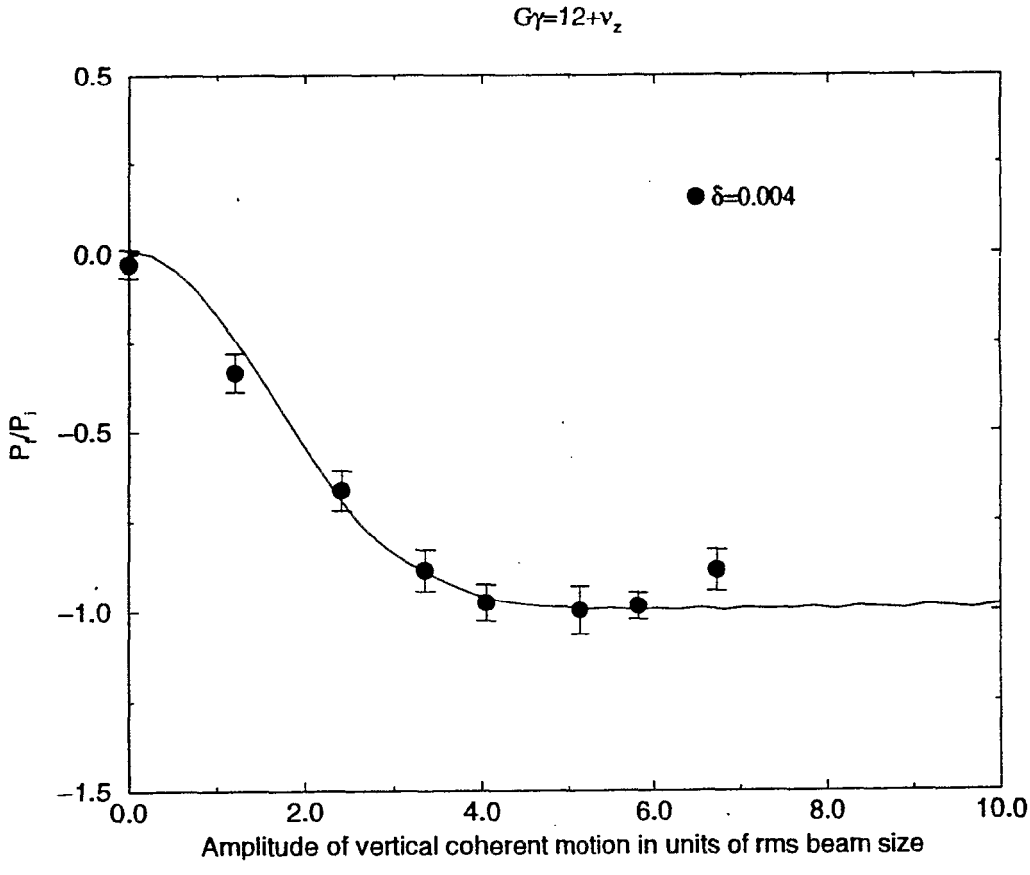

Total Spin Flip is generated

The RF dipole modulation tune was separated from the betatron tune by 0.004

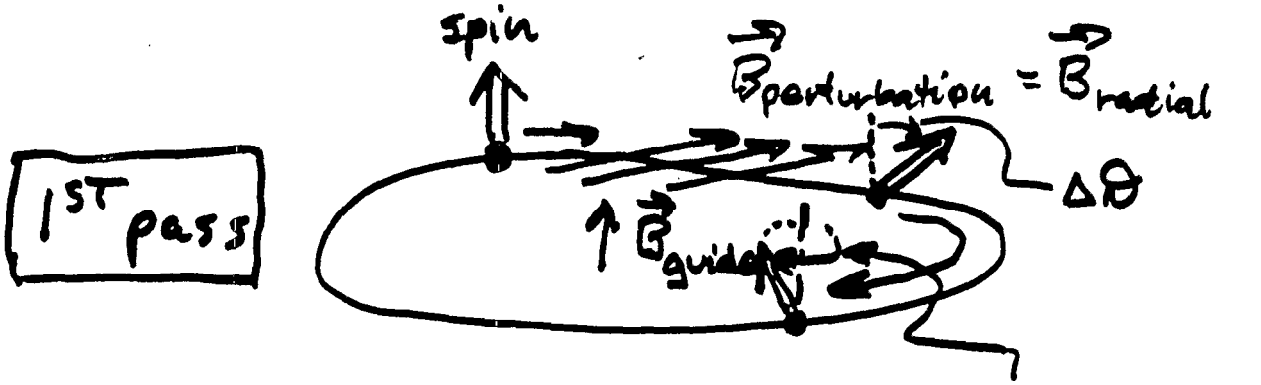

spin processes around $\vec{B}_{guide}$ by $\frac{g-2}{2}\gamma \times \vec{v}$

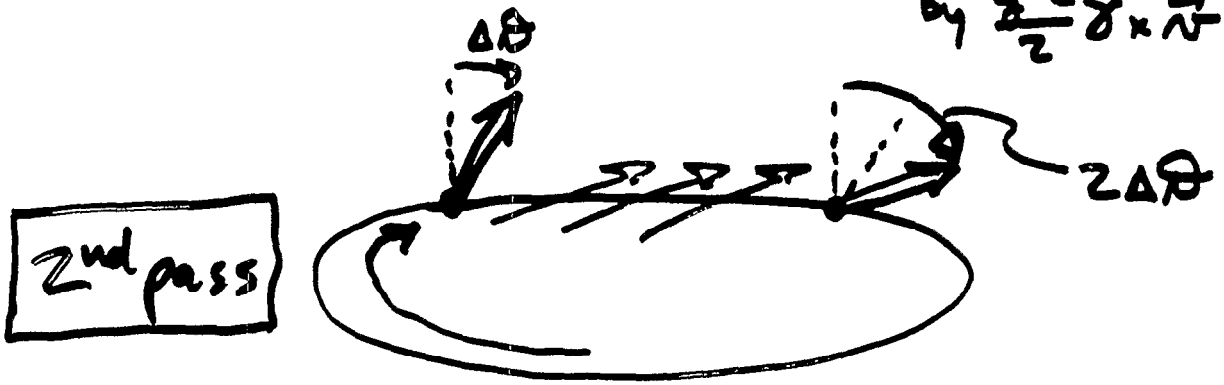

Siberian Snake:

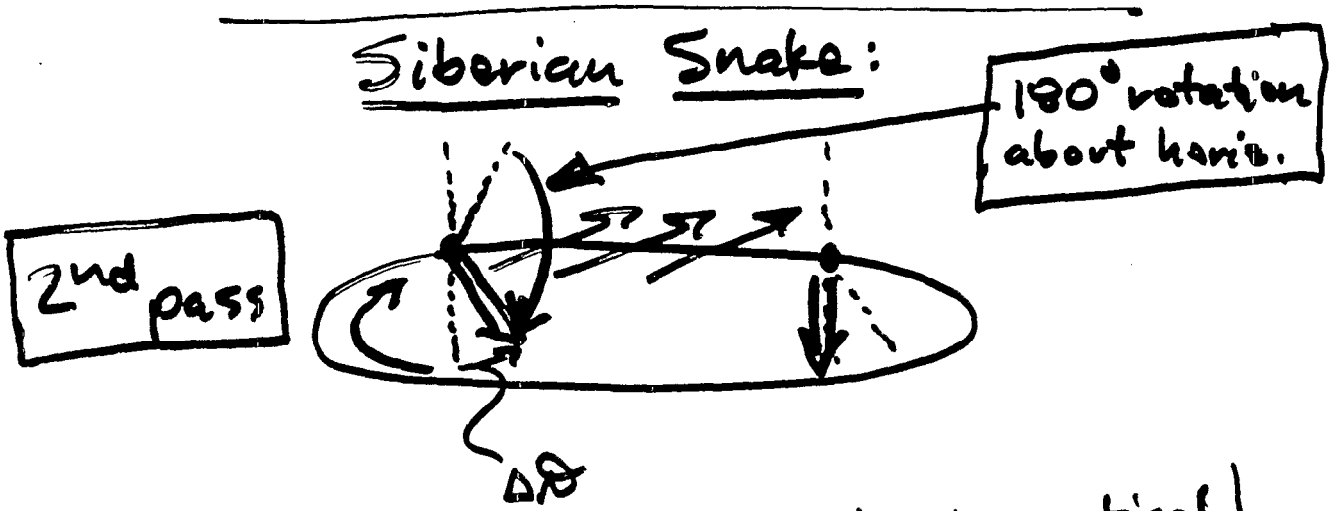

After 2 turns, polarization is vertical!

Shatunov, Ptitsin (1993): use 4 helical dipoles → snake.

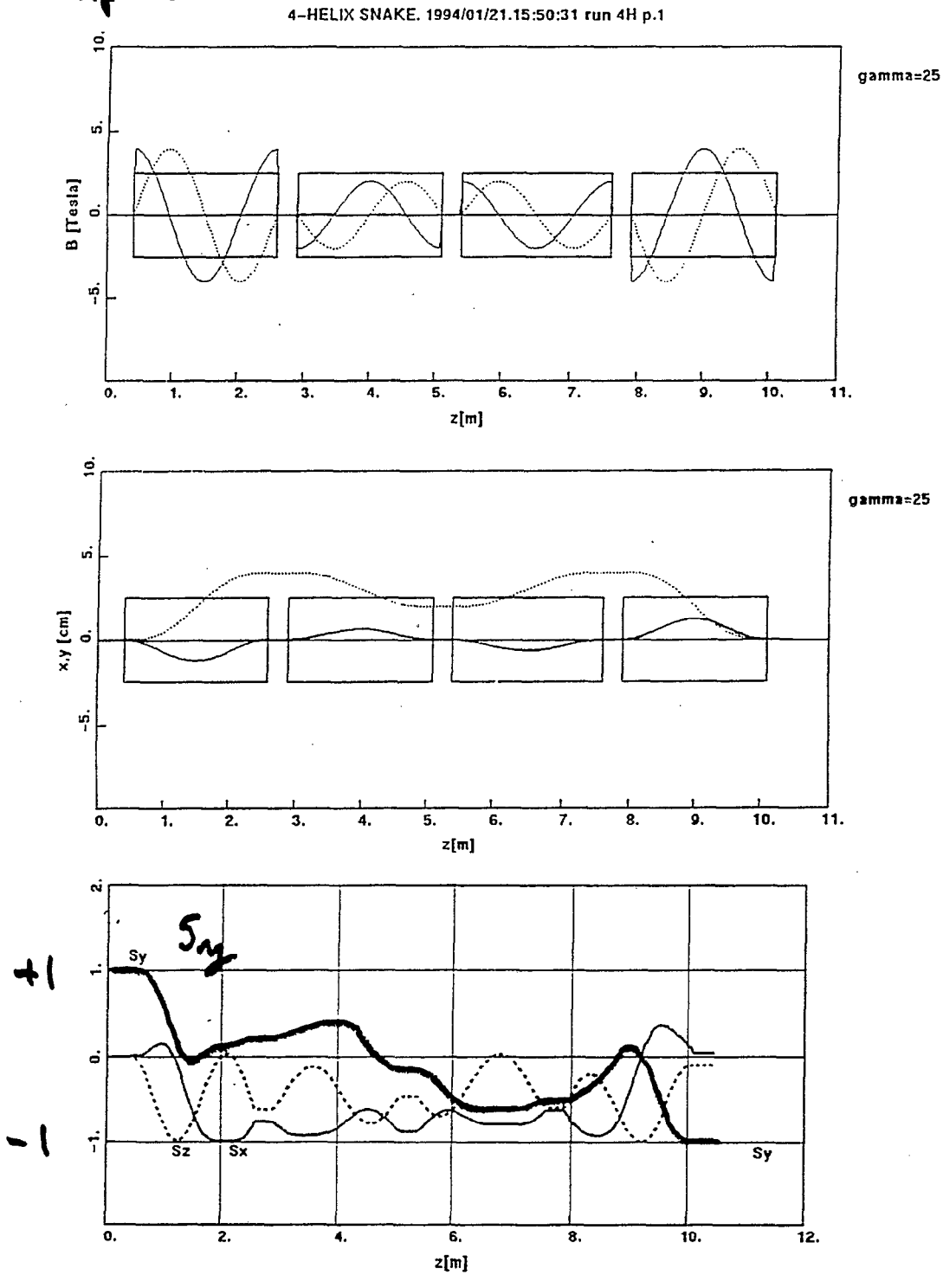

X (mm)
-40
-30
0
30
40
Y (mm)
-40
-30
0
30
40
z (m)
0
2
4
6
8
10

P00019S

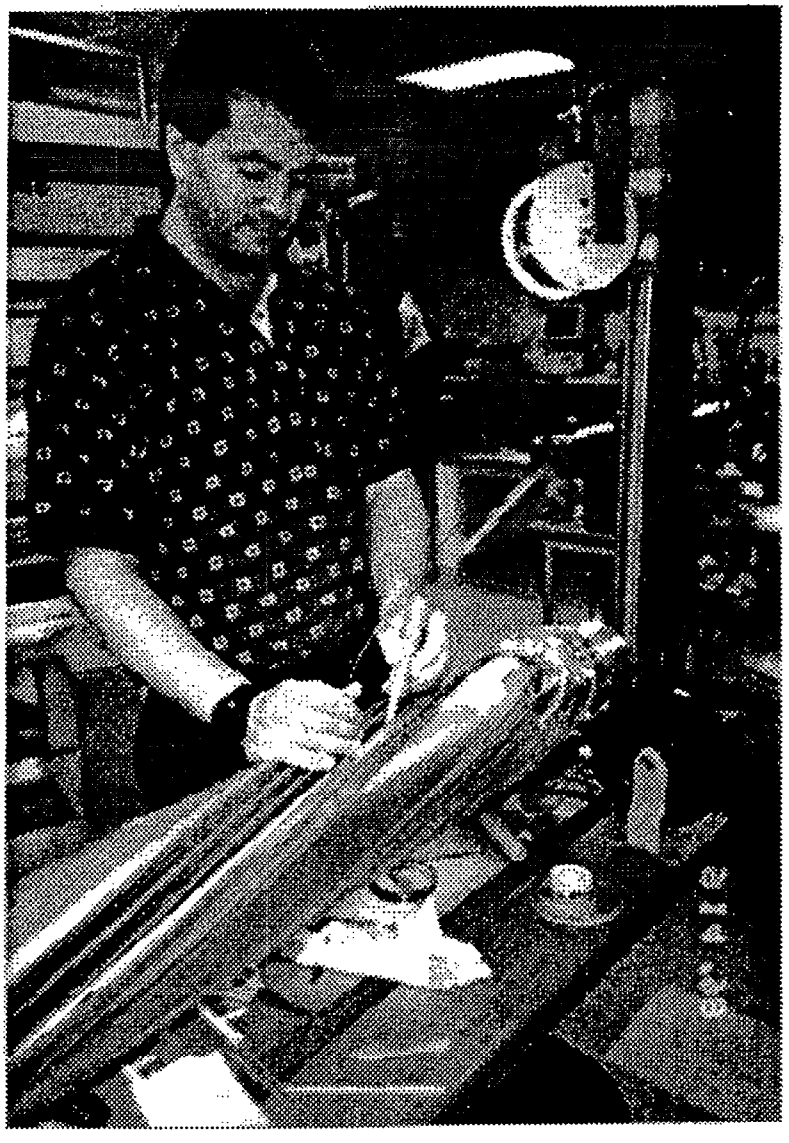

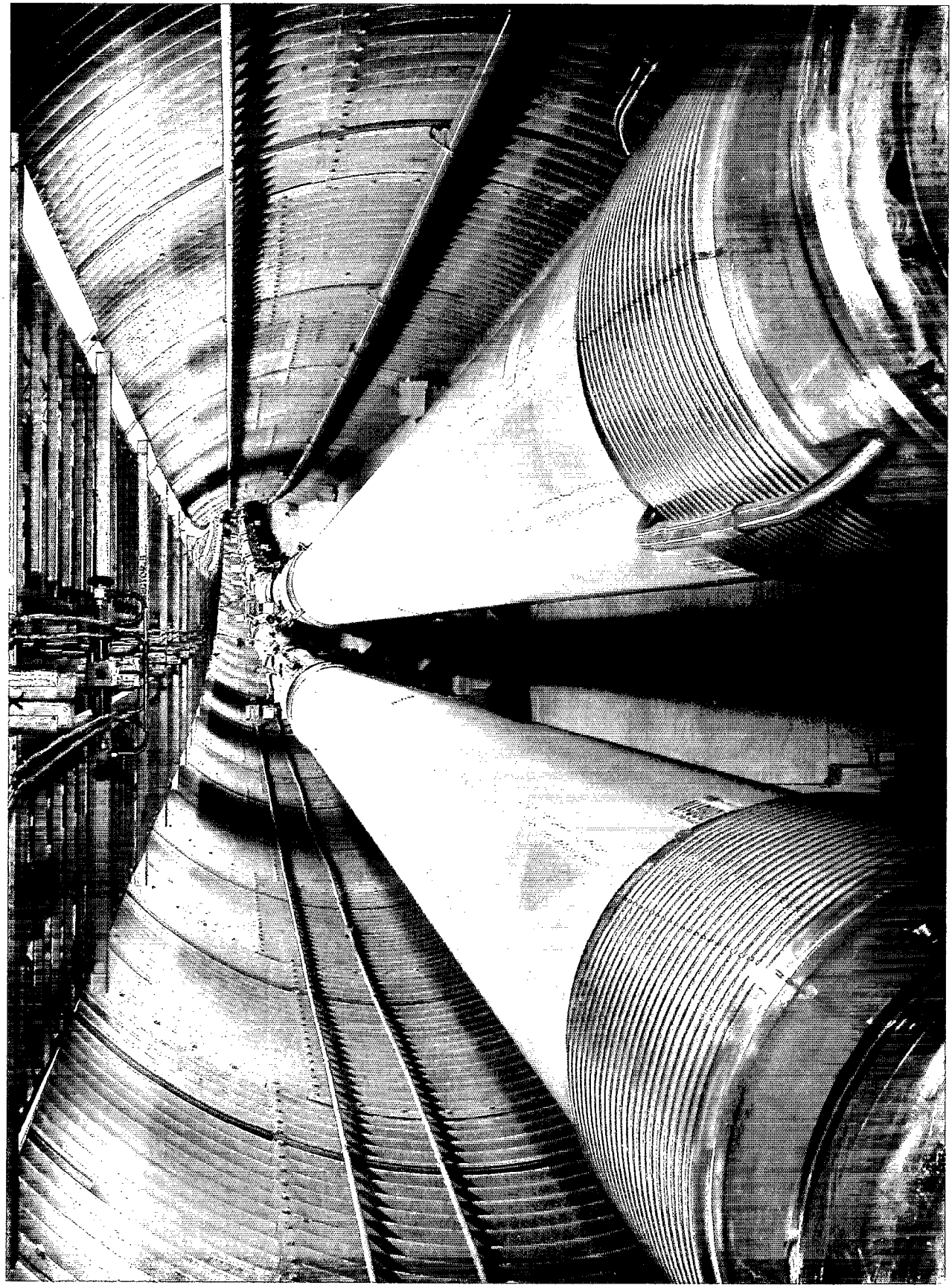

Measuring the beam polarization at RHIC:

- with electrons there are QED processes which can be calculated precisely: measure an asymmetry in scatter $\rightarrow P_{electron}$

- at low energy, use Stern Gerlach to separate spin states, measure P_{proton}
  - targets, sources

- at energies up to ~ 25 GeV use proton-proton elastic scattering at $-t = .15\,(GeV/c)^2$
  - empirical — analyzing power falls as $1/E$
  - calibrated with polarized target:

$$\underset{\text{beam}}{p\Uparrow} + p \rightarrow pp \qquad p + \underset{\text{target}}{p\Uparrow} \rightarrow pp$$

same A_N

- Coulomb-Nuclear interference is independent of E through RHIC energy range

$$\frac{N_{left} - N_{right}}{+} = .04\, P_{beam} \quad \text{for } p\Uparrow + \binom{C}{p} \rightarrow p + \binom{C}{p}$$

$-t = .003$

Beauty of CNI

Asymmetry calculable

$$A_N = \frac{G t_0 t \sqrt{t}}{m_p (t^2 + t_0^2)}$$

$$t_0 = \frac{8\pi\alpha Z}{\sigma_{tot}}$$

Weak beam momentum dependence

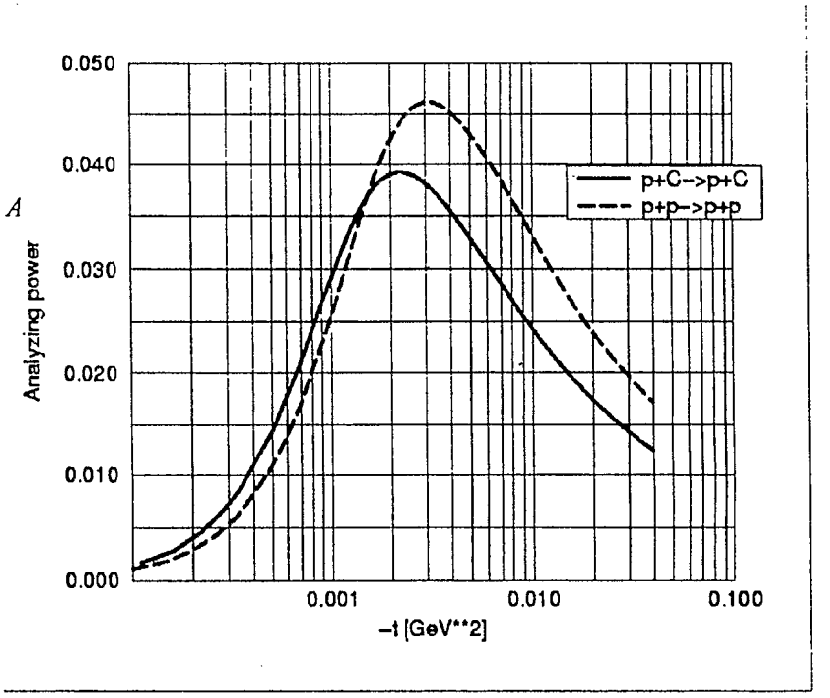

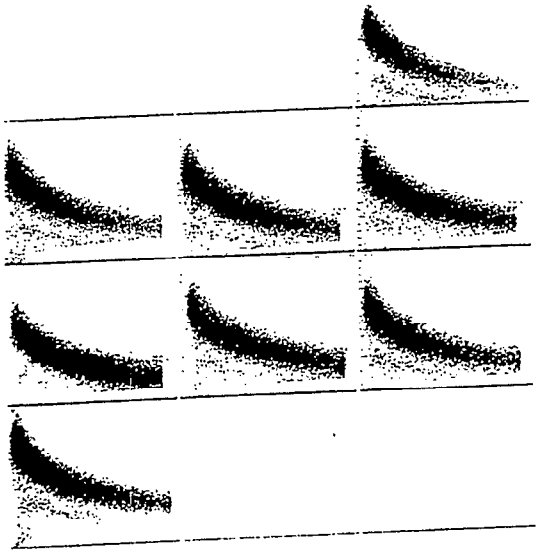

Bunched Beam / no squeeze

Polarimeter in RHIC

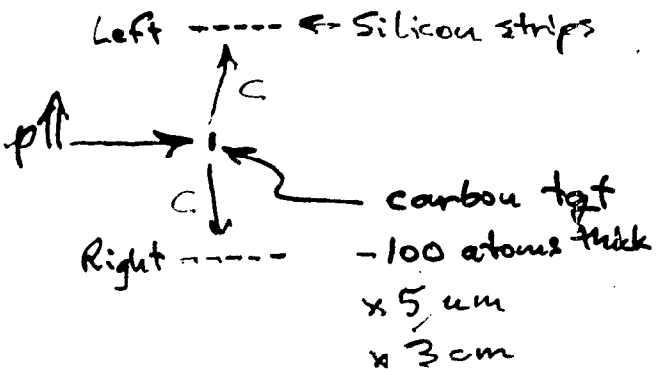

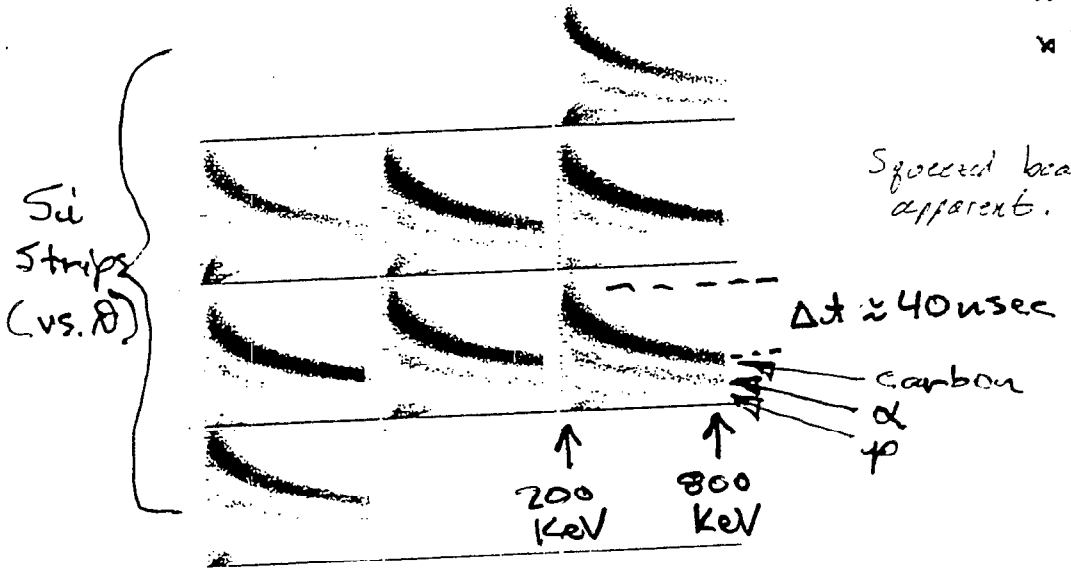

Squeezed beam ; α peak apparent.

$$\text{Asym} = \frac{\text{Left} - \text{Right}}{\text{Left} + \text{Right}} = k\, P_{beam} \left(\frac{g-2}{2}\right)_p \times \sigma_{total\,pc}$$

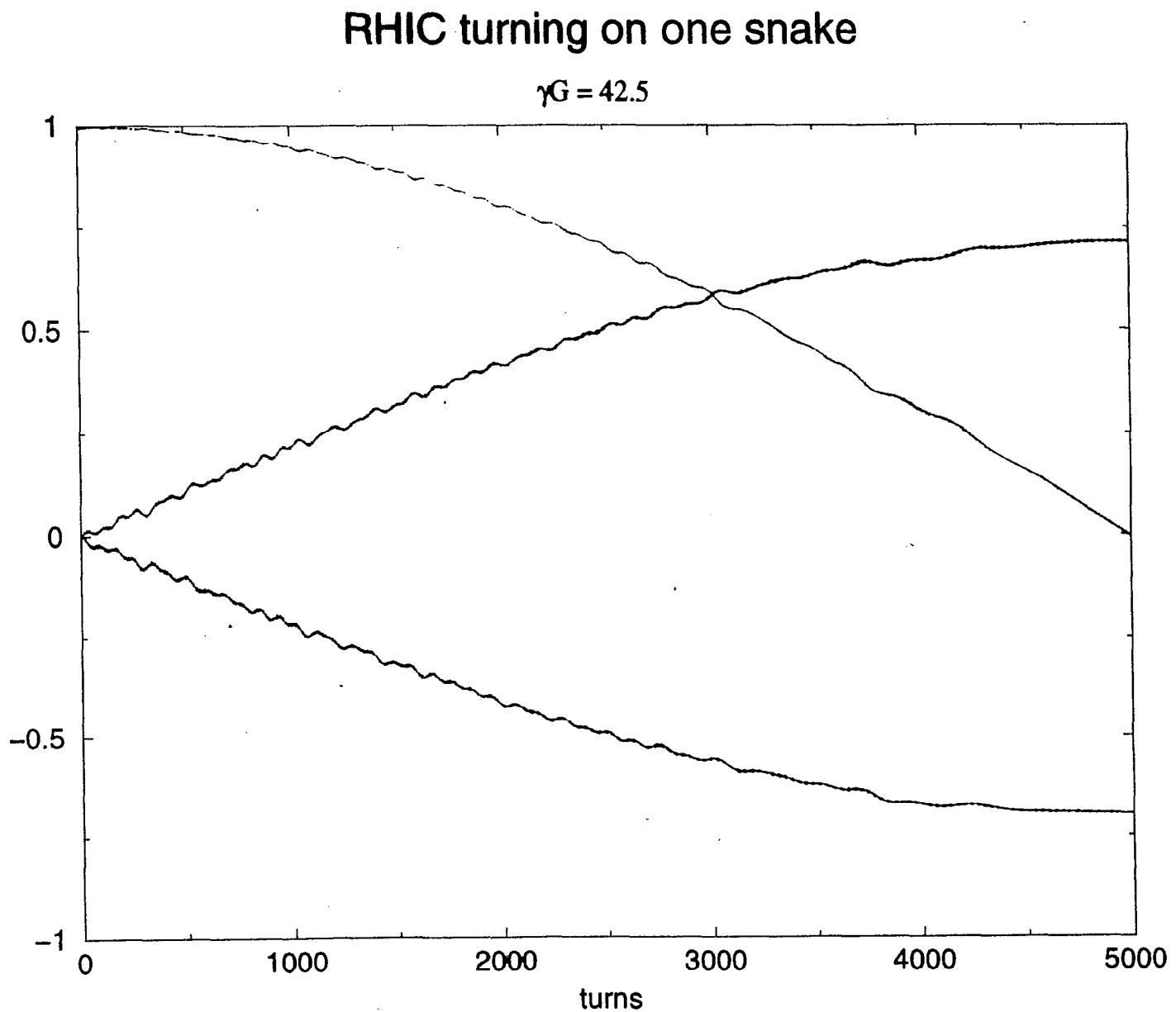
RHIC turning on one snake
γG = 42.5
1
0.5
0
−0.5
−1
< S >
0
1000
2000
3000
4000
5000
turns

Spin commissioning with a single Snake

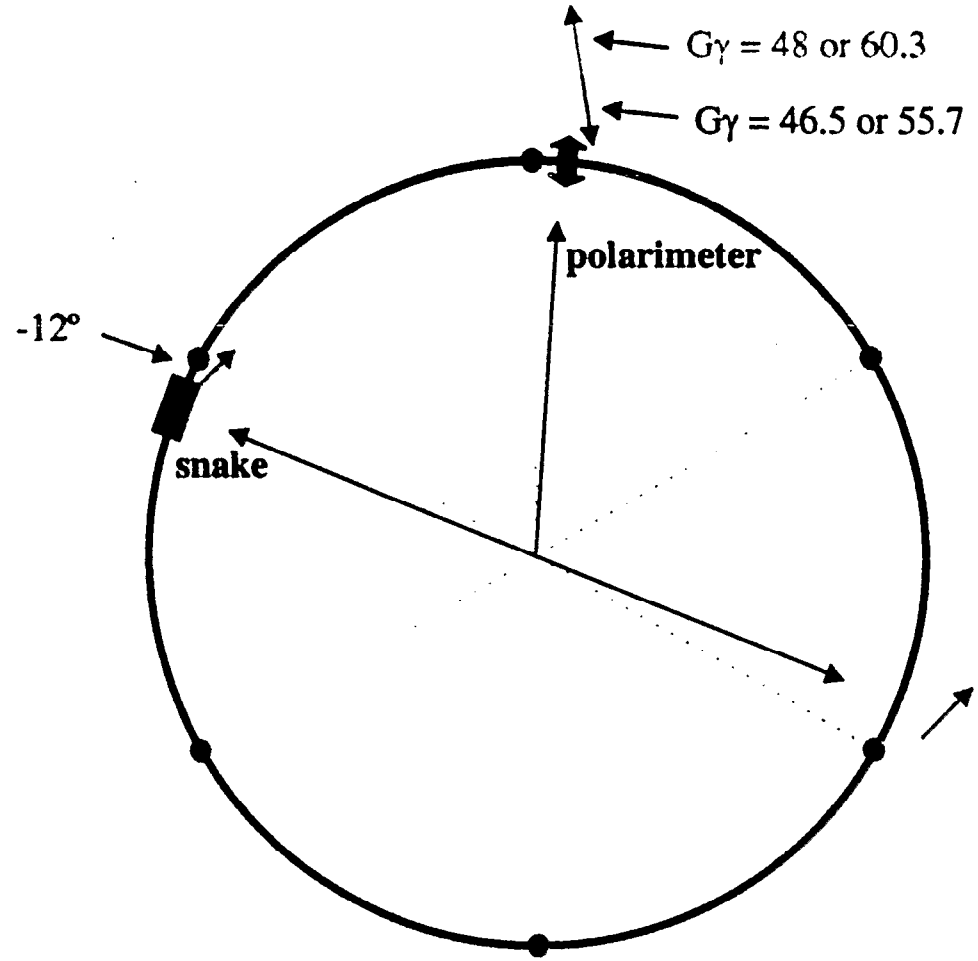

BROOKHAVEN
NATIONAL LABORATORY

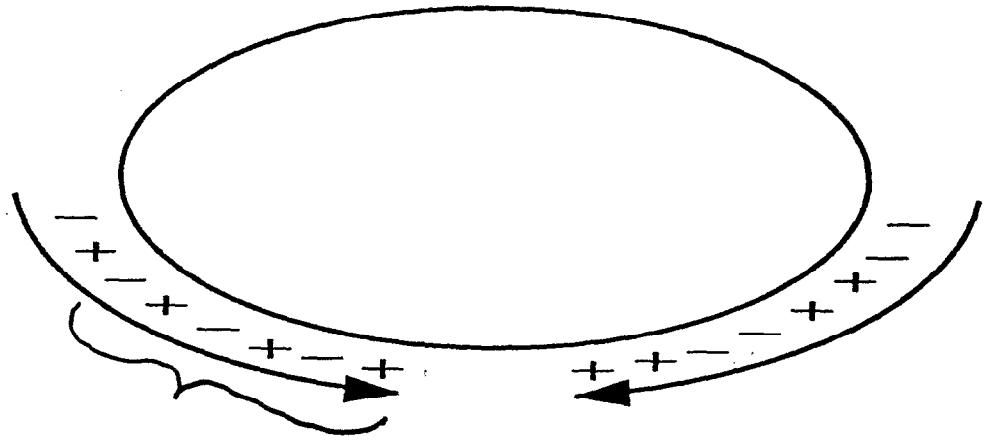

Commissioning:
loaded 6 bunches
- 2 μsec apart

2001 Spin run:
load 60 bunches
- 200 nsec apart

2002 Spin run:
load 120 bunches
- 100 nsec apart

Polarization with Snake magnet ON/OFF

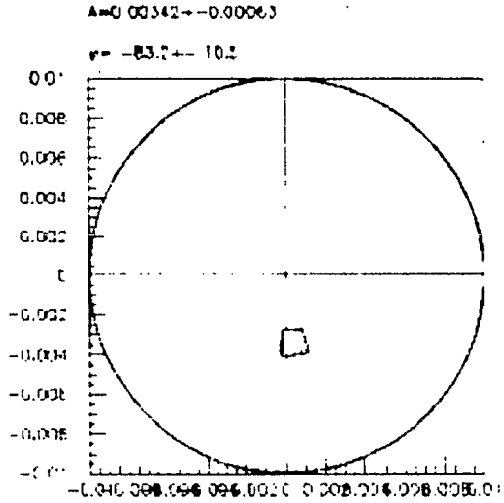

Gγ=46.5 Injection energy
Snake OFF Vertical polarization

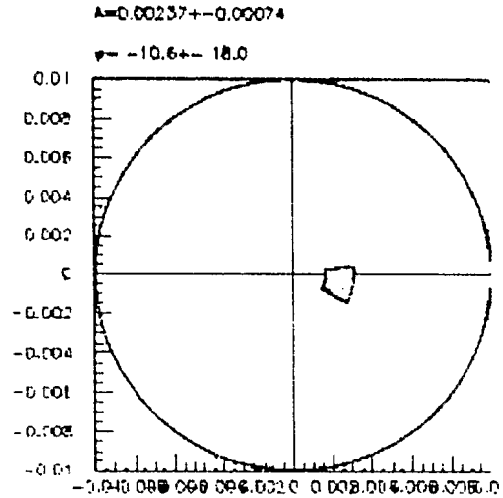

Gγ=46.5 Injection energy
Snake ON Horizontal polarization

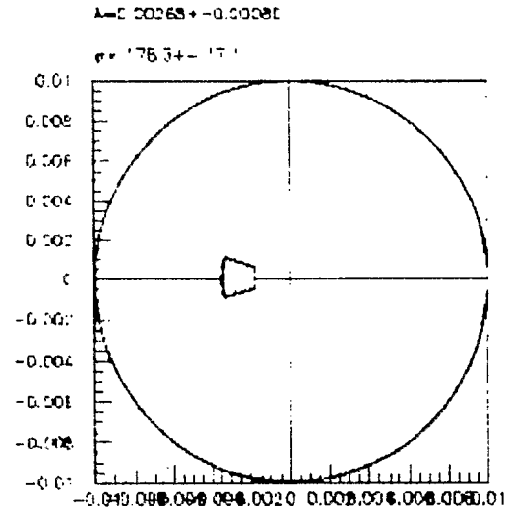

Gγ=48 Acceleration with Snake ON
Horizontal polarization

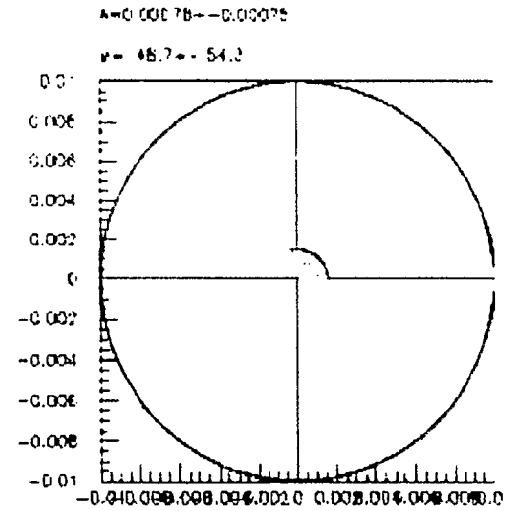

Gγ=48 Acceleration with Snake OFF
Polarization lost

Spin resonances in RHIC (w/o Snakes)

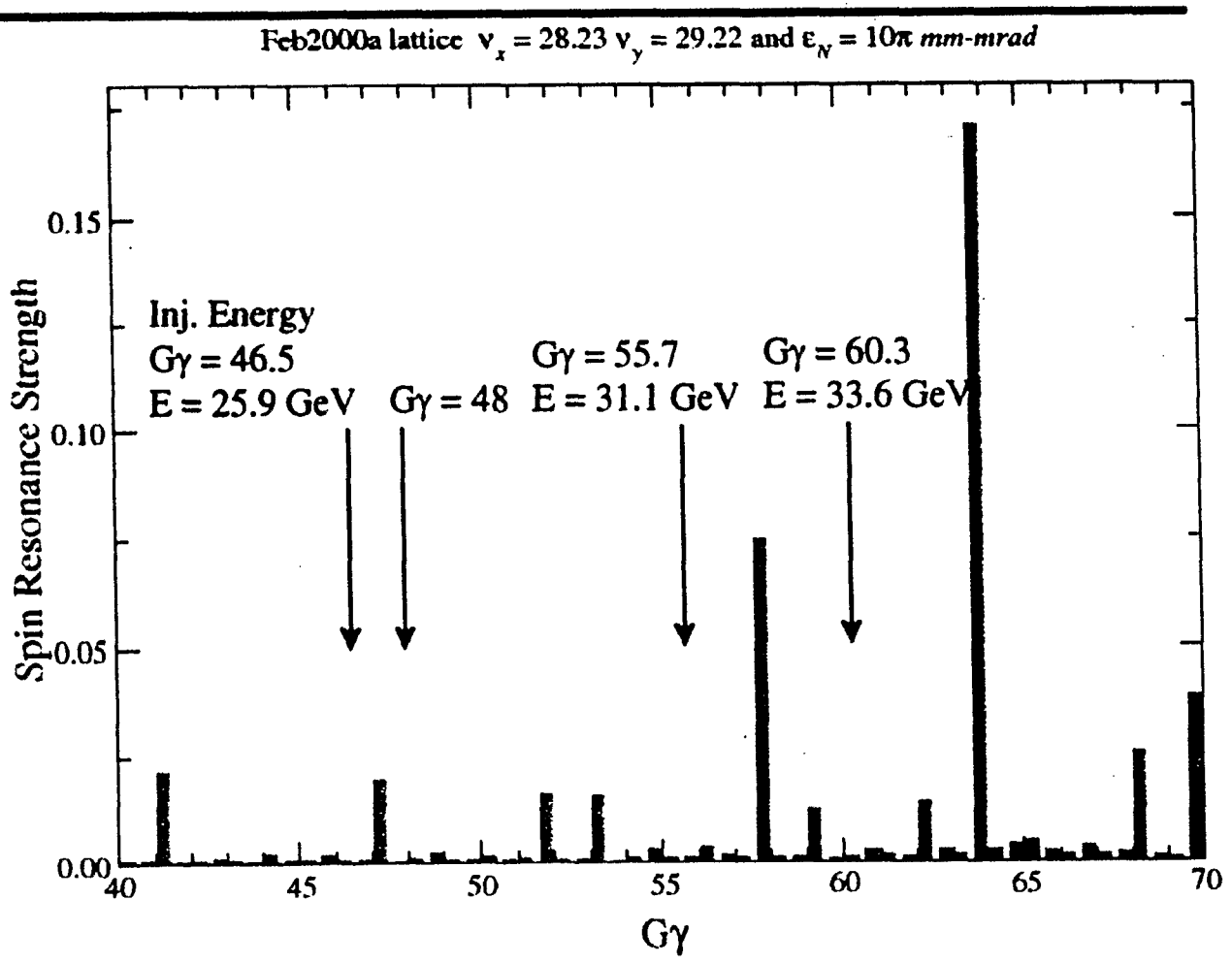

BROOKHAVEN
NATIONAL LABORATORY

Acceleration with single snake

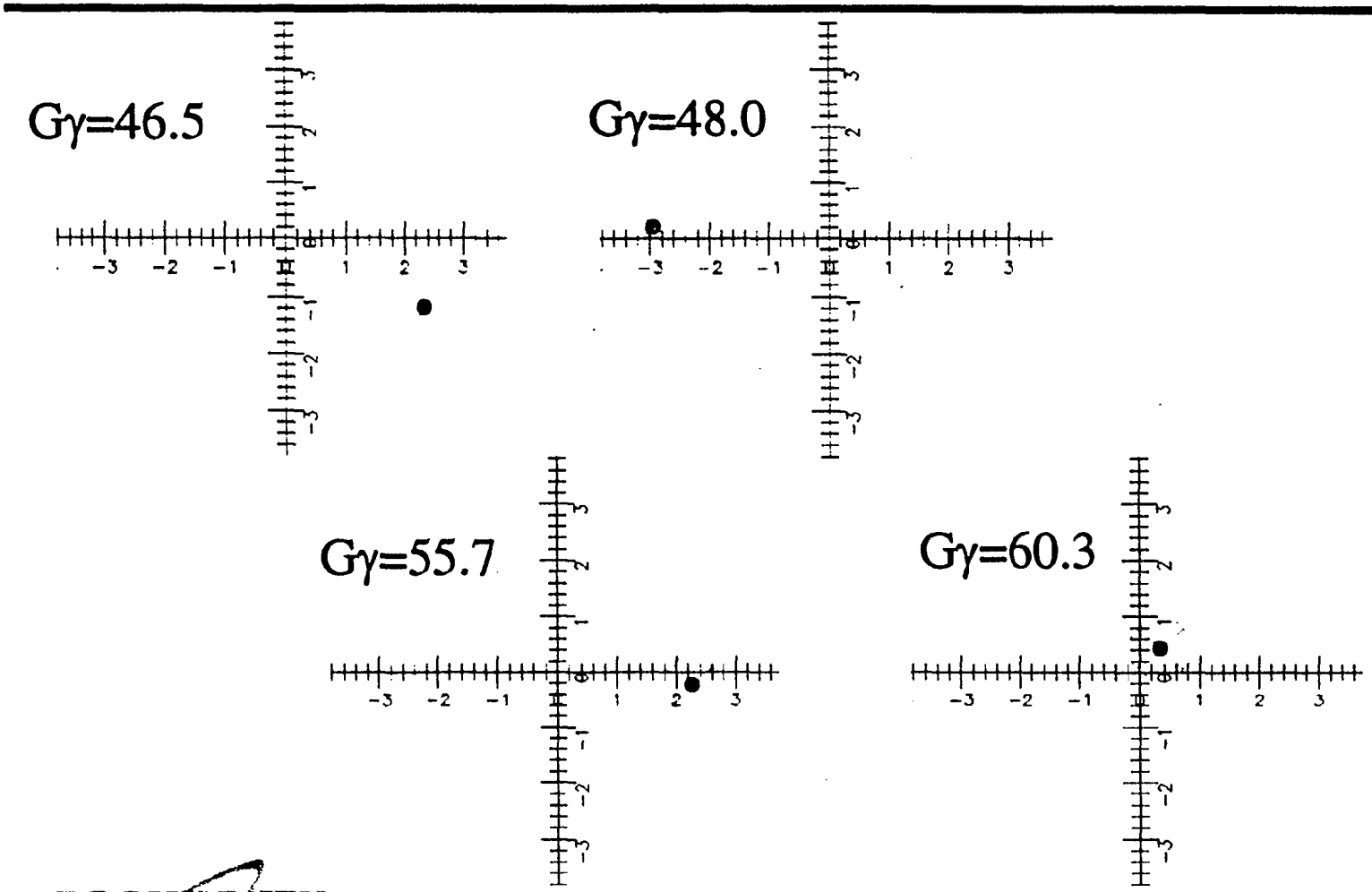

BROOKHAVEN
NATIONAL LABORATORY

Single Snake in RHIC ($E \leq 100$ GeV)

At $E = 100.53$ GeV: $G\gamma = 192 = 6 \times 32$
→ all IP's have same polarization
For snake axis at -52° → longitudinal polarization

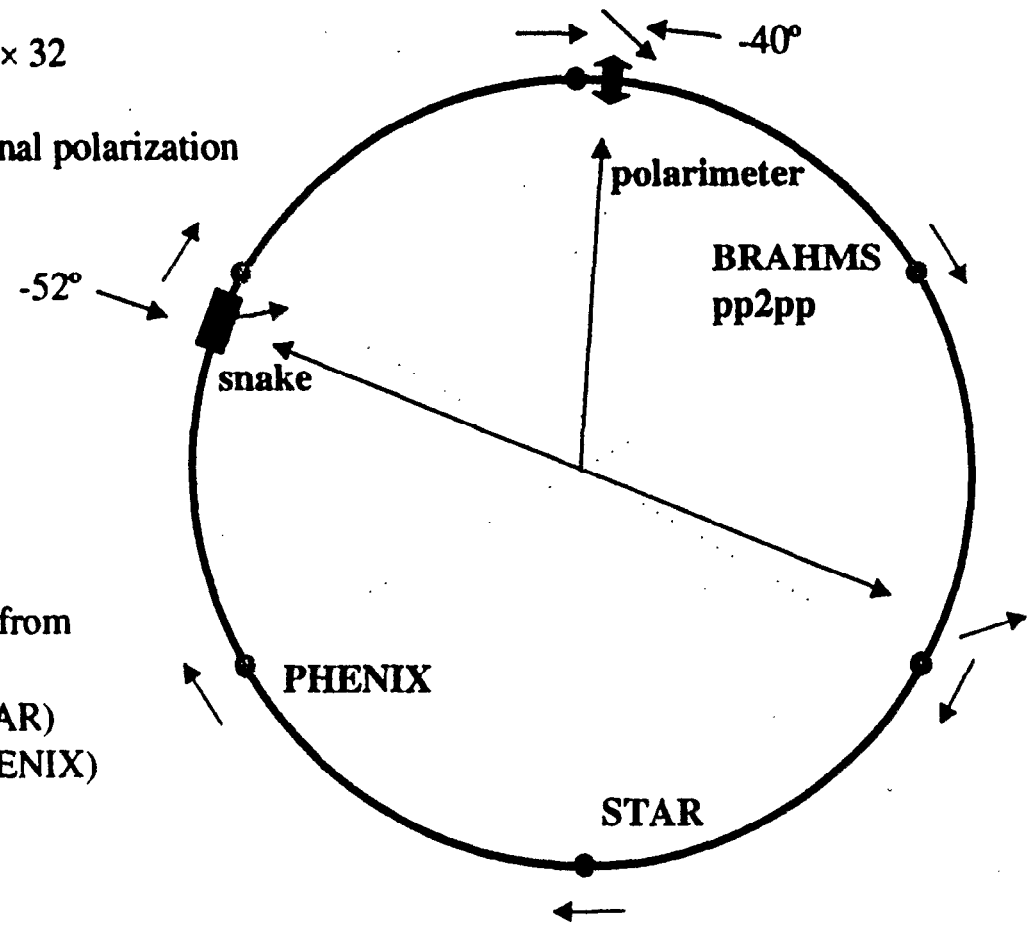

For $\Delta p/p = \pm 0.001$ max. deviation from long. polarization:
$32 \times \Delta p/p \times 360° = \pm 12°$ [0.98] (STAR)
$64 \times \Delta p/p \times 360° = \pm 24°$ [0.91] (PHENIX)

BROOKHAVEN
NATIONAL LABORATORY

RHIC Detectors

Built to handle low rate, high mult.
Au-Au
→ work for high rate, low multiplicity
pp

STAR — solenoid, TPC, EM calorimeter,
shower max. detector,
large coverage
→ γ, $e^{\pm}$, jets

PHENIX — side electron + photon detectors
with fine granularity;
forward muon detectors
→ γ, π^0, $e^{\pm}$, $\mu^{\pm}$

pp2pp — small angle pp expt. will measure
absolute polarization in coulomb-
nuclear interference region, study
spin in small angle scattering

STAR Detector

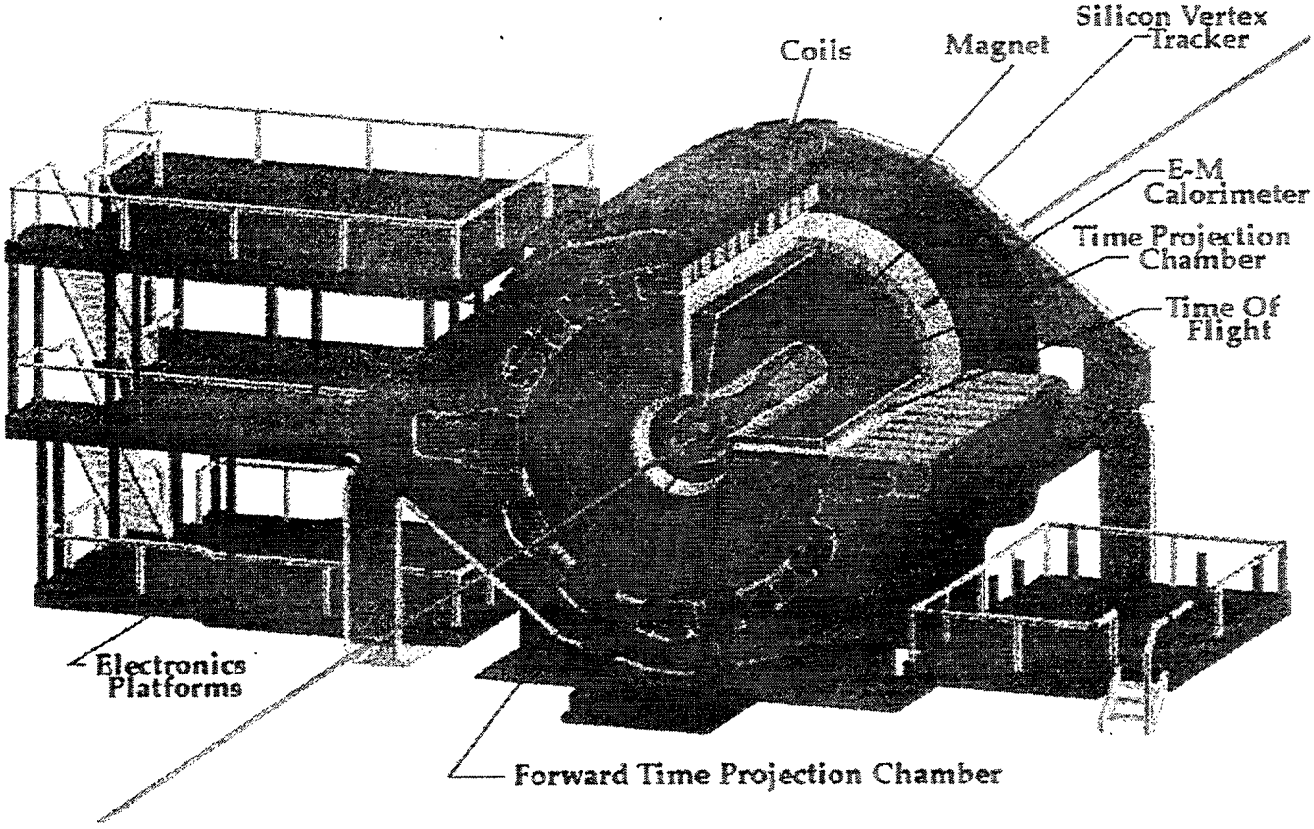

$q + g \rightarrow \gamma + q$ (STAR)

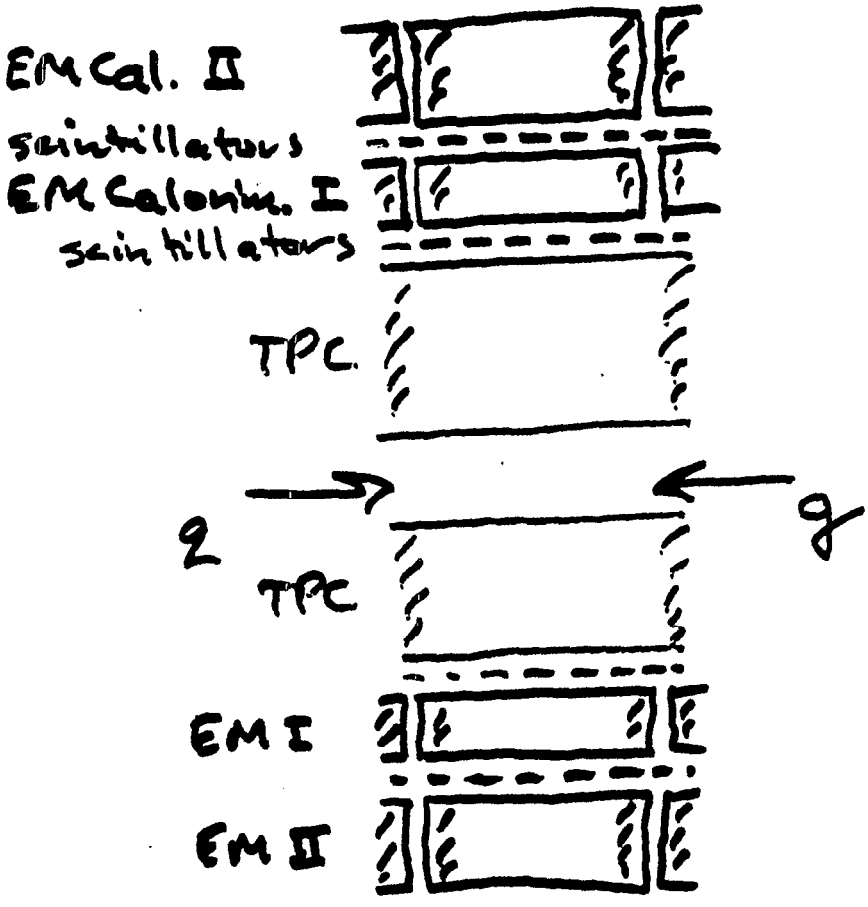

resolve π^0 to $p_\perp \lesssim 25$ GeV

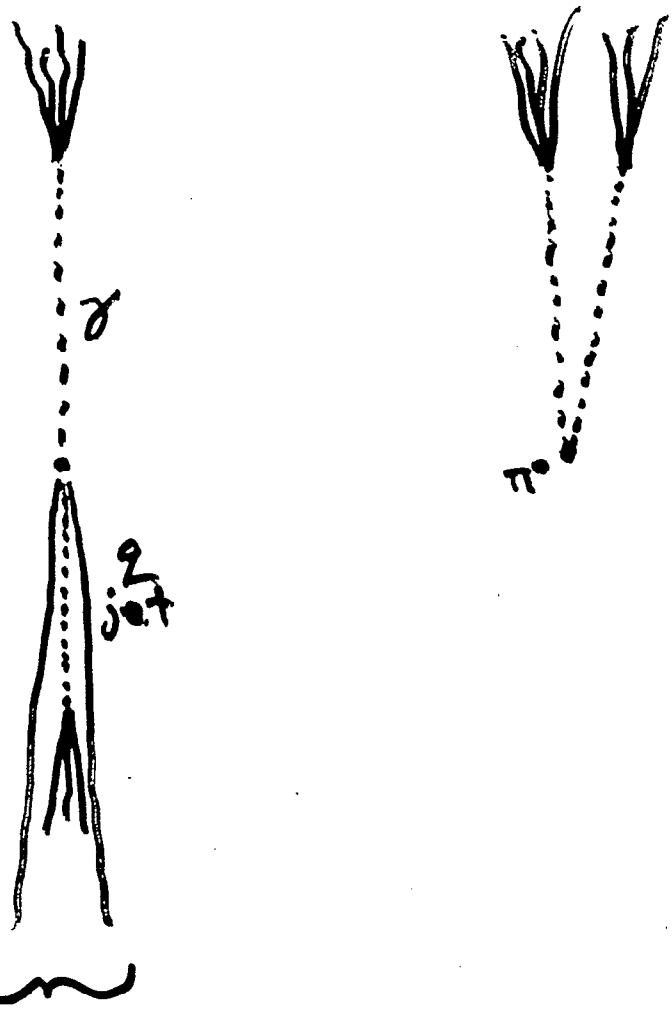

jet from adding
EM energy + charged energy

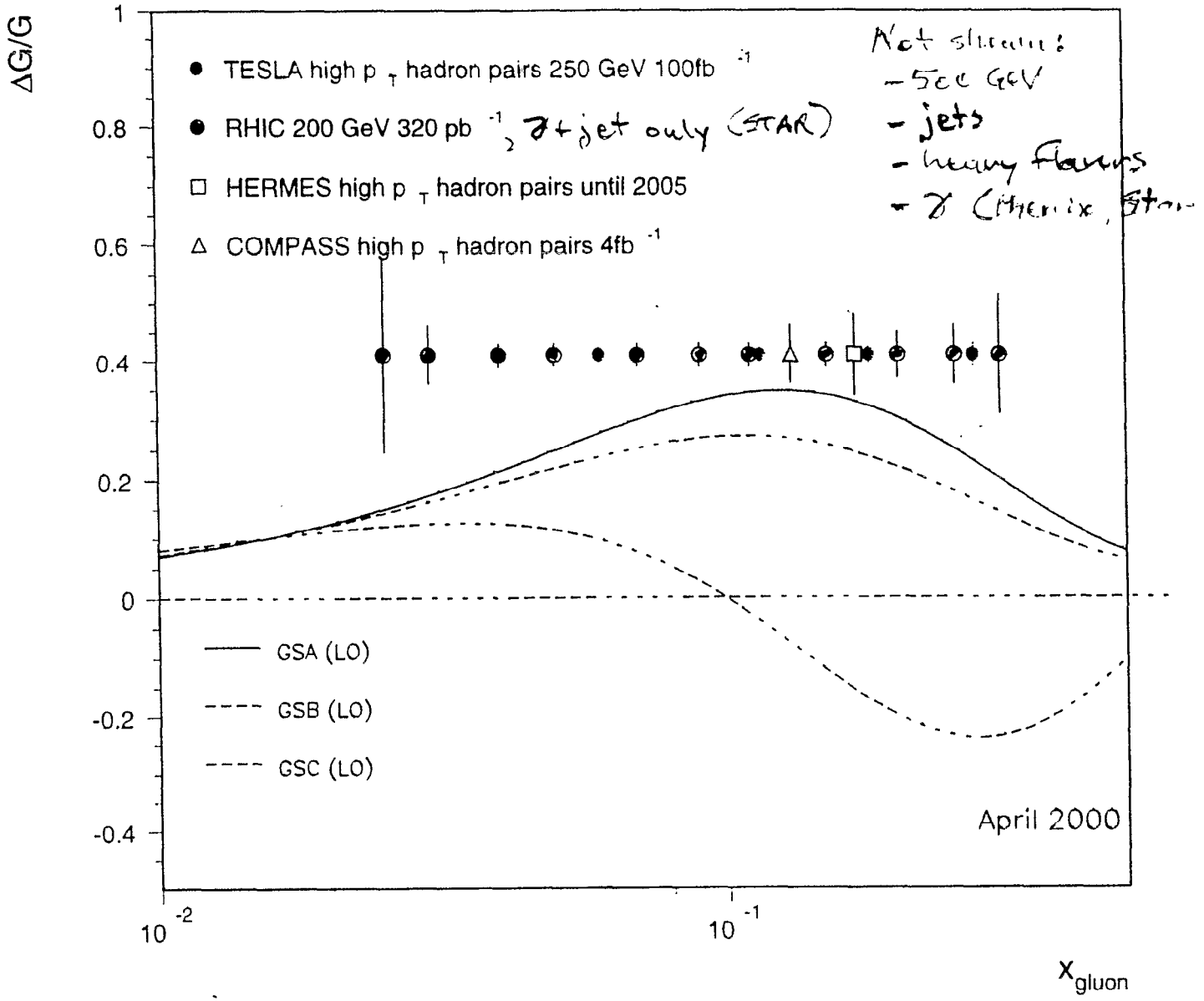
ΔG/G
1
0.8
0.6
0.4
0.2
0
-0.2
-0.4
TESLA high p T hadron pairs 250 GeV 100fb -1
RHIC 200 GeV 320 pb -1, γ+jet only (STAR)
HERMES high p T hadron pairs until 2005
COMPASS high p T hadron pairs 4fb -1
Not shown:
- 500 GeV
- jets
- heavy flavors
- γ (PHENIX, STAR
GSA (LO)
GSB (LO)
GSC (LO)
April 2000
10 -2
10 -1
x gluon

PHENIX Experiment at RHIC:

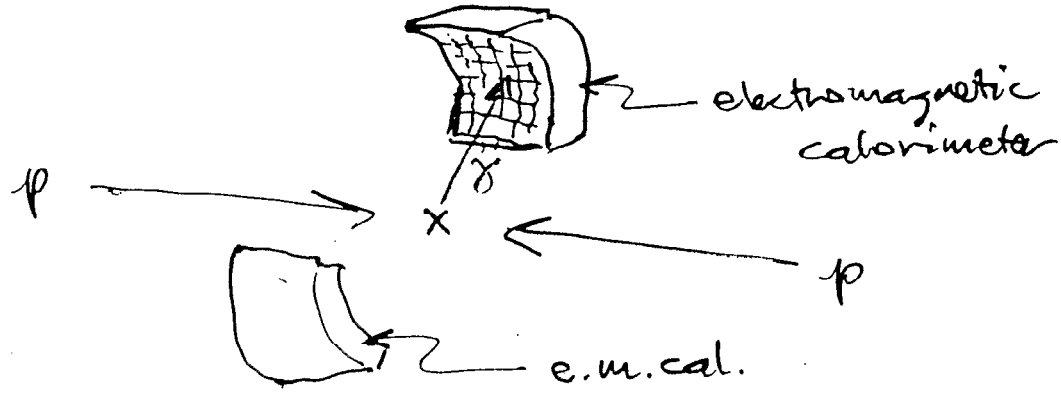

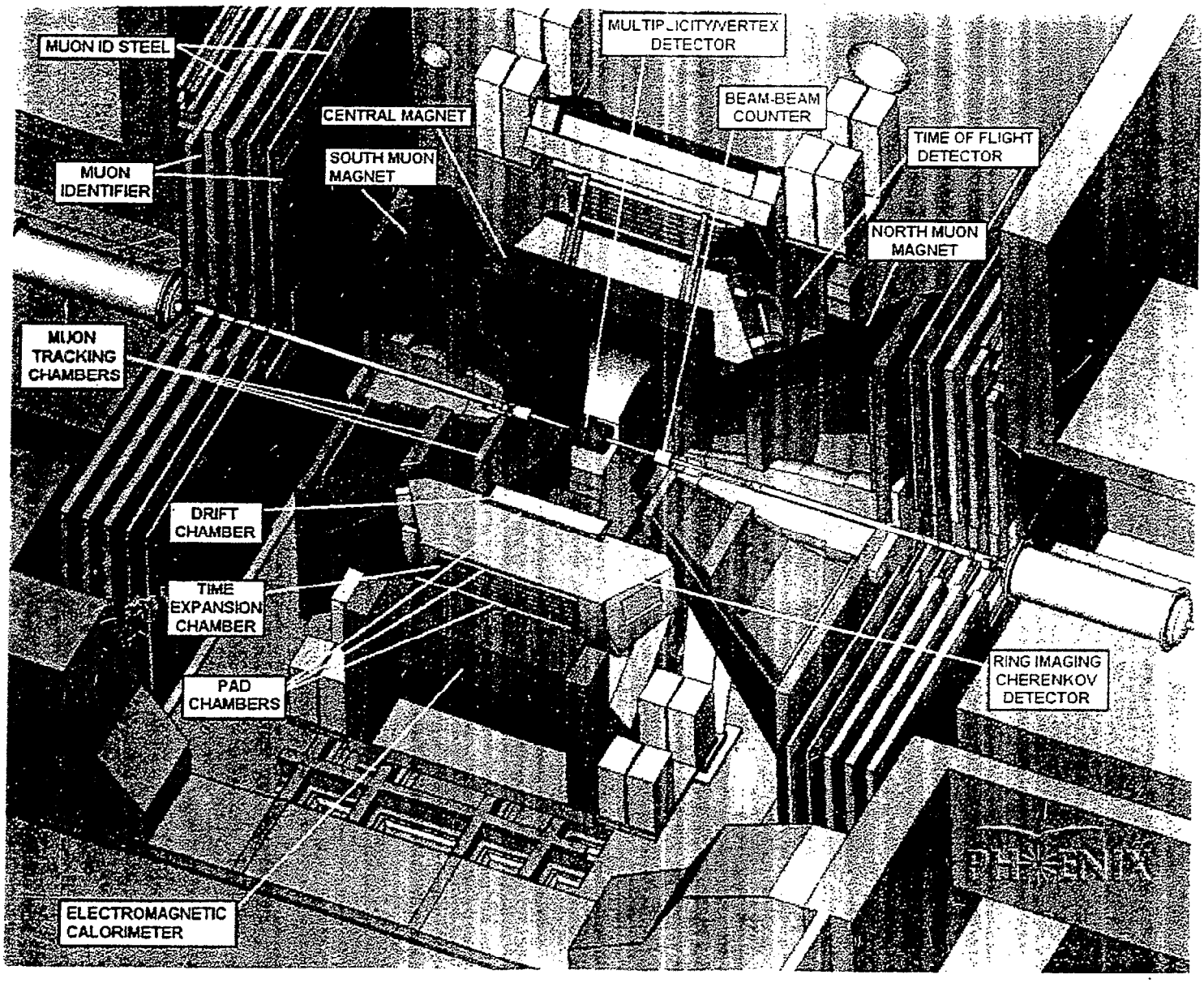

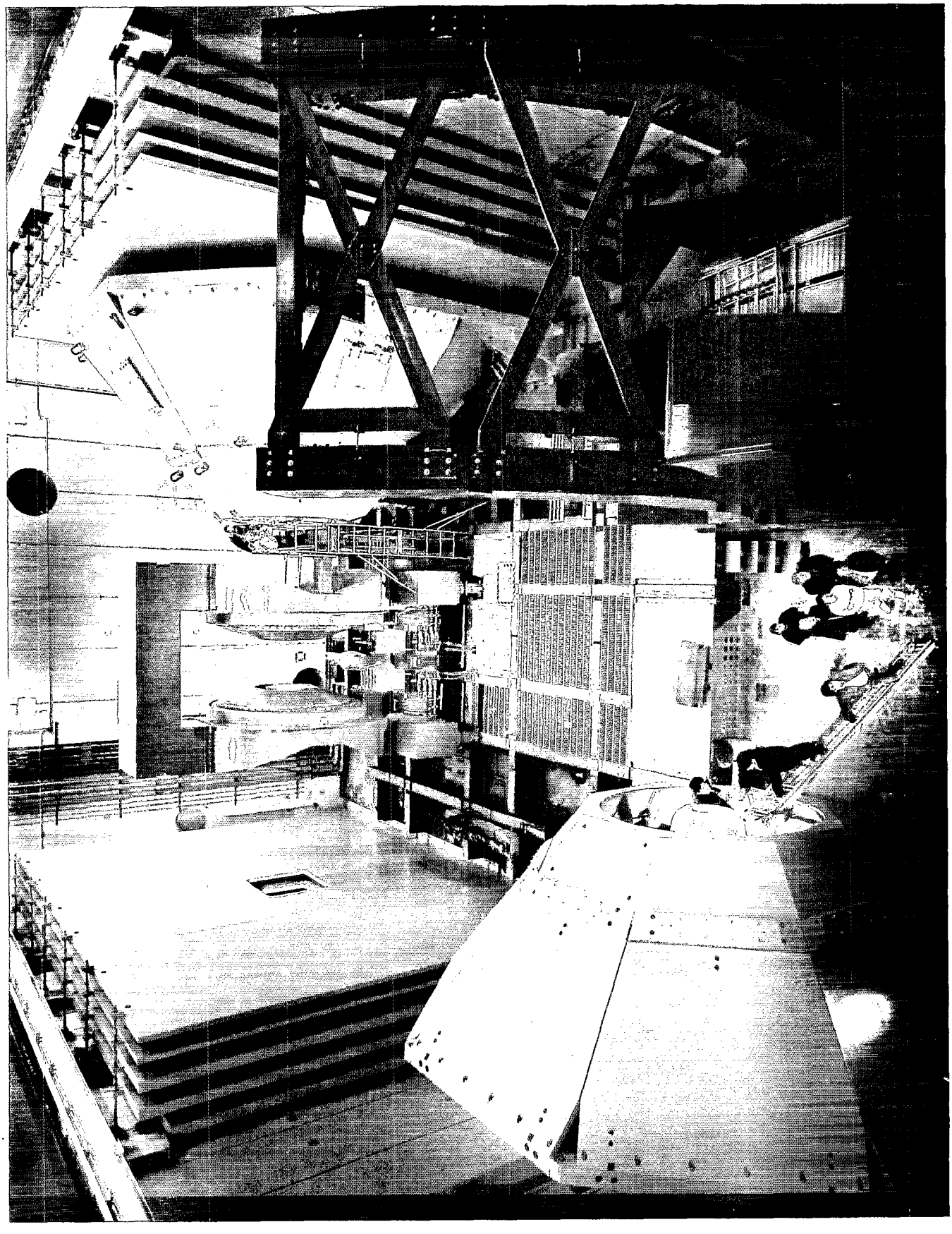

$\vec{p} + p \to W^+$

a)

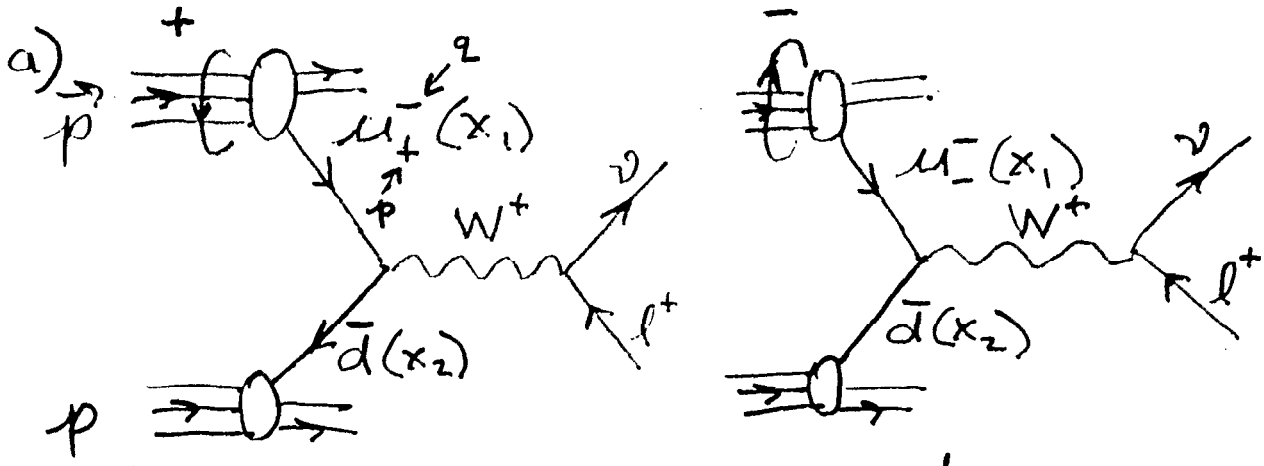

$$N(W^+)\Big|_{p_+ \to u} = N_0 u_+^-$$

$$N(W^+)\Big|_{p_- \to u} = N_0 u_-^-$$

$$\frac{N(W^+)\Big|_{p_+ \to u} - N(W^+)\Big|_{p_- \to u}}{+} = \frac{u_+^- - u_-^-}{+} = -\frac{\Delta u}{u}$$

$$x_1 = \frac{M_W}{\sqrt{s}} e^{\boxed{y_W}}$$

$$p_T^{lepton} = p_T^* = \frac{M_W}{2} \sin\theta^*$$ ← decay angle of ℓ^+ in W CM

$$y_\ell^* = \frac{1}{2} \ln\left[\frac{1+\cos\theta^*}{1-\cos\theta^*}\right]$$

$$\boxed{y_W} = y_\ell^{lab} - y_\ell^*$$

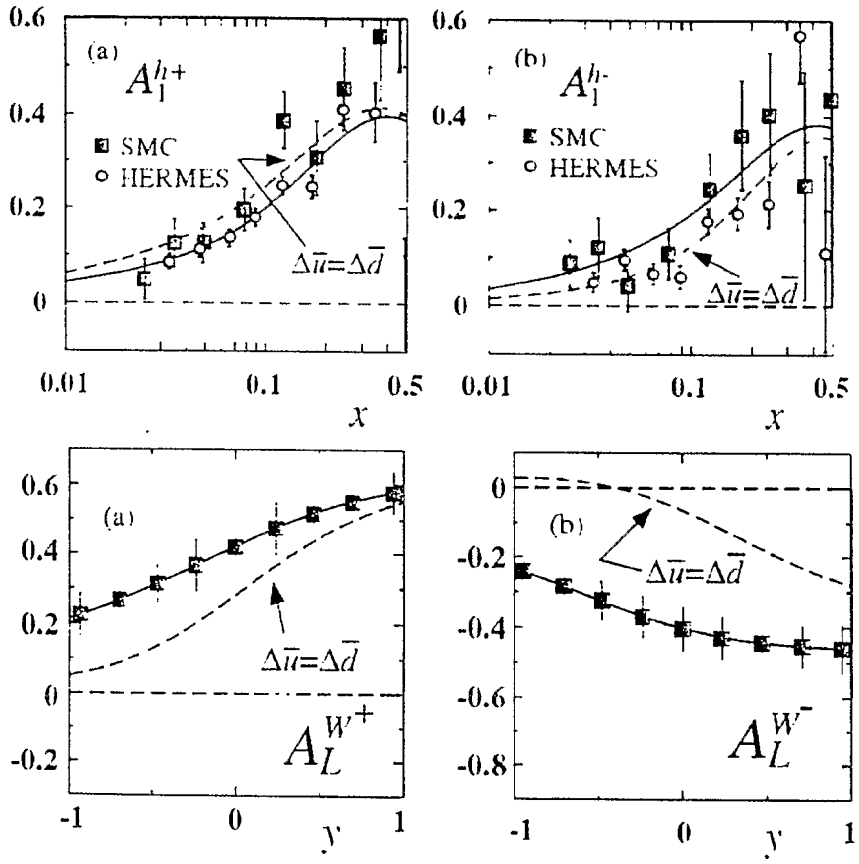
(a)
A_1^{h+}
SMC
HERMES
$\Delta\bar{u}=\Delta\bar{d}$
(b)
A_1^{h-}
SMC
HERMES
$\Delta\bar{u}=\Delta\bar{d}$
x
(a)
$\Delta\bar{u}=\Delta\bar{d}$
$A_L^{W^+}$
(b)
$\Delta\bar{u}=\Delta\bar{d}$
$A_L^{W^-}$
y

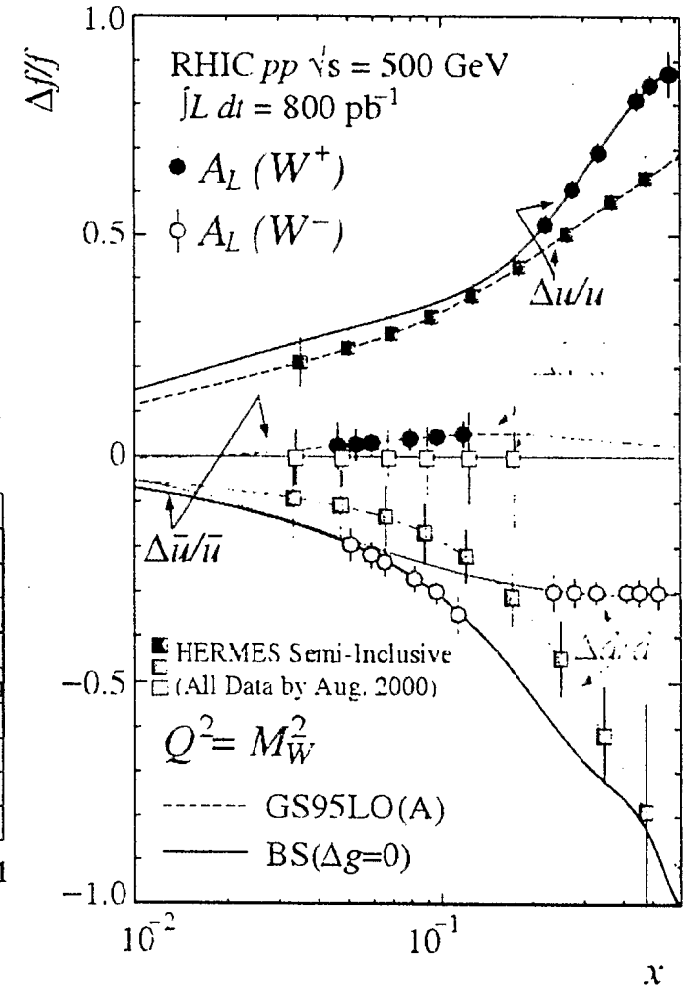
RHIC pp $\sqrt{s}$ = 500 GeV
$\int L\,dt$ = 800 pb^{-1}
$A_L\ (W^+)$
$A_L\ (W^-)$
$\Delta u/u$
$\Delta\bar{u}/\bar{u}$
$\Delta\bar{d}/\bar{d}$
HERMES Semi-Inclusive
(All Data by Aug. 2000)
$Q^2 = M_W^2$
GS95LO(A)
BS(Δg=0)
$\Delta f/f$
x

What I skipped:

- small angle pp elastic scattering with transverse and longitudinal spin, $\sqrt{s} = 20$ to 500 GeV – $pp2pp$ Expt.

- transversity: transverse spin structure of proton – STAR, PHENIX

- revisit transverse π asymmetries at $\sqrt{s} = 500$ – BRAHMS Expt.

- $\bar{u}/\bar{d}$ ratio from unpolarized $W^{\pm}$ production – PHENIX, STAR

- gluon polarization from
  - jet production – STAR
  - jet $\to \pi^{+,-,0}$ – PHENIX, STAR
  - open charm, bottom – PHENIX

- Λ fragmentation asymmetry – STAR

- gluon distribution from direct γ – PHENIX, STAR

We begin the RHIC spin program next year (2001).

We have an extensive range of exciting physics ahead, easily ~10 years of measurements.

Consider joining this adventure!

Physics of Proton-Antiproton Collisions at Tevatron CDF

Fumihiko Ukegawa[1]
(CDF Collaboration)[2]

Institute of Physics, University of Tsukuba
Tsukuba, Ibaraki, 305-8571 Japan

Abstract

The Collider Detector at Fermilab (CDF) collaboration performs an experiment at the Tevatron proton-antiproton collider at Fermilab in Batavia, Illinois, USA, using proton-antiproton collisions at a center-of-mass energy of $\sqrt{s} = 1.8$ TeV.

Since its inception in 1985, CDF has studied various aspects of elementary particle physics, such as quantum chromodynamics (QCD), electroweak physics, heavy quarks, and searches for new phenomena beyond the standard model of elementary particles.

Most recently, CDF collected a data sample corresponding to an integrated luminosity of 110 pb^{-1} during the period from 1992 to 1996 (Run I). CDF has observed production of top quark pairs in this data sample. CDF has also studied various hard QCD processes such as production of (a) high transverse momentum jets, (b) $W^{\pm}$ bosons, (c) lepton pairs through the Drell-Yan mechanism and Z^0 boson decay, and (d) heavy quarks both in open and hidden (quarkonium) forms.

After a brief introduction to the experiment and the particle detection with the CDF detector, we discuss some of these QCD processes and relevant CDF measurements. Finally, we mention B-physics results from Run-I data and prospects in the next data taking period Run II, which is scheduled to begin in spring 2001 and collect about 2 fb^{-1} of data in its first two years of operation.

[1] E-mail: ukegawa@hepsg3.px.tsukuba.ac.jp

[2] http://www-cdf.fnal.gov/

Physics of Proton-antiproton Collisions at Tevatron CDF (Mostly QCD)

Fumihiko Ukegawa
(CDF Collaboration)

Institute of Physics
University of Tsukuba

Riken School on Quarks, Hadrons and Nuclei
— QCD Hard Processes and the Nucleon Spin —

December 2 – 5, 2000
Echigo Yuzawa
Niigata, Japan

Contents

Introduction

CDF Experiment, Detector and Particle Detection

Gauge Boson Production

- $W^{\pm}$ Boson Production
- Z^0/Drell-Yan Production
- Prompt Photon Production

Heavy Quark Production

- b and c Quark Production
- Quarkonium Production

CDF Experiment

CDF is an experiment at the Tevatron $p\bar{p}$ collider at Fermilab.

CDF studies various aspects of elementary particle physics using $p\bar{p}$ collisions at $\sqrt{s} = 1.8$ TeV.
QCD is one of them.

CDF detector is a general purpose, $\sim 4\pi$ detector.

Brief History

- 1985: First collisions. ~20 events.
- 1987: 25 nb^{-1}. First physics results.
- 1988 - 1989: 4 pb^{-1}. Some intersting measurements.
- 1992 - 1996: 100 pb^{-1}. Top quark discovered.
- 2001 - 2007(?): 15 fb^{-1}. Higgs?

CDF Detector

- CDF : a general purpose detector with almost 4π coverage.
- Consists of
  - tracking chambers inside the 1.4 T solenoid
  - electromagnetic and hadron calorimeters
  - muon chambers

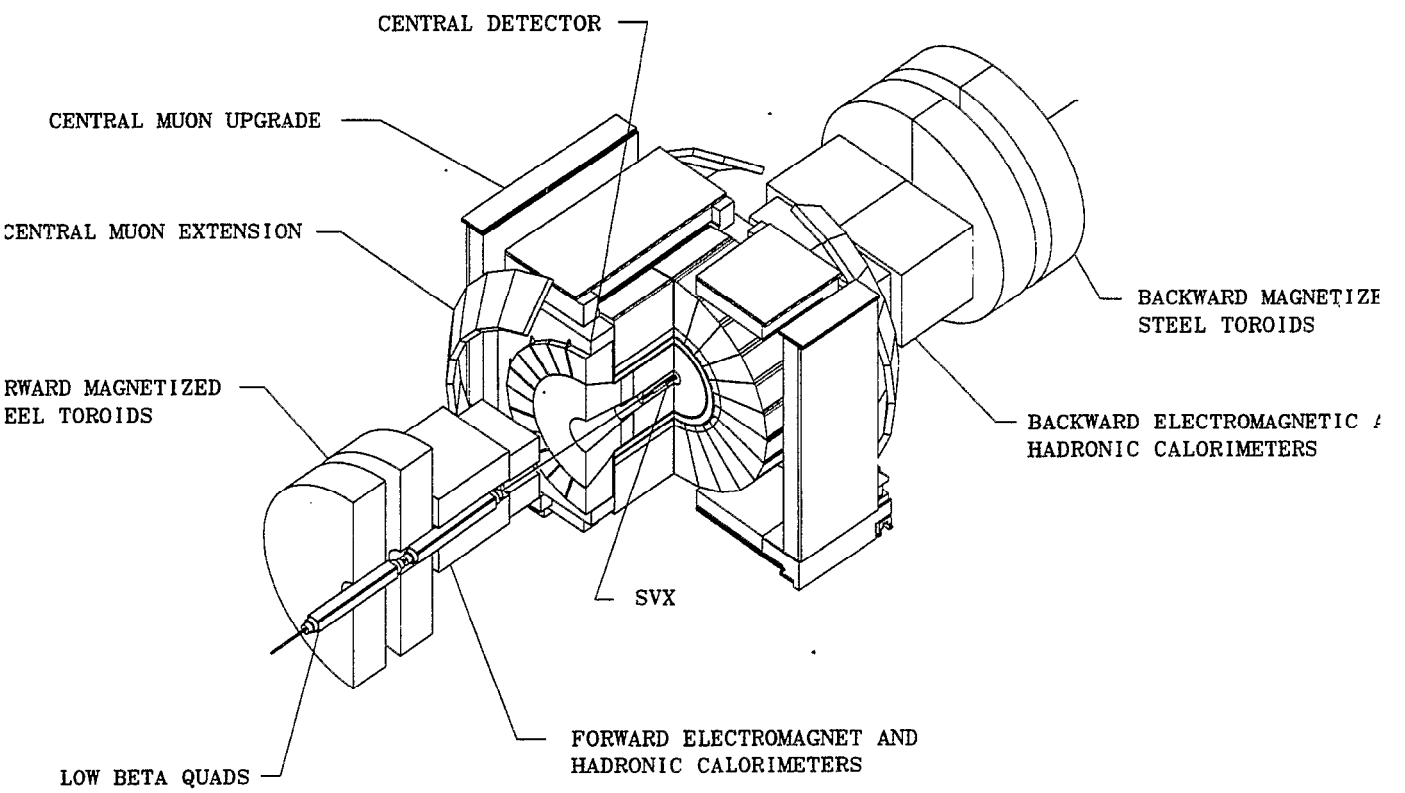

CDF detector, sliced in the plane with the beam axis. Only one quadrant is shown.

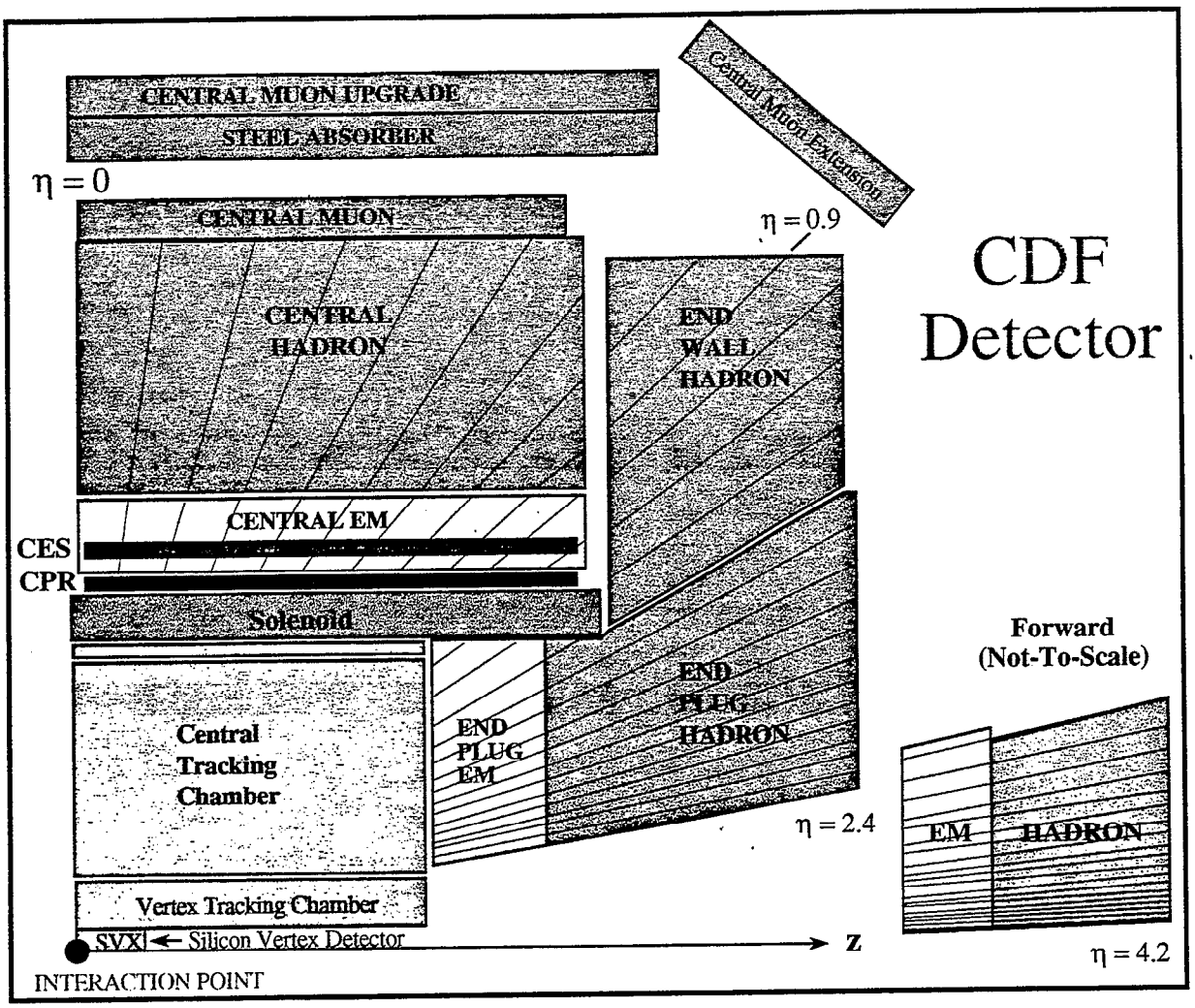

- SVX: silicon vertex detector
  VTX: vertex tracking chamber (TPC)
  CTC: central tracking chamber

  with

  preshower detector **and shower max detector**

- [illegible]

- Muon chambers

Central Tracking Chamber CTC :

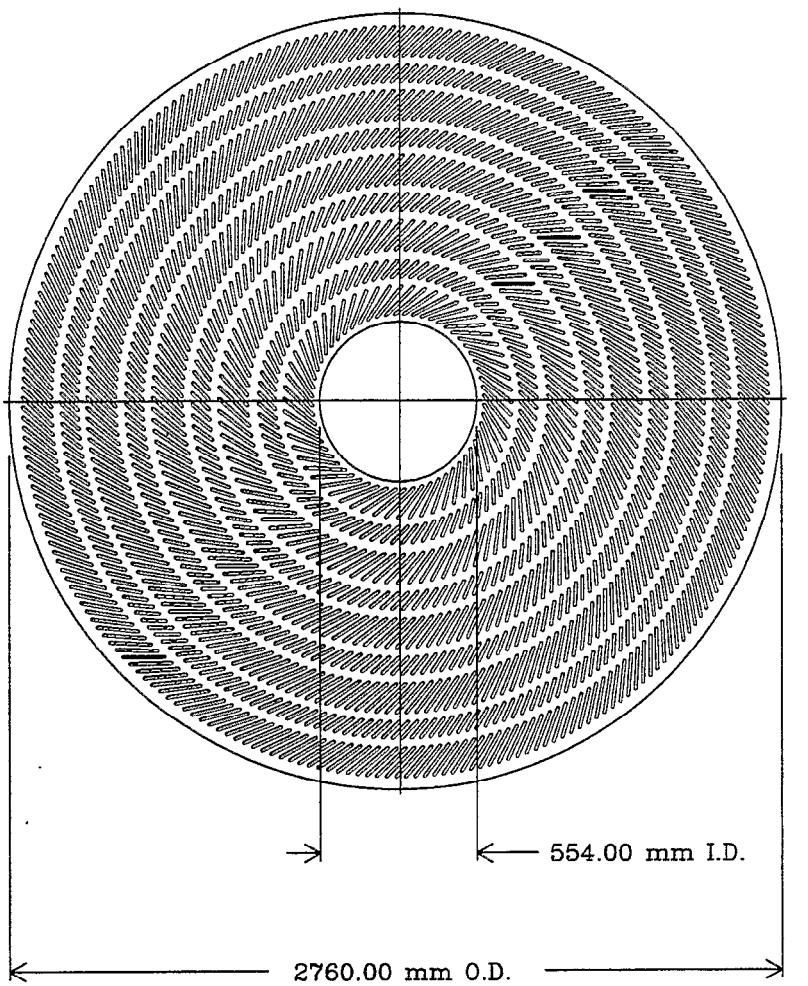

- Drift chamber inside 1.5 T B field.
- 1.4 m in radius, 3 m long.
- 84 measurement layers, grouped into 9 "super-layers".
- 12×5 axial layers, 6×4 stereo (3°) layers.
- Momentum resolution

$$\sigma/p_T \simeq 0.001\ p_T$$

with $p_T \equiv p \sin\theta$ in GeV/c.

Central Electromagnetic Calorimeter CEM :

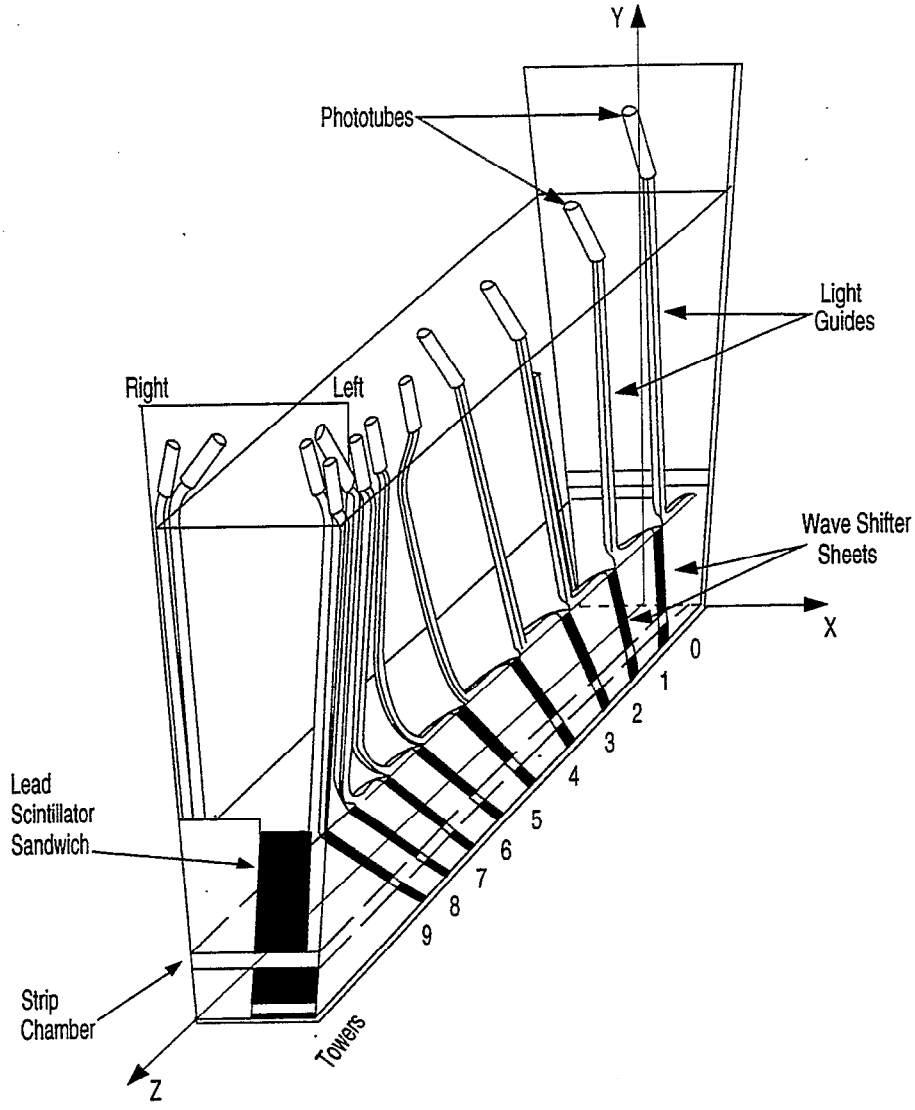

- Covers $\Delta\phi = 15°$, $|\eta| < 1.1$. 10 towers per wedge.
- 3-mm lead, 5-mm plastic scintillator, 31 layers. Total thickness $\simeq 18\, X_0$.
  Resolution $\sigma_E/E = 13.5\%/\sqrt{E \sin\theta}$.
- A layer of proportional chambers (CES) near shower maximum ($5.9\, X_0$).
  $\Delta(r\varphi) = 1.5$ cm, $\Delta z = 1.7, 2.0$ cm.

We measure

- Charged particle momenta with CTC.
- Electromagnetic and hadronic energies with calorimeters. ($e^{\pm}$, γ, hadrons)
- Detect/identify muons with muon chambers.
- Decay vertices of long-lived particles (e.g. B's) with silicon microstrip detector (SVX).

How Different Particles Look Like at CDF

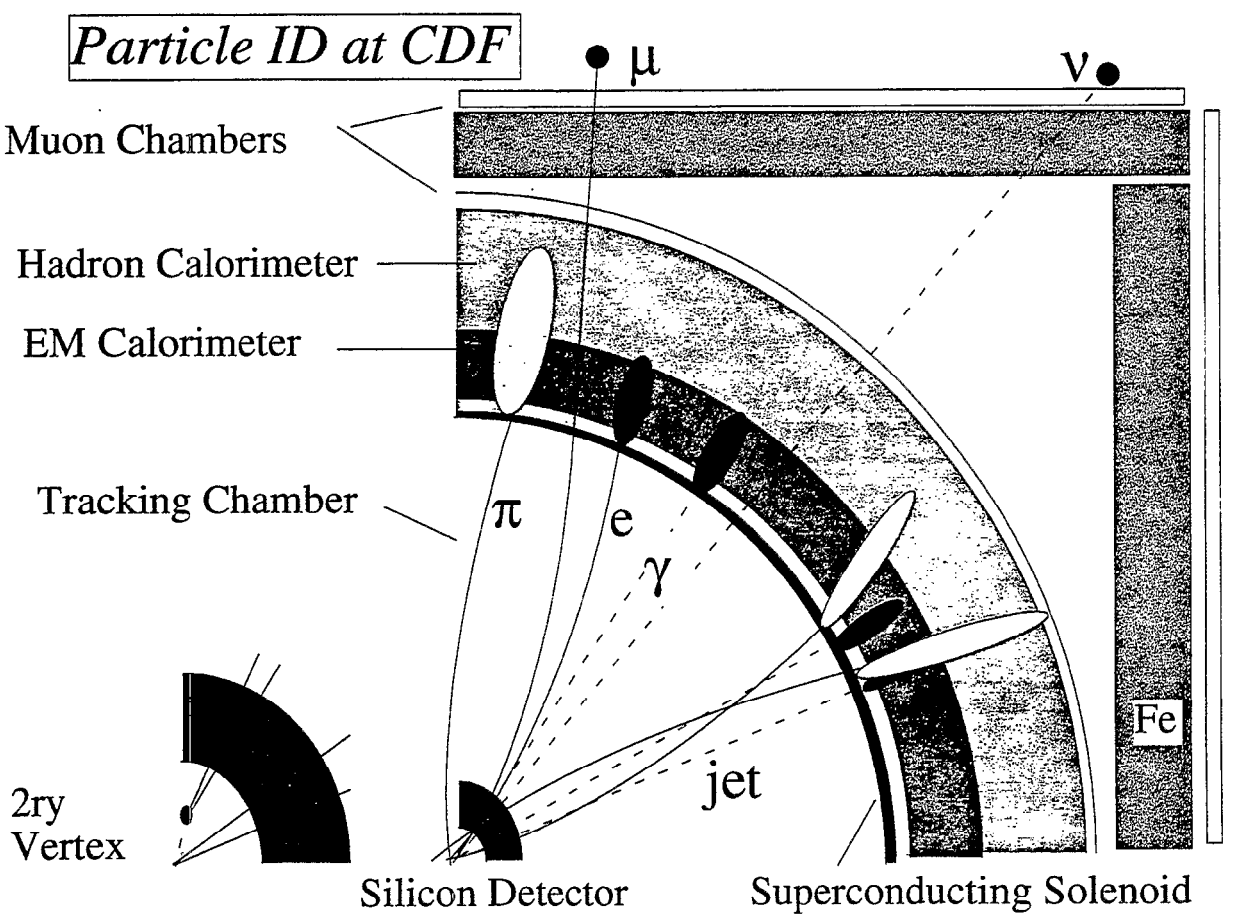

Z^0 and Drell-Yan $\ell^+\ell^-$ Production

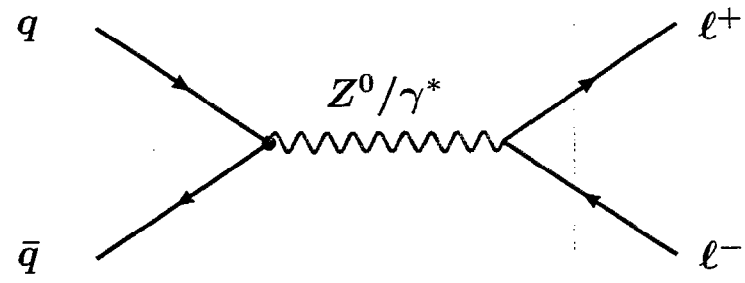

Z^0

- $M_{Z^0} = 90$ GeV$/c^2$, thus $\sqrt{x_1 x_2} = M_Z^0/\sqrt{s} \simeq 0.05 \rightarrow$ quarks at small x.
- Z^0 decays to $\ell^+\ell^-$, $q\bar{q}$.
  $\ell^+\ell^-$ final states very distinctive. $\mathcal{B} \simeq 3\%$.
- Require two high p_T leptons. $\ell = e$ or μ.
  Electrons :
  - Electromagnetic cluster in the calorimeter.
  - Longitidinal and transverse shower profiles consistent with electrons.
  - High p_T CTC track matched in positions and in E/p.

  Muons :
  - Track segments in the muon chambers.
  - High p_T CTC track matched in positions.
  - Energy deposit in calorimeters consistent with MIP.

CDF
$Z \rightarrow ee$ and $Z \rightarrow \mu\mu$ Events

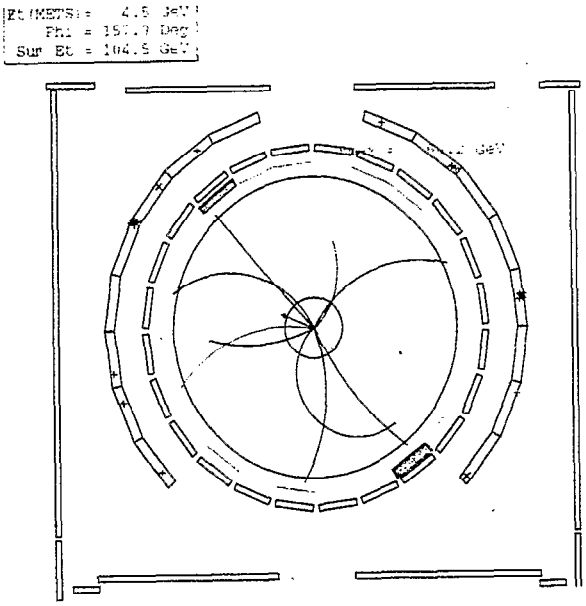

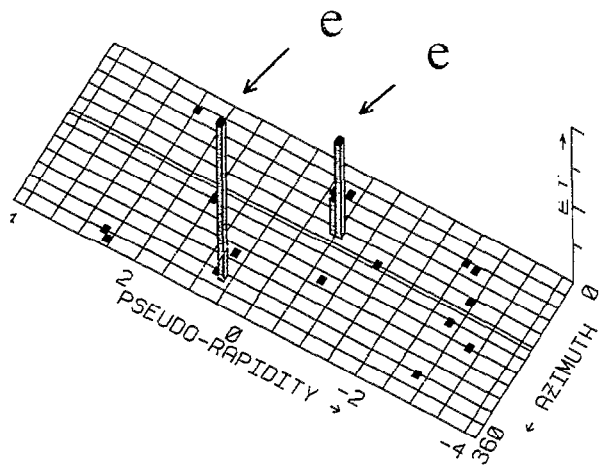

$E_T \cong 44$ and 36 GeV

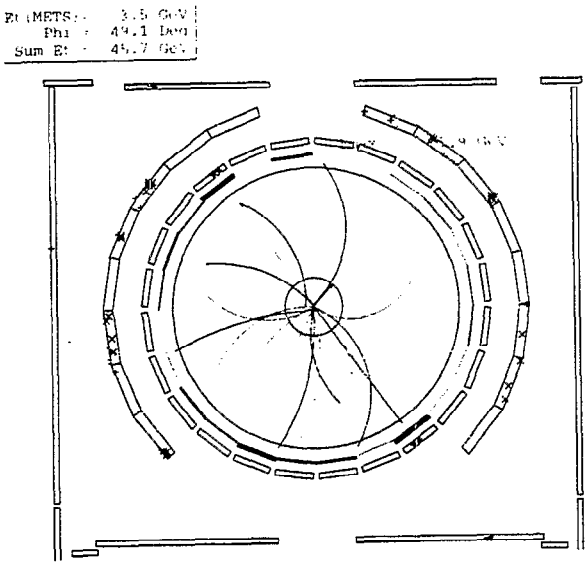

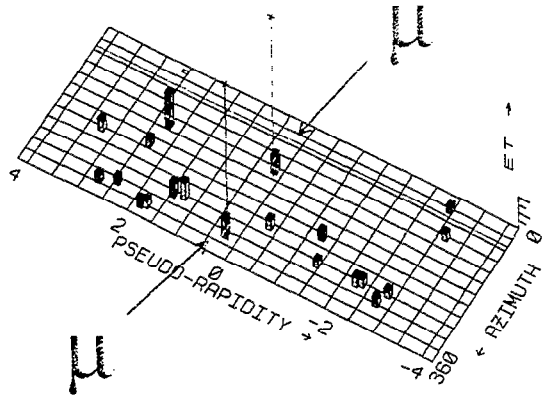

$P_T \cong 50$ and 32 GeV

Run 40323 Event34043 Z0.ANA]CENT ZS ELE CLEAN.DST 4SEP92 17:56:54 11-OCT-99

DAIS E transverse Eta-Phi LEGO Plot

METS: Etotal = 281.5 GeV, Et(scalar)= 84.8 Ge
Et(miss)= 3.5 at Phi= 352.8 Deg.

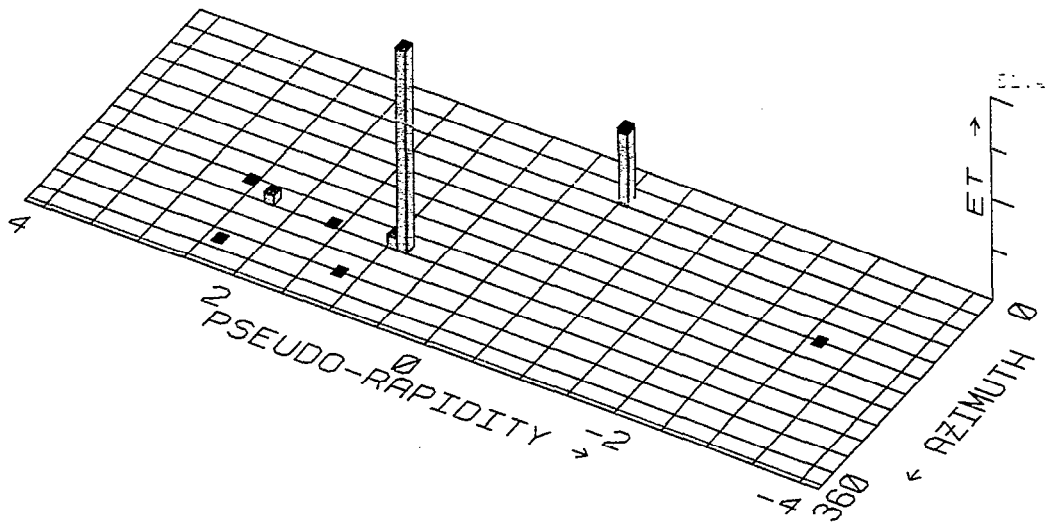

PHI: 55.
ETA: -0.60

Run 40323 Event34043 Z0.ANA]CENT ZS ELE CLEAN.DST 4SEP92 17:56:54 11-OCT-99

```
      *  WEST Wedge  3 Max Tower =     39.0392 GeV  *
* CEMD * AMP x16, x1 LEFT  towers 0 - 9
  0      0      0      0  1469 65535  1582     0      0      0
  0      0      0      0  1030  7957  1042     0      0      0
* CEMD * AMP x16, x1 RIGHT towers 0 - 9
  0      0      0      0  1279 65535  1477  1057      0      0
  0      0      0      0  1018  6986  1036     0      0      0
* CHAD * AMP x16, x1 LEFT  towers 0 - 7
  0      0      0      0  1000  1000  1000  1000
  0      0      0      0  1020  1237     0     0
* CHAD * AMP x16, x1 RIGHT towers 0 - 7
  0      0      0      0      0  1000     0     0
  0      0      0      0      0  1224     0     0
```

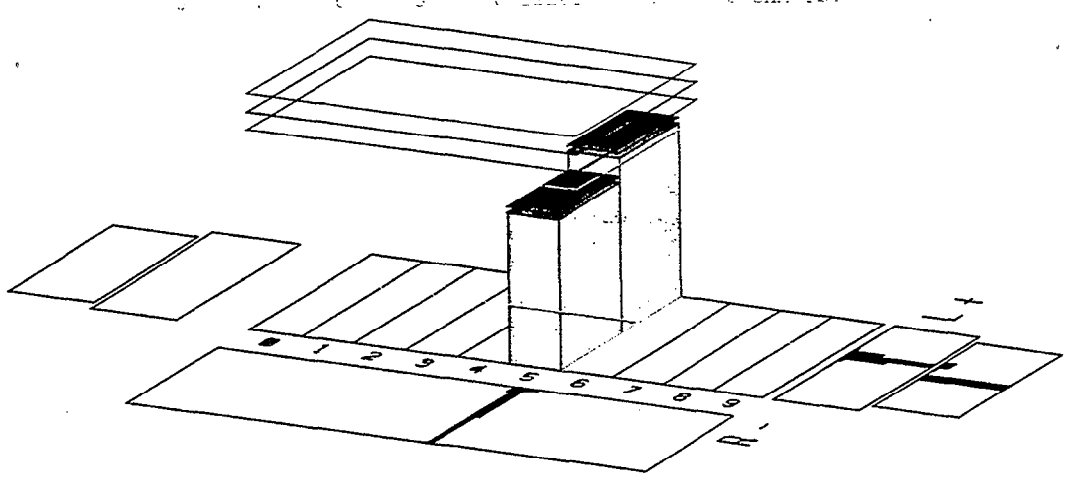

Min and Max(Channel = 74) Str GeV 0.000 9.562
Min and Max(Channel = 51) Wir GeV 0.000 10.049
Min and Max(Channel = 24) Pre fC 0.00 4393.51(= 8 MIPS)

PHI: 55.
ETA: -0.60

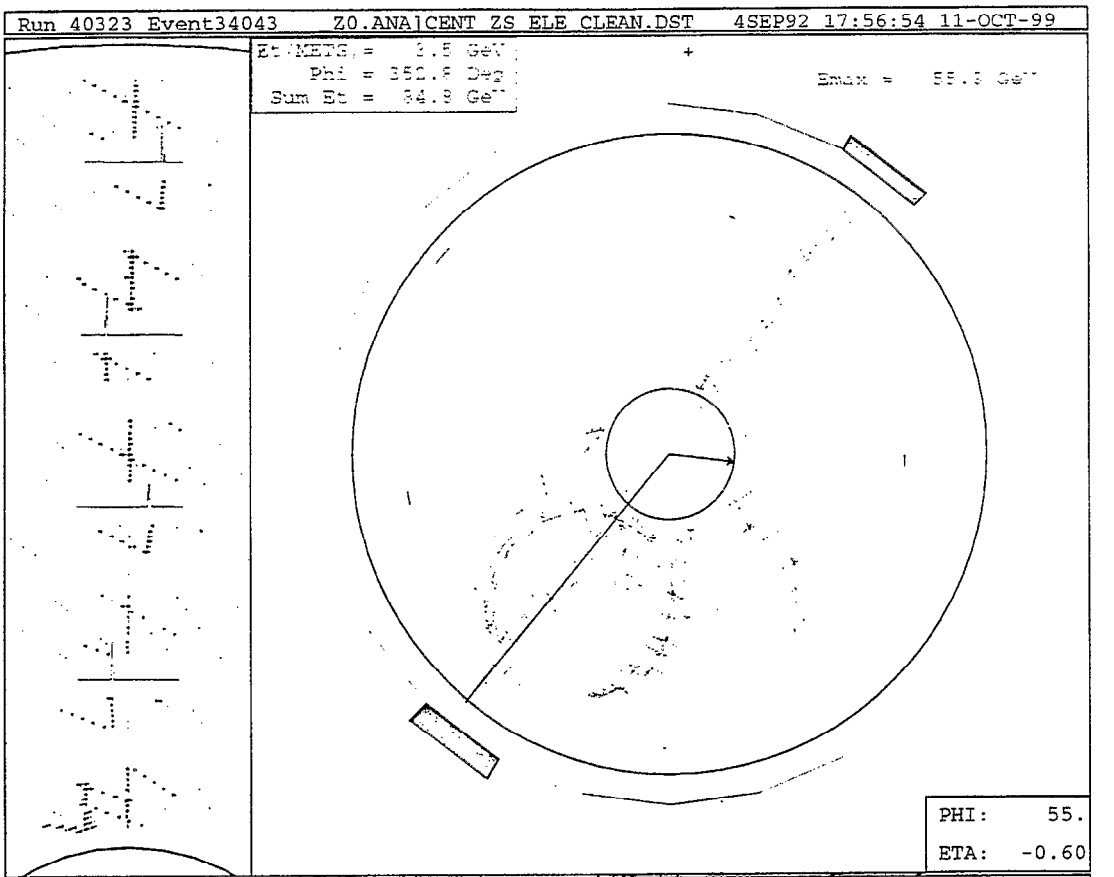
Run 40323 Event34043 Z0.ANA]CENT_ZS_ELE_CLEAN.DST 4SEP92 17:56:54 11-OCT-99
Phi = 352.8 Deg
Sum Et = 84.9 GeV
Emax = 55.3 GeV
PHI: 55.
ETA: -0.60

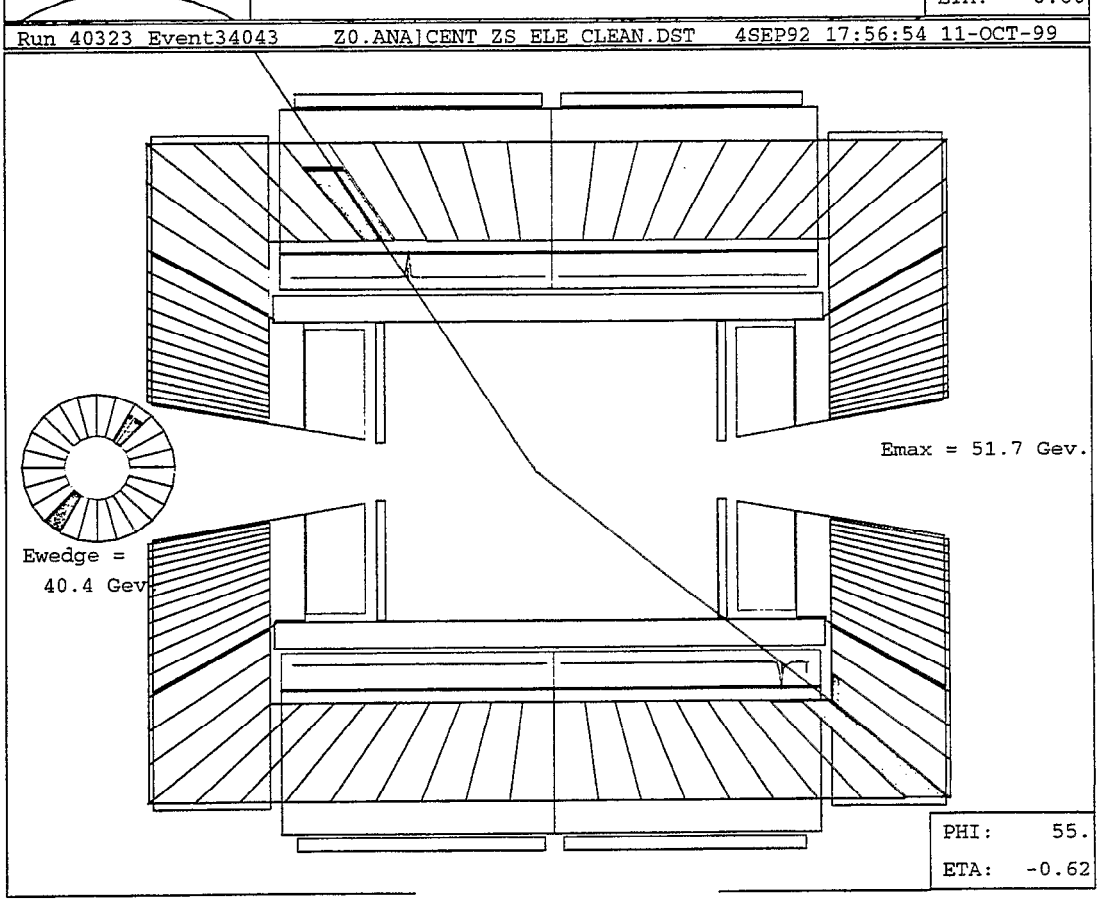
Run 40323 Event34043 Z0.ANA]CENT_ZS_ELE_CLEAN.DST 4SEP92 17:56:54 11-OCT-99
Emax = 51.7 Gev.
Ewedge =
40.4 Gev
PHI: 55.
ETA: -0.62

Dilepton mass spectra near Z^0

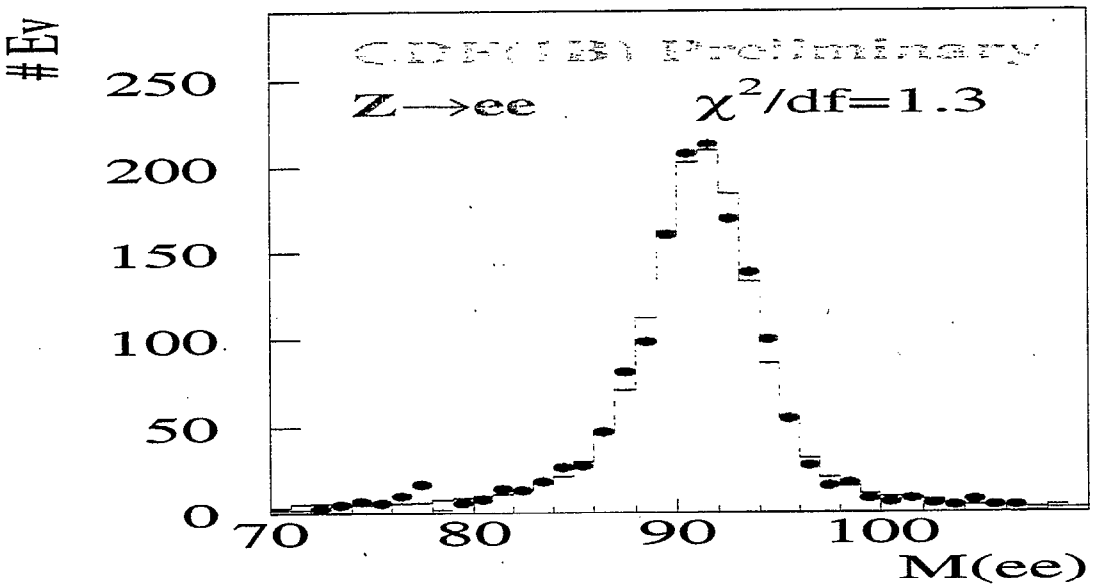

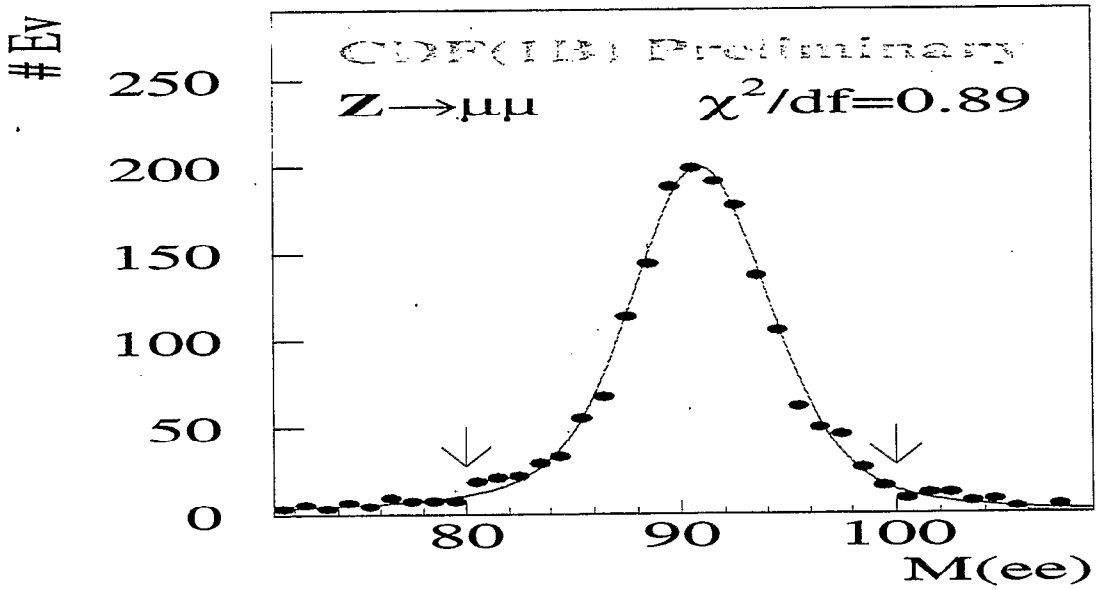

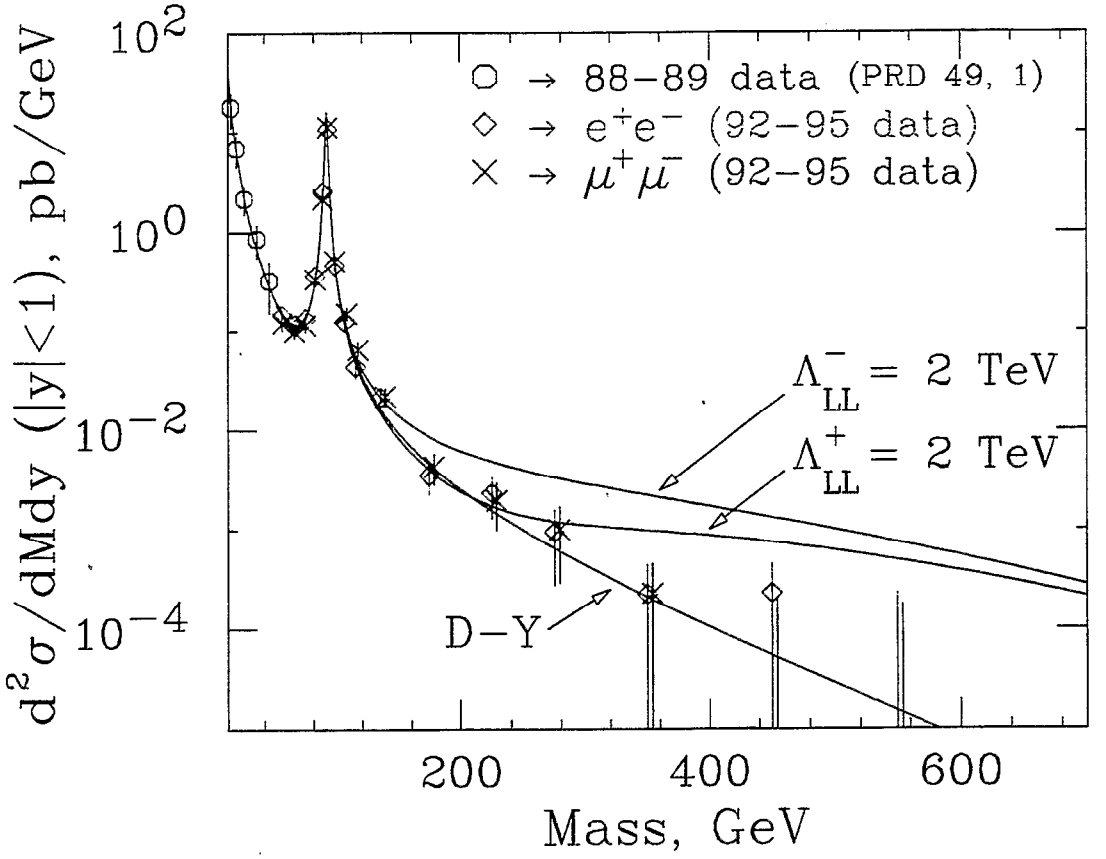

Kinematics

$$
\begin{aligned}
p_1 &= \frac{\sqrt{s}}{2}(x_1, 0, 0, x_1) \\
p_2 &= \frac{\sqrt{s}}{2}(x_2, 0, 0, -x_2) \\
\tau &\equiv M^2/s = p_1 \cdot p_2/s = x_1 x_2 \\
y_{\ell^+\ell^-} &= \frac{1}{2}\ln\left[\frac{E+p_z}{E-p_z}\right] = \frac{1}{2}\ln\left(\frac{x_1}{x_2}\right) \\
&\rightarrow x_1 = \sqrt{\tau}\exp(y), \quad x_2 = \sqrt{\tau}\exp(-y)
\end{aligned}
$$

For $M = 90$ GeV/c^2,

$$
\begin{aligned}
x_{\min} &= M^2/s = 0.0025 \\
y_{\max} &= \frac{1}{2}\ln(s/M^2) \simeq 3.0
\end{aligned}
$$

Z^0/DY Rapidity Distributions

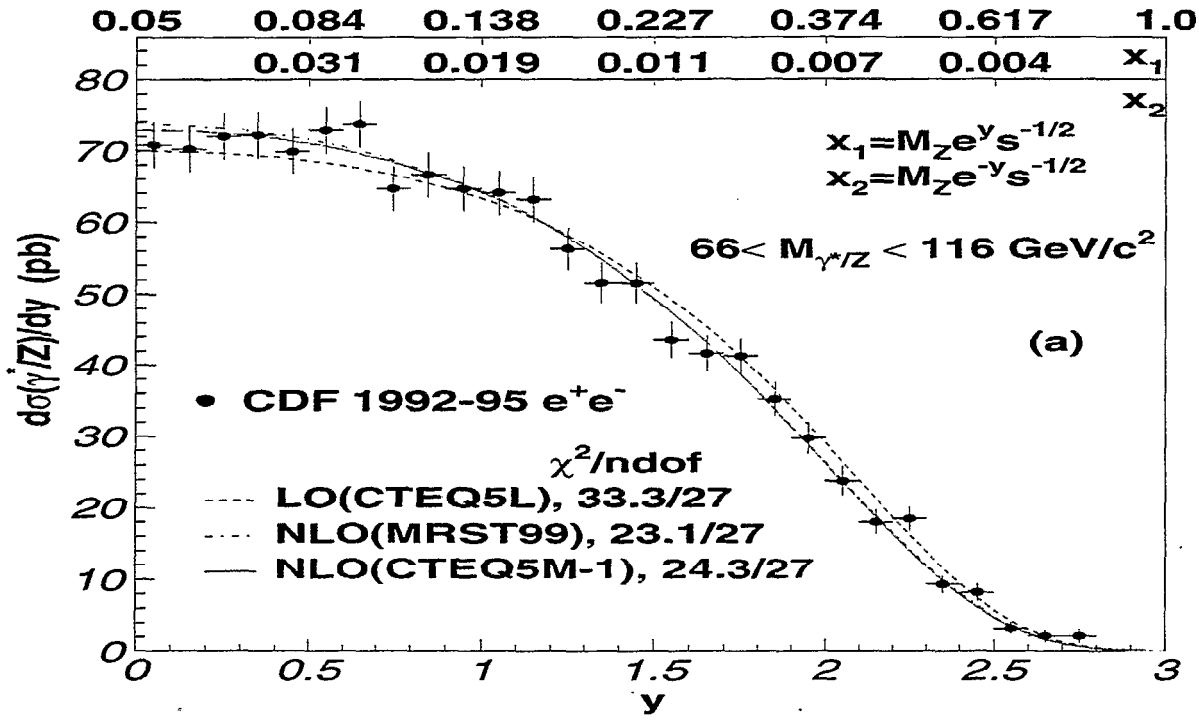

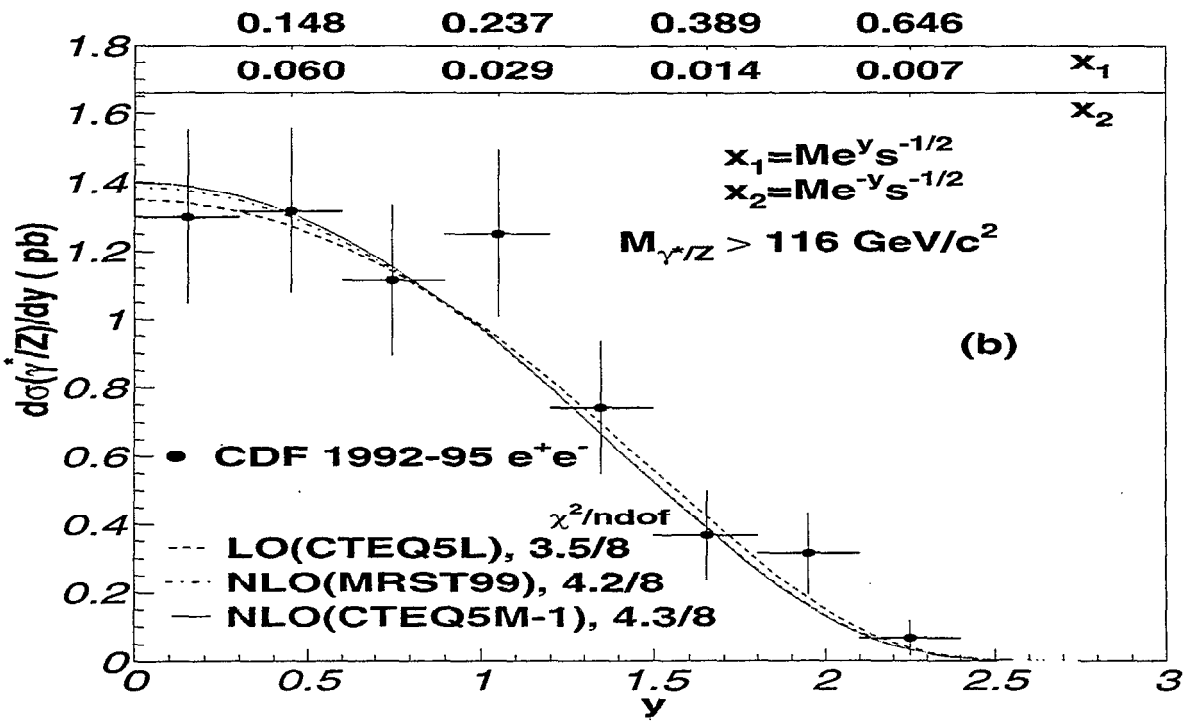

$$\int \left(\frac{d\sigma}{dy}\right) dy = 253 \pm 4 \pm 10 \text{ pb for } Z^0 \to \ell^+\ell^-.$$

W Boson Production

LO:

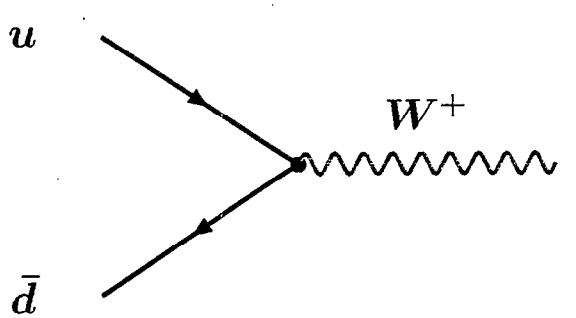

- $M_W = 80$ GeV$/c^2$, thus $\sqrt{x_1 x_2} = M_W/\sqrt{s} \simeq 0.04 \rightarrow$ quarks at small x.
- W^+ decays to $e^+\nu$, $\mu^+\nu$, $\tau^+\nu$, $u\bar{d}$, $c\bar{s}$.

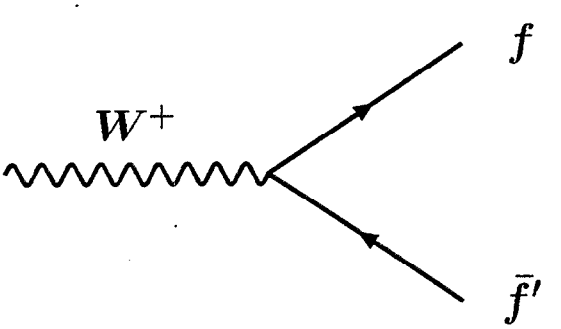

- $\ell^+\nu$ final states clean. $\mathcal{B} = 1/9$.
- How to detect the neutrino? We don't.
  $\rightarrow$ missing transverse energy.
  $$\vec{p}_T^{\,\nu} \equiv \vec{\not{E}}_T \equiv -\sum_i \vec{E}_T^{\,i}$$
  Sum is over all calorimeter towers.
- In LO, $\vec{p}_T^{\,W} \simeq 0$. Then $\vec{p}_T^{\,\ell} \simeq -\vec{p}_T^{\,\nu}$.

Run 41627 Event 748 F$W_Z DATA:[ANA]FIVE_WENU.DST 1NOV92 18:38:01 30-NOV-00

DAIS E transverse Eta-Phi LEGO Plot

METS: Etotal = 270.2 GeV, Et(scalar)= 93.8 Ge
Et(miss)= 37.7 at Phi= 314.4 Deg.

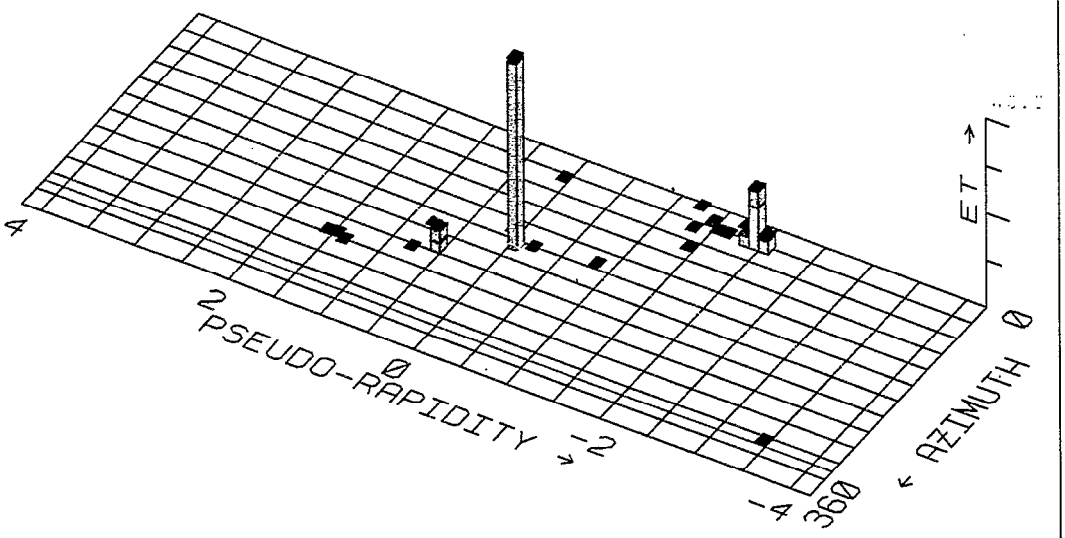

PHI: 160.
ETA: -0.10

Run 41627 Event 748 F$W_Z DATA:[ANA]FIVE_WENU.DST 1NOV92 18:38:01 30-NOV-00

Pt	Phi	Eta
z_1= -39.3,	5 trk	
-6.9	204	0.82
1.3	140	-0.16
1.3	242	1.81
-0.4	190	-0.03

4 rejectd trks

-0.6	27	-0.49
0.4	238	
0.4	339	
0.3	317	

Hit & to refresh

Et(METS)= 37.7 GeV
Phi = 314.4 Deg
Sum Et = 93.8 GeV

Emax = 42.8 GeV

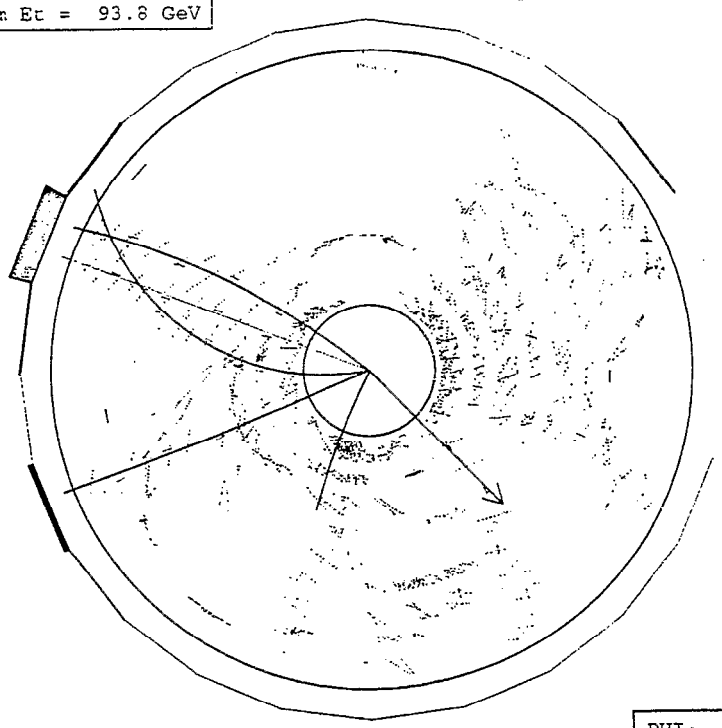

PHI: 159.
ETA: 0.12

How to reconstruct W?
Neutrino longitudinal momentum not known, so cannot form invariant mass.
$\rightarrow$ Transverse mass:

$$M_T^2 \equiv 2\, p_T^\ell\, p_T^\nu\, (1 - \cos\Delta\phi)$$

dN/dp_T^ℓ, dN/dp_T^ν show characteristic peak at $\sim M_W/2$ (Jacobian peak), and M_T at $\sim M_W$.

Require:

- **high p_T lepton (> 25 GeV/c).**
- **large missing E_T (> 25 GeV/c).**

This is usually enough to separate W's from BG.

Run Ib (90 pb^{-1}), electron channel.

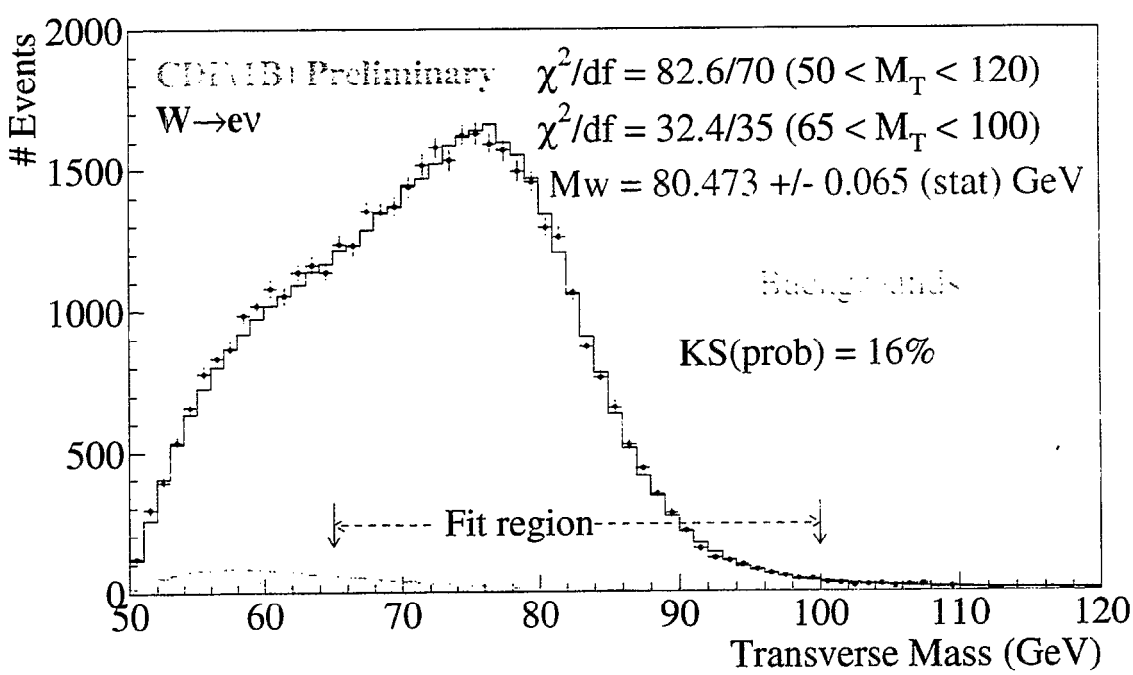

$\Rightarrow M_W = 80.443 \pm 0.079$ GeV/c^2 (CDF combined).

Somewhat sensitive to the Higgs mass thru radiative corrections.

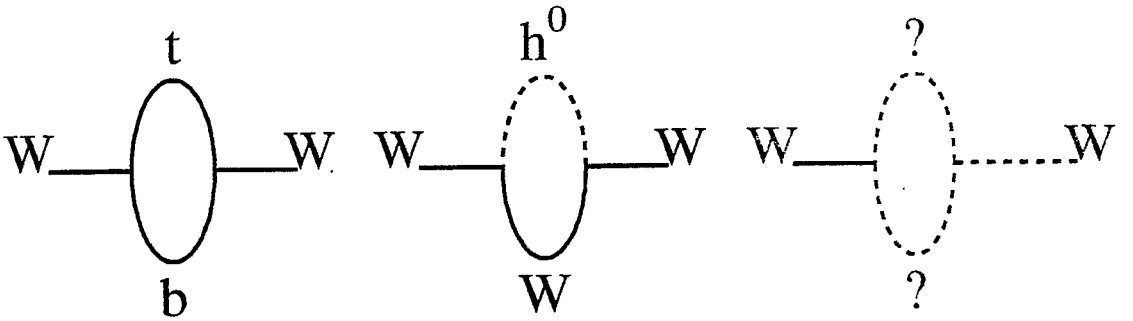

$\Delta M_W \propto M_T^2$ $\Delta M_W \propto \ln M_H$ New Physics

Constraints on the Higgs mass

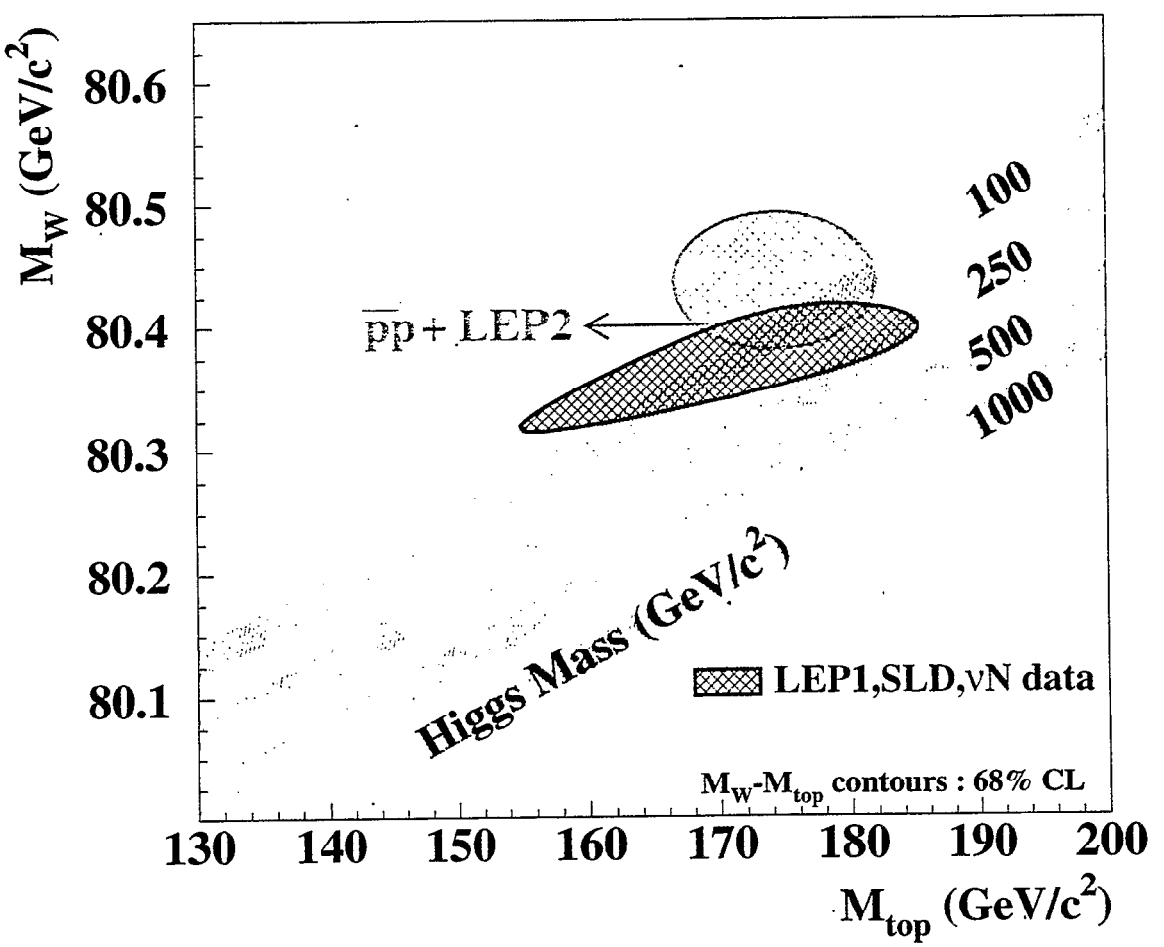

Measured Production Cross Section

$$\sigma(\bar{p}p \to W^+X) \cdot \mathcal{B}(W^+ \to \ell^+\nu)$$
$$+\ \sigma(\bar{p}p \to W^-X) \cdot \mathcal{B}(W^- \to \ell^-\bar{\nu})$$
$$= 2.49 \pm 0.12 \text{ nb}$$

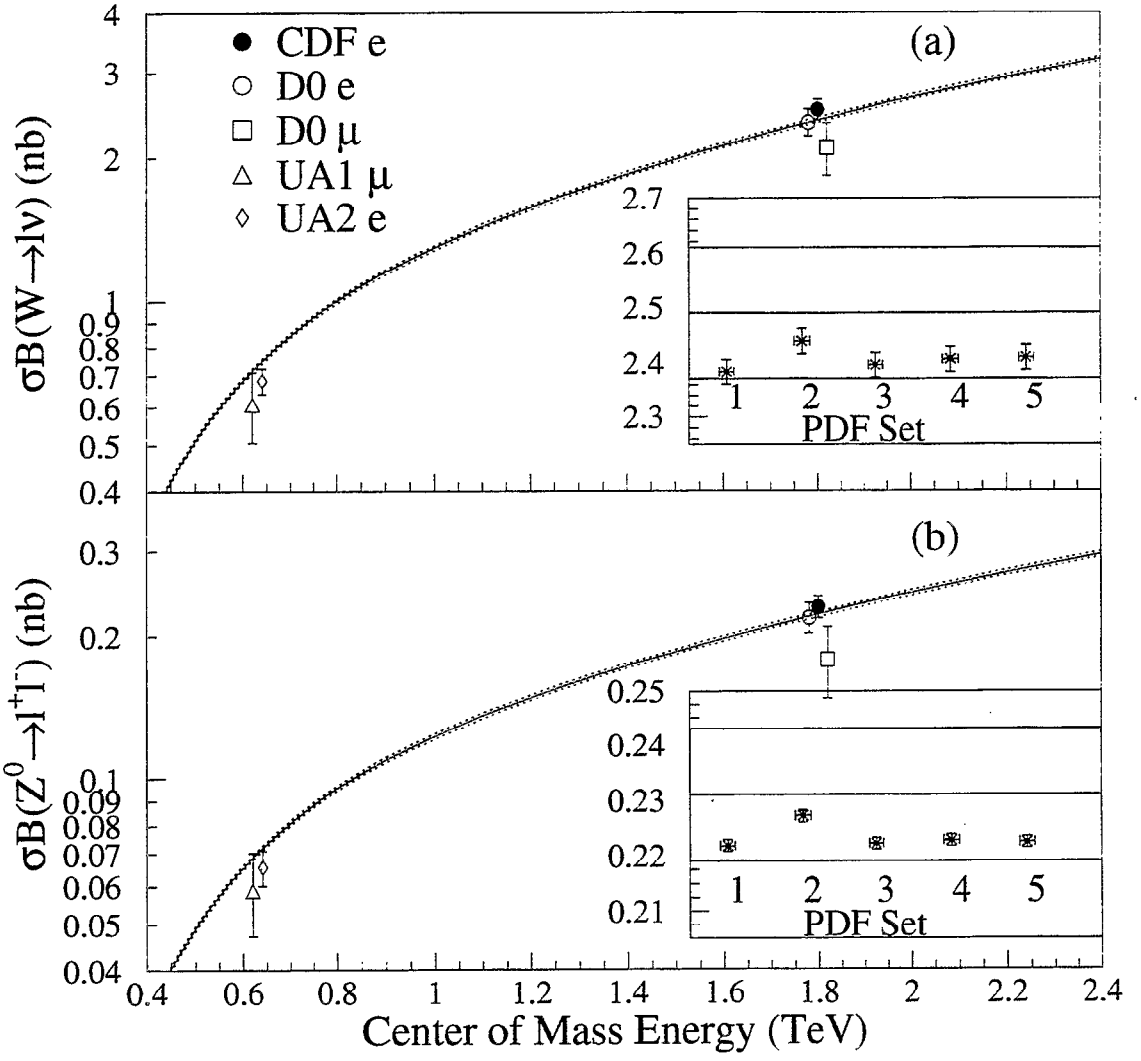

W Rapidity Distributions

Not symmetric around $y = 0$ even for $\bar{p}p$ collisions with valence dominance, because $u(x)$ is harder than $d(x)$.

W^+ tends to follow the u (p) direction ($y > 0$),
W^- tends to follow the $\bar{u}$ ($\bar{p}$) direction ($y < 0$).

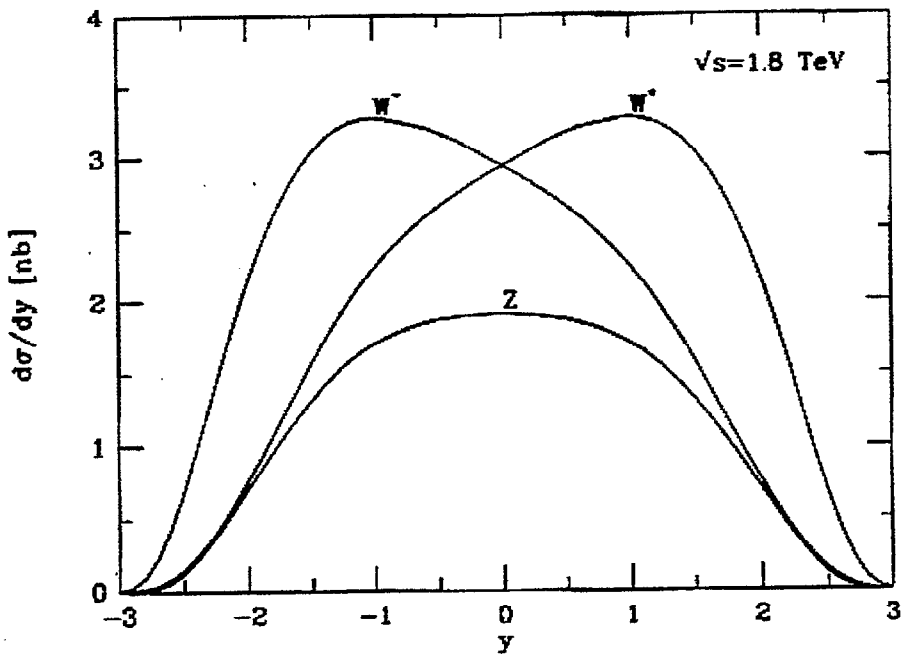

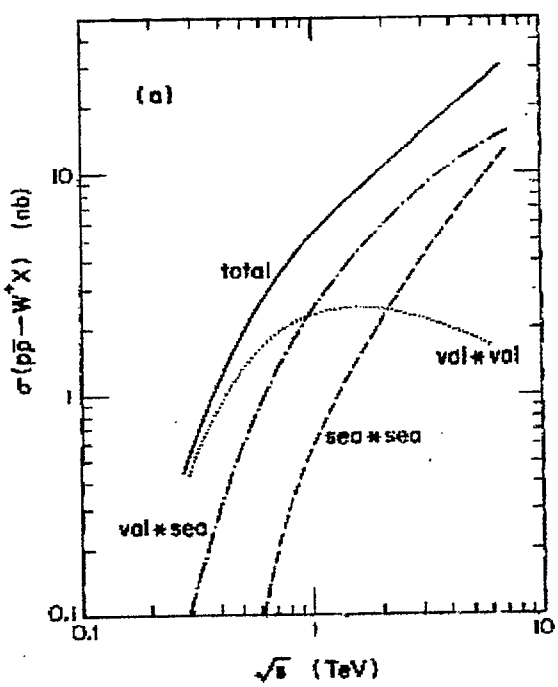

$W^{\pm}$ longitudinal momentum not measured:
$\rightarrow$ measure the lepton rapidity distribution.
Complication arises because $W^{\pm}$ is polarized.

$$u\bar{d} \rightarrow W^{+} \rightarrow \ell^{+}\nu \qquad d\bar{u} \rightarrow W^{-} \rightarrow \ell^{-}\bar{\nu}$$

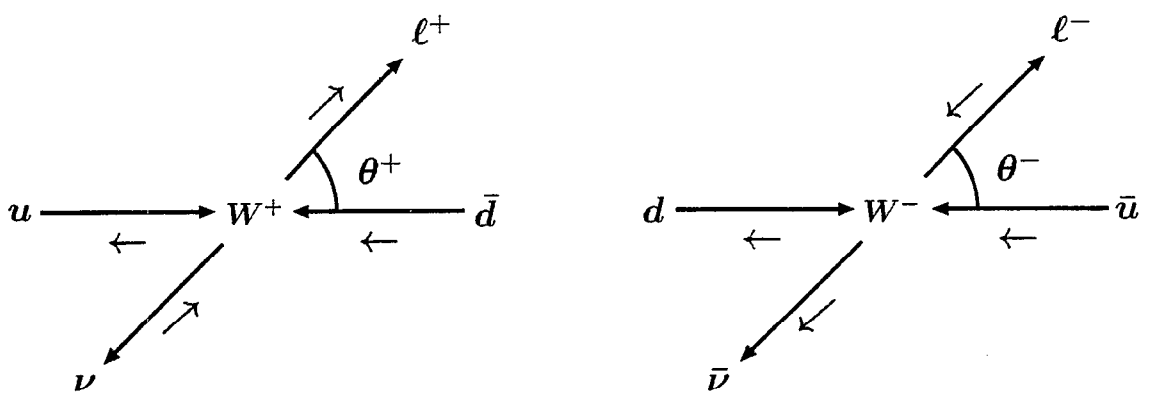

$$\frac{dN}{d\cos\theta^{+}} = |d^{1}_{1,-1}|^{2} \propto (1-\cos\theta)^{2} \;\Rightarrow\; \bar{p} \text{ direction}$$

$$\frac{dN}{d\cos\theta^{-}} = |d^{1}_{-1,-1}|^{2} \propto (1+\cos\theta)^{2} \;\Rightarrow\; p \text{ direction}$$

The two effects above are in opposite directions:
stronger one (structure function) wins.

Define asymmetry as

$$A(y) \equiv \frac{(d\sigma^{+}/dy) - (d\sigma^{-}/dy)}{(d\sigma^{+}/dy) + (d\sigma^{-}/dy)}$$

y: lepton rapidity.

Raw distribution

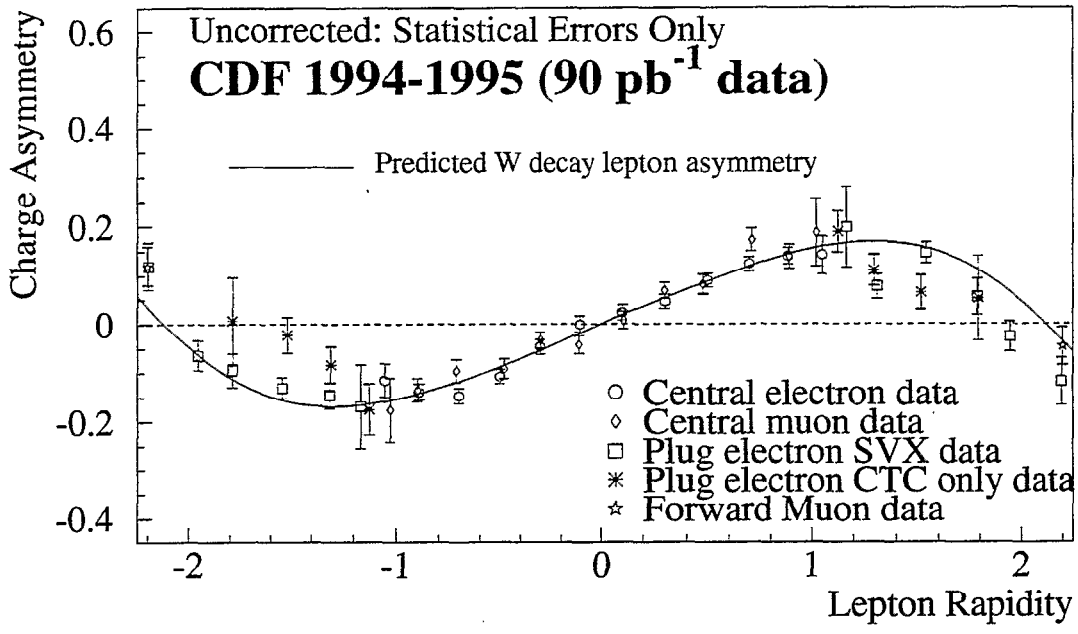

Corrected, and folded

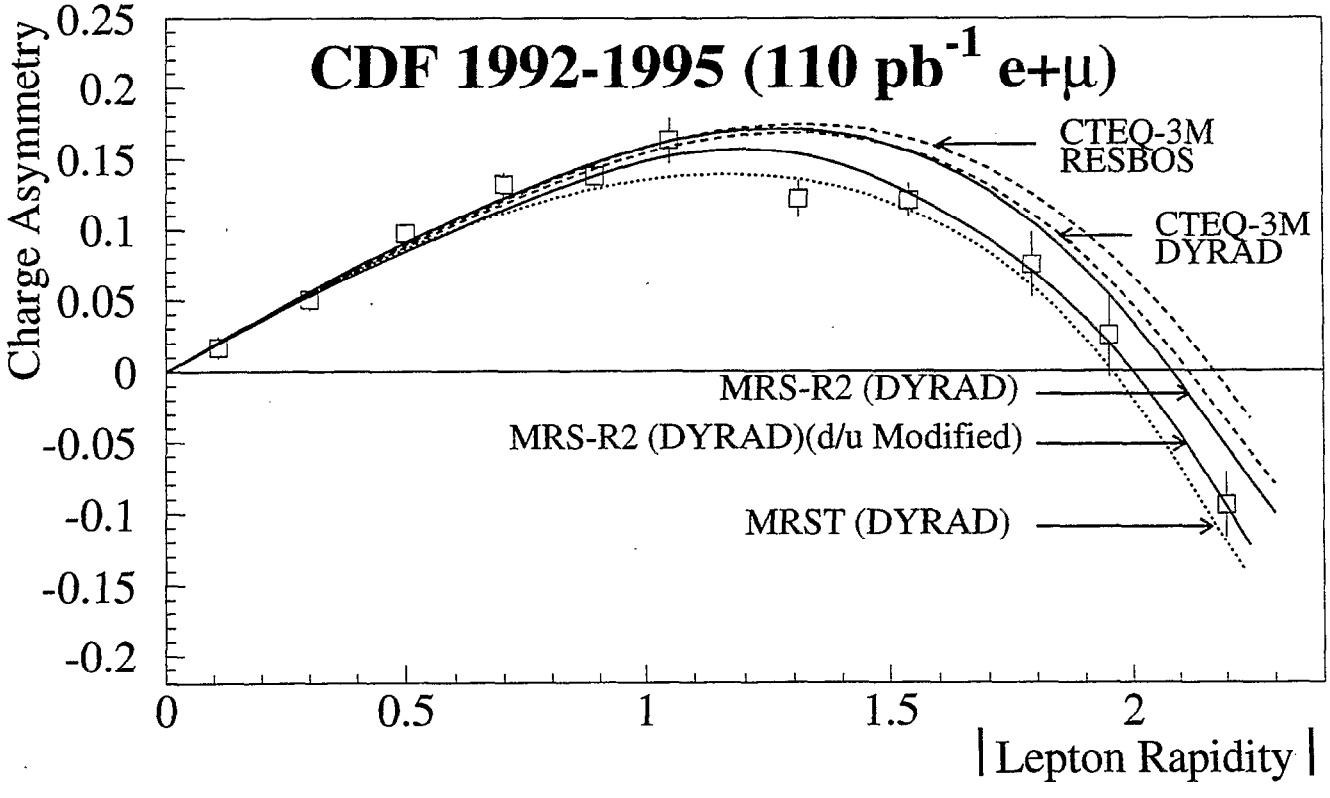

Prompt Photon Production

- **LO:**

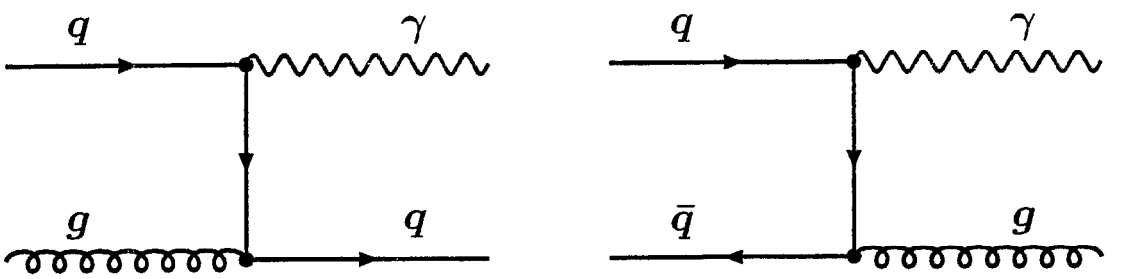

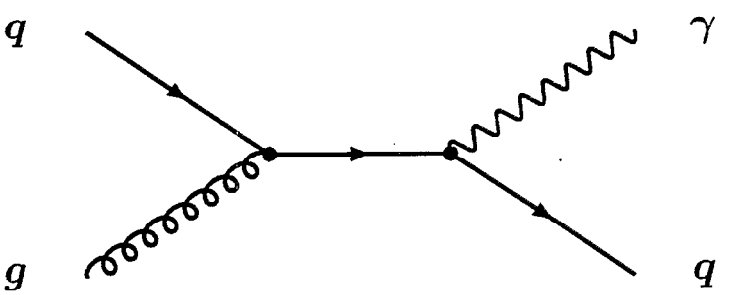

- **NLO: (examples)**

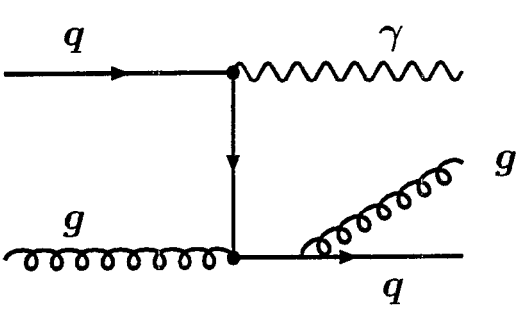

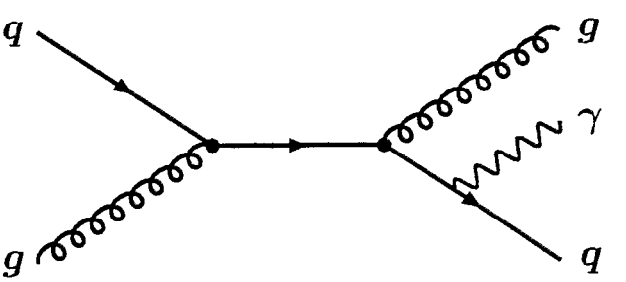

- **Sensitive to the quarks, as opposed to the gluons in case of jets.**

- Parton = photon. Energy-momentum well defined.
- Photon energy measured with calorimeter. Resolution better than for hadrons/jets.
- $\alpha_s \rightarrow \alpha$: cross section smaller than jets.

How to identify the photon?
Main BG: jets $\rightarrow$ leading $\pi^0 \rightarrow \gamma\gamma$,
energy deposit in electromagnetic calorimeter.

In principle separable, one photon vs. two photons.

Method I: Lateral shower profile using shower max detector CES.

Method II: Detect converted photon signal at preshow detector CPR.

I: Profile method

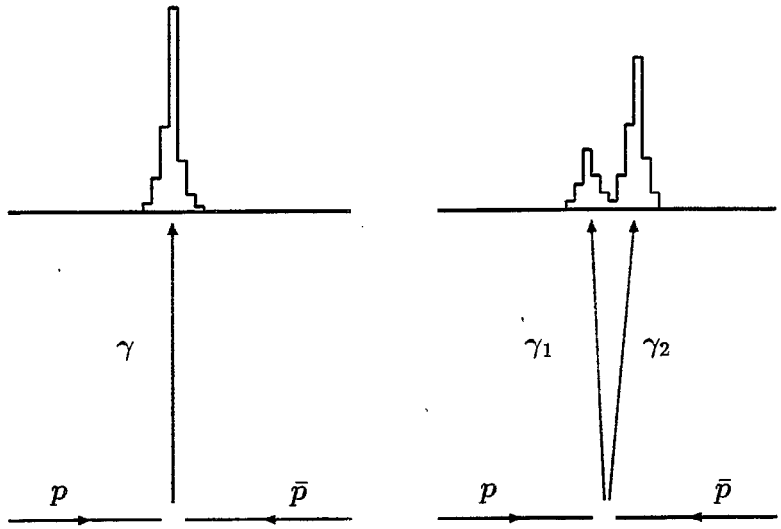

CES at $R = 181$ cm. Channel spacing ~ 1.5 cm.

$$d_{\min} = \frac{49}{p_T(\pi^0)} \text{ cm} \quad \text{with } p_T \text{ in GeV}/c.$$

Fit CES profile with single shower hypothesis.
Templates from electrons in real data and test beam.
χ^2 of the fit $\rightarrow$ larger for π^0, smaller for γ.

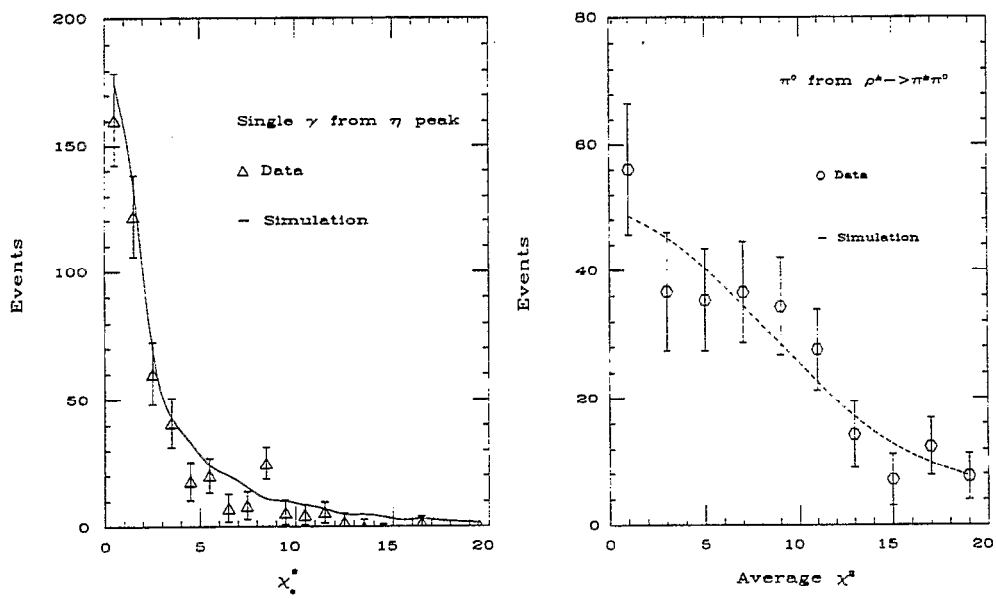

Count the raction with $\chi^2 < 4.0 \Rightarrow$ photon fraction.

Provides γ/π^0 separation up to ~ 30 GeV/c.

II: Conversion method

Photon conversion probability thru material thickness t is

$$P_\gamma(t) = 1 - \exp\left[-\frac{7t}{9X_0}\right].$$

For $\pi^0 \to 2\gamma$, the probability that at least one photon converts is

$$P_{\pi^0} = 1 - (1 - P_\gamma)^2 > P_\gamma.$$

Separation $P_{\pi^0} - P_\gamma$ is maximal for $P = 0.5$ or $t \sim 1.0\, X_0$.

CDF solienoid is $1.075\, X_0$ thick. Use it as the radiator, and detect converted photons just behind it. $\to$ CPR (proportional chamber).

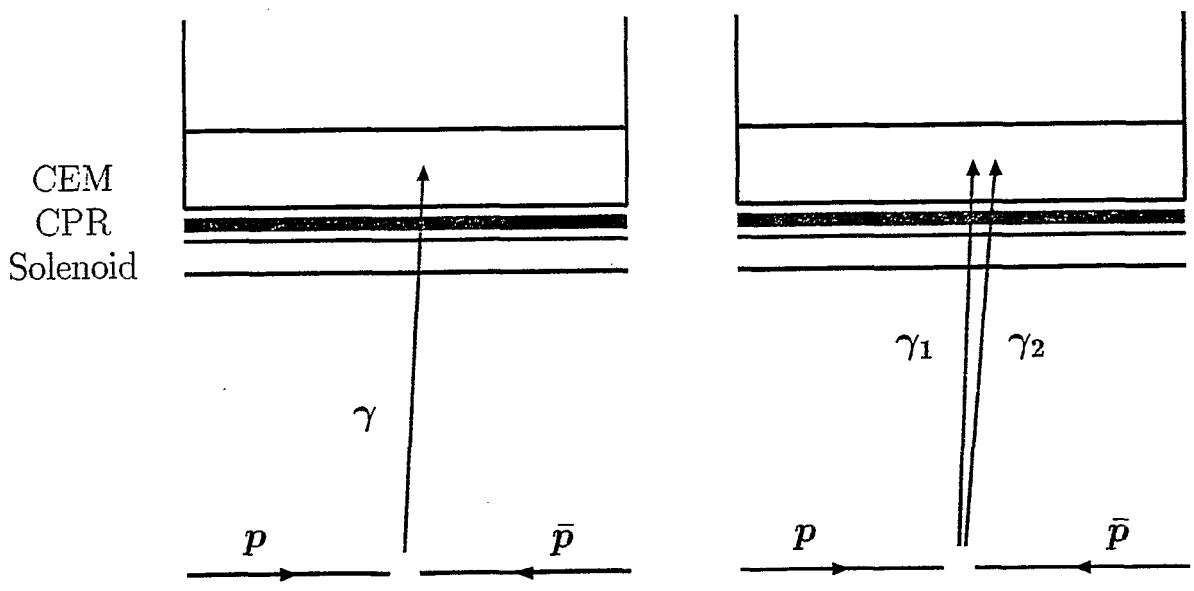

Measure the conversion probability P_{CPR} at CPR for photon candidates:

If $P_{\mathrm{CPR}} = P_\gamma$, all signal, if $P_{\mathrm{CPR}} = P_{\pi^0}$, all BG.

Somewhere in between $\to$ photon fraction.

Measure CES/CPR efficiencies in data :

ϵ for single γ's from $\pi^0/\eta \rightarrow \gamma\gamma$

ϵ for π^0 from $\rho^{\pm} \rightarrow \pi^{+}\pi^{0}$

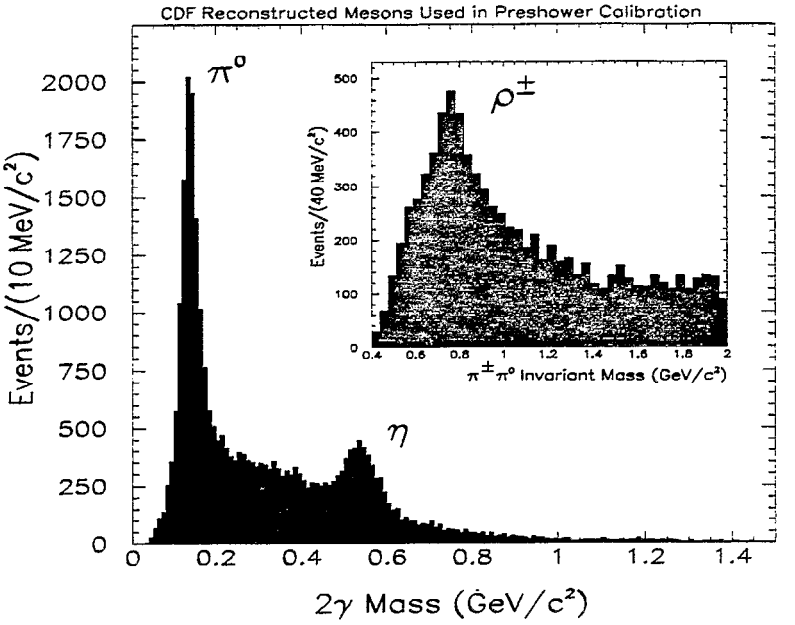

CDF Background Subtraction Methods

Fraction of Photons = $(\varepsilon_B-\varepsilon)/(\varepsilon_B-\varepsilon_\gamma)$

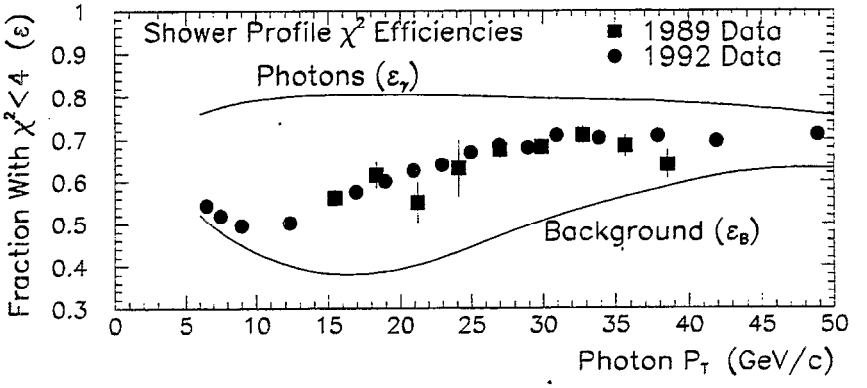

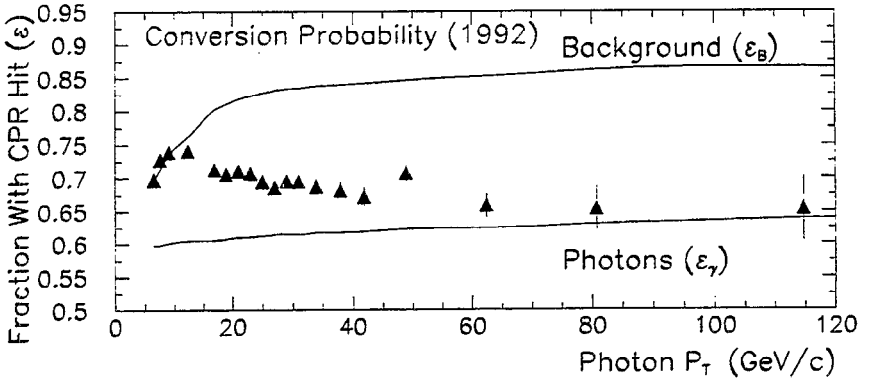

Single γ inclusive cross section (110 pb^{-1}).

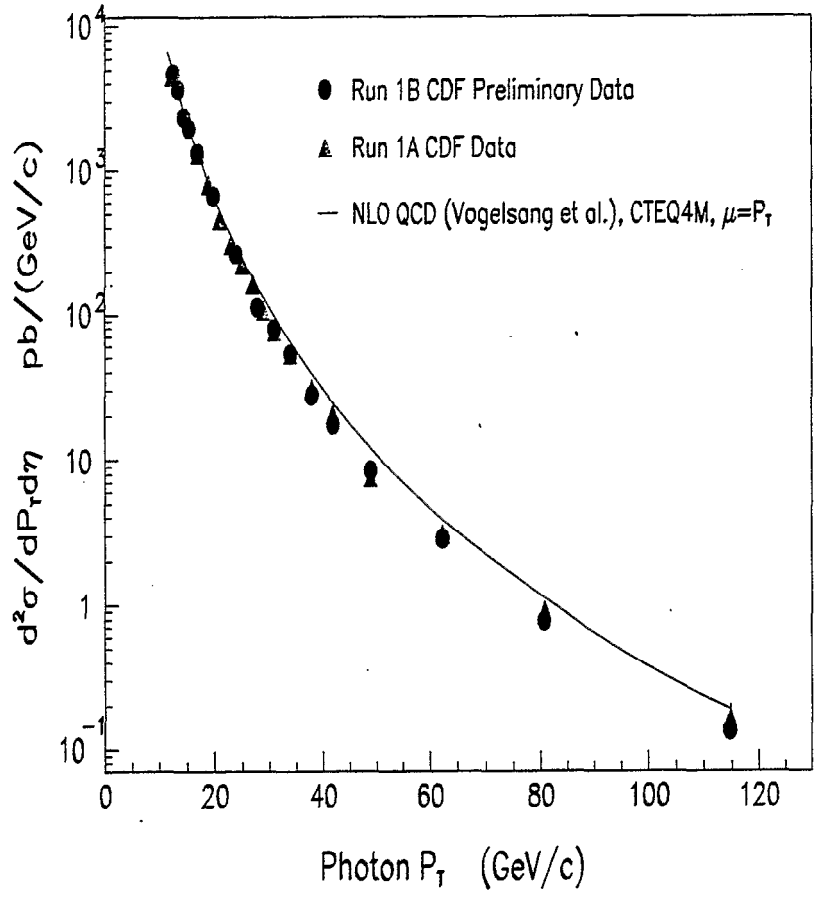

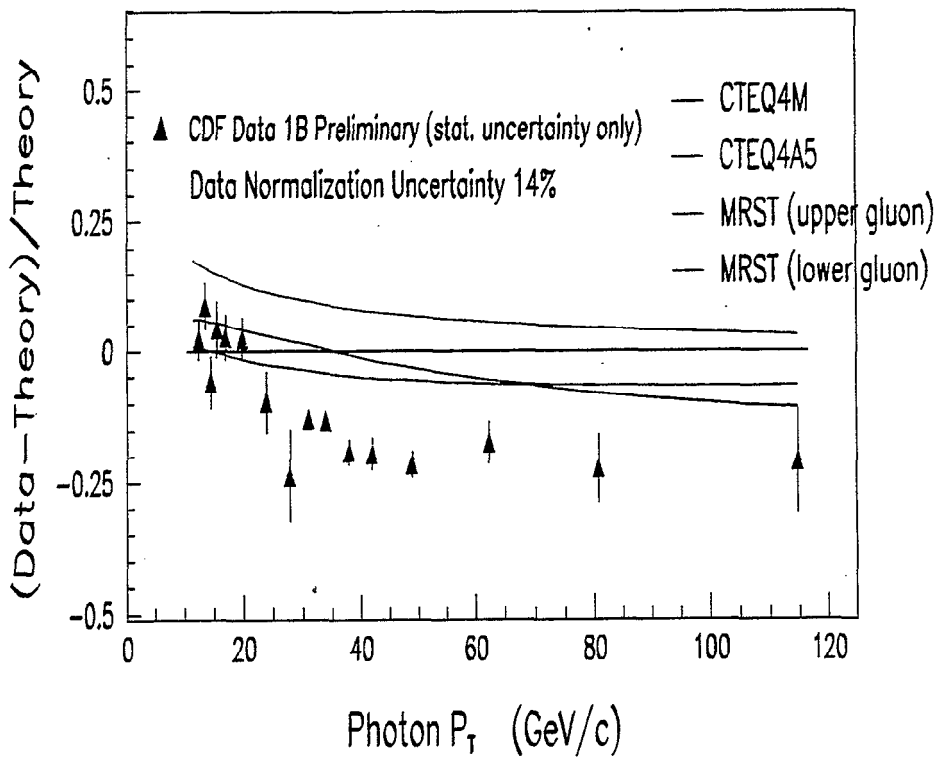

Photon + Charm Production

- Ideally Compton process probes the charm quark in proton.

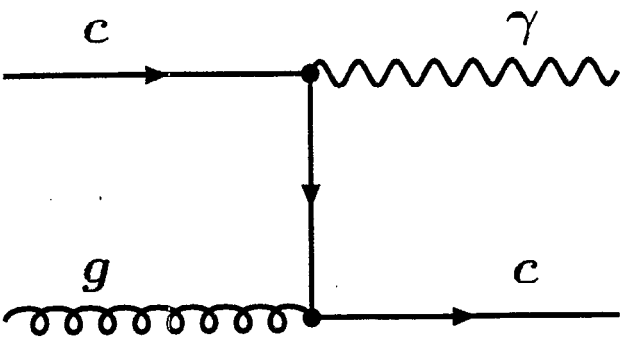

- However, other diagrams contribute, too.

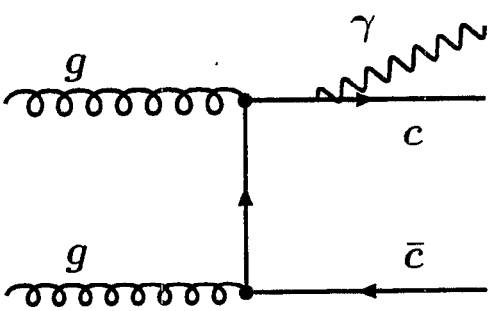

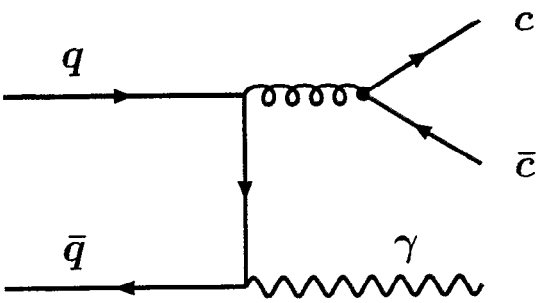

- In any case, measure $\gamma + c$ production cross section.

How to identify the charm quark?
Best if charm hadrons are fully reconstructed.

Charm Mesons

Quark comp.	J^P 0^-	Mass (MeV)	J^P 1^-	Mass (MeV)	Decay modes
$c\bar{u}$	D^0	1860	D^{*0}	2007	$\to D^0\pi^0$
$c\bar{d}$	D^+	1865	D^{*+}	2010	$\to D^0\pi^+$, $D^+\pi^0$
$c\bar{s}$	D_s^+	1970	D_s^{*+}	2112	$\to D_s^+\gamma$

$D^{*+} \to D^0\pi^+$ attractive,
because of the small Q value in the decay:

- Small background
- Good mass resolution in
  $\Delta M \equiv m(D^0\pi^+) - m(D^0)$.

Reconstruct D^0, usually use the decay modes
$D^0 \to K^-\pi^+$ $(BF = 3.8\%)$ and
$D^0 \to K^-\pi^+\pi^+\pi^-$ $(BF = 7.5\%)$.

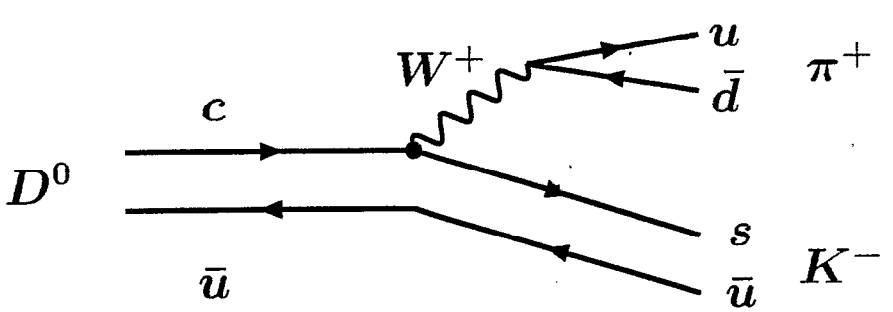

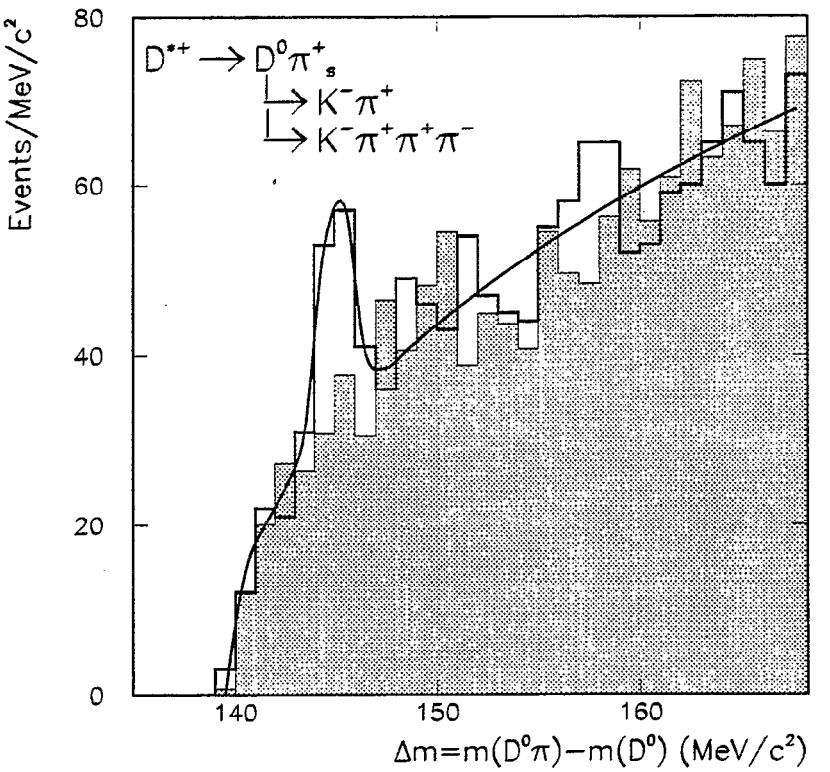
Events/MeV/c²
80
60
40
20
0
D*+ → D⁰π+s
→ K⁻π+
→ K⁻π+π+π−
140
150
160
Δm=m(D⁰π)−m(D⁰) (MeV/c²)

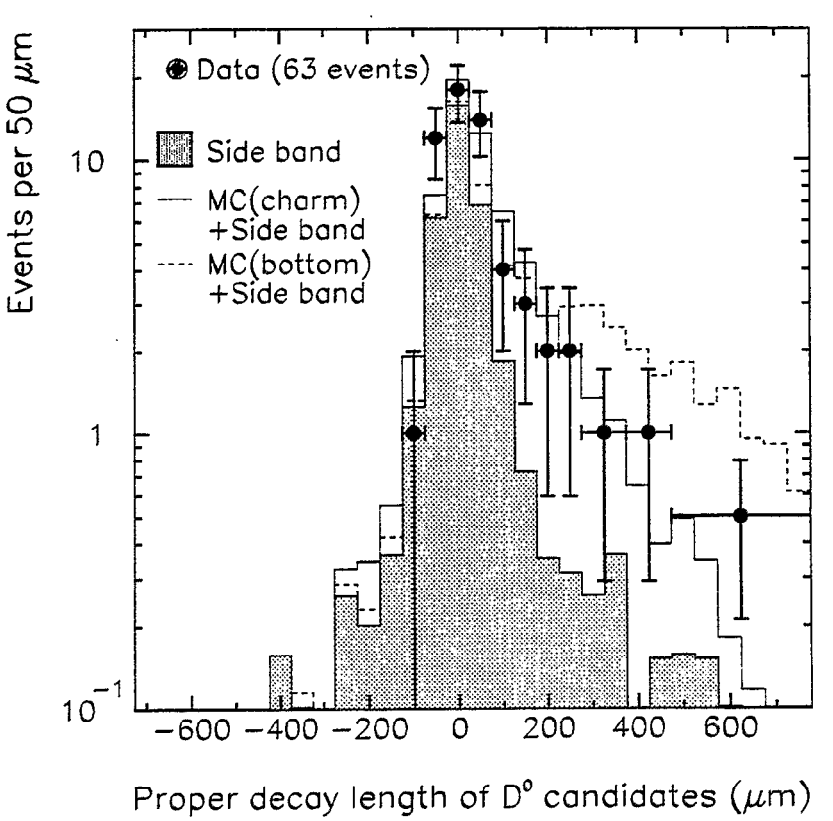
Events per 50 μm
Data (63 events)
Side band
MC(charm)
+Side band
MC(bottom)
+Side band
10
1
10⁻¹
−600 −400 −200 0 200 400 600
Proper decay length of D⁰ candidates (μm)

Heavy Quark Production

- Heavy quark mass $M_Q \gg \Lambda_{\rm QCD} \Rightarrow$ always a hard process.
  Perturbative QCD applicable for all momenta.
  LO:

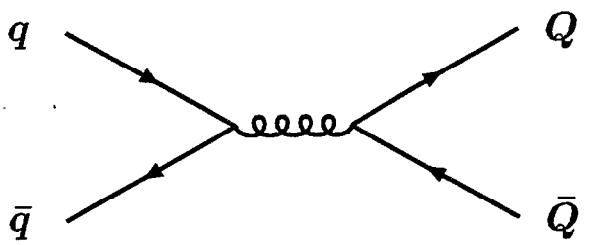

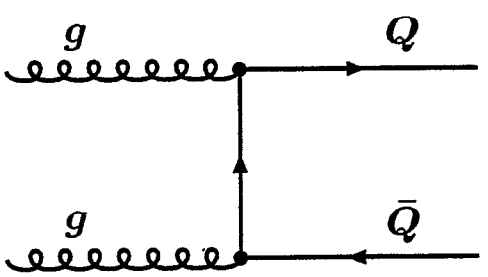

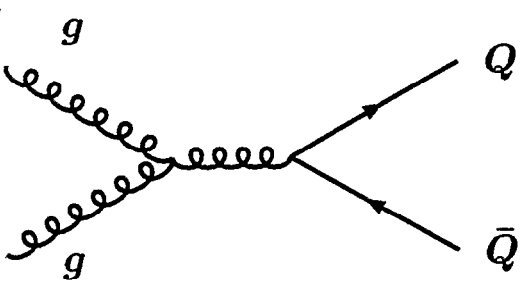

- NLO calculations available for
  - total cross sections
  - one-particle inclusive cross sections
  - two-particle correlations

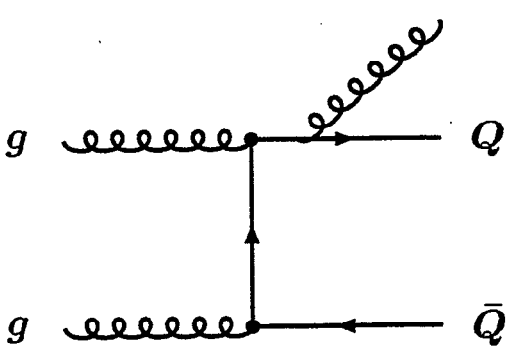

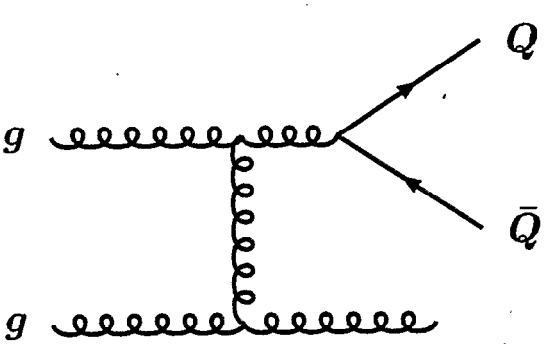

Bottom Quark Production

Correction to LO large, $\times 2.5$.
But p_T and rapidity distributions virtually unchanged.

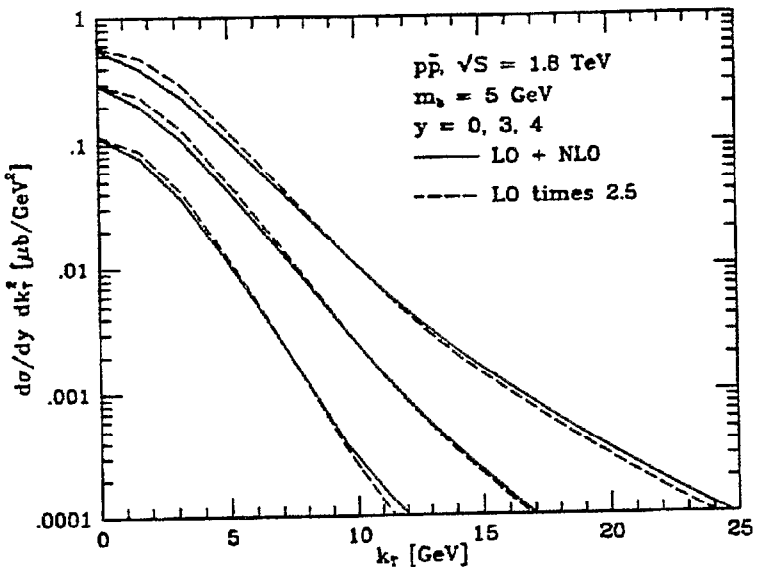

Dependence on renormalization scale μ not reduced in NLO.
Somewhat worrisome.

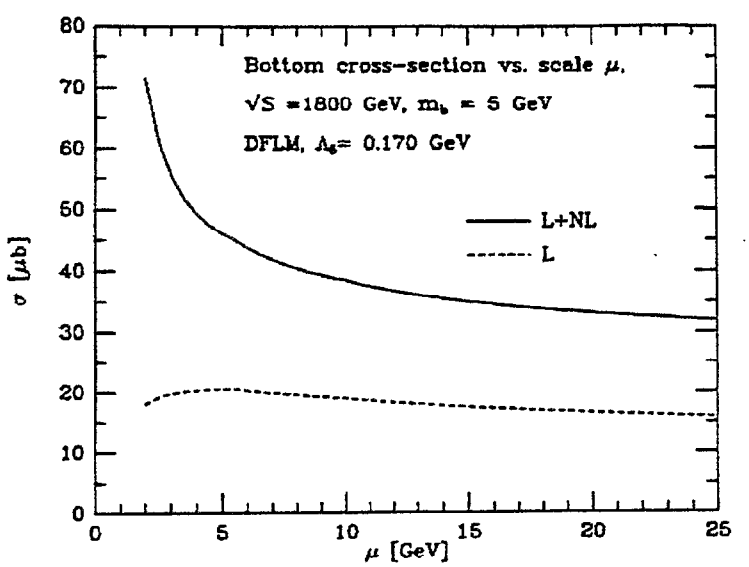

How to detect the b quark?
Have to identify its decay.

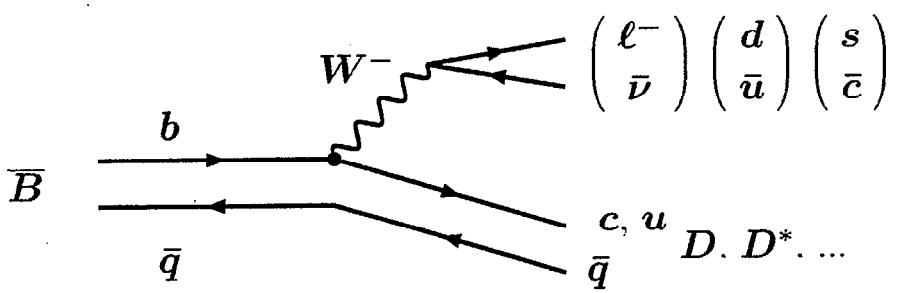

- 0-th order approximation :
  Decay of a heavy hadron $H_Q(\equiv Q\bar{q})$ is the decay of the heavy quark Q.
- b quark decays to c or u quark.
  $b \to c$ decay dominant, because $|V_{cb}| \gg |V_{ub}|$.
- Have to isolate among BG of q and g jets.
  $\Rightarrow$ use semileptonic decay and the lepton.
  Rate sizable : $\mathcal{B}(\overline{B} \to \ell^- \bar{\nu} X) = 10\%$.
  Main source of single leptons at low p_T (below $W^\pm$ and Z^0).
- B decays can also produce two leptons :
  - Sequential decays : $b \to \ell^- \bar{\nu} c$, $c \to \ell^+ \nu s$.
  - $\overline{B} \to J/\psi\, X$ via $b \to c\,\bar{c}s$, and $J/\psi \to \ell^+\ell^-$.

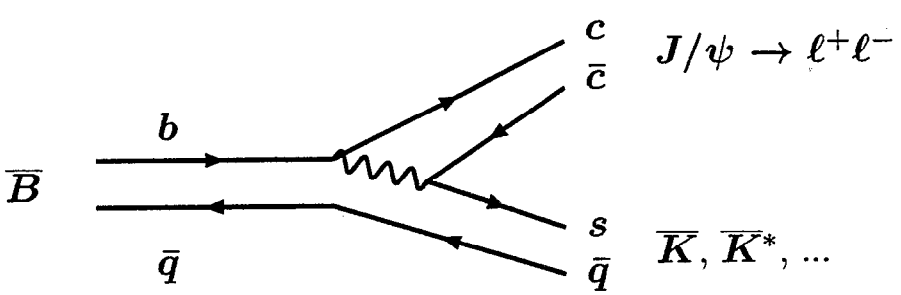

$$\mathcal{B}(\overline{B} \to J/\psi\, X) \simeq 1\%,\ \mathcal{B}(J/\psi \to \ell^+\ell^-) = 7\%.$$

Inclusive electron spectrum : 1988-89, PRL 71, 500 (1993).

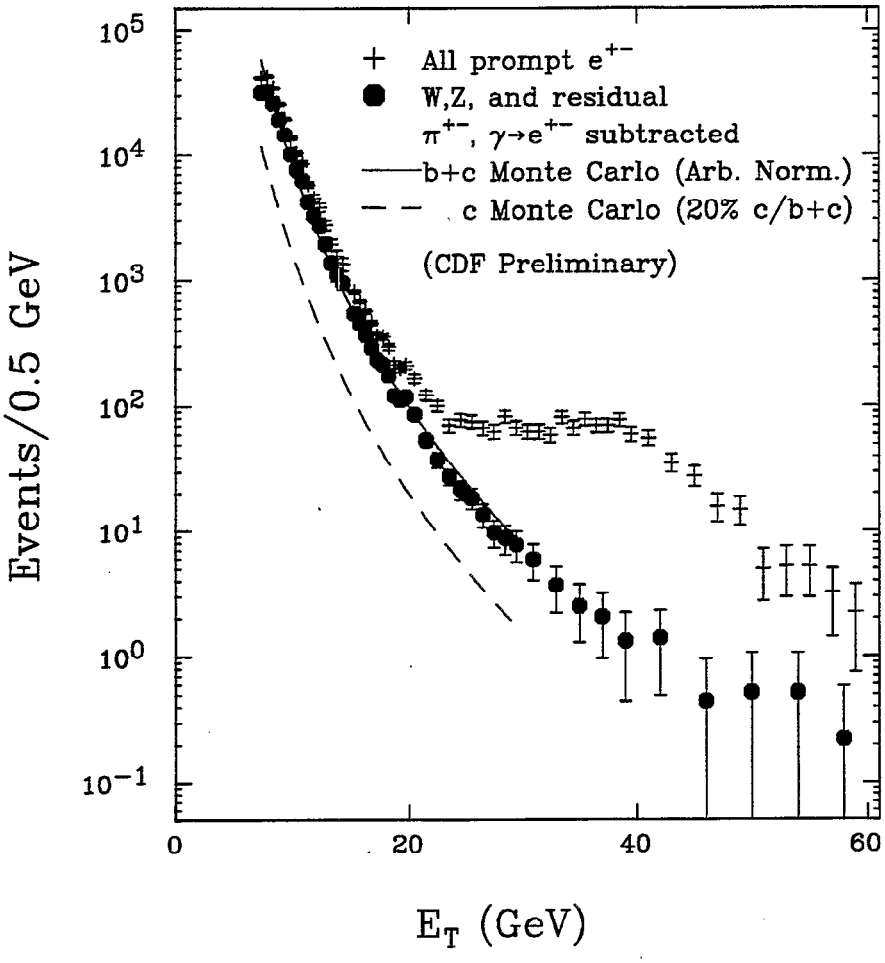

"Shoulder" above $\sim$ 25 GeV from $W^{\pm} \to e^{\pm}\nu$ and $Z^0 \to e^+e^-$.

Rest: $b \to e^-\bar{\nu}X$, $\bar{c} \to e^-\bar{\nu}X'$, hadron fakes.

$b \to \overline{B}$ fragmentation harder than $c \to D$.
Lepton momentum in the B rest frame larger than in the D.
$\Rightarrow$ bottom leptons enhanced over charm leptons.

$\overline{B} \to \ell^- \bar{\nu} D$, D^*, ... Should see the charm hadron associated with ℓ^-.

Reconstruct charm meson $D^0 \to K^- \pi^+$ near e^-.

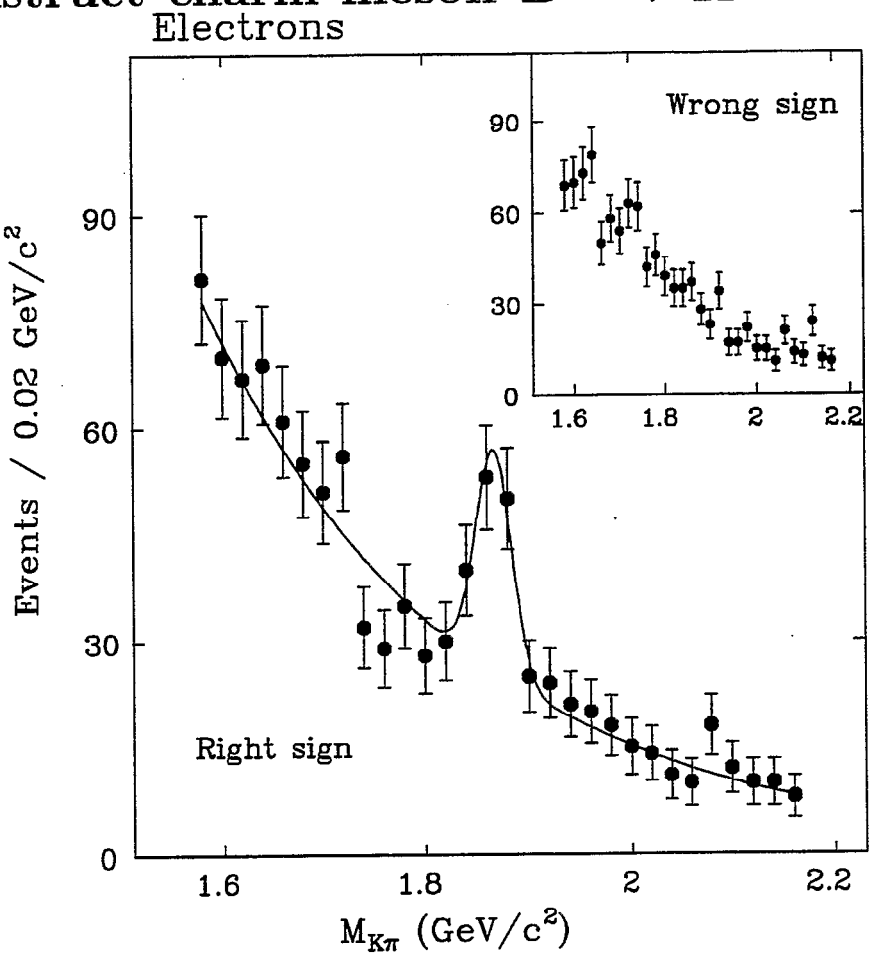

J/ψ and B decays

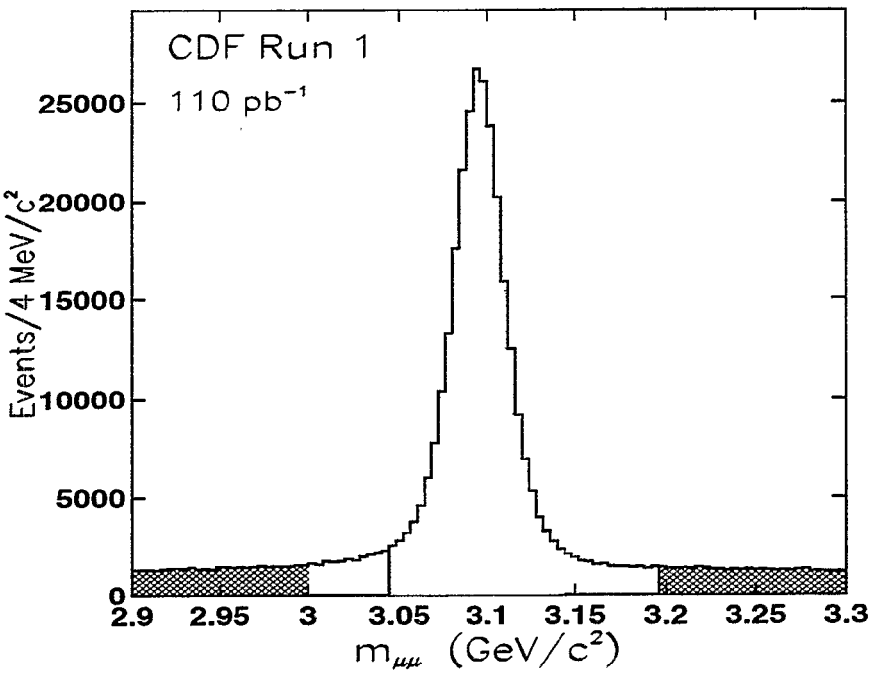

Decay length distribution

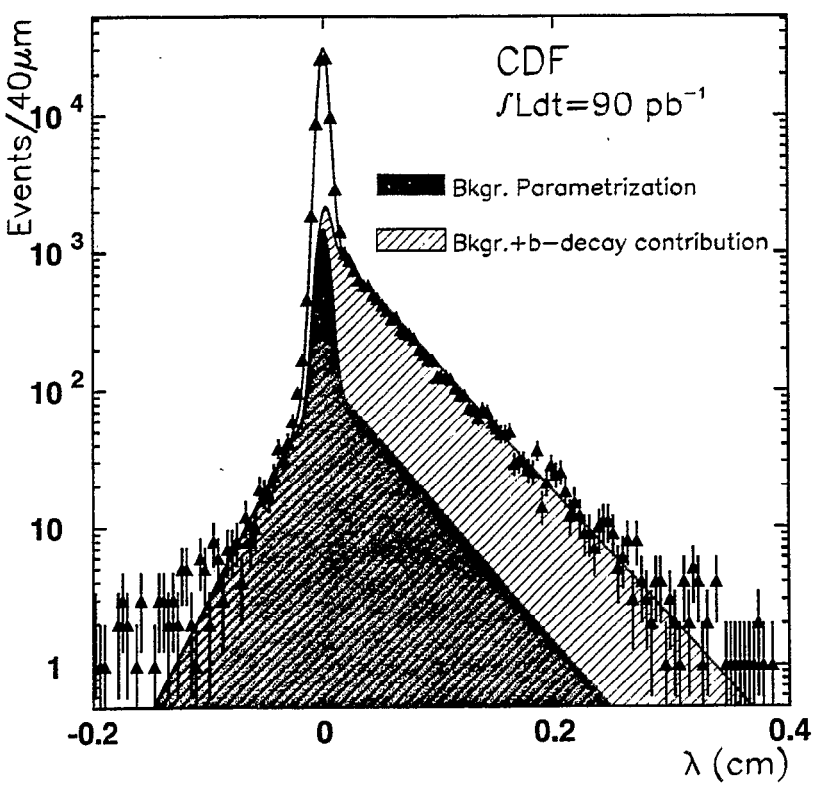

$\sim$ 20% of J/ψ's from B decays.

Production of J/ψ and $\psi(2S)$ from B decays

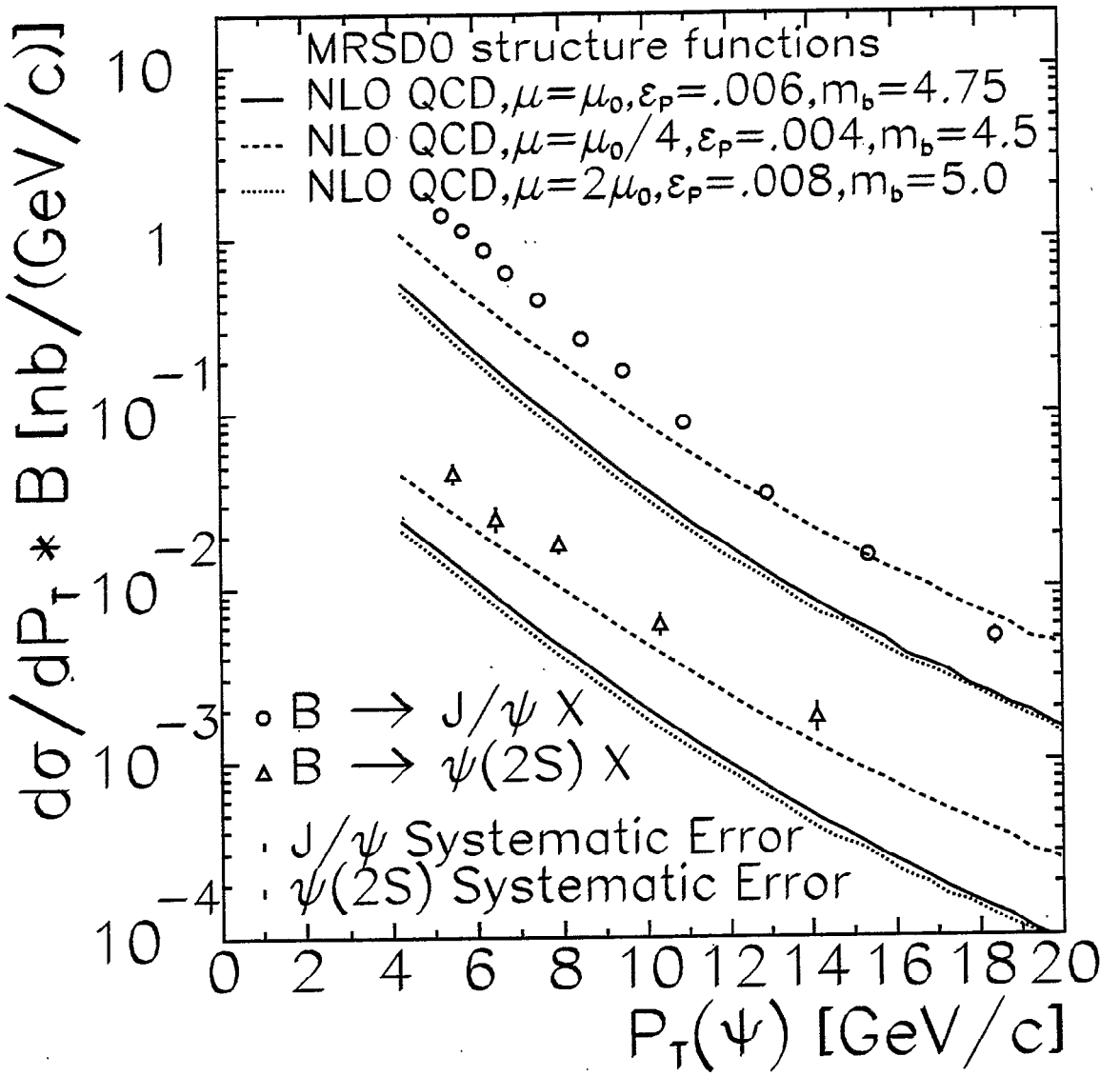

Higher than NLO QCD calculation with "normal" choices of scale μ, $\Lambda_{\rm QCD}$ and m_b.

Fully reconstructed $B^+ \to J/\psi K^+$ decays

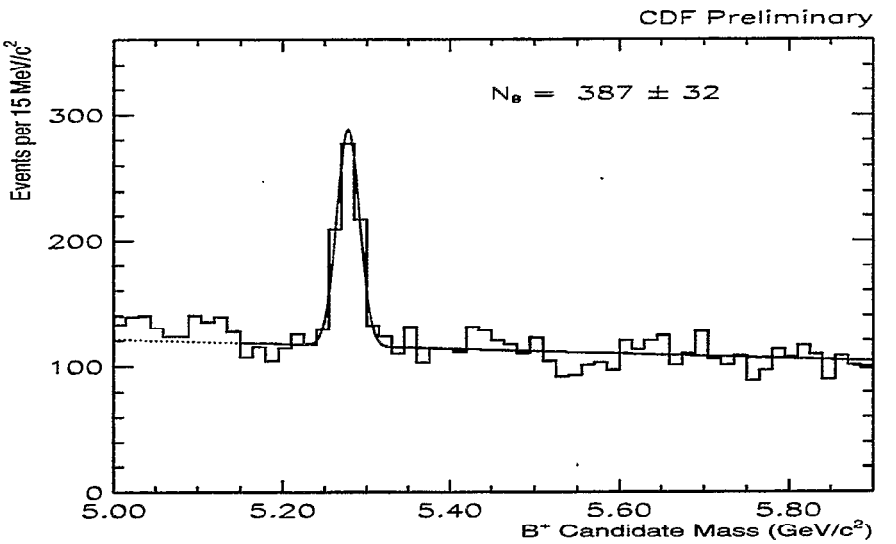

B^+ meson production cross section

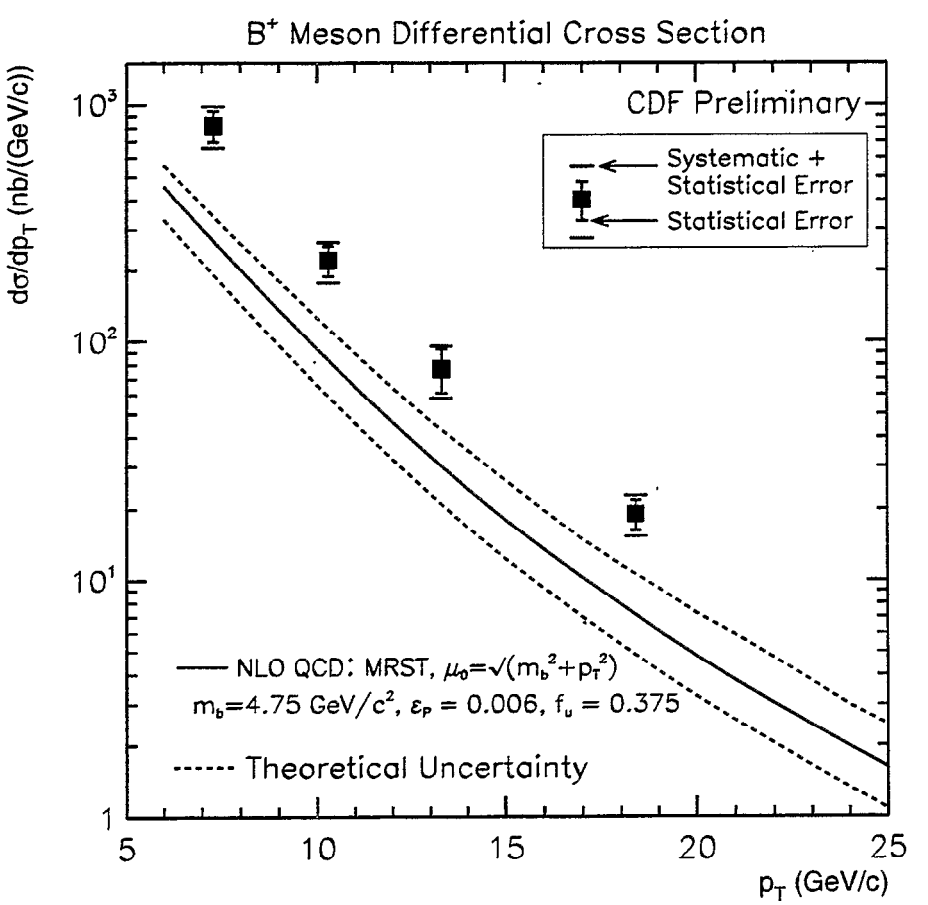

$\sigma(\bar{p}p \to B^+X) = 3.51 \pm 0.42 \pm 0.53$ μb for $p_T > 6$ GeV/c and $|y| < 1.0$.

Open Charm Production

Is charm heavy enough?
Otherwise similar to bottom.

Measure D^{*+} production.

Start with single μ sample ($p_T > 8$ GeV/c).
Use $D^{*+} \to D^0\pi^+$, $D^0 \to \mu^+\nu K^- X$.
Form $\Delta m \equiv m(\mu^+K^-\pi^+) - m(\mu^+K^-)$.

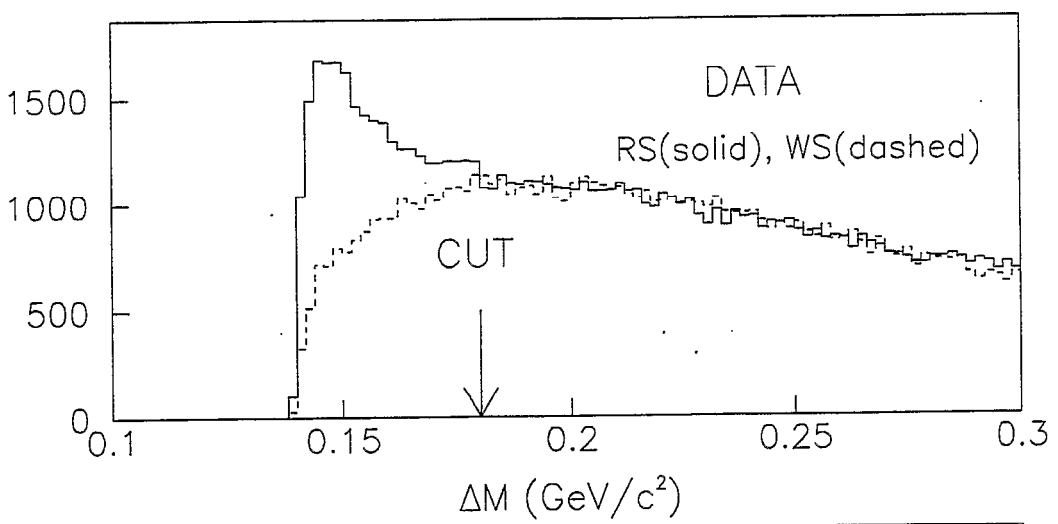

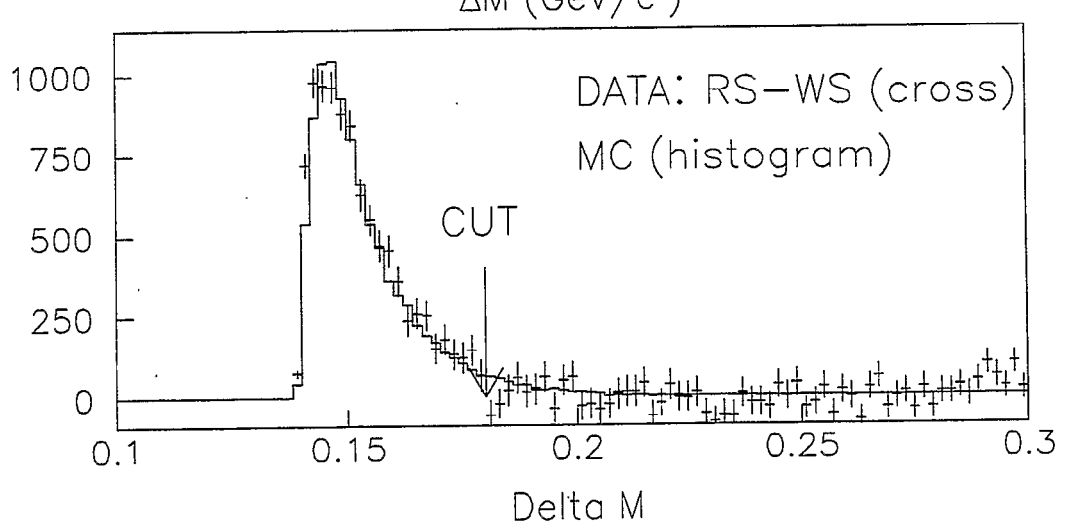

D^{*+} production

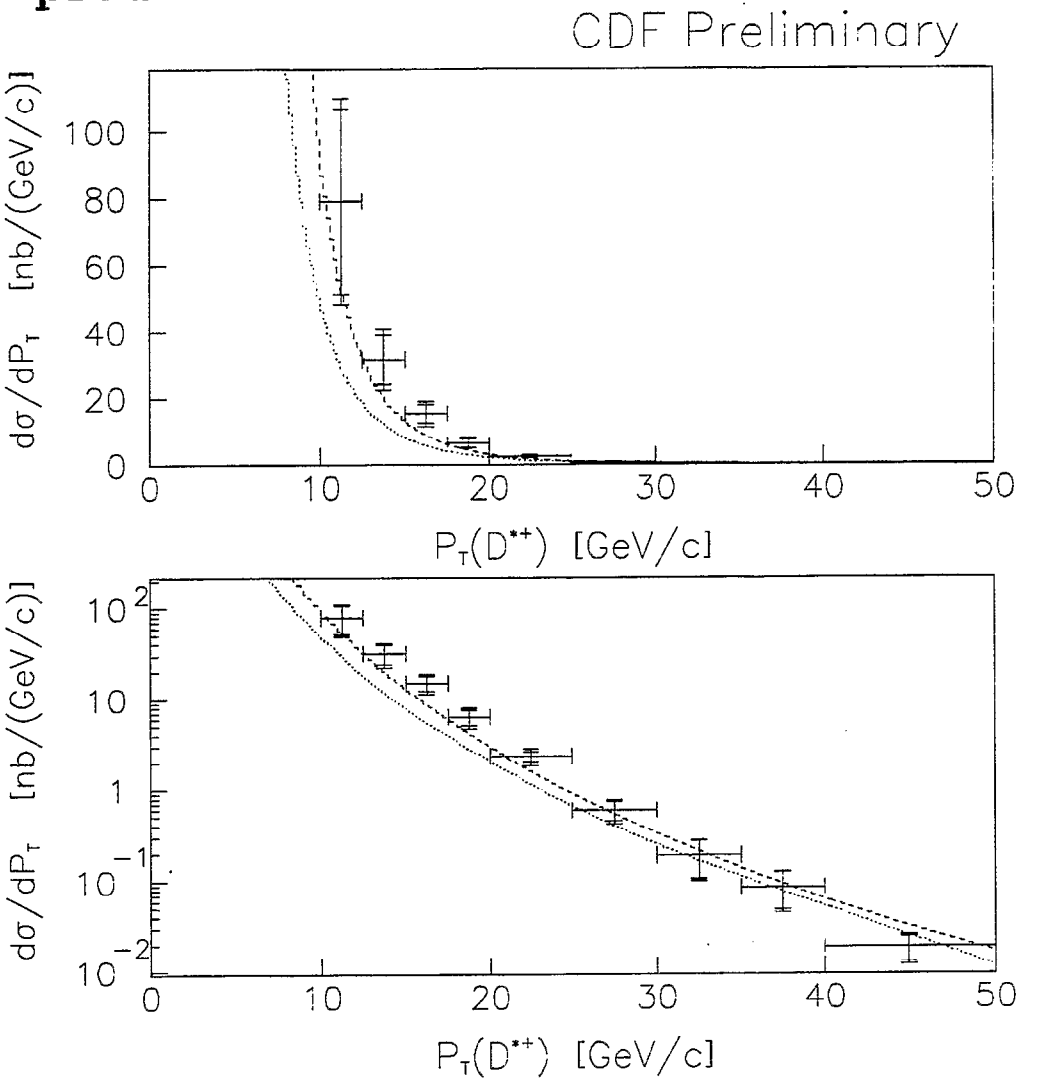

$\sigma(\bar{p}p \to D^{*+}X) = 347 \pm 65 \pm 58$ nb for $p_T > 10$ GeV/c and $|\eta| < 1.0$.
Theory : 240 nb, M. Cacciari (1998).

Onium Production

Quarkonia: bound states of heavy quark Q and its antiquark $\bar{Q}$.

$c\bar{c}$ states :
$L = 0,\ S = 0,\ J^P = 0^- :\ \eta_c$
$L = 0,\ S = 1,\ J^P = 1^- :\ J/\psi,\ \psi(2S),\ \ldots$
$L = 1,\ S = 1,\ J^P = 0^+,\ 1^+,\ 2^+ :\ \chi_{c0},\ \chi_{c1},\ \chi_{c2}$

Similarly for $b\bar{b}$:
$L = 0,\ S = 0,\ J^P = 0^- :\ \eta_b$
$L = 0,\ S = 1,\ J^P = 1^- :\ \Upsilon$
$L = 1,\ S = 1,\ J^P = 0^+,\ 1^+,\ 2^+ :\ \chi_{b0},\ \chi_{b1},\ \chi_{b2}$

$J/\psi \to 3g,\ \chi_{c(0,2)} \to 2g.$

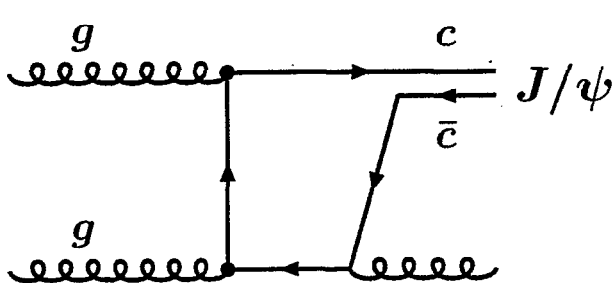

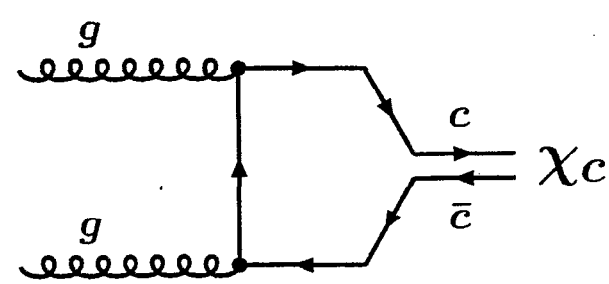

"Old" theory had predicted :
$\sigma(\psi(2S), \text{direct } J/\psi) \gg \sigma(\chi_c).$

CDF has found $\times 50$ direct J/ψ and $\psi(2S)$ yields than "color singlet model".

J/ψ and $\psi(2S)$ Production

Sources:

- $B \to J/\psi X$ **(lifetime, $\sim$ 20% of all)**
- **Direct** J/ψ
- **Direct** $\chi_c \to J/\psi\,\gamma$ **(not the case for** $\psi(2S)$**)**

The latter two have zero lifetime ("prompt") :

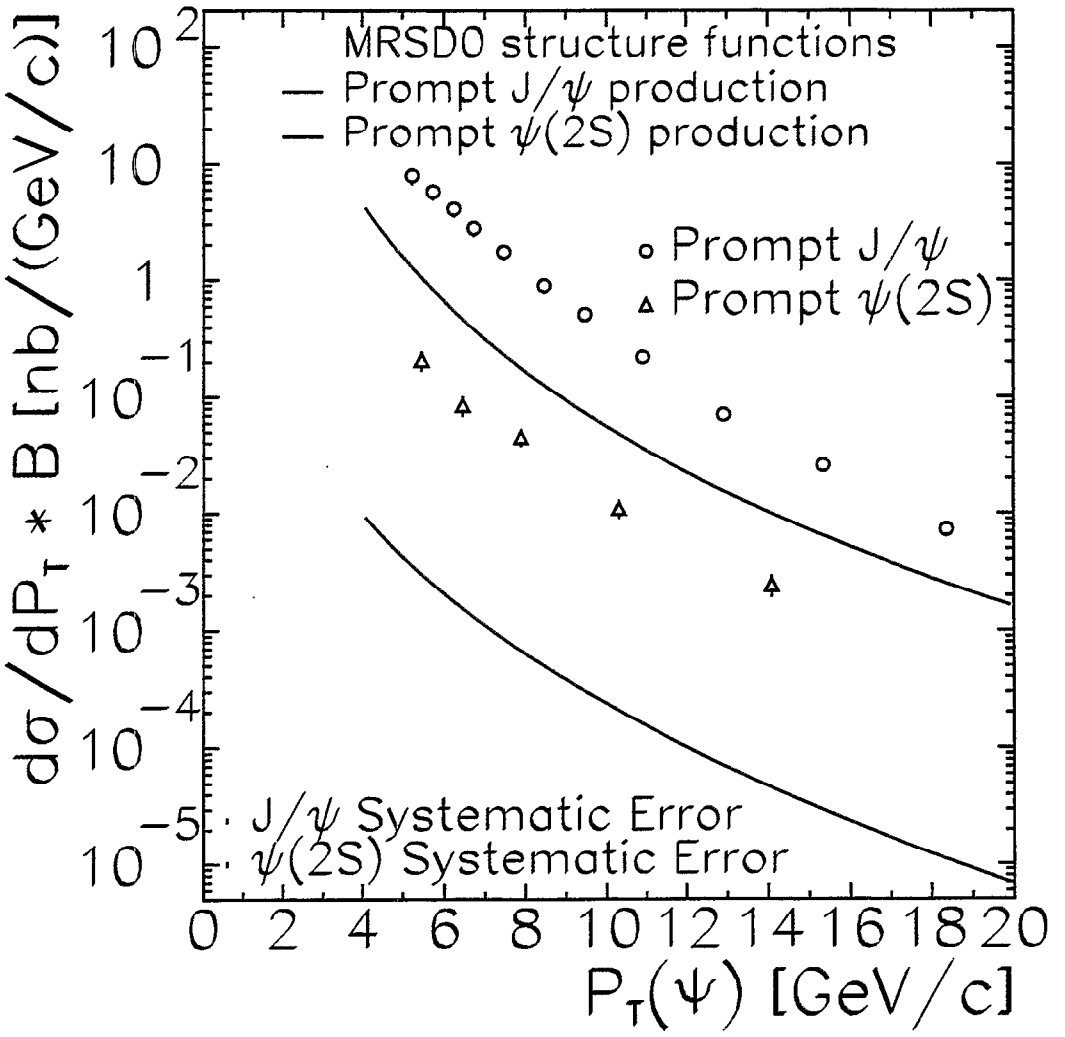

J/ψ from χ_c : $\chi_c \to J/\psi\,\gamma$

Identify γ with CEM/CES, combine it with J/ψ, calculate $\Delta M \equiv M(J/\psi\,\gamma) - M(J/\psi)$.

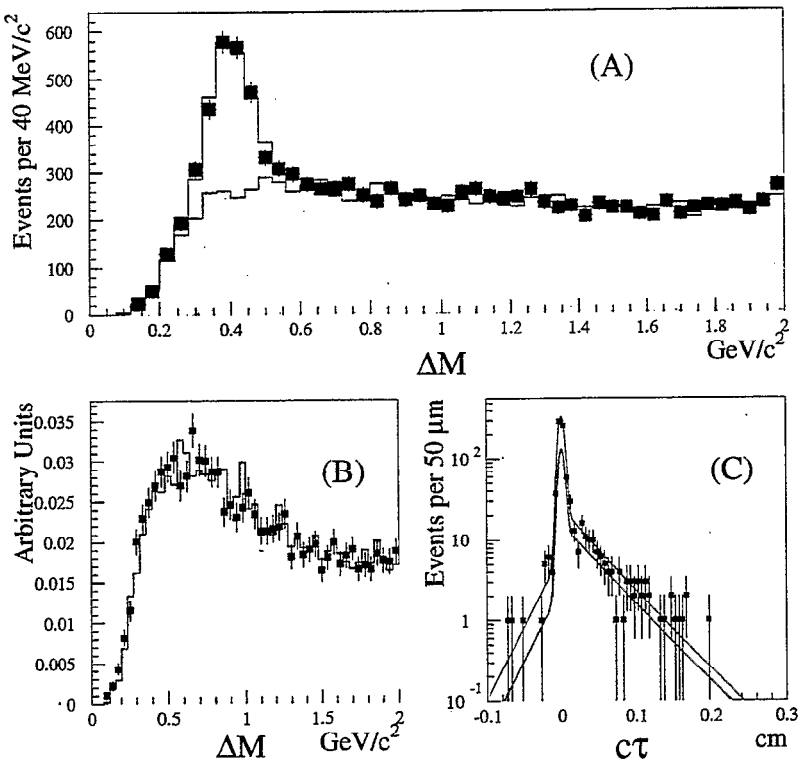

Use lifetime to subtract $B \to \chi_c X$.
Then extract sources of <u>prompt</u> J/ψ's.

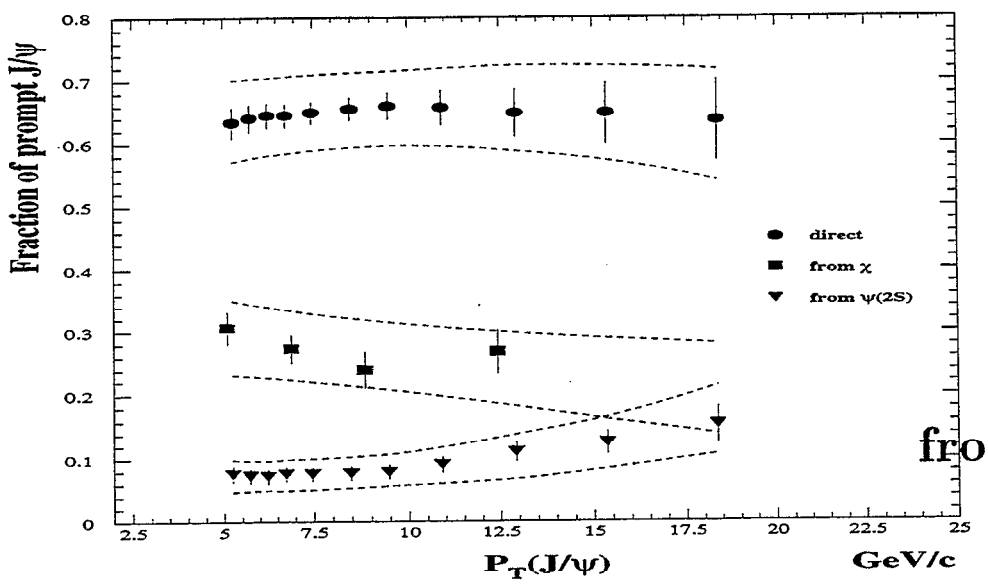

direct

from $\psi(2S)$

Prompt J/ψ Production Breakdown

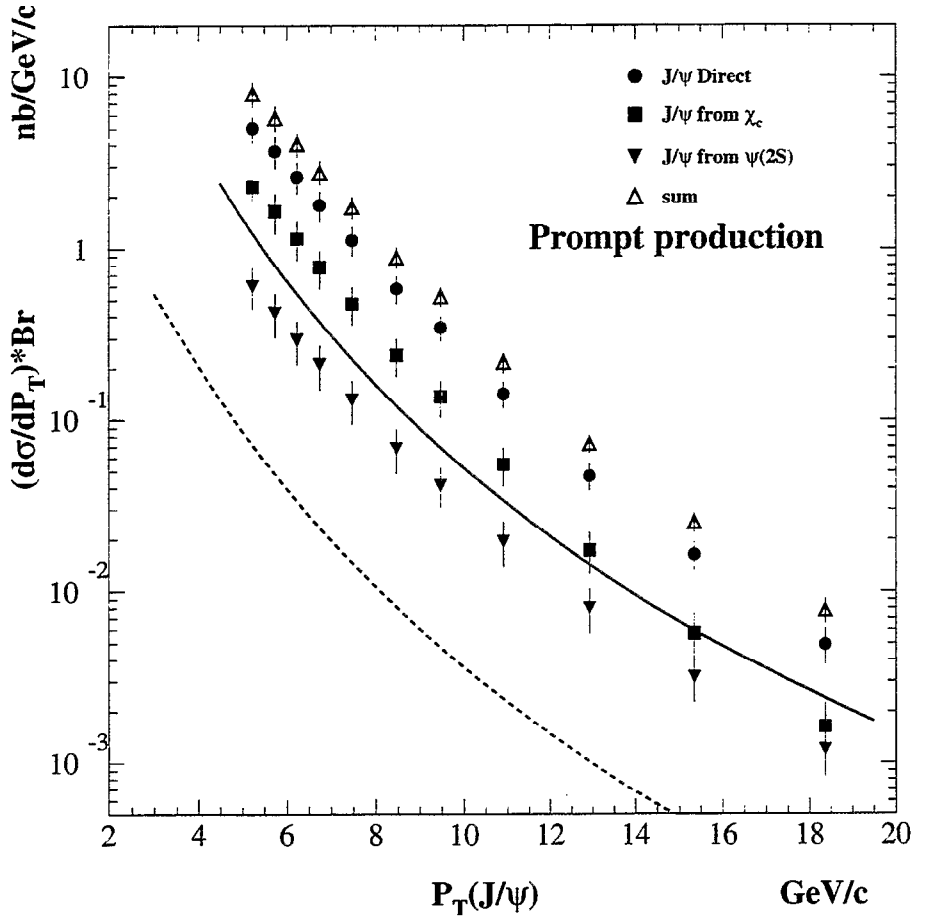

Direct production: both J/ψ and $\psi(2S)$ higher than prediction by a factor of ~ 50.

Other mechanisms must exist.
Gluon fragmentation?
Color octet?

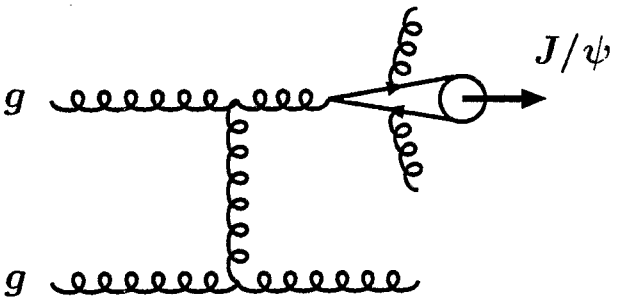

J/ψ and $\psi(2S)$ Polarization

Gluon fragmentation into ψ :

Gluons are massless ($p_T \gg m_\psi$) and thus transversely polarized.
ψ should inherit the gluon polarization.
Helicity angle:

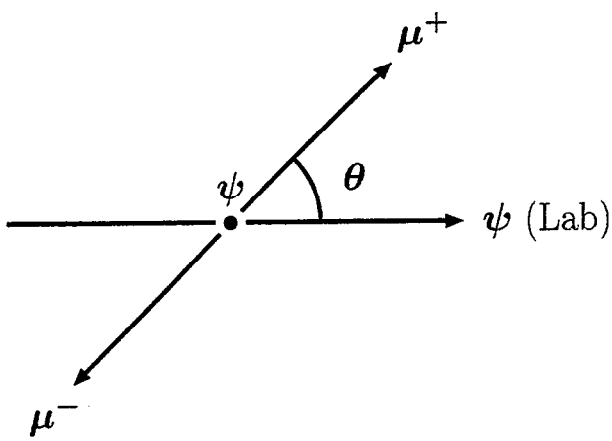

$$\frac{dN}{d\cos\theta} = 1 + \alpha\cos^2\theta$$

$\alpha = +1 \Rightarrow$ 100% transverse.
$\alpha = -1 \Rightarrow$ 100% longitudinal.

Prediction for direct production

Beneke and Krämer	$\alpha = 0.77 \pm 0.08$
Leibovich	$\alpha = 0.90 \pm 0.04$

at $p_T = 20$ GeV/c.

J/ψ and $\psi(2S)$ Polarization

J/ψ

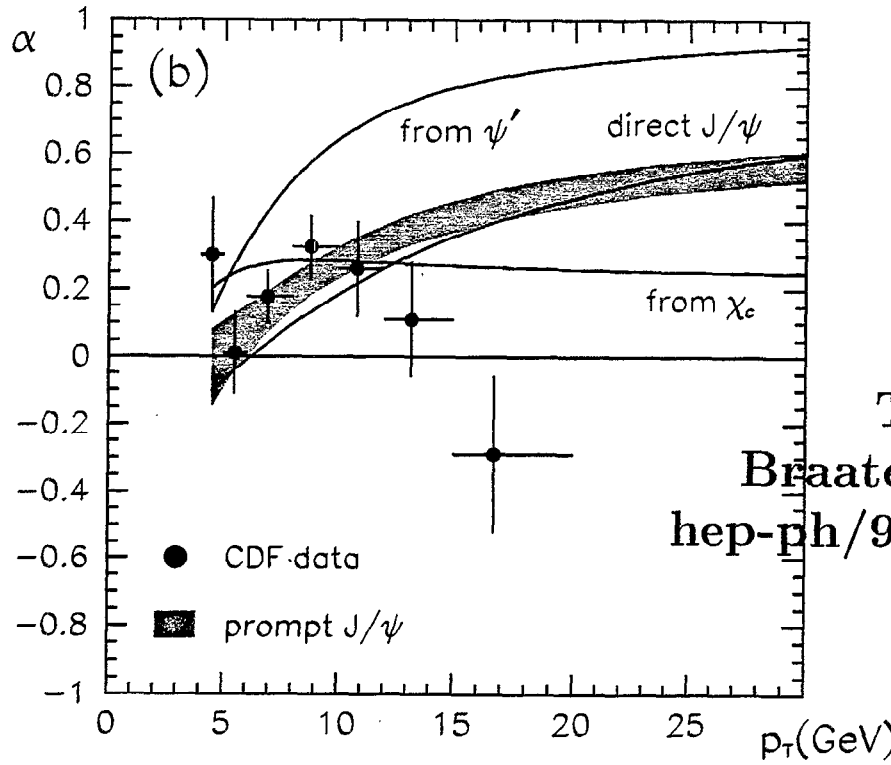

Theory:
Braaten *et al.*
hep-ph/9911436

$\psi(2S)$

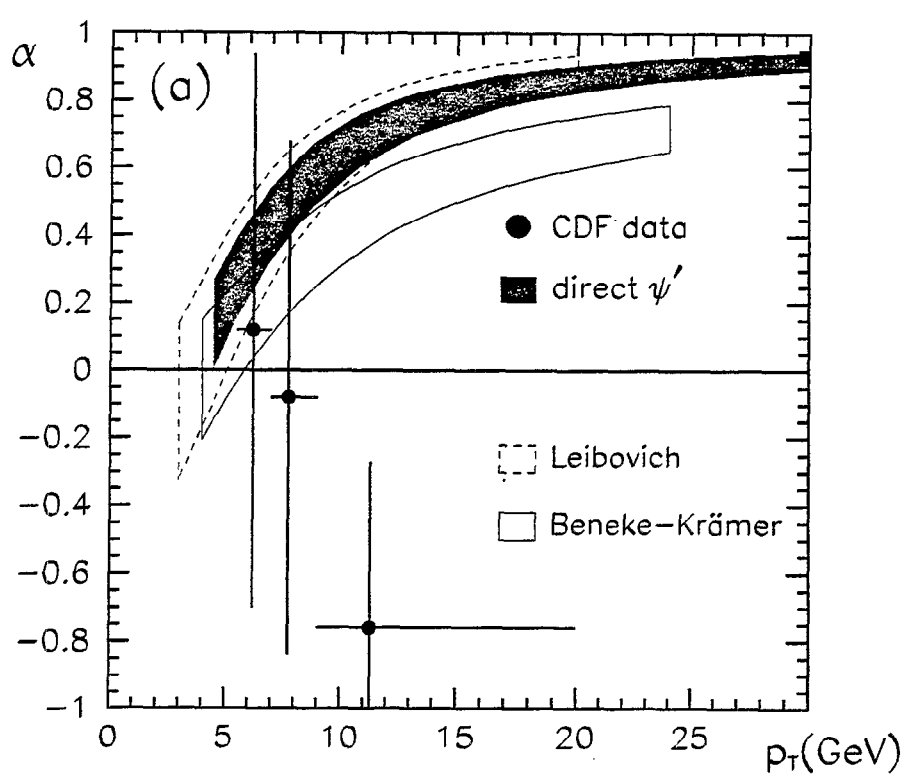

Phys. Rev. Lett. 85, 2886 (2000).

χ_c Production : separate χ_{c1} and χ_{c2}.

Need good energy resolution for photon :
$\Rightarrow$ use converted $\gamma \to e^+e^-$ (tracking momentum resolution better than calorimeter)

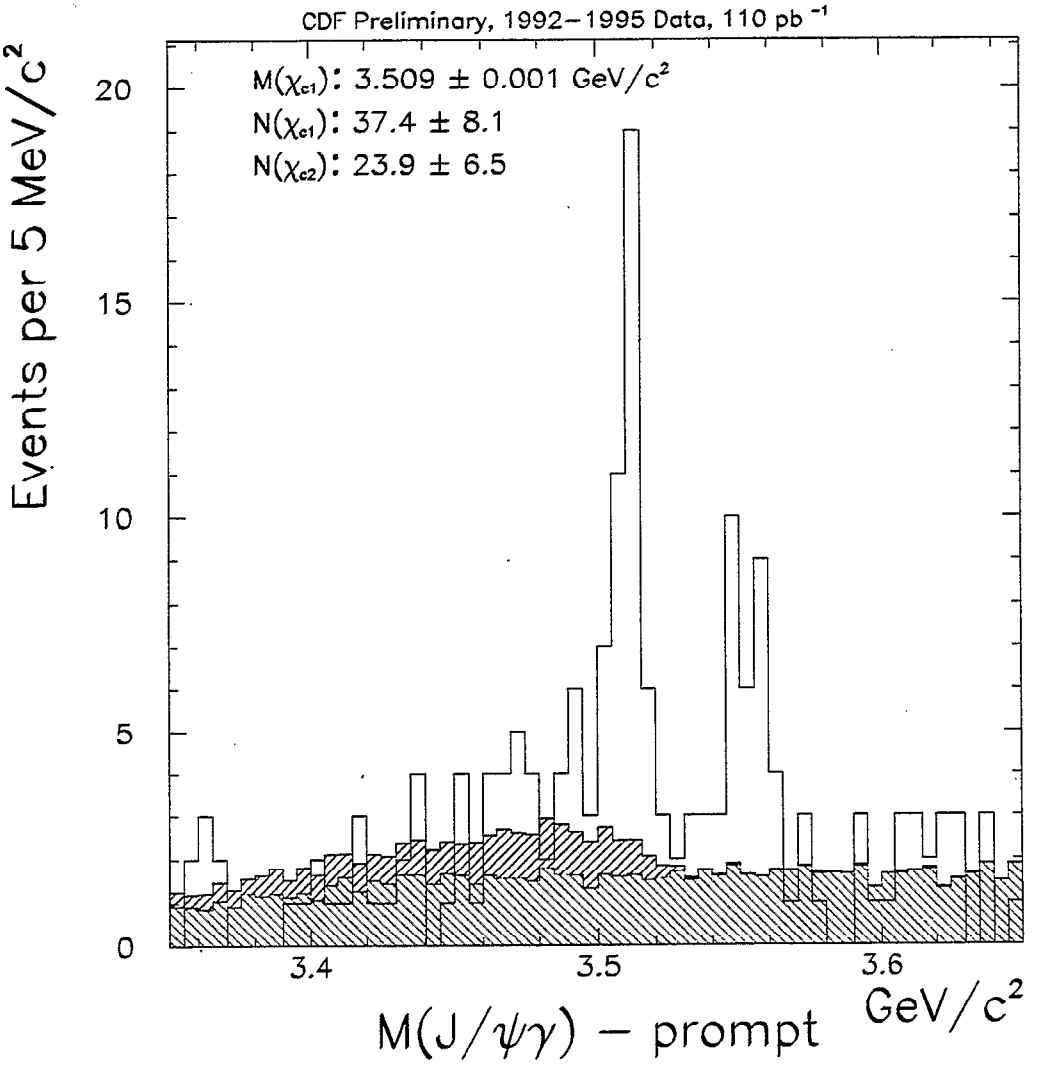

$$\frac{\sigma(\chi_{c2})}{\sigma(\chi_{c1})} = 0.89 \pm 0.33 \,^{+0.13}_{-0.10}$$

ϒ Production

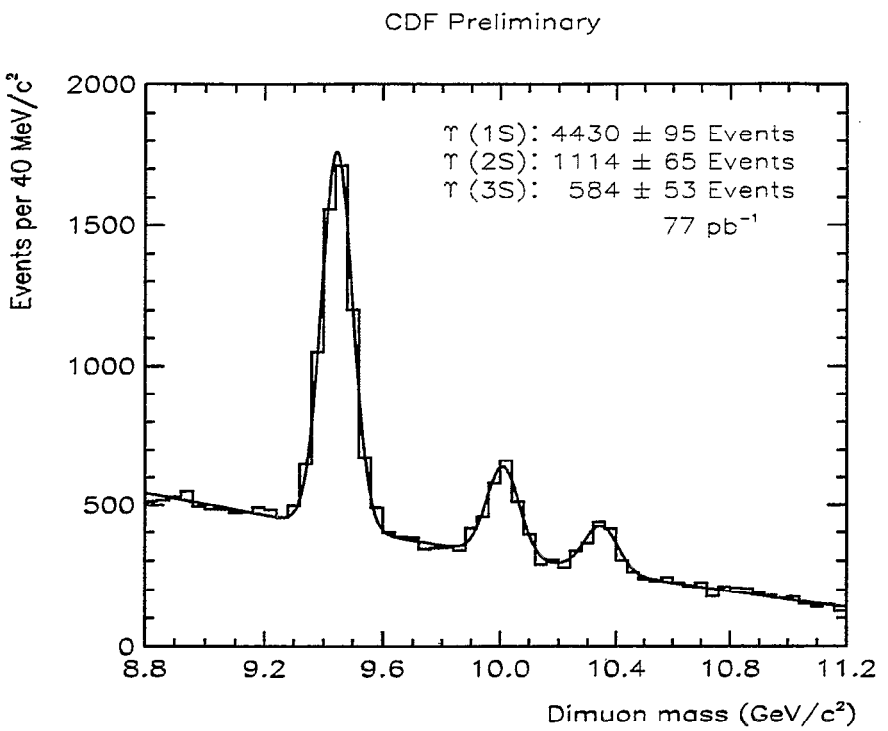

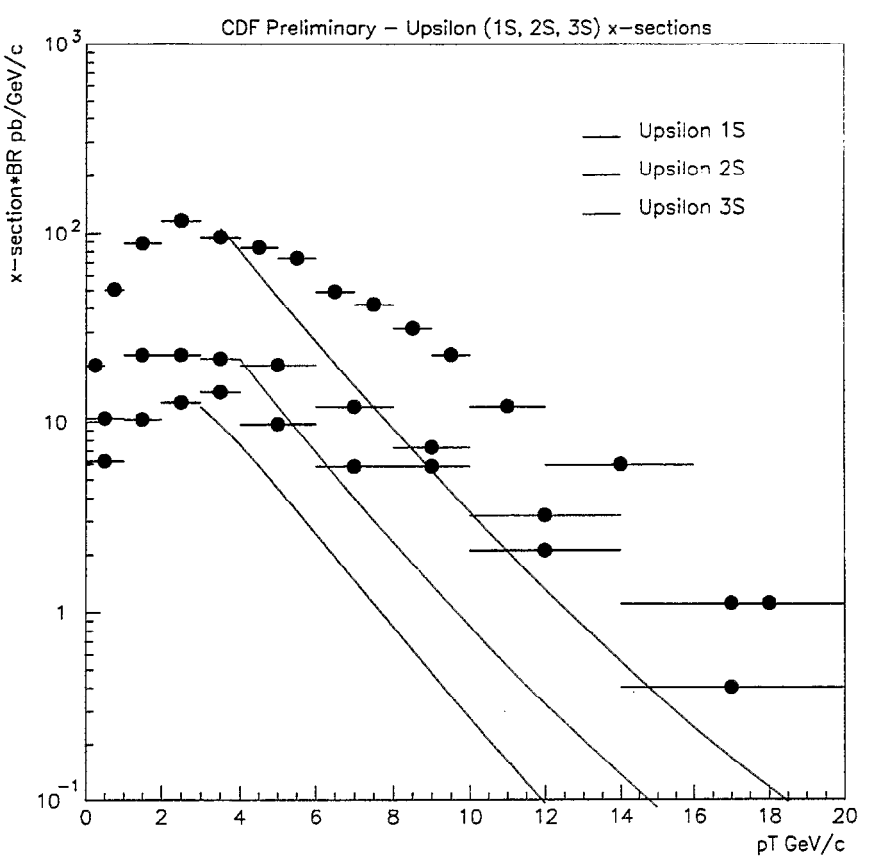

Weak Interaction:

Coupling of quarks and $W^{\pm}$ and Z^0 bosons

Examples:

- muon decay
- neutron β decay

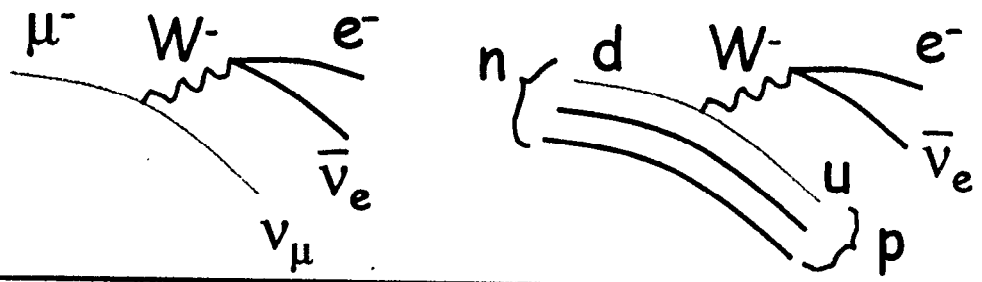

Heavy quarks *(s, c, b, t)* are unstable.
Transitions across generations possible: eg. $\Lambda^0 \rightarrow p\pi^-$ $(s \rightarrow u)$
$\rightarrow$ Quark flavors are not always conserved in C.C. weak int's.
Mass and flavor eigenstates connected by the CKM matrix.

$$V_{CKM} \equiv \begin{pmatrix} V_{ud} & V_{us} & V_{ub} \\ V_{cd} & V_{cs} & V_{cb} \\ V_{td} & V_{ts} & V_{tb} \end{pmatrix}$$

$$L \propto W_\mu \bar{U}_i \gamma^\mu V_{ij} D_j$$

$\bar{U} = (\bar{u}, \bar{c}, \bar{t})$

$D = \begin{pmatrix} d \\ s \\ b \end{pmatrix}$

Need to determine the elements V_{ij} experimentally.

B decays: Can probe five elements of V_{CKM}

$$V_{CKM} \equiv \begin{pmatrix} V_{ud} & V_{us} & V_{ub} \\ V_{cd} & V_{cs} & V_{cb} \\ V_{td} & V_{ts} & V_{tb} \end{pmatrix}$$

1: V_{cb}

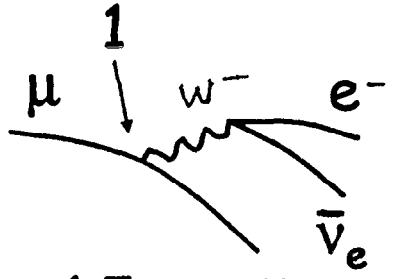

$\tau_b \sim 1.5$ ps

$\rightarrow |V_{cb}| \sim 0.04$

2: V_{ub}

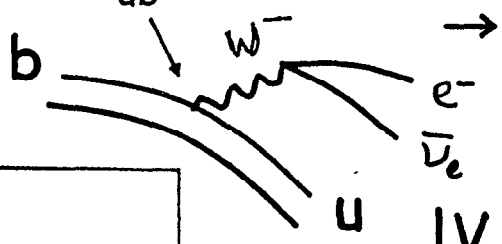

$|V_{ub}|/|V_{cb}| \sim 0.1$

V_{tb}, V_{ts}, V_{td} : *t* quark couplings.
In principle from *t* decays,
but hard in practice.
Can use *B* decay processes where
the *t* quark is involved in the loop,
e.g. particle-antiparticle oscillations
of the neutral *B* mesons.

Introduction

Why *B* Physics at a Hadron Machine ?

Because the production rates are high.

$e^+e^- \to b\bar{b} \sim 1$ nb at $\Upsilon(4S)$

~ 6 nb at Z^0

$p\bar{p} \to b\bar{b}\,x$ via strong interaction

$\sigma \sim 10\ \mu b$ at 1.8 TeV

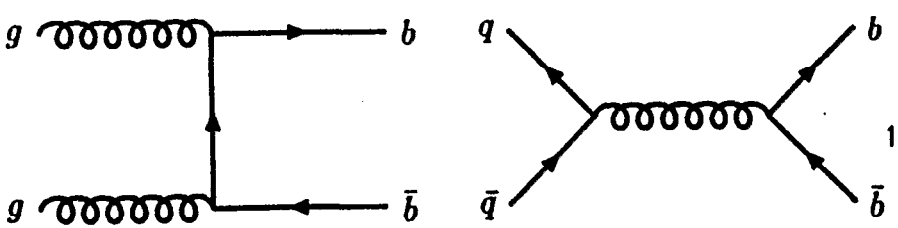

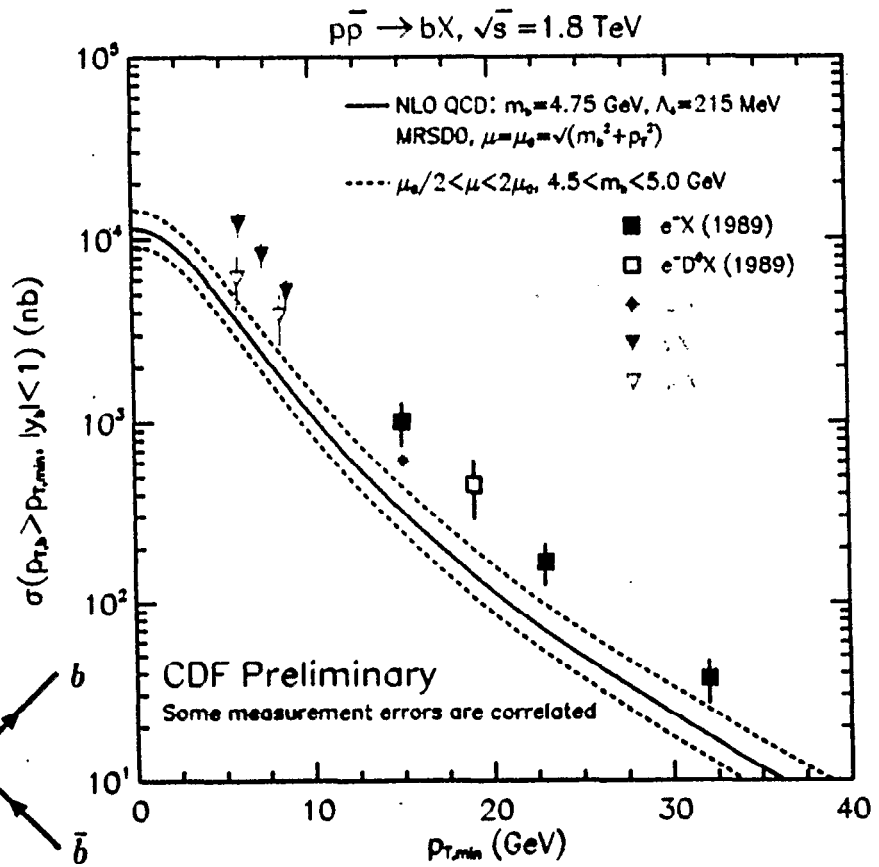

- Not only B^0, B^+, but also B_s^0, baryons, B_c
- Lorentz boost, $\beta\gamma \sim 2 - 4$.

  Vertex resolution not an issue.

Need to trigger on *B* decays, though.

So far relied on leptons:

- Single leptons (e, μ)
  - $B \to l^+ \nu X$

  $p_T > 8$ GeV/c
  $\langle p_T(B) \rangle \sim 20$ GeV/c
  purity ~ 40%

- Di-leptons (μμ, eμ)
  - $B \to J/\psi X$, $J/\psi \to \mu^+\mu^-$
  - $b \to e \nu X$, $\bar{b} \to \mu \nu X'$

  $p_T > 2$ GeV/c
  $\langle p_T(B) \rangle \sim 10$ GeV/c
  purity ~ 20% (J/ψ)

Signal $J/\psi \rightarrow \mu^+\mu^-$ Decay length dist.

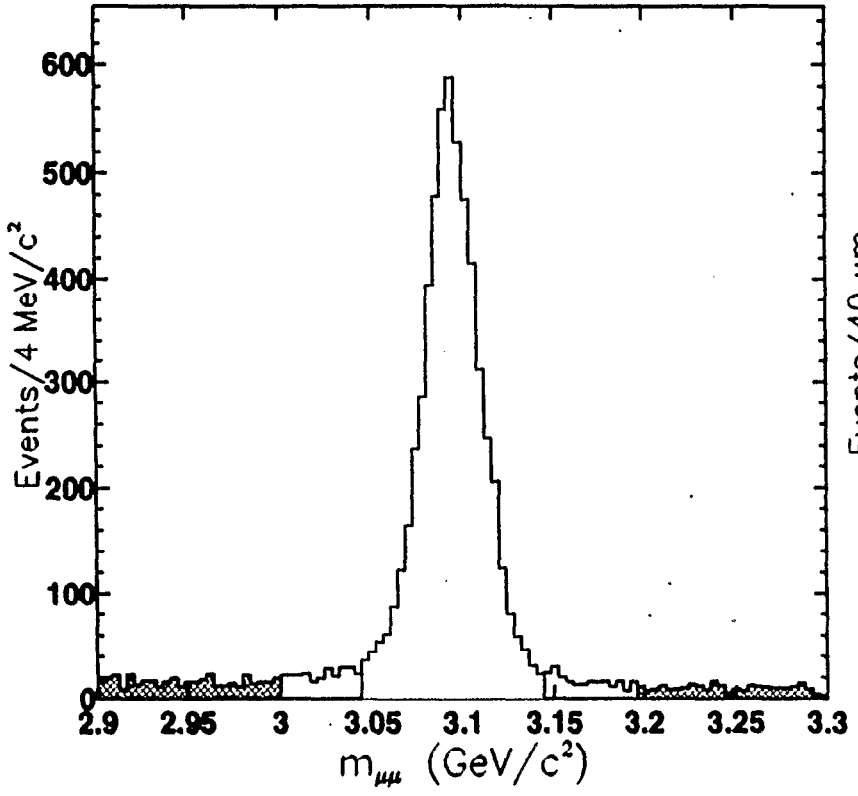

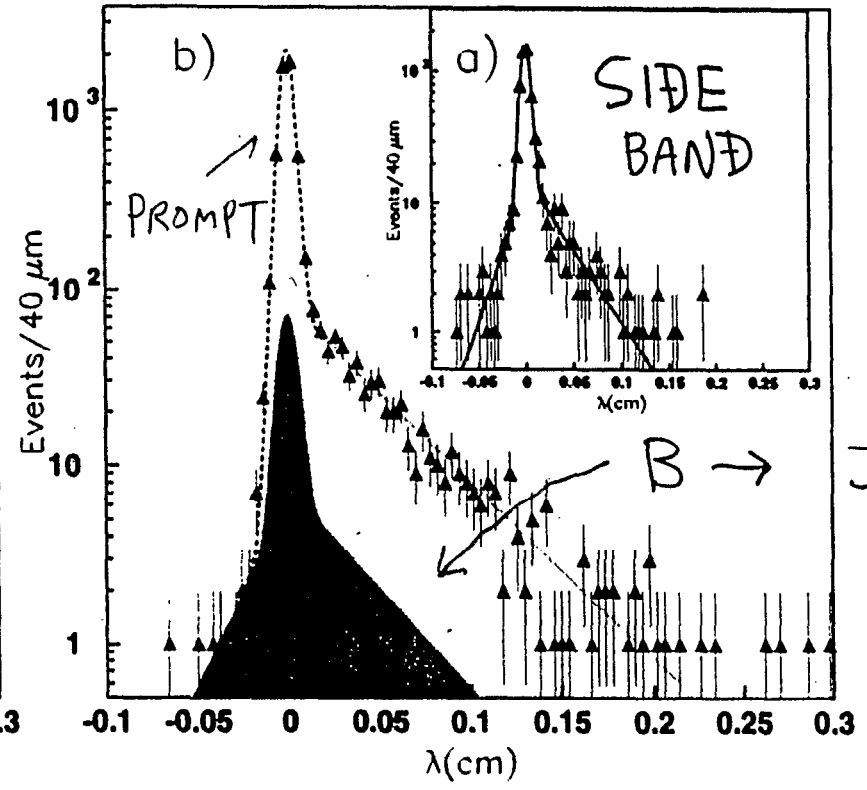

- ~ 240 k $J/\psi \rightarrow \mu^+\mu^-$.
- Mass resolution ~ 16 MeV/c².
- ~ 20% from *B* decays, others direct / $\chi_c \rightarrow J/\psi\gamma$.

Run-I CDF *B* physics results

WEAK INT.

- Mass measurements of B^+, B^0, B^0_s and Λ_b. ← QCD
- Lifetime measurements of B^+, B^0, B^0_s, Λ_b.
- B^0-$\bar{B}^0$ oscillations and flavor tagging.
- $\sin(2\beta)$ from $B^0/\bar{B}^0 \rightarrow J/\psi\, K^0_S$.
- B_c meson.
- Rare decay searches (FCNC decays)

QCD

- Inclusive *b* and *B* production.
- $b\bar{b}$ production correlations.
- *b*-quark fragmentation fractions, f_u, f_d, f_s ...
- Onium production (J/ψ, Υ)
  - Prompt and non-prompt (from *B*, χ_c) production
  - Production polarization

Lifetime Ratio $\tau(B^+) / \tau(B^0)$

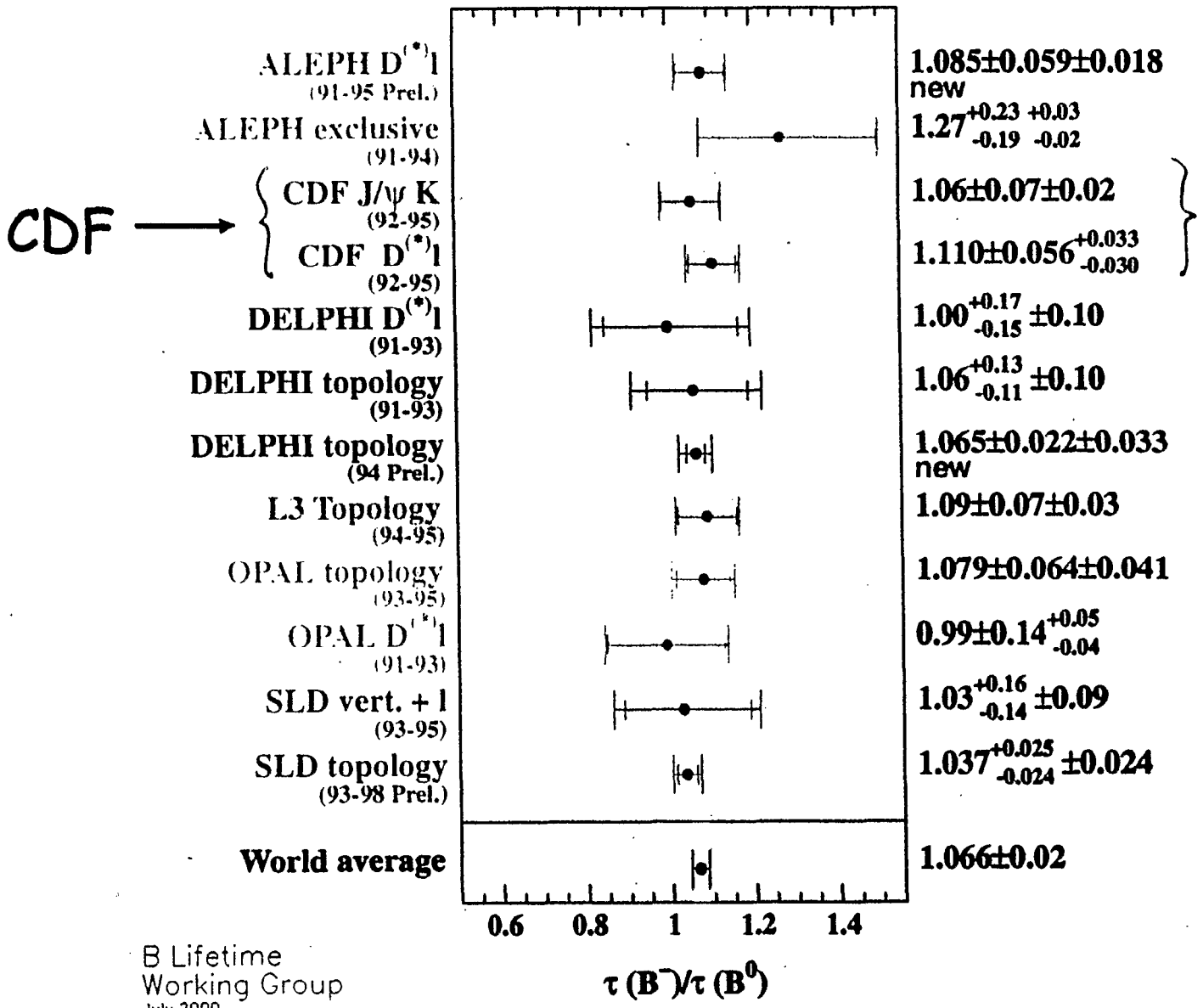

B Lifetime
Working Group
July 2000

B^0-$\bar{B}^0$ Oscillations

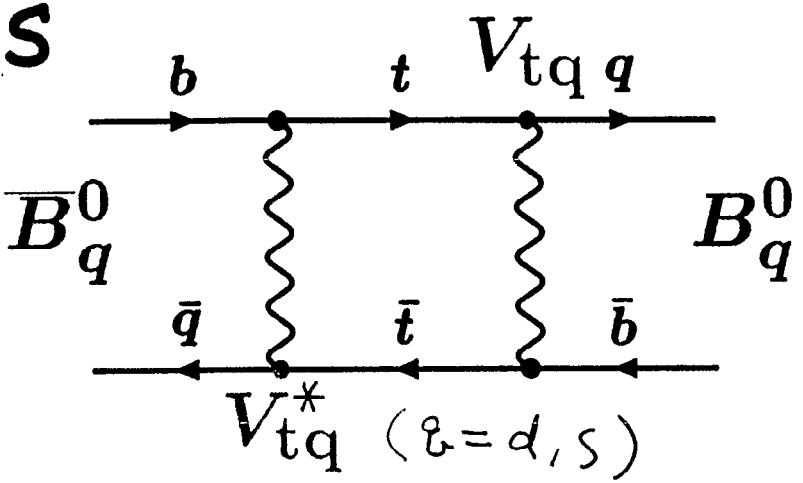

- 2nd order weak interaction.
- Decay probability:

$$P_{B^0 \to B^0}(t) = \frac{1}{2\tau} e^{-t/\tau} (1 + \cos \Delta m t) \qquad \text{Unmixed}$$

$$P_{B^0 \to \bar{B}^0}(t) = \frac{1}{2\tau} e^{-t/\tau} (1 - \cos \Delta m t) \qquad \text{Mixed}$$

$\tau \cong 1.5\ ps$

- Oscillation frequency = $\Delta m = m_H - m_L$:

  $\Delta m_q \propto |V_{tq}|^2$

- Eventually $\Delta m_s / \Delta m_d \to |V_{ts}| / |V_{td}|$

  with less theory uncertainty

Ingredients for B^0-$\bar{B}^0$ Oscillation Measurements

- Proper decay time $\quad ct = L_B/(\beta\gamma) = L_B \cdot \frac{m}{p}$
- Decay flavor ($B^0 \to l^+ \nu X$ vs $\bar{B}^0 \to l^- \nu X$)
- Production flavor, b or $\bar{b}$? Flavor tagging

Flavor tagging is the hardest part. (for CDF)

Conventional approach:

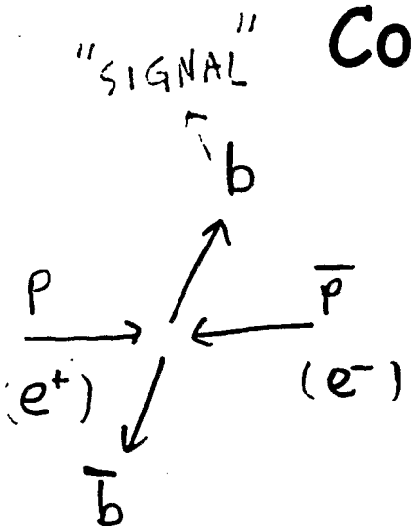

- identify the flavor of the other B
  - **semileptonic decay leptons,**
  - **(kaons) jet charge**
- infer the flavor of the signal B

Tagging Dilution

No tag is perfect. e.g. for lepton tag:

- Leptons from $b \to c \to l^+ \nu s$ B.R. SIMILAR. supp. by CUTS.
- B^0, B^0_s mixes. $\bar{\chi} \approx 0.13$
- Fakes.

Probability of misidentification W

"Dilution" $D \equiv 1 - 2W$.

Oscillation amplitude reduced by a factor D.

(unmixed - mixed) / total = $\cos(\Delta m\, t)$

$\to D \cos(\Delta m\, t)$

Tag effectiveness = εD^2,

ε is the efficiency of the tag.

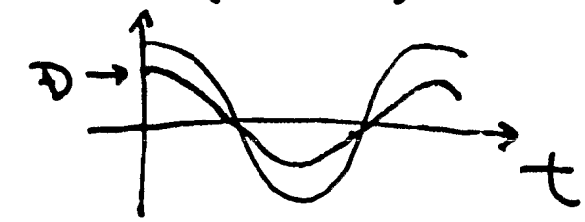

Mixing from l^- $D^{(*)}$ and same-side pion tag

Charm signal near l^-

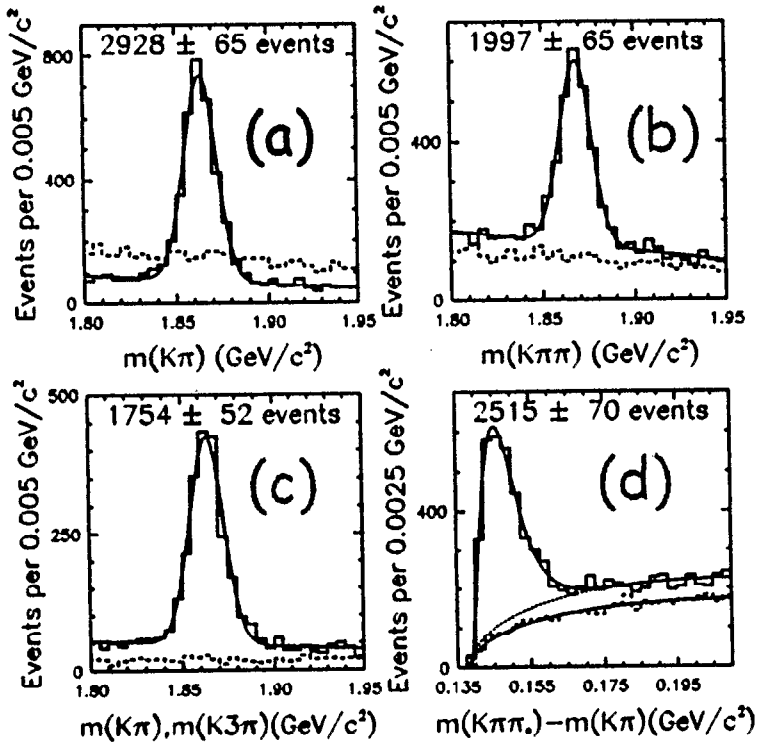

Asymmetry = (RS-WS) / Total

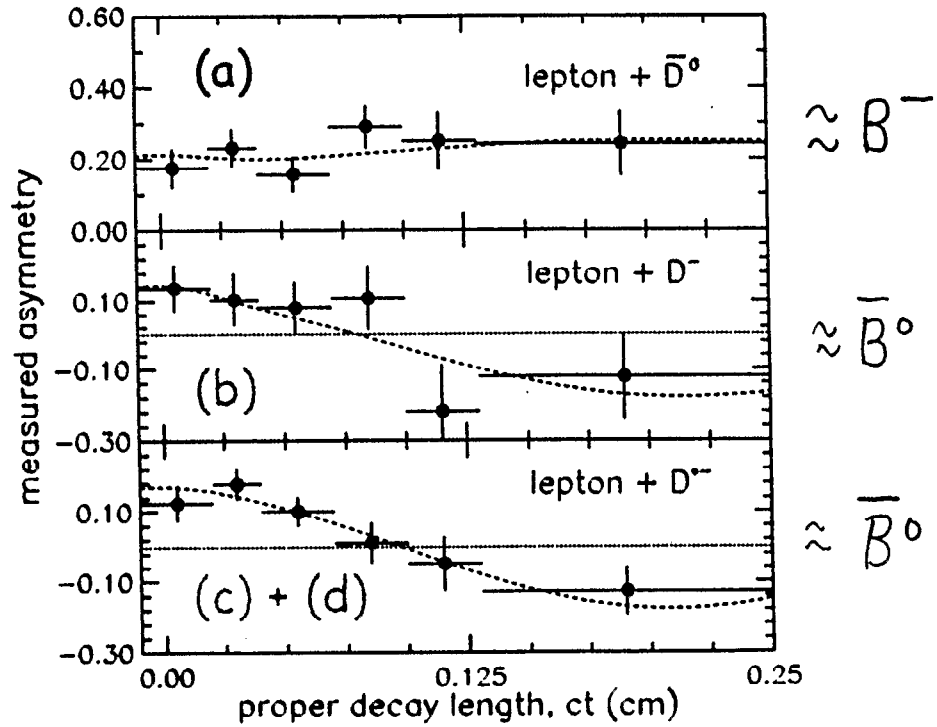

(a) $D^0 \to K^- \pi^+$. (b) $D^+ \to K^- \pi^+ \pi^+$.

(c) $D^{*+} \to D^0 \pi^+$,

$D^0 \to K^- \pi^+, K^- \pi^+ \pi^+ \pi^-$.

(d) $D^{*+} \to D^0 \pi^+$, $D^0 \to K^- \pi^+ \pi^0$.

$$\Delta m = 0.471^{+0.078}_{-0.068} \pm 0.034\, ps^{-1}$$

$$D(B^+) = 0.27 \pm 0.03 \pm 0.02$$

$$D(B^0) = 0.18 \pm 0.03 \pm 0.02$$

$\mathcal{E} \simeq 7000$

Dilepton Trigger

Mixing from l^- D^{*+} and lepton tag

Charm signal near l^-

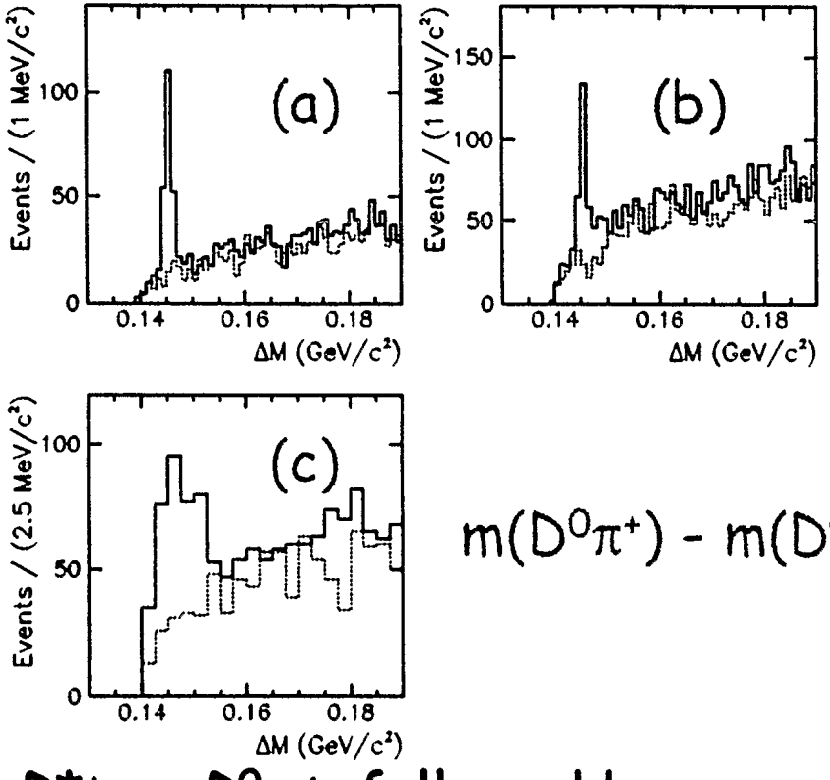

$m(D^0\pi^+) - m(D^0)$

Asymmetry = (RS-WS) / Total

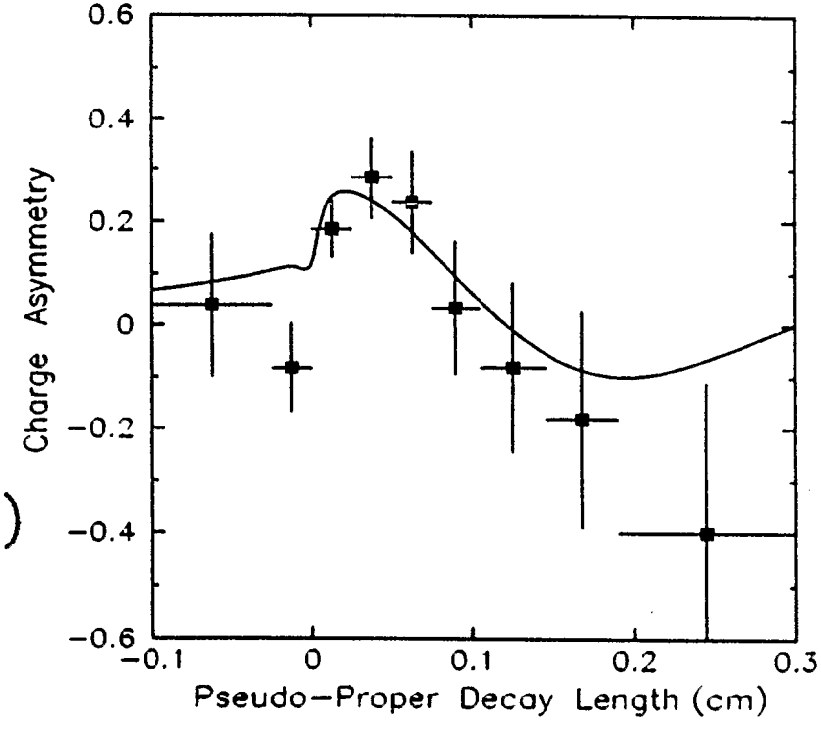

$D^{*+} \rightarrow D^0\pi^+$, followed by

(a) $D^0 \rightarrow K^-\pi^+$,

(b) $D^0 \rightarrow K^-\pi^+\pi^+\pi^-$.

(c) $D^0 \rightarrow K^-\pi^+\pi^0$.

530 SIGNAL

~80%

$$\Delta m = 0.516 \pm 0.099^{+0.029}_{-0.035}\, ps^{-1}$$

$W = 0.325 \pm 0.033 \pm 0.012$

$\rightarrow D = 0.350 \pm 0.070.$

CDF Δm_d Results

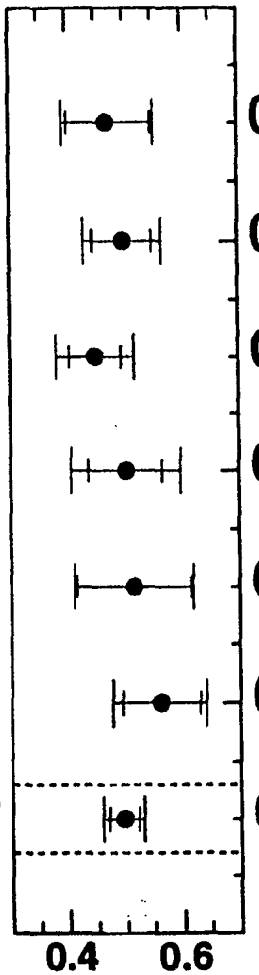

Δm_d [ps^{-1}]

D*lep / SST	$0.471 \,^{+0.078}_{-0.068} \pm 0.034$ ps^{-1}	PRL 80, 2057 (1998)
lep / Q^{jet},lep	$0.500 \pm 0.052 \pm 0.043$ ps^{-1}	PRD 60, 072003 (1999)
e / μ	$0.450 \pm 0.045 \pm 0.051$ ps^{-1}	Preliminary
μ / μ	$0.503 \pm 0.064 \pm 0.071$ ps^{-1}	PRD 60, 051101 (1999)
D*lep / lep	$0.516 \pm 0.099 \,^{+0.029}_{-0.035}$ ps^{-1}	PRD 60, 112004 (1999)
$D^{(*)}$ / lep	$0.562 \pm 0.068 \,^{+0.041}_{-0.050}$ ps^{-1}	Preliminary
Average	$0.495 \pm 0.026 \pm 0.025$ ps^{-1}	

ALSO $\Delta m_s > 5.8\ ps^{-1}$ (95% CL)

from $\bar{B}_s^0 \to \ell^- \bar{\nu} \phi X$

Δm_d Results

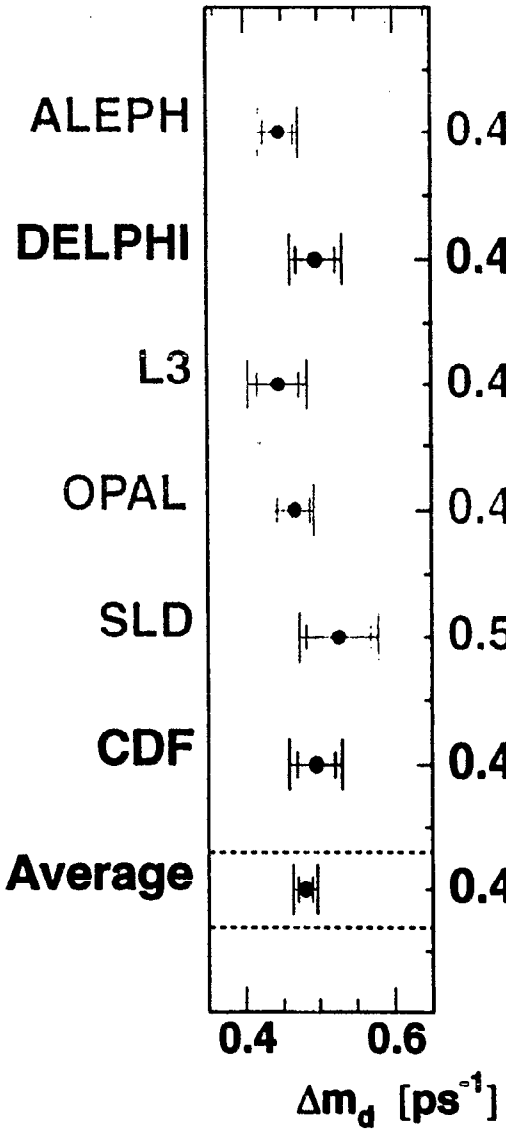

ALEPH	$0.446 \pm 0.020 \pm 0.018$ ps^{-1}
DELPHI	$\mathbf{0.497 \pm 0.027 \pm 0.023}$ **ps^{-1}**
L3	$0.445 \pm 0.028 \pm 0.028$ ps^{-1}
OPAL	$0.466 \pm 0.022 \pm 0.016$ ps^{-1}
SLD	$0.526 \pm 0.043 \pm 0.031$ ps^{-1}
CDF	$\mathbf{0.495 \pm 0.026 \pm 0.025}$ **ps^{-1}**
Average	$\mathbf{0.480 \pm 0.010 \pm 0.013}$ **ps^{-1}**

Δm_d world ave. now very precise.

Need better theory to improve precision in $|V_{td}|$.

Or, measure Δm_s.

m_{top}:
Another CDF contribution to *B* physics

$$|V_{td}| = (8.6 \pm 0.2 \pm 0.2 \pm 1.7) \times 10^{-3}$$

Δm_d theory $B_B \sqrt{f_B}$

• 信号のB粒子の近傍の粒子との相関を利用する方法

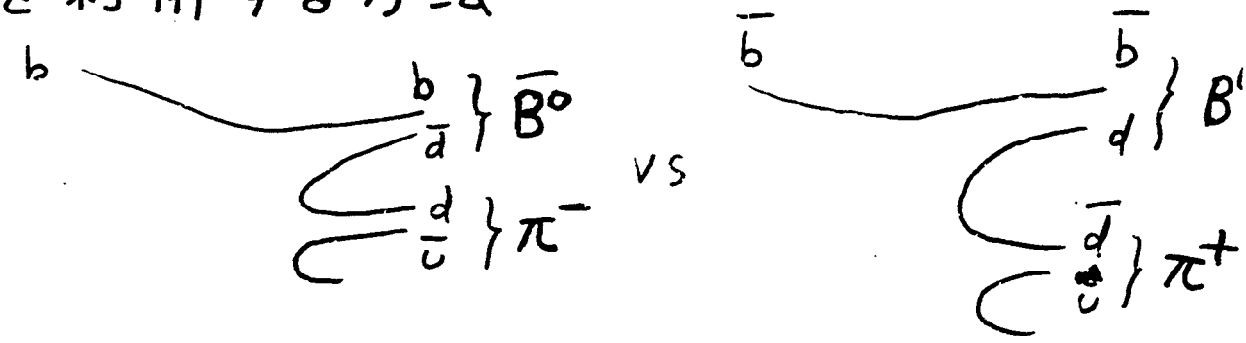

"SAME-SIDE TAGGING" SST

まとめ

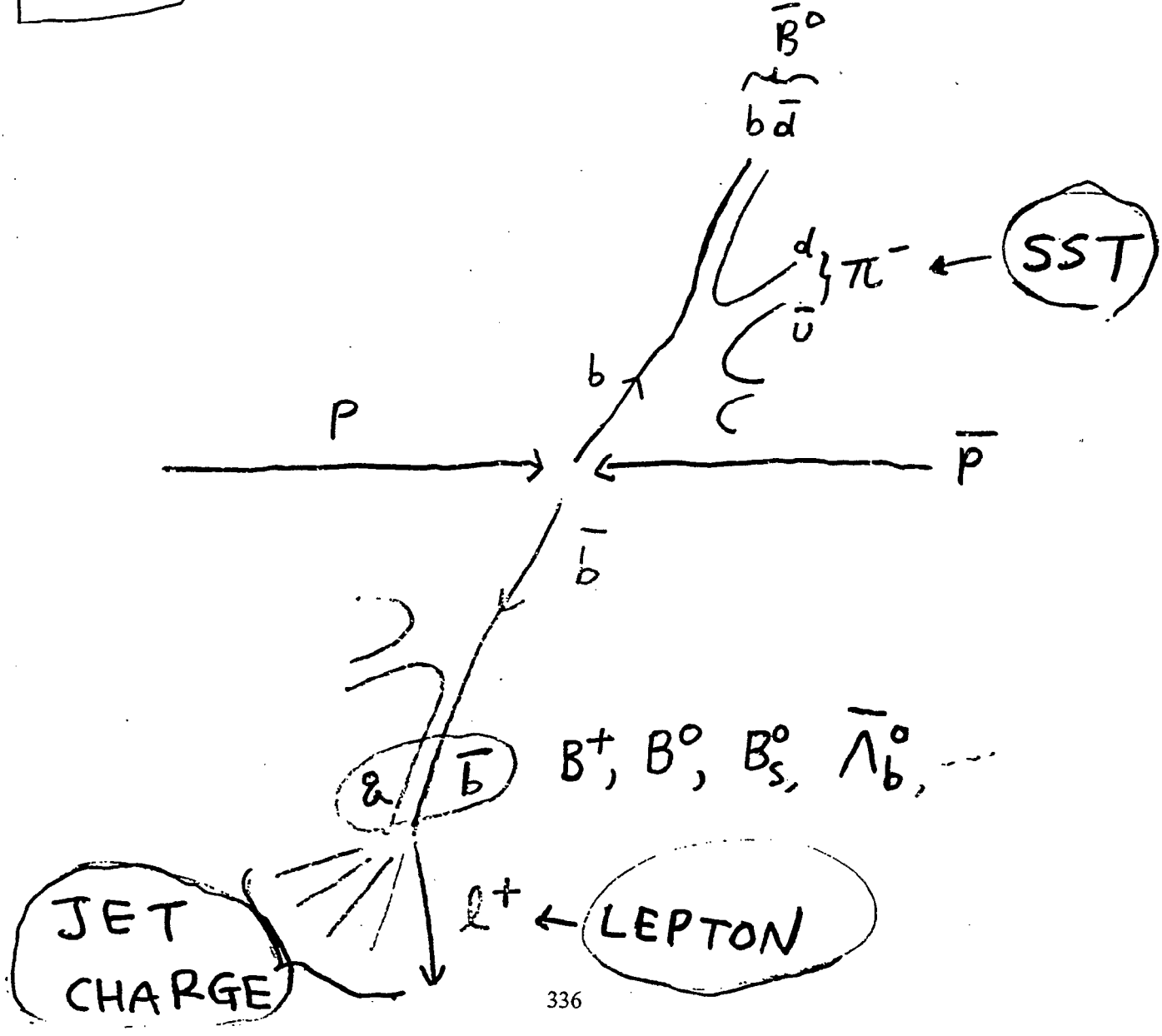

CP対称性の破れと小林・益川行列

CP対称性の破れ

⇔ 物理法則が粒子の反粒子の間で同等ではない.

小林・益川理論:

クオークが三世代(以上)あると

小林・益川行列は複素位相を持つ.

∴ 弱い相互作用のラグランジアンがCP変換のもとで不変でない

⇒ CP対称性の破れの起源となりうる.

小林・益川行列の近似形

(Wolfensteinによる)

$$V_{CKM} = \begin{array}{c} \\ u \\ c \\ t \end{array} \begin{array}{c} \begin{array}{ccc} d & s & b \end{array} \\ \begin{pmatrix} 1-\lambda^2 & \lambda & A\lambda^3(\rho-i\eta) \\ -\lambda & 1-\lambda^2 & A\lambda^2 \\ A\lambda^3(1-\rho-i\eta) & -A\lambda^2 & 1 \end{pmatrix} \end{array}$$

$\lambda = 0.22$

λ ρ η : $\mathcal{O}(1)$ の数

V_{CKM}：ユニタリ行列である.

$$VV^\dagger = V^\dagger V = \mathbb{1} = \begin{pmatrix} 1 & 0 & 0 \\ 0 & 1 & 0 \\ 0 & 0 & 1 \end{pmatrix}$$

$$V^\dagger = d\begin{pmatrix} V_{ud}^* & V_{cd}^* & V_{td}^* \\ V_{us}^* & V_{cs}^* & V_{ts}^* \\ V_{ub}^* & V_{cb}^* & V_{tb}^* \end{pmatrix} \qquad V = \begin{array}{c} \\ \begin{pmatrix} V_{ud} & V_{us} & V_{ub} \\ V_{cd} & V_{cs} & V_{cb} \\ V_{td} & V_{ts} & V_{tb} \end{pmatrix} \end{array} \quad b$$

(d行 b列)*

$$V_{ud}V_{ub}^* + V_{cd}V_{cb}^* + V_{td}V_{tb}^* = 0$$

おのおのは複素数：$z_1 + z_2 + z_3 = 0$

$\Leftrightarrow$ 複素平面上で三角形を作る

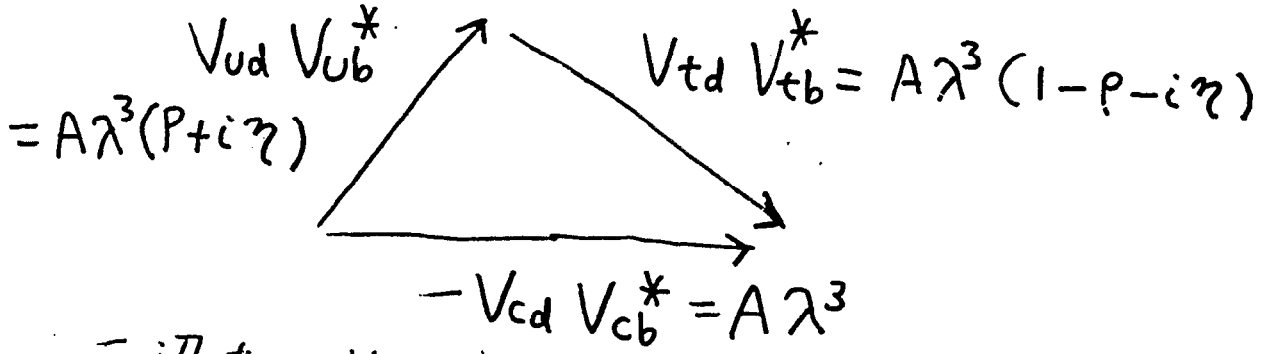

三辺を $-V_{cd}V_{cb}^* = A\lambda^3$ で割る.

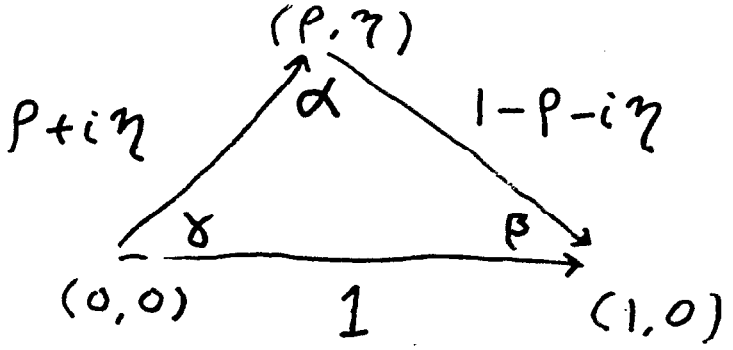

- 辺の長さ　クオーク間の遷移の強さ：$|V_{td}|, |V_{ub}|$
- 角度　CPの破れの大きさ

例② B^0 と $\bar{B}^0$ に共通の終状態 f ($f=\bar{f}$)
への崩壊：$\underbrace{B^0 \to \bar{B}^0}_{\text{粒子反粒子振動}} \to f$ が可能

$$\begin{tikzcd} B^0 \arrow[rr] \arrow[dr] & & f \\ & \bar{B}^0 \arrow[ur] & \end{tikzcd}$$

2つの経路の干渉（振幅）

$$A(t) \equiv \frac{\Gamma(B^0(t) \to f) - \Gamma(\bar{B}^0(t) \to f)}{\text{〃} \quad + \quad \text{〃}}$$

Carter, 三田 など $\to$ $= \pm \sin 2(\phi_M + \phi_f) \sin(\Delta m t)$

$\pm$：終状態 f の CP 固有値

$\sin 2(\phi_M + \phi_f)$：振幅

$\sin(\Delta m t)$：時間依存性

ϕ_M：$B^0\bar{B}^0$ 振動の位相 ($=\beta$)

ϕ_f：$B^0 \to f$ 崩壊の位相

例②-1 $\boxed{B^0/\bar{B}^0 \to J/\psi\, K^0_S}$

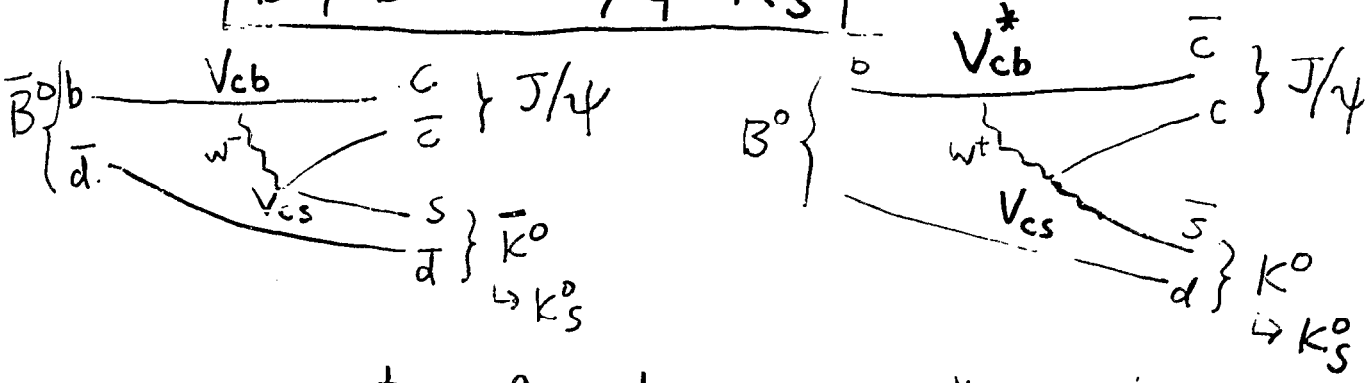

$CP|J/\psi K^0_S\rangle = -1$, $\phi_M = \beta$, $\phi_f = \mathrm{Arg}(V^*_{cb} V_{cs}) = 0$

$$\therefore A(t) = -\sin(2\beta)\sin(\Delta m t)$$

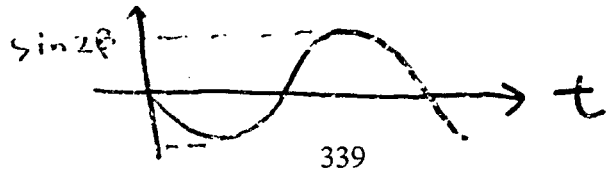

CP Violation in $B^0/\bar{B}^0 \to J/\psi\, K^0_S$

$$\boxed{CP \text{ viol.} \Leftrightarrow \Gamma(i \to f) \neq \Gamma(\bar{i} \to \bar{f})}$$

$$A(t) \equiv \frac{\Gamma(B^0 \to J/\psi K^0_S) - \Gamma(\bar{B}^0 \to J/\psi K^0_S)}{\Gamma(B^0 \to J/\psi K^0_S) + \Gamma(\bar{B}^0 \to J/\psi K^0_S)}$$

$$= -\sin(2\beta)\sin(\Delta m t)$$

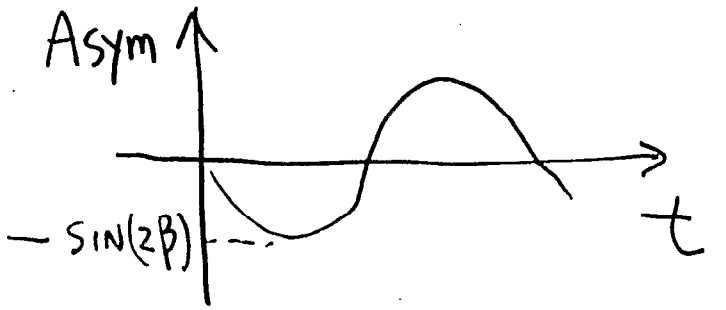

- Now the amplitude is the quantity of interest.
- Final state = $J/\psi\, K^0_S \to \mu^+\mu^-\pi^+\pi^-$ "Trivial"
- Initial state, B^0 or $\bar{B}^0$? Flavor Tagging LEPTON, JET Q, SAME-SIDE $\pi^\pm$
- Decay time: Not necessary at CDF, but helps.

$B^0/\bar{B}^0 \rightarrow J/\psi\, K^0_S$ ~ 400 signal ev. / 110 pb^{-1}

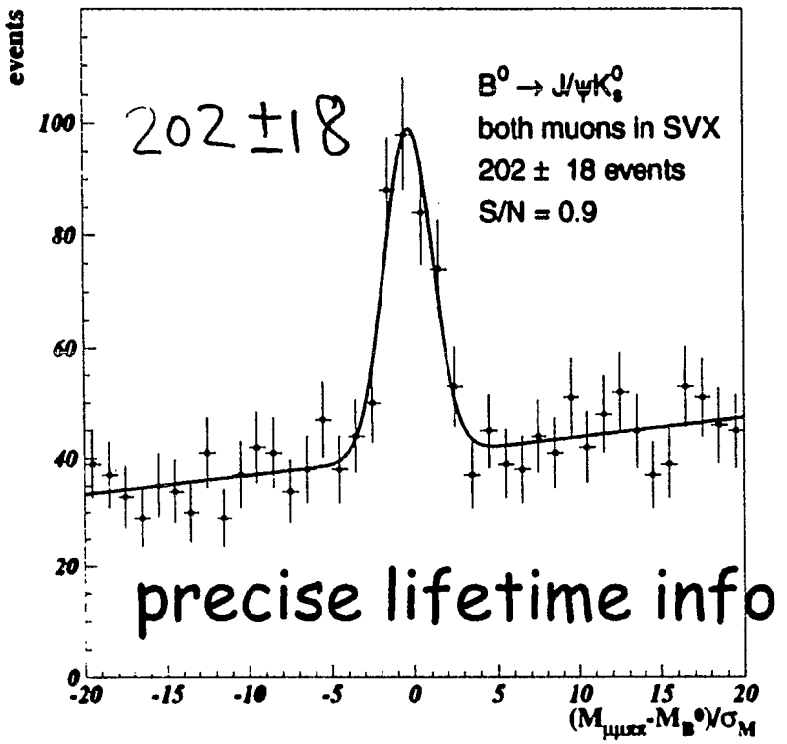

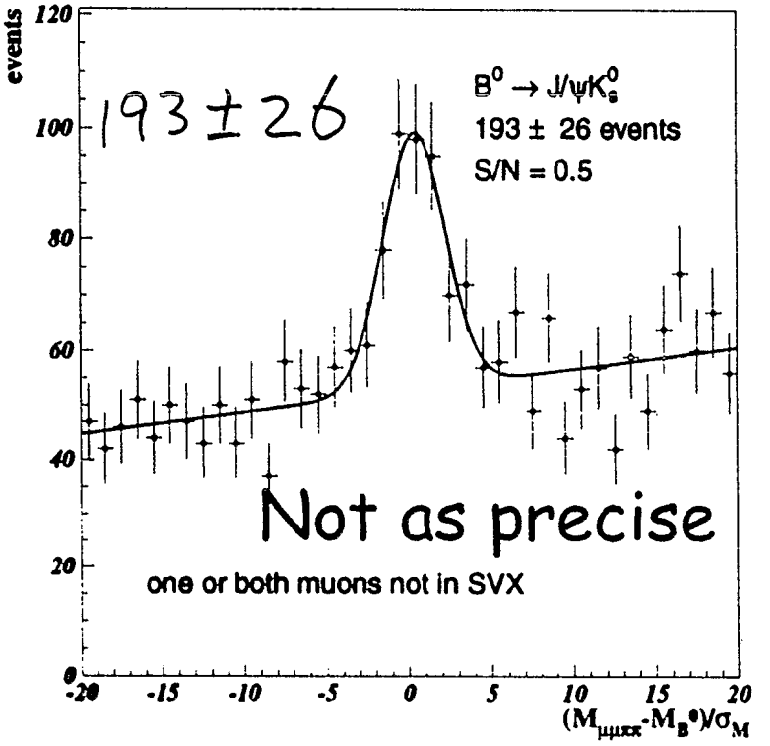

$$[\ \mathrm{Mass}(J/\psi\, K^0_S) - M(B^0)\ ]\ /\ \sigma_M$$

Apply 3 flavor tags, count B^0 vs $\bar{B}^0$.
Extract raw asymmetry = $D \sin(2\beta)$
Divide it by tag dilution $\rightarrow \sin(2\beta)$

Apply 3 Flavor Tagging Methods

- Same-side "pions"
- Leptons
- Jet charge

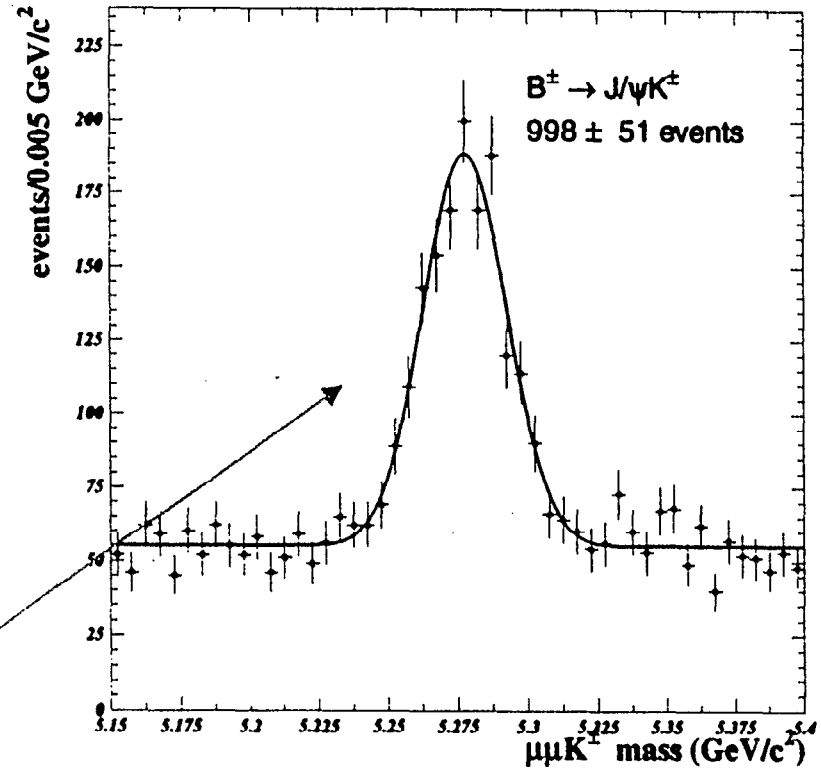

Measure tag dilution from ~ 1000 $B^+ \rightarrow J/\psi\ K^+$ decays.

(For SST, extrapolation of *lepton-D* meas.)

Tag	ε(%)	D(%)	εD²(%)
SST	70	17±3	2.1±0.5
Lepton	6.5	63±15	2.2±1.0
Jet Q	45	22±7	2.2±1.3
Total			6.3±1.7

Asymmetry

Precise lifetime sample:
Asymmetry vs. time.

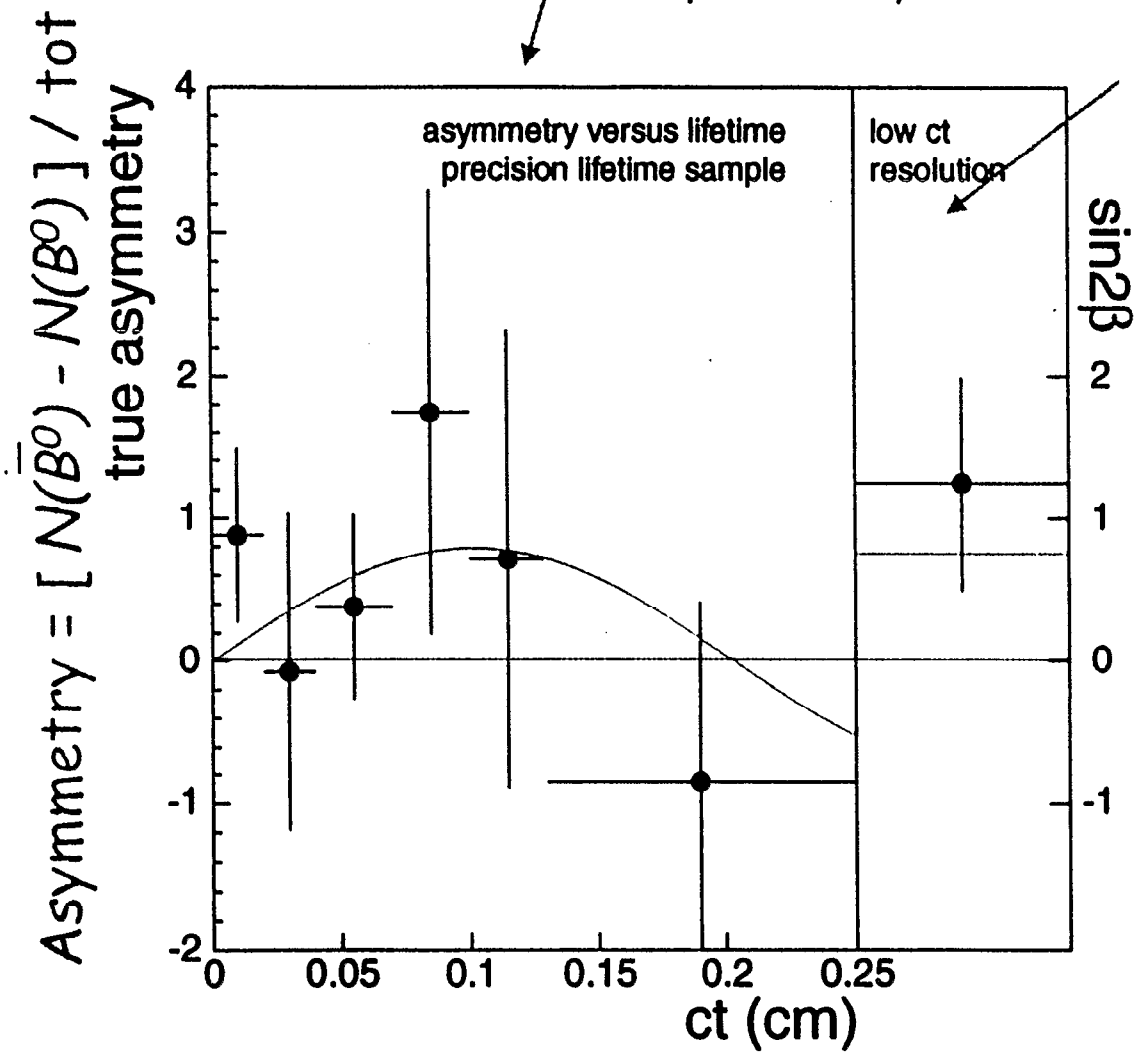

Less precise lifetime sample:
Time-integrated
Asym x $(1+x_d^2) / x_d$
= sin (2β)

$$\sin(2\beta) = +0.79 \; {}^{+0.41}_{-0.44}$$

(stat + syst).

MAIN SYST : DILUTION

PRD 61, 072005 (2000)

Constraints on the unitarity triangle

$\sin(2\beta) \rightarrow \beta$: four solutions, β_1, β_2, $\beta_1+\pi$, $\beta_2+\pi$ ($\beta_2=\pi/2-\beta_1$).

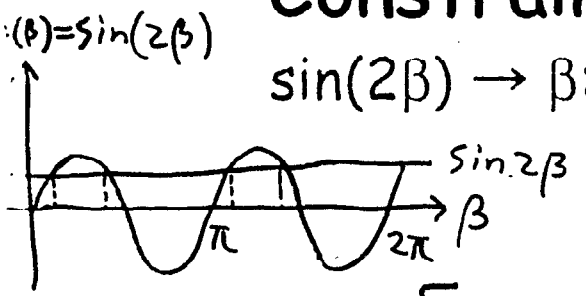

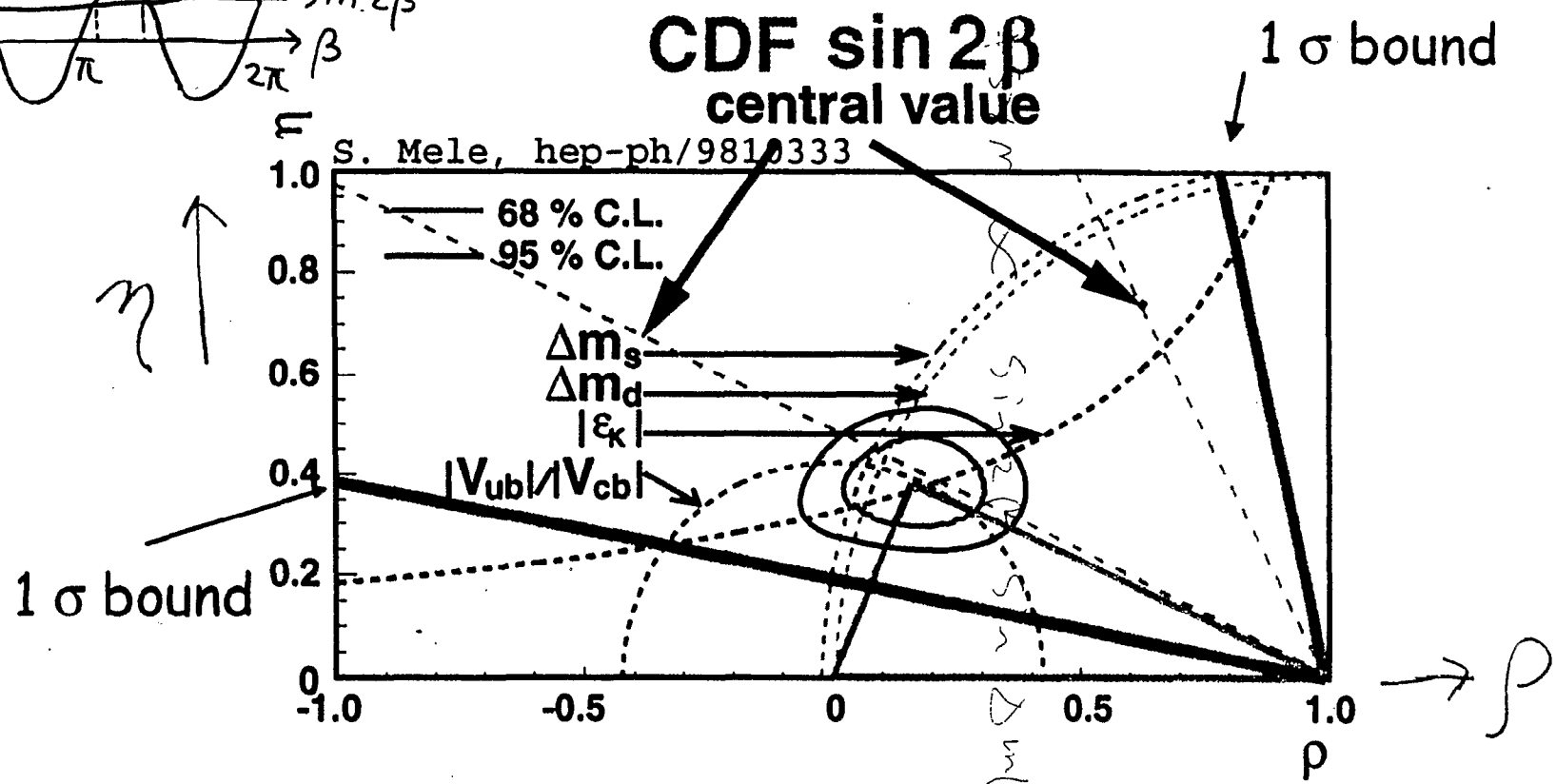

Not much constraint now, but should be interesting in Run-II.

Rare Decays $B \to K^{(*)} l^+ l^-$

- $b \to s$ FCNC transition
- Z^0 penguin and box diagram in addition to EM penguin.
- $|V_{ts}|$
- SM predicts B.R. ~ 10^{-7} to 10^{-6}.
- New physics could enhance it.
- Has yet to be observed.

PRL 83, 3378 (1999)

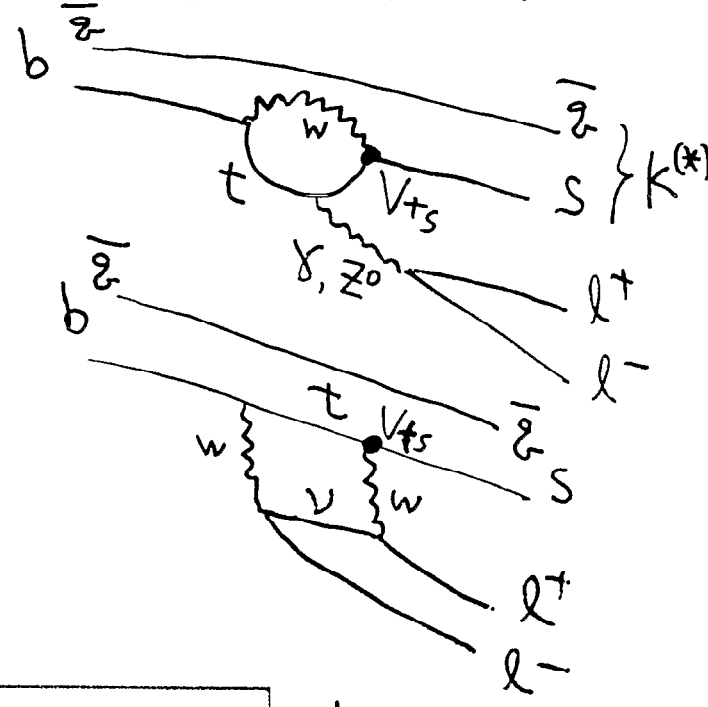

l^+l^- can be resonant, e.g. J/ψ, $\psi(2S)$.
$\to$ Indistinguishable from $b \to c\bar{c}s$
Look at non-resonant mass region.

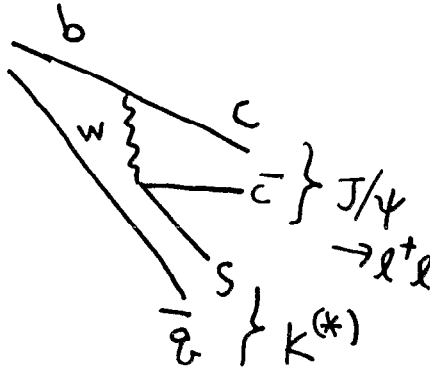

LOOK FOR EXCLUSIVE MODES

$B^+ \longrightarrow K^+ \mu^+ \mu^-$ 110 pb^{-1}

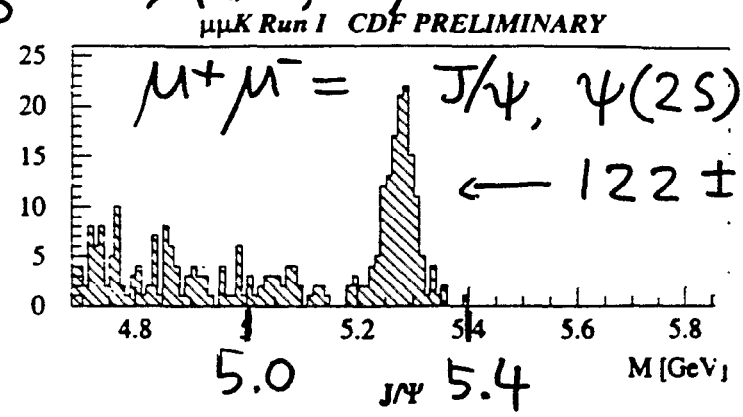

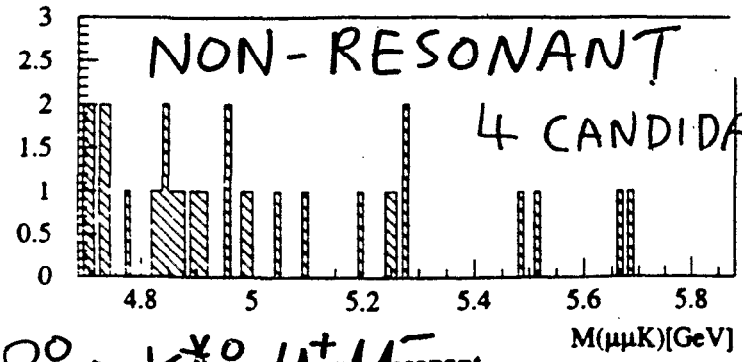

SM: $(5.9 \pm 2.1) \times 10^{-7}$

$BF < 5.2 \times 10^{-6}$ (90% CL)

$B^0 \rightarrow K^{*0} \mu^+ \mu^-$

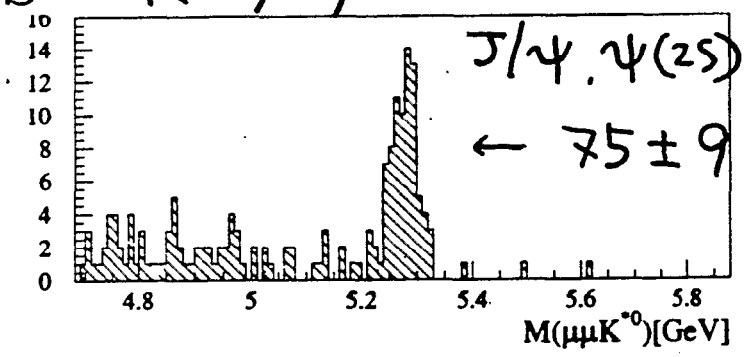

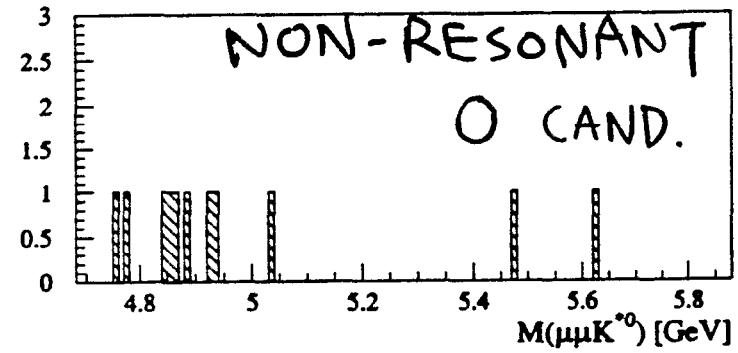

$BF < 4.0 \times 10^{-6}$ (90% CL)

SM: $(2.0 \pm 0.7) \times 10^{-6}$

Rare Decays $B \to K^{(*)} l^+ l^-$

- $b \to s$ FCNC transition
- Z^0 penguin and box diagram in addition to EM penguin.
- $|V_{ts}|$
- SM predicts B.R. ~ 10^{-7} to 10^{-6}.
- New physics could enhance it.
- Has yet to be observed.

PRL 83, 3378 (1999)

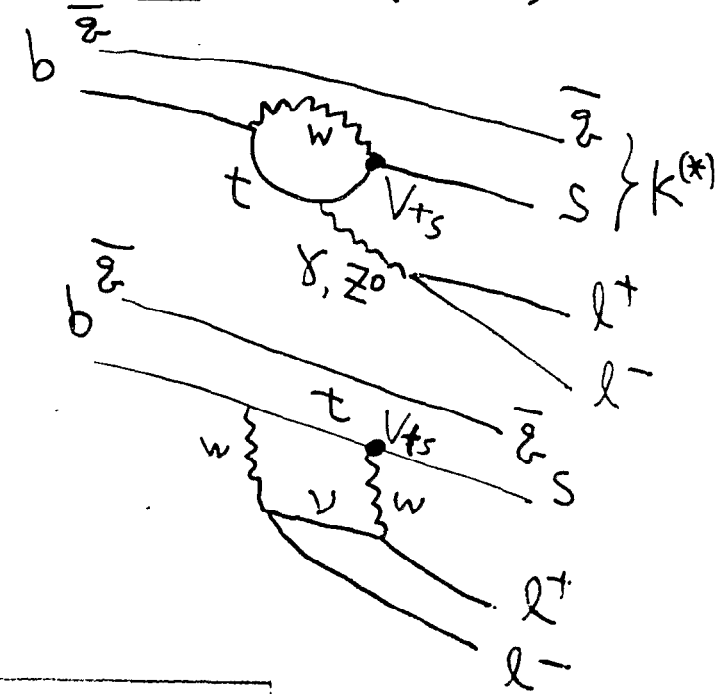

l^+l^- can be resonant, e.g. J/ψ, $\psi(2S)$.
$\to$ Indistinguishable from $b \to c\bar{c}s$
Look at non-resonant mass region.

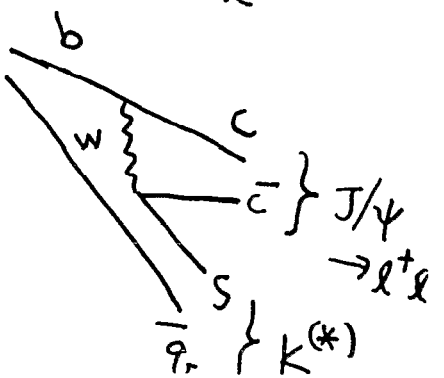

$B^+ \rightarrow K^+ \mu^+ \mu^-$

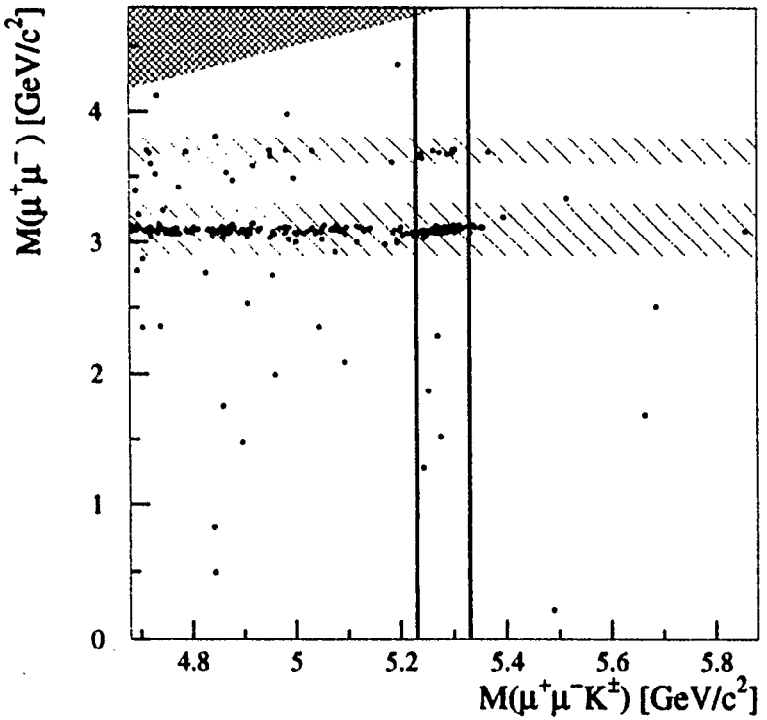

- 4 candidates
- BR < 5.2 X 10^{-6} @90% CL
- SM: (5.9 ± 2.1) X 10^{-7}

$B^0 \rightarrow K^{*0} \mu^+ \mu^-$

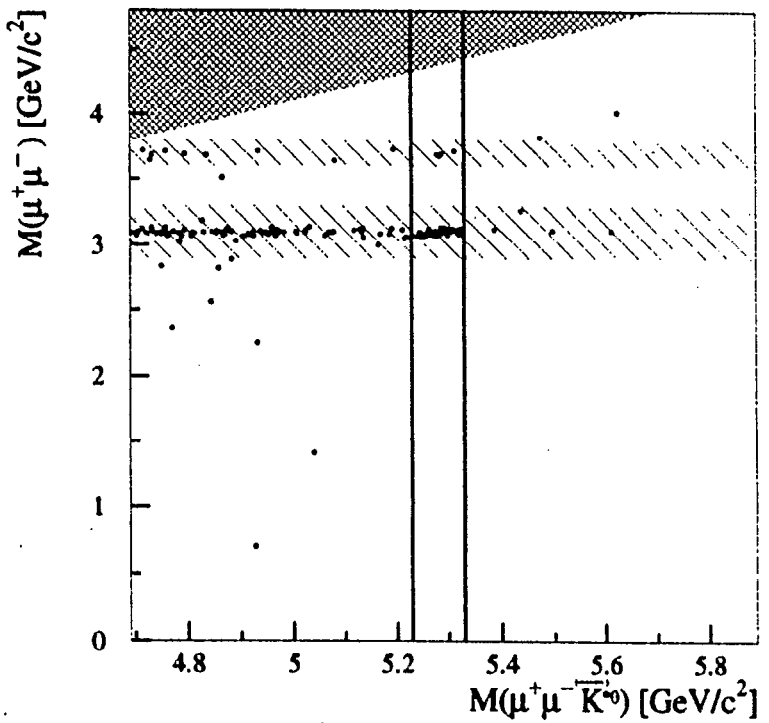

- 0 candidate
- BR < 4.0 X 10^{-6} @90% CL
- SM: (2.0 ± 0.7) X 10^{-6}

Expected signal ~ 0.5 event each.
Should see a handful of signal events in Run II.

Even Rarer Decays: $B^0, B^0_s \to l^+l^-$

- V_{td} for B^0, V_{ts} for B^0_s
- Helicity suppressed.
- B.R. very small.

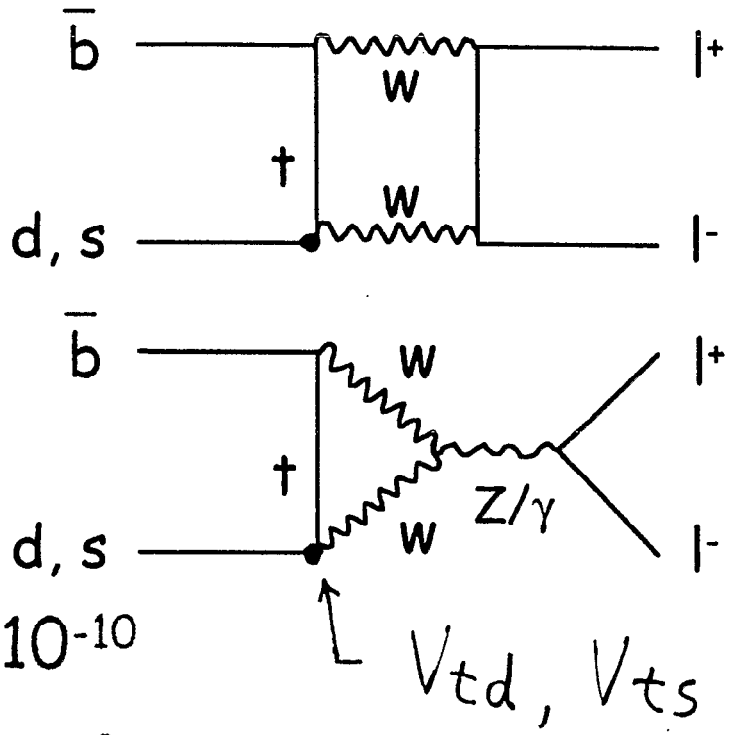

SM predictions:

- $B^0 \to \mu^+\mu^-$ $(1.5 \pm 1.4) \times 10^{-10}$
- $B^0_s \to \mu^+\mu^-$ $(3.5 \pm 1.0) \times 10^{-9}$
- $B^0 \to e^+e^-$ $(3.4 \pm 3.1) \times 10^{-15}$
- $B^0_s \to e^+e^-$ $(8.0 \pm 3.5) \times 10^{-14}$

Rare Decays $B^0, B^0_s \rightarrow \mu^+\mu^-$ PRD 57, 3811 (1998)

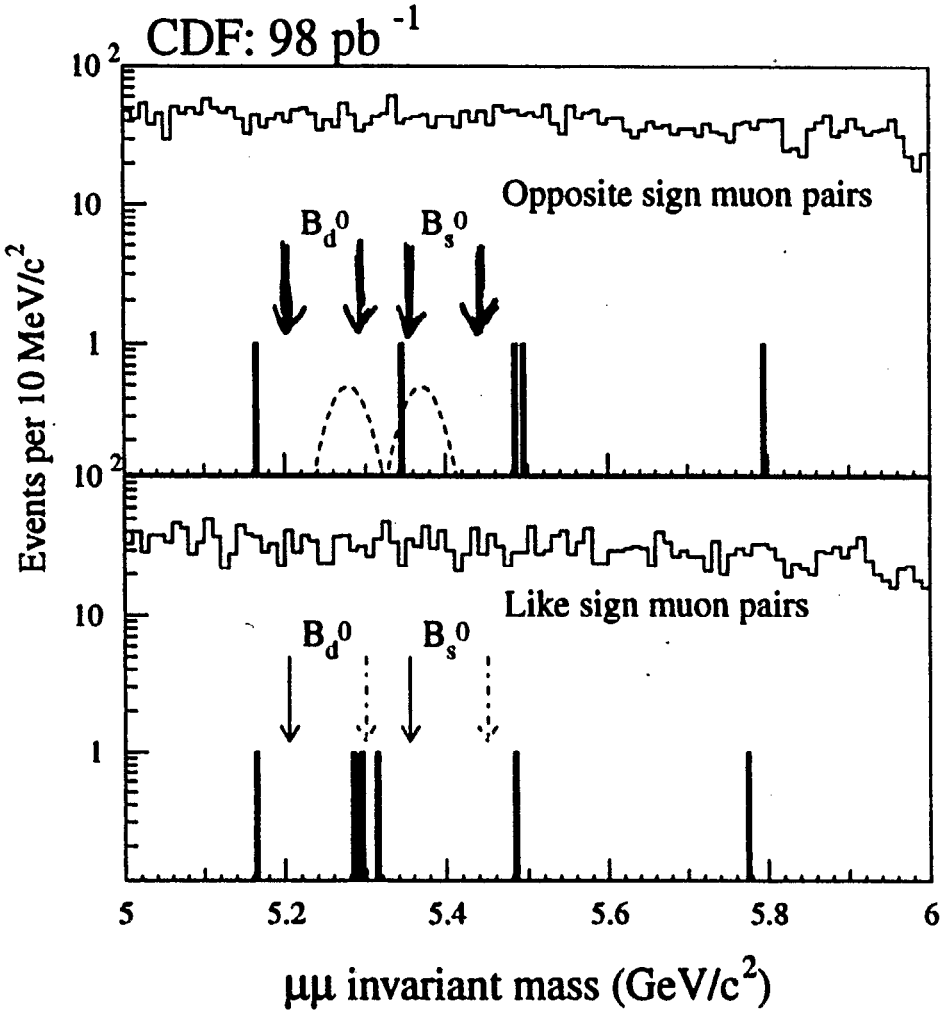

One candidate in the overlap region of B^0 and B^0_s mass windows.

B.R. < 8.6×10^{-7} for B^0

B.R. < 2.6×10^{-6} for B^0_s

@ 95% C.L.

Also looked for decays to $e^+\mu^-$, $e^-\mu^+$

B.R. < 4.5×10^{-6} for B^0

B.R. < 8.2×10^{-6} for B^0_s

Still long way to go...

PRL 81, 5742 (1998)

B Physics and CDF Run II

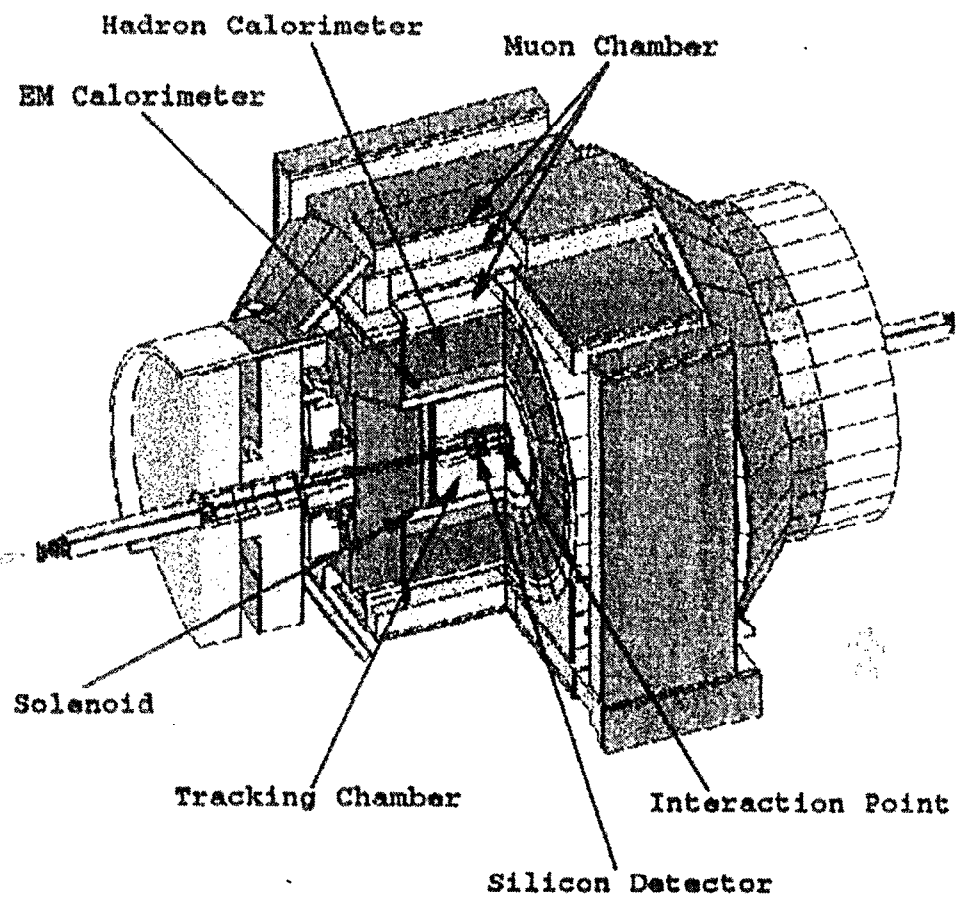

Accelerator

- $\sqrt{s}$ = 2000 GeV
- 6 bunches → 36, 108.
- New ~~150~~ 120 GeV Main Injector
- Luminosity = 10^{32} $cm^{-2}s^{-1}$
- $\int L\,dt$ = 2 fb^{-1} (2 years)

Detector

- Tracking system
- FE electronics
- Trigger/DAQ
- Plug calorimeter
- Extended muon coverage

Retained good momentum resolution & lepton ID.

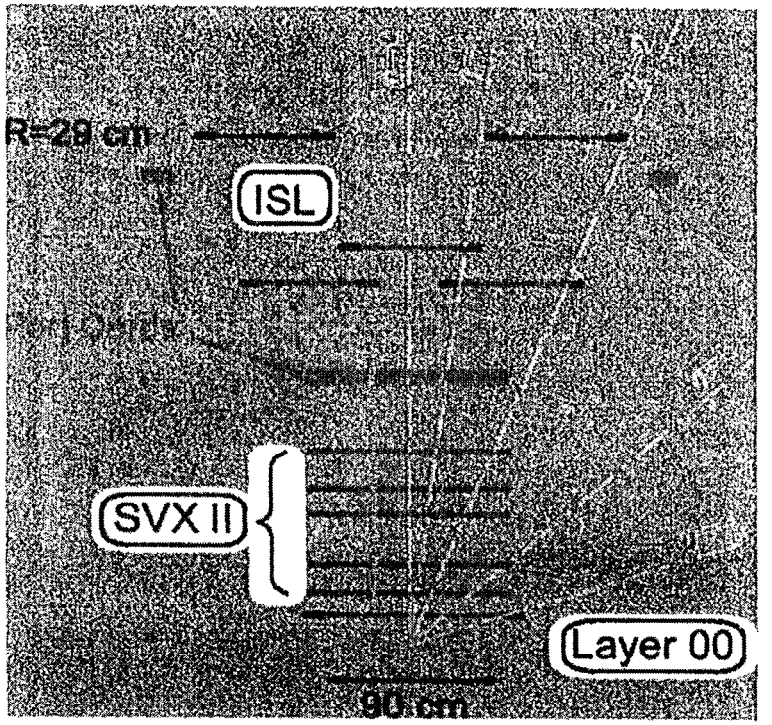

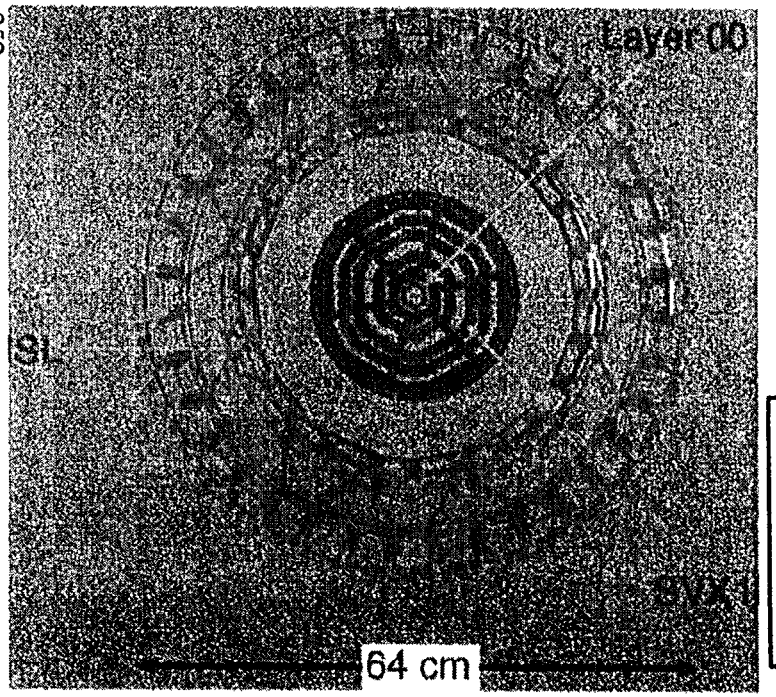

CDF-II silicon detectors

SVX II

- Radii 2.5 cm to 11 cm
- 5 layers
- Double-sided, 90° and 1.2° stereo
- Main vertex detector

Intermediate silicon layers (ISL)

- 3 more layers at R = 20 - 29 cm
- Construction similar to SVX II
- Precision tracking to higher eta.
- Aid linking from COT to SVX.

Significant Japanese contributions :

SVX II	Hiroshima, Okayama
ISL	Osaka City, Tsukuba

Silicon Vertex Trigger : SVT

Use silicon information at the 2nd level trigger

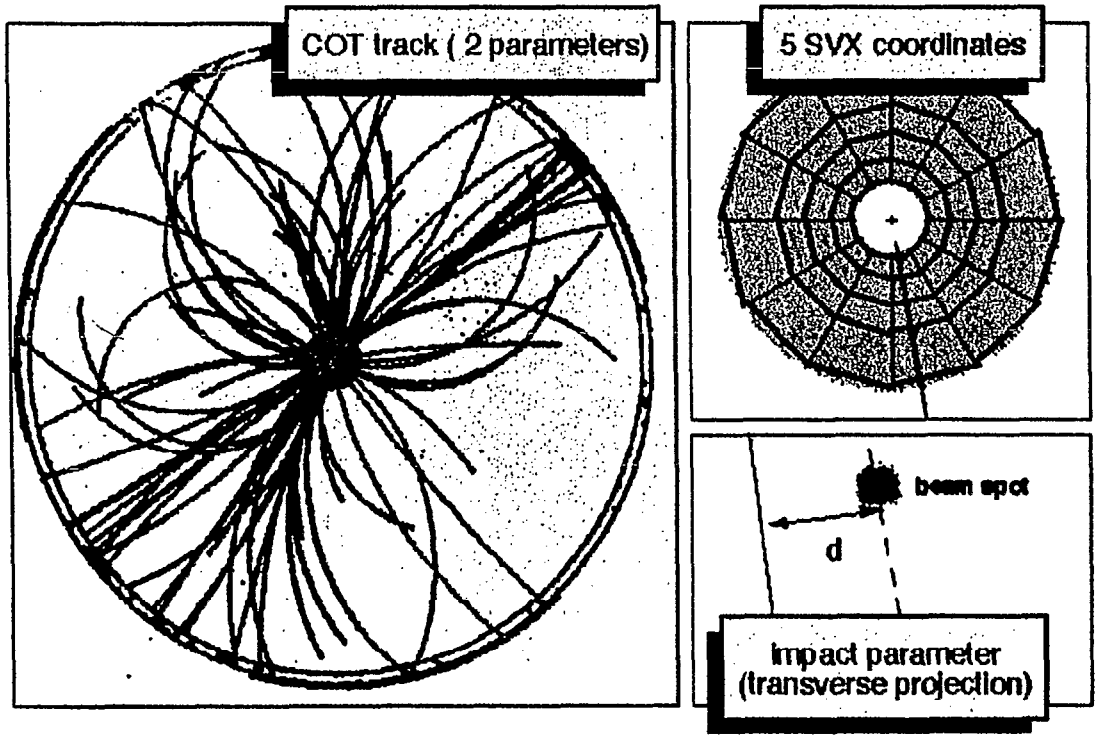

- Find a track in the main tracker COT.
- Extrapolate toward the SVX.
- Find SVX hits along the road.
- Calculate impact parameter wrt the primary vertex (beam spot).
- Resolution ~ 40 μm at 1 GeV/c.

Can trigger on all-hadronic final states such as

$B^0 \rightarrow \pi^+\pi^-, \quad B^0_s \rightarrow D_s^- \pi^+.$

New additions for *B* physics:	Time-of-flight counter Innermost Si layer

CDF-II TOF counter

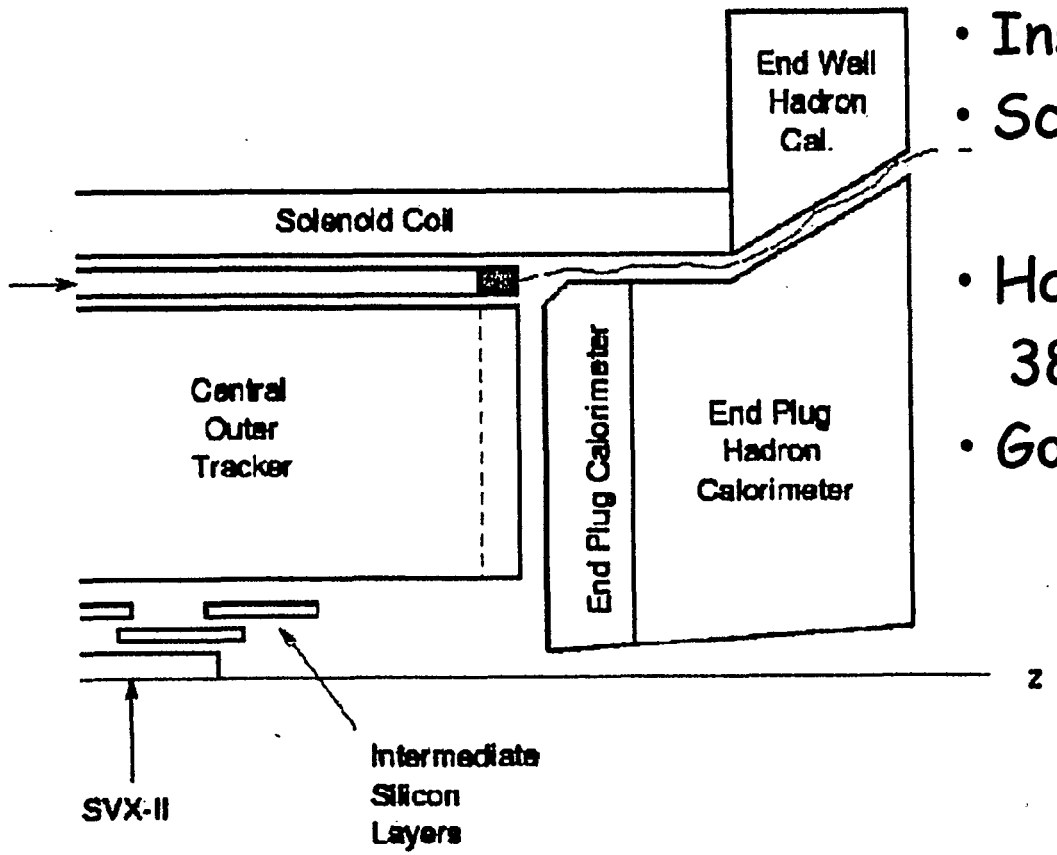

Detector

- Located at r = 1.4 m
- Inside 1.4 Tesla solenoid
- Scintillator Bicron BC408
  $4 \times 4 \times 270\ cm^3$ 216本
- Hamamatsu R7761 PMTs
  38 mm, 19-stage fine mesh
- Goal: $\sigma_T \sim 100$ ps

Purpose

- 2σ K/π separation
  up to 1.6 GeV/c
- *B* flavor tagging

Layer 00

Detector

- Single-sided
- At radius ~ 1.6 cm, minimize effect of multiple scattering.
- Can operate up to ~ 5 fb^{-1}

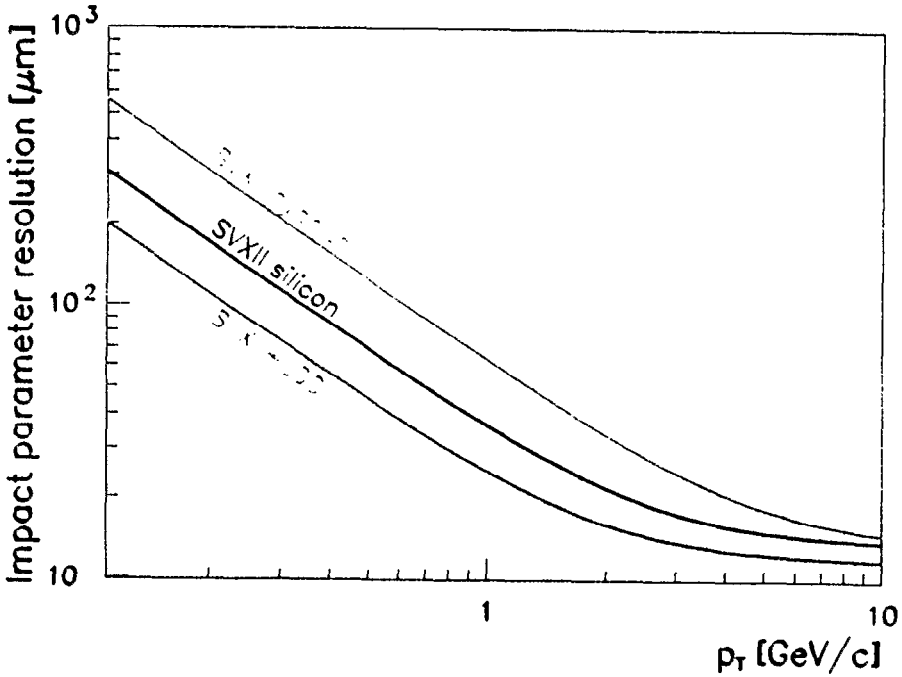

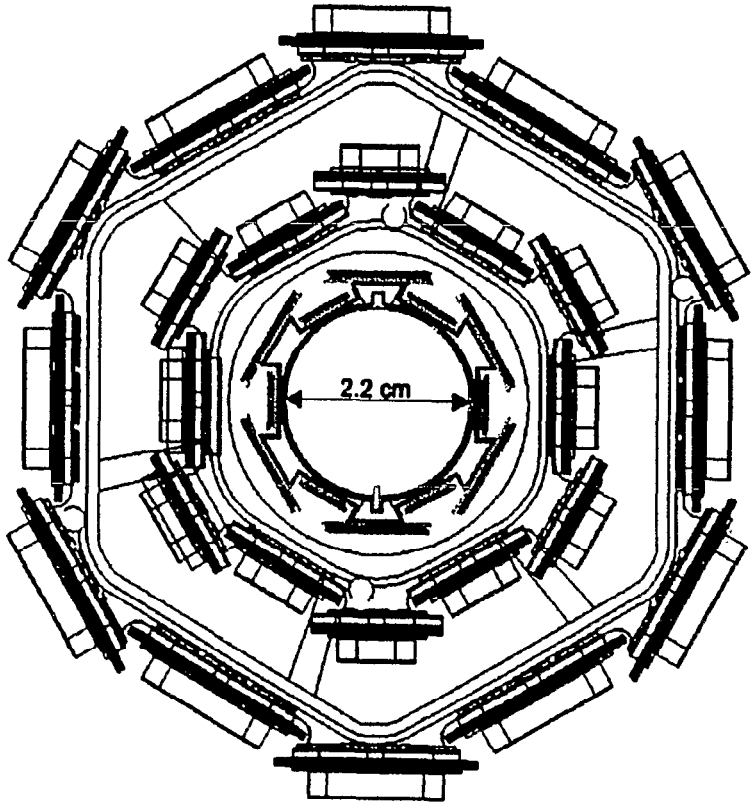

Purpose

Improve impact parameter resolution :

$\sigma \sim$ 9 μm for high p_T

$\oplus$ 10 μm alignment

Impact of TOF and Layer 00 on B^0_s mixing

Signal

- $B^0_s \rightarrow D^-_s \pi^+, D^-_s \pi^+ \pi^+ \pi^-$
- ~20 k events / 2 fb^{-1}

TOF

- Improves flavor tags.
- Helps at lower x_s.

Layer 00

- Improves vertex determination.
  → proper time resolution.
- Helps at higher x_s.

Once the oscillations are established, Δm_s will be determined to a few %.

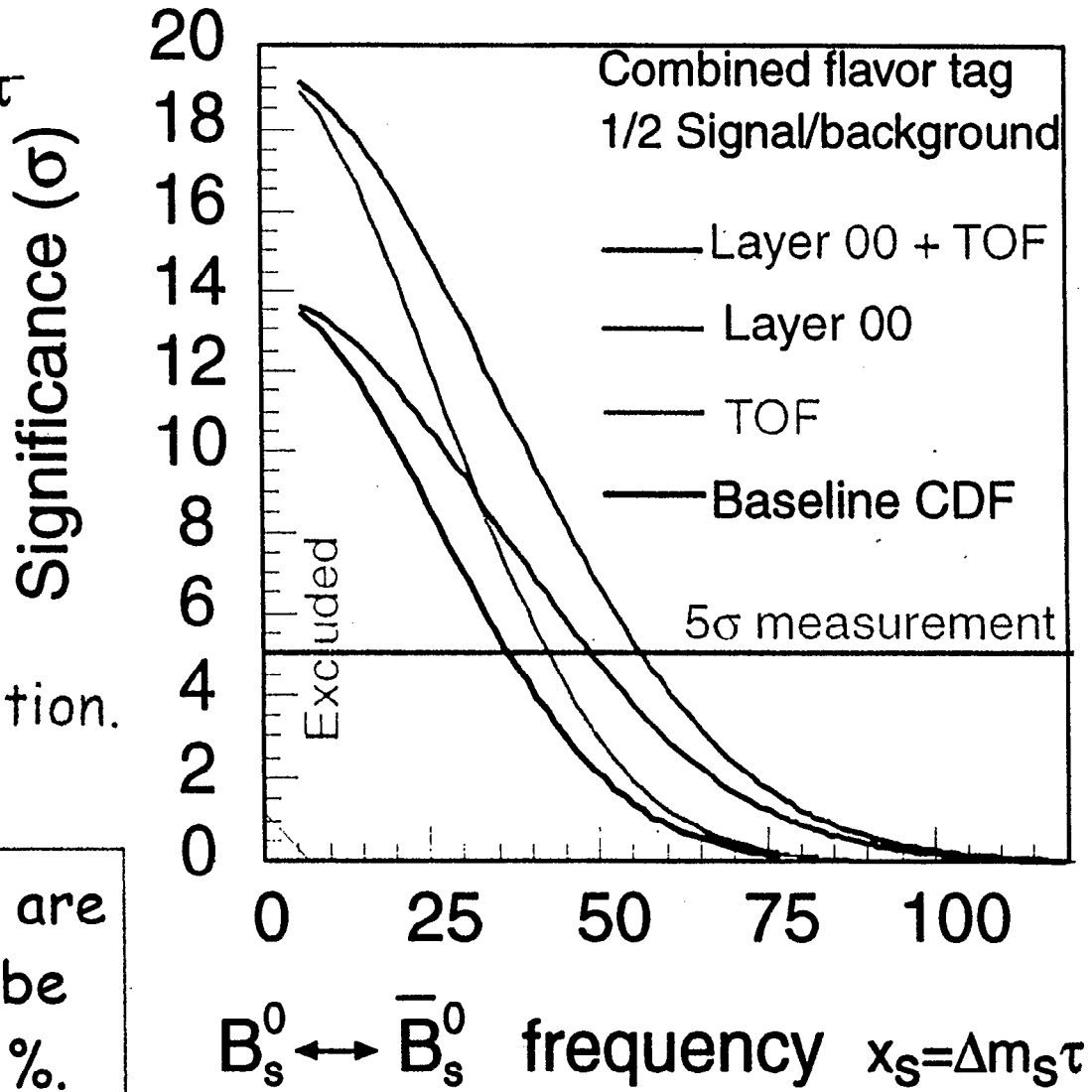

B Physics in CDF Run II Two Major Goals:

I. Precision $\sin(2\beta)$ from $B^0/\bar{B}^0 \rightarrow J/\psi\, K^0_S$

II. $B^0_s - \bar{B}^0_s$ Oscillation $\rightarrow \Delta m_s / \Delta m_d$

$\sin 2\beta = 0.79 \pm 0.084$

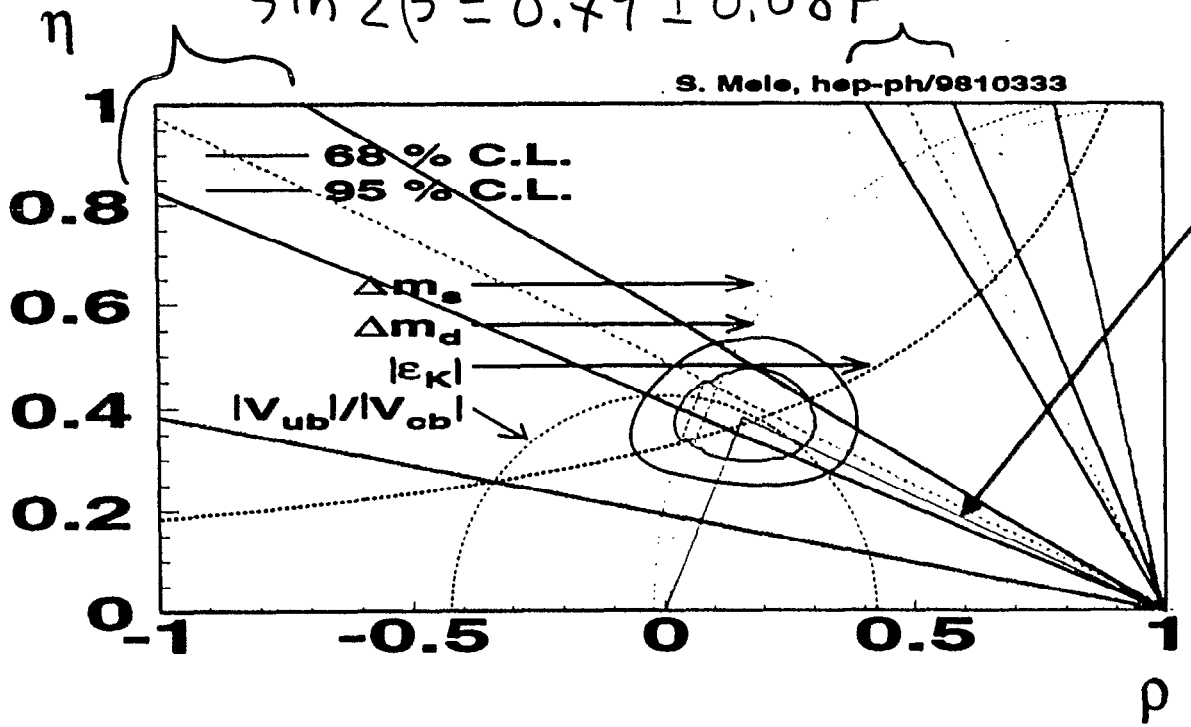

$|V_{td}| / \lambda |V_{ts}|$

Can be the first meaningful test of the unitarity triangle.

Run II projections

sin 2β precision from $J/\psi\ K^0_S$ (2 fb^{-1})

TDR: 10 k signal, εD^2 = 6.7% → ±0.084

New: 28 k signal, εD^2 = 9.1% → ±0.043

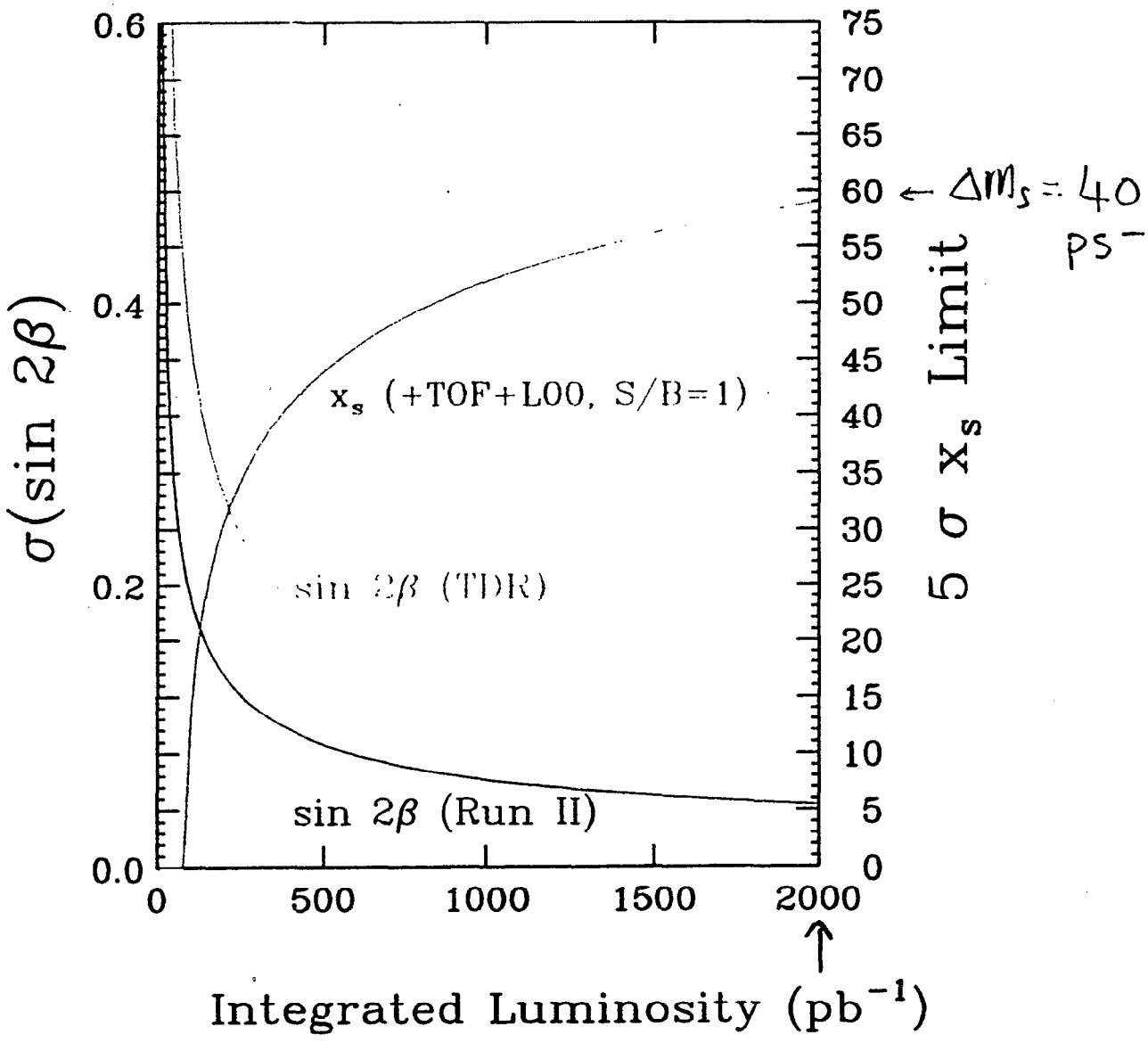

例②-2 $\boxed{B^0/\bar{B}^0 \to \pi^+\pi^-}$

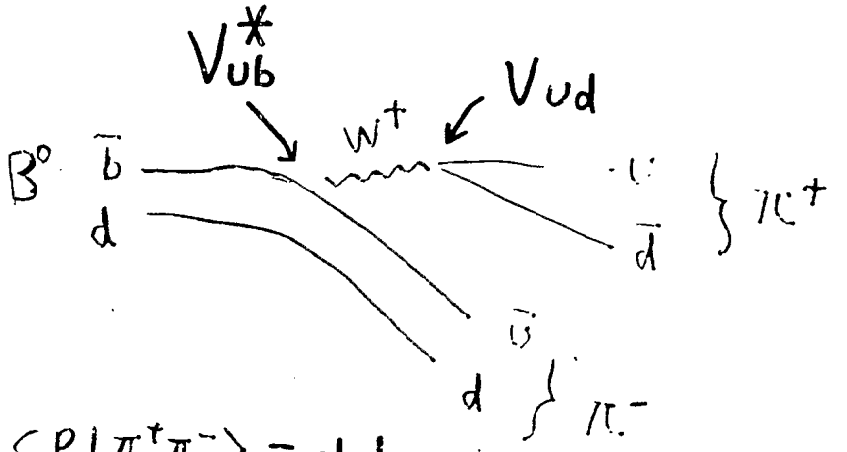

$\langle P|\pi^+\pi^-\rangle = +1$

$\Phi_m = \beta$ （$J/\psi K_S^0$ と同じ）

$\Phi_f = \mathrm{Arg}(V_{ub}^* V_{ud}) = \gamma$

$\therefore A(t) = \sin 2(\beta+\gamma)\cdot\sin(\Delta m t)$

三角形 $\alpha+\beta+\gamma=\pi$ $\therefore \beta+\gamma=\pi-\alpha$

$= \sin 2(\pi-\alpha)\cdot\sin(\Delta m t)$

$= -\sin(2\alpha)\cdot\sin\Delta m t$

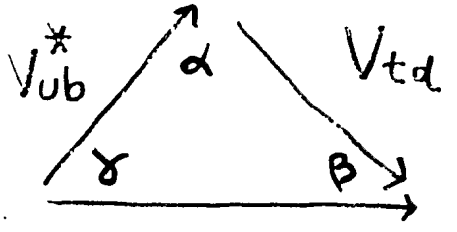

独立に

B粒子の崩壊：辺の長さと角度を両方測定することが可能である。

⇒ 理論を検証：整合性があるか？

例：三角形は閉じているか？

Run II (cont'd) Probing angle γ (phase of V_{ub})

- $B^0 \to \pi^+ \pi^-$ once thought to be the mode for $\sin 2(\pi-\gamma-\beta)$.
  (assuming $b \to u$ tree dominance over penguin)
- CLEO finds much larger $K^- \pi^+$ and tiny $\pi^+ \pi^-$.
- Not just small rates, but also means penguin pollution.
  $\to$ Relation to $\sin(2\alpha)$ less clear.
- Strategies proposed, but are challenging experimentally...

New approach : R. Fleischer, Phys. Lett. B 459, 306 (1999).
Throw in $B^0_s \to K^+K^-$, measure asymmetries in both B^0 and B^0_s.

In general, for a decay $B^0 \to f$ (f = CP eigenstate) :

$$A_{CP}(t) = A^{dir} \cos(\Delta m t) + A^{mix} \sin(\Delta m t).$$

A^{dir} : "direct" CP violation, A^{mix} : CP violation thru mixing.

Experimentally, measure 4 A's from $B^0 \to \pi^+ \pi^-$ and $B^0_s \to K^+K^-$.

Then extract β, γ and penguin and tree decay amplitudes.

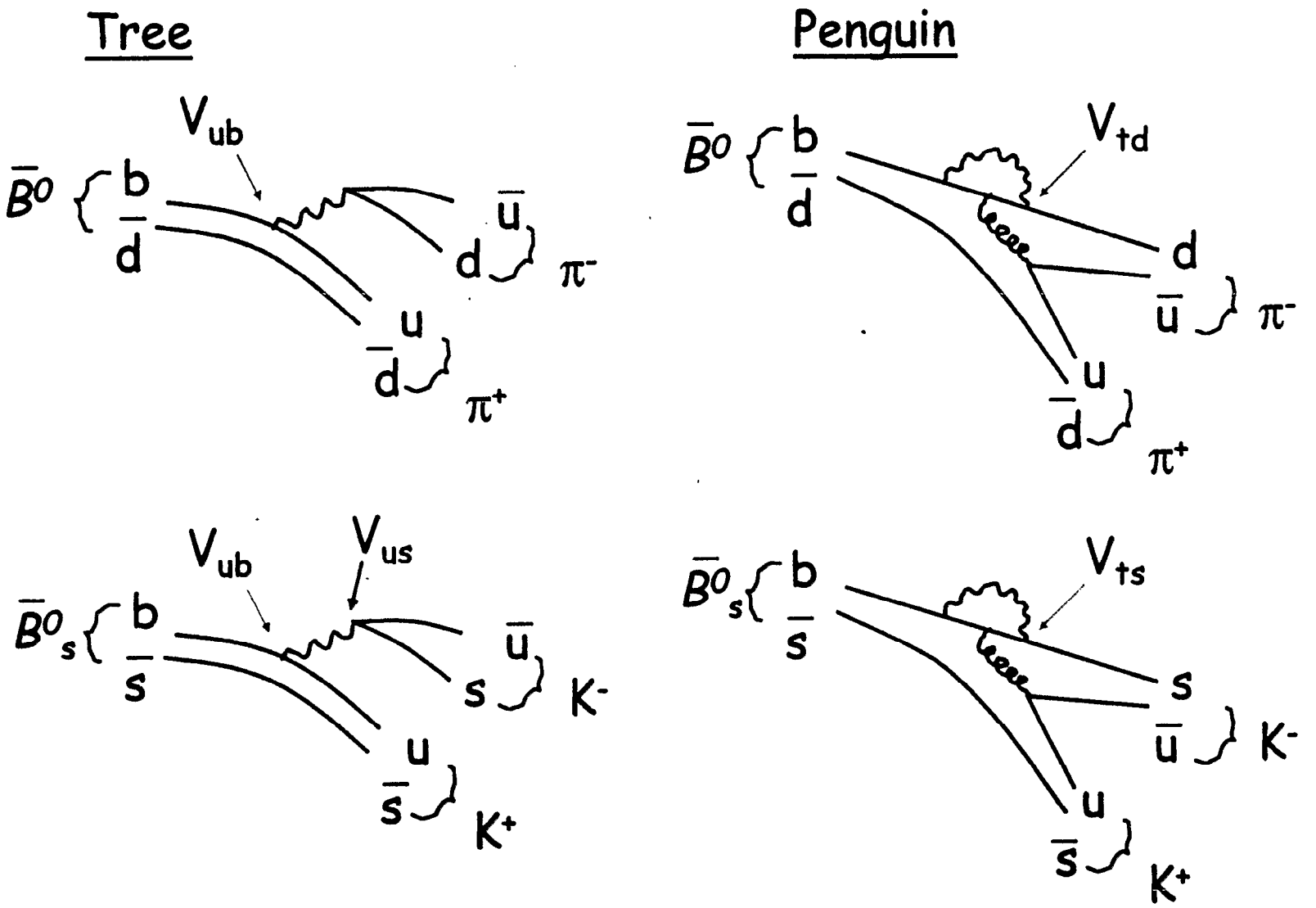
Tree
Penguin
V_{ub}
V_{td}
V_{us}
V_{ts}
$\bar{B}^0$
$\bar{B}^0_s$
b
$\bar{d}$
$\bar{s}$
$\bar{u}$
d
s
u
π^-
π^+
K^-
K^+

Angle γ (phase of V_{ub}) continued

Four CP asymmetries to measure. ($\lambda = \sin\theta_c$)

- $A^{dir}(B^0 \to \pi^+\pi^-) = -2d \sin\theta \sin\gamma / (1 - 2d\cos\theta\cos\gamma + d^2)$
- $A^{mix}(B^0 \to \pi^+\pi^-) = [\sin 2(\beta+\gamma) - 2d\cos\theta \sin(2\beta+\gamma) + d^2 \sin 2\beta] / [1 - 2d\cos\theta\cos\gamma + d^2]$
- $A^{dir}(B^0_s \to K^+K^-) \sim 2(\lambda^2/d)\sin\theta\sin\gamma$
- $A^{mix}(B^0_s \to K^+K^-) \sim 2(\lambda^2/d)\cos\theta\sin\gamma$

If no penguin,
$A^{dir} = 0$ (B^0, B^0_s)
$A^{mix} = \sin 2(\beta+\gamma)$ (B^0)
$A^{mix} = \sin(2\gamma)$ (B^0_s)

Four unknowns to extract :

- β, γ = angles of the unitarity triangle.
- d = ratio of penguin (P) to tree (T) decay amplitudes,
  θ = phase of "P/T"
  $d\, e^{i\theta} \equiv \lambda |V_{cb}/V_{ub}| / (1-\lambda^2/2)\, [P/(T+P)]$

Expect ~5 k $B^0 \to \pi^+\pi^-$, ~10 k $B^0_s \to K^+K^-$
$\to$ angle γ to ~10°.

Summary

- CDF does *B* physics pretty well.
- Run-I results cover virtually all aspects of *B* physics.
- Run II should produce further interesting results, in particular
  - $\sin(2\beta)$ precision of $\pm(0.043$ to $0.084)$.
  - Δm_s up to ~ 40 ps^{-1}.
  - angle γ to ± 10 degrees.

Heavy Quarkonium and QCD[1]

Hirotsugu Fujii
University of Tokyo at Komaba, Tokyo 153-8902

Heavy quarkonium (Φ) is a QCD bound state of a heavy quark (Q) and its antiquark ($\bar{Q}$). The asymptotic freedom may justify the use of the perturbative approach to the properties of the quarkonium. In fact the scales relevant to Φ form a hierarchy:

$$m_Q \gg m_Q v \sim P_{Q\bar{Q}} \gg m_Q v^2 \sim \epsilon_{\rm BE} \gg \Lambda_{\rm QCD},$$

where $v \sim \alpha_s(\epsilon_{\rm BE})$ is the relative velocity of quarks in Φ, $P_{Q\bar{Q}}$ the relative momentum, $\epsilon_{\rm BE}$ the binding energy.

First we discussed the hadroproduction[2] and the interaction of Φ, assuming the factorization into the hard and soft parts. For the hadroproduction the color singlet model (CSM) failed to predict the total cross section and p_T dependence. In the color octet model (COM) the $Q\bar{Q}$ pair is produced in the color octet state, and then evolves into the singlet resonance in the time scale of $\epsilon_{\rm BE}^{-1}$ by emitting/absorbing soft gluon(s). This latter, soft part is described by the unknown matrix elements in the NRQCD framework which we can tune to reproduce the experimental data.

The COM predicts the transverse polarization for the produced Φ at high p_T, while the Tevatron data showed opposite tendency. The k_T factorization calculation for the hard part was applied very recently to the χ_c production and then to the J/ψ production with the result that the COM contributions are substantially reduced from those in the collinear approximation.

Next we discussed the quarkonium interaction with light hadrons ($h's$). The small size of Φ allows us to expand the soft gluon fields into a series of the multipoles. We showed that the quarkonium interaction with h is weak because of 1) the smallness of quarkonium (color transparency) and 2) the softness of the gluons in h.

In the second part, I talked about the J/ψ suppression observed at CERN-SPS, and discussed its interpretation along with the line of the COM. The suppression data up to S-U, fitted with $\sigma_{abs} \sim 7$ mb (baseline), are understood as a suppression of the pre-resonance state in the COM. Then the Pb-Pb data are found further below the baseline, which is called 'anomalous' suppression. The data shows step-like behavior; There is a claim of the χ_c-melting followed by the ψ melting because 30% of the observed J/ψ comes from χ_c decay, though E_T fluctuation may give another likely explanation.

There are many uncertainties we have to clear before make any final conclusion about the QGP formation. Since RHIC is capable of doing a systematic study by changing the parameters, $\sqrt{s}$ and A, we can learn much more details about the heavy ion events and unveil the physics of QGP. We note at the same time the progress is strongly required in the related area such as in the quarkonium hadroproduction; The united efforts in neighboring fields are needed to uncover the new physics hiding in ultra-relativistic heavy ion collisions. It is one of the interesting features in this fields of the heavy ion physics.

[1]Suggested by Prof. D. Kharzeev, who unfortunately couldn't come and give his lecture at the school.
[2]The diffractive production gives us a place to study a different aspect of QCD.

Heavy Quarkonium and QCD

— an intuitive view —

H. FUJII (U. Tokyo)

Plan

1. Heavy Quark and Quarkonium
2. Why Heavy Quark/Quarkonium?
3. Quarkonium Production
4. Quarkonium Interaction
5. Quarkonium as Hard Probe of QGP
6. Base-line and Anomalous Suppression
7. Concluding Remarks

Heavy Quarks and Quarkonia

$\Lambda_{QCD} \sim 0.2\,GeV$

- Quark Mass

$u(1 \sim 5MeV)$	$c(1.15 \sim 1.35GeV)$	$t(174.3GeV)$
$d(3 \sim 9MeV)$	$s(75 \sim 170MeV)$	$b(4.0 \sim 4.4GeV)$

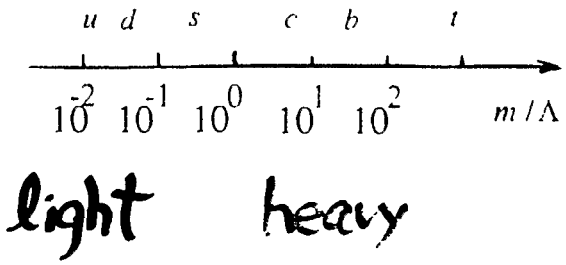

- Quarkonia : $Q\bar{Q}$ bound states.
  - Spin-1

state	$J/\psi(1S)$	$\chi_{cJ}(1P)$	$\psi'(2S)$	$\Upsilon(1S)$	$\chi_{bJ}(1P)$	$\Upsilon'(2S)$
$M_{[GeV]}$	3.1	3.5	3.7	9.6	9.9	10.0

- Open Charm/Beauty $Q\bar{q}$, $q\bar{Q}$

state	$D(0^-)$	$D^*(1^-)$	$B(0^-)$	$B^*(1^-)$
$M[GeV]$	1.9	2.0	5.3	5.3

Why Interesting?

- Heavy <u>quarks</u> are <u>heavy</u>: $m_Q \gg \Lambda_{QCD}$
  - pQCD is meaningful
  - Good probe of gluon densities

- Heavy <u>quarkonia</u> are <u>small</u>: $1/m_Q\alpha$
  - Use multipole/OPE expansion
  - Good probe of softer gluon fields

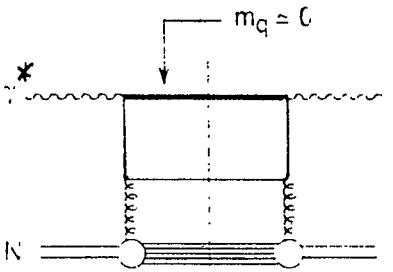

$\tau \sim \frac{1}{\sqrt{-q^2}}$

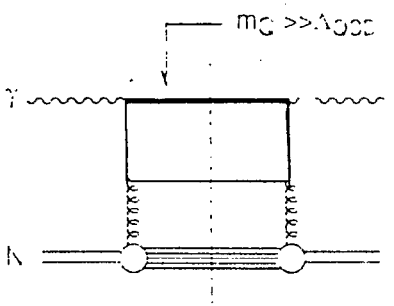

$\tau \sim \frac{1}{2m_Q}$

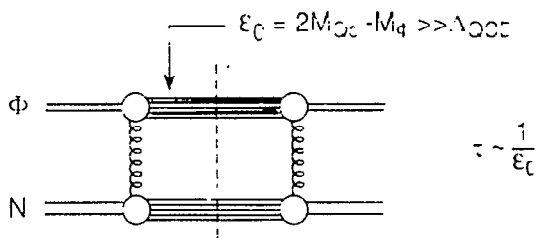

$\tau \sim \frac{1}{\varepsilon_Q} \sim \frac{1}{m_Q \alpha^2}$

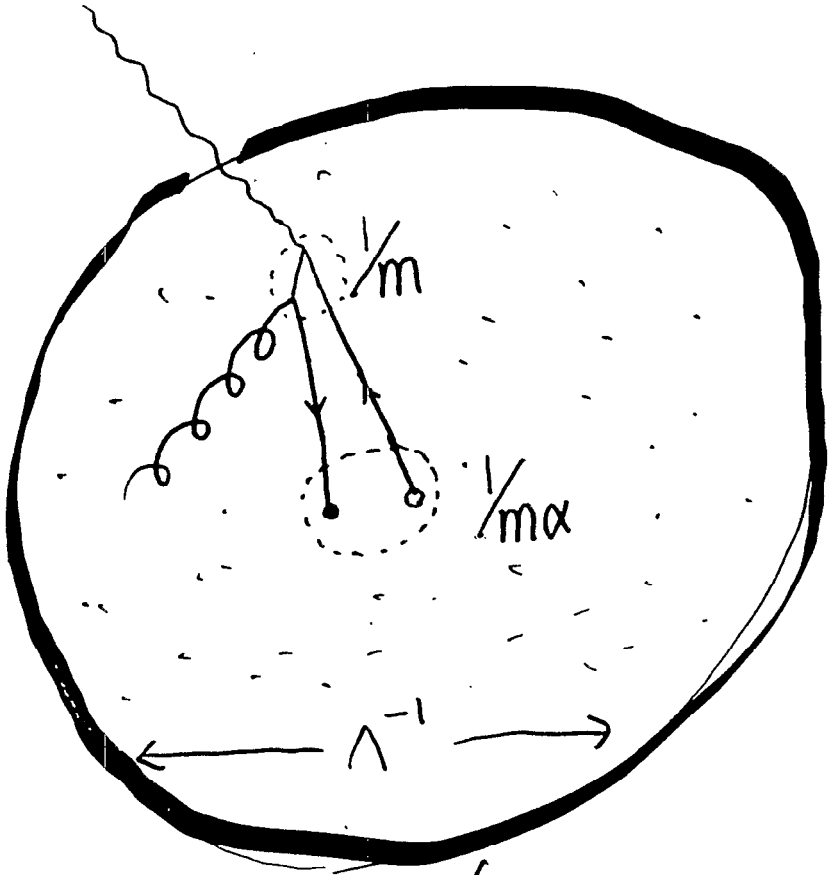

a hadron

Hydrogen-like

$$E(r) = \frac{1}{2m}\frac{1}{r^2} - \frac{\alpha}{r}$$

$$E'(r) = -\frac{1}{mr^3} + \frac{\alpha}{r^2} = 0$$

$$\boxed{\begin{aligned} r &\sim \frac{1}{m\alpha} \\ E_0 &\sim m\alpha^2 \end{aligned}}$$

Why Interesting?

- Heavy quarkonia are simple gluon source
  - Good theoretical framework to study small-x physics

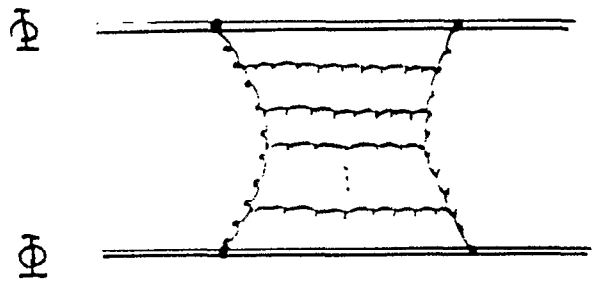

- Q'm spectroscopy on the lattice $\rightarrow \Lambda_{QCD}$

  $\Upsilon, \Upsilon', \Upsilon'', \chi_{cJ}$ splitting

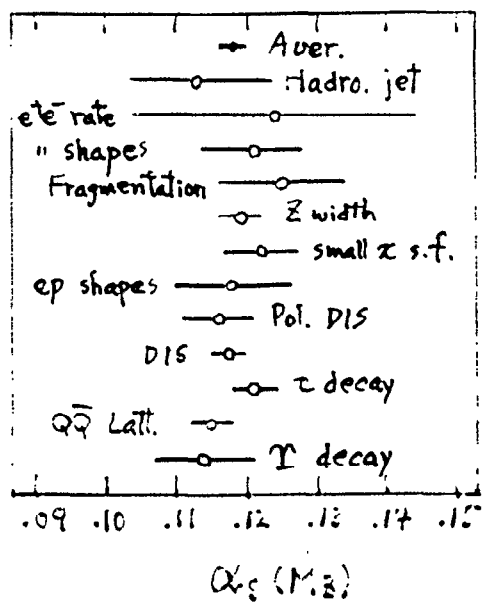

- ...

Why Interesting?

- Quark Deconfinement Matsui-Satz
  - Color screening in dense medium→no bound state!

$$V(r,\mu)=\frac{\sigma}{\mu}\left[1-e^{-\mu r}\right]-\frac{\alpha}{r}e^{-\mu r}$$

  - Static, long-range effect
  - at hadronization, too far apart for J/ψ

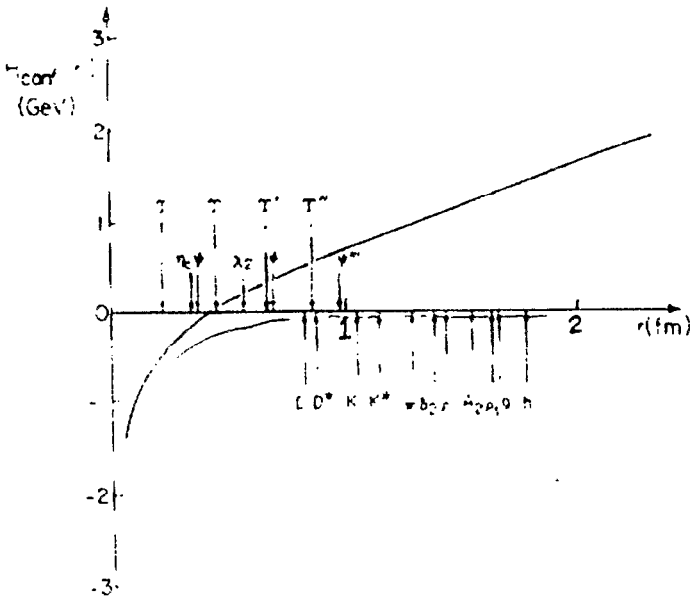

r of mesons vs the Cornel potential

	Ψ(1S)	Ψ(2S)	χ(1P)
μ_D[GeV]	0.68	0.35	0.35
T/T_C	1.2	1	1

Hierarchy

We assume ...

production	quarkonia		light hadrons
m_Q	$\gg$ $m_Q v$	$\gg$ $m_Q v^2$	$\gg$ Λ_{QCD}
	$\sim p_{Q\bar{Q}}$	$\sim \epsilon_0$	
	$\sim 1/r_{Q\bar{Q}}$		

In reality,

$m_c \sim 1.3$ GeV $\quad m_c v^2 \sim 0.5$ GeV $\quad \Lambda_{QCD} \sim 0.2$ GeV

Q'm Production Mechanism

- Motivation for CSM
  - Pair Creation: Rel Quantum effect, fast $\sim 1/2m_Q$
  - NR bound state: Internal motions are slow $\sim 1/m_Q\alpha^2$

2-step production

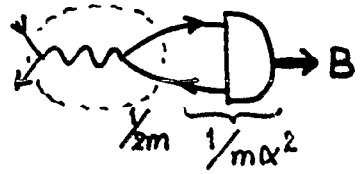

★ Eg. $e^+e^- \to \mu^+\mu^-$ b.s.

$$\mathcal{M}(e^+e^- \to B) = \sqrt{2M}\int d^3k\, \tilde{\psi}^*(k)\frac{1}{\sqrt{2E_k}}\frac{1}{\sqrt{2E_{-k}}}\overbrace{\langle \mu^+\mu^- | S | e^+e^- \rangle}^{k\text{-indept. for } k \ll m_\mu} = \sqrt{\frac{2}{M}}\psi(0)(-2e^2)$$

$\simeq$

$$\therefore\ \sigma^{\text{unp}}(e^+e^- \to B) = \frac{64\pi^3}{M^3}\alpha \cdot |\psi(0)|^2 \cdot \delta(s - M^2)$$

★ For Ψ, project onto the dominant Fock state

$J/\psi \cdots c\bar{c}(^3S_1)$

$\chi_J \cdots c\bar{c}(^3P_J)$

$$\mathcal{M}(\psi + X) = \hat{\mathcal{M}}(c\bar{c}(^3S_1) + X)\, R_\psi(0) \to d\sigma(\psi X) = d\hat{\sigma}(c\bar{c}(^3S_1)X) \cdot \underbrace{R_\psi^2(0)}_{\text{known!}}$$

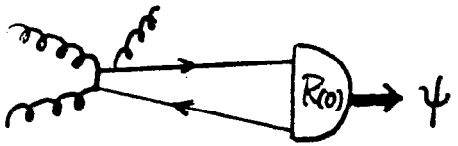

$$\Gamma(\psi \to e^+e^-) = \frac{4\alpha^2}{9m_c^2} \cdot 4\pi |\psi(0)|^2$$

Q'm Production Mechanism(CSM)

- <u>hadro-production in CSM</u>
  - ★ Abusolutely normalized prediction!
  - ★ Sensitive to gluonic structure!

$\sigma(ab \to J/\psi\, X) =$ 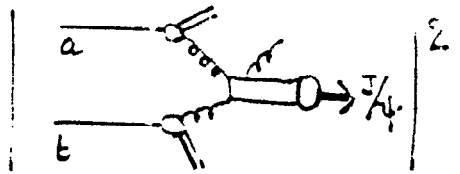

$$= \sum_{ij} \int dx_i\, dx_j\, G_{i/a}(x_i)\, G_{j/b}(x_j)\, \hat{\sigma}(ij \to c\bar{c}(^3S_1)X)\, R^2_\psi(0).$$

known

NB.

- Just a model: factorization is assumed
- IR divergence in χ-state production
- Rel. Corr. $O(v)$; ...$v^2 \sim 1/3$ for ψ
- <u>Fails in describing the data@Tevatron</u>: total x-sec, P_T-dep.
- Fragmentation is important at high p_t

Q'm Production Mechanism(COM)

- Why Color Octet?
  - Three scales:

$$m_Q \gg m_Q v = r_{Q\bar{Q}}^{-1} \gg m_Q v^2 = \varepsilon_{Q\bar{Q}}$$

  - on-shell g, $k \sim k^0 \sim m_Q v^2$ slow, g^*, $k \sim m_Q v$, $k^0 \sim m_Q v^2$ fast, and included in the potential.
  - NRQCD, expansion in v

$$\Phi >= (\underline{Q}\underline{\bar{Q}})_1 > + O(v) (\underline{Q}\underline{\bar{Q}})_8 g > + \cdots$$

Bodwin, Braaten, Lepage

- Color Octet Model (COM)
  - produce $Q\bar{Q}_8$, bound to Q'm
  - IR div in χ can be cancelled
  - $\langle O^{\Phi}_{1,8} \rangle$ unknown parameters

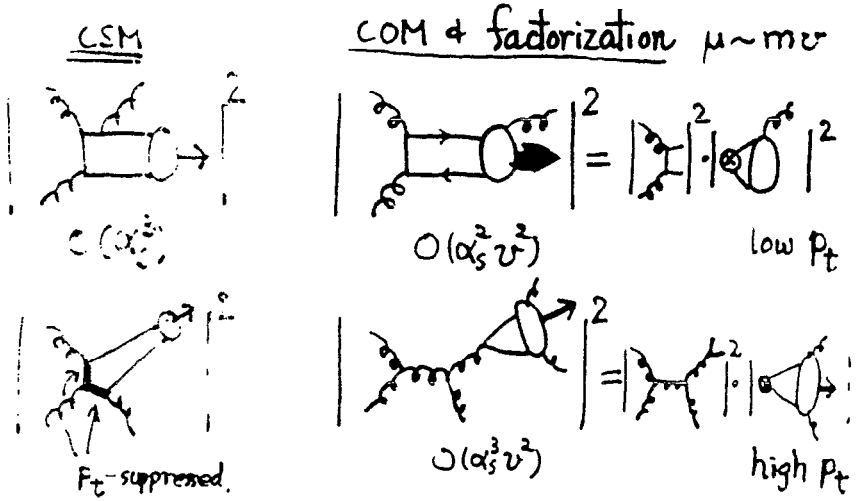

$$\sigma(ab \to \Phi X) = \sum_{ij} \int dx_i dx_j \, G_{i/a}(x_i) G_{j/b} \sum_{\{\theta\}} \hat{\sigma}(ij \to \bar{Q}[1,8]; {}^{2S+1}L_J; X) \cdot \langle O^{\Phi}_{1,8}({}^{2S+1}L_J) \rangle$$

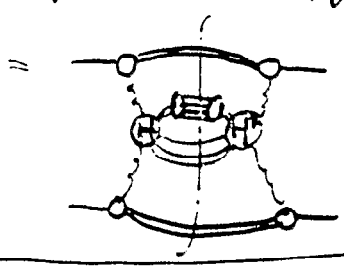

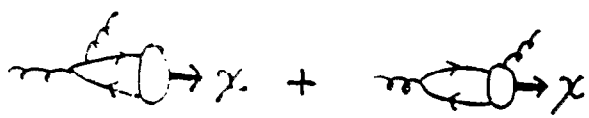

$p\bar{p} \longrightarrow J/\psi X$ hep-ph/9611218

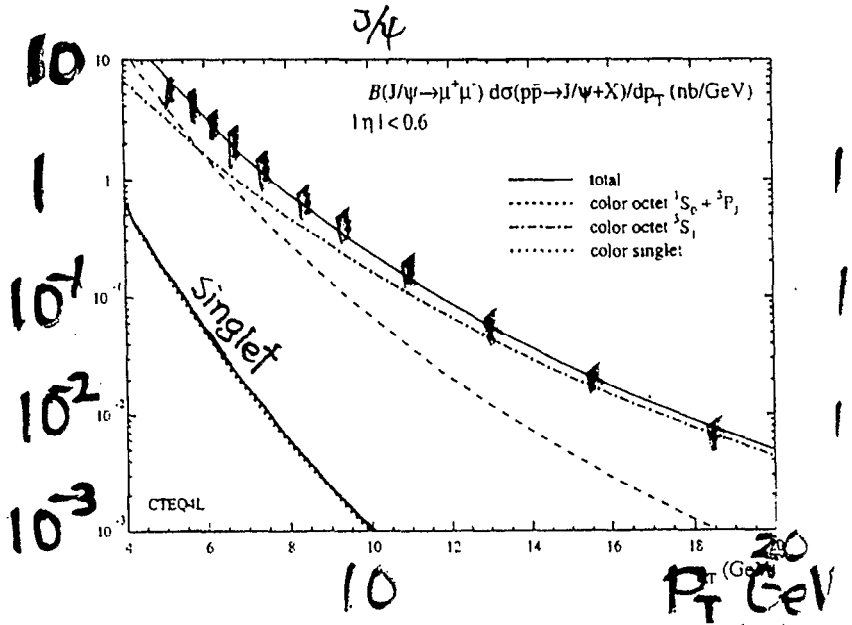

FIG. 1. Fit of color octet contributions to direct J/ψ production data from CDF ($\sqrt{s}=1.8$ TeV, pseudorapidity cut $|\eta|<0.6$). The theoretical curves are obtained with CTEQ4L parton distribution functions, the corresponding $\Lambda_4=235$ MeV, factorization scale $\mu=(p_t^2+4m_c^2)^{1/2}$ and $m_c=1.5$ GeV. The fitted color octet matrix elements are given as the central values in Table I.

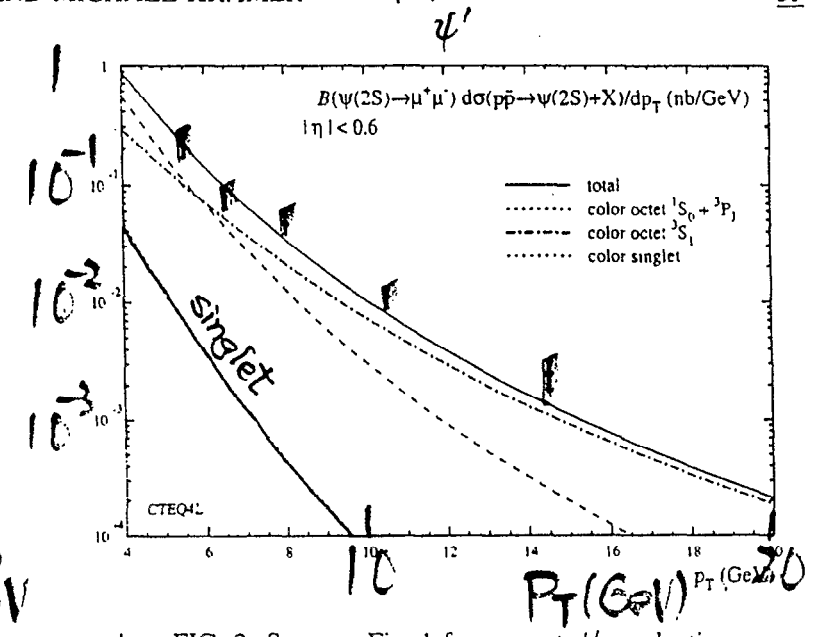

FIG. 2. Same as Fig. 1 for prompt ψ' production.

where $f_{i/p}$ and $f_{j/\bar{p}}$ denote the parton densities and λ specifies the helicity state. At nonvanishing transverse momentum, the leading partonic subprocesses $i+j\rightarrow c\bar{c}[n]+k$ occur at order α_s^3. To obtain the short-distance cross section for a given $c\bar{c}$ state n, we expand, in the rest frame of the heavy quark pair, the partonic amplitude in the relative momentum of the heavy quarks and decompose the amplitude in spin and color. The amplitude squared for $i+j\rightarrow\psi^{(\lambda)}+X$ can now be written as

try implemented in the decomposition of $\langle \mathcal{O}^{\psi^{(\lambda)}}_{n;kl}\ldots\rangle$; they can be found in [6]. For the $S=0$, $L=0$ intermediate state, each helicity state contributes one third of the unpolarized cross section. For the P wave intermediate state, one must first sum over all orbital angular momentum states L_z and then project with the polarization vector $\epsilon(\lambda)$ of the quarkonium. The short-distance coefficients that enter $d\hat{\sigma}_{ij}^{(\lambda)}[n]$ can now be written as

$$A_{ij}[n]+B_{ij}[n][\epsilon(\lambda)\cdot k_1]^2+C_{ij}[n][\epsilon(\lambda)\cdot k_2]^2 + D_{ij}[n][\epsilon(\lambda)\cdot k_1][\epsilon(\lambda)\cdot k_2], \tag{4}$$

Q'm Production Mechanism

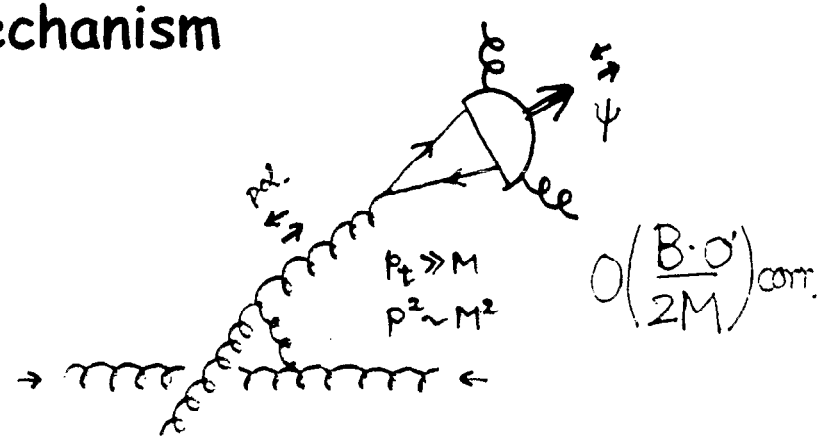

- Testing the COM
  - Soft part, process independent? → Fig.
  - Polarization of ψ @ high p_t → Fig.
  - χ_2 production, $\chi_2 \to \psi + \gamma$
    D. Kharzeev + R. Jaffe
- Solution?
  - k_T factorization → Fig.
  - Rel. Corr. ?
  - Others?

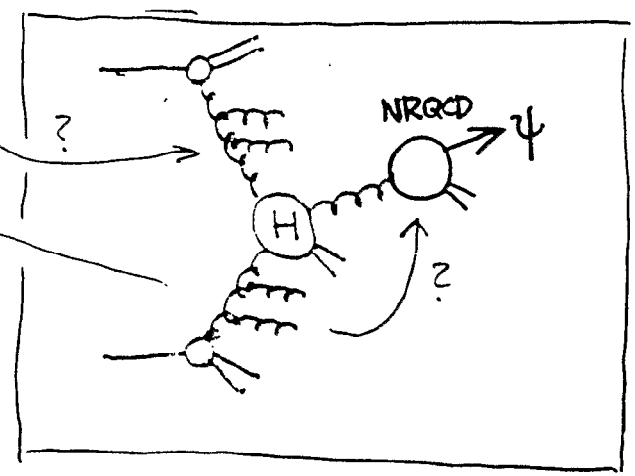

Mizukoshi hep-ex/9911384

fig 4

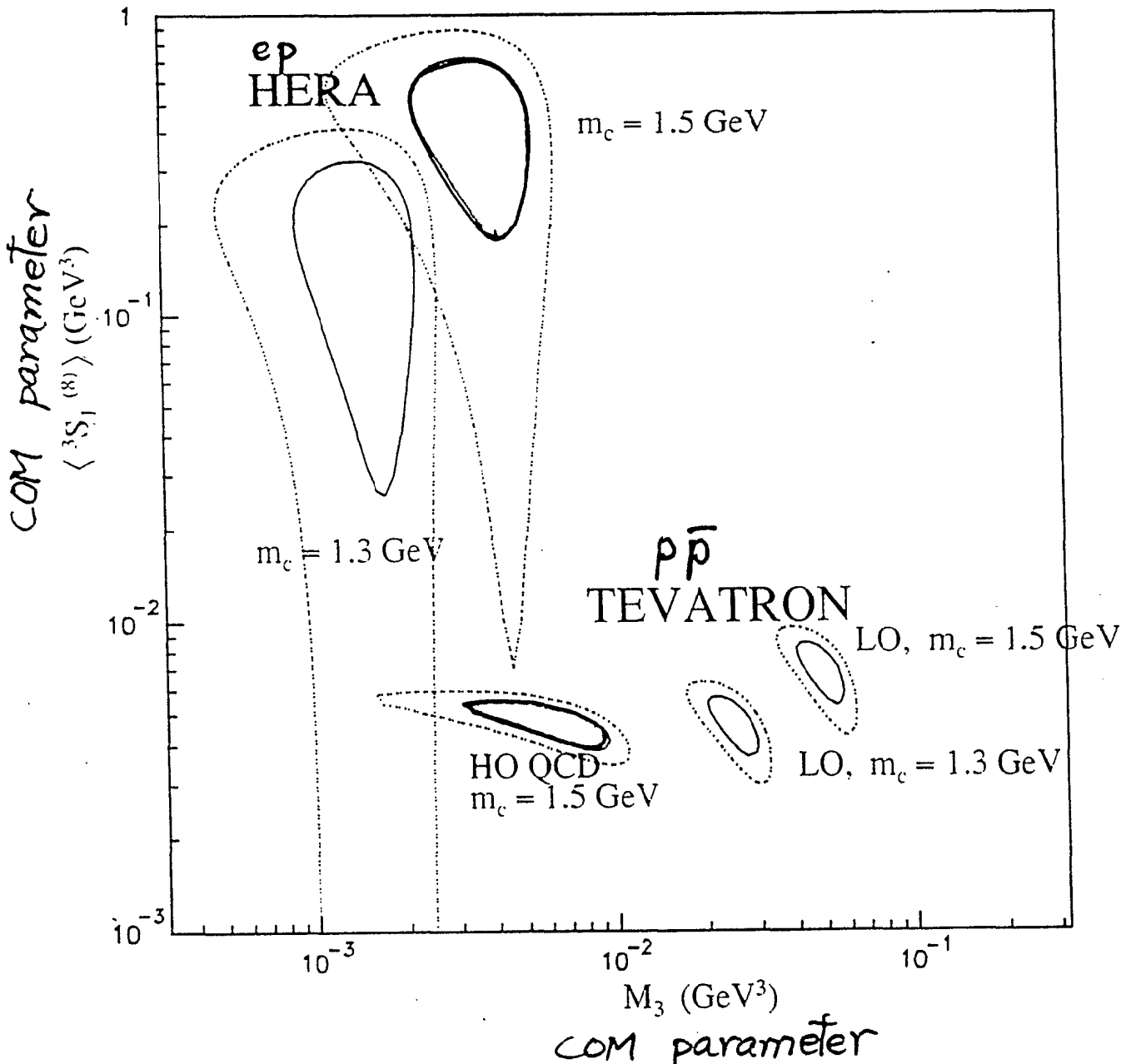

Helicity Frame

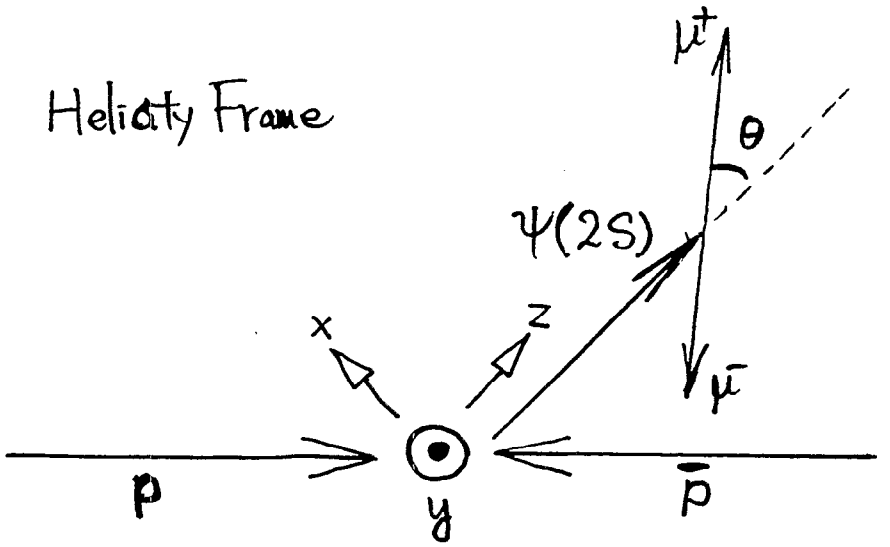

θ: angle between μ^+ in $\psi(2S)$ rest frame and direction of $\psi(2S)$ in lab frame

$$w(\cos\theta) = \frac{3}{2(3+\alpha)}(1+\alpha\cos^2\theta)$$

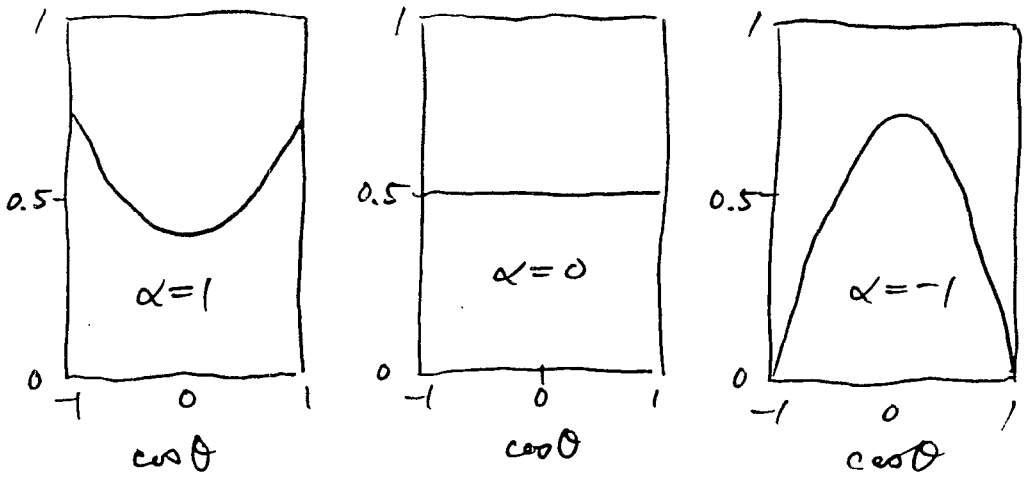

Ngo, CDF/MIT APS Centennial Meeting / March 20-26, '99

COM matrix elements large

PDF	$\langle O_1^{J/\psi}(^3S_1)\rangle$	$\langle O_8^{J/\psi}(^3S_1)\rangle$	$M_r^{J/\psi}$	$\langle O_1^{\psi'}(^3S_1)\rangle$	$\langle O_8^{\psi'}(^3S_1)\rangle$	$M_r^{\psi'}$	$\langle O_1^{\chi_{c0}}(^3P_0)\rangle$	$\langle O_8^{\chi_{c0}}(^3S_1)\rangle$
I	1.34 ± 0.10	4.42 ± 0.73	8.75 ± 0.87	6.50 ± 0.64	4.20 ± 1.00	1.30 ± 0.45	3.63 ± 1.27	3.55 ± 2.05
II	1.38 ± 0.10	3.95 ± 0.66	6.59 ± 0.69	6.70 ± 0.66	3.66 ± 0.88	0.78 ± 0.36	3.74 ± 1.31	-0.75 ± 1.77
unit	GeV^3	$10^{-3}\mathrm{GeV}^3$	$10^{-2}\mathrm{GeV}^3$	$10^{-1}\mathrm{GeV}^3$	$10^{-3}\mathrm{GeV}^3$	$10^{-2}\mathrm{GeV}^3$	$10^{-1}\mathrm{GeV}^3$	$10^{-4}\mathrm{GeV}^3$

TABLE I. NRQCD matrix elements. The labels I and II refer to MRST98LO and CTEQ5L, respectively. The value of r for $M_r^{J/\psi}$ is 3.44 for I and 3.45 for II. The value of r for $M_r^{\psi'}$ is 3.46 for both I and II.

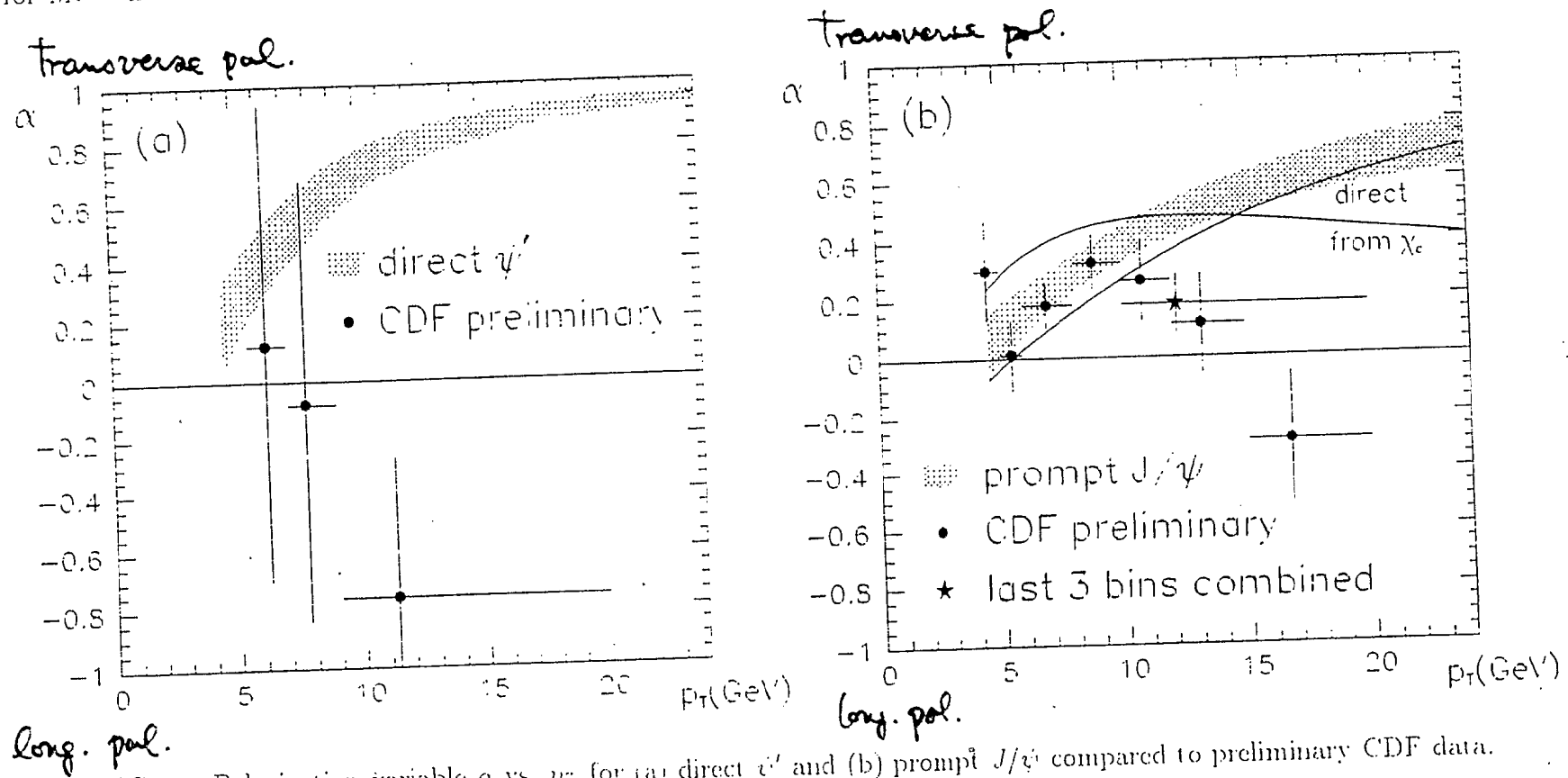

FIG. 1. Polarization variable α vs. p_T for (a) direct ψ' and (b) prompt J/ψ compared to preliminary CDF data.

allow the polarization to be measured with higher precision and out to larger values of p_T. If the result continues

[1] G.T. Bodwin, E. Braaten, and G.P. Lepage, Phys. Rev. D 51, 1125 (1995); 55, 5855(E) (1997).

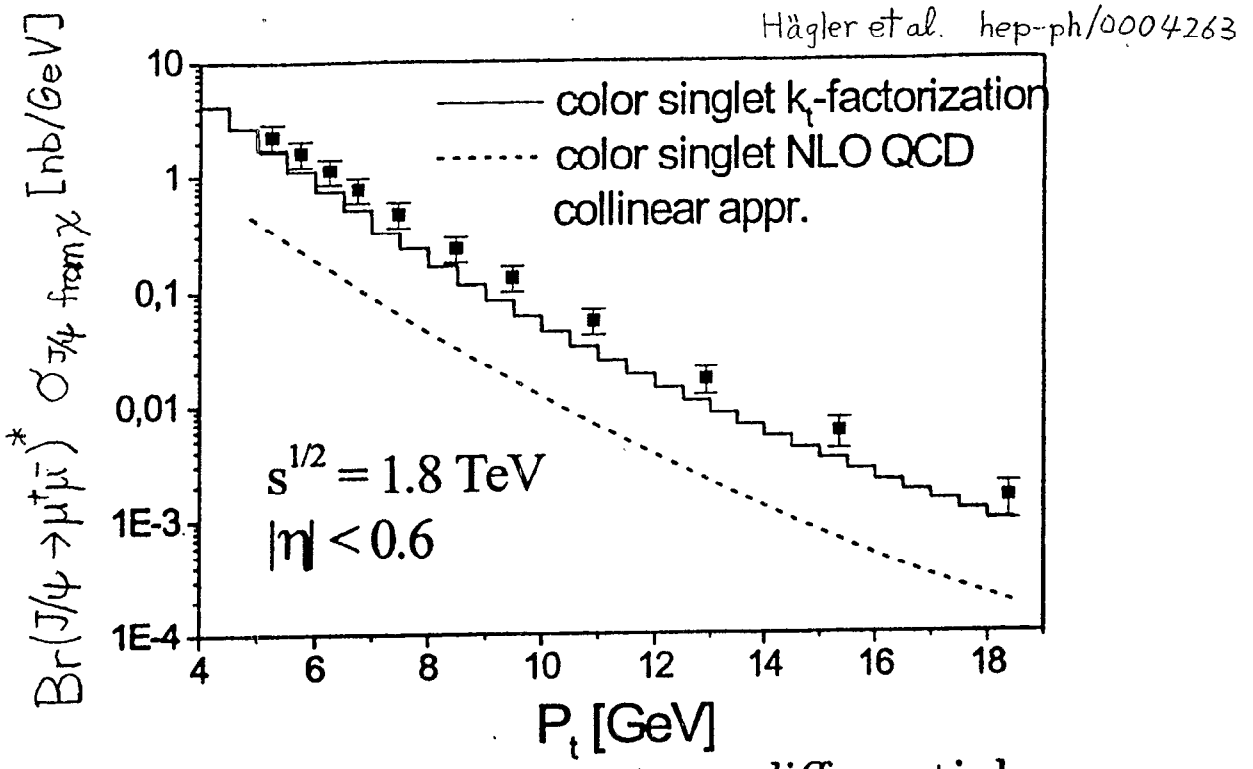

The transverse momentum differential cross sec-
in comparison to the data and a NLO QCD calculation

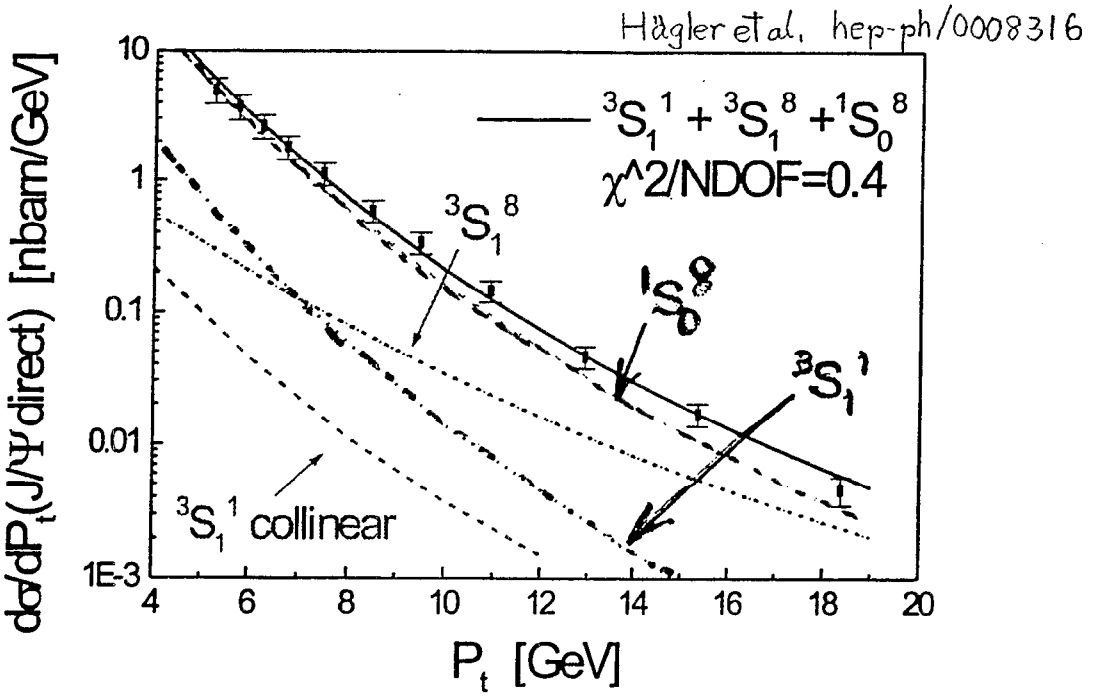

FIG. 2. Direct J/Ψ production

Quarknium Production

Assuming the factorization, (otherwise...)

- COM may not be the full story

But

- Eg. k_T-fact. calc. still needs COM contrib., although it's substantially reduced.

$J/\psi,\ \psi' \cdots$

Quarkonium Interaction

$u \sim \epsilon_0 \sim m v^2$

- Sufficiently massive Q'm, $\Lambda_{QCD} \ll \varepsilon_0$
- Small Dipole in Soft External Fields
  - Soft; $q^0 \ll \varepsilon_0$
  - Leading term ... $E \cdot E$
  - $(v \times r) \cdot B \ll r \cdot E$, because $v = p/m_Q \sim \alpha_s$
  - HARD: Polarizability $\sim r^2/\varepsilon_0$ small
    - Color Transparency
  - SOFT: Needs $\langle E \cdot E \rangle$

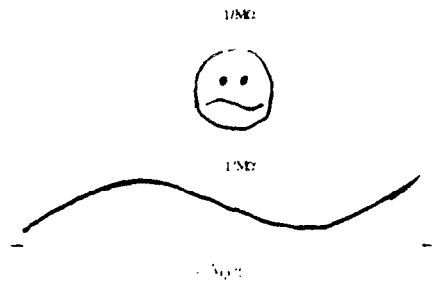

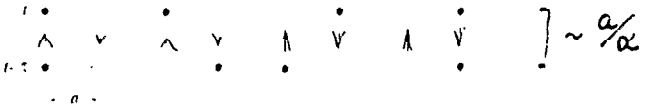

$\sim a/\alpha$

$$= \frac{1}{N} \mathrm{tr}(\tau^a \tau^b) \int_0^\infty d\tau\, (ig)\left(A^{0a}(t, \tfrac{a}{2}) - A^{0a}(t, -\tfrac{a}{2})\right) \cdot e^{-\partial_T \tau} (ig)\left(A^{0b}(t-\tau, \tfrac{a}{2}) - A^{0b}(t-\tau, -\tfrac{a}{2})\right)$$

$$= -\frac{g^2}{2N} \int_0^\infty d\tau\, a \cdot \partial A^{0a}(t, 0)\, e^{-\partial_T \tau}\, a \cdot \partial A^{0a}(t-\tau, 0)$$

Taylor exp'd. in τ

$$= -\frac{g^2}{2N} \sum_n \frac{1}{\partial_T}\, a \cdot \partial A^{0a}(t, 0) \left(\frac{\partial_0}{\partial_T}\right)^n a \cdot \partial A^{0a}(t, 0)$$

Q'm w.f. $\longrightarrow$

$$\boxed{-\sum_n \frac{g^2}{2} \underbrace{a^2 \frac{1}{\varepsilon_0} d_n \frac{1}{\varepsilon_n^{n-2}}}_{\text{Onium}} \cdot \underbrace{E^a (\partial_0)^{n-2} E^a}_{\text{Ext. field}}}$$

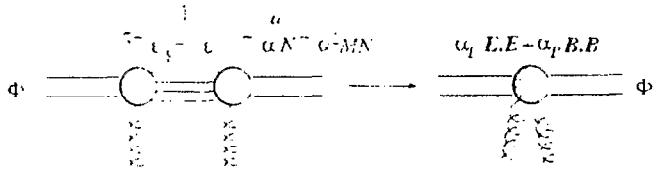

How to extract the info about Q'm Int.

NB: q^0 must be small to justify our treatment

- Ex.1; Q'm-π Int.

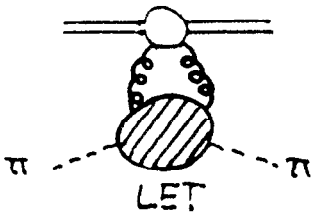

$$M = \frac{a^2}{\varepsilon_0} d_2 < \pi \left| \frac{g^2}{2} E^2 \right| \pi >$$

- Generally, $\langle h|E^2|h\rangle$ not known
- Use Low Energy Theorem to get an estimate

$$M \cong \frac{a^2}{\varepsilon_0} d_2 \cdot \frac{4\pi^2}{9} q^2$$

- $\frac{1}{2} g^2 E^2 \sim \frac{4\pi^2}{9} \theta_\mu^\mu$
- $\langle \pi | \theta_\mu^\mu | \pi \rangle \cong q^2 + 2m_\pi^2$

- Good for elastic scatttering : $\sigma \propto \frac{a^4}{\epsilon_0^2} q^4$
- No good for transition, $\Phi' \to \Phi\pi\pi$
  - $M_{\Phi'} - M_\Phi = O(\epsilon_0)$ is our 'HARD' scale.

Application; $\pi\Phi$ interactions

— $\pi J/\psi$ Elastic Cross Section —

$$\sigma(s) = \frac{1}{4\pi s}\frac{M^2}{2\mathbf{p}_{\rm CM}^2}\underbrace{\left(\frac{d_2}{c_0}a_0^2\right)^2}_{\sim r_Q^6}\left(\frac{4\pi^2}{b}\right)^2\int_0^{4\mathbf{p}_{\rm CM}^2} d(-t)\, \underbrace{t^2}_{\sim q^4}$$

- Chiral symmetry: Low momentum suppression, t^2

  $\Longrightarrow$ At low energies the $\pi\Phi$ interaction is very weak.

- The cross section is of order, 0.01 mb;

  $\Longrightarrow$ much smaller than the geometrical size of J/ψ.

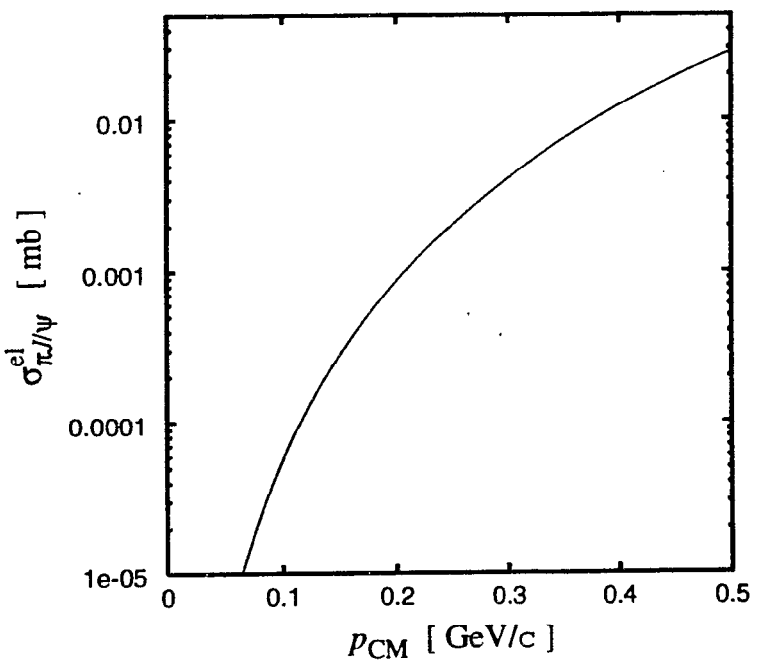

How to extract the info about Q'm Int.

NB: q^0 must be small, how to approach to physical region...

- Ex.2; Parton Model: Gluon structure

$$M = \frac{a^2}{\varepsilon_0} \sum_{n=2,\text{even}} \varepsilon^{2-n} d_n < h \frac{g^2}{2} E (D_0)^{n-2} E | h >$$

$$= a^2 \varepsilon_0 \sum_{n=2,\text{even}} d_n < h | O_n | h > \left(\frac{\lambda}{\varepsilon_0} \right)^n \qquad \lambda = \frac{p \cdot K}{M} \sim p^0$$

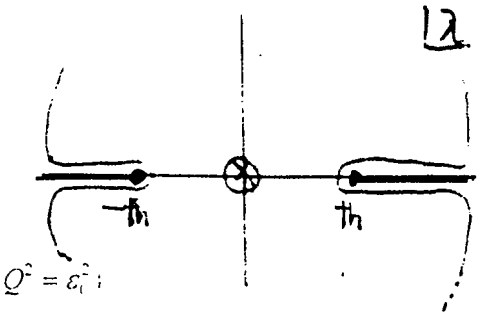

- Sum rule $\frac{2}{\pi} \int_{-1}^{1} d\lambda \lambda^{-n} \sigma_{\Phi h}(\lambda) = a^2 \varepsilon_0 d_n < O_n > \varepsilon_0^{-n}$

- Suggests gluonic parton model; $< O_n > = \int dx x^{n-2} g(x, Q^2 = \varepsilon_0^2)$

$$\sigma_{\Phi h}(\lambda) = \int_0^1 dx g(x) \sigma_{\Phi g}(x\lambda) \cdot \theta(x\lambda / \varepsilon_0 - 1)$$

$$\sigma_{\Phi g}(q^0) = \text{const} \cdot a^2 \cdot \frac{(q^0/\varepsilon_0 - 1)^{3/2}}{(q^0/\varepsilon_0)^5} \quad \ldots$$

No Tayler exp. in τ.

Parton dist.

$$g(x) = g_2 (k+1)(1-x)^k, \quad g_2 \sim 0.5, \quad k = 4 \text{ for } N$$

$$\therefore \sigma_{J/\psi N}(\lambda) = 2.5\,\text{mb} \left(1 - \frac{\lambda_0}{\lambda}\right)^{6.5}$$

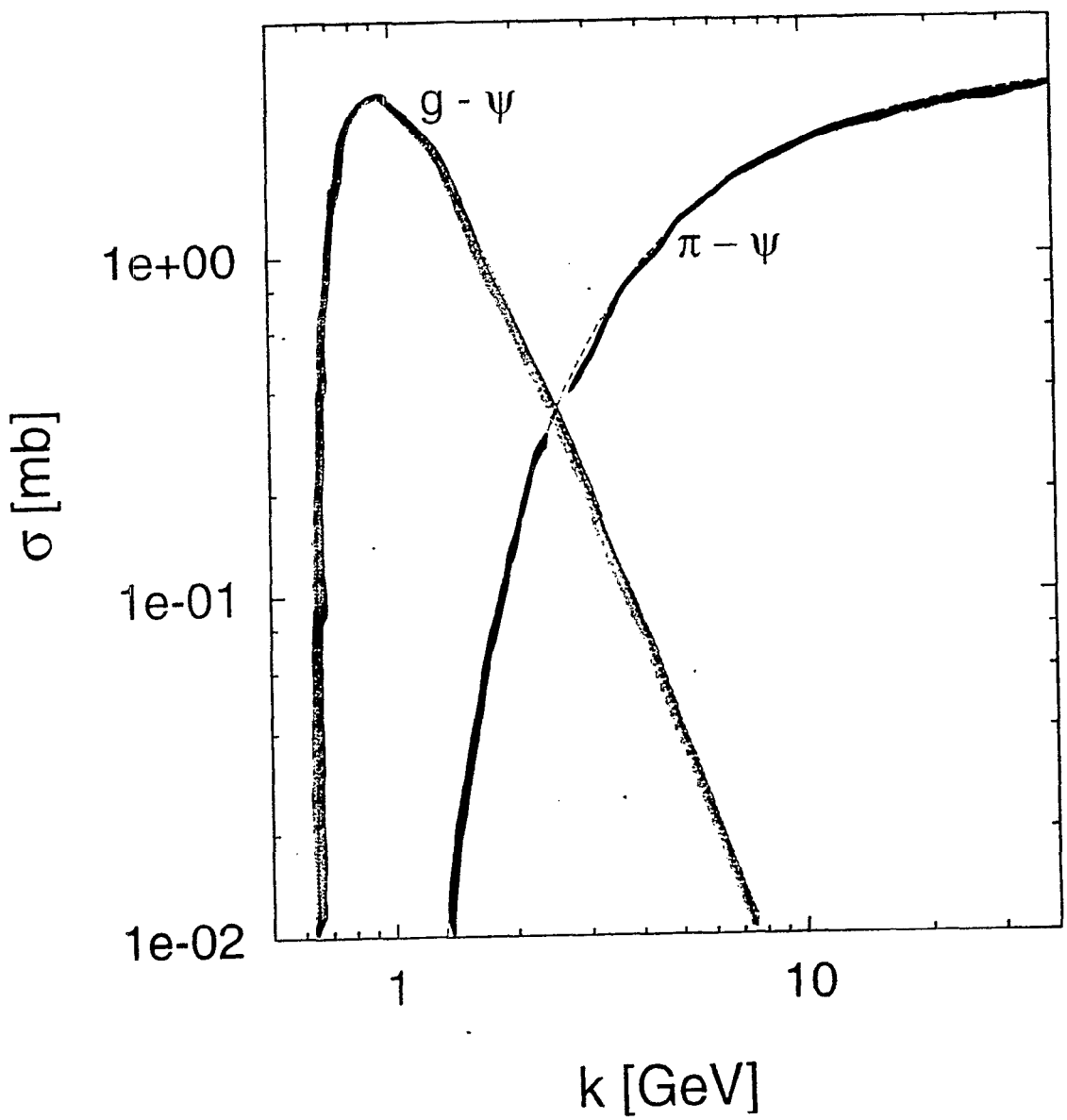
g - ψ
π − ψ
1e+00
1e-01
1e-02
σ [mb]
1
10
k [GeV]

Physics

- Photo-dissociation

  $q^0 \sim \epsilon_0$ effective.

- $\sigma_{\Phi h}(\lambda) = \int_0^1 dx\, g(x)\, \sigma_{\Phi g}(x\lambda) \cdot \theta(x\lambda/\epsilon_0 - 1)$

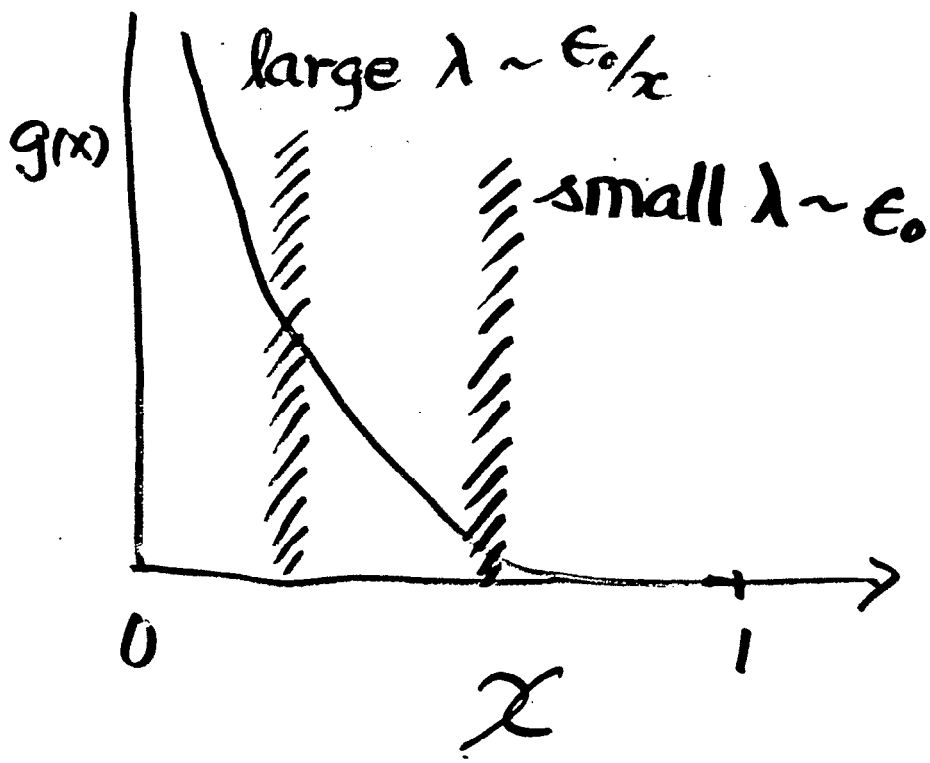

Q'n Interaction

For sufficiently heavy onia,

- multi-pole exp. applied $\quad r_{Q\bar{Q}} \ll \Lambda_{QCD}^{-1}$
- interaction is weak $\quad \sim a^2/\epsilon_0$

$$\sim (a^2/\epsilon_0)^2 \times q^4$$

elastic $\qquad$ pion

- w/ parton model

low-energy light hadrons hardly break quarkonia, because their gluonic content is <u>soft</u>.

Quarkonia as hard probe of QGP

~Introduction~

QCD dynamics

- properties of hadron (nucleon)
- " QCD matter

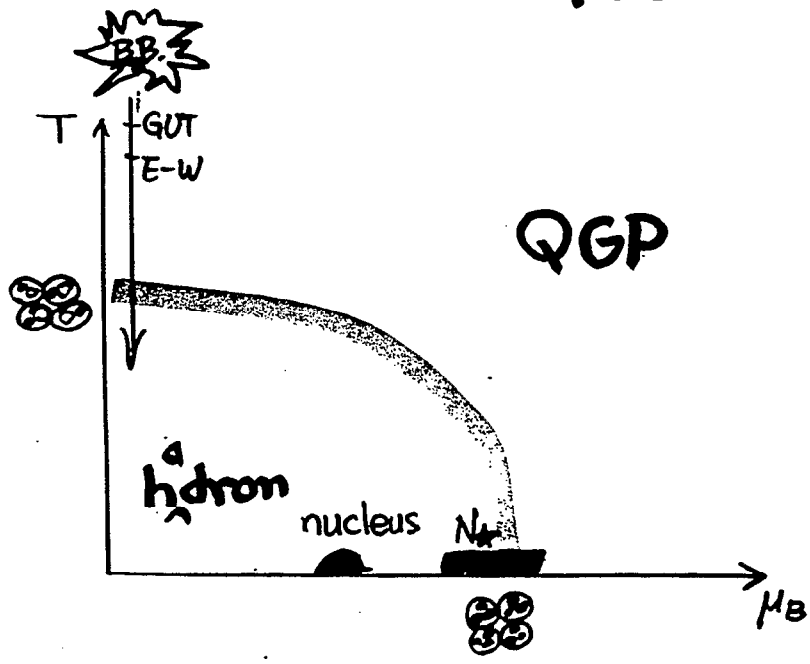

- Quark-hadron transition is the only one, which can be studied in the Laboratory.

- Big HI Accels.

fixed	BNL-AGS		$\sqrt{s} \sim 4$ GeV
	CERN-SPS	Pb-Pb	$\sqrt{s} \sim 17$ GeV
collider	BNL-RHIC	Au-Au	$\sqrt{s} \sim 130$ GeV

Quarkonia as hard probe of QGP

- Possible QGP signatures
  - Strangeness: hard gluons+χ-restoration $E_g \sim T$, $m_s : 0.5 \to 0.1$ GeV
    (Hadronic back ground)
  - J/ψ, ψ', χ: color screening
    (Hadronic FSI w/N, π, ,ρ,,,)
  - Thermal dilepton, γ:
    (DY b.g. etc.)

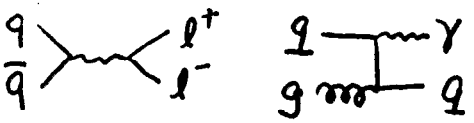

  - Collective flow: EOS, many scatterings ..... Phase Tr. → Softening
  - Low mass dilepton: mass-shift of ρ
    (broadening of width? No direct rel to QGP)
  - HBT interferometry: size at freeze-out
  - Hadron yield ratio
  - ...

CERN announcement

Cf. U. Heinz

- Initial Energy Density ε_0 in Pb+Pb@SPS
  - Bjorken's formula (1-dim, free stream)

$$\varepsilon_{Bj}(\tau_0) = \underbrace{\frac{1}{\pi R^2}}_{\text{overlap}} \underbrace{\frac{1}{2\tau_0}}_{\text{length}} \frac{dE_T}{dy}\Big|_{y=0}$$

$63\,\mathrm{fm}^2$ $2\,\mathrm{fm}$ $400\,\mathrm{GeV}$

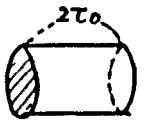

$$\longrightarrow \boxed{\varepsilon_{Bj}^{Pb\text{-}Pb}(1\,\mathrm{fm}/c) = 3.2 \pm 0.3\ \mathrm{GeV/fm}^3}$$

- LQCD estimate.

$$\boxed{\begin{array}{l} T_c \simeq 170\ \mathrm{MeV} \longleftrightarrow \varepsilon_c \simeq 0.6\ \mathrm{GeV/fm}^3 \\ T \simeq 220\ \mathrm{MeV} \longleftrightarrow \varepsilon \simeq 3.5\ \mathrm{GeV/fm}^3 \end{array}}$$

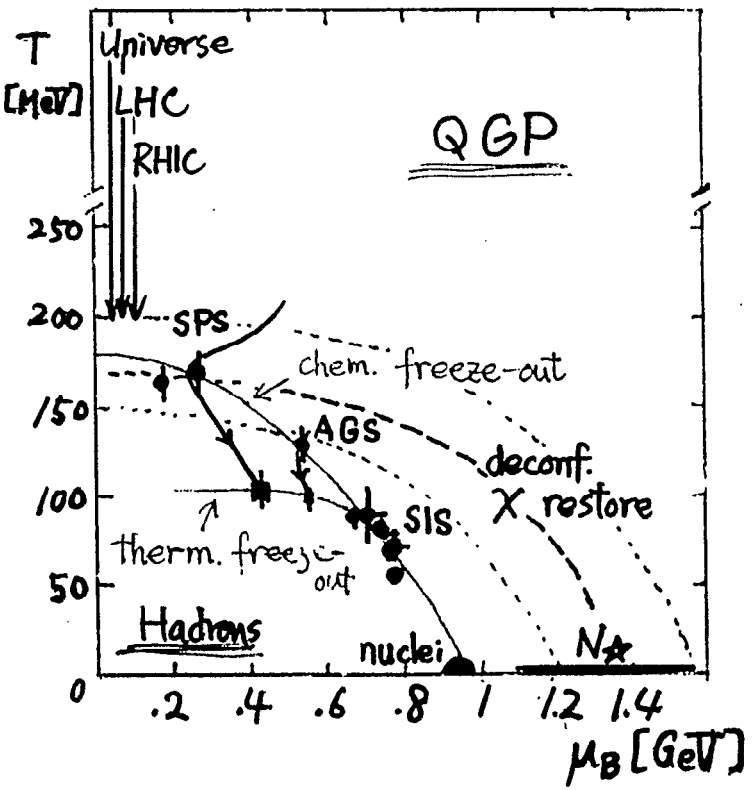

3 Important signatures at CERN-SPS

- Strangeness enhancement+Chem Equilib
  - Handron Yield →Tc~170MeV~LQCD estimate
  - Global strangeness Enhancement
  - Large enhancement $\Omega+\bar{\Omega}$
- J/ψ suppression
  - 'normal' upto S+U
  - 'anomalous' for Pb+Pb
- Low-mass dilepton enhancement
  - Rho meson modification?

Standard

E.g.

- Strangeness: Ω enhancement

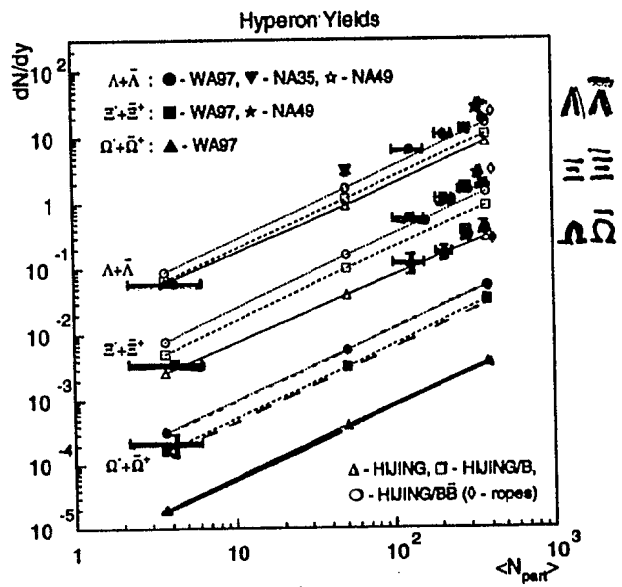

HIJING/$B\bar{B}$

Vance-Gyulassy

- Anomalous J/ψ suppression: NA50

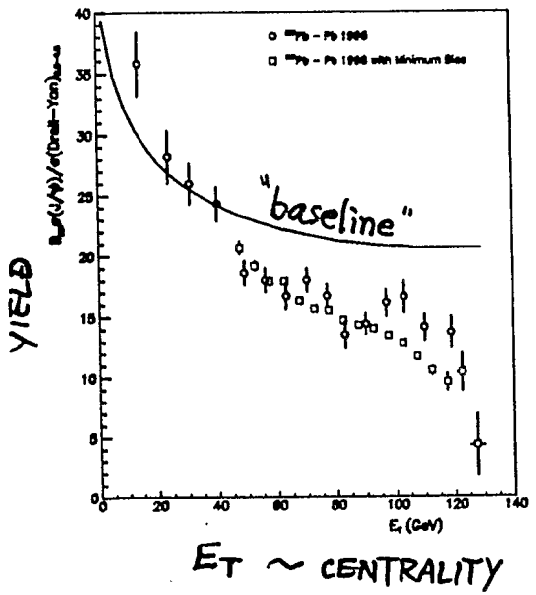

$E_T \sim$ CENTRALITY

something happened (Touched QGP?)

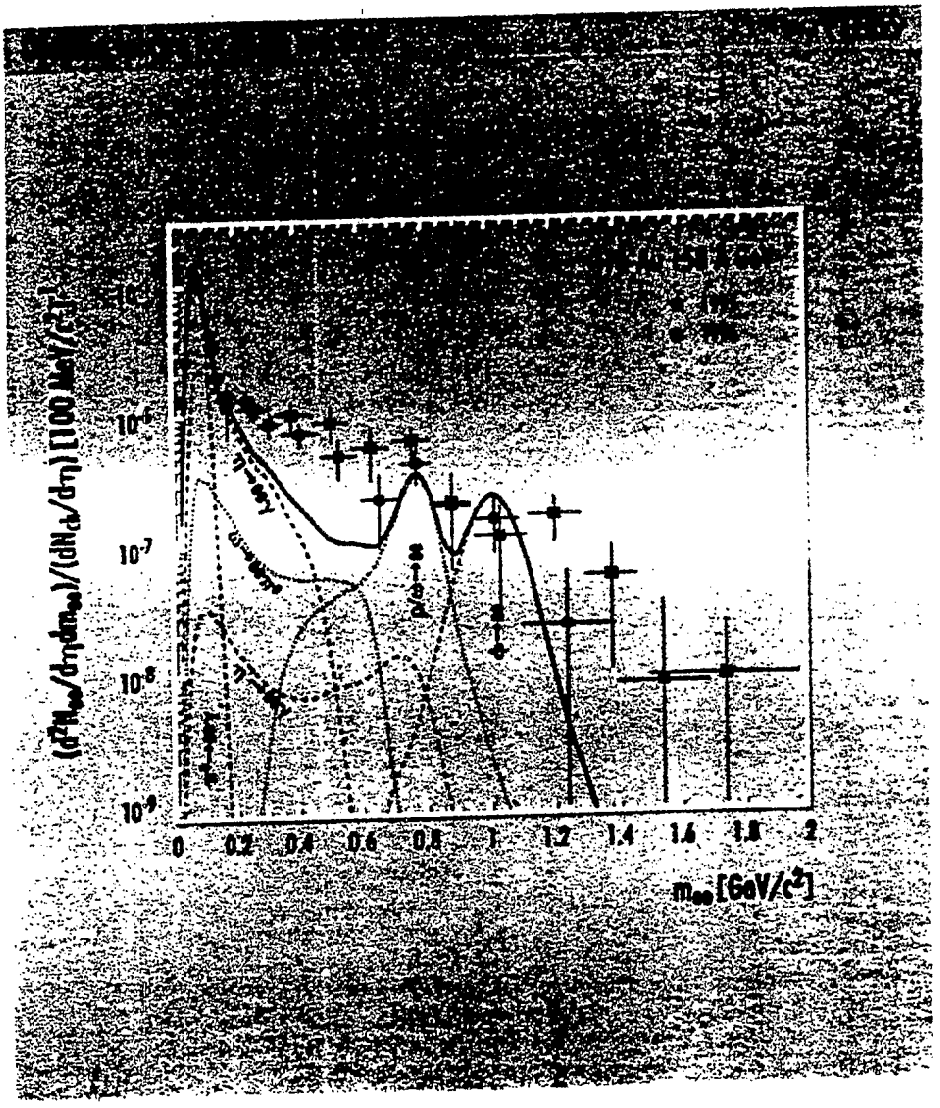
$(d^2N_{ee}/d\eta dm_{ee})/(dN_{ch}/d\eta)$ [100 MeV/c^2]$^{-1}$
10^{-6}
10^{-7}
10^{-8}
10^{-9}
0
0.2
0.4
0.6
0.8
1
1.2
1.4
1.6
1.8
2
m_{ee} [GeV/c^2]

Idea of J/ψ supp. as QGP signal

1. Color screening ··· J/ψ melt in QGP

Static, global effect. Matsui-Satz..

			Satz
	$\psi(1S)$	$\psi(2S)$	$\chi(1P)$
μ_D(GeV)	0.68	0.35	0.35
T/T_c	1.2	1	1

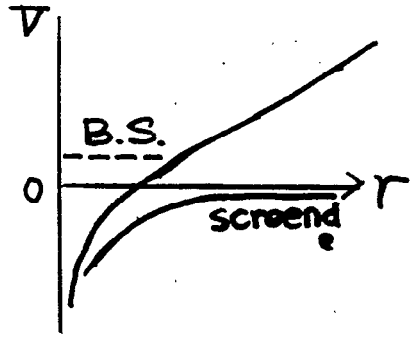

2. Gluon Dissociation

Incoherent, local effect.

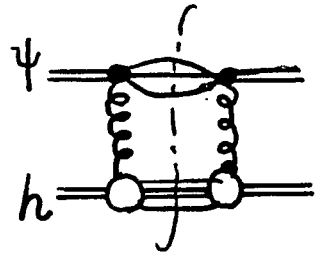

- Break-up threshold
  $\Delta E = 2M_D - M_\psi = 0.64$ GeV.

Average gluon mom. at T=.2GeV

- hadronic phase : Thermal dist. of π, ···
  $\langle k \rangle_{conf} \sim 0.6T = 0.1$ GeV
- QGP phase : Thermal dist. of g, q
  $\langle k \rangle_{deconf} \sim 3T = 0.6$ GeV

We expect ...

- Heavy quarks produced only in early stages (hard collisions)

- { No bound state in Debye screened potential
  Hard gluons in QGP prevent $Q\bar{Q}$ from being bound.

- @ hadronization, too far apart for J/ψ.

- Small final-state interactions w/ light hadrons
  (- nucleons
  - produced hadrons (π, ρ, ...)
  = comovers.

- CARTOON

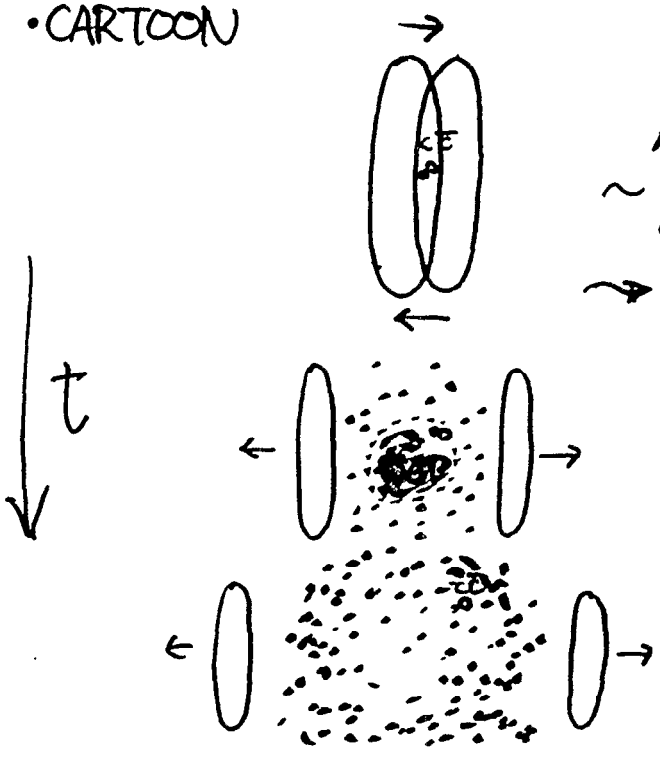

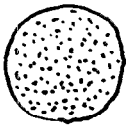

AB coll. @ High energy

~ colls. of parton beam.

$\rightarrow \sigma_{c\bar{c}}^{AB} \sim \sigma_{c\bar{c}}^{pp} \cdot A \cdot B$

p-A

$$\sigma_\psi^{pA} \neq \sigma_\psi^{pp} \cdot A \cdot B$$

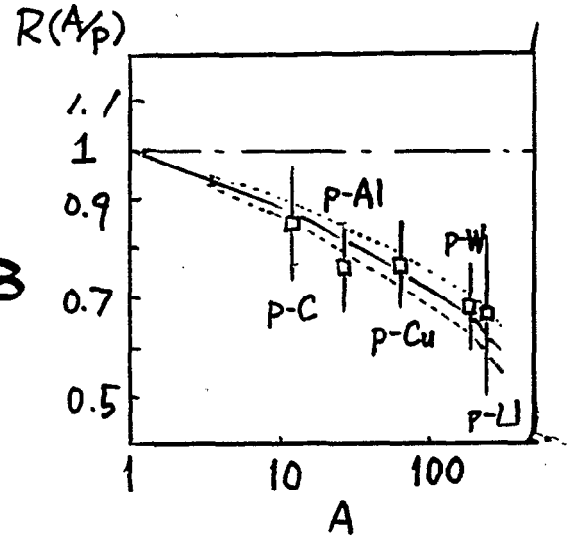

Suppression factor — nucleon density

$$S \propto e^{-\rho\, \sigma_{abs}\, \text{"}L\text{"}}$$

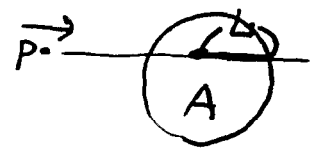

$$\sigma_{abs} = 6.9 \pm 1.1\ \text{mb}.$$

(Glauber approac

Larger than $\sigma_{geo} = 2 \sim 3$ mb.

$r_\psi \sim 0.3$ fm

$r_{\psi'} \sim 0.7$ fm

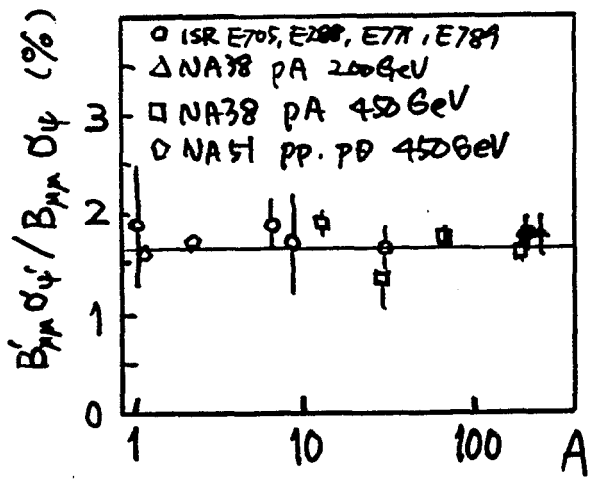

ratio ψ'/ψ is indept. of A

→ ψ' suppression is the same as ψ.

Interpretation

★ If assume the COM dominance in the production,

- Big x-sec $\sigma_{abs} \cong 7mb > \sigma_{geo} \simeq 2 \sim 3mb$

  ← Larger color charge of CO state : $\times \frac{9}{4}$

- The same suppression for ψ and ψ'

  ← Formation time $(\tau_0 \sim \frac{1}{B.E.}) \times \gamma \sim$ a few fm

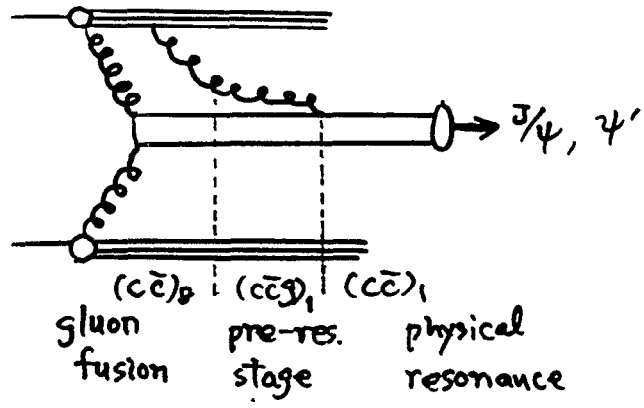

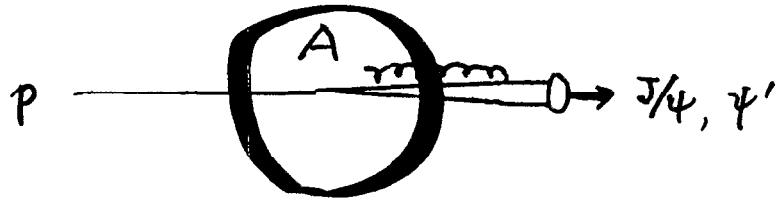

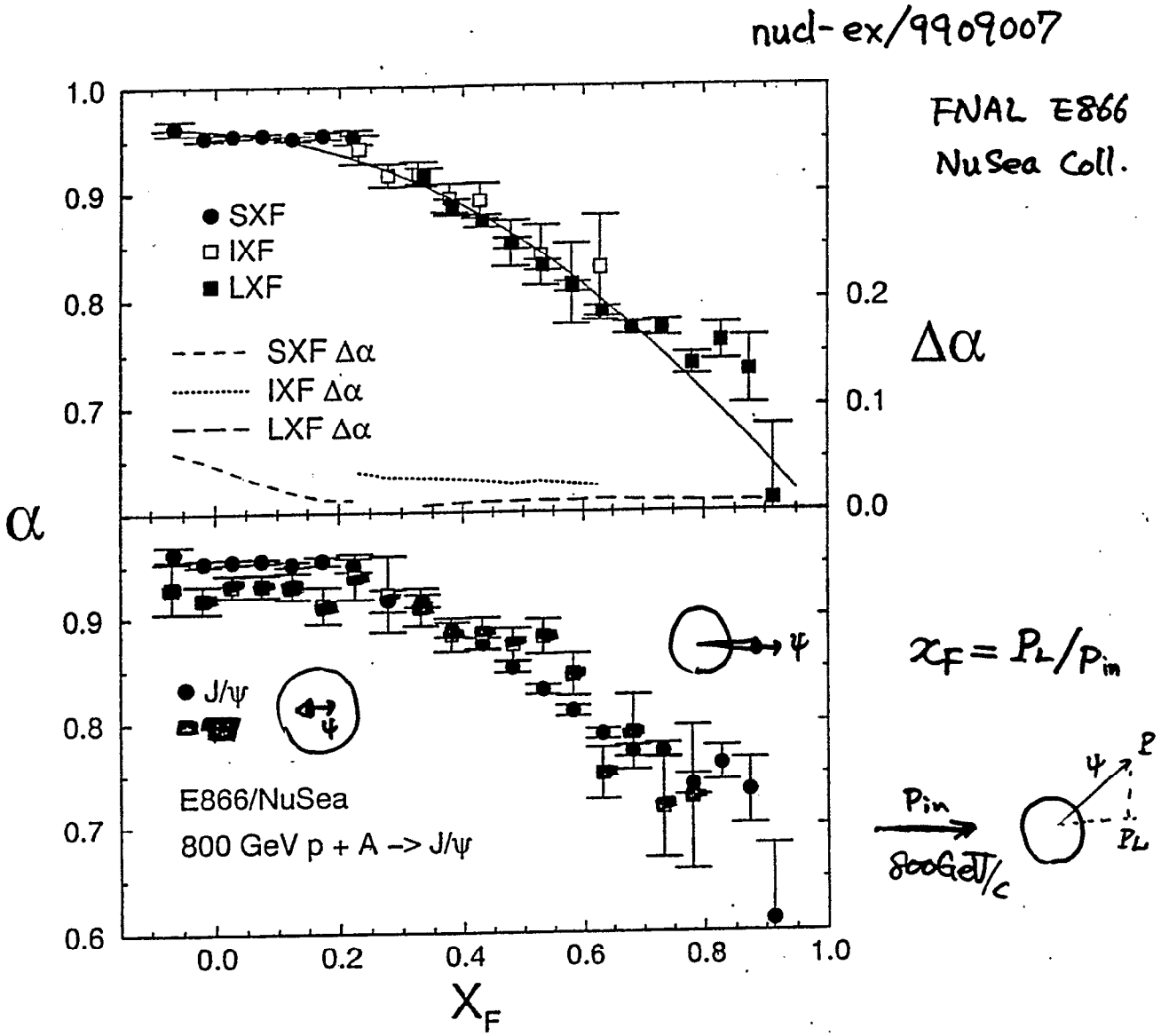

FIG. 3. α for the J/ψ versus x_F for the three different data s (top) and for the J/ψ and ψ' after the data sets are com- ıed (bottom). Values are corrected for the p_T acceptance, discussed in the text. These corrections ($\Delta\alpha$) have a maxi- ım value of 0.06 and are shown using the right-hand vertical .le in the top panel. The relative systematic uncertainty be- een α for the J/ψ and ψ' is estimated to be 0.003, while : absolute systematic uncertainty is 0.01 in α; neither is in- ded here. The solid curve represents the parameterization cussed in the text.

A-B

- Suppression factor ... A-B ...

$B\sigma(J/\psi)/\sigma(DY)$

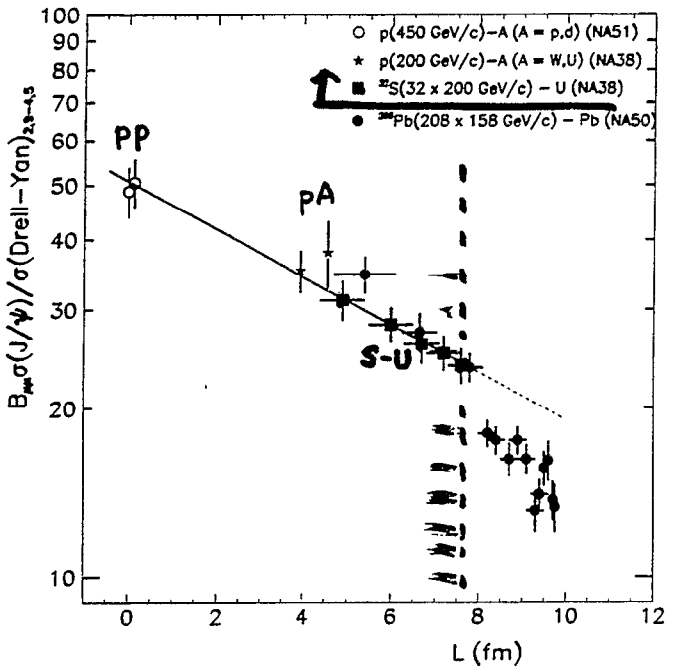

$\sigma(DY) \propto A \cdot B$

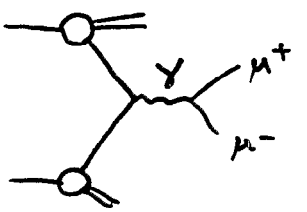

Data can be described by the same x-sec.

$\sigma_{abs} \sim 7mb$

up to S-U coll. @ $\sqrt{s} = 17$ GeV.

$\therefore$ p-p ~ p-A ~ A-B

A-B dependence can be described by the same σ_{abs} : 'normal' suppression.

cf. For S-U, ψ' is more suppressed than ψ.

reflecting the fact $\Gamma_{\psi'} > \Gamma_{\psi}$, $B.E._{\psi'} < B.E._{\psi}$

Extrapolation to Pb+Pb; Anomalous Suppression of psi:

extrapol. of normal supp.

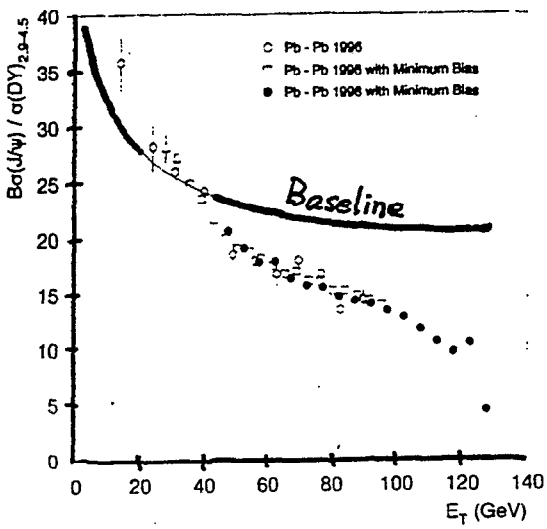

comover fit

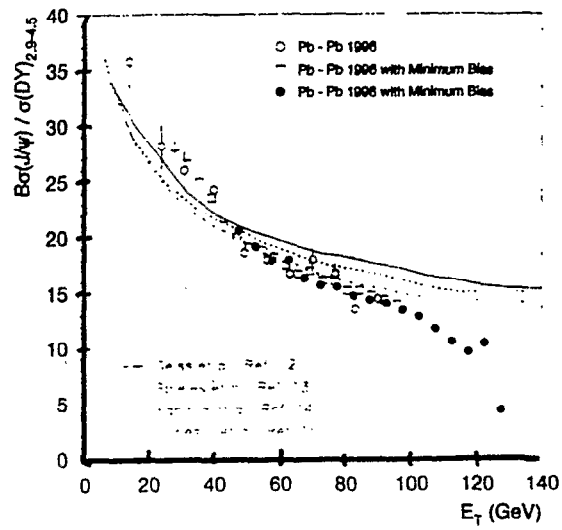

- Comovers Scinario may be ruled out ...
- 2-Step Melting of psi? (Satz) or E_T fluctuation?

Exp./Theory

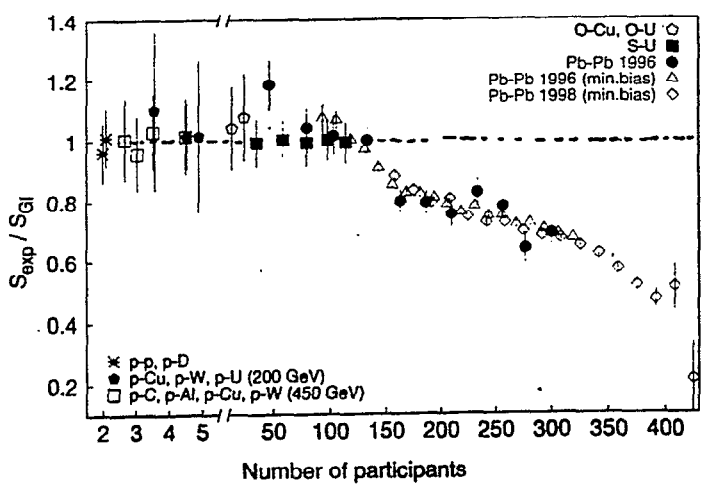

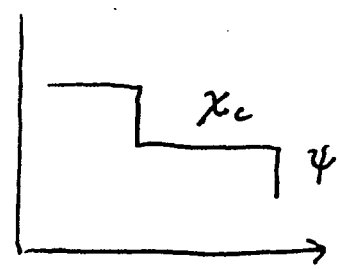

30% of obsd. ψ comes from χ_c dec

Does "anomalous" suppression have been established?

Final State Effects

- Check the COM:
  Polarization of J/ψ at CDF: negative! ... No need COM??
  (A.Schäfer et al.)
- Comovers ...surely they are there: $\psi\pi \to D\bar{D}^*, \psi\rho \to D\bar{D}^*$...
  - thousands of pions
  - pQCD approach...interact weakly (color transparency)
  - Hadronic eff.Lag. ... D-meson exch(range 0.1fm!)
  - Non-Rel quark model ... OGE + quark exch.

  largely different.
  - Expt'l check? ... hadronic P_T broadening of J/ψ?
- screening + gluon dissociation ....both should be taken into account; Transport Simulation Model by (C.M.Ko et al)

Initial State Effects

- parton energy loss, gluon shadowing, ...

have to study the production- and interaction of quarkonia !

Really a threshold?

- small E_T data ... will be done
- change E, A systematically
- Is there any other obs. which shows the threshold?

Redlich QM'99

$J/\psi + \pi \longrightarrow D\bar{D}^*$

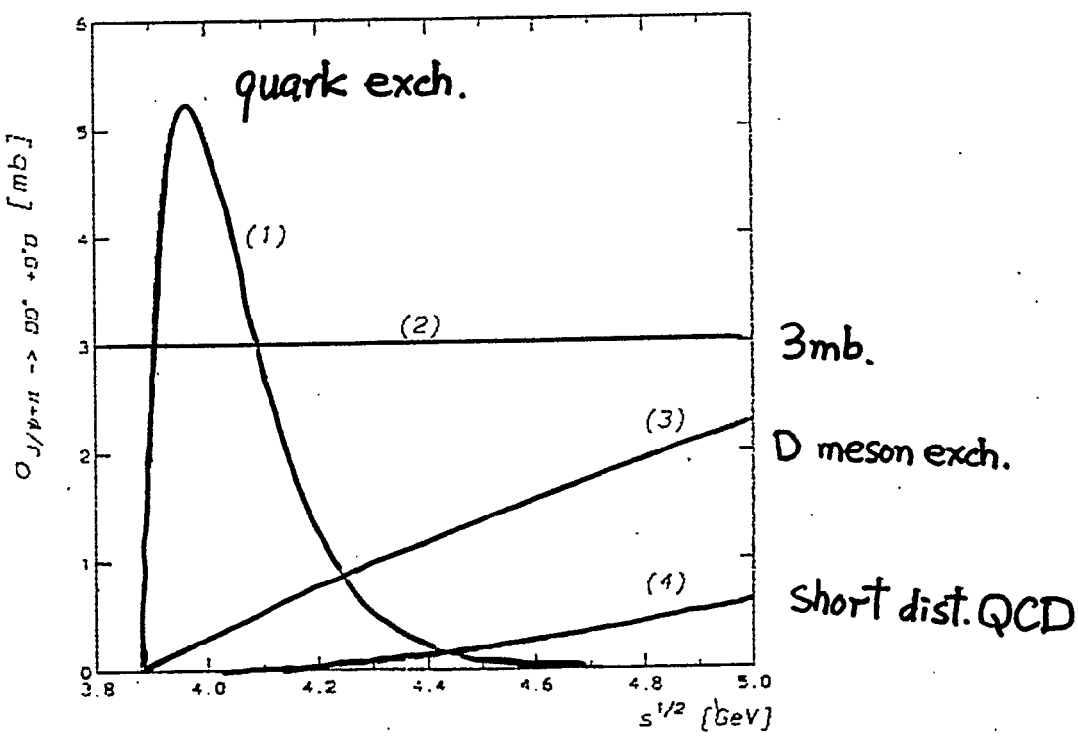

(1) quark-exchange model K. Martins, D Blaschke, E. Quack
(2) $\sigma_{J/\psi+\pi}$=3 mb
(3) meson-exchange model S. Matinyan, B. Muller
(4) short-distance QCD D. Kharzeev, H. Satz

* $T \simeq 200$ MeV or so,

the behavior near threshold is important.

Concluding Remark.

- For QGP,
  one signal is not enough.
  we need various correlated evidences

- For J/ψ supp.
  COM gives us a simple picture for 'normal' suppression

  But... the status in understanding the Q'm production (int. τ_{00}) is controversial yet.

- To understand QGP, need solid results, tools, progresses in various related areas.
  This is one of the interesting + important aspects of the HI physics.

RIKEN Winter School
Quarks, Hadrons and Nuclei
~QCD Hard Processes and the Nucleon Spin~
December 1-5, 2000

Organization of the School

International Advisory Committee:

G. Bunce (RBRC), K. Hagiwara (KEK), K. Imai (Kyoto), M. Ishihara (RBRC), R. Jaffe (MIT), J. Kodaira (Hiroshima), T. Morii (Kobe), T. Uematsu (Kyoto)

Organizing Committee:

T. Ichihara (RIKEN/RBRC), H. En'yo (Kyoto), S. Kumano (Saga), Y. Koike (Niigata), N. Saito (RIKEN/RBRC, co-chair), T.-A. Shibata (TITECH/RIKEN, co-chair), K. Naito (RIKEN), T. Hatsuda (Tokyo), N. Hayashi (RIKEN), K. Yazaki (TWCU/RIKEN, co-chair), T. Yamanishi (Fukui), Y. Watanabe (RIKEN/RBRC)

Lecturers:

G. Bunce (RBRC), H. Fujii (Tokyo), X.-D. Ji (Maryland), W.-D. Nowak (DESY), F. Ukegawa (Tsukuba), M. Wakamatsu (Osaka)

Tutors:

T. Hatsuda (Tokyo), N. Ishii (RIKEN), J. Kodaira (Hiroshima), K. Naito (RIKEN), Y. Yasui (RIKEN)

Secretary:

Y.Kishino (RIKEN)

RIKEN Winter School
Quarks, Hadrons and Nuclei
~QCD Hard Processes and the Nucleon Spin~
December 1-5, 2000

List of the Students of the School

Abuki, Hiroaki	University of Tokyo, Doctor Course abuki@nt.phys.s.u-tokyo.ac.jp
Alam, Jan-e	University of Tokyo, Postdoctor alam@nt.phys.s.u-tokyo.ac.jp
Bernreuth, Stefan	Tokyo Institute of Technology, Postdoctor bernreut@chiral.nucl.phys.titech.ac.jp
Fukushima, Kenji	University of Tokyo, Doctor Course fuku@nt1.c.u-tokyo.ac.jp
Furusawa, Hirofumi	Niigata University, Master Course hiro@nt.sc.niigata-u.ac.jp
Hori, Michihiro	Hiroshima University, Doctor Course michi@theo.phys.sci.hiroshima-u.ac.jp
Huang, Han Wen	Kobe University, Postdoctor huanghw@radix.h.kobe-u.ac.jp
Izumi, Etsuko	Ochanomizu University, Master Course g0040501@edu.cc.ocha.ac.jp
Kamihara, Nobuyuki	Tokyo Institute of Technology, Master Course kamihara@nucl.phys.titech.ac.jp
Mawatari, Kentaro	Kobe University, Master Course mawatari@radix.h.kobe-u.ac.jp
Mineo, Hirofumi	University of Tokyo, Doctor Course mineo@nt.phys.s.u-tokyo.ac.jp
Morii, Kazushige	Hiroshima University, Doctor Course moriikz@theo.phys.sci.hiroshima-u.ac.jp
Nagashima, Makiko	Ochanomizu University, Doctor Course g0070508@edu.cc.ocha.ac.jp
Ohsuga, Hiroshi	Tokyo Institute of Technology, Master Course hiroshi@nucl.phys.titech.ac.jp
Oyama, Satoshi	Kobe University, Doctor Course satoshi@radix.h.kobe-u.ac.jp
Tanaka, Hidekazu	Tokyo Institute of Technology, Master Course thide@nucl.phys.titech.ac.jp
Tanaka, Marie	Hanomizu University, Master Course goo40513@edu.cc.ocha.ac.jp

RIKEN Winter School
Quarks, Hadrons and Nuclei
~QCD Hard Processes and the Nucleon Spin~
December 1-5, 2000

Program of the School

Dec. 1 (Fri)		
	17:30	Registration
	18:00	Reception
Dec. 2 (Sat)		
	9:00 - 10:00	Ji(1)
	10:30 - 11:30	Nowak(1)
	Lunch	
	13:30 - 14:30	Wakamatsu(1)
	15:00 - 16:00	Bunce(1)
	16:30 - 17:30	Ukegawa(1)
	Dinner	
	20:00 -	Discussion
Dec. 3 (Sun)		
	9:00 - 10:00	Nowak(2)
	10:30 - 11:30	Ji(2)
	Lunch	
	13:30 - 14:30	Fujii(1)
	15:00 - 16:00	Ukegawa(2)
	16:30 - 17:30	Wakamatsu(2)
	Banquet	
Dec. 4 (Mon)		
	9:00 - 10:00	Ji(3)
	10:30 - 11:30	Nowak(3)
	Lunch	
	Excursion	
	Dinner	
	20:00 -	Discussion
Dec. 5 (Tue)		
	9:00 - 10:00	Fujii(2)
	10:30 - 11:30	Bunce(2)
	Lunch	
	End of School	

Winter School

Pictures

Additional RIKEN BNL Research Center Proceedings:

Volume 35 – RIKEN Winter School – Quarks, Hadrons and Nuclei – QCD Hard Processes and the Nucleon Spin – BNL-

Volume 34 – High Energy QCD: Beyond the Pomeron – BNL-

Volume 33 – Spin Physics at RHIC in Year-1 and Beyond – BNL-52635

Volume 32 – RHIC Spin Physics V – BNL-52628

Volume 31 – RHIC Spin Physics III & IV Polarized Partons at High Q^2 Region – BNL-52617

Volume 30 – RBRC Scientific Review Committee Meeting – BNL-52603

Volume 29 – Future Transversity Measurements – BNL-52612

Volume 28 – Equilibrium & Non-Equilibrium Aspects of Hot, Dense QCD – BNL-52613

Volume 27 – Predictions and Uncertainties for RHIC Spin Physics & Event Generator for RHIC Spin Physics III – Towards Precision Spin Physics at RHIC – BNL-52596

Volume 26 – Circum-Pan-Pacific RIKEN Symposium on High Energy Spin Physics – BNL-52588

Volume 25 – RHIC Spin – BNL-52581

Volume 24 – Physics Society of Japan Biannual Meeting Symposium on QCD Physics at RIKEN BNL Research Center – BNL-52578

Volume 23 – Coulomb and Pion-Asymmetry Polarimetry and Hadronic Spin Dependence at RHIC Energies – BNL-52589

Volume 22 – OSCAR II: Predictions for RHIC – BNL-52591

Volume 21 – RBRC Scientific Review Committee Meeting – BNL-52568

Volume 20 – Gauge-Invariant Variables in Gauge Theories – BNL-52590

Volume 19 – Numerical Algorithms at Non-Zero Chemical Potential – BNL-52573

Volume 18 – Event Generator for RHIC Spin Physics – BNL-52571

Volume 17 – Hard Parton Physics in High-Energy Nuclear Collisions – BNL-52574

Volume 16 – RIKEN Winter School - Structure of Hadrons - Introduction to QCD Hard Processes – BNL-52569

Volume 15 – QCD Phase Transitions – BNL-52561

Volume 14 – Quantum Fields In and Out of Equilibrium – BNL-52560

Volume 13 – Physics of the 1 Teraflop RIKEN-BNL-Columbia QCD Project First Anniversary Celebration – BNL-66299

Volume 12 – Quarkonium Production in Relativistic Nuclear Collisions – BNL-52559

Volume 11 – Event Generator for RHIC Spin Physics – BNL-66116

Volume 10 – Physics of Polarimetry at RHIC – BNL-65926

Volume 9 – High Density Matter in AGS, SPS and RHIC Collisions – BNL-65762

Volume 8 – Fermion Frontiers in Vector Lattice Gauge Theories – BNL-65634

Volume 7 – RHIC Spin Physics – BNL-65615

Volume 6 – Quarks and Gluons in the Nucleon – BNL-65234

Additional RIKEN BNL Research Center Proceedings:

Volume 5 – Color Superconductivity, Instantons and Parity (Non?)-Conservation at High Baryon Density – BNL-65105

Volume 4 – Inauguration Ceremony, September 22 and Non -Equilibrium Many Body Dynamics – BNL-64912

Volume 3 – Hadron Spin-Flip at RHIC Energies – BNL-64724

Volume 2 – Perturbative QCD as a Probe of Hadron Structure – BNL-64723

Volume 1 – Open Standards for Cascade Models for RHIC – BNL-64722

For information please contact:

Ms. Pamela Esposito
RIKEN BNL Research Center
Building 510A
Brookhaven National Laboratory
Upton, NY 11973-5000 USA

Phone: (631) 344-3097
Fax: (631) 344-4067
E-Mail: pesposit@bnl.gov

Ms. Tammy Heinz
RIKEN BNL Research Center
Building 510A
Brookhaven National Laboratory
Upton, NY 11973-5000 USA

(631) 344-5864
(631) 344-2562
theinz@bnl.gov

Homepage: http://quark.phy.bnl.gov/www/riken.html
http://penguin.phy.bnl.gov/www/riken.html

RIKEN BNL RESEARCH CENTER

RIKEN Winter School

Quarks, Hadrons and Nuclei

~QCD Hard Processes and the Nucleon Spin~

December 1-5, 2000

Li Keran

Nuclei as heavy as bulls
Through collision
Generate new states of matter.
T.D. Lee

Copyright©CCASTA

Speakers:

G. Bunce
H. Fujii
X.-D. Ji
W.-D. Nowak
N. Saito
T.-A. Shibata
F. Ukegawa
M. Wakamatsu
K. Yazaki

Organizers: Naohito Saito, Toshi-Aki Shibata, and Koichi Yazaki